

D-A065 518 AIR FORCE FLIGHT DYNAMICS LAB WRIGHT-PATTERSON AFB OHIO F/G 11/9
CONFERENCE ON AEROSPACE POLYMERIC VISCOELASTIC DAMPING TECHNOLO--ETC(U)
JUL 78 L ROGERS

UNCLASSIFIED

AFFDL-TM-78-78-FBA

NL

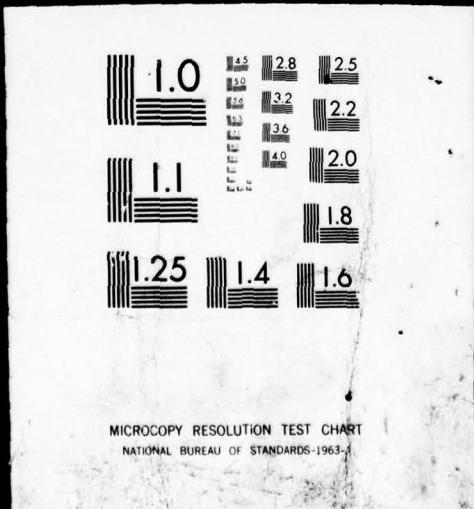
OF 6
AD 65518



FRIED

| OF

AD
AO 65518



14 AFFDL-TM-78-78-FBA

13.5
1 LEVEL II

ADVANCED METALLIC STRUCTURES
ADVANCED DEVELOPMENT PROGRAM OFFICE
STRUCTURAL MECHANICS DIVISION
AIR FORCE FLIGHT DYNAMICS LABORATORY
AIR FORCE WRIGHT AERONAUTICAL LABORATORIES
AIR FORCE SYSTEMS COMMAND
WRIGHT PATTERSON AFB OH 45433

AD A0 655518

16 48646

17 50



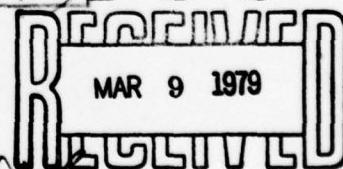
CONFERENCE ON
AEROSPACE POLYMERIC
VISCOELASTIC DAMPING
TECHNOLOGY
FOR THE 1980's held

DDC FILE COPY

7-8 FEBRUARY 1978
DAYTON, OHIO.

Technical rept.

DDC



DR LYNN ROGERS
EDITOR

12 553p

11 JULY 1978

012070
79 03 02 029

APPROVED FOR PUBLIC RELEASE, DISTRIBUTION UNLIMITED

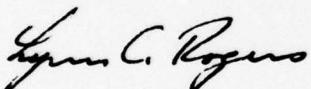
SP

NOTICE

When Government drawings, specifications, or other data are used for any purpose other than in connection with a definitely related Government procurement operation, the United States Government thereby incurs no responsibility nor any obligation whatsoever; and the fact that the Government may have formulated, furnished, or in any way supplied the said drawings, specifications, or other data, is not to be regarded by implication or otherwise as in any manner licensing the holder or any other person or corporation, or conveying any rights or permission to manufacture, use, or sell any patented invention that may in any way be related thereto.

This report has been reviewed by the Information Office (IO) and is releasable to the National Technical Information Service (NTIS). At NTIS, it will be available to the general public, including foreign nations.

This technical report has been reviewed and is approved for publication.



DR. LYNN ROGERS
Project Engineer

FOR THE COMMANDER



WILLIAM R. JOHNSTON
Acting Program Manager
Advanced Metallic Structures
Advanced Development Program Office
Structural Mechanics Division

Copies of this report should not be returned unless return is required by security considerations, contractual obligations, or notice on a specific document.

63211F

Unclassified

SECURITY CLASSIFICATION OF THIS PAGE (When Data Entered)

REPORT DOCUMENTATION PAGE		READ INSTRUCTIONS BEFORE COMPLETING FORM
1. REPORT NUMBER AFFDL-TM-78-78-FBA	2. GOVT ACCESSION NO.	3. RECIPIENT'S CATALOG NUMBER
4. TITLE (and Subtitle) CONFERENCE ON AEROSPACE POLYMERIC VISCO-ELASTIC DAMPING TECHNOLOGY FOR THE 1980'S		5. TYPE OF REPORT & PERIOD COVERED Conference Report
7. AUTHOR(s) Compiled by Dr. Lynn Rogers		6. PERFORMING ORG. REPORT NUMBER
9. PERFORMING ORGANIZATION NAME AND ADDRESS AFFDL/FBA Wright-Patterson Air Force Base, OH 45433		10. PROGRAM ELEMENT, PROJECT, TASK AREA & WORK UNIT NUMBERS Project 486U Task 486U5000
11. CONTROLLING OFFICE NAME AND ADDRESS AFFDL/FBA Wright-Patterson Air Force Base, OH 45433		12. REPORT DATE July 1978
14. MONITORING AGENCY NAME & ADDRESS (if different from Controlling Office)		13. NUMBER OF PAGES 575
		15. SECURITY CLASS. (of this report) Unclassified
		15a. DECLASSIFICATION/DOWNGRADING SCHEDULE
16. DISTRIBUTION STATEMENT (of this Report) Distribution Statement A Approved for Public Release; distribution unlimited		
17. DISTRIBUTION STATEMENT (of the abstract entered in Block 20, if different from Report) DDC REF ID: A6511100 MAR 9 1979 B		
18. SUPPLEMENTARY NOTES		
19. KEY WORDS (Continue on reverse side if necessary and identify by block number) Damping, Viscoelastic, Vibration Damping, Vibration Control, Noise Control, High Cycle Fatigue Control, Resonant Fatigue Control, Attenuation, Abatement		
20. ABSTRACT (Continue on reverse side if necessary and identify by block number) The purpose of this report is to make available the technical papers presented at the Conference on Aerospace Polymeric Viscoelastic Damping Technology for the 1980's. The papers contained herein have been reproduced directly from the original manuscripts.		

DD FORM 1 JAN 73 1473 EDITION OF 1 NOV 65 IS OBSOLETE

Unclassified
SECURITY CLASSIFICATION OF THIS PAGE (When Data Entered)

79 03 02 029

SECURITY CLASSIFICATION OF THIS PAGE(When Data Entered)

~~SECURITY CLASSIFICATION OF THIS PAGE (When Data Entered)~~

FOREWORD

This report was prepared by the Advanced Metallic Structures Advanced Development Program Office under Project 486U, "Advanced Metallic Structures." It was administered under the direction of the Air Force Flight Dynamics Laboratory, Air Force Systems Command. Dr. Lynn Rogers served as Project Engineer.

The technical papers contained in this report were presented at the Conference on Aerospace Polymeric Viscoelastic Damping Technology for the 1980's, which was held at the Ramada Inn-Stratford House, Dayton, Ohio, 7-8 February 1978. Dr. Lynn Rogers served as Conference Chairman.

Gratitude and appreciation is expressed to Mr. Joseph Militello, Mrs. Audrey Sachs, and Mrs. Jennie L. Long, University of Dayton, for the excellent job accomplished as Coordinator, Conference Administrator, and Conference Secretary, respectively. Gratitude is also expressed to the Conference Technical Advisors: Dr. J.P. Henderson, Air Force Materials Laboratory; Dr. D.L.G. Jones, Air Force Materials Laboratory; Mr. A.D. Nashif, Anatrol Corporation; and Mr. D.H. Whitford, University of Dayton Research Institute. Gratitude is also expressed to Mr. George Peterson, Deputy Director, Air Force Wright Aeronautical Laboratories, and Colonel George Cudahy, Director, Mr. Keith Collier, Chief Scientist, and Mr. William H. Goesch, Deputy Program Element Manager, Air Force Flight Dynamics Laboratory for their support of the Conference and their expressed interest and support of this technical area.

The report was submitted by the author on 11 July 1978.

Publication of this report does not constitute Air Force approval of the findings or conclusions presented. It is published only for the exchange and stimulation of ideas.

ACCESSION for	
NTIS	White Section <input checked="" type="checkbox"/>
DDC	Buff Section <input type="checkbox"/>
UNANNOUNCED <input type="checkbox"/>	
JUSTIFICATION	
BY	
DISTRIBUTION AVAILABILITY CODES	
Dist. AFPL and/or SPECIAL	
A	

TABLE OF CONTENTS

	<u>Page</u>
KEYNOTE ADDRESS: The Role of Damping Technology In Reliability and Life Cycle Cost of Future Air Force Systems	
G. P. Peterson, Air Force Wright Aeronautical Laboratories, Wright-Patterson Air Force Base, Ohio	1
INTRODUCTION	
Dr. Lynn Rogers, Conference Chairman Air Force Flight Dynamics Laboratory Wright-Patterson Air Force Base, Ohio	7
Introduction To Damping Materials and Systems For Vibration Control in Structures	
D. I. G. Jones, Air Force Materials Laboratory Wright-Patterson Air Force Base, Ohio	11
Measurement of Materials and System Damping	
R. Plunkett, University of Minnesota, Department of Aerospace Engineering and Mechanics, Minneapolis, Minnesota	97
Summary of Constrained Damping Literature	
R. A. DiTaranto, Widener College Chester, Pennsylvania	109
Vibration Damping Analysis by Finite Elements	
F. K. Bogner and R. A. Brockman, University of Dayton Research Institute, Dayton, Ohio	127
Damped Vibration Theory: A State-Of-The-Art Assessment	
F. C. Nelson, Department of Mechanical Engineering Tufts University, Medford, Massachusetts	155
Selected 3M Materials, Properties, Environmental Resistance and Applications	
D. B. Caldwell, 3M Company, Industrial Specialties Division, St. Paul, Minnesota	165
Developments in Damping Technology	
E. J. O'Keefe, Specialty Composites Corporation Acoustics R&D, Newark, Delaware	183
Selected E-A-R Damping Materials and Applications	
E. H. Berger, EAR Corporation Indianapolis, Indiana	197
Necessary Steps for Successful Viscoelastic Damping Applications	
Dr. Lynn Rogers, Air Force Flight Dynamics Laboratory Wright-Patterson Air Force Base, Ohio	219

TABLE OF CONTENTS (CONT.)

	<u>Page</u>
Spatial and Temporal Temperature Distribution Considerations D. B. Paul, Air Force Flight Dynamics Laboratory Wright-Patterson Air Force Base, Ohio	225
Fourier Analysis in the Laboratory and in the Field M. L. Drake, University of Dayton Research Institute Dayton, Ohio	253
A Thoroughly Engineered Application of Damping Technology to Jet Engine Inlet Guide Vanes Lynn C. Rogers, Air Force Flight Dynamics Laboratory Wright-Patterson Air Force Base, Ohio	
and	
Michael L. Parin, University of Dayton Research Institute Dayton, Ohio	277
High Modulus Graphite Fiber Constrained Layer Damping Treatment for Heavy Aerospace Structures J. Soovere, Lockheed-California Company Aeromechanics Department, Burbank, California	295
Airframe Structural Damping Evaluations and Applications H. W. Bartel, Lockheed-Georgia Company, Advanced Structures, Marietta, Georgia	321
Viscoelastic Damping Applications B-1 Aircraft A. G. Tipton, Los Angeles Division, Rockwell International, Los Angeles, California	331
Modal Damping Measurements on Pabst Adhesively Bonded Airframe Fuselage Structure R. Gordon, Air Force Flight Dynamics Laboratory Wright-Patterson Air Force Base, Ohio	
and	
J. Sharp, Aeronautical Systems Division Wright-Patterson Air Force Base, Ohio	357
Damping for Enhanced Reliability in Vibroacoustic Environments R. N. Hancock and J. A. Hutchinson Vought Corporation, Vibroacoustics, Dallas, Texas	367
Hamilton Standard Electronics Presentation - Slides Only W. Ammerman Hamilton Standard Electronics Windsor Locks, Connecticut	385

TABLE OF CONTENTS (CONCLUDED)

	<u>Page</u>
Examples of the Use of Additive Elastomeric Damping Treatments to Control Vibration Problems in Air Force Systems C. M. Cannon, University of Dayton Research Institute Dayton, Ohio	397
SMRD Damping Applications J. M. Medaglia and C. V. Stahle General Electric Company, Space Division Philadelphia, Pennsylvania	419
The Influence of Damping on Acoustic Transmission Loss of Panels L. L. Faulkner Battelle, Columbus Laboratories Columbus, Ohio	451
Vibration Reduction of Airborne Optical System Using Light Weight Constraining Damping Technique C. P. Lui Hughes Aircraft Company, Laser Division Culver City, California	461
Property Measurement and Application of Elastomer Dampers A. J. Smalley Mechanical Technology Inc., Machinery Dynamics Section Latham, New York	481
ASTM Damping Materials Testing Specification Activity E. E. Dennison Gilbert/Commonwealth Association, Power Engineering Division, Jackson, Michigan	533
DAMP IT: A Proposed Advanced Development Program Dr. Lynn Rogers Air Force Flight Dynamics Laboratory Wright-Patterson Air Force Base, Ohio	539
CONFERENCE SUMMARY	551
AGENDA	555
ATTENDANCE LIST	561

KEYNOTE ADDRESS

THE ROLE OF DAMPING TECHNOLOGY
IN RELIABILITY AND LIFE CYCLE COST
OF FUTURE AIR FORCE SYSTEMS

G. P. Peterson
Air Force Wright Aeronautical
Laboratories
Wright-Patterson Air Force Base,
Ohio

KEYNOTE ADDRESS

THE ROLE OF DAMPING TECHNOLOGY IN RELIABILITY AND LIFE CYCLE COST OF FUTURE AIR FORCE SYSTEMS

G. P. Peterson
Air Force Wright Aeronautical Laboratories

I'd like to welcome all of you to Dayton and just say a few words from my perspective. Hopefully, this will convey to you from a management standpoint the kind of environment that we see for the kind of technologies that the four laboratories at Wright-Patterson are involved in.

There is no doubt that there is, and will continue to be, a tremendous degree of activity in terms of the reduction of life cycle cost, and that is keyed around the O&S cost. We certainly in the last five to ten years in all the labs have made a hard run, and are still making a hard run, at the reduction of acquisition costs. I think you will see a substantial increase in the O&S cost reduction activity. Although I cannot forecast completely at this juncture, some of the Air Force Wright Aeronautical Laboratories have gone a lot harder in that direction than some of the others, but I think they're all pointed that way. The reason for that is not simply that it's a popular bandwagon and we might as well all climb on. I think it's done primarily from a dollars and cents point of view. It simply says that there are some substantial problems in the field. We have a tremendous investment year in and year out in resolving those problems and, therefore, technologies which can impact on them are going to wind up with extremely high priorities in terms of their development.

Along those lines, payoff is very important; Lynn Rogers has a car with a license plate that has "DAMP IT" on it. I was wondering what "DAMP IT" meant. It says in the program, Dynamics Abatement and Major Payoff, that's where the "DAMP" comes from, and the "IT" is for Integrated Technology. But if you take the payoff out, you just have "DAM IT". One of the major things everyone, certainly we and the Logistic Command, are going to have to do a much better job on, is to try to come up with as hard an analysis as we can in terms of those payoffs; because those payoffs will determine where resources are applied, both yours and ours. Certainly for those of you from industry, as you look to your management in terms of their support, the questions are, "How much do I have to put up?", "When do I get it back?", and "How much do I get back?". Those questions are basic ones for all of us in the kind of environment where front-end money and front-end people resources are tough to come by. Those questions are going to have to be answered a lot better. So for those of you

who deal in product form, either in the manufacture or the supply of it, or for those of you who are here from the ALC's or AFLC or the ALD, that kind of data is extremely important. The opening up of pipelines to provide that kind of information is extremely important in terms of where we apply our resources. But I will come back to my point that, without a doubt, we see a substantial payoff in working that arena. I don't believe we've reached the point where we're leveling off. That curve is still on the upswing in terms of the applications of those resources and, as we get closer and closer to those kinds of problems, we find more and more opportunities or places to spend our money. Therefore, as we look at a fascinating technology with high promise, such as damping, it must compete with other high payoff technologies; it has to compete in a dollar and cents arena and win your support as well as ours.

I know from when I was in the Materials Laboratory that Jack Henderson who is a super guy, and Dave Jones who is a super guy, and believe me, both super salesmen, are damn tough to hold off; they keep coming and that's good. That kind of tension in the system is necessary. That kind of pressure is good, it is positive and I urge you all to develop that kind of aggressive, persevering attitude with the technology if you have an interested role in it because that kind of entrepreneurship and that kind of hard drive is absolutely required to sell management on providing the necessary resources to get the job done.

In addition to that drive, you need data, you need information, and you need good ideas. That's why I'm particularly pleased to look at this group today, which as indicated by the invitation list, represents a cross-section of the kind of people who either have that data or can get that data and certainly will have the opportunity to develop and conceive the kind of approaches we are going to need to make this technology real.

It already is, at least in my limited perspective, a real technology in terms of some of the things we're seeing going into the propulsion area now, again pioneered by some of the people in the Materials Laboratory and the Propulsion Laboratory. That opportunity in the propulsion area is one that we're almost there on, at least in one case. Coming off that base, I believe we'll see an opening of further applications with that type of damping solution. I believe though as I look at the program and look at where we stand now with the technology, we see other opportunities in terms of going to higher temperature damping solutions. Also, we see the opportunity to a great extent in the airframe, avionics, and equipment areas; in fact, any place there's a vibration problem. As we seek to expand coming off this initial, successful experience, it's extremely important that we define those areas, that we provide the data, the analysis that substantiates what's the problem, what can we do about it, how much is it going to cost, and what the payoff is. That kind of data is extremely important both to your management and mine if we're going to make the right kinds of decisions. I urge you all, and this meeting is a good place to start, to put

the story together in a clear way. There are lots of people with lots of ideas; all of which are going to save money: if you just give me a dollar now, I'll save you ten in a year or two or three. Therefore, those of you who can muster the most evidence, the clearest story, are the ones who are going to wind up with the kind of resources that its going to take to get the job done.

Most of what I've talked about so far deals with O&S, and it deals with possible field solutions. That's extremely important. Obviously, I am not standing here saying that there will not be another new airplane, but I cannot forecast exactly when that will happen. Thus, as we look to investments now, and a return on those investments, technology which can play against existing vehicles, currently in the inventory or those now in development and scheduled to go into the inventory is extremely important. This is because it's only through the applications of technology to those vehicles that we may get a relatively near or midterm kind of return. That kind of return is important to all of us.

I also believe that it is extremely important that I don't overemphasize the field fix and the O&S business. We still have in the laboratories a vital role to play in terms of the next systems, whether they be space, aircraft, or missile systems and in that role the use of this kind of technology in the front end, in the design-in end, is extremely important as well. So, I don't want to leave you with the impression that we're talking about technology now as simply something you shove out in the field. This kind of technology will play in both arenas and therefore is doubly attractive.

I would urge one other thing. In the drive to increase the applications spectrum, moving from what may be organic technology (primarily with aluminum foil and adhesives, etc.) in propulsion applications, moving into airframe, missile, laser potential applications, and expanding that application spectrum, I would urge you all not to forget the fundamental research base which really leads to a thorough understanding of what it is you're doing. That fundamental base, the solid scientific understanding of the basic principles, is something I believe is extremely important. I know, having lived through the composites business, that it still, in certain minds, has an aura of black magic ("I don't know how they do it but they mix up some magic hocus-pocus and they smear it on and it works somehow, but I don't quite understand why."). As long as you've got that stamp on a technology, management will resist utilization and it will find only a specialty sort of utility. I believe with the kind of potential we see with this technology, that while on the one hand we drive toward increasing the applications spectrum, we must also pay a tremendous amount of attention to the fundamental base, acquiring a thorough understanding of what we're doing, how we're doing it, why it works. That understanding for both the Government as well as industry is key if we're going to use this kind of technology intelligently.

There are entrepreneurs now for advanced development damping activity; now is also a very good time to take a look at what we call our 6.1 or basic research base in terms of understanding the fundamentals and basic principles. As we move into further applications, I believe that we also ought to ensure that there is a research base activity that builds that understanding hand-in-hand, and most importantly, ahead of the applications, or we greatly increase the risk of potential problems in the future.

I can truthfully say I believe this is an exciting technology area. I wouldn't have agreed to keynote it if I hadn't believed that it has a tremendous potential. I believe that the people involved can say this with great confidence from the Air Force side, are hard driving, they've got their heads screwed on right, they're dynamic. I hope this conference will not damp them out but will add to their determination and also provide important guidance and input.

Therefore, I would urge you all to get on the air and get in as much discussion and dialogue as you possibly can during the conference. I would certainly welcome talking with any of you, who, coming off of this conference, have some clear thoughts in your mind as to what ought to happen, how things ought to go, ideas that you see or impressions that you've got, convictions, etc. We face some tough decisions coming up very shortly in terms of where we put our resources. I think that anything you might have to offer would certainly be of interest to me. I, therefore, open up the communication channels in terms of mail or a call or whatever it is that turns you on in terms of the way you'd like to communicate in getting back to me with whatever your thoughts or comments might be on this subject. It's one of considerable importance to us and we're going to go through some agonizing decisions over the coming months in terms of budget, people resources, and so your inputs I can honestly say would be very valuable.

I wish you, and I know you'll have, a super conference, a terrific conference. I wish the best to you all. I hope to hear from you. Thank you.

INTRODUCTION

**Dr. Lynn Rogers
Conference Chairman
Air Force Flight Dynamics
Laboratory
Wright-Patterson Air Force Base,
Ohio**

INTRODUCTION

Dr. Lynn Rogers
Conference Chairman
Air Force Flight Dynamics Laboratory

This conference is sponsored by the Advanced Metallic Structures Advanced Development Program Office in the Structural Mechanics Division at the Air Force Flight Dynamics Laboratory. Among the many purposes and benefits of the conference, two should be mentioned; namely, information exchange and program identification. By way of program identification and definition, it is hoped to receive inputs and to reach a consensus on general technology needs and opportunities based on a review of past applications and state of the art to determine problems, payoffs, and limitations.

No conference on damping technology should fail to mention the pioneering role of the Air Force Materials Laboratory in sponsoring and advancing damping technology. With the emergence of a technology base in polymeric materials and their utilization in practical vibration damping, the Air Force Flight Dynamics Laboratory has responsibility for airframe, avionics, and accessories applications, while the Air Force Materials Laboratory has the responsibility for the propulsion area.

Recent cost estimates indicate that vibration-induced failures costs the Air Force over \$200M annually. This does not include degraded performance or operational readiness. Vibration is a problem in the Air Force, as well as to the rest of the world.

Many of those problems could be greatly abated with proper use of polymeric viscoelastic damping. Of course, not all vibration problems can be alleviated with damping, but the benefits have not begun to be tapped.

While viscoelastic damping is a specialty within the specialty of vibration engineering, and while there is somewhat of an art to certain types of applications, basic scientific and engineering principles apply and can be mastered. Those who are unwilling or unable to invest the necessary time and energy in developing adequate understanding and skills and who, nevertheless, embark on an application of damping, most often achieve very poor results. A shot in the dark rarely hits the target. The worst result from these situations is usually not that the vibration problem was not solved, but that a very lasting and very negative attitude toward viscoelastic damping is formed throughout the involved organizations. To memorialize this often found situation, the definition given in Figure 1 is offered.

DEFINITION OF DAMPING

SOMETHING WE TRIED IN '66,
IT DIDN'T WORK
AND SO WE HAVEN'T TRIED IT ANYMORE

OF COURSE:

- IT WAS A TOUGH (VIBRATION, NOISE, RESONANT FATIGUE) PROBLEM
- OUR GUY'S WORKED HARD ON IT
- TRIED EVERYTHING
- BRAINSTORMED THE OLD HEADS
- RAN OUT OF TIME
- RAN OUT OF FUNDS
- SOMEBODY SAID LET'S TRY DAMPING - WE HAVE 3 DAYS LEFT

Figure 1

**INTRODUCTION TO DAMPING MATERIALS AND SYSTEMS
FOR VIBRATION CONTROL IN STRUCTURES**

**D. I. G. Jones
Air Force Materials Laboratory
Wright-Patterson Air Force Base, Ohio**

I. INTRODUCTION

Structures and machines are normally designed to meet innumerable criteria which are defined by the use for which the structure or machine is intended, and which include (a) geometrical and tolerance factors, (b) external static loading and strength considerations, (c) external dynamic loads and loads resulting from movement within and/or of the structure or machine, and (d) dynamic response characteristics. The first two of these factors have little to do, directly, with noise and vibration phenomena although their influence on the second pair of factors can be very marked. The third factor, namely external loads and internal loads generated by movements within the structure or machines, can produce serious noise and vibration problems, as for example the noise emanating from meshing gear teeth in an engine transmission. However, it is very often the dynamic response characteristics of the machine or structure which amplify and aggravate these sources of noise and/or vibration and thereby cause even more serious problems. Examples of such phenomena include (a) sonic fatigue, where the resonant response characteristics of aircraft skin structure coupled with intense noise from jet engines leads to high stresses and early failure, (b) resonances of jet engine fan or turbine blades which can couple with multiples of the shaft rotation speed to generate undesirable vibration induced stresses, unless the

utmost care is taken to avoid these resonances, (c) rotating shafts, where critical speeds can occur at or near design rotation speeds and lead to shaft whirling problems unless care is again taken, (d) gear systems, which tend to resonate at certain speeds unless care is taken to avoid these conditions by careful geometrical design or by the use of more appropriate gear materials, (e) thin panels, plates and shells in machines and structures which often vibrate excessively and act as serious secondary sources of noise, (f) pipes and tubes in engines which can vibrate excessively in response to engine induced excitation and fail prematurely, (g) modern steel frame buildings which can vibrate excessively under wind and earthquake loading.

Now it must be clearly understood that noise control problems can be exceedingly difficult to resolve because, although resonance amplified vibration may be at their root, possibly in an inaccessible location, many other parts of the structure will serve to amplify, transmit and/or re-radiate the output of the original source. Vibration control problems are usually somewhat simpler to resolve because the vibration problem is usually identifiable as directly associated with some abnormal dynamic behavior of the part affected, and not with some far distant point which may be the source as in the case of some noise problems. It follows, therefore, that if a noise problem is directly and intimately linked with local abnormal dynamic behavior of a part of a structure, some

noise reduction may be achieved by controlling the vibration, whereas if it is not, a solution will be far more difficult to achieve. We shall now discuss in more depth the available technology for control of vibration problems in structures and machines, bearing in mind that this technology must be utilized with knowledge and care, and recognizing that it can also be used to solve many problems of noise control, but certainly not all. The one phenomenon which dominates the dynamic behavior of structures and machines is resonance. To understand what this means, let us consider the simple mass-spring system illustrated in Figure 1.

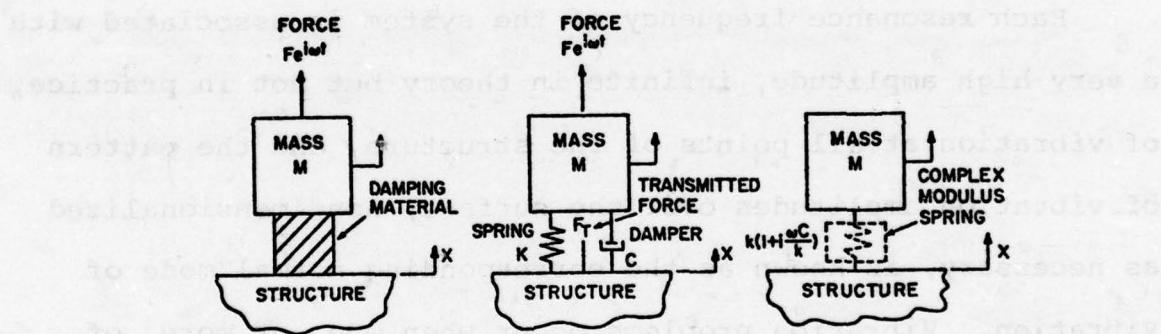


Figure 1. Mass - Spring - Damper System

This system consists of a mass M connected through a spring of modulus K to a rigid surface. A force is now applied to the mass at a finite frequency of oscillation. At very low frequencies, the mass simply moves steadily as

the force varies with time. As the frequency increases, the inertia force $-M\ddot{X}$ gradually increases until it is eventually exactly equal and opposite to the force KX of the spring and the amplitude of the vibration $|X|$ can then build up indefinitely to an infinitely large value, at least in theory, and the particular frequency at which this occurs is known as the resonance frequency. At higher frequencies, the inertia force $-M\ddot{X}$ become extremely large and the mass M tends to "stand-still". So much for a very simple structure. For a more complex structure or machine, similar phenomena occur but with more than one resonance. See Figures 2 to 4.

Each resonance frequency of the system is associated with a very high amplitude, infinite in theory but not in practice, of vibration at all points of the structure, and the pattern of vibration amplitudes over the surface, nondimensionalized as necessary, is known as the corresponding normal mode of vibration. Vibration problems occur when one, or more, of these resonant frequencies occur at frequencies where significant excitation exists, so that high amplitudes arise and cause failure or malfunction.

Vibration control is the technology available for (a) moving the resonance peaks to less sensitive values, (b) reducing the magnitude of the exciting forces at the source, (c) changing the mode shapes in a favorable manner and/or

(d) reducing the height of the resonance peaks. Technique (a) is widely used to design shafts, turbines and other rotating machines so that resonant peaks do not fall directly over frequencies of significant excitation. The procedure is not always perfect because it is difficult to make a large number of resonant frequencies always avoid a large number of excitation frequencies under all speed conditions; moreover, it is not possible at all if the excitation is of significant magnitude over a broad frequency range and not merely at a number of discrete frequencies. Technique (b) is clearly desirable at all times, but definite limits exist as to what reduction in the excitation can be achieved. Technique (c) is difficult to apply since it demands a remarkably precise knowledge of the dynamic response of the structure, but is certainly a possible approach in some instances, usually in conjunction with technique (a). Technique (d) will consistently reduce the severity of a vibration problem, but demands a totally different technology from the first three techniques, which essentially involve either reducing the magnitude of the excitation or making geometrical changes in the structure. In order to reduce the amplitude at each resonance to a low value, relative to that customarily measured, energy must be dissipated in the structure before it has the opportunity of generating high resonant amplitudes. This is what is meant by damping, and useful damping can be introduced into a structure only by using materials or techniques which dissipate much larger amounts of energy than resonating structures customarily do.

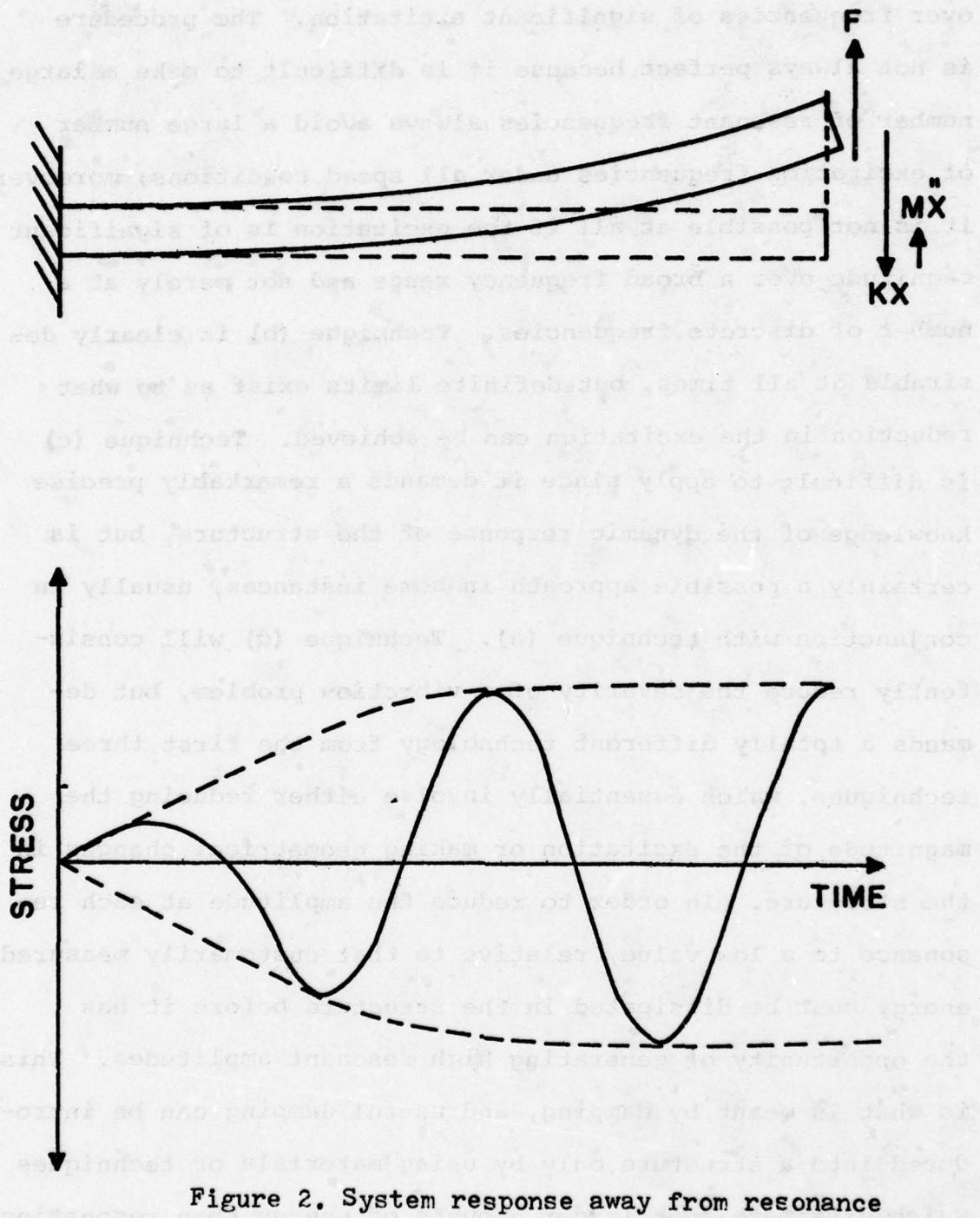


Figure 2. System response away from resonance

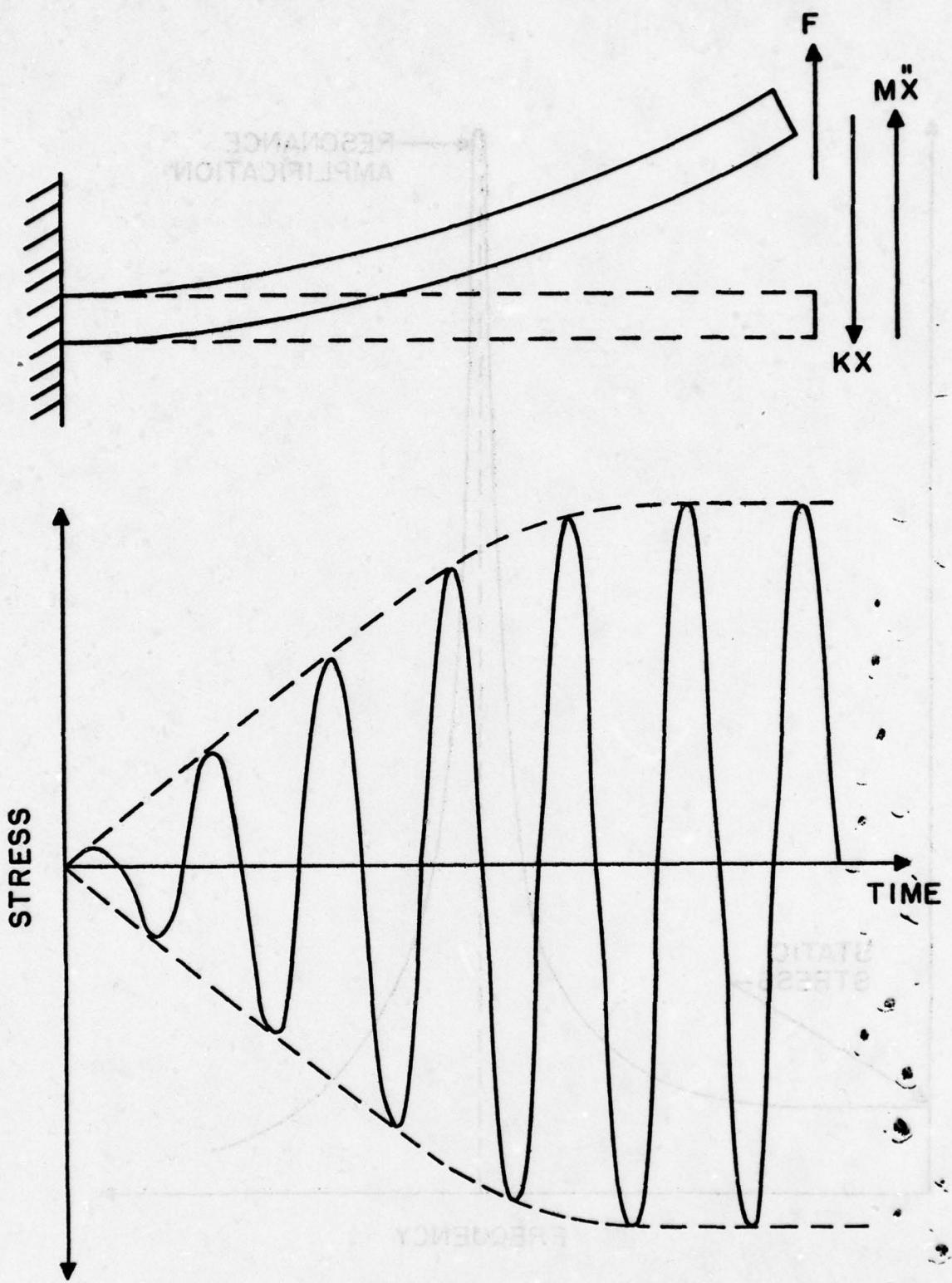


Figure 3. System response at resonance

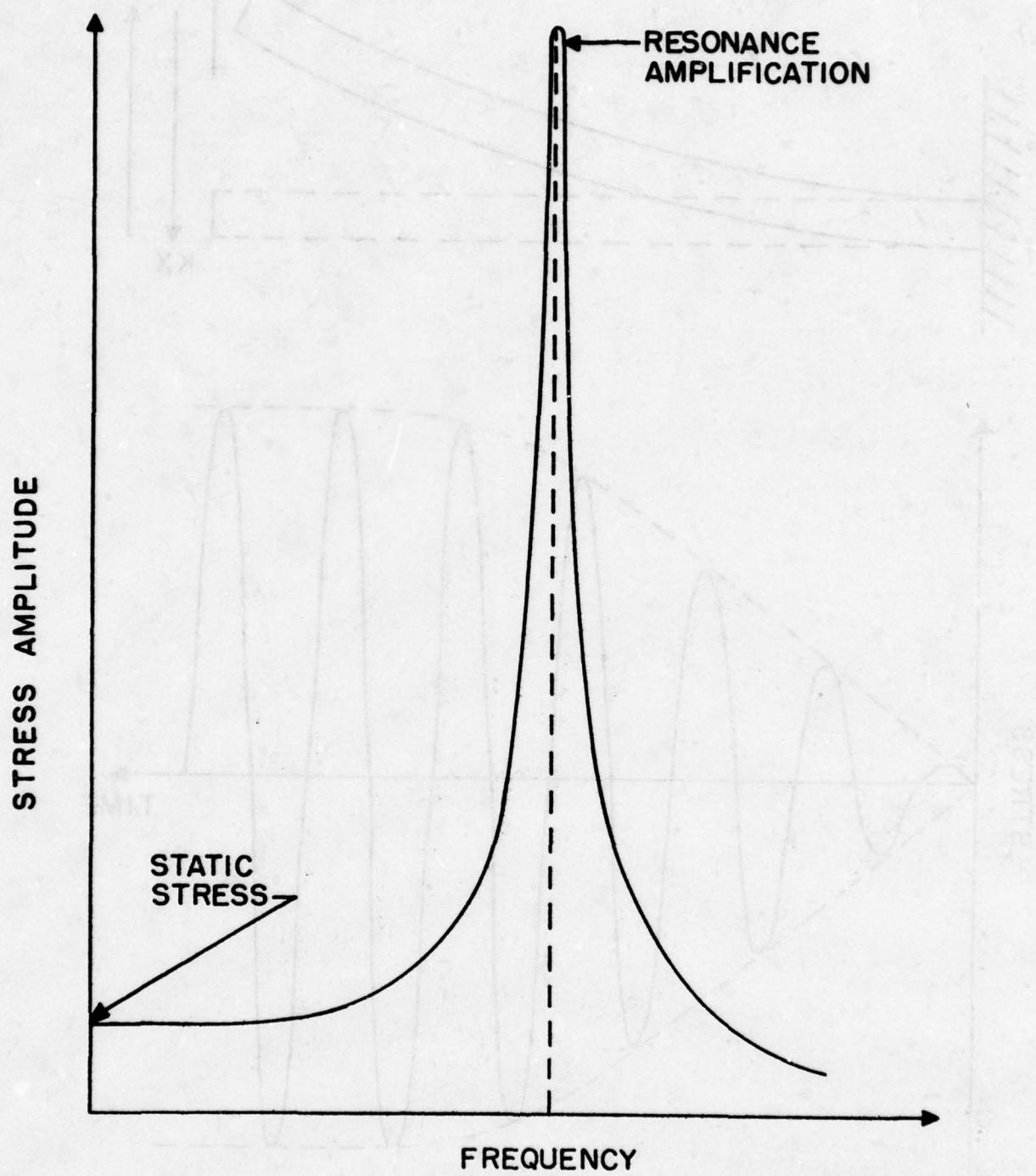


Figure 4. Idealised response spectrum

2. SOURCES AND CHARACTERIZATION OF DAMPING

Most materials used for structural purposes are not noteworthy for the amount of energy which they are capable of dissipating under cyclic strain and, indeed, such behavior would be regarded as unacceptable for most design purposes unless dynamic response criteria were of primary importance. However, it is true that all materials, when strained cyclically, do dissipate some energy no matter how little it may be and therefore all materials normally possess damping in some degree. A useful way of introducing the concept of damping is in terms of the various types of stress-strain curves which can be observed in simple specimens of various types of material when they are uniaxially strained, cyclically, to various amplitude levels. Once a steady state has been reached, after several cycles, the stress-strain curve of a material will not be a straight line, as for a perfectly elastic material, but will instead be a closed loop known as a hysteresis loop. The shape of this loop will depend on the material itself, environmental factors such as temperature, frequency, and the strain amplitude. No matter what the shape may be, the area enclosed by the stress-strain loop will be a direct measure of the energy dissipated per unit volume per cycle, and hence a measure of the damping. This damping behavior arises from a wide variety of internal sources including grain boundary effects, point defect relaxations, thermoelastic effects, eddy

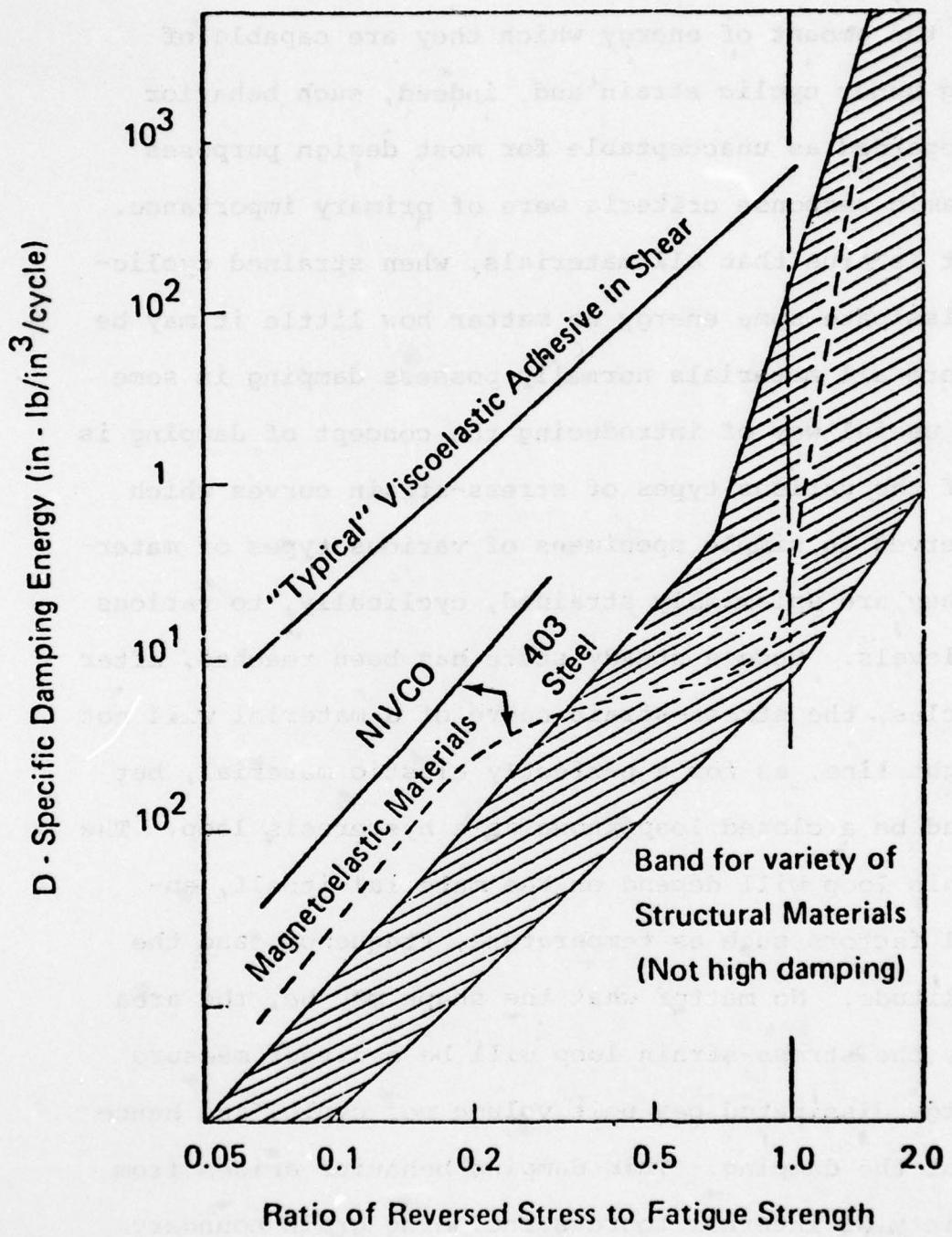


Figure 5. Dissipative behavior of various materials

currents in metals and alloys and interactions between chains of large molecules in elastomeric materials. Further details may be followed up in the literature, particularly in the work of Lazan [1]. See Figure 5.

As a broad rule, the damping behavior of most elastomeric, or rubberlike, materials is the most readily amenable to characterization and analysis as compared with, say, the metallic class of materials. In the case of most elastomeric material specimens, subjected to uniaxial cyclic strain, the steady state stress-strain curve is essentially an ellipse, as illustrated in Figure 6.

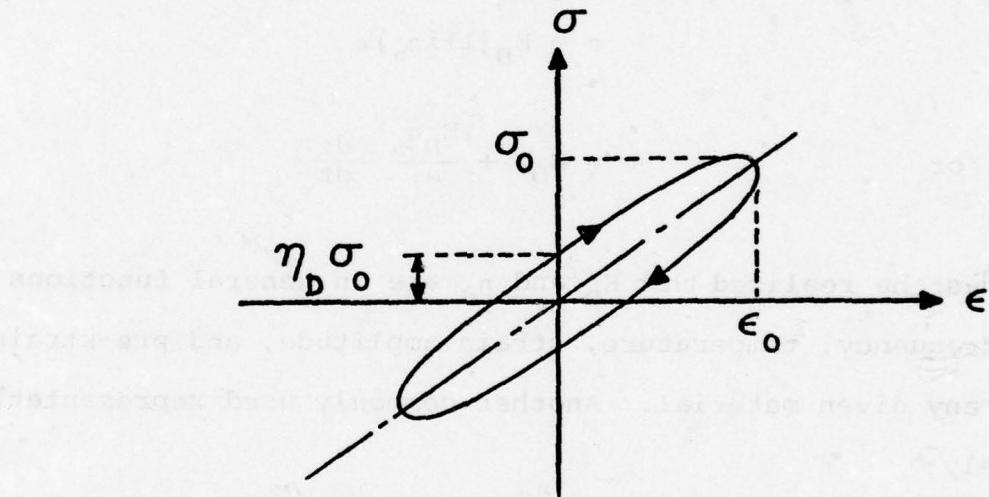


Figure 6. Elliptical hysteresis loop

The degree of simplicity which evolves from this particular fact is best realized by writing down the equation of the ellipse, then inserting a sinusoidally varying strain $\epsilon = \epsilon_0 \sin \omega t$ and calculating, from the equation of the ellipse,

the stress necessary to produce the motion indicated thereby. The result [2, 3] is an exceedingly simple representation of the material behavior in which the real moduli E or G of a perfectly elastic material are replaced by complex moduli $E_D(1+i\eta_D)$ or $G_D(1+i\eta'_D)$ which are, of course, meaningful in a direct sense only if the strain and stress vary as $\exp(iwt)$ in the time domain. This complex arithmetic approach then allows one to directly apply any solutions which are obtainable for the perfectly elastic case by merely changing over to complex arithmetic. Those who are less familiar with complex numbers can equally well work with a real number representation. These two representations may be written as:

$$\sigma = E_D(1+i\eta_D)\epsilon$$

or

$$\sigma = E_D\epsilon + \frac{E_D\eta_D}{\omega} \frac{d\epsilon}{dt}$$

It must be realized that E_D and η_D are in general functions of frequency, temperature, strain amplitude, and pre-strain for any given material. Another commonly used representation, namely

$$\sigma + A \frac{d\sigma}{dt} = B\epsilon + C \frac{d\epsilon}{dt}$$

is equivalent for $\epsilon = \epsilon_0 \exp(iwt)$, if A, B, and C are chosen appropriately to simulate as closely as possible the actual variation of E_D and η_D with frequency. By means of these simple stress-strain relationships, one can obtain some idea of the meaning of E_D and η_D , as applied to the vibrations of a simple system.

So much for characterization. The way in which the large number of available elastomeric materials differ from each other is in the variation of E_D and η_D with frequency, temperature, strain amplitude and prestress, temperature being by far the most important factor since E_D can vary by as much as four orders of magnitude over a narrow temperature range in some cases. The variation of Young's Modulus E_D and loss factor η_D with temperature for an elastomer, at fixed frequency and cyclic strain amplitude, are typically of the form shown in Figure 7. Three distinct temperature regions are observed, namely the glassy region, the transition region and the rubbery region. In the glassy region, E_D is high and η_D is low; in the transition region E_D varies rapidly with temperature and η_D is high, and in the rubbery region E_D varies more slowly with temperature and η_D is lower than in the transition region, although not as low as in the glassy region. At the very highest temperatures, irreversible thermal decomposition of the material occurs.

Although the variation of complex modulus properties with frequency is less drastic than with temperature, it is often important. For a typical material, graphs of E_D and η_D versus temperature for a number of frequencies might look as in Figure 8.

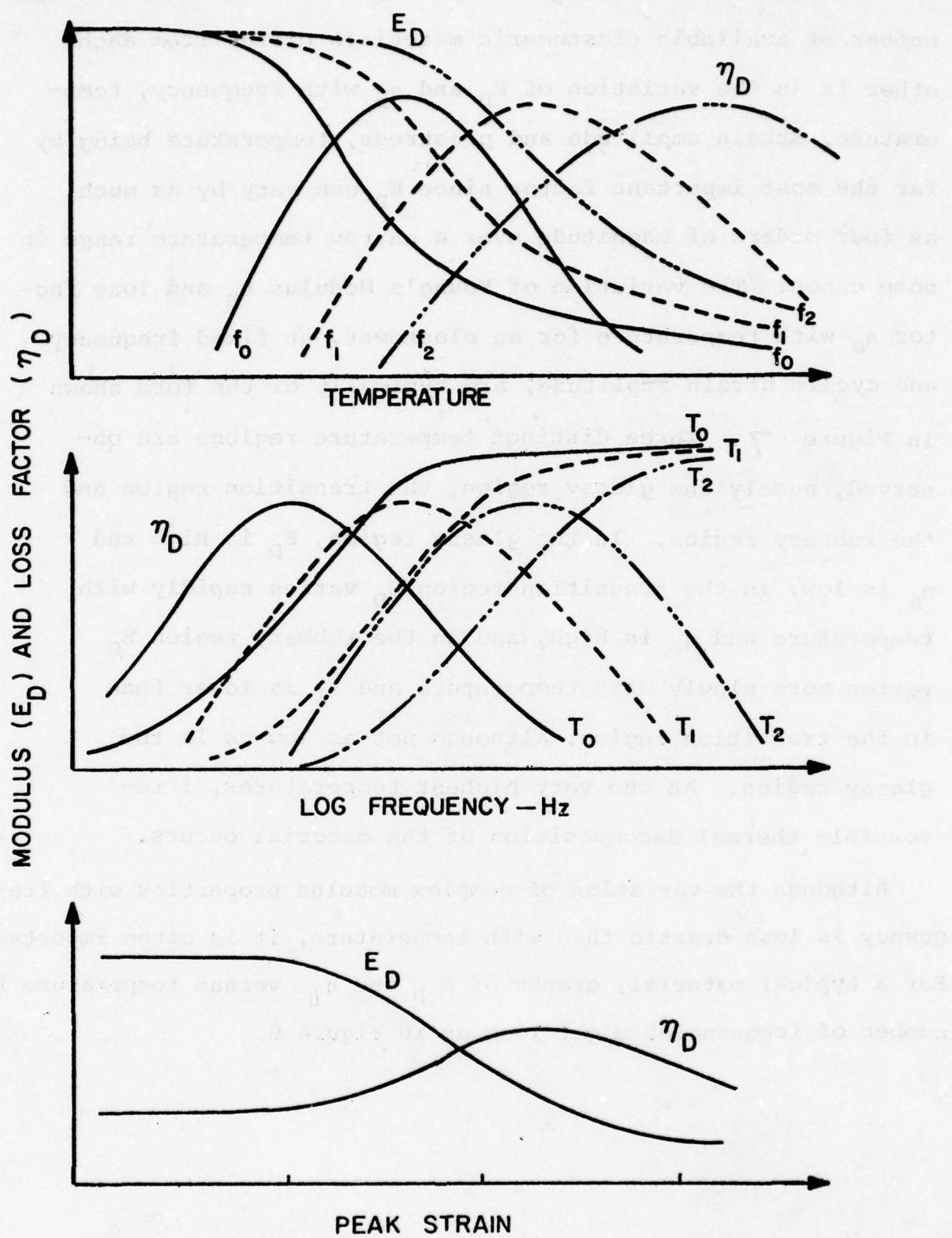


Figure 7. Idealised damping material behavior

Temperature - frequency equivalence

If the effects of frequency on damping material behavior are taken into account, one of the most useful techniques for presenting the experimental data is by means of the temperature-frequency equivalence (reduced frequency) for linear rheological materials [1,2,4]. In this approach, $(T_0 \rho_0 / T\rho) \times E_D$ and η_0 are plotted against the so-called reduced frequency parameter $f.a_T$, where f is the actual frequency, a_T is a function of the absolute temperature T , and T_0 is a reference temperature, again on the absolute scale. Usually T_0/T and the density ratio ρ_0/ρ are regarded as 1.0 over a wide temperature range and are ignored. The preparation of "master curves" of E_D and η_0 against $f.a_T$ is extremely useful for extrapolating test results obtained under a wide but still limited set of conditions. For example, in a test series one may have data over the frequency range 100 to 1000 Hz and a temperature range from 0°C to 100°C and wish to estimate the properties at 50°C and 2 Hz. In order to achieve this, one first uses the available data to produce a best fitting set of master curves. The process is most satisfactorily accomplished empirically by judging the factor a_T on the basis of the shift needed to make the curve of $\log E_D$ versus \log (frequency) as in Figure 8, at temperature T_i ($T_i = \pm 1, 2, \dots$), match as closely as possible the curve of E_D versus frequency at temperature T_0 , while at the same time matching the curves of η_0 versus frequency at temperatures T and T_0 , to produce curves like those shown in Figure 9. In this way, the limitations of the measuring techniques can be at least partly compensated for. Typically, a_T will vary with temperature in the manner illustrated in Figure 9. Figures 10 to 12 show the data reduction for polyisobutylene.

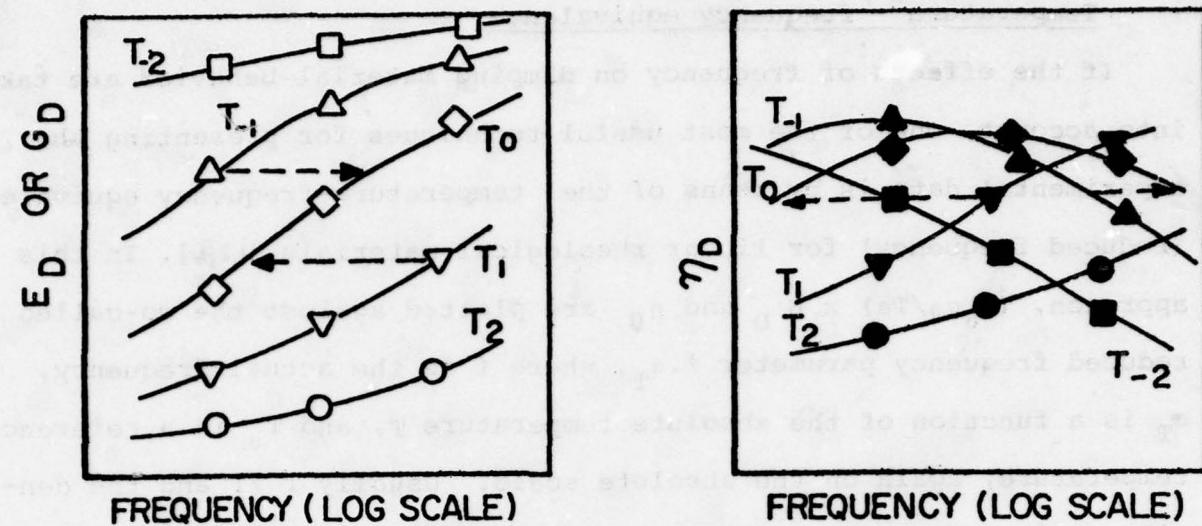


Figure 8. Damping behavior as function of frequency

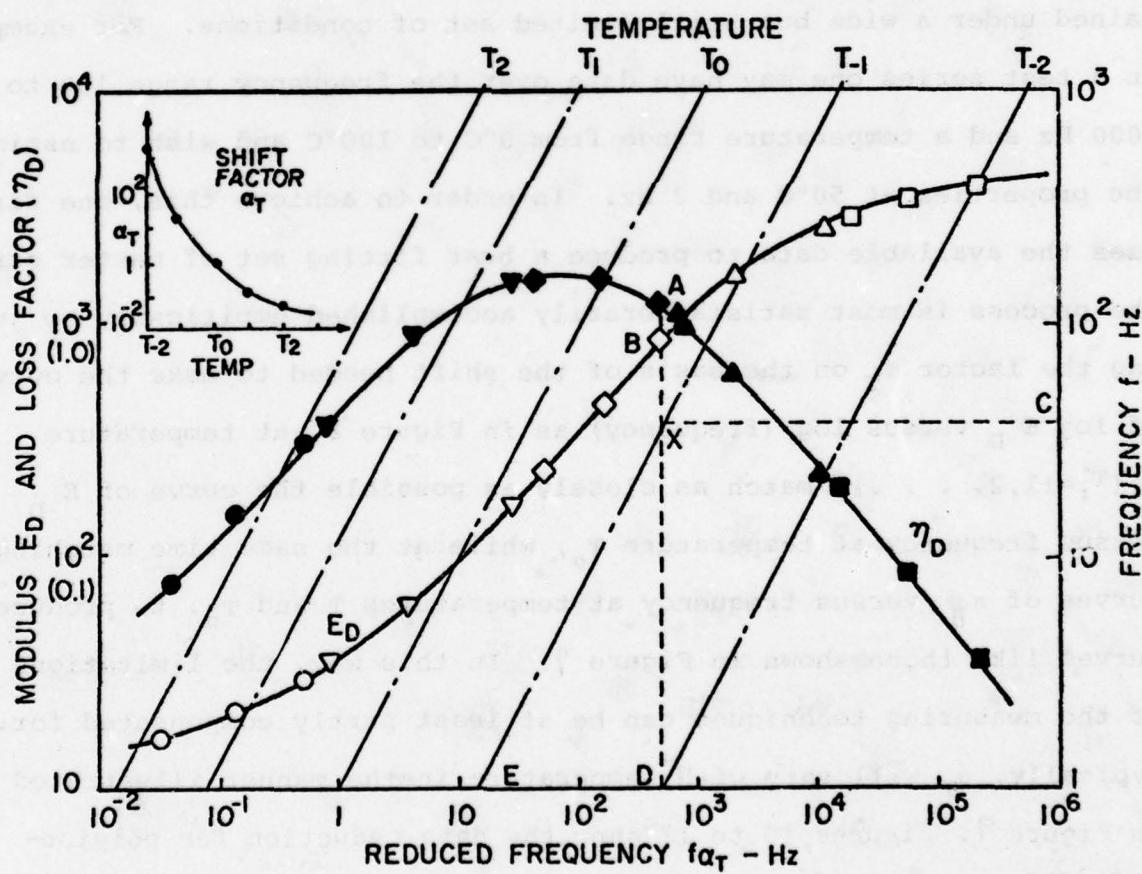


Figure 9. Reduced frequency/Reduced temperature scheme

TABLE II. Young's Modulus, E , vs. Temperature, T , for Polyisobutylene

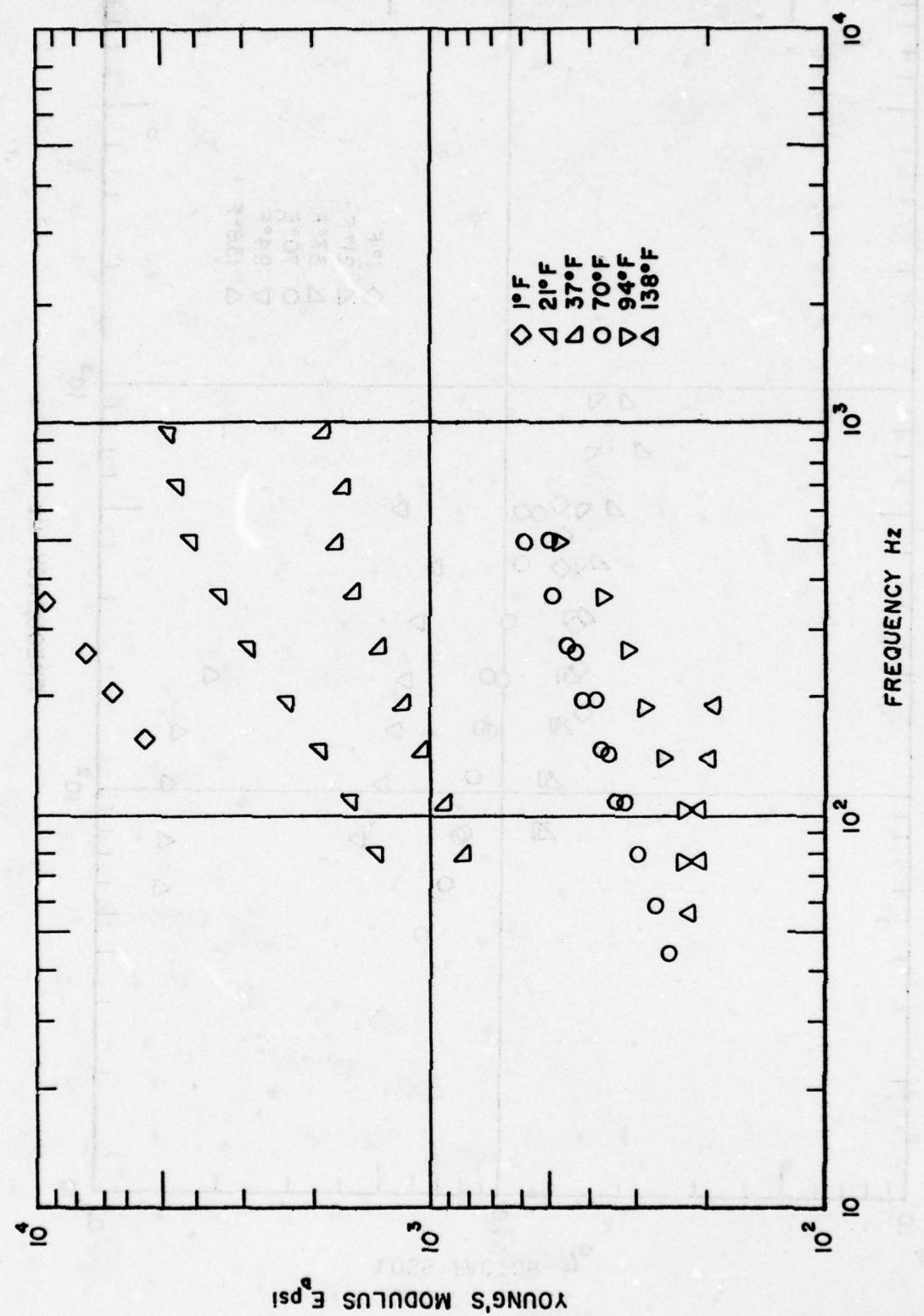


Figure 10. Modulus versus frequency for Polyisobutylene

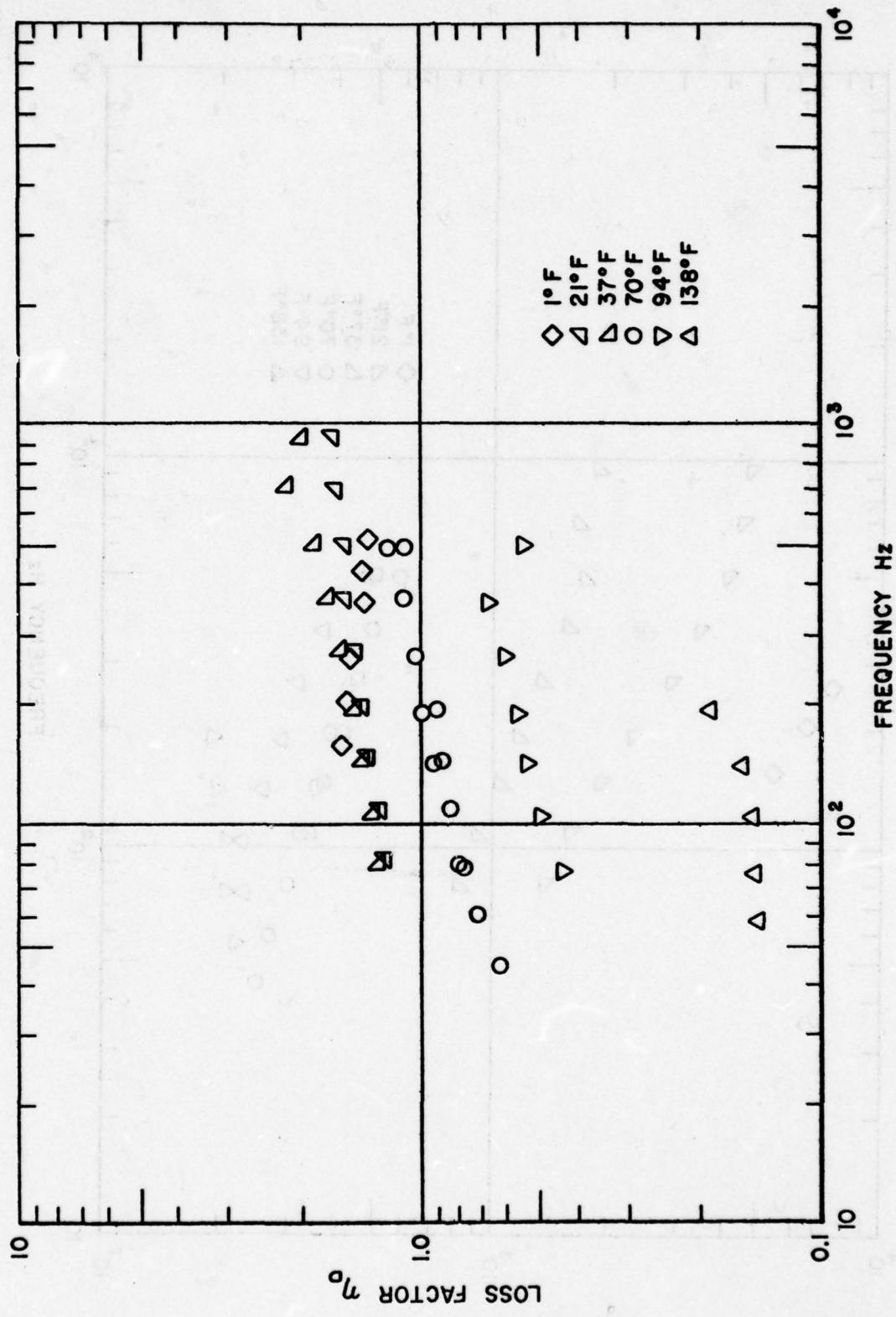


Figure 11. Loss factor versus frequency for Polyisobutylene

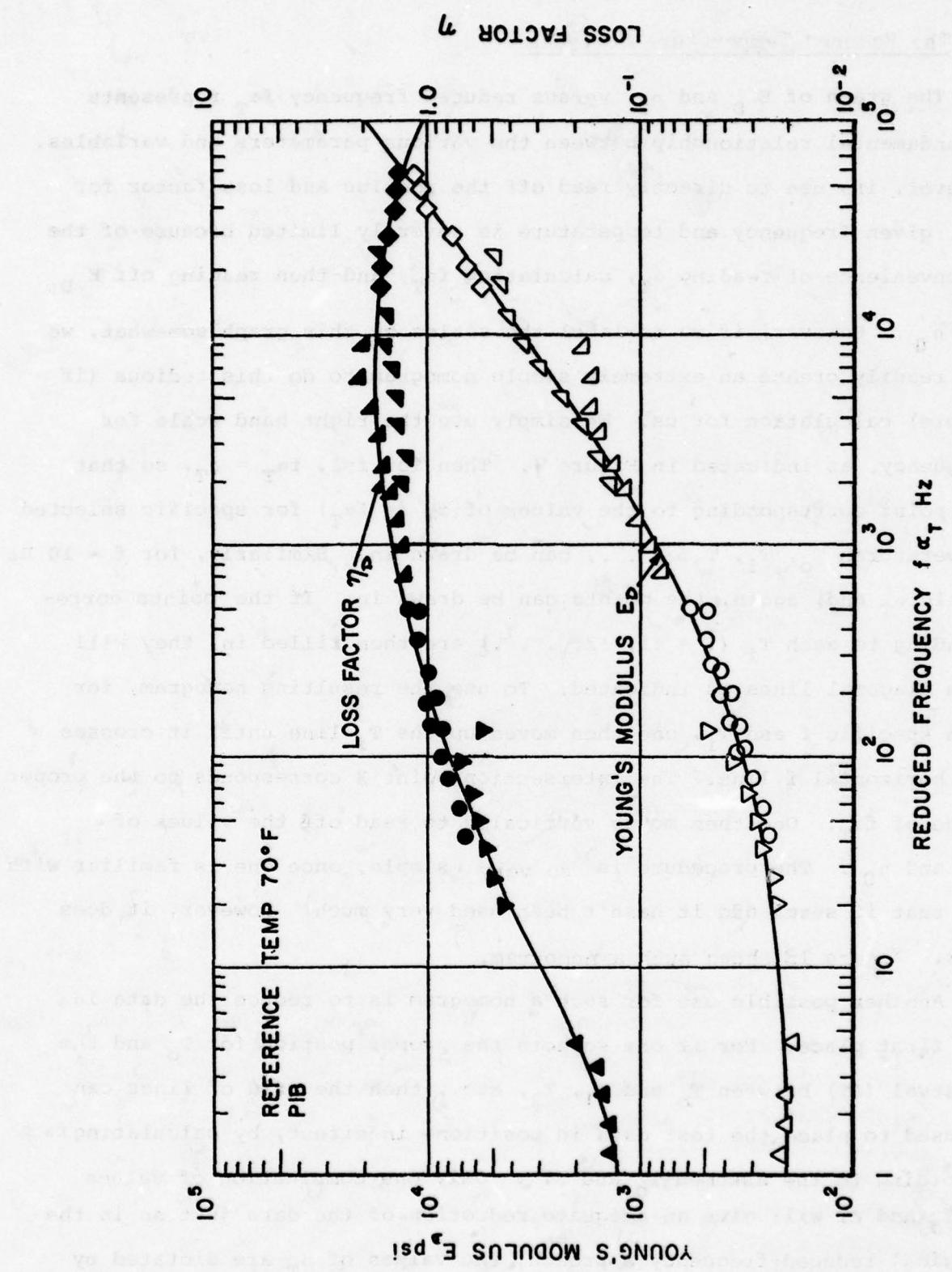


Figure 12. Reduced variables for Polyisobutylene

The Reduced Temperature Nomogram

The graph of E_D and η_D versus reduced frequency $f\alpha_T$ represents a fundamental relationship between the various parameters and variables. However, its use to directly read off the modulus and loss factor for any given frequency and temperature is severely limited because of the inconvenience of reading α_T , calculating $f\alpha_T$, and then reading off E_D and η_D . However, if we re-label the scales on this graph somewhat, we can readily create an extremely simple nomogram to do this tedious (if simple) calculation for us. We simply use the right hand scale for frequency, as indicated in Figure 9. Then for $f=1$, $f\alpha_T = \alpha_T$, so that the point corresponding to the values of α_T ($= f\alpha_T$) for specific selected temperatures T_0, T_1, T_2, \dots , can be drawn in. Similarly, for $f = 10$ Hz $f\alpha_T = 10 \alpha_T$ and, again, the points can be drawn in. If the points corresponding to each T_i ($i = \pm 1, \pm 2, \dots$) are then filled in, they will form diagonal lines as indicated. To use the resulting nomogram, for each specific f and T_i , one then moves up the T_i line until it crosses the horizontal f line. The intersection point X corresponds to the proper value of $f\alpha_T$. One then moves vertically to read off the values of E_D and η_D . The procedure is so very simple, once one is familiar with it, that it seems odd it hasn't been used very much. However, it does work. Figure 13 shows such a nomogram.

Another possible use for such a nomogram is to reduce the data in the first place. For if one selects the proper position for T_0 and the interval (ΔT) between T_0 and T_1, T_2 , etc., then the grid of lines can be used to place the test data in position- in effect, by calculating $f\alpha_T$ according to the assumed T_0 and ΔT . Only one combination of values of T_0 and ΔT will give an adequate reduction of the data just as in the original reduced-frequency approach, the values of α_T are dictated by

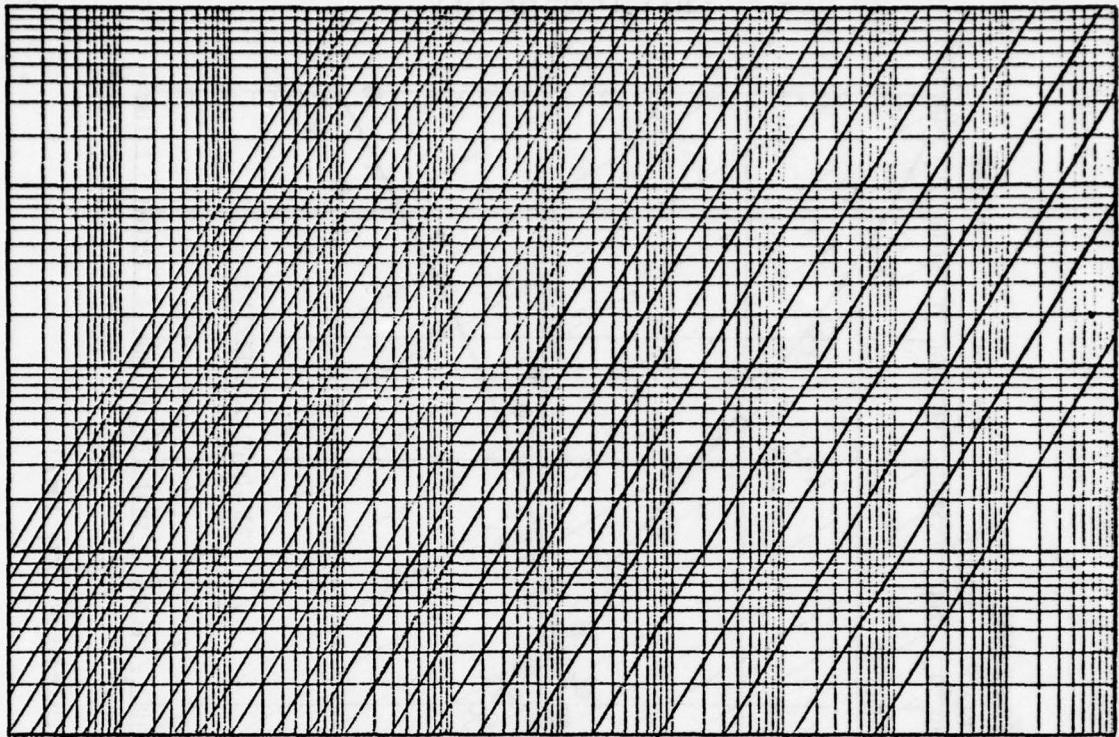


Figure 13. Typical Reduced Temperature Nomogram

the test data. The collapse of the data is easily achieved once the temperature scale is properly selected. This is clearly a matter of judgement, but not more so than in the case of any other types of scale, or in producing the reduced - frequency graphs in the first place. Figures 14 to 21 show typical results for some available materials. Figure 22 shows the graph of α_T versus temperature curve for several of these materials, from which the nomogram was constructed.

$$\log \alpha_T = \frac{-12(T-T_0)}{525+(T-T_0)} \quad [32]$$

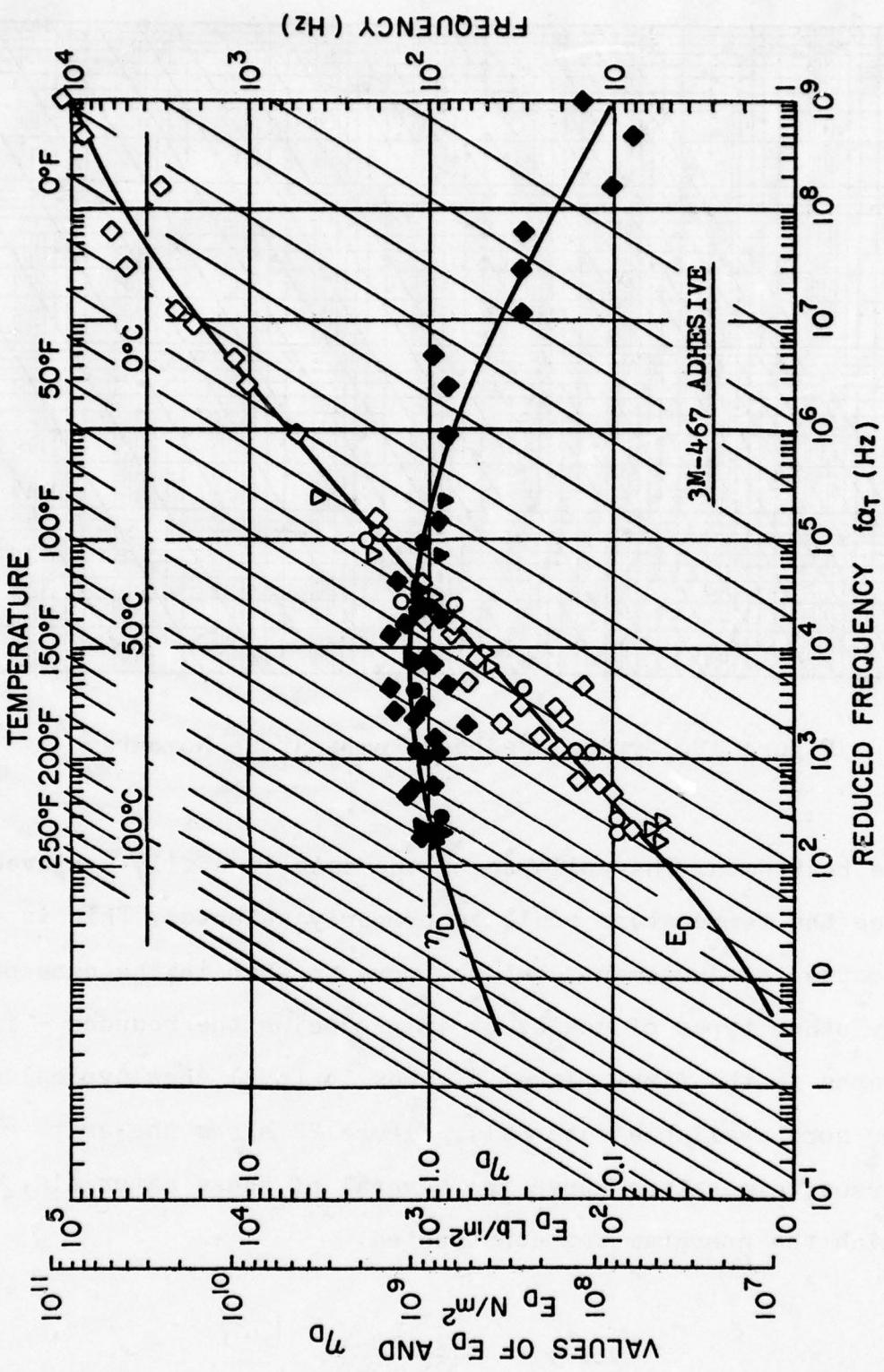


Figure 14. Reduced temperature curves for 3M-467 adhesive

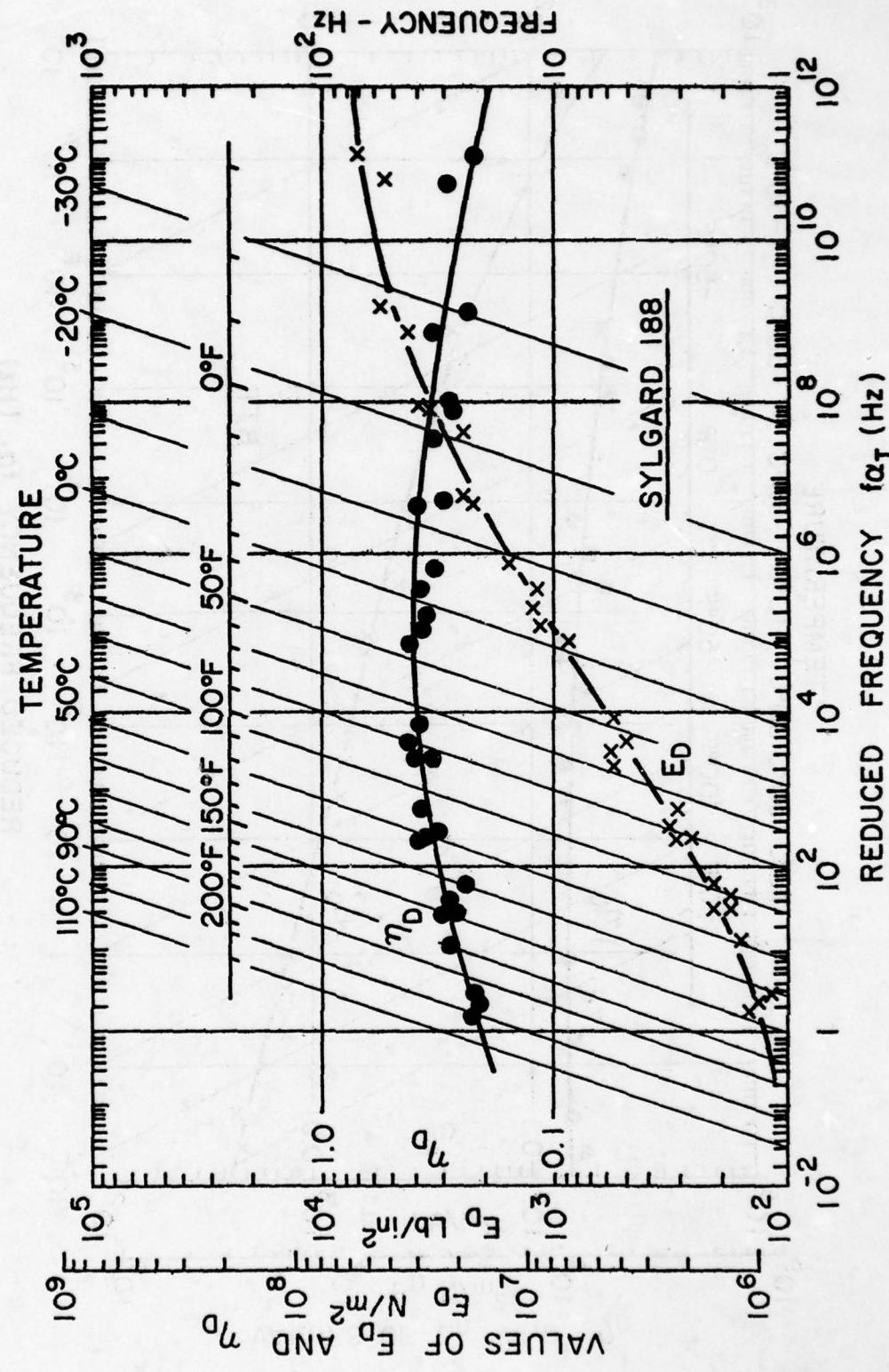


Figure 15. Reduced temperature curves for sample of
Sylgard 188 potting compound.

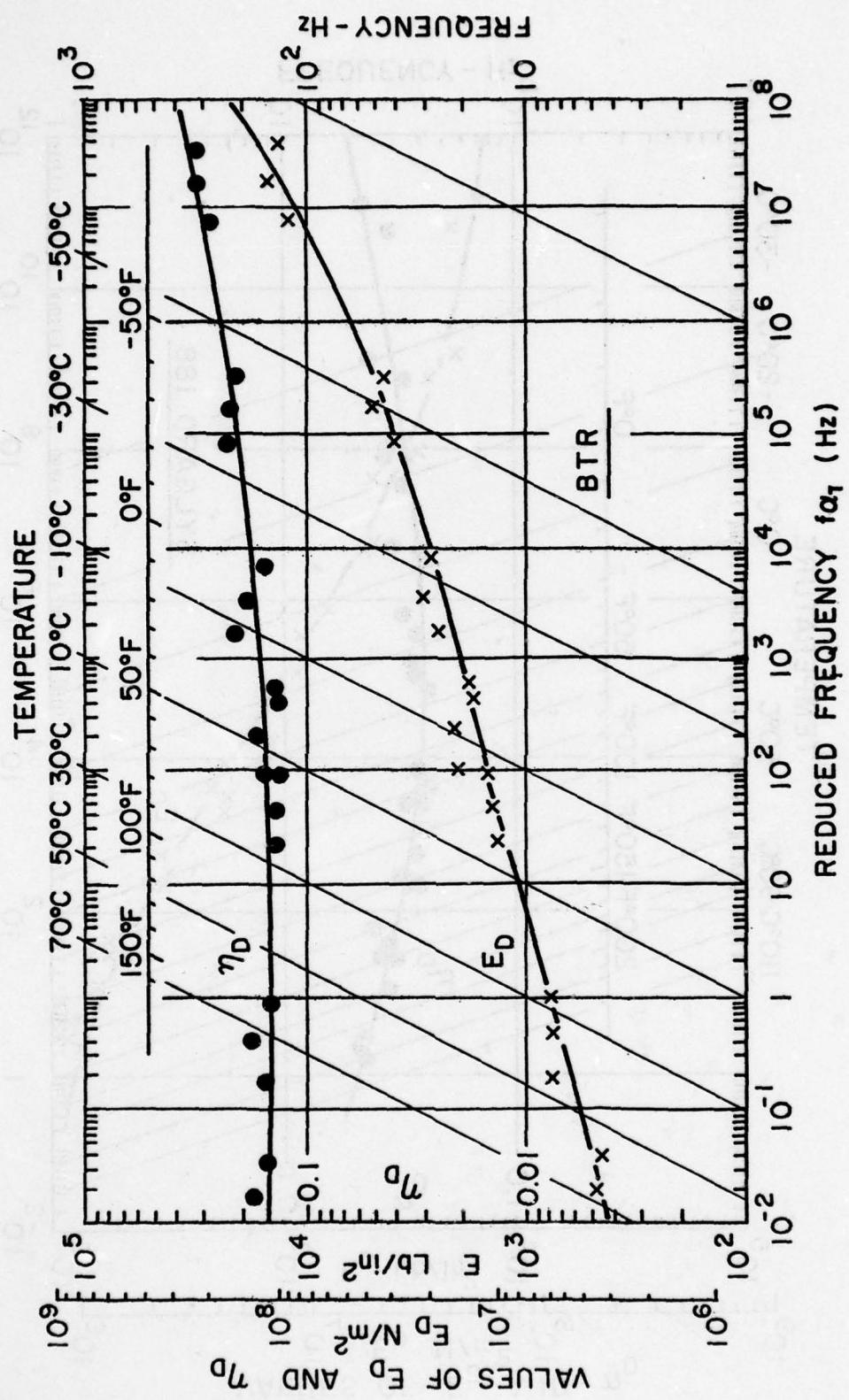


Figure 16. Reduced temperature curves for BTR silicone

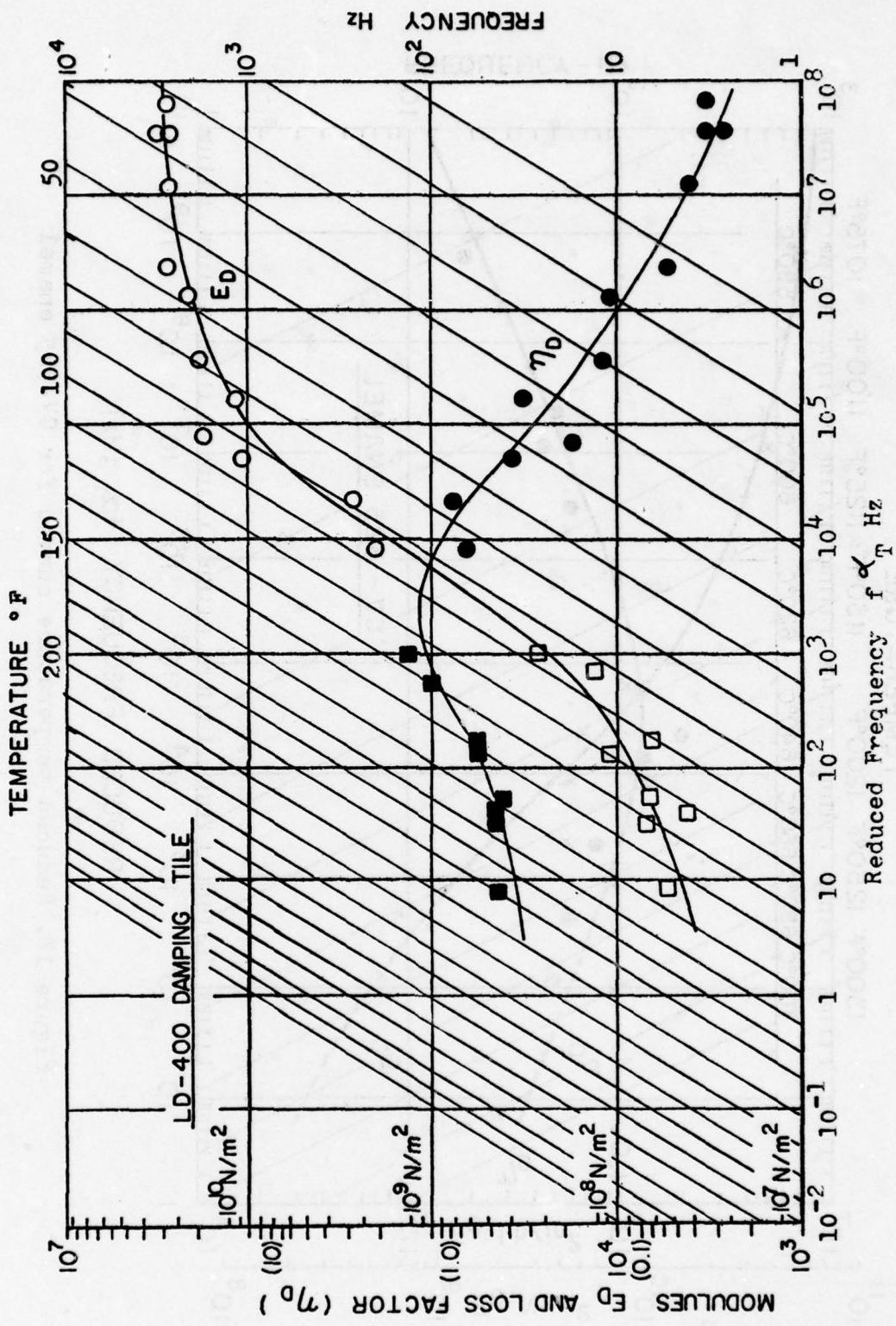


Figure 17. Reduced temperature curves for LD-400 Damping tile

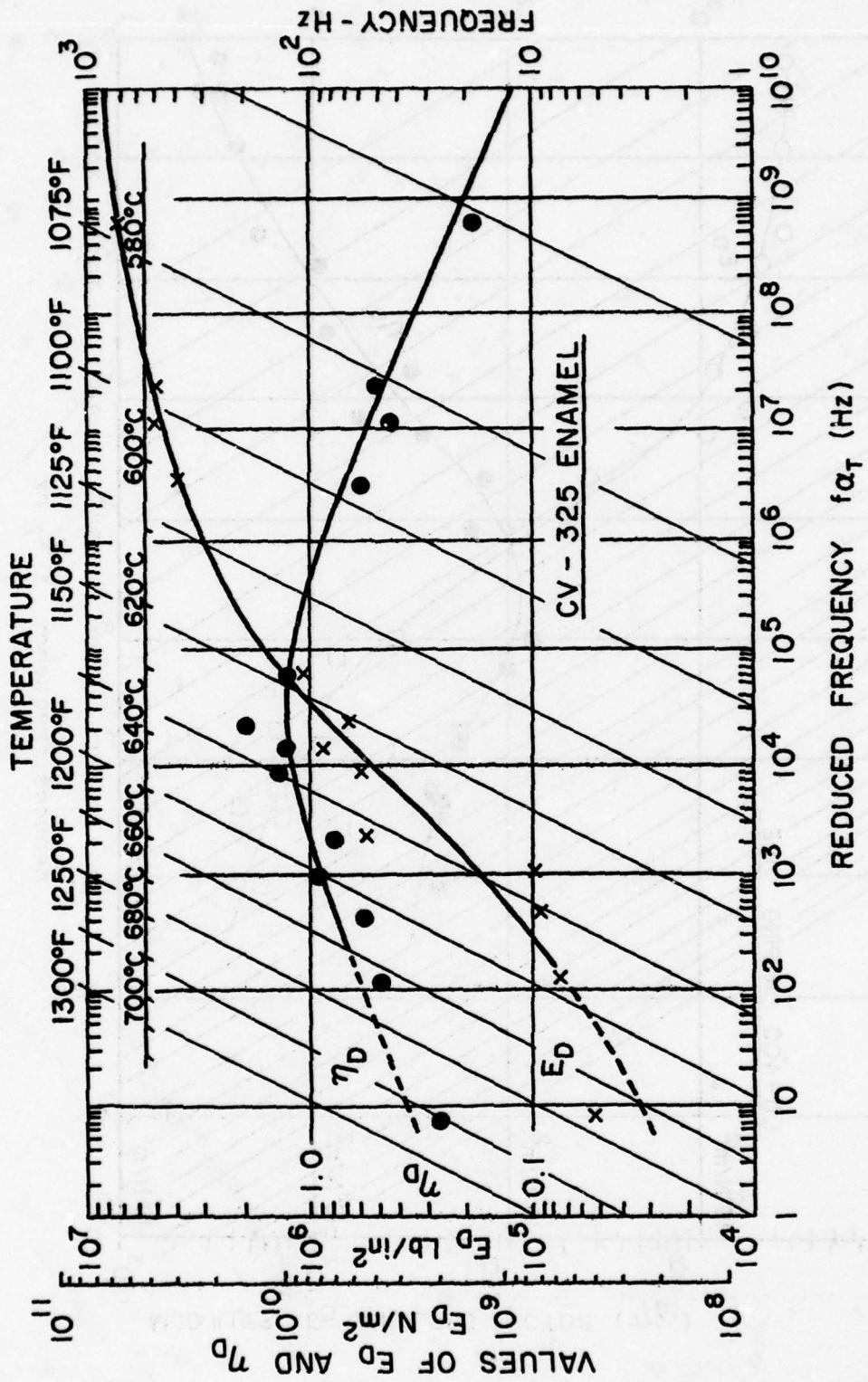


Figure 18. Reduced temperature curved for CV-325 enamel

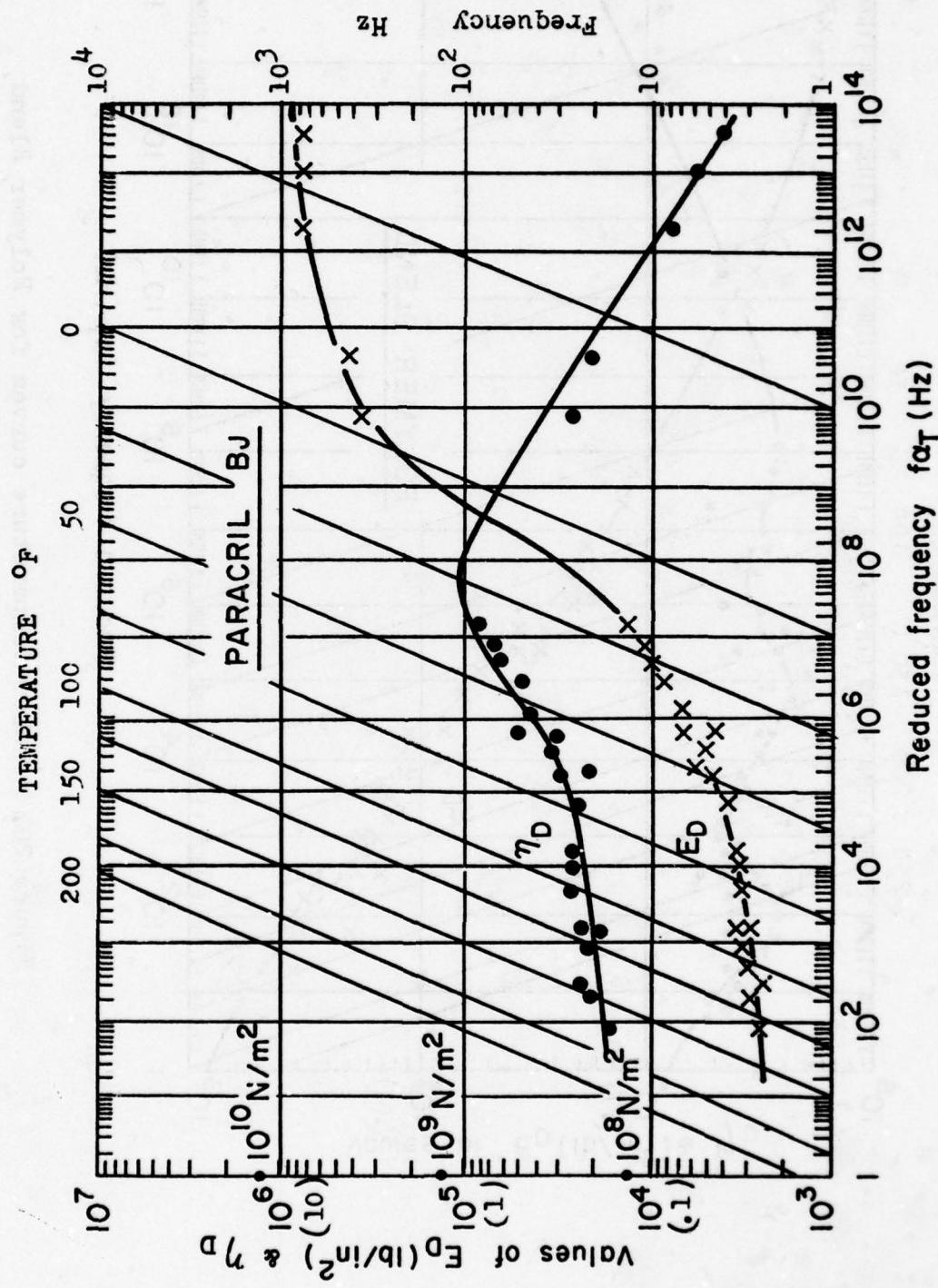


Figure 19. Reduced temperature curves for Paracril-BJ
Nitrile rubber

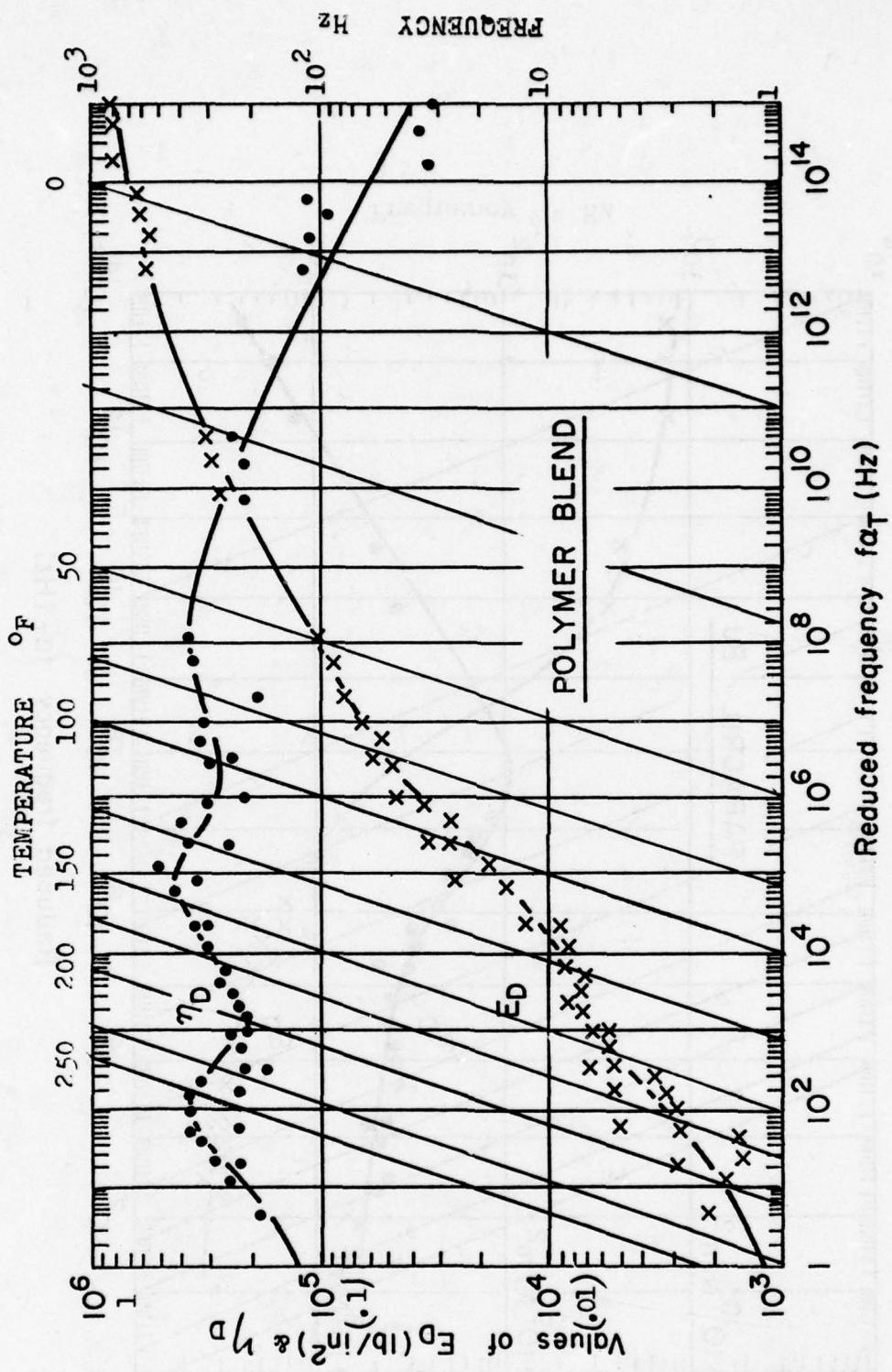


Figure 20. Reduced temperature curves for Polymer Blend

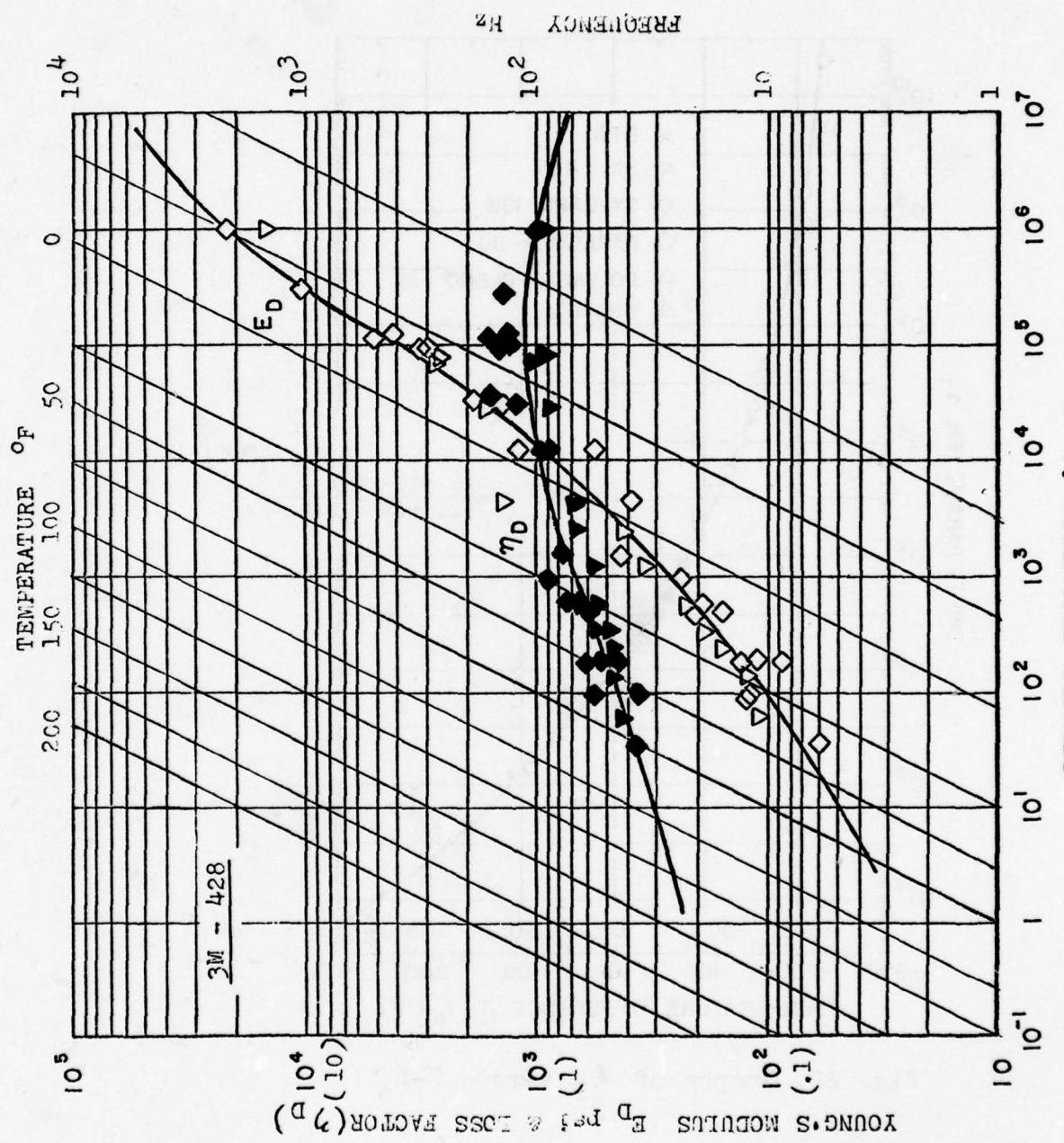


Figure 21. Reduced Temperature curves for 3M-428

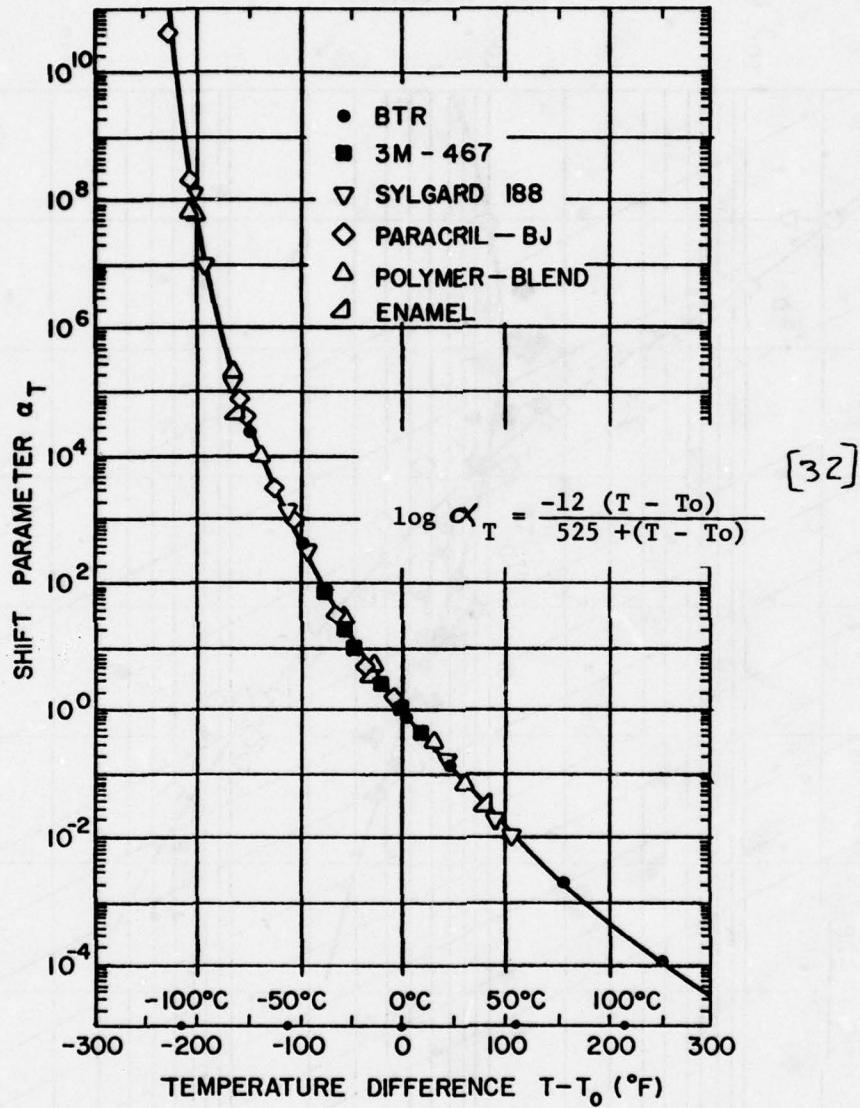


Fig. 22. Graphs of α_T versus $T - T_0$

For a typical structural alloy, the hysteresis loop is usually thin and cusped, as sketched in Figure 23 so that the damping is very low. As the material is strained into the plastic range, the loop will thicken and hence the damping will increase, but only at the expense of operating the material in a region where it may fail in a relatively small number of cycles.

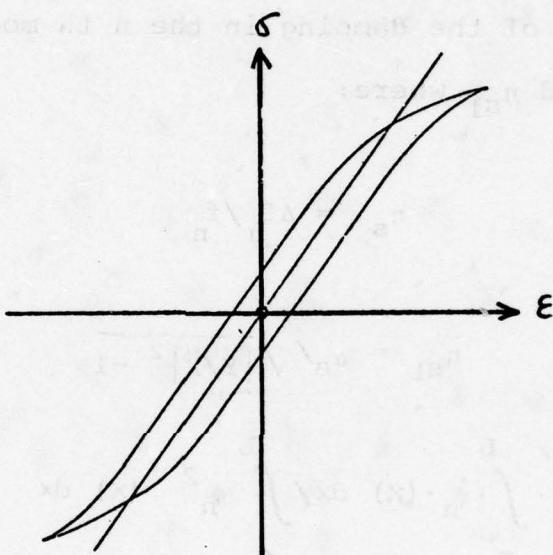


Figure 23. Cusped hysteresis loop

This behavior is characteristic of most commonly used structural alloys and one has to examine somewhat less common alloy systems before one may encounter higher levels of damping at low strain levels, relative to the point at which plasticity effects become significant. Alloy systems which exhibit high damping behavior include some of the Manganese-copper alloys, Iron-Aluminum alloys and magnesium alloys

Resonant vibration tests on cantilever beams are often used to obtain a measure of the damping properties of the beam material. If, in these tests, one can measure the resonant frequency f_n of the n th mode, the "half-power" bandwidth Δf_n defining the points on either side of the response peak where the amplitude is 0.707 times the peak amplitude, the peak acceleration \ddot{Y} at the tip and the input acceleration \ddot{X} at the root, then a measure of the damping in the n th mode is given by two numbers η_s and η_{s1} where:

$$\eta_s = \Delta f_n / f_n$$

$$\eta_{s1} = \alpha_n / \sqrt{|\ddot{Y}/\ddot{X}|^2 - 1}$$

and
$$\alpha_n = \int_0^L \phi_n(x) dx / \int_0^L \phi_n^2(x) dx$$

where $\phi_n(x)$ is the n th normal mode of the cantilever beam.

These quantities can be used to obtain a simple measure of the variation of the beam damping in each mode as a function of peak strain amplitude at the root of the beam, on the surface, and/or frequency and temperature. The quantities η_s and η_{s1} are not a direct measure of the damping behavior of the material itself unless the material is linear i.e. η_s and η_{s1} are independent of strain amplitude, but do give a qualitative [5-9] insight into the suitability of a given alloy for damping purposes.

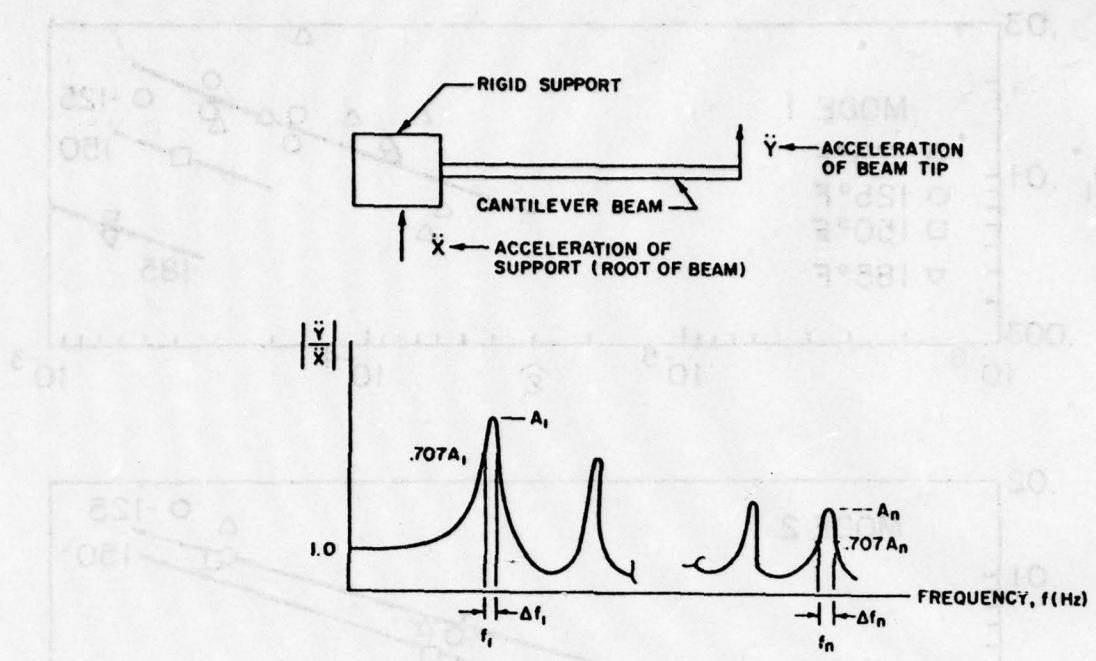


Fig. 24. Response curve of the acceleration ratio, $\frac{\ddot{Y}}{\ddot{X}}$, for a cantilever beam. \ddot{Y} is the acceleration of the tip of the beam and \ddot{X} is the applied acceleration at the root of the beam.

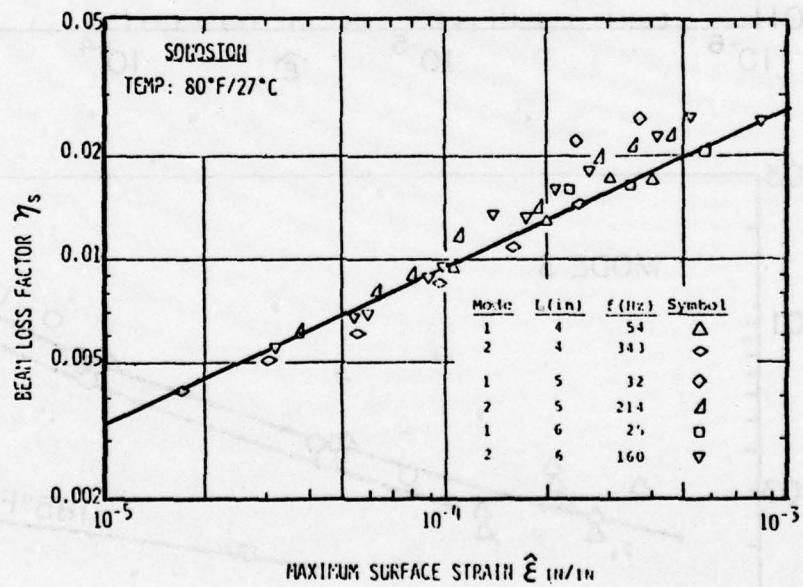


Figure 25. Variation of η_s with strain for Sonoston

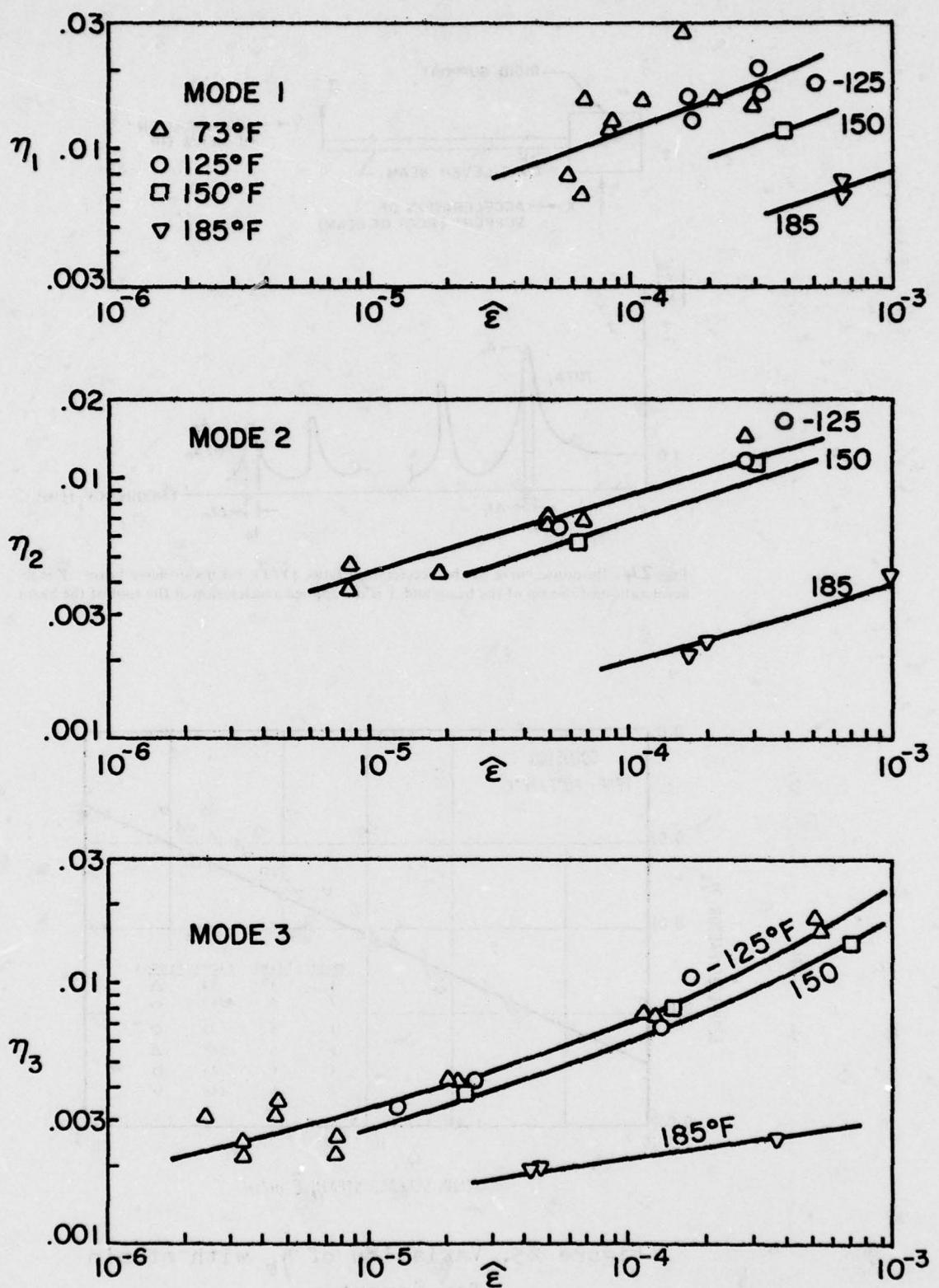


Figure 26. Variation of η_n with temperature for Sonoston

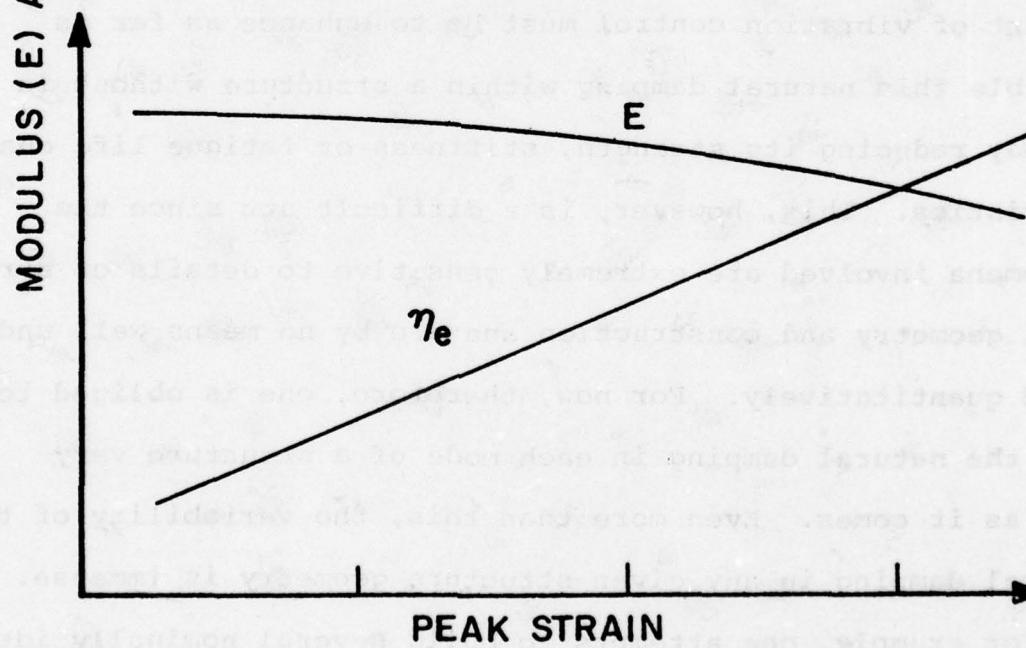
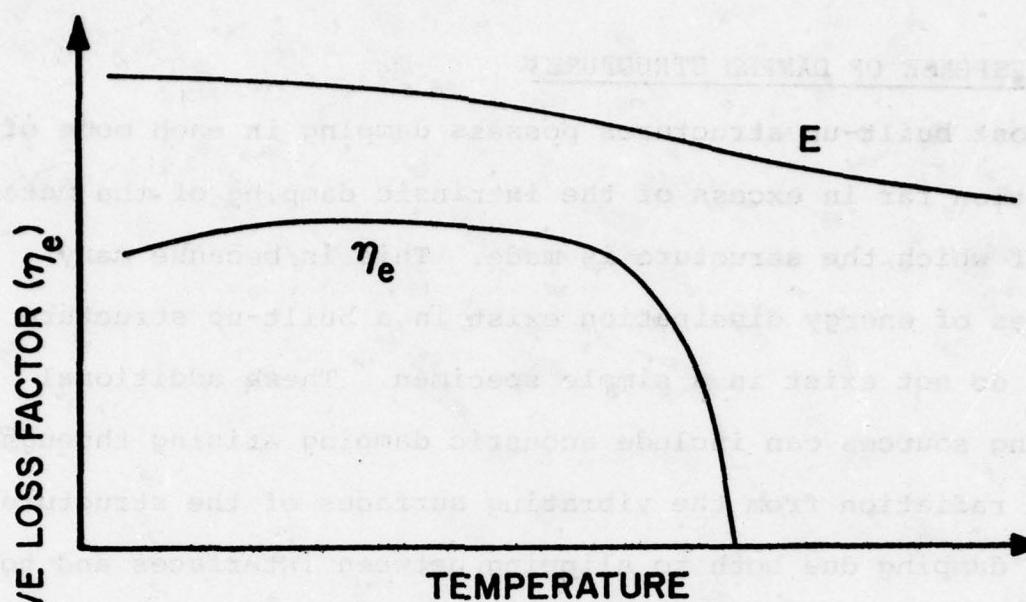


Figure 27. Idealized variation of modulus and loss factor

3. RESPONSE OF DAMPED STRUCTURES

Most built-up structures possess damping in each mode of vibration far in excess of the intrinsic damping of the material of which the structure is made. This is because many sources of energy dissipation exist in a built-up structure which do not exist in a simple specimen. These additional damping sources can include acoustic damping arising through sound radiation from the vibrating surfaces of the structure, joint damping due both to slipping between interfaces and to "air-pumping" caused by transverse relative motion of overlapping metal sheets [10] and air pumping through holes in bounding surfaces enclosing finite volumes of air, as structural surfaces which surround the volume vibrate. One aspect of the art of vibration control must be to enhance as far as possible this natural damping within a structure without in any way reducing its strength, stiffness or fatigue life characteristics. This, however, is a difficult art since the phenomena involved are extremely sensitive to details of structural geometry and construction and are by no means well understood quantitatively. For now, therefore, one is obliged to take the natural damping in each mode of a structure very much as it comes. Even more than this, the variability of the natural damping in any given structure geometry is immense. If, for example, one attempts to build several nominally identical structures using normal fabrication techniques, the

measured values of the modal loss factor in any given mode may vary by a factor of as much as ten, typically varying from $\eta_s = 0.002$ to $\eta_s = 0.02$. This unpredictability, as much as anything else, makes reliance on natural damping a rather uncertain affair, because the displacements and stresses at resonance under sinusoidal excitation are inversely proportional to η_s , and the stresses and displacements under random excitation are inversely proportional to $\sqrt{\eta_s}$

Unconstrained Layer Treatments

The free or unconstrained layer treatment is by far the simplest way of introducing damping into a sheet metal type of structure. The treatment consists of a layer of an appropriate elastomeric material bonded, by a suitable adhesive, to those vibrating surfaces of the structure which are vibrating primarily in a bending type of mode as shown in Figure 28. As these surfaces bend, the treatments on the surfaces are deformed cyclically in tension-compression and so dissipate energy.

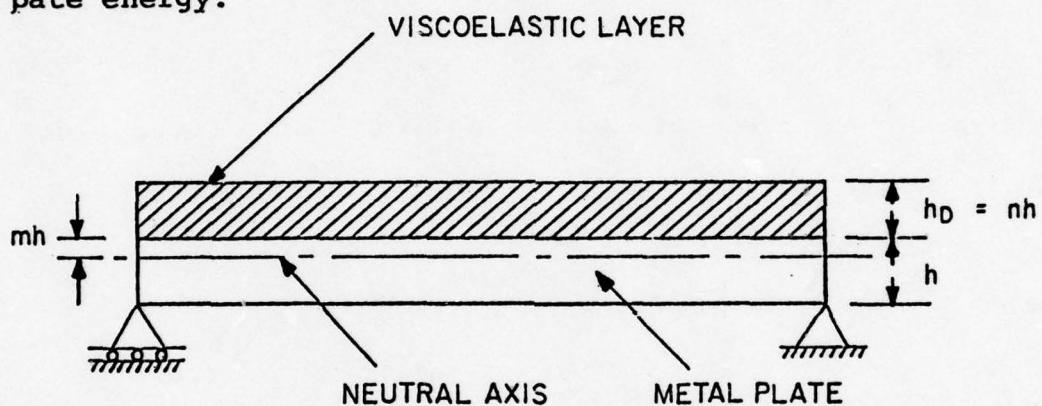


Figure 28. Unconstrained layer treatment

If an unstiffened beam of thickness h and Young's Modulus E is fully covered by a layer of viscoelastic material of thickness h_D with complex Young's Modulus $E_D(1+in_D)$, then the damping n_s in a mode of vibration, defined as $n_s = \Delta f_n/f_n$ where f_n is the n th resonant frequency and Δf_n is the "half-power" bandwidth, is:

$$\eta_s = \frac{n \cdot en}{1+ne} \left[\frac{3 + 6n + 4n^2 + 2en^3 + e^2 n^4}{1 + 2en(2 + 3n + 2n^2) + e^2 n^4} \right] \quad (1)$$

$$\left(1 + \frac{\rho_D n}{\rho}\right) \left(\frac{f_r}{f_n}\right)^2 = \frac{1 + 2en(2 + 3n + 2n^2) + e^2 n^4}{1 + en} \quad (2)$$

where $n = h_D/h$ and $e = E_D/E$. These now classic equations were originally derived by Dr. H. Oberst and Dr. K. Frankenfeld in 1952 [11]. In these equations, ρ_D is the density of the damping material, ρ is that of the beam and f_r is the resonant frequency of the n th mode of the damped beam. If, instead of an unstiffened beam, the treatment is applied to an unstiffened plate, these equations still apply, provided that the Poisson's ratio v_D of the viscoelastic material is approximately equal to that of the beam or plate material, v .

An alternative form [12] of the above equations is of considerable value, particularly in view of the possibility of extending them to apply to stiffened plates. These equations are:

$$\eta_s = \eta_D / (1 + A/Be) \quad (3)$$

$$\left(1 + \frac{\rho_D n}{\rho}\right) \left(\frac{f_r}{f_n}\right)^2 = (A + Be)/2 \quad (4)$$

where

$$A = \frac{(1 - n^2 e)^3 + (1 + [2n + n^2]e)^3}{(1 + ne)^3} \quad (5)$$

and

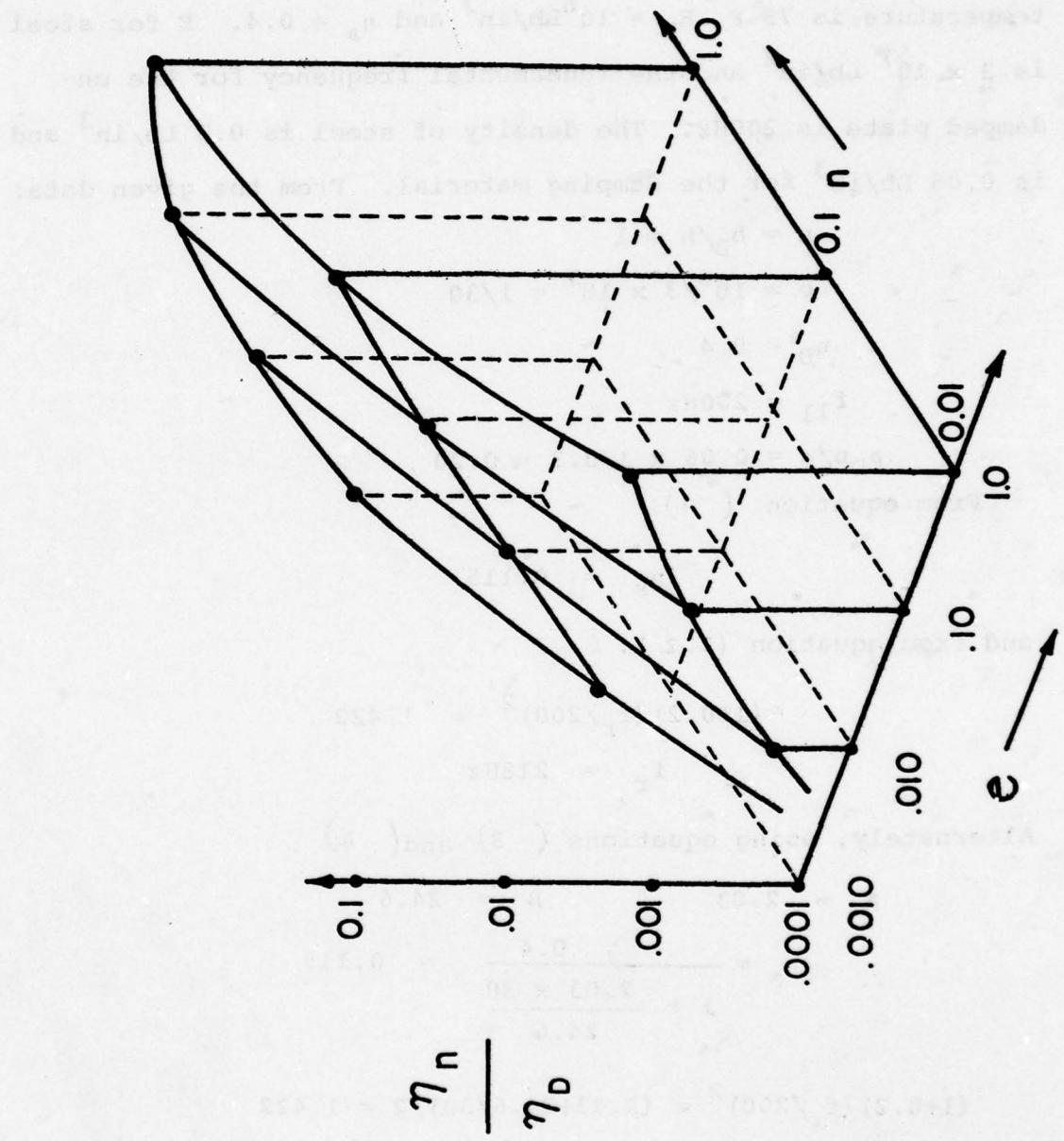
$$B = \frac{(2n + 1 + n^2 e)^3 - (1 - n^2 e)^3}{(1 + ne)^3} \quad (6)$$

Needless to say, the two sets of equations are identical, as may readily be verified.

Design Procedure

The plate geometry is given, the undamped resonant frequencies f_n are known, and E_D and η_D are assumed known for the damping material as functions of temperature and frequency. For given thickness ratio n , one then chooses the mode to be considered and makes a first guess at the frequency f_r of that mode for the damped system. Using equation (4), a new value of f_r is calculated using values of E_D and η_D corresponding to the initial value of f_r . The process is repeated until the two values of f_r converge. Then, from equation (3) the value of η_s is calculated. The process is repeated over the desired temperature range. If the damping behavior so achieved is not suitable, one may either increase n or choose another material with a more suitable peak damping temperature. The most important criterion, as equation (1) clearly shows, is that the product $E_D n$ be as large as possible at the temperature where maximum damping is required.

Figure 29. Damping versus e and n for free layer treatment



Sample Calculation

Find the loss factor η_s and the resonant frequency in the fundamental mode of a rectangular steel plate, clamped at all four edges, of thickness $1/4$ inch, if the plate is damped by means of a layer of viscoelastic material, $1/4$ inch thick. The temperature is $75^\circ F$, $E_D = 10^6 \text{ Lb/in}^2$ and $\eta_D = 0.4$. E for steel is $3 \times 10^7 \text{ Lb/in}^2$ and the fundamental frequency for the undamped plate is 200Hz . The density of steel is 0.3 Lb/in^3 and is 0.06 Lb/in^3 for the damping material. From the given data:

$$n = h_D/h = 1$$

$$e = 10^6/3 \times 10^7 = 1/30$$

$$\eta_D = 0.4$$

$$f_{11} = 200\text{Hz}$$

$$\rho_D n / \rho = 0.06 \times 1/0.3 = 0.20$$

∴ From equation (1):

$$\eta_s = 0.115$$

and from equation (2.2) :

$$(1+0.2)(f_r/200)^2 = 1.422$$

$$\therefore f_r = 218\text{Hz}$$

Alternately, using equations (3) and (4) :

$$A = 2.03 \quad B = 24.6$$

$$\therefore \eta_s = \frac{0.4}{1 + \frac{2.03 \times 30}{24.6}} = 0.115$$

$$(1+0.2)(f_r/200)^2 = (2.03+24.6/30)/2 = 1.422$$

$$f_r = 218\text{Hz as before}$$

Damping of Stiffened Plates

The presence of stiffeners in a sheet metal type of structure will serve to reduce the effectiveness of a free layer treatment. The prediction of the effect of such a treatment on modal damping is very difficult in general, and is beset with many assumptions. If, as is often the case for structures having thin stiffened skin type construction, the treatment is applied over all the surfaces which deform primarily in bending, the damping in each mode can be estimated from the equations

$$\eta_s \doteq \eta_b / [1 + (A - 2 + \beta_{nm})/Be] \quad (7)$$

$$(1 + \rho_D n / \rho) (f_r / f_{nm})^2 \doteq 1 + (A - 2 + Be) / \beta_{nm} \quad (8)$$

where A and B are defined as before and:

$$\beta_{nm} = \frac{2\xi_{nm}^4 \iint_S \phi_{nm}^2 dx dy}{\iint_D \left[\left(\frac{\partial^2 \phi_{nm}}{\partial \Delta^2} \right)^2 + \left(\frac{L}{\epsilon} \right)^4 \left(\frac{\partial^2 \phi_{nm}}{\partial \delta^2} \right)^2 + 2\nu \left(\frac{L}{\epsilon} \right)^2 \left(\frac{\partial^2 \phi_{nm}}{\partial \Delta^2} \right) \left(\frac{\partial^2 \phi_{nm}}{\partial \delta^2} \right) \right] dx dy} \quad (9)$$

It is exceedingly difficult to calculate β_{nm} in general because the detailed information on mode shapes is usually not available. One can estimate β_{nm} in some idealized cases but in the event of one encountering a practical problem, perhaps the best procedure is to apply a treatment consisting of a

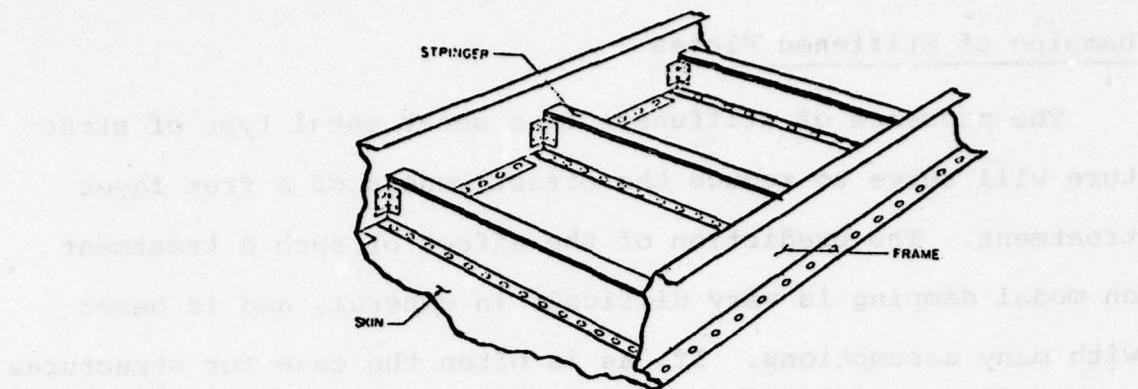
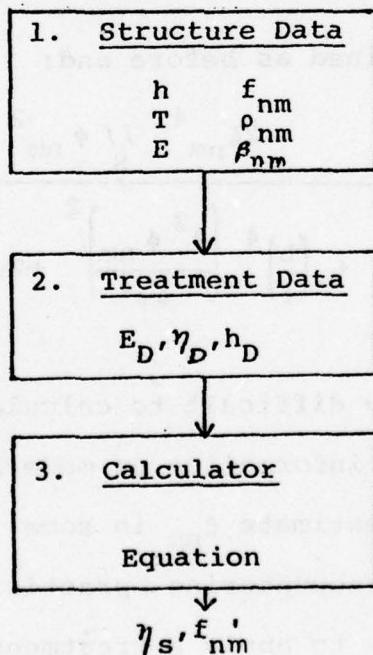


Figure 30. Skin-stringer structure

known, suitable, viscoelastic material in known thickness and over the entire surface involved in the vibration modes of interest. Measured response records can then be used to estimate η_s and one would then use equations 7 and 8 in reverse to estimate β_{nm} . From this point onwards, one could then use the equations directly to estimate the effects of other treatment thicknesses and/or other treatment materials.



Sample Calculation

The plate of the previous example is stiffened while the same damping treatment is retained over the whole surface.

The loss factor is reduced to 0.04. Estimate β_{nm} for the fundamental mode, and the added thickness of material needed to return n_s to its unstiffened plate value.

From equation (7), using the same values of n and e:

$$0.04 = \frac{0.4}{1 + (2.03 - 2 + \beta_{nm}) / (24.6/30)}$$

$$\therefore \frac{30}{24.6} (0.03 + \beta_{nm}) = 9.0$$

$$\beta_{nm} = \frac{9.0 \times 24.6}{30} - 0.03 = 7.37$$

We must now guess at a new value of n needed to raise n_s to a value of 0.115. By trying several value of n, we eventually find that it must be equal to 1.84 to raise the loss factor to the desired level.

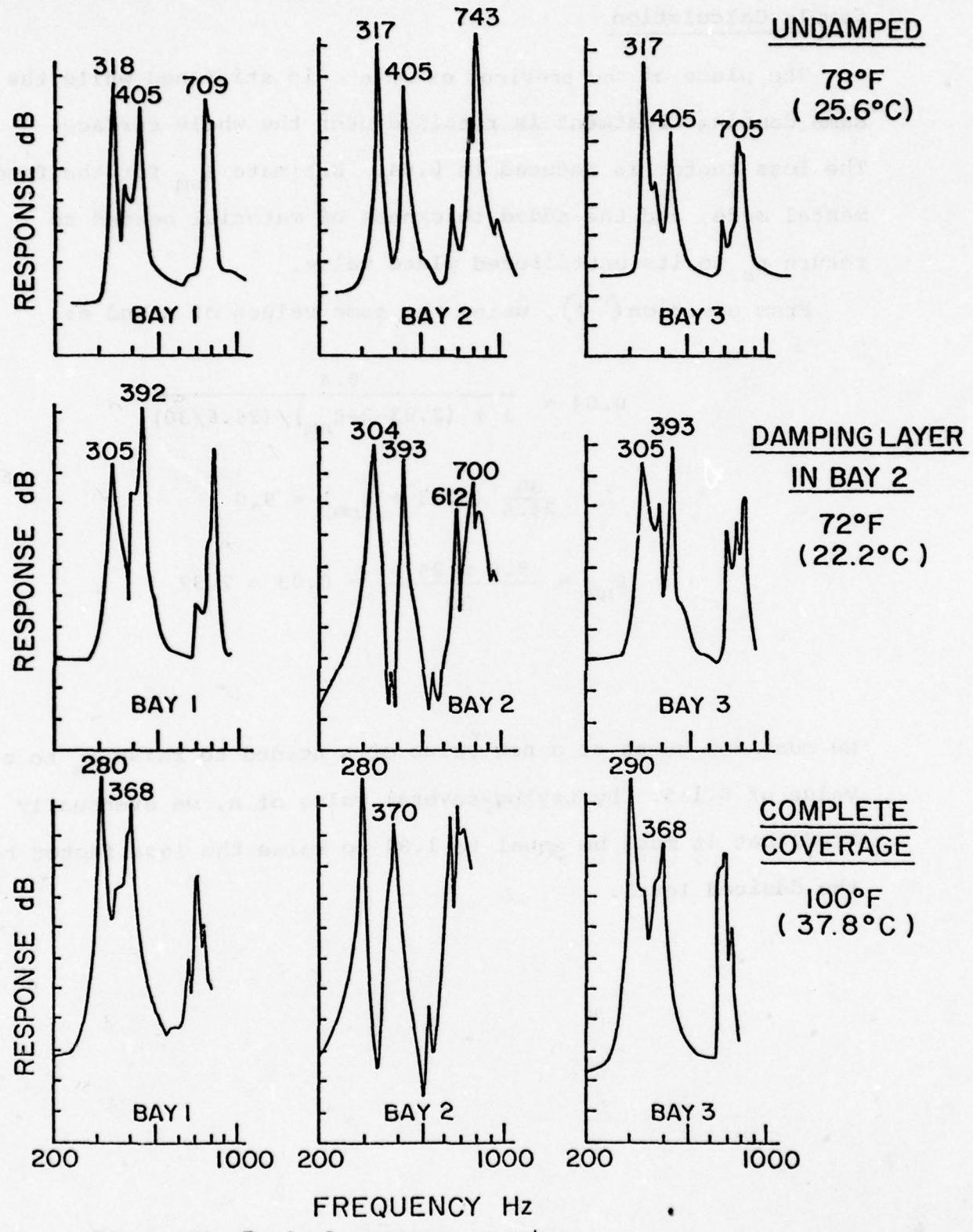


Figure 31. Typical response spectra

Constrained layer treatments

Sandwich panel construction is widely used with honeycomb cores wherever high stiffness is required. Cores having viscoelastic properties are also attractive, although boundary attachment problems are not readily overcome. Some typical sandwich constructions are illustrated in Figure 32.

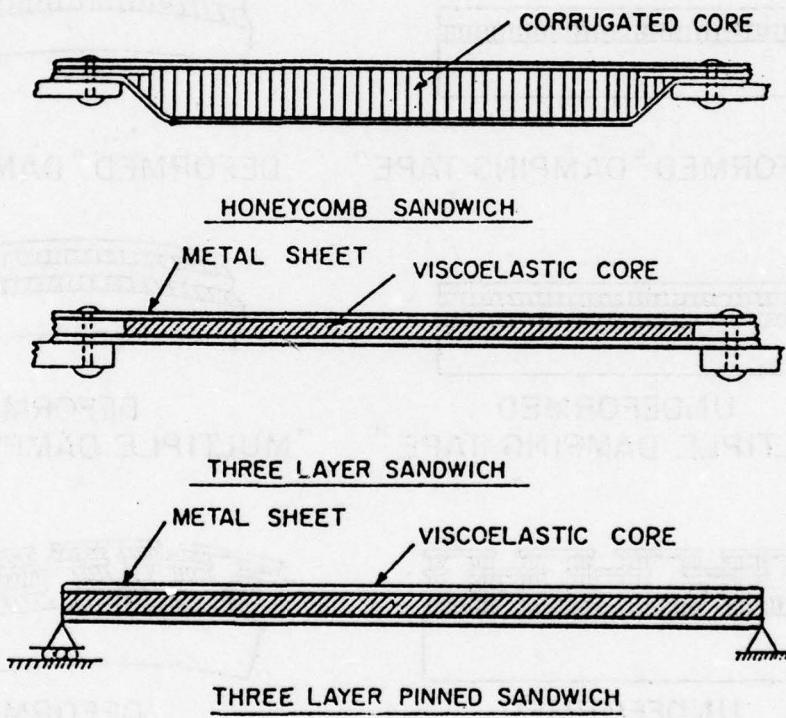
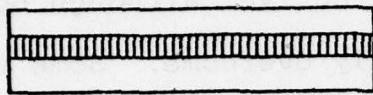
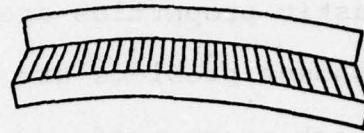


Figure 32. Typical sandwich constructions

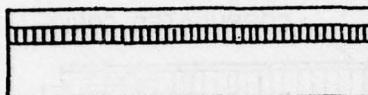
Constrained layer damping treatments are usually more efficient than free layer treatments because the requirement that the damping material be both stiff and "lossy" can be relaxed, the necessary stiffness being provided instead by stiff metallic or composite layers which force the relatively soft damping material to deform in shear instead of tension-compression, as illustrated in Figure 33.



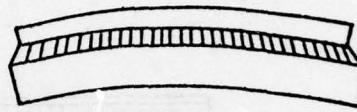
UNDEFORMED "SANDWICH"



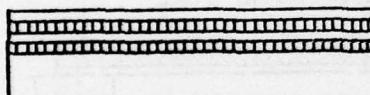
DEFORMED "SANDWICH"



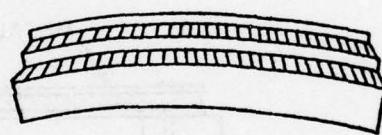
UNDEFORMED "DAMPING TAPE"



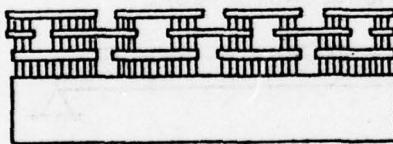
DEFORMED "DAMPING TAPE"



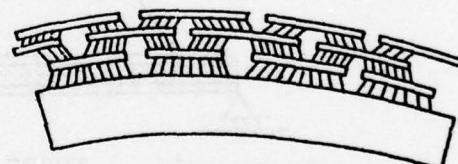
UNDEFORMED
"MULTIPLE DAMPING TAPE"



DEFORMED
"MULTIPLE DAMPING TAPE"



UNDEFORMED
"CUT" TREATMENT



DEFORMED
"CUT" TREATMENT

Fig. 33. Constrained layer treatments - mechanical behavior

Sandwich system

The simplest constrained layer system is the sandwich system, consisting of two identical beams joined together by an intermediate layer of the damping material. The equation derived by Ross, Kerwin and Ungar are well-known and accepted for this case [13].

$$E^*I = \frac{E_1 h_1^3}{12} + E_2^* h_2 \left(\frac{h_2^2}{12} + h_{21}^2 \right) + E_3 h_3 \left(\frac{h_3^2}{12} + \frac{g^* E_1 h_1 h_{31}}{E_1 h_1 + g(E_1 h_1 + E_3 h_3)} \right) - E_2^* h_2 h_{31} \left(\frac{\frac{E_1 h_1 (h_{21}/2 + h_2/12) + 2g^* E_3 h_3 h_{21}}{E_1 h_1 + g(E_1 h_1 + E_3 h_3)}} \right) \quad (10)$$

where:

$$h_{31} = (h_1 + h_3)/2 + h_2 \quad h_{21} = (h_1 + h_2)/2$$

$$E^* = E(1+i\eta) \quad E_2^* = E_2(1+i\eta_2) \quad (11)$$

$$g^* = g(1+i\eta_2) \quad g = \frac{G_2}{E_3 h_3 h_2} \left(\frac{l}{n\pi} \right)^2$$

g is the "shear parameter"

In these equations, E^*I is the effective flexural rigidity of the entire system.

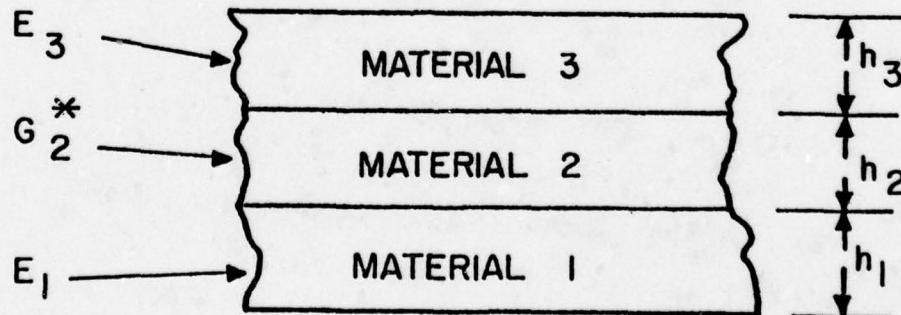


Figure 34. Sandwich treatment

These equations now contain an important new parameter, namely the "shear parameter" g . This depends on the shear modulus G_2 of the center layer and on the semi-wavelength ℓ/n of the beam in the n^{th} mode. Strictly speaking, therefore, only pinned-pinned boundary conditions may be considered. However, provided that the proper semi-wavelength is used, the equations appear to be applicable to other boundary conditions. Once $E*I$ has been calculated, one can deduce the modal damping since:

$$\eta'_{\text{n}} = \frac{\text{Im}(E*I)}{\text{Re}(E*I)} \quad (12)$$

and

$$\frac{(\rho_e h_e)(\omega'_{\text{n}})^2 \ell^4}{\text{Re}(E*I)} = \xi_{\text{n}}^4 \quad (13)$$

where ξ_{n} is the n^{th} eigen value of the beam (for pinned-pinned case $\xi_{\text{n}} = n\pi$). Hence, ω'_{n} can be calculated.

Damping in Symmetric viscoelastic sandwich panels

If the panel boundaries are assumed to be pinned or simply supported, the damping and stiffness characteristics of the panel can be estimated from the equations [14, 15]:

$$\eta_s = \frac{3\eta_D \psi_{nm} (1+n)^2}{(1 + \psi_{nm})^2 + \eta_D^2 + 3(1+n)^2(1+\psi_{nm} + \eta_D^2)} \quad (14)$$

$$\left[1 + \frac{\rho_D h_D}{2\rho h} \right] \left(\frac{f_r}{f_o} \right)^2 = 1 + \frac{3(1+n)^2 (1+\psi_{nm} + \eta_D^2)}{(1+\psi_{nm})^2 + \eta_D^2} \quad (15)$$

$$\psi_{nm} = \frac{(r^2+1)}{(1-v^2)} \frac{\pi^2}{2} \frac{E}{G_D} \left(\frac{h}{\lambda} \right)^2 n \quad (16)$$

where $n = h_D/h$, λ is the half wavelength in one direction and r is the ratio of λ to the half wavelength in the other direction, and v is Poisson's ratio for the outer sheets.

If the boundaries are clamped, which would be a closer approximation to what one might use in a practical application, one can estimate the size of the equivalent pinned plate of the same aspect ratio simply by varying the pinned plate dimensions until the observed natural frequencies are the same as those for the clamped plate in the appropriate mode, in lieu of a more exact analysis. See references [16] to [19] for more information.

Sample Calculation

A steel sandwich plate is 12 inches long by 20 inches wide by 3/16 inch net thickness. The outer sheets are of thickness 1/16 inch each, of Young's modulus $E = 3 \times 10^7$ Lb/in², and the core layer is 1/16 inch thick with Young's modulus of 360 Lb/in² and loss factor of 1.4. The plate is pinned along all four sides. Calculate the damping and the resonant frequency for the fundamental mode. The density of the damping material is 0.04 Lb/in³. For the undamped plates, each of thickness 1/16 inch, the equation of motion is:

$$\frac{Eh^3}{12(1-\nu^2)} v^4 w - \rho h w^2 w = 0$$

For the fundamental mode $w = \sin(\pi x/12) \sin(\pi y/20)$ if the x and y axis are defined as being along the 12 inch and 20 inch sides respectively, with the origin at a corner. Substituting into the equation of motion given, for $\nu = 1/3$:

$$\frac{Eh^3}{12(1-\nu^2)} \left[\frac{1}{12^2} + \frac{1}{20^2} \right]^2 - \rho h w_{11}^2 = 0$$

$$\text{whence } w_{11}^2 = \frac{3 \times 10^7 \times (1/16)^2 \times 386(400+144)}{0.3 \times 12 (8/9) (400 \times 144)}$$

$$\therefore f_{11} = 184 \text{ Hz}$$

For the damped plate, we note that $n = 1$ and $\eta_D = 1.4$. Therefore, by equation

$$\therefore \psi_{11} = \frac{[(12/20)^2 + 1]\pi^2 \times 3 \times 10^7 \times (1/16)^2 \times 1}{(1-1/9) 2 \times (360/3) \times 12^2} = 50.9$$

From equation (14):

$$n_s = \frac{3 \times 1.4 \times 50.9(2)^2}{(51.9)^2 + (1.4)^2 + 3 \times 4(51.9+1.96)} \\ = 0.252$$

and, from equation (15):

$$\left[1 + \frac{0.04 \times 1}{2 \times 0.3} \right] \left(\frac{f_r}{184} \right)^2 = 1 + \frac{3(2)^2(1+50.9 + 1.96)}{(51.9)^2 + 1.96} \\ \therefore 1.067 \left(\frac{f_r}{184} \right)^2 = 1.12$$

$$\therefore f_r = 184 \times 1.025 = 189 \text{ Hz}$$

Multiple Constrained Layer Treatments

Figure 35 illustrates the various geometries of multiple layer damping treatments which have been examined analytically and experimentally. The very simplest constrained layer treatment consists simply of a thin layer of viscoelastic material attached to the surface of the structure and constrained by a stiff layer, usually of metal, on the outer surface. Multiple layers are produced simply by repeating the pattern. The advantages of this type of treatment are manifold. For example, since the mechanism of energy dissipation is primarily through shear deformation of the viscoelastic material as the surface deforms in bending, the viscoelastic material need not have an exceptionally high shear modulus to be effective, as is the case for a free layer treatment. Furthermore, by choosing very stiff constraining layers one can further enhance the damping capability and, finally, by

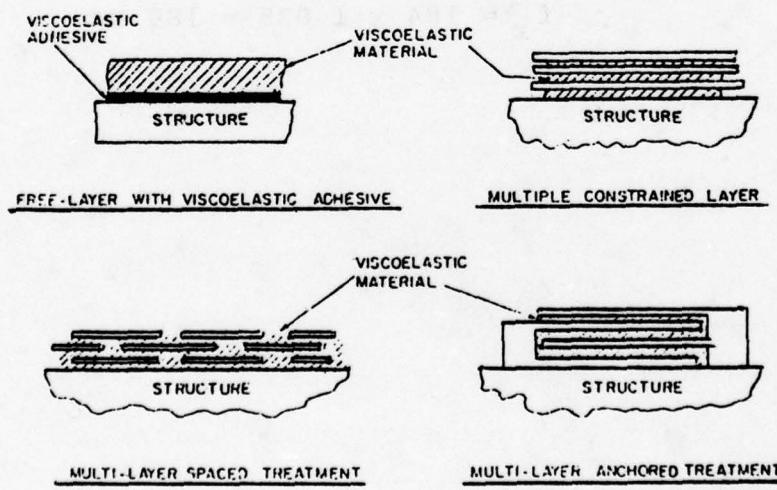


Figure 35. Typical multiple layer treatments

choosing appropriate different materials for each viscoelastic layer, one can optimize the damping to some degree to be effective over a wider temperature or frequency range than one usually achieves with a single viscoelastic material between each constraining layer

Unlike the free layer treatment, the analysis of constrained layer treatments is generally difficult and analysis and experimental data are not always in good agreement, although the qualitative behavior of these systems seems to be well understood [20 - 21]. For a designer's purposes semi-empirical data, based on experiments, are often preferable although the price paid for this approach is the limited number of parameters which can be varied. A comprehensive program to evaluate multiple constrained layers on simple beams, for example, would have to consider wide variations in the number of layers N , the complex shear modulus $G_D (1+i\eta_D)$ of the viscoelastic layers [or $E_D (1+i\eta_D)$], the modulus E_C of the constraining layer, the viscoelastic material thickness h_D , the constraining layer thickness h_C , the modal half-wavelength λ_n in the n th mode, the length L and the thickness h of the beam, the modulus E of the beam and the boundary conditions. This total of at least ten parameters can easily lead to the necessity for conducting an enormous number of response tests and would become highly impractical if a large number of values of each parameter had to be examined. Fortunately, however, analysis can help greatly in showing which non-dimensional groups of parameters are the most promising to look into.

In fact, elementary theory seems to show that many of the parameters can be combined into a single "shear parameter" defined by $E_D \lambda_n^2 / E_C h_C h_D$ which, when combined with the geometrical ratios h_D/h_C and h_D/h , the modulus ratio E_C/E , and N , reduces the total number of independent parameters from ten to five. Even further reduction can be achieved by representing the behavior of the multiple layer treatment in terms of an equivalent complex Young's modulus $E_\epsilon(1+in_\epsilon)$, for which E_ϵ/E_C and n_ϵ/n_D depend strongly only on $E_D \lambda_n^2 / E_C h_C h_D N$ and h_C/h_D , thereby eliminating the ratios h_C/h , E_C/E and N , at least to a degree of approximation. The number of important parameters is then reduced to two and experimental data reduction is greatly simplified.

Equivalent Complex Moduli

Extensive tests [22,23] have been carried out on a clamped-clamped aluminum beam, seven inches long, one inch wide and 0.050 inches thick, for a large number of different multiple constrained layer treatments. Typical measured graphs of η_s and $(1+\rho_D n/\rho) (f_r/f_n)^2$ versus $E_D \lambda_n^2$ are plotted in Figure 36. From these graphs, using equations (3) and (4) in reverse, one can deduce the values of E_e and η_e for each selected value of $E_D \lambda_n^2$. Typical graphs of E_e/E_C and η_e/η_D versus $E_D \lambda_n^2/E_C h_D h_C N$ are shown in Figure 37. To extend the data to unstiffened plates, it is necessary only to replace the beam shear parameter $\phi_n = E_D \lambda_n^2/E_C h_C h_D$ by a plate shear parameter $\phi_{nm} = E_D \lambda_{nm}^2/(r^2 + 1)E_C h_C h_D N$ where λ_{nm} is the half wavelength of the nm th mode and r is the ratio of λ_{nm} to the distance between the other two node lines bounding a segment of a mode. For example, for a 10 in. by 8 in. plate pinned on all four edges, λ_{11} for the fundamental mode is 8 in. and $r = 8/10$.

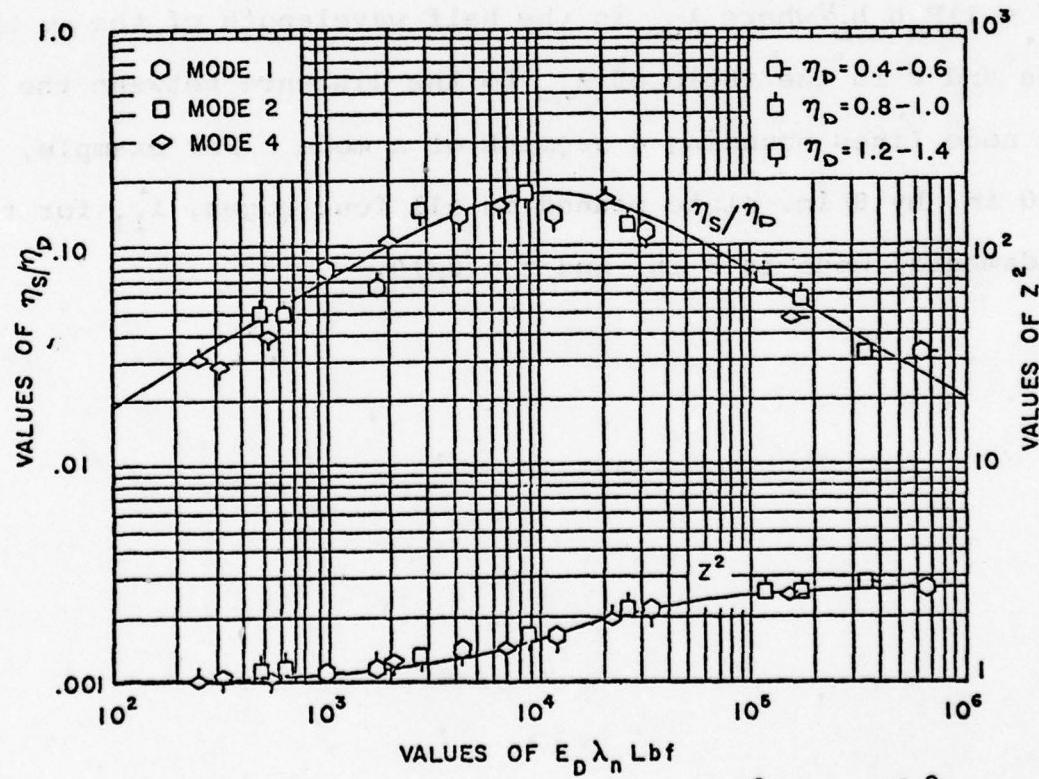
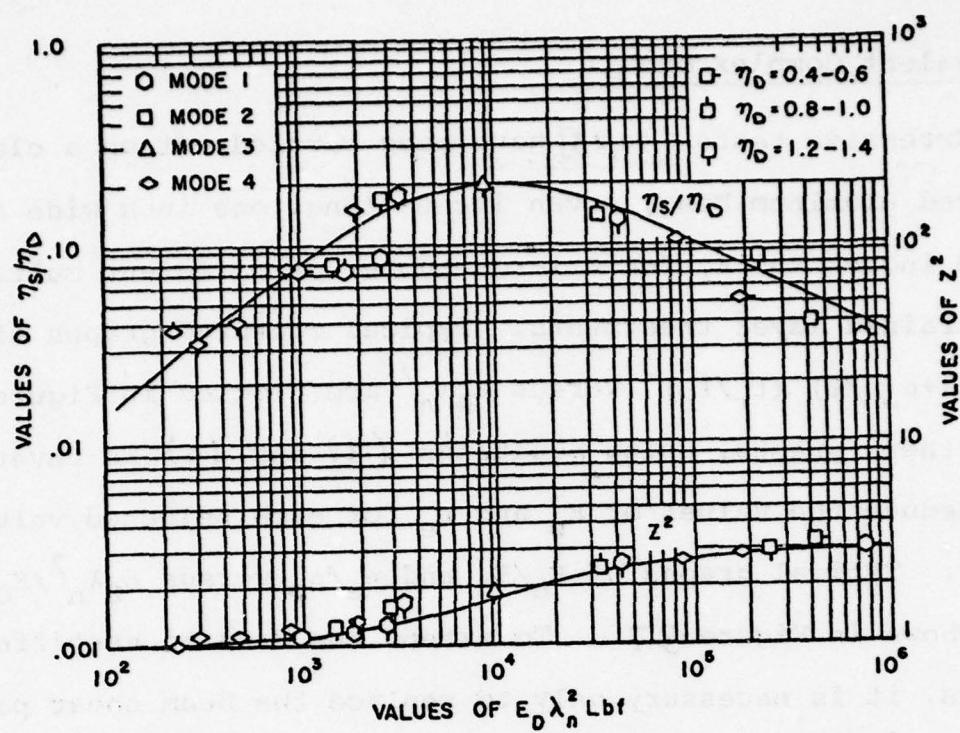


Fig. 36. Typical graphs of η_s/η_D and z^2 vs. $E_D \lambda_n^2$

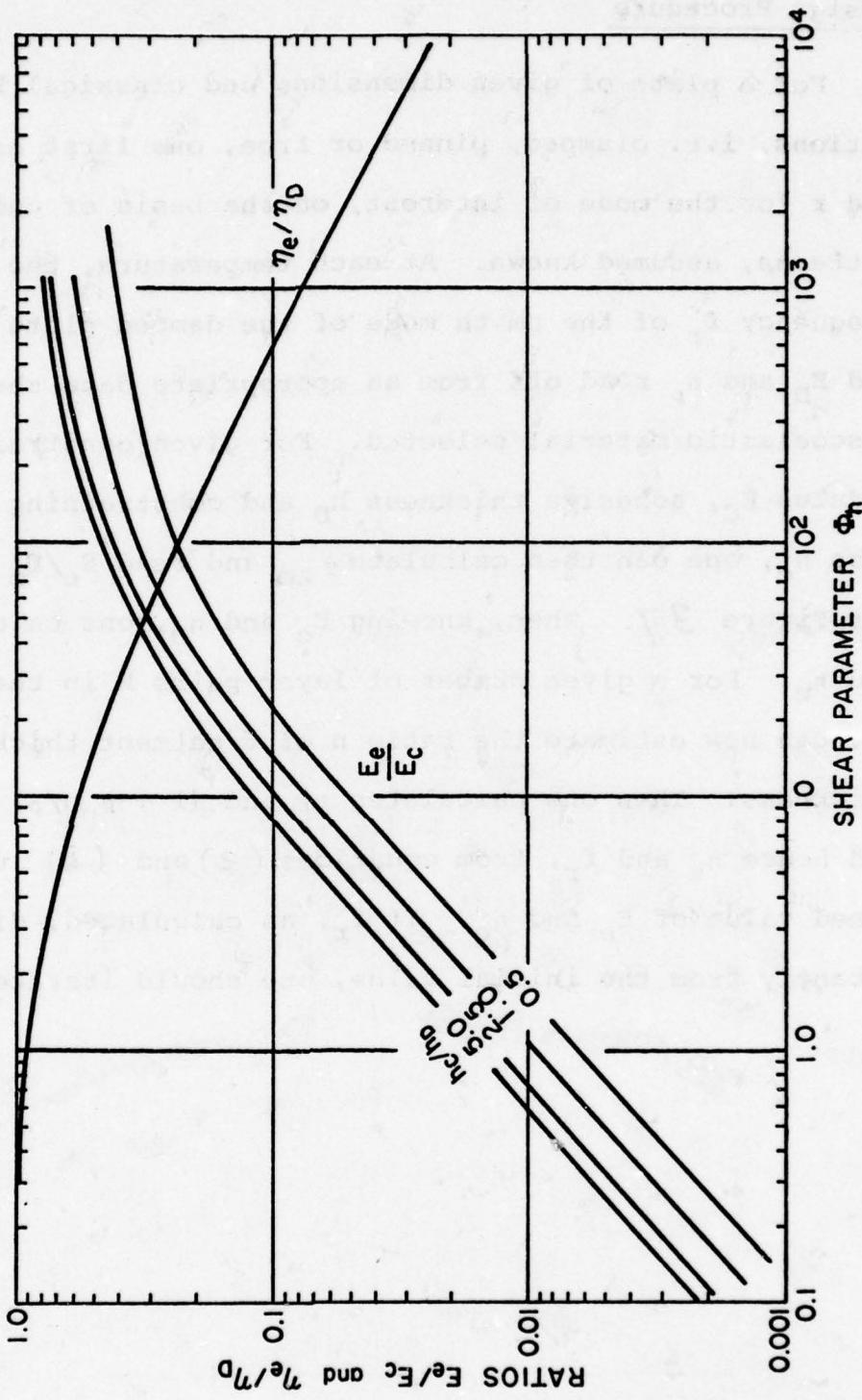
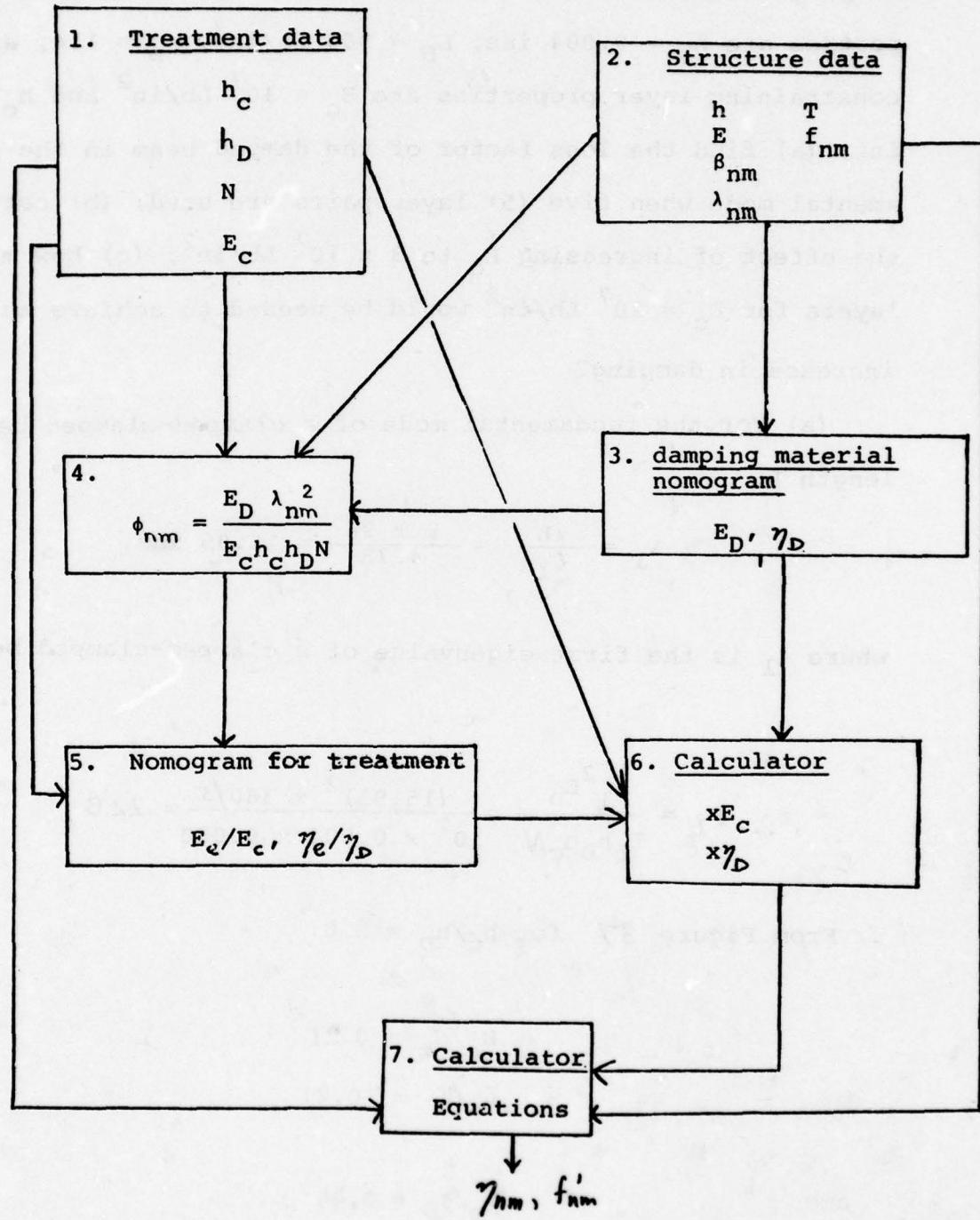


Figure 37. Graphs of E_e/E_c and η_e/η_D against Φ_n

Design Procedure

For a plate of given dimensions and classical boundary conditions, i.e. clamped, pinned or free, one first estimates λ_{nm} and r for the mode of interest, on the basis of undamped modal patterns, assumed known. At each temperature, the resonant frequency f_r of the nm th mode of the damped plate is guessed and E_D and η_D read off from an appropriate data sheet for the viscoelastic material selected. For given constraining layer modulus E_C , adhesive thickness h_D and constraining layer thickness h_C , one can then calculate ϕ_{nm} and read E_e/E_C and η_e/η_D off Figure 37. Then, knowing E_C and η_D , one calculates E_e and η_e . For a given number of layer pairs N in the treatment, one can now estimate the ratio n of treatment thickness to plate thickness. Then one calculates η_s and $(1 + \rho_D n / \rho) (f_r/f_{nm})^2$, and hence η_s and f_r , from equations (3) and (4) using the determined value of E_e and η_e . If f_r , as calculated, differs significantly from the initial value, one should iterate.

Schematic procedure for calculating performance of multiple constrained layer treatment on structure.



Sample Calculation

A clamped-clamped steel beam of length 2 ft. and thickness 0.25 inches is to be damped by a multiple layer constrained damping treatment over the whole surface. If the adhesive properties are $h_D = 0.004$ ins, $E_D = 360$ Lb/in², $\eta_D = 1.4$, and the constraining layer properties are $E_C = 10^7$ Lb/in² and $h_C = 0.020$ ins; (a) find the loss factor of the damped beam in the fundamental mode when five (5) layer pairs are used; (b) estimate the effect of increasing E_C to 3×10^7 Lb/in²; (c) how many layers for $E_C = 10^7$ Lb/in² would be needed to achieve an equal increase in damping?

(a) For the fundamental mode of a clamped-clamped beam of length L:

$$\lambda_1 = \frac{\pi L}{\xi_1} = \frac{\pi \times 24}{4.73} = 15.95 \text{ ins.}$$

where ξ_1 is the first eigenvalue of a clamped-clamped beam

$$\therefore \phi_1 = \frac{\lambda_1^2 E_D}{E_C h_D h_C N} = \frac{(15.95)^2 \times 360 / 5}{10^7 \times 0.004 \times 0.020} = 22.8$$

∴ From Figure 37 for $h_C/h_D = 5.0$:

$$E_C/E_C = 0.21$$

$$\therefore E_e/E = 0.21$$

and

$$\eta_e/\eta_D = 0.44$$

$$\therefore n_e = 0.44 \times 1.4 = 0.616$$

Therefore, from equation (1) or (3), with $n = 5(0.004 + .020)/0.25 = 0.48$:

$$n_s = 0.234$$

(b) If we now increase E_c to 3×10^7 , then ϕ_1 becomes

$$\phi_1 = 22.8/3 = 7.6$$

$$\therefore E_e/E_c = 0.095$$

$$\therefore E_e/E = 0.095 \times 3 = 0.285$$

and

$$n_e/n_D = 0.62$$

$$\therefore n_e = 0.62 \times 1.4 = 0.868$$

Therefore, by equation (1) or (3)

$$n_s = 0.372$$

(c) In order to estimate the number of layers with $E_c = 10^7 \text{ lb/in}^2$ needed to achieve the above loss factor we must simply repeat the calculation procedure (a) with $N = 6, 7, 8 \dots$ until this value of n_s is equalled or exceeded. For $N = 11$ we have:

$$\gamma_s = 0.368$$

Tuned Damping Devices

The various layered damping treatments operate effectively only in structures and modes of vibration for which high surface strains occur. For structures which have low surface strains involving non-platelike behavior, as in the case of very highly curved elements, the tuned damper concept may be of greater utility. Essential prerequisites for a tuned damper to be of value are that the damper be located at a point of high amplitude response, such as an anti-node of a mode, and that the frequency spectrum of the response have a single resonance, a number of widely separated resonances or a number of widely separated groups of modes.

Let us first consider the damper itself in isolation, in order to understand the principle of action [24 - 28].

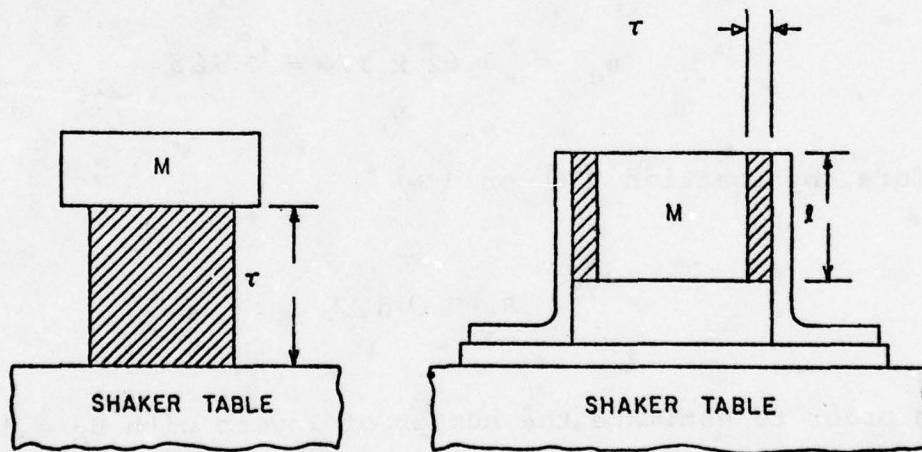


Figure 38. Typical tuned damper concepts

Figure 38 shows an idealized sketch of a tuned damper, consisting of a mass attached to a spring exhibiting viscoelastic damping behavior. This simple tuned damper is essentially a simple single degree of freedom system.

The force exerted on the structure by the damper, resulting from an excitation $X \exp(i\omega t)$ at the point of attachment, is:

$$F = -K(Y-X)(1+i\eta) \exp(i\omega t)$$

$$= \frac{-M\omega^2 X}{1-M\omega^2/K(1+i\eta)} \quad (17)$$

At the frequency for which $M\omega^2/K=1$, we see that:

$$F = \frac{-i X K}{\eta_D} = \frac{\dot{X}K}{\eta\omega}$$

indicating that the force F is opposing the velocity X i.e. it is a damping force. By proper choice of M, K and η_D , one can in principle design a damper to introduce a high degree of damping into a number of structures. One can also calculate the energy dissipation in the damper. Typical results are shown in Figure 39.

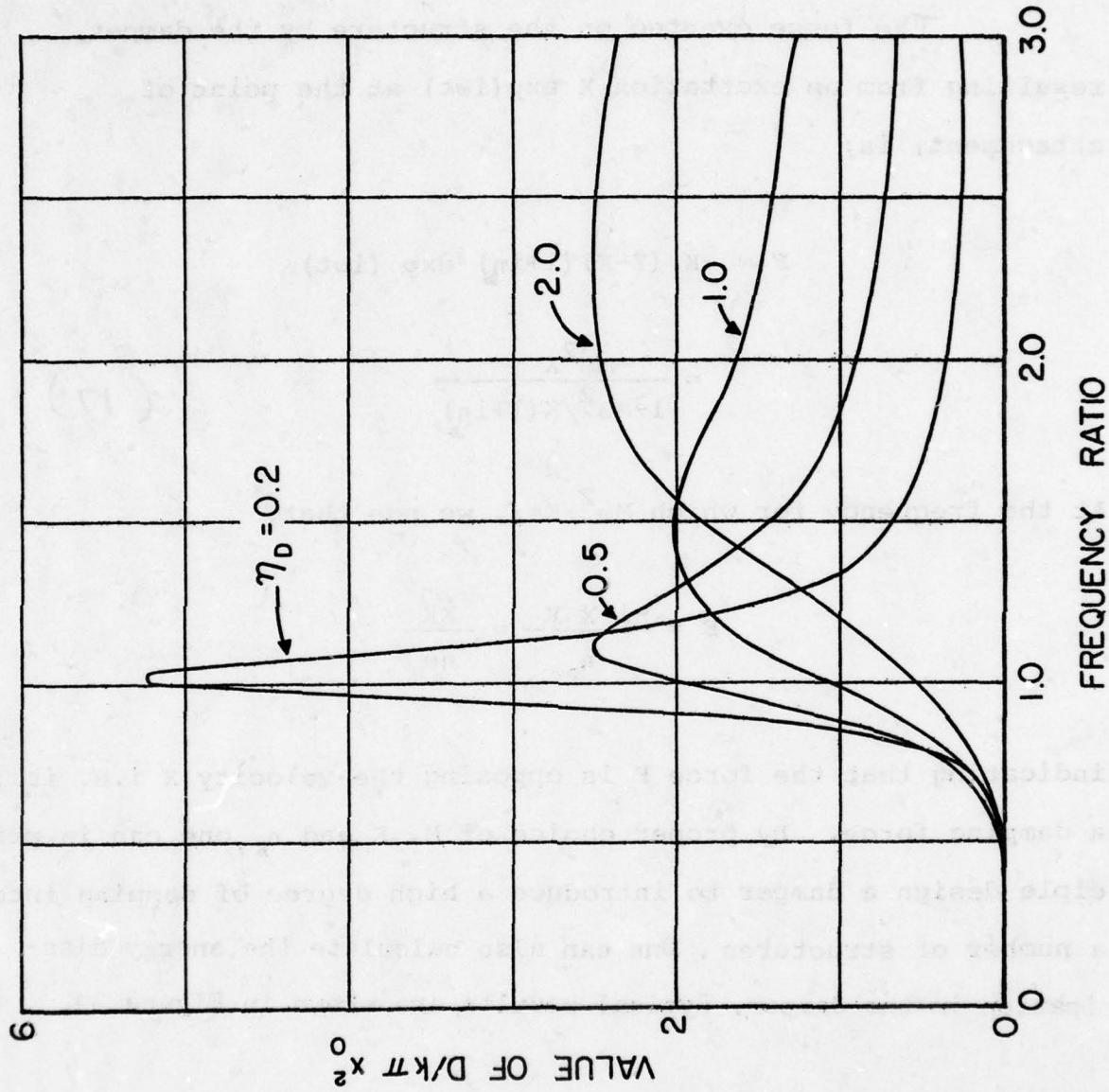


Figure 39. Graphs of $D/\pi k X_0^2$ versus frequency ratio

Tuned Dampers in simple structures

If the structure is relatively simple, to the extent that it either has only a single resonance or a number of very widely separated resonances, a tuned damper can be designed very readily simply by ensuring that the damper frequency $\omega_D = \sqrt{K/M}$ is close to the frequency of the mode to be damped.

The effect of the damper on the response of the structure is to split the original single mode into two [26] The lower frequency branch corresponds to the damper mass M and the structure surface moving essentially in-phase while the higher frequency peak corresponds to the mass and surface moving essentially out of phase. The effect of moving the damper frequency ω_D relative to the frequency ω_n of the mode in question to emphasize one of the peaks at the expense of the other, with an optimum damping case occurring when the two response peaks are of equal amplitude.

For simple structures meeting the requirements of a single resonance peak or widely separated resonances, the response behavior of the damped system near the lowest frequency can be written in the form:

$$\frac{W}{W_0} = \frac{1}{1 - \left(\frac{\omega}{\omega_1}\right)^2 - \frac{\psi_c (\omega/\omega_1)^2}{1 - (\omega/\omega_D)^2 / (1 + i\eta_s)}} \quad (18)$$

where W_0 is the static displacement under the applied forces at zero frequency and ψ_e is an effective mass given by:

$$\psi_e = \left(\frac{M}{M_s} \right) \gamma_1$$

where M_s is the mass of the structure and γ_1 is a non-dimensional parameter depending on the mode shape and the damper location. Calculation of γ_1 will be difficult in general, although it is easily worked out for simple cases.

Equation (18) shows that the response W/W_0 at any frequency ω and any point in the structure depends only on the effective mass ψ_e , the frequency ratio ω_D/ω_1 , and the damper loss factor η_d . For given η_d and ψ_e , therefore, varying ω_D/ω_1 will alter the tuning of the damper and vary the relative amplitude of the two response peaks generated by the damper, as in Figure 40.

Figure 41 shows the variation of the value of $n_s = (|W_0^2/W^2| - 1)^{-1/2}$ with ω_D/ω_1 for typical values of η_d and ψ_e .

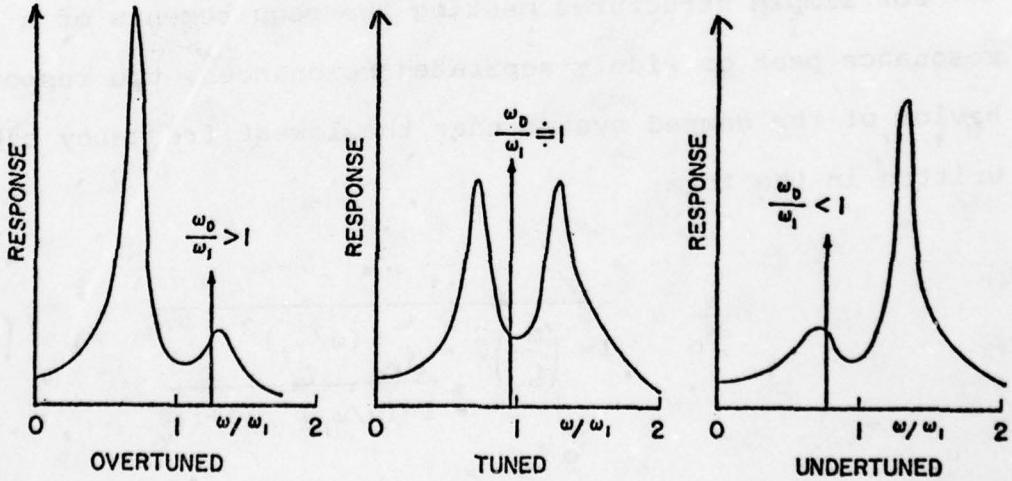


Figure 40. Typical response spectra for simple structure

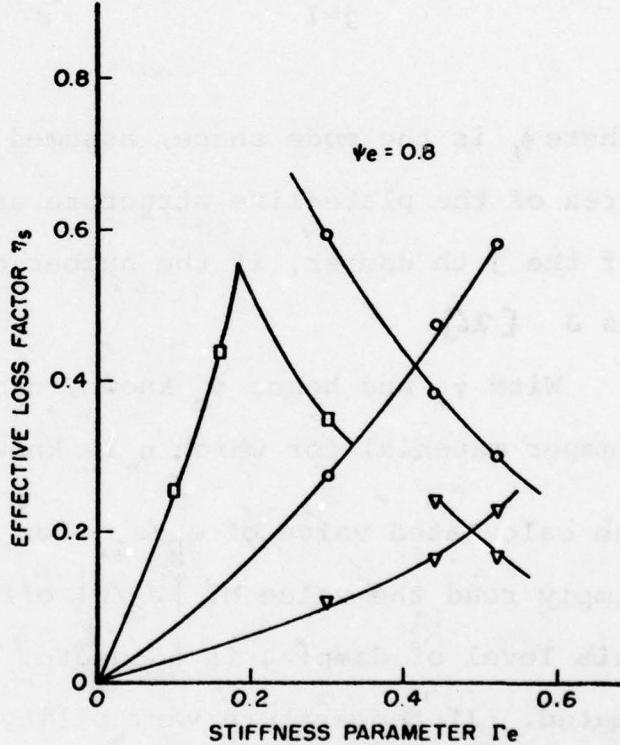
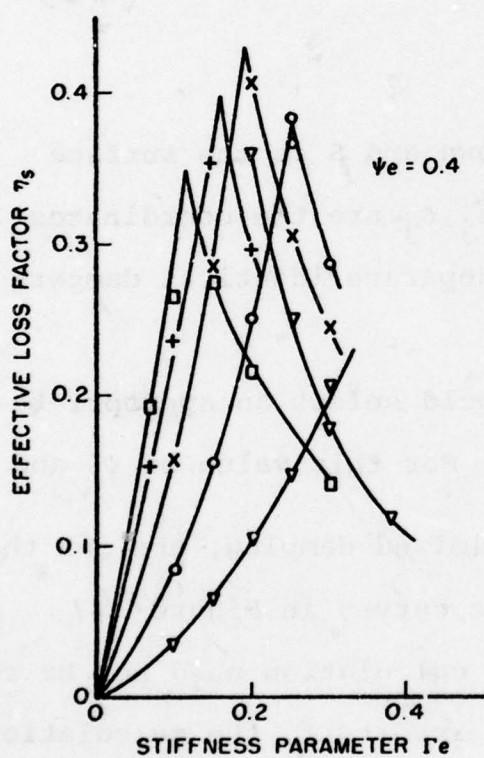
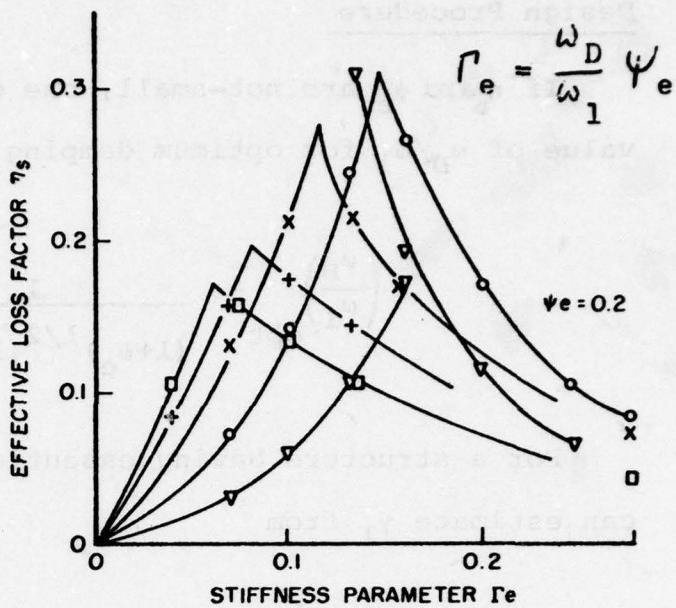
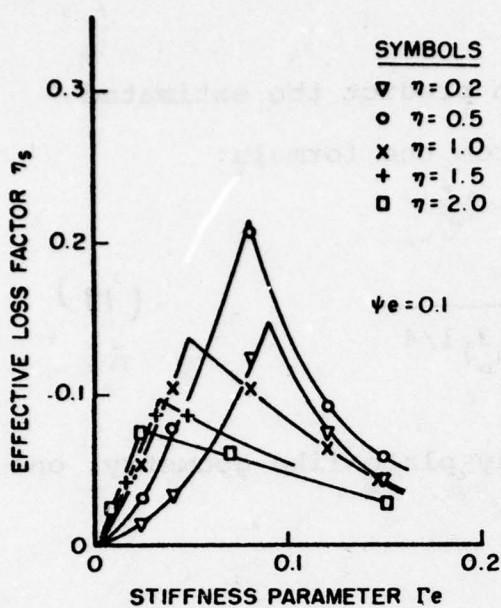


Figure 41. Graphs of Effective Loss Factor η_s Against Stiffness Parameter Γ_e (Shaker Excitation)

Design Procedure

If η_b and ψ_e are not small, one can predict the estimated value of ω_D/ω_1 for optimum damping from the formula:

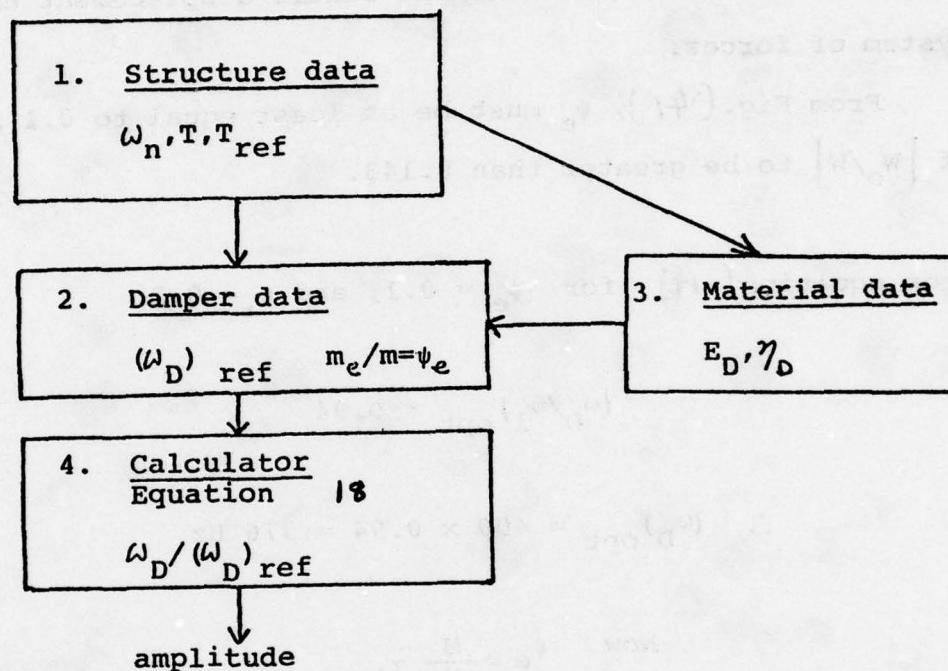
$$\left(\frac{\omega_D}{\omega_1}\right)_{\text{opt}} = \frac{1}{(1+\psi_e)^{1/2} (1+\eta_b^2)^{1/4}} \quad (19)$$

For a structure having essentially plate-like geometry, one can estimate γ_1 from

$$\gamma_1 = \sum_{j=1}^J \phi_1^2 (\Delta_j, \delta_j) / \int_S \phi_1^2 (\Delta, \delta) d\Delta d\delta \quad (20)$$

where ϕ_1 is the mode shape, assumed known and S is the surface area of the plate-like structure and Δ_j, δ_j are the coordinates of the j th damper, if the number of separate identical dampers is J [26].

With γ_1 and hence ψ_e known, one would select an appropriate damper material for which η_b is known. For this value of ψ_e and the calculated value of ω_D/ω_1 for optimized damping, one can then simply read the value of $|\omega_o/\omega|$ off the curves in Figure 41. If this level of damping is adequate, the calculation need not be repeated. If temperature variability is important, the calculation should be repeated at several temperatures.



Sample Calculation

A structure has a single resonance peak at 400 Hz. the mass of the structure is 10 lb. and the tuned damper is to be placed at a location for which γ_1 is estimated to be 3.0. Using a viscoelastic material having a Young's modulus of 1000 Lb/in² and a loss factor of 0.2, design a damper which will reduce the peak response to less than seven (7) times the static displacement under any system of forces.

From Fig. (41), ψ_e must be at least equal to 0.1 for the value of $|W_o/W|$ to be greater than 0.143.

From equation (19), for $\psi_e = 0.1$, and $\eta_d = 0.2$:

$$(\omega_D/\omega_1)_{opt} = 0.94$$

$$\therefore (\omega_D)_{opt} = 400 \times 0.94 = 376 \text{ Hz}$$

Now $\psi_e = \frac{M}{M_s} \gamma_1$

$$\therefore 0.1 = \frac{M}{10} \times 3$$

$$\therefore M = 0.33 \text{ lb.}$$

But $(\omega_D)_{opt}^2 = \frac{K}{M} = \frac{E_D S K_T}{hM}$

where $E_D = 1000 \text{ Lb/in}^2$, S is the cross-sectional area of the damper, assumed of cylindrical shape as in Figure 38, h is the length and K_T is a shape factor given by [29]:

$$K_T = 1 + \beta (S/S')^2$$

where S' is the non-load carrying area of the specimen and β is a non-dimensional quantity equal to about 2.0 for an unfilled elastomer and 1.5 for a filled elastomer. For a cylindrical specimen of radius R , therefore:

$$(376 \times 2\pi)^2 = \frac{1000 \pi R^2 (1+R^2/4h^2)}{h (0.33/386)}$$

$$\therefore \frac{R^2}{h^2} \left\{ 1 + \frac{R^2}{4h^2} \right\} = \frac{1.52}{h}$$

Any values of h and R which satisfy this equation will therefore be acceptable dampers. For $R/h = 1$, for example:

$$\frac{1.52}{h} = 1 \left(1 + \frac{1}{4} \right) = \frac{5}{4}$$

$$\therefore h = 1.21 \text{ ins}$$

$$\text{and } R = 1.21 \text{ ins}$$

If, on the other hand we were to design a shear type damper of the type illustrated in Figure 38, the procedure would be as follows. As before:

$$(\omega_D)^2_{\text{opt}} = \frac{K}{M} = \frac{G_D S K_S}{hM}$$

where G_D is the shear modulus, usually about one third (1/3) the Young's Modulus E_D , S is the load carrying area, h is the thickness of the shear layers and K_S is now given by [30]:

$$K_S = \frac{1}{1 + h^2/3 \cdot 6 \cdot K^2}$$

and K is the radius of gyration of the shear layer cross section about the neutral axis of bending. For a rectangular shear layer, $K = l/\sqrt{12}$

$$\therefore (376 \times 2\pi)^2 = \frac{333 (2lb)}{h(0.33/386)(1+h^2/3l^2)}$$

$$\therefore \frac{h}{l} \left(1 + \frac{h^2}{3l^2}\right) = 0.1406$$

For $h/l = 0.1$,

$$\begin{aligned} b &= 0.1 (1+0.01/3)/0.140 \\ &= 0.717 \text{ ins.} \end{aligned}$$

If we now let $l = 1$ in., $h = 0.1$ in. If $l = 2$ in., $h = 0.2$ in. and so on.

Tuned Dampers in Complex Structures

When tuned dampers are applied to complex structures possessing many closely spaced resonances, the simplicity of the foregoing is lost and the effect of the dampers on the structural response is dependent on the exact nature of the structural geometry, so that no relatively general design concepts can be formulated.

It can be said, however, that if the modes of vibration of interest extend over more than an octave band of frequency, have widely dissimilar energies associated with them and/or have many node lines, then tuned dampers are not likely to be of much value in reducing structural response. If, however, the modes of vibration of interest do fall within an octave band, do have similar energies and have few node lines, then we may say that tuned dampers will be very effective indeed. This type of response behavior is exactly what we observe in the case of the skin-stringer class of structure.

A typical skin-stringer structure is illustrated in Figure 30. In this type of structure, the mode of vibration are typically divided into groups or bands of modes corresponding to (a) no nodes within the bays, (b) one, two or more node lines within the bays parallel to the stiff frames and (c) one, two or more node lines within each bay parallel to the stringers. The frequency limits of each band depend critically on the aspect ratio of each bay, namely the ratio of frame separation to stringer separation. If the aspect ratio is small, the first band having

no mode lines within each bay will be separated from the others whereas for high aspect ratios the bands will all tend to overlap. In practice this means that tuned dampers are not likely to be of much utility for aspect ratios greater than about two (2). For aspect ratios less than two, however, several investigations [27, 31] have shown that tuned dampers can be very effective. Figure 42 shows the effect in a typical case

No general design rules are available even in this case, however, beyond the fact that one should tune the damper so that its resonant frequency lies near the center of the band and the damper loss factor η_D should be as high as possible.

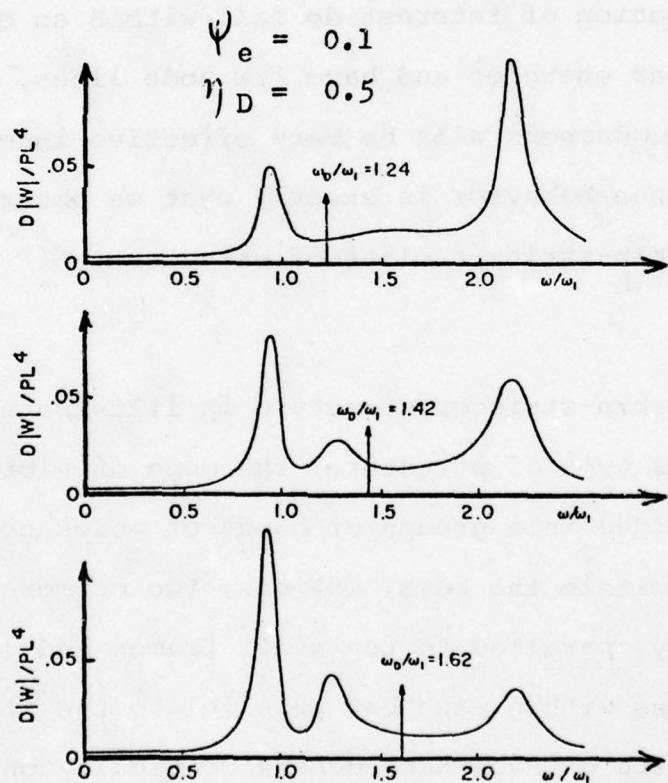


Figure 42. Typical response spectra for complex structure

4. NOMENCLATURE

A	resonance amplification factor or dimensionless constant as in text
A';B';C'	constants
B	dimensionless constant
D	flexural rigidity or subscript denoting damping materials according to test
E	Young's modulus of elastic material
E _D	real part of Young's modulus
E _C	constraining layer modulus
E _e	effective Young's modulus
exp	exponential function
e	E _D /E - modulus ratio
f	frequency (Hz)
f _n	n th natural frequency
f _{nm}	n m th natural frequency
f _r	resonant frequency of damped system
F	Force
G _D	real part of shear modulus
h	thickness of plate or beam
h _D	thickness of damping material
h _C	thickness of constraining layer
i	$\sqrt{-1}$
K	spring stiffness or radius of gyration
K _S , K _T	shape factors
L, l	lengths
M	mass
M _s	mass of structure

n	h_D/h - thickness ratio
N	number of layers
R	radius
r	ratio of λ_n to half wavelength of plate in normal direction
s, s'	areas
t	time
T, T_0	absolute temperatures
w, w_b	displacements
x	velocity
x	coordinate along beam
X, Y	displacement amplitude
\ddot{x}, \ddot{y}	accelerations
y	instantaneous displacement

α_n	dimensionless constant
α_T	temperature shift factor
β, β_{nm}	dimensionless constant
α	non dimensional parameter
δ	y/t
Δ	x/L
η_D	loss factor in tension-compression
η'_D	shear loss factor
η_e	effective loss factor
r, η_s, η_s	loss factors - see text
$\lambda, \lambda_n, \lambda_{nm}$	modal half wavelengths
ν, ν_D	Poisson's ratio
ξ_{nm}	$n m$ th eigenvalue
ρ, ρ_o, ρ_D	densities
σ	stress
ϕ_{nm}	$n m$ th normal mode. Also shear parameter
ψ_e	effective mass ratio
ψ_{nm}	inverse shear parameter
ω	frequency (rad/sec)
ω_D	damper natural frequency
$\hat{\epsilon}$	maximum strain
ϵ, ϵ_o	strains

D-A065 518 AIR FORCE FLIGHT DYNAMICS LAB WRIGHT-PATTERSON AFB OHIO F/G 11/9
CONFERENCE ON AEROSPACE POLYMERIC VISCOELASTIC DAMPING TECHNOLO--ETC(U)
JUL 78 L ROGERS

UNCLASSIFIED

2 OF 6
AD A0 65 61 B

AFFDL-TM-78-78-FBA

NL





5. REFERENCES

1. B.J. Lazan, Damping of Materials and Members in Structural Mechanics, Pergamon Press, New York, 1968.
2. J.C. Snowdon, Vibration and Shock in Damped Mechanical Systems, John Wiley and Sons Inc., New York, 1968.
3. D.I.G. Jones, J.P. Henderson and A.D. Nashif, "Reduction of Vibrations in Aerospace Structures by Additive Damping" Shock and Vibration Bulletin 40, Part 5, pp 1-18, Dec. 1969.
4. J.D. Ferry, Viscoelastic Properties of Polymers, John Wiley and Sons Inc., New York, 1961.
5. D. Birchon, "Hidamets, metals to reduce noise and vibration", Engineer, London, 5 Aug. 1966.
6. G.E. Bowie, J.F. Nachman and A.N. Hammer, "Exploitation of Cu-Rich Damping Alloys; Part I-The search for Alloys with high damping at low stress", American Society of Mechanical Engineers Paper 71 - Vibr. - 106, 1971.
7. G.F. Weissmann and W. Babington, "A high damping Magnesium Alloy for Missile Application", The Journal of Environmental Sciences, October 1966.

3. P. Sridharan and R. Plunkett, "Damping in Porcelain Enamel Coatings", Air Force Materials Laboratory Report AFML-TR-71-193, July 1972.
9. T. Parsons, W. Yates and F. Schloss, "The Measurement of dynamic properties of materials using a transfer technique", Naval Ship Research and Development Center, Research and Development Report - 2981, 1969.
- 10 E.E. Ungar, "Energy Dissipation at Structural Joints; Mechanisms and Magnitudes", Air Force Flight Dynamics Laboratory Report FDL-TDR-64-98, July 1964.
- 11 H. Oberst, "Über die Dämpfung der Biegeschwingungen dünner Bleche durch festhaltende Beläge", Acustica 2, leaflet 4, AB 191-194, Part I, 1952, and 4, p 433, Part II, 1954.
- 12 D.I.G. Jones, "Effect of Free Layer Damping on response of stiffened plate structures", Shock and Vibration Bulletin 41, Part 2, pp 105-120, Dec. 1970.
- 13 D. Ross, E.E. Ungar and E.M. Kerwin, Jr., "Damping of Plate Flexural Vibrations by means of viscoelastic laminae", Structural Damping, American Society of Mechanical Engineers, 1959.

14. D.J. Mead, "The effect of certain damping treatments on the response of idealized aeroplane structures excited by noise", Air Force Materials Laboratory Report AFML-TR-65-284, August 1965.

15. E.J. Richards and D.J. Mead, editors, Noise and Acoustic Fatigue in Aeronautics, John Wiley and Sons, New York, 1968.

16. A.D. Nashif and T. Nicholas, "An Analytical and experimental investigation of a two-layer damping treatment", Shock and Vibration Bulletin 39, Part 4, p 53, 1969.

17. P. Grootenhuis, "Vibration control with viscoelastic materials", Environmental Engineering, No. 38, May 1969.

18. A.D. Nashif and T. Nicholas, "Attenuation of vibrational amplitudes through the use of multiple layered damping treatments", American Society of Mechanical Engineers, Paper 71-Vibr-40, 1971.

19. D.J. Mead and S. Markus, "Loss factors and resonant frequencies of encastre damped sandwich beams", Journal of Sound and Vibration, Vol. 12, No. 1, pp 99-112, 1970.

20. D.I.G. Jones and W.J. Trapp, "Influence of Additive Damping on resonance fatigue of Structures", Journal of Sound and Vibration, Vol. 17, No. 2, pp 157-185, 1971.

21. A.D. Nashif and T. Nicholas, "Vibration Control by a multiple layered damping treatment", Shock and Vibration Bulletin 41, pp 121-131, 1970.
22. D.I.G. Jones, "Design of constrained layer treatments for broad temperature damping", Shock and Vibration Bulletin 44, Part 5, 1 - 12, 1974.
23. D.I.G. Jones, A.D. Nashif and M.L. Parin, "Parametric study of multiple-layer damping treatments on beams", J. Sound and Vibration 29(4), 423-434, 1973.
24. J.P. Henderson, "Energy dissipation in a Vibration damper utilizing viscoelastic suspension", Shock and Vibration Bulletin 35, Part 7, pp 213-229, April 1968.
- 25 A.D. Nashif, "Development of practical tuned dampers to operate over a wide temperature range", Shock and Vibration Bulletin 38, Part 3, pp 57-69, 1968.
26. D.I.G. Jones, "Response and damping of a simple beam with tuned dampers", Journal of the Acoustical Society of America, Vol. 42, No. 1, pp 50-53, July 1967.
- 27 D.I.G. Jones, "Effect of isolated tuned dampers on response of multispan structures", Journal of Aircraft, Vol. 4, p 343, 1967.

28. D.I.G. Jones and G.H. Bruns, "Effect of tuned viscoelastic dampers on response of multi-span structures", Shock and Vibration Bulletin 36, Part 4, p 49, 1967.
- 29 J.C. Snowdon, Vibration and shock in damped mechanical systems Wiley, New York, 1968.
- 30 A.B. Davey and A.R. Payne, Rubber in Engineering Practice, Palmerton Publishing Co. Inc., New York, pp 118-119, 1964.
31. J.P. Henderson, "Vibration analysis of curved skin-stringer structures having tuned elastomeric dampers", Air Force Materials Laboratory Report AFML-TR-72-240, 1972.
32. L. C. Rogers and A. D. Nashif, "Computerized Processing and Empirical Representation of Viscoelastic Material Property Data and Preliminary Constrained Layer Damping Treatment Design," Shock and Vibration Bulletin, 48, 1978.

MEASUREMENT OF MATERIAL AND SYSTEM DAMPING

R. Plunkett
University of Minnesota
Department of Aerospace Engineering
and Mechanics
Minneapolis, Minnesota

MEASUREMENT OF MATERIAL AND SYSTEM DAMPING

Robert Plunkett
Professor, Aerospace Engineering and Mechanics
University of Minnesota
Minneapolis, MN 55455

ABSTRACT

Damping factor is defined in terms of energy and it is shown that damping factors due to different mechanisms are additive. It is shown that damping is only effective at resonance and that its effectiveness depends in part on the type of excitation. Different techniques of measuring damping in the laboratory and in service are listed.

Introduction

Decisions about the appropriate use of damping treatments to control the dynamic response of structural systems are heavily dependent on what we measure and how we measure it. Field measurements of system damping tell us what may be accomplished and whether it has been; laboratory measurements of material damping furnish the information necessary for design purposes. This paper does not pretend to be a complete coverage of all the technical details; its only purpose is to point out the premises, results and problems. The underlying theory is covered in the six survey papers and volumes listed as references. Reference 1 is very complete but out of print. References 1 through 4 cover both theory and technical literature through 1965. References 5 and 6 are more readily available and are more recent but do not cover the recent literature very thoroughly.

Before we can discuss measurement, we must know what we are measuring. We shall confine ourselves to a consideration of damping effects in the linear response region of normal structures, those in which damping is relatively small. The dynamics response of such a structure depends primarily on the mass and stiffness distribution; unless there are large changes in geometry, both of these are independent of amplitude of motion and thus define linear dynamic response. Because of this linearity, superposition holds and the powerful techniques of modal decomposition and spectral response may be used. If such a structure is subjected to a deformation pattern whose spacial distribution does not change while the amplitude of the deformation is taken through one complete cycle from equilibrium to positive loading back through equilibrium to equal negative loading and return to equilibrium, the necessary loading distribution will be almost a linear function of the

the deformation if this deformation has a sinusoidal time variation. Careful measurement will show some hysteresis in this almost linear plot and this hysteresis corresponds to energy dissipation or damping. The definition of system damping factor is:

$$\eta_s = \frac{\Delta W_s}{2\pi U_s} \quad (1)$$

where

$$\Delta W_s = \int F dx = \int F v dx$$

In this expression, ΔW_s is the net work done on the system in one such cycle and is therefore the energy dissipated or lost by the system as defined. U_s is the deformation energy stored in the system at its maximum deformation.

Because of this definition, if there are several mechanisms for energy dissipation or transfer, the system damping factor is equal to the sum of the factors found for each mechanism separately:

$$\begin{aligned} \eta_s &= \frac{\Delta_1 W_s + \Delta_2 W_s + \Delta_3 W_s + \dots}{2\pi U_s} \\ &= \eta_{1s} + \eta_{2s} + \eta_{3s} + \dots \end{aligned} \quad (2)$$

Since the effects of different damping mechanisms are additive, it makes little sense to point out that a certain damping treatment increases damping by so many times. In addition, there is little point in adding a damping treatment with an η of 0.01 if the original value is 0.05; it would be very useful if one started from 10^{-3} .

The next concern is how to determine ΔW_s . We have already noted that energy added to a system by a concentrated force is equal to the work done. By the same reasoning, the energy stored and energy dissipated per unit volume of a material is

$$\begin{aligned} u &= \frac{1}{2}(\sigma : \epsilon)_{\text{max}} \\ \Delta w &= \int \sigma : \dot{\epsilon} dt \end{aligned} \quad (3)$$

where $:$ stands for tensor scalar multiplication. From these definitions we get the definition of complex modulus for sinusoidal strain:

$$E^* = E' + iE'' = E'(1 + i\eta) \quad (4)$$

η is a constant for polymeric materials and some metals at low strain levels. In References 1 and 2, it is shown that if η depends on strain level:

$$\eta_{1s} = \frac{\int \eta(\epsilon) \epsilon^2 dV}{\int \epsilon^2 dV} \quad (5)$$

so that a small volume, like a fillet, at high strain level does not lead to high damping.

Effects of Damping

Damping is useful for control of vibration only near resonance. If one examines the graphs of forced response of a single degree of freedom system as a function of damping which are given in any elementary text on vibration theory, one finds that damping has no influence on vibration amplitude at frequencies which are more than ηf_n higher or lower than the resonant frequency. This has somewhat different implications for different types of excitation.

I. Sinusoidal Excitation

For steady state sinusoidal excitation of a single degree of freedom linear system the velocity response is:

$$\text{If } f(t) = f_0 e^{i\omega t} = f_0 \cos \omega t$$

$$v(t) = \frac{v_0}{(\beta - \frac{1}{\beta}) + i\eta} e^{i\omega t} \quad (6)$$

$$= \frac{v_0}{[(\beta - \frac{1}{\beta})^2 + \eta^2]^{1/2}} \cos(\omega t + \theta)$$

$$\text{where } \beta = \frac{\omega}{\omega_n} = \frac{f}{f_n}$$

We may express the frequency response as

$$V(\omega) = f_0 H(\omega; \eta) \quad (7)$$

$$\text{where } H(\omega; \eta) = [(\beta - \frac{1}{\beta}) + i\eta]^{-1/2}$$

is the complex frequency response with η as a parameter. Thus if we double the damping we reduce the resonant amplitude by 2 but have little effect away from resonance.

II. Stochastic Excitation

For random excitation, as in the case of jet noise or turbulence, the response may be found from the spectrum. If we transform from the time domain to the frequency domain for a single measured excitation:

$$\begin{aligned} \text{if } & f(t) \rightarrow F(\omega) \\ \text{then } & v(t) \rightarrow V(\omega) \end{aligned} \quad (8)$$

where

$$V(\omega) = F(\omega) H(\omega; \eta)$$

If we average over a large number of measurements we get the power spectral density and

$$S_v(\omega) = |H(\omega; \eta)|^2 S_f(\omega) \quad (9)$$

where S_f is the power spectral density of the exciting force and S_v is that of the velocity. In this case, it can be shown that the RMS value of v is inversely proportional to the square root of η so that we must increase η by 4 to reduce v by 2.

III. Transient Excitation

The maximum shock amplitude for a step shock excitation such as a landing shock, a sonic boom or a bumper crash is very insensitive to damping. The maximum dynamic amplitude for a step input to an undamped system is twice the static displacement; it requires an η of 0.5 to reduce this by 25%. What does happen is that the transient vibration dies out faster as the damping is increased. If the transient excitation is oscillatory, as in earthquakes, damping does affect the response spectrum but usually by even less than it does for stochastic processes.

IV. Self Excited Oscillations

The technical requirement for self excited oscillations is that the system damping be less than zero as in flutter or brake squeal. This means that the amplitude depends on non-linear effects rather than on the normal kinds of damping. As a result, increasing the damping will have almost no effect until the critical value is reached. Then, a very small increase in damping will eliminate the vibration completely.

We see that changes in damping are only of importance for frequencies near resonance and that the net effect depends markedly on which one of the four types of excitation is operative.

Measurement Technique

A number of specific measurement techniques are described in references 4 and 6. They can all be grouped into four categories.

I. Decay

If we excite a material or system at its resonant frequency and turn off the excitation, the amplitude of sinusoidal vibration will decay exponentially. It is shown in handbooks that:

$$\eta = \frac{1}{n} \ln \frac{x_{k+n}}{x_k} \quad (10)$$

where x_i is the positive magnitude of a given peak. If we make a logarithmic plot of the envelope of the vibration as a function of time with a level recorder, the damping will be proportional to the slope. Figure 1 shows such a decay curve for an annealed tool steel decaying from 500 microstrain to 2 microstrain. The damping (slope) is large at large strain, changes by a factor of about 10 at 50 microstrain and then increases again. This last effect is due to Coulomb friction at the base of the cantilever beam being tested.

II. Driven

If a system is driven at resonant frequency, we can find the damping by measuring the input vibratory force, the vibration amplitude at the driven point and the vibration amplitude of the system. Then:

$$\eta = \frac{\text{Energy Input}}{2\pi U_s}$$

III. Driven-Frequency Sweep

If a system is driven by a constant force while sweeping the excitation frequency, the ratio of resonant amplitude to the amplitude at frequencies well below resonance is equal to $1/\eta$. In addition the dimensionless frequency bandwidth is equal to η (Ref. 4).

IV. Impact Excitation

If a vibratory system is impacted by an instrumented hammer, the time response and the force-time trace can be put into the frequency domain by a FFT computer. An experimental approximation to $H(\omega)$, equation 7, can be found from the complex ratio of the two spectra. η can be found by suitable curve fitting to $H(\omega)$. This method works best for lightly damped systems which can be struck on stiff parts of the structure.

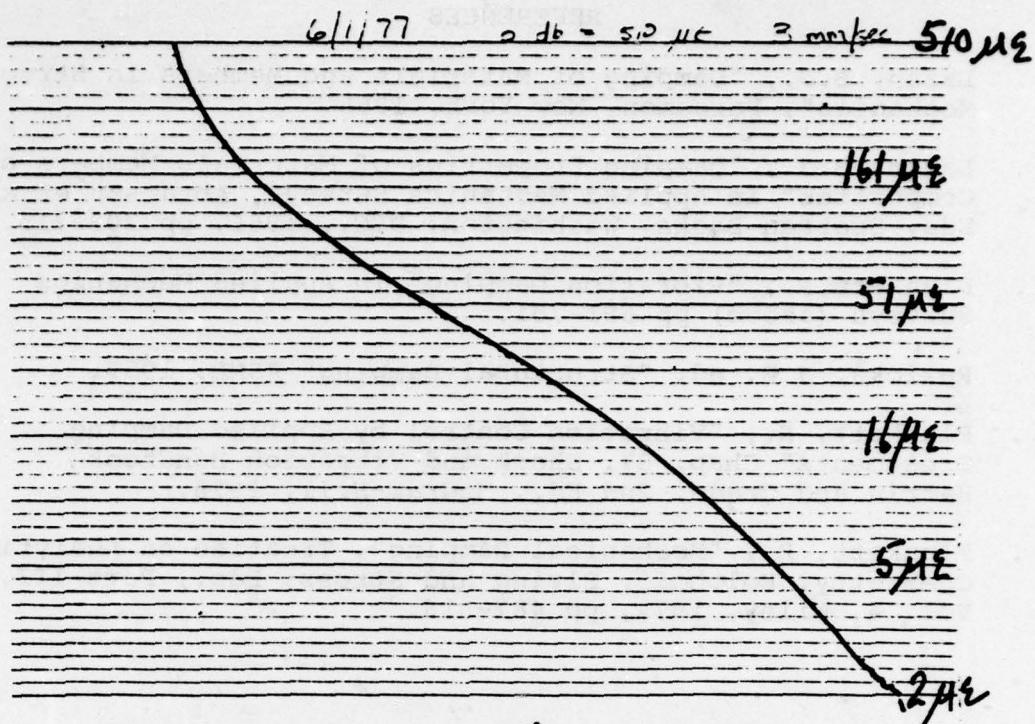
Operating Systems

Operating conditions can sometimes change the damping drastically. A lift vehicle in vacuum or an airplane in flight will usually have much lower damping than would be measured on the ground. One of the above procedures may be used during operation. For example, a sinusoidal exciter can be mounted in a wing for a frequency sweep. Decay can be measured from impact excitation. The power spectral density can be measured for a system subjected to turbulent flow

conditions where we know the turbulent spectrum to be relatively flat. If this is done, we must watch out for two natural frequencies close enough together to affect the results. Fig. 2 shows the averages of 128 samples of a cylinder in turbulent cross flow. The top graph shows two resonances at 142 and 159 Hz interfering enough to make the damping measurement impossible. The bottom graph indicates a damping constant of about 0.01 to 0.02. One of the best methods for finding system damping under operating conditions is to change the damping by a known amount and measure the resulting amplitude change.

REFERENCES

- 1). Lazan, B.J., "Damping of Materials and Members in Structural Mechanics", Pergamon, New York, 1968.
- 2). Lazan, B.J., "Damping Properties of Materials Members and Composites" in Applied Mechanics Surveys, Abramson et al. Eds, Spartan Books, Washington, D.C., 1966, pp 703-715.
- 3). Plunkett,R., "Vibration Damping" in Applied Mechanics Surveys (above) pp 691-701.
- 4). Ruzicka, J.E. ed. "Structural Damping" ASME, 1959.
- 5). Plunkett, R., "Vibration Control by Applied Damping Treatments" Chap. 37, Shock and Vibration Handbook , Harris and Crede, 2nd Ed., McGraw-Hill, 1976.
- 6). Plunkett, R., "Mechanical Damping", Treatise on Analytical Chemistry, Kolthoff, Elving and Stross, Eds., Part III, Vol. 4, Wiley, 1977, pp 487-516.



DECAY CURVE - NONLINEAR

Figure 1

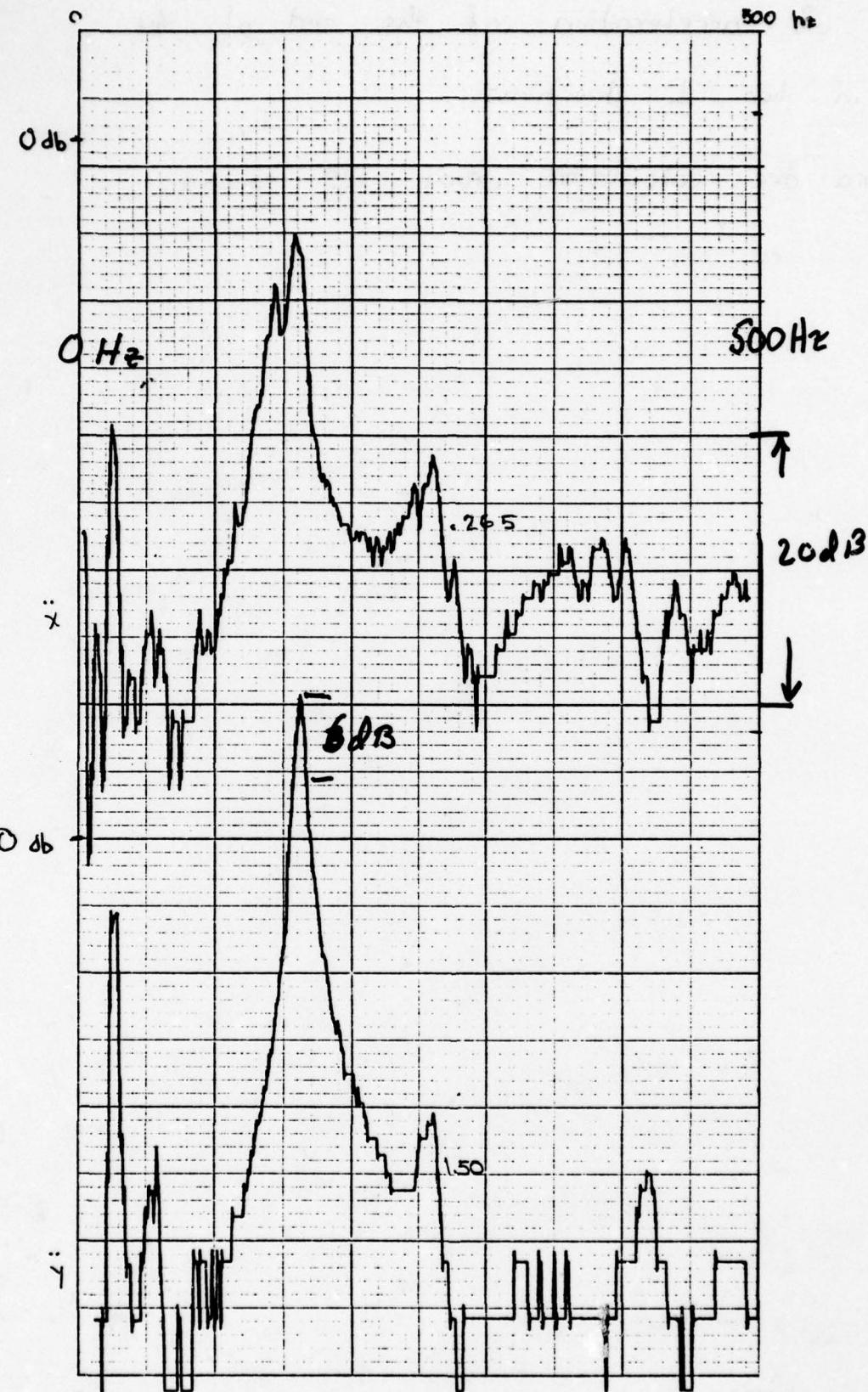


Figure 2

Plots are of acceleration of the end of the cylinder in two L directions.

The spectra are calculated from 128 spectra.
averaged

SUMMARY OF CONSTRAINED DAMPING LITERATURE

**R. A. DiTaranto
Widener College
Chester, Pennsylvania**

SUMMARY OF CONSTRAINED DAMPING LITERATURE

R. A. DiTaranto, Ph.D.
Professor of Engineering
Widener College
Chester, PA 19013

ABSTRACT:

A personal view is presented of the work accomplished in the field of constrained viscoelastic damping. This is followed by a comprehensive review of the field written by Professor B. C. Nakra which is included with additional references.

INTRODUCTION

Two recent articles by Professors B. C. Nakra, I.I.T. New Delhi, India and F. C. Nelson, Tufts University respectively contain 105 and 29 pertinent references summarizing constrained viscoelastic damping. The review articles are found in "The Shock and Vibration Digest." (Vol. 8(6) 1975 and Vol. 9(7) 1977). Professor Nakra's excellent article is reproduced herein with the kind permission of the Shock and Vibration Information Center.

Rather than repeat the same material presented in the articles I would like to chronicle the interest and work accomplished in this field. As in most summarizations, I am sure I will neglect to mention individuals and organizations who have played a role in studying this field. I apologize for these omissions due to the lack of time and possibly my ignorance of their contributions.

DISCUSSION

Oberst's paper in 1952 analyzing the damping capability of a viscoelastic material trowelled onto a beam is recognized as the first engineering paper on unconstrained layered damping. Schwarzl published a paper in 1958 "Forced Bending and Extensional Vibration of a Two-Layer Compound Linear Viscoelastic Beam."

In 1959, Ross and Kerwin of Bolt, Beranek and Newman investigated the damping capability of a tape having a viscoelastic adhesive and a thin flexible backing. The tape when adhered to a beam introduced damping through shearing of the viscoelastic material. Thus, the constrained layer damping was first analyzed. Ross and Kerwin used an effective beam stiffness approach to determine the natural frequency and associated loss factor. To accomplish this, they assumed sinusoidal mode shapes, which restricted their results to infinitely long or simply-supported beams. Their results demonstrated the typical curve of an increase, peaking, followed by a decrease in the loss factor as the shearing capability of the viscoelastic increased. Also the natural frequencies followed the pattern of the uncoupled natural frequencies of the beams for low shear carrying ability until the two elastic 'beams' act as an integral one at the high shear carrying capacity of the viscoelastic layer. Ungar and others at B.B. & N. added to the understanding of the constrained layer damping using a stored and loss energy approach.

During the early sixties, the U.S. Navy Ship Silencing Division initiated a Structural Damping Program in which constrained layer damping was considered. Blasingame and I did some work with the results of Kerwin, et al followed by a need to assess the effect of boundary conditions other than simply-supported. In 1965 my paper "Theory of Vibratory Bending for Elastic and Viscoelastic Layered Finite Length Beams" was published. The result was a sixth order differential equation which required the use of six boundary conditions for a solution of the natural frequencies and associated loss factors. The case of a simply supported beam agreed with the results already obtained by Ross & Kerwin. In 1966 Nakra and Grootenhuis arrived at the same equation at Imperial College, London as part of a doctoral dissertation. At the Institute of Sound and Vibration Research, Mead and Markus rederived the sixth order differential equation using plate theory. Mead made some valuable contributions to the interpretations of the equation and he and Markus solved the natural frequencies and associated loss factors for an encastered beam using a high speed digital computer.

Professor Grootenhuis has continued to make contributions to the field at Imperial College; Professor Nakra has led the field at I.I.T. New Delhi India and Professor Markus has published in the field from Czechoslovakia.

In the U.S.A., T. Nicholas has contributed to the field with his work at Columbia University and Wright-Patterson Air Force Base. D.I.G. Jones, J. P. Henderson and A. D. Nashiff have been active in the field for the Air Force.

An interesting International Symposium on "The Damping of the Vibrations of Plates by Means of a Layer" was held at Leuven, Belgium September 1967, sponsored by the Belgium and French Acoustical Societies. The papers were contributed from England, France, Germany, Belgium, Holland, Italy, Russia and U.S.A. There was a mixture of applied and theoretical papers. A list of the papers comprise the Appendix.

After the sixth order differential equation was developed for the constrained damping, work has been concerned with plates; inclusion of higher order effects (rotatory inertia and elastic shear); use of more than three layers; effect of a discontinuous constraining layer; unsymmetrically layered beams; optimization of Damping; practical use of the constrained layer damping.

The use of constrained layer damping has been extended to rings and cylinders. Free and forced vibrations of rings and cylinders has been reported by DiTaranto, Nelson, F.C., Markus, S., and Lu, Douglass and Thomas of the U.S. Navy Ships Research and Development Lab, Annapolis, Maryland.

Y.P. Lu has analyzed and obtained computed results for a ring using the actual shear modulus and loss factor values versus frequency of a tested configuration and has shown good agreement with test.

It is obvious that I have not been able to give all the details concerned with this field and that much more work has and is going on. I am sure that the other speakers will fill in the gaps and will especially inform us of the actual beneficial uses of constrained damping layered materials.

VIBRATION CONTROL WITH VISCOELASTIC MATERIALS

B.C. NAKRA



Suitable arrangements of elastic and viscoelastic materials are being used in vibration control. The viscoelastic materials are so arranged so that they are subjected to deformations when exposed to vibration. Some high molecular weight polymers exhibit viscoelastic properties.

Conventional approaches for controlling vibrations have avoided resonance due to coincidence of excitation frequency and any natural frequency of a system. This approach cannot be of practical use when vibrations occur over a wide frequency range, as, for example, in turbojet and rocket engines, in which the high acoustic energy level could excite vibrations from very small to frequencies higher than 10,000 Hz. In such cases, a number of resonances of structural elements might be excited. Limitation of resonant vibration amplitudes lies in providing damping in the system. The materials usually chosen for strength and rigidity do not have appreciable internal damping. Efforts to produce high damping alloys with high fatigue strength have not been very successful [23]. Manganese copper alloys give a maximum loss factor of 0.05. The loss factor for polymers may lie between 0.01 and 2.0 [24,25].

When viscoelastic materials are used for vibration control, they are arranged so that they are subjected to shear or direct strains. The simplest arrangement is the unconstrained one in which a layer of viscoelastic material is attached to an elastic one. During flexural vibrations of such an arrangement, direct alternating strains are induced in the viscoelastic layer. In constrained construction a viscoelastic layer is sandwiched between the elastic layers; the result is predominantly shear strain in the viscoelastic layer during flexural vibration. Damping tapes [87] consisting of thin metal foil covered with a viscoelastic adhesive and used on an existing vibrating structure is a constrained type of arrangement. Several layers of viscoelastic materials may be used to improve the damping characteristics [1, 2, 61, 98]. Another technique involves the use of viscoelastic material at the edges of panels [58]. When there is not sufficient

localized strains for effective damping from viscoelastic materials, a small mass suspended on a viscoelastic damper and attached to the vibrating structure is used. Such devices are known as tuned dampers [31]. The inertial effect of the mass, when excited by structural vibration, can induce cyclic strains in the viscoelastic material and dissipate vibration energy.

Properties of Viscoelastic Materials

The properties of viscoelastic materials depend upon frequency, temperature, and strain. Several means of classification can be used to specify the properties of linear viscoelastic materials; these include complex modulus, creep function, stress relaxation function, differential operator form, or a hypothetical model composed of an array of springs and dashpots. All of the forms can be related [9, 29]. Reviews of methods for finding the properties of viscoelastic materials have been published [32, 73]. For sinusoidal motion the deformation produced in a viscoelastic material is not in phase with force but lags by an angle, the tangent of which is the loss factor of the material. The ratio of stress to strain is a complex modulus for a viscoelastic material. Complex shear, or Young's modulus can be obtained experimentally. With one method [26] for obtaining the complex shear modulus of viscoelastic materials, frequency, temperature, and strain amplitude can be varied independently. With another technique [68] forced vibration resonance tests are done on an elastic cantilever that is coated on both sides with the viscoelastic material. A guide to some high damping materials and their properties has been published [99]. Efforts to find materials capable of withstanding a temperature range from -40 to 200°C without reduction of damping to low values have been reported [57]. Oberst [74] has published a review of the development of high damping polymers.

Damping Effectiveness

The measurement of the effectiveness of damping in a complex system using viscoelastic materials is based

*Professor, Mechanical Engineering Department, Indian Institute of Technology, Hauz Khas, New Delhi-29, India

on the assumption that the resonant response of a continuous system at any vibration mode is analogous to a lumped parameter spring mass system [94]. On the basis of this assumption, criteria have been derived for assessing the damping effectiveness of a system [52]. The following is a generalized equation of motion for resonant harmonic response:

$$-mp^2 q + k(1+i\eta_s)q = f_0.$$

In the equation q is generalized displacement, m and k are generalized mass and stiffness respectively, p is frequency, f is the amplitude of the generalized harmonic excitation, and η_s is the system loss factor. Usually η_s is the ratio of imaginary to real part of the complex generalized stiffness. It has been pointed out [52] that η_s in itself is not a sufficient criterion for assessing damping effectiveness. As damping treatment changes, the stiffness and mass of the structure change. The quantity $k\eta_s$ is the displacement response effectiveness. If the excitation is inertial, such as occurs at the ends of a beam subjected to sinusoidal motion, the displacement response effectiveness is η_s and not $k\eta_s$ [62]. Criteria for damping effectiveness for harmonic and band-limited white noise excitations have been reported [10] that account for variation of mass, stiffness, and loss factor on the mean square particle velocity of the structure.

Damping Arrangements

Unconstrained Damping Arrangements

Initial work on flexural vibration analysis of an unconstrained arrangement containing viscoelastic material bonded to elastic material was carried out in the early 1950s [49, 75]. In other experimental work [30] a thin layer of bitumen emulsion containing Schist powder on steel plates was used. Mead [53] reported an investigation of a vibrating stringer-skin combination using "Aquaplas" damping compound. Damping in an unconstrained arrangement depends on thickness, stiffness, and loss factor of the viscoelastic material. It has been pointed out [93] that in a two-layered beam, flexural and extensional vibrations are coupled; this paper also contains an analysis of forced vibration of the arrangement. A similar study was reported for two-layered plates. Equations for flexural vibrations of two-layered

beams, including the rotary, translatory, and transverse effects, have been derived [82]. The effects of rotary inertia and shear deformation on the free vibration of a two-layered damped beam are of significance at high frequencies [71].

Baumgarten and Pearce [7] analyzed transverse vibrations of thin free-free beams and plates having viscoelastic coatings and concluded that, when the coatings are of thin or moderate thickness compared to the plate, viscoelastic material on only one side of the beam or plate is most effective; at greater thickness tow symmetrical coatings, one on each side of the elastic base layer, are preferable. The propagation of normal waves in damped cylindrical shells and the effect of damped coatings on the losses produced have been investigated [95].

Constrained Damping Arrangements

A constrained damping arrangement is a sandwich-type construction in which the middle viscoelastic layer is constrained by two elastic face layers. It is also known as a sandwich damping or shear damping arrangement. Plass [79] analyzed such an arrangement; both outer layers were considered to be very thin, and shear effect in the core was included. An analysis for the vibration damping of a three-layered arrangement, taking into account the shear deformation of the viscoelastic core, has been reported [44]. A general analysis was reported [87] that included both shear and extensional damping effects and the influence of various geometric and physical parameters. Damping optimum for a given shear parameter is dependent on the mode of vibration and the in phase shear modulus of the viscoelastic material. Shear damping in a three-layered arrangement is more effective than that in the extensional one in a two-layered arrangement [45, 87]. The use of a stiff spacer between viscoelastic and elastic layers induces large strains in the viscoelastic layer, resulting in higher damping.

An alternative method for finding loss factor of composite structures [100, 101] is to define the loss factor in terms of energy concepts, taking the energy storage and dissipative mechanisms in the structure, in accordance with those in arrays of viscoelastic springs. Whittier [102] reported an approximate analysis of sinusoidal excitation of a sandwich

cantilever made up of a thin viscoelastic layer, a spacer, the beam to be damped, and a constraining cover.

Flexural vibration analysis of beams or plates using the constrained damping technique has been reported [11, 16-19, 54, 62, 63, 83, 84, 89, 90, 103-105]. Mead [54] analyzed the flexural vibration of a symmetrical simply-supported sandwich plate with a viscoelastic core. Equations for the flexural vibration of three-layered arrangement having a viscoelastic core have been derived [16, 62] for beams and plates [17]. Detailed results for damping of sandwich beam effectiveness have been reported [18, 19]. Experimental evaluations of damping in a constrained arrangement have been given [89, 104], as have design data for loss factor and resonant frequencies [90, 91]. The three-layered configuration has been analyzed [11, 103, 105]. It has been shown [63] that the extensional effect in a stiff thick core, which is often ignored in constrained arrangements, may be significant for low-order resonant modes. An analysis by Rao and Nakra [83, 84] includes the effects of rotary, longitudinal, and transverse inertia; these effects are important at frequencies of practical interest. An approximate analysis for the flexural vibration of a simply-supported three-layered beam having a nonlinear viscoelastic core has been published [64]. Korites and Nelson [47] concluded that the loss factor in constrained arrangements is reduced by dissipative heating. Work on three-layered sandwich shells with viscoelastic cores [38, 77] and for laminated rings [20, 50] has been carried out.

Multiple-Layered Arrangements

Arrangements having more than three layers are included in multiple-layered arrangements. Ungar and Ross [98] formulated a theory for evaluating the damping effectiveness of multiple tapes applied to an elastic structure. They indicated that the number of tapes has a negligible effect on damping at high frequencies and an appreciable effect at low frequencies. Theoretical analyses of layered beams symmetrically arranged with alternate elastic and viscoelastic layers [1] and for unsymmetrically arranged multiple-layered beams have been published [3]. Results of the influence of the number of layers and the thickness ratio of viscoelastic to elastic layers have

been given [2] for beams using constant size, weight, and static stiffness criteria. It is concluded that the loss factor of the system can be increased by increasing the number of layers; however, weight, size, and static stiffness also increase. Design data for the loss factor of a symmetrical multiple-layered configuration having "n" identical elastic layers and thin viscoelastic layers constrained between them have been published [91].

It has been shown [61, 62] that to achieve damping over a wide range of shear parameter values an arrangement of two dissimilar viscoelastic materials is preferred to a three-layered one. Either a four-layered sandwich with two viscoelastic layers between the two elastic faces [61] or a five-layered sandwich with alternate elastic and viscoelastic layers can be used. Analyses of multicored beams and beams with constrained viscoelastic layers on both sides of an elastic beam have been reported [65, 66]. Analysis of multiple-layered arrangements is cumbersome, and attempts have been made [33, 34, 69] to simplify the analysis with an approximate method, in which damping is in terms of an equivalent free layer treatment.

Discontinuous Damping

Partially damped arrangements or those having cuts have been analyzed. The effects of partial coverage for constrained layer viscoelastic treatment have been published [46, 72, 78, 81]. Length optimization of cuts in the constrained treatment has been worked out [80], and a general expression for the loss factor of beams with partial damping treatment applicable to any vibrating mode shape has been derived [51]. An extension [96] of the work by Plunkett and Lee [80] is for square plates covered with alternating layers of viscoelastic material and thin metal sheets and having the constraining layer in segments. Experimental and theoretical results for radial driving point impedance of a damped composite ring, with a finite number of mass segments attached to the periphery of the ring by a viscoelastic material, have been reported [21].

Random and Shock Excitations

The effectiveness of unconstrained damping on structures subjected to random excitation has been

evaluated [53]. Clarkson and Cicci [13] concluded that the addition of unconstrained damping to stiffened skin structures that are subjected to broad-band acoustic excitation reduce rms response by a factor of about three; the weight added is about two percent. Kaul et al [42, 43] reported analytical studies on unconstrained and constrained arrangements subjected to white noise random excitation. Because complex modulus representation for viscoelastic materials can be used only for harmonic vibrations, a different characterization must be used for viscoelastic materials for random and shock excitations.

Jones [39, 40] reported analytical studies for the transverse displacement shock response of two-layered elastic-viscoelastic plates subjected to a rectangular pulse type shock; he assumed that the stress-strain law for the viscoelastic material corresponded to that of a linear viscoelastic solid or a three-element type model. Chawla and Nakra [12] analyzed three-layered beams having viscoelastic cores and subjected to half sine impact; the core material was assumed to be a linear viscoelastic solid. They studied the effects of various parameters on the peak response during and after application of shock and on the decay of vibrations. Analysis of three-layered beams having a viscoelastic core modeled as four elements, for rectangular shock and for rectangular shock pulse excitation, has been done [67]. Kapur and Nakra [41] showed that rotary and longitudinal inertias have a substantial effect on the transient response (half sine pulse shock excitation of low duration) of a three-layered beam having a four element type viscoelastic core.

Solutions for Various Boundary Conditions

Little work has been done on the analysis of damped structures with end conditions other than simply-supported ones. It has been shown [22] that the composite loss factor versus frequency of a three-layered laminated beam with a viscoelastic core is unaffected by the type of end restraints. As has been pointed out [77], however, the damping effect differs, depending upon the boundary conditions. Evaluation of the response of viscoelastic damped structures for different boundary conditions is cumbersome. The finite difference method has been used [1]. Mead and Markus [55] studied the forced response of three-layered damped sandwich beams in

terms of the forced damped normal modes for specific excitation. The technique has been used to evaluate the loss factor and resonant frequencies for fixed-fixed boundary conditions [56] and for a damped sandwich cantilever [76]. Asnani and Nakra [4] have used the Ritz method for finding the forced response of damped sandwich beams with fixed-fixed and cantilever types of boundary conditions.

Tuned Viscoelastic Dampers

The effect of tuned dampers consisting of a small mass suspended on a viscoelastic damper has been studied [31, 35]. A flexible beam joined by viscoelastic links to the ends of a vibrating structure has been analyzed [70]. Large vibratory amplitude reductions were possible when the weight of the structure was increased slightly. Several possible practical configurations with tuned damping devices containing high temperature vitreous enamels have been described [36].

Viscoelastic Boundary Damping

Experimental and analytical investigations on the effect of using viscoelastic material at the support junctions of beams and plates have been done [58]. System damping may be increased by proper application of the above techniques; the increase, however, would be small compared to that in the multilayer technique. Quantitative evaluation of the damping has been reported [59, 60].

Applications

The use of viscoelastic damped substructures for supporting aircraft and missile components has been reported [6, 14, 37, 86, 92]. Use of antidrumming materials for noise reduction in such machines as compressors and turbines has also been carried out [8]. Reduction of noise and vibration of crank case and cylinder block walls in an engine having a separate load carrying structure with attached highly damped outer walls incorporating viscoelastic materials has been published [5].

Sandwich damping treatment has been applied to concrete structures [27]. The foundation for a concrete railway bridge deck incorporated a damping material between the concrete members in order to

reduce disturbances resulting from vibrations of the bridge deck. The damping material consisted of bitumen reinforced with rubber latex. Viscoelastic building dampers have been used at the junction of floors and walls in multistoried buildings [15]. Turner [97] reported that a viscoelastic damping material was used for noise reduction in a ship. A graphite loaded viscoelastic material reduced the noise by about six dB. A two-stage anti-vibration mounting consisting of a subframe of damped sandwich construction has been employed [28] for machinery isolation. An acoustic enclosure based on the viscoelastic damping technique has been reported for a piling hammer [25].

Conclusion

One handicap in the use of viscoelastic materials is the adverse environmental effect. Efforts to find viscoelastic materials capable of withstanding a broad temperature range without appreciable change of properties have been numerous [15, 48, 57, 74]. Not enough data are available on fatigue properties or on damping properties of viscoelastic materials due to shear and direct strains at different temperatures and frequencies. Much of the work that has been done has been restricted to simple idealized structural configurations subjected to harmonic excitations; the viscoelastic material is treated linearly. The algebra involved in finding solutions for various boundary conditions is involved. Use of computer-aided techniques would be of interest. It would also be useful to have a procedure for obtaining an optimized arrangement for damping effectiveness, keeping in mind the static stiffness, weight, and size requirements.

References

1. Agbasiere, J.A. and Grootenhuis, P., "Flexural Vibration of Symmetrical Multilayer Beams with Viscoelastic Damping," *J. Mech. Engr. Sci.*, **10**, p 269 (1968).
2. Asnani, N.T. and Nakra, B.C., "Vibration Damping Characteristics of Multilayered Beams with Constrained Viscoelastic Layers," ASME Paper No 73-DE-C (1973).
3. Asnani, N.T. and Nakra, B.C., "Vibration Analysis of Multilayered Beams Involving Viscoelastic Layers," *J. Instn. Engr. India*, **50**, pp 187-193 (1970).
4. Asnani, N.T. and Nakra, B.C., "Forced Vibration Analysis of Sandwich Beams with Viscoelastic Core," *J. Aero. Soc. India*, **24**, pp 288-294 (1972).
5. Austen, A.E.W. and Priede, T., "Noise of Automotive Diesel Engines - Its Causes and Reduction," *SAE Trans.*, **74**, p 719 (1966).
6. Baker, J.K., "Practical Example of the Attenuation of Vibrations by Sandwich Damping," *J. Soc. Environ. Engr.* (38) pp 9-11 (1969).
7. Baumgarten, J.R. and Pearce, B.K., "The Damping Effect of Viscoelastic Materials: Part I, Transverse Vibration of Beams with Viscoelastic Coatings; Part II, Transverse Vibration of Plates with Viscoelastic Coatings," *J. Engr. Indus., Trans. ASME*, **93**, pp 645-655 (1971).
8. Betzhold, C.H., Kurz, J., and Oberst, W., "Some Applications of Antidrumming Materials and Sound Barrier Mats Composed of Plastics to Machines," *Proc. Intl. Symp. Assoc. Belge Acousticiens*, Leuven (1967).
9. Bland, D.R., *The Theory of Linear Viscoelasticity*, Pergamon Press (1960).
10. Barisov, L.P., Kanaev, B.A., Rybak, S.A., and Tartakovskii, B.D., "Criteria for Comparing the Effectiveness of Vibration Absorbing Coatings," *Soviet Physics Acoustics*, **20**, pp 217-220 (1974).
11. Chatterjee, A. and Baumgarten, J.R., "An Analysis of Viscoelastic Damping Characteristic of a Simply Supported Sandwich Beam," *J. Engr. Indus., Trans. ASME*, **93**, pp 1239-1244 (1971).
12. Chawla, D.R. and Nakra, B.C., "Transient Response of Sandwich Simply Supported Beam with Linear Viscoelastic Core," *Proc. 15th Congr: Theor. Appl. Mech.*, Sindri, pp 69-78 (1970).

13. Clarkson, B.L. and Cicci, F., "Method for Reducing the Response of Integrally Stiffened Structures to Random Pressures," *J. Engr. Indus., Trans. ASME*, 91, pp 1203-1209 (1969).
14. Cooney, J.P. and Thorn, R.P., "Considerations in the Selection of Viscoelastic Materials for Constrained and Unconstrained Layer Damping Treatments," *ASME Paper No 64-WA/RP-8* (1964).
15. Dahlquist, C.A., "A Family of Viscoelastic Materials for Diverse Damping Applications," *ASME Paper No 71 Vibr.* 47 (1971).
16. Di Taranto, R.A., "Theory of Vibratory Bending for Elastic and Viscoelastic Layered Finite Length Beams," *J. Appl. Mech., Trans. ASME*, 32, p 881 (1965).
17. Di Taranto, R.A. and McGraw, J.R., "Vibratory Bending of Damped Laminated Plates," *J. Engr. Indus., Trans. ASME*, 91, pp 1081-1090 (1969).
18. Di Taranto, R.A. and Blasingame, W., "Composite Loss Factor of Selected Laminated Beams," *J. Acoust. Soc. Amer.*, 40, pp 187-194 (1966).
19. Di Taranto, R.A. and Blasingame, W., "Composite Damping of Vibrating Sandwich Beams," *J. Engr. Indus., Trans. ASME*, 89, pp 633-638 (1967).
20. Di Taranto, R.A., "Free and Forced Response of a Laminated Ring," *J. Acoust. Soc. Amer.*, 53, pp 748-757 (1973).
21. Di Taranto, R.A., Lu, Y.P., and Douglas, B.E., "Forced Response of a Discontinuously Constrained Damped Ring," *J. Acoust. Soc. Amer.*, 54, pp 74-79 (1973).
22. Di Taranto, R.A. and Blasingame, W., "Effect of End Constraints on the Damping of Laminated Beams," *J. Acoust. Soc. Amer.*, 39, pp 405-407 (1966).
23. Grootenhuis, P., "The Control of Vibrations with Viscoelastic Materials," *J. Sound Vib.*, 11, pp 421-433 (1970).
24. Grootenhuis, P., "Vibration Control with Viscoelastic Materials," *J. Soc. Environ. Engr.*, (38) pp 3-9 (1969).
25. Grootenhuis, P., "Damping Mechanisms in Structures and Some Applications of the Latest Techniques," *Proc. Symp. on Appl. of Exptl. Theor. Struct. Dynam.*, Southampton, pp 17.1-17.26 (1972).
26. Grootenhuis, P., "Measurement of the Dynamic Properties of Damping Materials," *Proc. Intl. Symp. Assoc. Belge Acousticiens*, Leuven (1967).
27. Grootenhuis, P., "Sandwich Damping Treatment Applied to Concrete Structures," *Trans. Royal Soc.* A263, p 455 (1968).
28. Grootenhuis, P. and Ewins, D.J., "Multi-Directional Vibration Isolation," *Proc. Symp. Soc. Environ. Engr.* London (1972).
29. Gross, B., *Mathematical Structure of the Theories of Viscoelasticity*, Herrman and Cie, Paris (1953).
30. Itterbeck, V. and Myncke, H., "Vibration of Plates Covered with a Damping Layer," *Acustica*, 3, p 207 (1953).
31. Jones, D.I.G., Nashif, A.D., and Adkins, R.L., "Effect of Tuned Dampers on Vibrations of Simple Structures," *AIAA J.*, 5, pp 310-315 (1967).
32. Jones, D.I.G., "Temperature-Frequency Dependence of Dynamic Properties of Damping Materials," *J. Sound Vib.*, 33, pp 451-470 (1974).
33. Jones, D.I.G., Nashif, A.D., and Parin, M.L., "Parametric Study of Multiple Layer Damping Treatment on Beams," *J. Sound Vib.*, 29, pp 423-434 (1973).
34. Jones, D.I.G., "Damping of Stiffened Plates by Multiple Layer Treatment," *J. Sound Vib.*, 35, pp 417-427 (1974).
35. Jones, D.I.G., "Response and Damping of a Simple Beam with Tuned Dampers," *J. Acoust. Soc. Amer.*, 42, pp 50-55 (1967).

36. Jones, D.I.G., Nashif, A.D., and Stargardter, H., "Vibrating Beam Dampers for Reducing Vibrations in Gas Turbine Blades," *J. Engr. Power, Trans. ASME*, 97, pp 111-116 (1975).
37. Jones, D.I.G. and Trapps, W.J., "Influence of Additive Damping on Resonant Fatigue of Structures," *J. Sound Vib.*, 17, pp 157-185 (1971).
38. Jones, I.W. and Salerno, V.L., "The Effect of Structural Damping on Forced Vibrations of Cylindrical Sandwich Shells," *J. Engr. Indus., Trans. ASME*, 88, pp 318-324 (1966).
39. Jones, I.W., "Non-periodic Vibrations of Layered Viscoelastic Plates," PhD Thesis, Polytech. Inst., Brooklyn (1967).
40. Jones, I.W., "Damping of Plate Vibrations by Means of Attached Viscoelastic Materials," *U.S. Naval Res. Lab. Shock Vib. Bull.*, No 39, Pt 4, pp 63-72 (1969).
41. Kapur, A.D. and Nakra, B.C., "Effects of Rotary and Longitudinal Inertias on Transient Response of a Beam with Unconstrained Viscoelastic Layers," *J. Acoust. Soc. India*, 1, pp 109-114 (1973).
42. Kaul, O.N., Gupta, K.N., and Nakra, B.C., "Response of a Viscoelastic Sandwich Beam to White Noise Random Excitation," 18th Congr. Theor. Appl. Mech., Madras (1973).
43. Kaul, O.N., Gupta, K.N., and Nakra, B.C., "White Noise Random Excitation of a Two-Layered Beam Arrangement," *Proc. 19th Congr. Theor. Appl. Mech.*, Kharagpur (1974).
44. Kerwin, E.M., "Damping of Flexural Waves by a Constrained Viscoelastic Layer," *J. Acoust. Soc. Amer.*, 31, p 952 (1959).
45. Kerwin, E.M. and Ross, D., "A Comparison of the Effectiveness of Homogeneous Layers and Constrained Layers of Viscoelastic Materials in Damping Flexural Waves in Plates," *Proc. 3rd. Intl. Congr. on Acoustics*, Stuttgart (1959).
46. Kerwin, E.M. and McQuillan, R.J., "Plate Damping by a Constrained Viscoelastic Layer: Partial Coverage and Boundary Effects," *Bolt Beranek and Newman Rep. No 760* (1960).
47. Korites, B.J. and Nelson, F.C., "The Influence of Dissipative Heating on the Loss Factor of a Viscoelastically Damped Beam," *J. Engr. Indus., Trans. ASME*, 91, pp 975-980 (1969).
48. Lee, H., "New Polymers for Structural Adhesives, Honeycombs and Reinforced Composites," *ASME Paper No 65-AV-22* (1965).
49. Lienard, P., "Étude d'une Méthode de Mesure du Frottement Interieur de Revêtements Plastiques Travailleur en Flexion," *La Recherche Aéronautique*, 20, p 11 (1951).
50. Lu, Y.P., Douglas, B.E., and Thomas, E.V., "Mechanical Impedance of Damped Three-Layered Sandwich Rings," *AIAA J.*, 11, pp 300-304 (1973).
51. Markus, S., "Damping Mechanism of Beams Partially Covered by Constrained Viscoelastic Layer," *Acta Technica CSAV*, No 2, pp 179-194 (1974).
52. Mead, D.J., "Criteria for Composing Effectiveness of Damping Treatments," *Noise Control*, 7, p 27 (1961).
53. Mead, D.J., "The Effect of a Damping Compound on Jet Afflux Excited Vibrations," Part I: *Aircraft Engr.* 32, pp 64-72 (1960); Part II: *Aircraft Engr.* 32, pp 106-113 (1960).
54. Mead, D.J., "The Double Skin Damping Configuration," *Univ. Southampton, ASSU Rep. No 160* (1962).
55. Mead, D.J. and Markus, S., "The Forced Vibrations of a Three-Layer Damped Sandwich Beam with Arbitrary Boundary Conditions," *J. Sound Vib.*, 10, pp 163-175 (1969).
56. Mead, D.J. and Markus, S., "Loss Factor and Resonant Frequency of Encastre Damped Sandwich Beams," *J. Sound Vib.*, 12, pp 99-112 (1970).

57. Mechel, F., "Structural Configurations for Increasing Fatigue Life," Proc. Intl. Symp. Assoc. Belge Acousticiens, Leuven (1967).
58. Mentel, T.J., "Vibrational Energy Dissipation at Structural Support Junctions," Proc. Colloq. Struct. Damping ASME, pp 89-116 (1959).
59. Mentel, T.J., "Viscoelastic Boundary Damping of Beams and Plates," J. Appl. Mech., Trans. ASME, 31, pp 61-71 (1964).
60. Mentel, T.J., "Joint Interface Damping," J. Engr. Indus., Trans. ASME, 89, pp 773-784 (1967).
61. Nakra, B.C. and Grootenhuis, P., "Structural Damping Using a Four-Layer Sandwich," J. Engr. Indus., Trans. ASME, 94, pp 81-86 (1972).
62. Nakra, B.C., "Vibrations of Viscoelastically Damped Laminated Structures," PhD Thesis, Univ. London, (1966).
63. Nakra, B.C. and Grootenhuis, P., "Extensional Effect in Constrained Viscoelastic Layers," Aeronaut. Quart., 25, pp 225-231 (1974).
64. Nakra, B.C., "Vibration Analysis of a Sandwich Beam with Nonlinear Viscoelastic Core," J. Sci. Engr. Res., 13, pp 137-145 (1969).
65. Nakra, B.C., "Vibration Analysis of Multicored Beams Involving Viscoelastic Layers," Proc. 12th Congr. on Theor. Appl. Mech., India, pp 155-163 (1967).
66. Nakra, B.C., "Vibration Analysis of Sandwich Beams with Constrained Viscoelastic Layers on Both Sides," J. Aeron. Soc. India, 25, pp 35-39 (1973).
67. Nakra, B.C. and Chawla, D.R., "Shock Response of a Three-Layer Sandwich Beam with Viscoelastic Core," J. Aeron. Soc. India, 23, pp 135-139 (1971).
68. Nashif, A.D., "New Method for Determining Damping Properties of Viscoelastic Materials," U.S. Naval Res. Lab. Shock Vib. Bull., No 36, Pt 4, pp 37-46 (1967).
69. Nashif, A.D. and Nicholas, T., "Attenuation of Vibrational Amplitudes Through the Use of Multiple-Layered Damping Treatments," ASME Paper No 71 - Vibr -40 (1971).
70. Nashif, A.D. and Jones, D.I.G., "A Resonant Beam Tuned Damping Device," J. Engr. Power, Trans. ASME, 91, pp 143-148 (1969).
71. Nicholas, T., "The Effect of Rotary Inertia and Shear Deformation on the Flexural Vibrations of a Two-Layered Viscoelastic Beam," U.S. Naval Res. Lab. Shock Vib. Bull., No 38, pp 13-28 (1968).
72. Nokes, D.S. and Nelson, F.C., "Constrained Layer Damping with Partial Coverage," U.S. Naval Res. Lab. Shock Vib. Bull., No. 38 (1968).
73. Nolle, A.W., "Methods for Measuring Dynamic Mechanical Properties of Rubber-like Materials," J. Appl. Phys., 19, p 753 (1948).
74. Oberst, H., "Reduction of Noise by the Use of Damping Material," Trans. Royal Soc., A263 p 241 (1968).
75. Oberst, H., "Ueber die Dampfung der Biegeschwingungen dünner Bleche durch fest haftende Beläge," Part I: Acustica, 2 (1952); Part II: Acustica, 4 (1954).
76. Oravsky, V., Markus, S., and Simkova, O., "A New Approximate Method of Finding the Loss Factors of a Sandwich Cantilever," J. Sound Vib. 33, pp 335-352 (1974).
77. Pan, H.H., "Axisymmetric Vibration of a Circular Sandwich Shell with a Viscoelastic Core Layer," J. Sound Vib., 9, pp 338-348 (1969).
78. Parfitt, G.G., "The Effect of Cuts in Damping Tapes," Proc. 4th Intl. Congr. Acoustics, Copenhagen, pp 21-28 (1962).
79. Plass, H.J., "Damping of Vibrations in Elastic Rods and Sandwich Structures by Incorporation of Additional Viscoelastic Materials," Proc. 3rd Midwest. Conf. Solid Mech., p 48 (1957).

80. Plunkett, R. and Lee, C.T., "Length Optimization for Constrained Viscoelastic Layer Damping," *J. Acoust. Soc. Amer.*, 48, pp 150-161 (1970).
81. Pulgarno, L.J., "Effectiveness of Partial Coverage for Constrained Layer Damping Treatments," 64th Meeting, *Acoust. Soc. Amer.*, Washington (1962).
82. Pujara, K.K. and Nakra, B.C., "Forced Vibrations of Two-Layered Beam Arrangements," *J. Sci. Engr. Res.*, 12, pp 117-124 (1968).
83. Rao, Y.V.K.S. and Nakra, B.C., "Influence of Rotary and Translatory Inertia on the Vibrations of Unsymmetrical Sandwich Beams," *Proc. 15th Congr. on Theor. Appl. Mech.*, India, pp 301-314 (1970).
84. Rao, Y.V.K.S. and Nakra, B.C., "Vibrations of Unsymmetrical Sandwich Beams and Plates with Viscoelastic Cores," *J. Sound Vib.*, 34, pp 309-326 (1974).
85. Ren, N. and Yu, Y.Y., "Vibrations of Two-Layered Plates," AFOSR Rep. No 65-1423 (1965).
86. Rosen, H. and Veilleux, E.D., "Designing Damping into Laminated Structures," *Mach. Des.*, 32, p 24 (1960).
87. Ross, D., Ungar, E.E., and Kerwin, E.M., "Damping of Plate Flexural Vibrations by Means of Viscoelastic Laminae," *Proc. Colloq. Struct. Damping ASME*, pp 49-87 (1959).
88. Ross, D. and Kerwin, E.M., "Damping of Flexural Vibrations in Plates by Free and Constrained Viscoelastic Layers," *Bolt Beranek and Newman Rept. No 632* (1959).
89. Ruzicka, J.E., "Damping Structural Resonances Using Viscoelastic Shear Damping Mechanisms," Parts I and II, *J. Engr. Indus., Trans. ASME*, 83, p 403 (1961).
90. Ruzicka, J.E., Derby, T.F., Schubert, D.W., and Pepi, J.S., "Damping of Structural Composites with Viscoelastic Shear Damping Mechanisms," NASA CR-742 (1967).
91. Ruzicka, J.E. and Derby, T.F., "Loss Factor and Resonant Frequency of Viscoelastic Shear Damped Structural Composites," *NASA CR-1269* (1969).
92. Ruzicka, J.E., "Vibration Response Characteristics of Viscoelastic - Damped Structures," *U.S. Naval Res. Lab. Shock Vib. Bull.*, No 34, Pt 5, pp 155-175 (1965).
93. Schwarzl, F., "Forced Bending and Extensional Vibration of a Two-Layer Compound Linear Viscoelastic Beam," *Acustica*, 8, p 164 (1958).
94. Skudrzyk, E., "Vibrations of a System with Finite or Infinite Number of Resonances," *J. Acoust. Soc. Amer.*, 3, p 1140 (1958).
95. Tartakowsky, B.D., Michailow, R.N., and Naumkina, N.I., "Low Order Normal Wave Propagation in Damped Cylindrical Shells," *Proc. Intl. Symp. Assoc. Belge Acousticiens*, Leuven (1967).
96. Torvik, P.J. and Strickland, D.Z., "Damping Additions for Plates Using Constrained Viscoelastic Layers," *J. Acoust. Soc. Amer.*, 51, pp 985-991 (1972).
97. Turner, A.E., "The Use of Damping Materials for Noise Reduction of a Passenger Ship," *J. Sound Vib.*, 10, p 187 (1969).
98. Ungar, E.E. and Ross, D., "Damping of Flexural Vibrations by Alternate Viscoelastic and Elastic Layers," *Proc. 4th Midwest. Conf. Solid Mech.* (1959).
99. Ungar, E.E. and Hatch, D.K., "Selection Guide to High Damping Materials," *Product Engr. (N.Y.)*, 32, p 44 (1961).
100. Ungar, E.E. and Kerwin, E.M., "Loss Factors of Viscoelastic Systems in Terms of Energy Concepts," *J. Acoust. Soc. Amer.*, 34, p 954 (1962).
101. Ungar, E.E., "Loss Factors of Viscoelastically Damped Beam Structures," *J. Acoust. Soc. Amer.*, 34, p 1082 (1962).

102. Whittier, J.S., "Effect of Configurational Additions Using Viscoelastic Interfaces on Damping of a Cantilever Beam," W.A. - D.C. Rep. 58-568 (1959).
103. Yan, M.J. and Dewell, E.H., "Governing Equations for Vibrating Constrained-Layer Damping of Sandwich Plates and Beams," J. Appl. Mech., Trans. ASME, 39, p 1041 (1972).
104. Yin, T.P., Kelly, T.J., and Berry, J.E., "A Quantitative Evaluation of Constrained Layer Damping," J. Engr. Indus., Trans. ASME, 89, pp 773-784 (1967).
105. Yu, Y.Y., "Damping of Flexural Vibrations Sandwich Plates," J. Aero. Space Sci., 29, pp 790-803 (1962).

Additional References

- Nelson, F.C. "Techniques for Design of Highly Damped Structures," The Shock and Vibration Digest, Vol. 9 (7) pp 3-11 (1977) has 29 references.
- International Symposium on "The Damping of the Vibrations of Plates by Means of a Layer" Edited by H. Myncke - Leuven Belgium, September 1967.

H. OBERST (Farbwerke Hoechst AG - Frankfurt/M)

Vibration damping of metal structures, especially by optimized amorphous high polymers

M. A. HECKL (Müller BBN GmbH - München)

The effect of damping layers on waves of different types

Y. JULLIEN (Centre de Recherches Physiques - Marseille)

Recherche d'un matériau de revêtement à équation d'état généralisée, conduisant à une loi de frottement non linéaire optimale

B. D. TARTAKOWSKI, N. I. NAUMKINA, G. M. AVILOVA (Academy of Science - Moscow)

On the three-layer optimized vibrodamping construction

F. LINHARDT (Farbwerke Hoechst AG - Frankfurt/M)

Measurements of the dynamic-mechanical properties of vibration damping materials and damped metal plates

B. D. TARTAKOWSKI, W. E. FRISHBERG, G. S. LUBASHEVSKI (Academy of Science - Moscow)

On multichannel technique for investigation of vibration structures with distributed parameters

R. DI TARANTO (P.M.C. College - Chester)

Analytical investigations of the damping of sandwich beams having a thin viscoelastic layer

F. MECHEL (Ludwigshafen - RH)

Structural configurations for increasing fatigue life

P. GROOTENHUIS (Imperial College of Science and Technology - London)

Measurement of dynamic properties of damping materials

P. KOCH, H. J. KOPINECK, B. MEUTHEN, W. TAPPE (Hoesch AG - Dortmund)

Laminated sheets for high vibration damping-manufacturing, properties, practical applications

D. J. MEAD (Department of aeronautics and astronautics - The University Southampton)

The use of stiffened sandwich plates on aircraft

A. MARTIN (UTAC - Cachan)

*Application de la technique des revêtements sensibles à la détermination
des modes de vibration des éléments de carrosserie*

F. H. VAN TOL Technische Physische Dienst TNO - TH - Delft)

*Scale model investigations of damping layers applied for noise reduction
aboard ships*

K. KURZ, CH. BETZHOLD, W. OBERST (Dr. Stankiewicz GmbH - Celle)

*About the application of antidrumming materials at engines and the
separation of the noise components*

CH. BETZHOLD, K. KURZ, W. OBERST (Dr. Stankiewicz GmbH - Celle)

*Some applications of antidrumming materials and sound barrier mats,
composed of plastics, for machines*

**B. D. TARTAKOWSKI, R. N. MICHAILOW, N. I. NAUMKINA (Academy
of Science - Moscow)**

Low-order normal wave propagation in damped cylindrical shells

**B. D. TARTAKOWSKI, O. G. SHWILKINA, M. M. EFRUSSI (Academy
of Science - Moscow)**

Transmission loss of metal plates with vibrodamping coverings

P. FRYER, A. FRY, R. STEPHENS (Imperial College - London)

A new method for measuring sound transmission through plates

A. FRY, P. FRYER, R. STEPHENS (Imperial College - London)

Sound transmission through plates of various structures

B. H. S. SHARP, J. W. BEAUCHAMP (Building Research Station - Garston)

The influence of damping materials on the transmission loss of panels

T. D. KUDRJAWTSEWA (Academy of Science - Moscow)

Sound transmission through a multilayer damping periodic construction

**L. P. BORISOV, B. D. TARTAKOWSKI, W. B. CHERNISHOW (Academy
of Science - Moscow)**

On sound radiation of homogeneous and armed damped plates

- Lu, Y.P.' Douglas, B.E., "On the Forced Vibration of Three-Layer Damped Sandwich Beam" J.Sound Vib. 32 pp 513-516 (1974).
- Chandrasekharan, M.P., Ghosh, A., "Damping Characteristics of Elastic-Viscoelastic Composite Shafts" J.Sound Vib. 37 pp 1-15 (1974).
- Nandra Kishore, N., Ghosh, A., "Damping of Elastic-Viscoelastic Composite Curved Bars and Helical Springs" J.Sound Vib. 43 pp 621-632 (1975).
- Rao, D.K. "Transverse Vibration of Pre-Twisted Sandwich Beams" J.Sound Vib. 44 pp 159-168 (1976).
- Hyer, M.V., Anderson, W.J., Scott, R.A., "Non-linear Vibrations of Three Layer Beams With Viscoelastic Case I-Theory" 46 (1) pp 121-136 (1976).
- Lu, Y.P., "An Analytical Formulation of the Forced Responses of Damped Rings" 48 (1) pp 27-33 (1976).
- Markus, S., "Damping Properties of Layered Cylindrical Shells, Vibrating in Axially Symmetric Modes" 48 (4) pp (511-524) (1976).
- Mead, D. "Governing Equations for Vibrating Constrained Layer Damping Sandwich Plates and Beams," J.A.M. 40 pp 639-640 (1973).
- Srinivas, S. "Viscoelastic Damping Free Vibrations of Laminates" U.S. Naval Res. Lab. Shock & Vib. Bulletin 43 (4) pp 163-173 (June 1973)
- Nelson, F.C.; Sullivan, D.F. "The Forced Vibrations of a Three Layered Damped Circular Ring" ASME Paper 77 - DET - 154.
- Carne, T.G. "Constrained-Layer Damping Examined by Finite Element Analysis" GMR-1926 Presented at Soc. Eng. Sc. Meeting, Austin, TX October, 1975.

VIBRATION DAMPING ANALYSIS BY FINITE ELEMENTS

**F. K. Bogner
R. A. Brockman
University of Dayton Research Institute
Dayton, Ohio**

1. INTRODUCTION

The problem of dissipating vibratory energy in aerospace structures to prevent resonant fatigue failures has long been an important consideration in structural design. It is well known that certain viscoelastic materials can be used to achieve considerable reduction in resonant amplitudes when applied in the form of a coating or a constrained-layer damping treatment¹. Until recently, however, the design of layered structures with damping treatments has been accomplished largely by the use of gross approximations or cut-and-try experimental methods.

In the past ten to fifteen years, investigators have shown an increased interest in developing analytical tools for designing effective damping treatments. Particular emphasis has been placed on certain specialized cases commonly encountered in practice, such as three-layer sandwich^{2,3} and periodic structures^{4,5}. A few fairly general analyses for linear viscoelastic structures have been reported;^{6,7} however, these are intended for structures of a diverse nature, and may be expensive or impractical for use in preliminary design or parametric studies.

The present study involves the development of a pilot program for finite element analysis of steady-state, forced vibrations of layered and stiffened viscoelastic structural panels (Figure 1). Considerable attention is given to representation of general through-the-thickness geometry, which is of particular interest in evaluating damping treatment concepts, and in correlating experimental data. The panel may consist of a number of layers, each of which can be treated either as thin plates or three-dimensional solids, having direction-dependent (orthotropic) viscoelastic material properties. Provision is made for offset stiffeners on the panel surfaces, as well as discrete tuned damping elements. A unique feature of the finite element analysis is complete compatibility of all one-, two- and three-dimensional elements, not only in displacements but in bending slopes as well. Slope discontinuities due to transverse

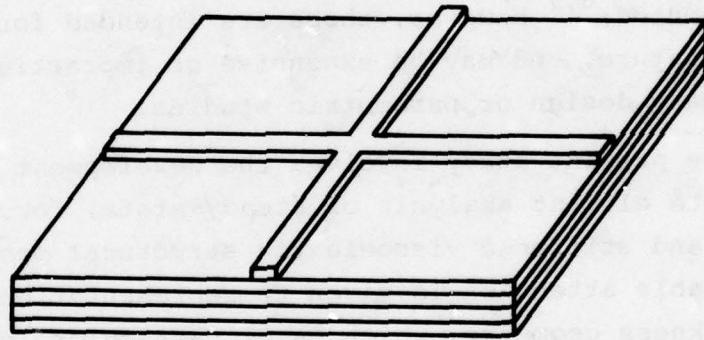


Fig. 1. Layered, Stiffened Viscoelastic Panel

shear deformation in individual layers are also taken into account. Several examples which demonstrate the accuracy and capabilities of the method are presented later in this paper.

2. SCOPE OF A PILOT PROGRAM

Although the work presented here formally represents a pilot study, the computer program developed to obtain the reported results is quite comprehensive in many respects. The primary restriction of the pilot program is that it is applicable to a narrow class of structural geometries. Within the defined problem class, however, the analysis is quite general with respect to such items as state-of-the-art finite elements, data generation, material characterization, equation solving, and problem size. The expenditure of a significant amount of effort on the development of an out-of-core, complex equation solver, and large matrix assembly and manipulation procedures, makes the subject program particularly efficient as far as pilot efforts are concerned. The reason for producing a comprehensive and efficient trial program is to show conclusively that a more general finite element analysis capability can be a valuable tool for the analysis and design of structures with viscoelastic damping, and to provide a useful base for further analytical developments.

The computer program is written in FORTRAN EXTENDED language for the CDC 6600. When assembled without overlay directives, the compiled code occupies about 130K octal (45K decimal) words of central memory. Several characteristics of the subject computer program are discussed below in more detail.

Structure Class

The class of structures to which the analysis is applicable is composed of flat, rectangular panels with beam stiffeners. The panels are multiple layered with each layer being either a classical plate or a three-dimensional solid at the discretion of the user. Also, each layer can include independent viscoelastic damping properties. The beam stiffeners are classical

beams which include the effects of bending, torsion, and axial deformation. Any layer can be stiffened independently with an arbitrary number of beams which are parallel to the panel edges. The offset of stiffeners not placed at the panel midsurface is accounted for in the analysis.

Response Analysis

The pilot program is capable of performing both static and forced harmonic vibration analyses. Presently, the program output is restricted to the complex displacements, and the corresponding displacement amplitudes and phase angles of the nodes of a finite element model. For convenience, frequency sweeps can be made in a single submission of the program to generate the characteristic amplitude versus frequency plots and to locate resonance points.

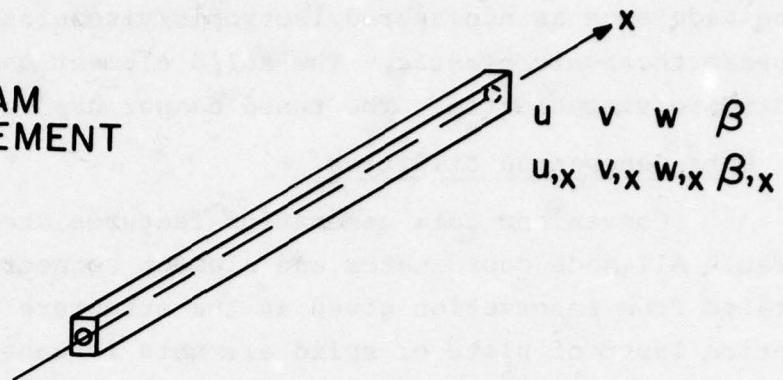
Finite Element Library

At present, four elements reside in the finite element library of the program; these are a beam element, a plate element, a solid element, and a simple tuned damper element. All of the continuum elements are based on Hermite cubic interpolation of the variables. Referring to Figure 2, the beam element has two nodes and 16 degrees of freedom; the plate element has 48 degrees of freedom distributed among four nodes; and the solid element has 8 nodes with 96 degrees of freedom. Since the continuum elements are all based on Hermite cubic interpolation, they are mutually compatible in both displacements and bending slopes. Slope discontinuities due to shear deformation in adjacent layers can be permitted, however. Consistent mass and damping matrices are utilized for all elements.

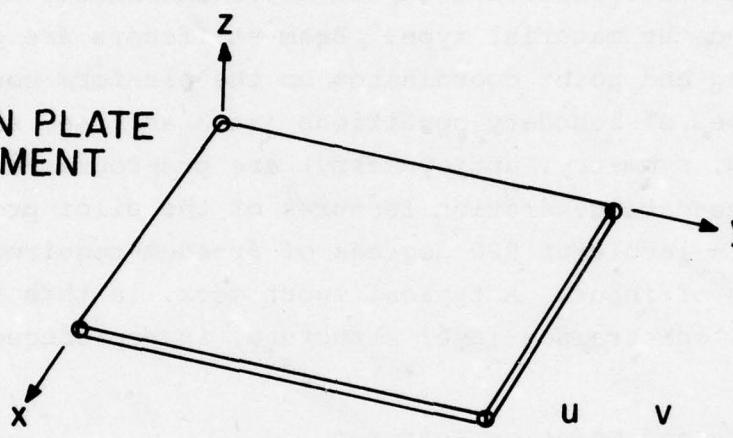
Material Properties Library

Each of the four finite element types has individual flexibility of material properties characterization. The beam element is simply isotropic and elastic. The plate element can at most be layered/orthotropic/viscoelastic. Sub-classifications

BEAM ELEMENT



THIN PLATE ELEMENT



THREE-DIMENSIONAL SOLID ELEMENT

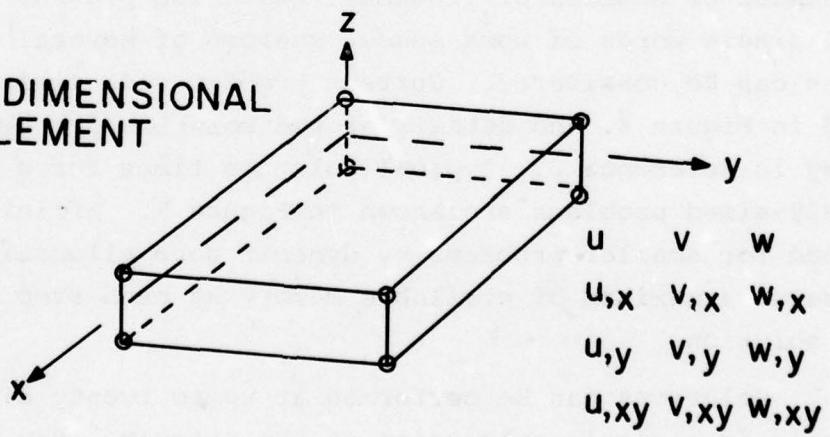


Fig. 2. Continuum Finite Elements

can be made such as nonlayered/isotropic/viscoelastic or layered/orthotropic/elastic. The solid element can at most be orthotropic/viscoelastic. The tuned damper has complex stiffness.

Data Generation Utilities

Convenient data generation features are built into the program. All node coordinates and element connectivity data are generated from information given at the structure boundaries. An entire layer of plate or solid elements is generated by simply specifying data referring to the layer thickness, the element type, and the material type. Beam stiffeners are generated by specifying end point coordinates on the planform boundary. Also, common types of boundary conditions (such as free, simple support, clamped, symmetry, antisymmetry) are preprogrammed. As an example of the data generation features of the pilot program, a recent analysis involving 920 degrees of freedom required a total of only 18 lines of input. A typical input deck, in this instance for a stiffened, constrained-layer structure, is reproduced in Figure 3.

Programming and Solution Features

The subject finite element analysis code has been developed for maximum efficiency on problems of moderate size, but is relatively open-ended with respect to problem complexity (i.e., number of degrees of freedom). With the present allocation of 14000 single words of work space, systems of several thousand equations can be considered. Current problem size limits are pictured in Figure 4, and details of the solution process are discussed in Reference 8. Typical solution times for a few moderately-sized problems are shown in Figure 5. Efficiency is maintained for smaller problems by dynamic core allocation, which makes use of a maximum of available memory at each step in the problem solution.

Solutions can be performed at up to twenty discrete frequencies in a single submission of the program. For subsequent analyses the initial matrix calculations are automatically reused

NDRI / AFML CONSTRAINED-LAYER TEST SPECIMEN			6 X 9 IN. PLANFORM	CL/STF EDGES +
LUM. 2024 (50 MIL) / ISD-110 (4 MIL)	/ ALUM.	2024 (10 MIL)	100 DEGREES F.	+
SD PROPERTIES C = 920. PSI	FTA = 1.00	CIRCLE FIT RESONANCE 253.5 HZ.		
3 4 3 2 1 2	9			
1 1 0.1				
2 3 0.3				
1.E7 1.E7				
2 0.1				
0. 0.				
920. 1.557				
1 1.E7 1.E7				
0.1 0.1				
0. 0.				
0. 1.5				
0. 1 4 3				
1 1 0.05				
2 2 0.004				
1 1 0.01				
1 2 1 1				
1 2 4 1				
1 3 1 1				
252. 253.				
253. 253.3				
253. 253.7				
254. 255.				
256. 256.				

Fig. 3. Computer Program Input for Stiffened Constrained-Layer Damping Specimen Analysis

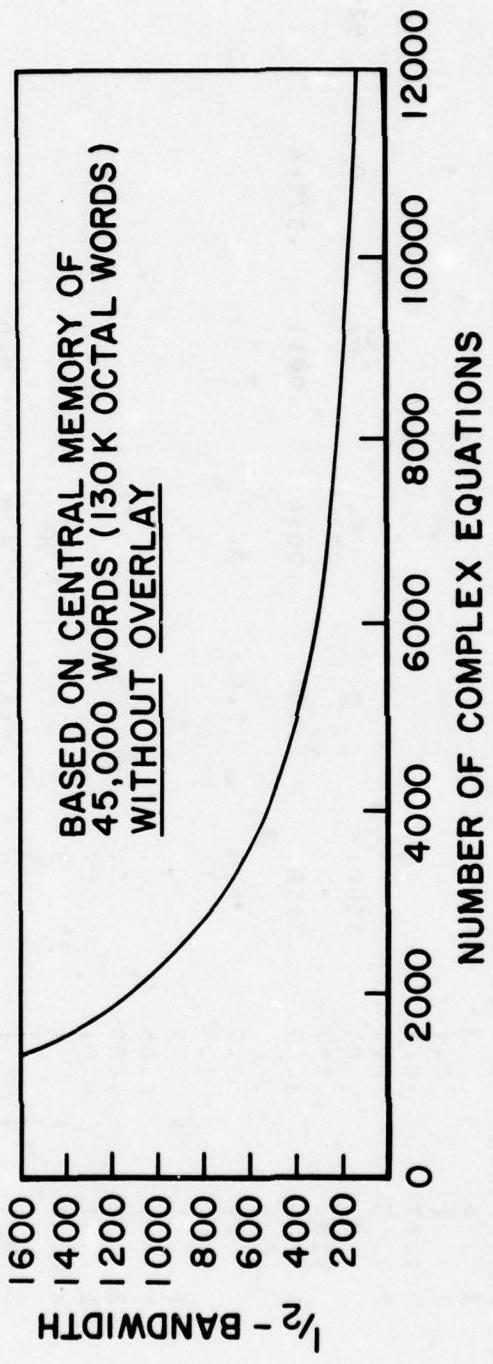


Fig. 4. Approximate Problem Size Limits

Problem	Number Equations	Half- Bandwidth	Complex Equations Solution Time (sec)
THIN PLATE	41	30	0.6
" "	82	60	2.4
" "	177	70	17.0
" "	205	138	24.5
" "	354	140	73.5
CANTILEVER BEAM	152	48	8.6
" "	154	50	9.7
CONSTRINED-LAYER PLATE	80	60	2.4
SANDWICH BEAM	234	102	30.9
" "	920	108	180.0
FIVE-LAYER SANDWICH	288	102	37.9

Fig. 5. Typical Execution Times for Equation Solution

at additional frequencies, thereby reducing matrix assembly times by approximately 99 percent. Identical elements are detected by the program so that computational effort at the element stage is reduced to a minimum.

3. EQUATIONS OF MOTION

The equation of virtual work for a three-dimensional body in Cartesian coordinates can be written as⁹

$$\iiint_V (S_{mn} \delta e_{mn} + \rho u_m \delta \dot{u}_m) dV = \iint_{\partial V_\sigma} F_m \delta u_m dA, \quad (1)$$

where S_{mn} are the stresses, e_{mn} are the strains, u_m represents the Cartesian displacements, and ∂V_σ is that portion of the boundary over which applied forces are prescribed. For the steady state dynamic problem, both the applied loads and the response are assumed to vary harmonically in time,

$$\begin{aligned} F_m &= p_m \exp(i\omega t) & e_{mn} &= \epsilon_{mn} \exp(i\omega t) \\ u_m &= U_m \exp(i\omega t) & S_{mn} &= \sigma_{mn} \exp(i\omega t) \end{aligned} \quad (2)$$

where $i = \sqrt{-1}$ and ω is the forcing frequency. In general, the functions p_m , u_m , ϵ_{mn} and σ_{mn} of (2) are complex valued. A linear constitutive law of the form

$$\sigma_{mn} = C_{mnkl} \epsilon_{kl} \quad (3)$$

is assumed where C_{mnkl} is complex-valued and satisfies the symmetry conditions

$$C_{mnkl} = C_{klmn} = C_{nmkl} = C_{mnlk}. \quad (4)$$

Combining (1) through (4), the virtual work equation can be written as the variation $\delta \pi_S = 0$, where

$$\begin{aligned} \pi_S = \frac{1}{2} \iiint_V & (C_{mnkl} \epsilon_{mn} \epsilon_{kl} - \omega^2 \rho \dot{U}_m \dot{U}_m) dV \\ & - \iint_{\partial V_\sigma} p_m U_m dA. \end{aligned} \quad (5)$$

The strain amplitudes ε_{mn} in (5) are understood to be defined implicitly in terms of the complex displacements as

$$\varepsilon_{mn} = \frac{1}{2} (U_{m,n} + U_{n,m}), \quad (6)$$

so that the complex energy functional π_S is a function only of the displacement amplitudes U_m . It should be mentioned that, despite the similarity of (5) to the Lagrangian potential of the body, the functional π_S is in general indefinite due to the non-ordered nature of the complex field; the true displacements $U_m(x,y,z)$ render π_S a stationary value, but not a minimum, with respect to the set of all kinematically admissible displacements of the structure. It is important to note also that initial displacement and velocity conditions do not appear in the governing equations, since only a particular (i.e., steady-state) solution of the problem is sought.

To obtain the discrete governing equations corresponding to (5), a representative element of the structure is considered, over which the displacement fields

$$U_m = \underline{\underline{N}}^T \underline{x}_m \quad (7)$$

are assumed; the total displacement vector of an element is then

$$\underline{x}_e^T = [\underline{x}_1^T \quad \underline{x}_2^T \quad \underline{x}_3^T]. \quad (8)$$

Use of the matrix forms of Equations (3) and (6) in (5) then yields the governing discrete equation

$$(\underline{\underline{K}} - \omega^2 \underline{\underline{M}}) \underline{x} - \underline{P} = \underline{0}, \quad (9)$$

where \underline{x} is the union of the element degrees of freedom,

$$\underline{x} = \underline{U} \underline{x}_e. \quad (10)$$

The contributions of individual finite elements to (9) are assembled by familiar methods⁹ which are not detailed here. The characteristic (mass, stiffness) matrices of the beam, plate, and solid finite elements considered here are evaluated through the use of Equation (9) in its one-, two- and three-dimensional forms, respectively.

4. FINITE ELEMENT DISCRETIZATION

The present finite element development contains elements in one, two, and three dimensions, as shown in Figure 6. In each instance, the approximating displacement state is based upon the Hermite cubic interpolation formula, which provides for full displacement and slope compatibility and a high degree of modelling efficiency¹¹.

Beam Element

The beam element formulation is based upon the Bernoulli-Euler assumptions of elementary beam theory, and assumes an elastic, isotropic material. Effects of rotatory inertia and offset of the beam axis from reference nodal points are included in the analysis. All displacements on the beam axis, as well as the torsional angle of twist, are approximated by the one-dimensional Hermite interpolation (Figure 6):

$$F(x) = \sum_{i=1}^2 [H_{0i}(x) f_i + H_{1i}(x) F_{xi}]. \quad (11)$$

The resulting element therefore possesses sixteen degrees of freedom. No warping is included in the development of the beam finite element. However, the polar inertia is considered to be independent of bending moments of inertia to permit approximate corrections for thin-walled sections,¹² and shear-area correction factors may be introduced to simulate transverse shear deformation effects.

Thin Plate Element

A thin flat plate element is provided for modelling panel layers which are adequately represented by a classical theory of thin plates. The particular element employed here has been shown to yield excellent results for elastic problems of thin plates, cylindrical shells, and layered orthotropic sandwich construction.^{11,13}

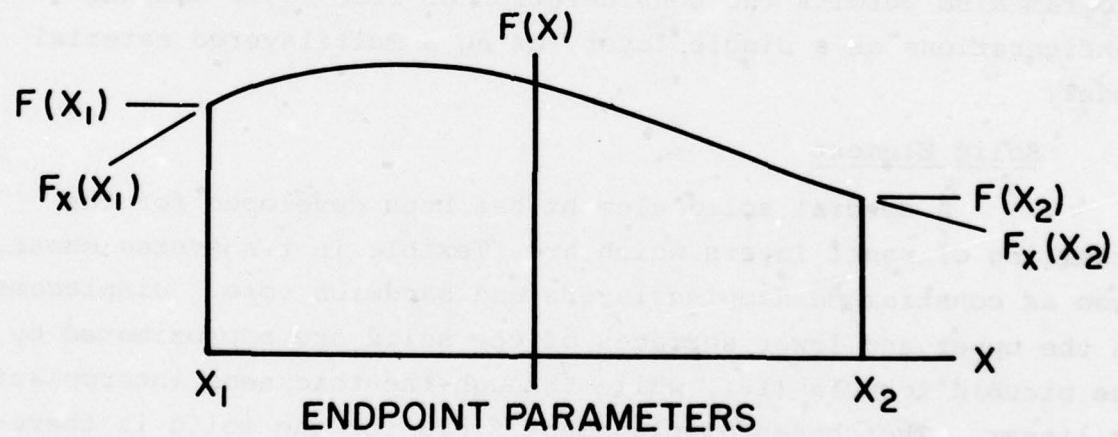
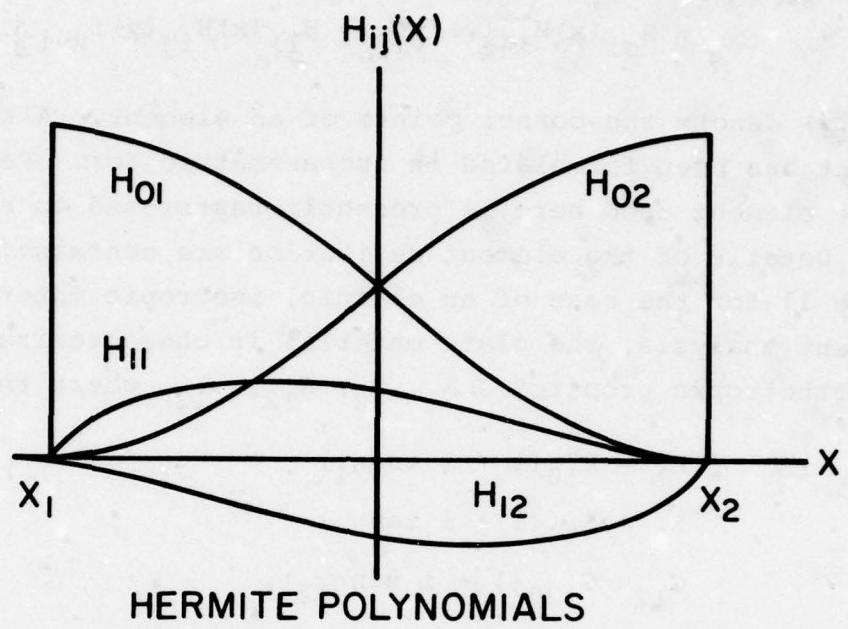


Fig. 6. Hermite Bicubic Polynomials and Endpoint Parameters

The components of displacement for the plate element are represented by the two dimensional Hermite bicubic formula,¹¹

$$f(x,y) = \sum_{i=1}^2 \sum_{j=1}^2 [H_{0i}(x) H_{0j}(y) f_{ij} + H_{1i}(x) H_{0j}(y) f_{xij} \\ + H_{0i}(x) H_{1j}(y) f_{yij} + H_{1i}(x) H_{1j}(y) f_{xyij}] \quad (12)$$

where (i,j) denote the corner points of an element. Although such an element has been formulated in isoparametric form (Reference 13), the plate element used here is presently restricted to rectangular meshes. Details of the element derivation are contained in Reference 11 for the case of an elastic, isotropic material. In the present analysis, the plate material is characterized by the planar orthotropic properties E_1 , E_2 , G_{12} , ν_{12} , where the moduli

$$E_1 = E_{10}(1 + i \tan \gamma_1) \\ E_2 = E_{20}(1 + i \tan \gamma_2) \\ G_{12} = G_{120}(1 + i \tan \gamma_{12}). \quad (13)$$

Effects due to offset of the principal orthotropic axes (1,2) with respect to the structural axes (x,y) are considered. The computer program also permits the consideration of free-layer damping configurations as a single layer, using a multilayered material model.

Solid Element

A special solid element has been developed for the modelling of panel layers which are flexible in transverse shear, such as constrained damping layers and sandwich core. Displacements in the upper and lower surfaces of the solid are approximated by the bicubic formula (12), while through-the-thickness interpolation is linear. The chosen displacement field for the solid is therefore fully compatible in both displacement and slope with the beam and plate elements, while permitting relative deformations in transverse shear between adjacent layers. Three-dimensional orthotropic viscoelastic properties are used for the material

description. The solid finite element, which has 96 degrees of freedom, has been found to give excellent results, even for the analysis of very thin layers and for plate-bending problems.

5. NUMERICAL EXAMPLES

The steady-state viscoelastic finite element analysis has been used to analyze a number of layered panel configurations, and shows excellent agreement with both analytical and experimental results. Representative analyses involving commonly-used damping treatment configurations are presented here, and compared with experimental results.

Beam with Free-Layer Damping Treatment

A cantilever beam constructed from 0.0379 inch aluminum with a 0.102-inch thick free-layer damping treatment is pictured in Figure 7. The finite element model shown consists of two plate elements in the aluminum base layer, and two solid elements representing the damping layer, resulting in a total of 84 unconstrained degrees of freedom. Analysis results for the second bending mode of the beam are shown in Figure 8. The finite element analysis shows good agreement with experiment, as the calculated resonance is less than three percent different from the measured resonant frequency. Results of a conventional beam analysis are in error by approximately 5.5 percent. Loss factors based upon resonant amplification factor at the beam tip are $\eta=0.002$ from the beam analysis, and $\eta=0.001$ by the finite element solution. The results plotted in Figure 8 were determined by analysis at 20 different frequencies, and required 74 seconds of processing time for the total solution.

Stiffened Constrained-Layer Plate

The 6 by 9 inch constrained-layer specimen shown in Figure 9 has also been analyzed by the present finite element method. Both ends of the panel are fixed to solid blocks, and the sides are stiffened by one-inch deep aluminum angles attached to the uppermost aluminum layer. The finite element model

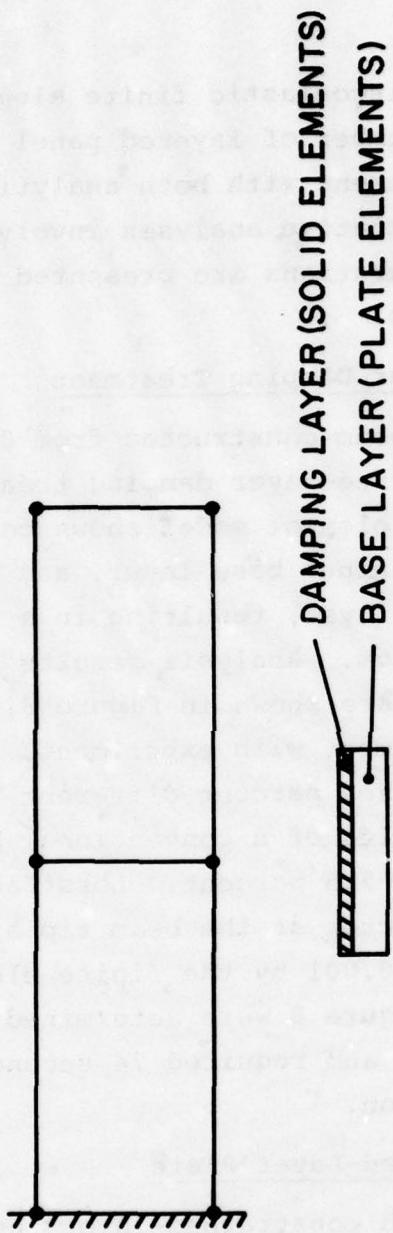


Fig. 7. Beam with Free-Layer Damping Treatment

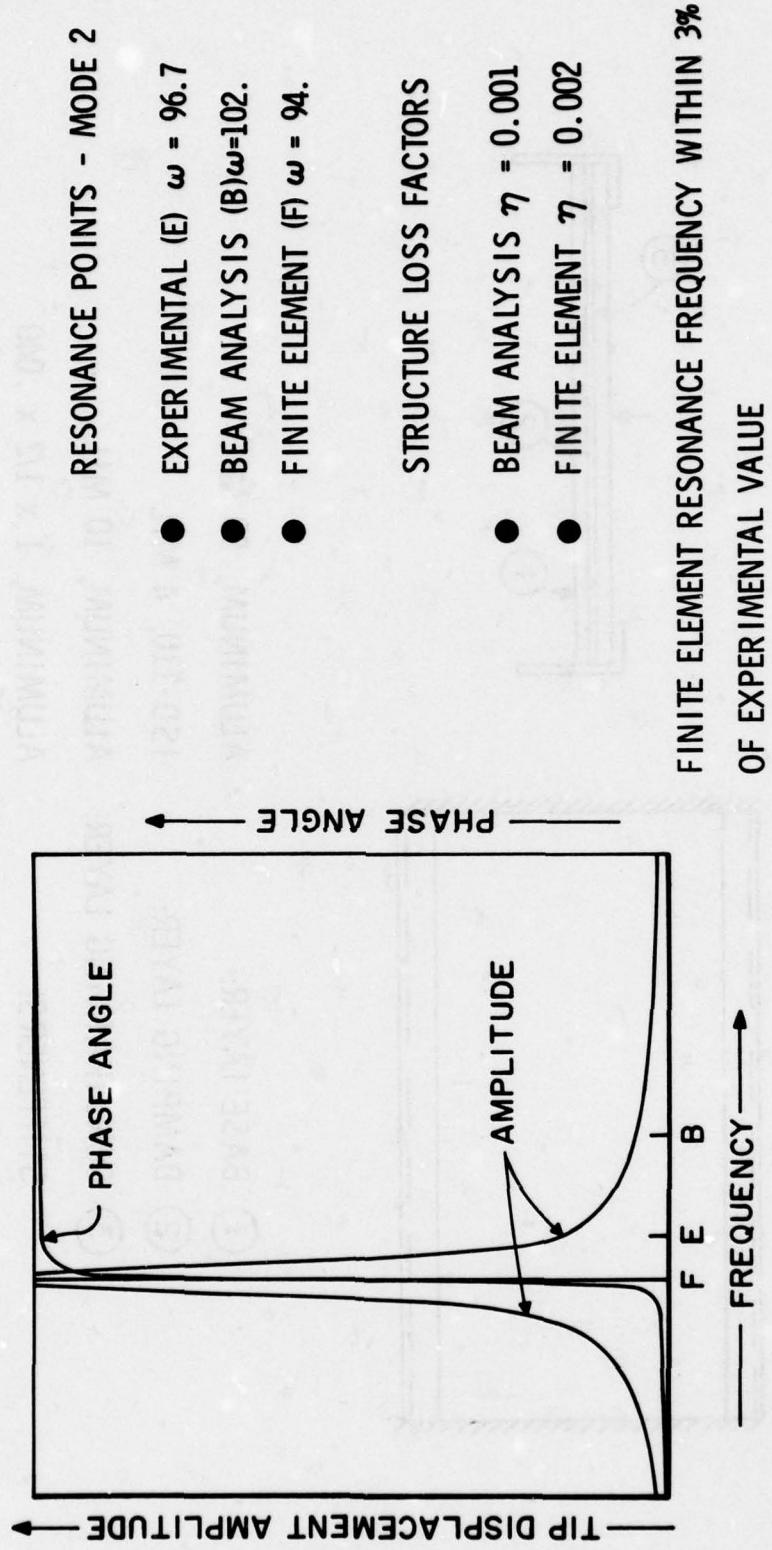
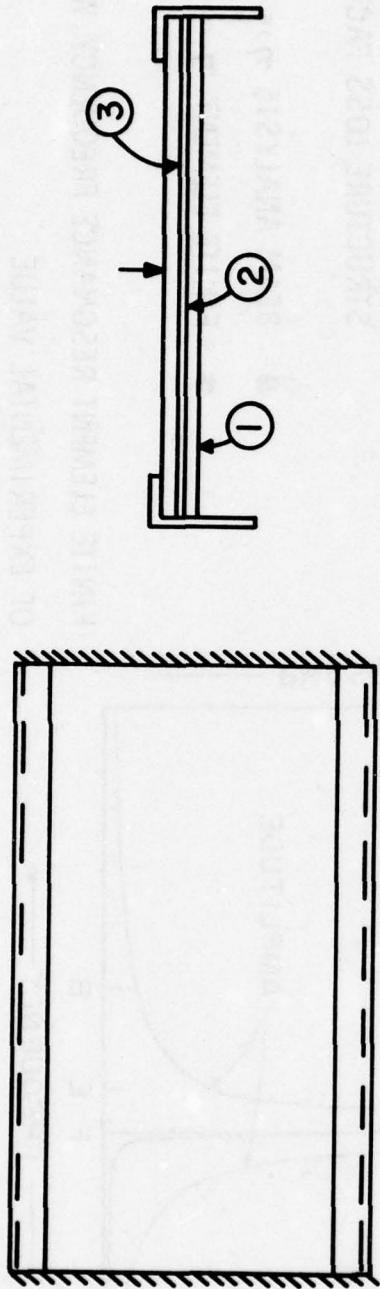


Fig. 8. Analysis Results for Free-Layer Beam



- ① BASE LAYER: ALUMINUM, .50 MIL
- ② DAMPING LAYER: ISD-110, .4 MIL
- ③ CONSTRAINING LAYER: ALUMINUM, .10 MIL
- STIFFENERS: ALUMINUM, 1 x 1/2 x .040

Fig. 9. Stiffened Constrained-Layer Plate

(Figure 10) consists of eight thin plate elements in the base and constraining layers, and four, three-dimensional elements used to represent the damping layer, which is relatively flexible in transverse shear. Central displacement and phase angle results for the constrained-layer specimen at a temperature of 70°F are plotted versus frequency in Figure 11. The predicted frequency of 261 Hz at peak amplitude is seen to be only 1.9 percent greater than the experimental first-mode resonance of 255.5. Similar results for temperatures ranging to 100°F are shown in Figure 12; the upper frame of the figure shows the variation of damping layer modulus and loss factor over the temperature range of interest. Comparisons of loss factor results were not possible for this example due to a lack of experimental data.

6. CONCLUSIONS

A finite element technique for the analysis of viscoelastic damping in layered panel structures has been presented, and demonstrated in the solution of forced vibration problems for some common damping treatment configurations. Excellent agreement is obtained with analytical and experimental results, even for coarse element grids. The computer program is oriented toward efficient solution of problems of moderate size, and includes extensive data generation capabilities.

The accuracy and efficiency demonstrated by the reported pilot computer program certainly warrants the further development of finite element analysis methods for viscoelastic damping applications. A number of areas exist in which further development is needed. These include analysis of curved panels, isoparametric finite elements, consideration of rotating and initially-stressed parts, and, ultimately, extension to automated structural design and optimization of damping characteristics.

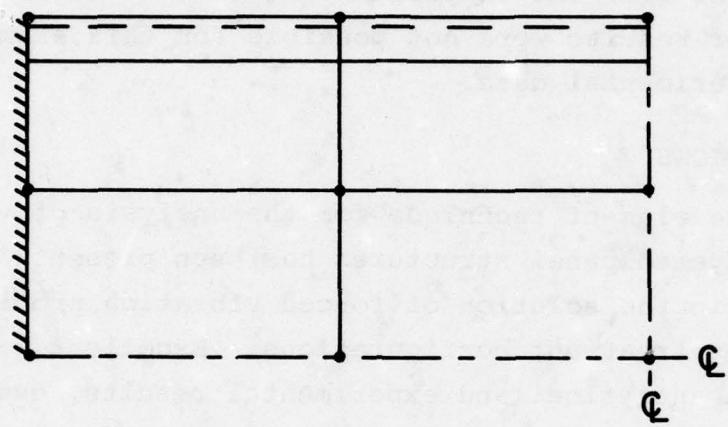


Fig. 10. Constrained-Layer Plate Finite Element Model

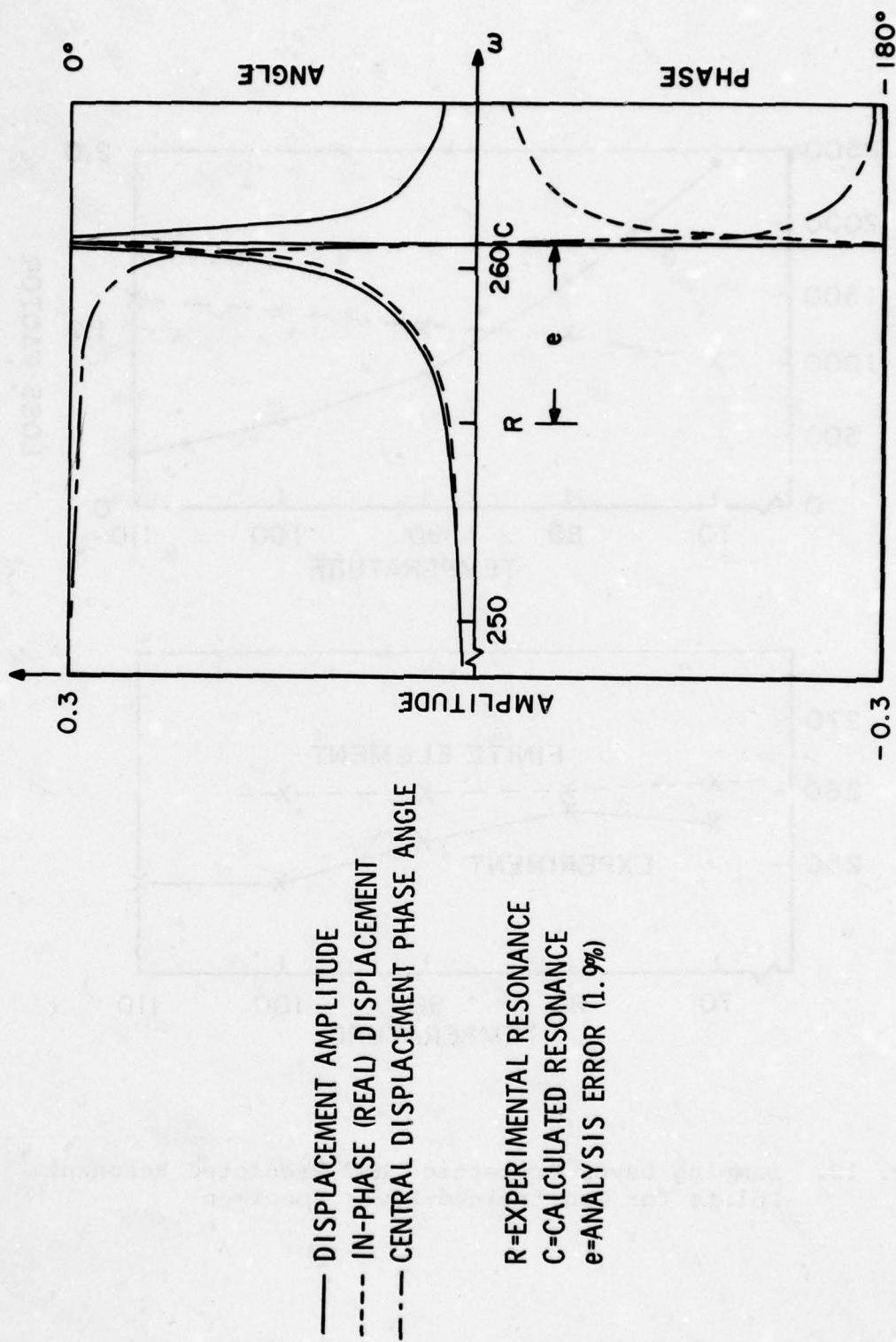


Fig. 11. Analysis Results for Constrained-Layer Plate

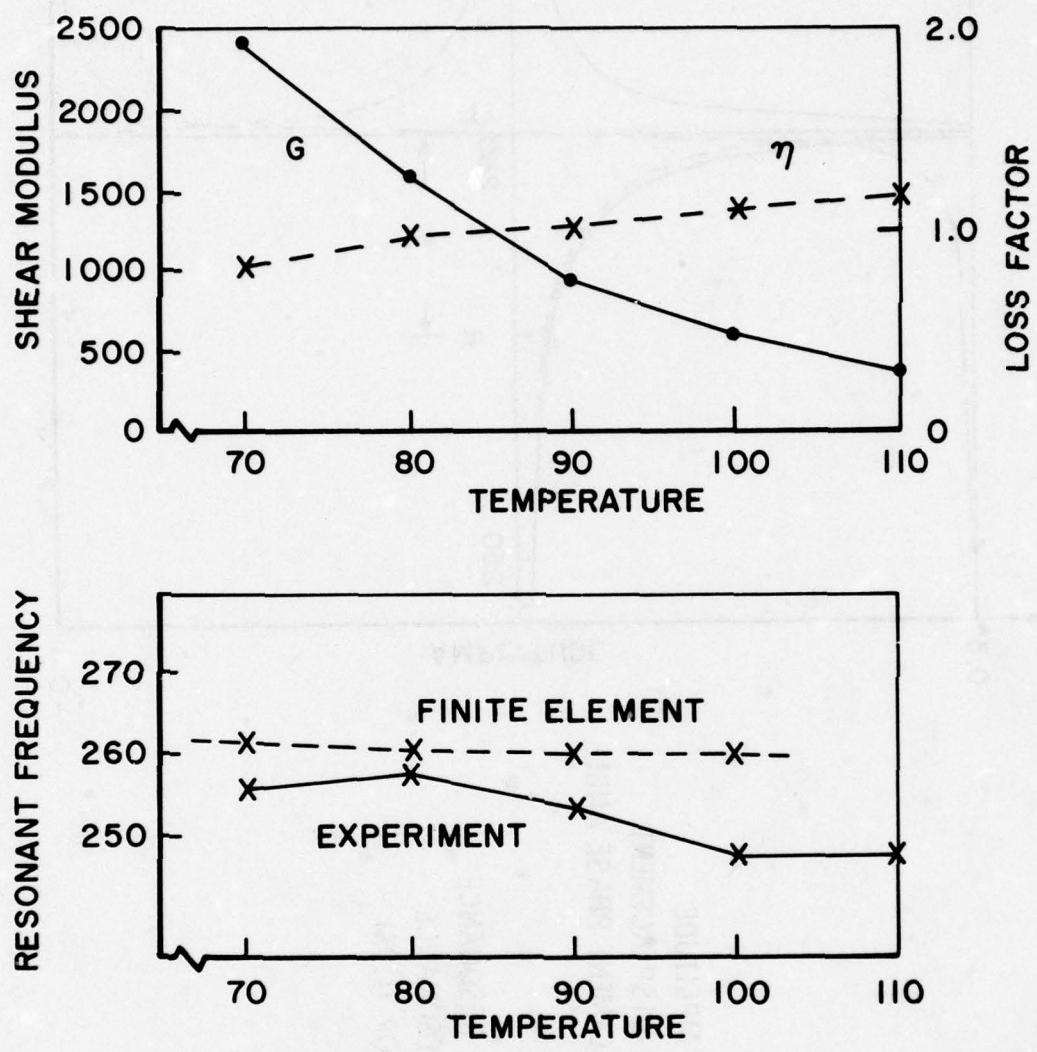


Fig. 12. Damping Layer Properties and Predicted Resonant Points for Constrained-Layer Specimen

ACKNOWLEDGEMENT

The developments presented in this paper were sponsored by the Air Force Materials Laboratory, Wright-Patterson Air Force Base, Ohio, under the direction of Dr. John P. Henderson. Experimental results were provided by Mr. Michael Drake of the University of Dayton Research Institute.

REFERENCES

1. Oberst, H., "Reduction of Noise by the Use of Damping Materials," Royal Aero. Soc., Vol. 263, 1968, pp 441-453.
2. Chatterjee, A., and J. R. Baumgarten, "An Analysis of Viscoelastic Damping Characteristics of a Simply-Supported Sandwich Beam," Trans. ASME, J. of Eng. for Industry, Vol. 93, No. 4, November 1971.
3. Yu, Yi-Yan, "Damping of Flexural Vibrations of Sandwich Plates," J. Aero. Soc., Vol. 29, 1962, pp 790-803.
4. Sen Gupta, G., "Natural Flexural Waves and the Normal Modes of Periodically-Supported Beams and Plates," J. Sound Vib., Vol. 13, No. 1, 1970, pp 89-101.
5. Henderson, J. P., "Vibration Analysis of Curved Skin-Stringer Structures Having Tuned Elastomeric Dampers," AFML-TR-72-240, October 1972.
6. Zienkiewicz, O. C., M. Watson, and I. P. King, "A Numerical Method of Viscoelastic Stress Analysis," Int. J. Mech. Sci., Vol. 10, 1968, pp 807-827.
7. White, J. L., "Finite Elements in Linear Viscoelasticity," AFML-TR-68-150, 1968.
8. Brockman, R. A., "Solution of Large Systems of Complex-Valued Linear Equations," UDR-TM-77-09, University of Dayton Research Institute, Dayton, Ohio, August 1977.
9. Malvern, L. E., Introduction to the Mechanics of a Continuous Medium. Prentice-Hall, 1969.
10. Zienkiewicz, O. C., The Finite Element Method in Engineering Science. McGraw-Hill Publishing Co., London, 1971.
11. Bogner, F. K., "Finite Deflection, Discrete Element Analysis of Shells," AFFDL-TR-67-185, December 1968.

12. Timoshenko, S. P., and D. H. Young, Elements of Strength of Materials. D. Van Nostrand Co., 1968.
13. Brockman, R. A., "Finite Element Method for the Finite Displacement Analysis of Sandwich Composite Panels," UDR-TR-77-65, University of Dayton Research Institute, Dayton, Ohio, December 1977.

**DAMPED VIBRATION THEORY:
A STATE-OF-THE-ART ASSESSMENT**

**F. C. Nelson
Department of Mechanical Engineering
Tufts University
Medford, Massachusetts**

One question of interest which arises with increasing frequency is how to best set up and analyze nonlinear systems so as to have a minimum likelihood of end up with undesirable effects.

DAMPED VIBRATION THEORY: A STATE-OF-THE-ART ASSESSMENT

F. C. Nelson

Department of Mechanical Engineering
Tufts University
Medford, Massachusetts 02155

ABSTRACT

A review of the state-of-the-art in the formulation and solution of damped-vibration problems is presented. Particular emphasis is placed on problems with non-proportional or hysteretic damping. The availability of this technology in existing computer programs is assessed and comment is made about current patterns of usage and areas which deserve further development.

INTRODUCTION

The technology for solving damped eigenvalue problems and damped vibration response problems exists but is little used. Wider knowledge and more use of this technology, especially at the design stage, could increase the reliability and life of structures subjected to severe vibroacoustic environments.

This paper will survey this technology with particular emphasis on the solution of equations of motion which have either nonproportional or hysteretic damping. Computer programs which incorporate this technology will be mentioned. Comment will also be made about current patterns of usage and suggestions will be made about areas where further research is needed.

FORMULATION IN PHYSICAL AND MODAL COORDINATES

Lumped parameter or finite element modeling of a structure produces a set of coupled equations of motions which can be concisely written in matrix form. For n such equations the matrix equations of motion become

$$[m]\{\ddot{x}\} + [c]\{\dot{x}\} + [k]\{x\} = \{f(t)\} \quad (1)$$

where $[m]$, $[c]$ and $[k]$ are the $n \times n$ mass, damping and stiffness matrices and $\{x\}$ and $\{f(t)\}$ are the $n \times 1$ displacement and forcing function matrices. Because $\{x\}$ represents the physical coordinates, equation (1) will be referred to as the physical equations of motion.

Techniques for the numerical integration of equation (1) have been described in reference [1]. Direct integration at this stage places no restrictions on the form of $[c]$ and allows step-wise changes in $[c]$ and $[k]$ to simulate nonlinearities in damping and stiffness. However, since all elements of $\{x\}$ must be considered, a major computational effort is required when n is large.

If the structural behavior is linear, it is advantageous to change from physical coordinates $\{x\}$ to modal coordinates $\{q\}$. The modal equations are

$$\{\ddot{q}\} + [\Phi]^T [c] [\Phi] \{\dot{q}\} + [\omega^2] \{q\} = [\Phi]^T \{f(t)\} \quad (2)$$

where $[\Phi]$ is the $n \times n$ modal matrix whose columns are the undamped eigenvectors associated with equation (1), $[\omega^2]$ is the $n \times n$ (diagonal) spectral matrix whose elements are the corresponding undamped eigenvalues, and $\{x\} = [\Phi]\{q\}$. Techniques for finding $[\Phi]$ and $[\omega^2]$ are discussed in ref. [2]. The advantage of a modal formulation lies in the fact that it is often possible to anticipate that the structural response will be dominated by a few normal modes (i.e. eigenvectors) and

equations (2) can be truncated to include only these dominant modes. The order of eq. (2) is then much less than n and numerical integration will require much less time.

Let us now consider the term $[\Phi]^T [c] [\Phi]$ in some detail since it is the only term which couples together the modal equations of motion.

PROPORTIONAL DAMPING

If one assumes

$$[c] = a_0 [m] + a_1 [k] \quad (3)$$

the term $[\Phi]^T [c] [\Phi] = [\tilde{c}]$ will be diagonal and the modal equations will be uncoupled. This type of damping is called proportional damping. Since eq. (3) has only two free constants, only two elements of $[\tilde{c}]$ can be specified. Caughey has generalized eq. (3) so that any number of the elements in $[\tilde{c}]$ can be specified. Proportional damping is more fully discussed in ref. [3].

NONPROPORTIONAL DAMPING

If $[\Phi]^T [c] [\Phi]$ is nondiagonal, the damping is called nonproportional. However, the desire to have a diagonal damping matrix is a strong one since uncoupled modal equations permit the physical response to be easily visualized as a superposition of the responses of a series of modal oscillators. The response spectrum analysis method, which is widely used in seismic analysis of structures, is based on this perception.

To achieve this desire for a diagonal damping matrix even for nonproportional damping, two approximations are often used.

- (1) Compute $[\Phi]^T [c] [\Phi]$ and neglect the off-diagonal terms. In Ref. [4] Warburton and Soni have studied the errors associated with this approximation and propose a criterion for judging when the errors are acceptable.
- (2) Replace $[\Phi]^T [c] [\Phi]$ by a diagonal viscous damping matrix whose elements are assigned by experience. This substitute matrix is called the equivalent viscous modal damping matrix.

It is important to realize that it is not necessary to use either of these approximations to solve a nonproportionally damped structure by modal superposition. One can use damped vibration theory. To illustrate this point, three different formulations of damped vibration theory will now be described.

THE COMPLEX MODE METHOD

This method was introduced by Frazer, Duncan and Collar in the 1930's and more fully developed by Foss in his classic paper of 1958, see Ref. [5]. If one adds to equation (1), the trivial equation

$$[m]\{\ddot{x}\} - [m]\{\dot{x}\} = 0$$

the resulting equations may be written

$$\begin{bmatrix} [0] & [m] \\ [m] & [c] \end{bmatrix} \begin{Bmatrix} \{\ddot{x}\} \\ \{\dot{x}\} \end{Bmatrix} + \begin{bmatrix} -[m] & [0] \\ [0] & [k] \end{bmatrix} \begin{Bmatrix} \{\dot{x}\} \\ \{x\} \end{Bmatrix} = \begin{Bmatrix} \{0\} \\ \{f(t)\} \end{Bmatrix} \quad (4)$$

By setting $\{f(t)\} = \{0\}$ and assuming $\{x\} = \{\psi\}e^{\lambda t}$, equation (4) becomes an eigenvalue problem with modal matrix $[\Psi]$ and spectral matrix $[\lambda]$. The coordinate transformation

$$\begin{Bmatrix} \{\dot{x}\} \\ \{x\} \end{Bmatrix} = [\Psi]\{q\}$$

will produce an uncoupled set of modal equations and permit a straightforward application of modal superposition. The identical procedure can be applied to the modal equation of motion, eq. (2), rather than the physical equation of motion as done above. This leads to sparser matrices than those contained in eq. (4).

There is a serious computational price to this method: $[\Psi]$ is composed of $2n$ complex eigenvectors and $[\lambda]$ of $2n$ complex eigenvalues, both in complex conjugate pairs. The use of complex modes and frequencies to obtain analytical solutions to real vibration problems is detailed in Chapter 9 of reference [6]. Computer algorithms based on this method are also available. Gupta has presented an algorithm in ref. [7] and has incorporated it into a modal superposition program called DAMP*. Recently, this method has been used to compute receptances for damped structures, ref. [8], and this opens the way for substructure analysis using complex modes.

THE CHARACTERISTIC PHASE LAG METHOD

This method was introduced by Fraeijs de Veubeke in 1948 and circulated more widely in ref. [9].

Assume that all forces are sinusoidal and in-phase. Then eq. (1) can be written

$$[m]\{\ddot{x}\} + [c]\{\dot{x}\} + [k]\{x\} = \{f\} \cos\Omega t$$

Assume that this equation has solution

* available from COSMIC (Computer Software Management and Information Center), University of Georgia, Athens, GA 30601

$$\{x\} = \{\gamma\} \cos(\Omega t - \theta).$$

This requires

$$([k] - [m]\Omega^2)\tan\theta - [c]\Omega\{\gamma\} = \{0\} \quad (5)$$

$$([k] - [m]\Omega^2)\cot\theta + [c]\Omega\{\gamma\} = \{f\} \quad (6)$$

Equation (5) is an eigenvalue problem with spectral matrix $[\Gamma_\theta]$ and modal matrix $[\Gamma]$. Equation (6) yields an associated force matrix $[F]$ where

$$[F] = [\{f\}_1 | \{f\}_2 | \dots].$$

Each force vector $\{f\}_i$ is associated with an eigenvalue θ_i and an eigenvector $\{\gamma\}_i$. Notice that the eigenvalues are phase angles rather than frequencies (hence the name for the method). It can be shown that the force distribution $\{f\}_i$ excites only the mode shape $\{\gamma\}_i$; hence, these modes are sometimes called damped forced modes.

The fact that $[\Gamma_\theta]$, $[\Gamma]$ and $[F]$ depend on the forcing frequency Ω and must be recalculated every time Ω changes has discouraged wide use of this method. A reconsideration of the method in light of modern computing techniques would be useful. Also, the availability of the Fast Fourier Transform may permit the efficient use of the method for forcing other than sinusoidal.

The above discussion places no restriction on the form of $[c]$. In reference [10], Mead seizes on the concept of damped forced modes and shows that if $[c]$ corresponds to hysteretic damping in the form $[c] = i[h]$, the dependence of the various modal quantities on the forcing frequency vanishes. The method then becomes very attractive. In fact, if $[h] = \eta[k]$, the damped forced modes become identical to the undamped normal modes. The great utility of Mead's modification of this method is illustrated in reference [11].

THE COMPLEX STIFFNESS METHOD

Damping is called hysteretic if the damping force is proportional to the displacement and in antiphase with the velocity. This definition results in an energy dissipation per cycle which is independent of frequency. The most common, although not the only, way of expressing this definition in mathematical form is to introduce a complex stiffness matrix, i.e.

$$[\underline{k}] = [k]_R + i\eta[k]_I$$

where $[k]_R$ contains all the elastic stiffnesses and the real part of the viscoelastic stiffnesses. $[k]_I$ contains the imaginary parts of the viscoelastic stiffnesses. All viscoelastic elements are assumed to have the same loss factor η .

This method of incorporating hysteretic damping into a

a structure is valid for sinusoidal forcing. If we adopt the complex exponential notation, sinusoidal forcing may be written in the form

$$\{f(t)\} = \operatorname{Re} [\underline{f} e^{i\Omega t}]$$

where $(_)$ indicates a complex quantity.

The physical equations of motion take the form

$$[-\Omega^2 [m] + i\eta[k]_I + [k]_R] \{\underline{x}\} = \{\underline{f}\} \quad (7)$$

Modal equations are obtained by using a transformation based on the undamped eigenvectors associated with eq. (7).

$$\{\underline{x}\} = [\Phi] \{\underline{q}\}.$$

It can be shown that

$$[\Phi]^T [m] [\Phi] = [I]$$

$$[\Phi]^T [k]_R [\Phi] = [\omega^2]$$

$$[\Phi]^T [k]_I [\Phi] = [p^2]$$

hence the modal equation

$$\begin{bmatrix} [\omega^2] - \Omega^2 [I] & -\eta [p^2] \\ \eta [p^2] & [\omega^2] - \Omega^2 [I] \end{bmatrix} \begin{Bmatrix} \{\underline{q}\}_R \\ \{\underline{q}\}_I \end{Bmatrix} = \begin{Bmatrix} [\Phi]^T \{\underline{f}\}_R \\ [\Phi]^T \{\underline{f}\}_I \end{Bmatrix} \quad (8)$$

where $\{\underline{q}\}$ and $\{\underline{f}\}$ have been separated into their real and imaginary parts.

The $2n \times 2n$ matrix in eq. (8) is skew-symmetric and sparse so solution can be fairly efficient. This efficiency can be improved by using modal truncation. However, the stiffness and loss factor of real viscoelastic materials vary with temperature and frequency. In particular then, for a given temperature, $[\Phi]$ will be a function of the natural frequencies -- but these frequencies can not be found until the stiffness of the viscoelastic material is known. Clearly, an iterative procedure is required.

Lalanne and his colleagues have developed a perturbation method which minimizes the amount of computer calculation and permits the use of real material properties in the solution of eq. (8), see ref. [12]. In addition, they have developed a computer program, ASTRE*, which uses complex stiffness isoparametric solid elements. ASTRE has been successfully used to solve thick, curved structures damped by viscoelastic layers.

* Information on this program is available from Prof. M. Lalanne, Institut National des Sciences Appliquees, Laboratoire de Mecanique des Structures, 69621 Villeurbanne, France

CONCLUSIONS

Both analysts and designers desire conceptual simplicity and computational efficiency. However, when it comes to damped vibration problems, this desire manifests itself in different ways for different people. Those who prefer as much physical reality as possible tend, in the author's experience, to choose numerical integration of the modal equations. Those who prefer mathematical simplicity tend to replace the actual damping distribution with an equivalent viscous modal damping matrix and then use modal superposition. The methods of damped vibration theory discussed above have the potential to satisfy both groups, especially when the damping is large. However, it is clear that advances in computational efficiency are needed as well as a wider understanding of the simplicity and usefulness of these methods.

REFERENCES

1. Tillerson, J. R., "Selecting Solution Procedures for Non-linear Structural Dynamics," Shock Vib. Dig., Vol. 7, No. 4, pp. 2-13, 1975.
2. Bishop, R. E. D., Gladwell, G. M. L., Michaelson, S., The Matrix Analysis of Vibration, Cambridge Univ. Press, 1965.
3. Wilson, E. L. and Penzien, J., "Evaluation of Orthogonal Damping Matrices," Int'l J. Numerical Methods in Engr., Vol. 4, pp. 5-10, 1972.
4. Warburton, G. B. and Soni, S. R., "Errors in Response Calculations for Non-Classically Damped Structures," Earthquake Engr. and Structural Dyn., Vol. 5, pp. 365-376, 1977.
5. Foss, K. A., "Co-ordinates which Uncouple the Equations of Motion in Damped Linear Dynamic Systems," Jour. of Appl. Mech., Vol. 25, pp. 361-364, 1958.
6. Hurty, W. C. and Rubinstein, M.F., Dynamics of Structures, Prentice-Hall, 1964.
7. Gupta, K. K., "Eigenproblem Solution of Damped Structural Systems," Int'l J. Numerical Methods in Engr., Vol. 8, pp. 877-911, 1974.
8. Kung, W-C, Hohenemser, K. H., "Eigenvalue Analysis for Coupled Large Linear Damped Structures," Computer Methods in Appl. Mechanics, Vol. 12, p. 69-75, 1977.
9. Fraeijs de Veubeke, B.M., "A Variational Approach to Pure Mode Excitation Based on Characteristic Phase Lag Theory," A.G.A.R.D. Report 39, 1956.
10. Mead, D. J., "The Existence of Normal Modes of Linear Systems with Arbitrary Damping," Symposium on Structural Dynamics, Loughborough Univ. of Tech., Vol. I, pp. c.5.1-15, 1970.
11. Mead, D. J., Markus, S., "The Forced Vibration of a Three-Layer, Damped Sandwich Beam with Arbitrary Boundary Conditions," J. Sound Vib., Vol. 10, pp. 163-175, 1969.
12. Lalanne, M., Paulard, M., Trompette, P., "Response of Thick Structures Damped by Viscoelastic Material with Application to Layered Beams and Plates," Shock and Vib. Bull. 45, pp. 65-71, 1975.

**SELECTED 3M MATERIALS, PROPERTIES,
ENVIRONMENTAL RESISTANCE AND APPLICATIONS**

**D. B. Caldwell
3M Company
Industrial Specialties Division
St. Paul, Minnesota**

3M VISCOELASTIC MATERIALS

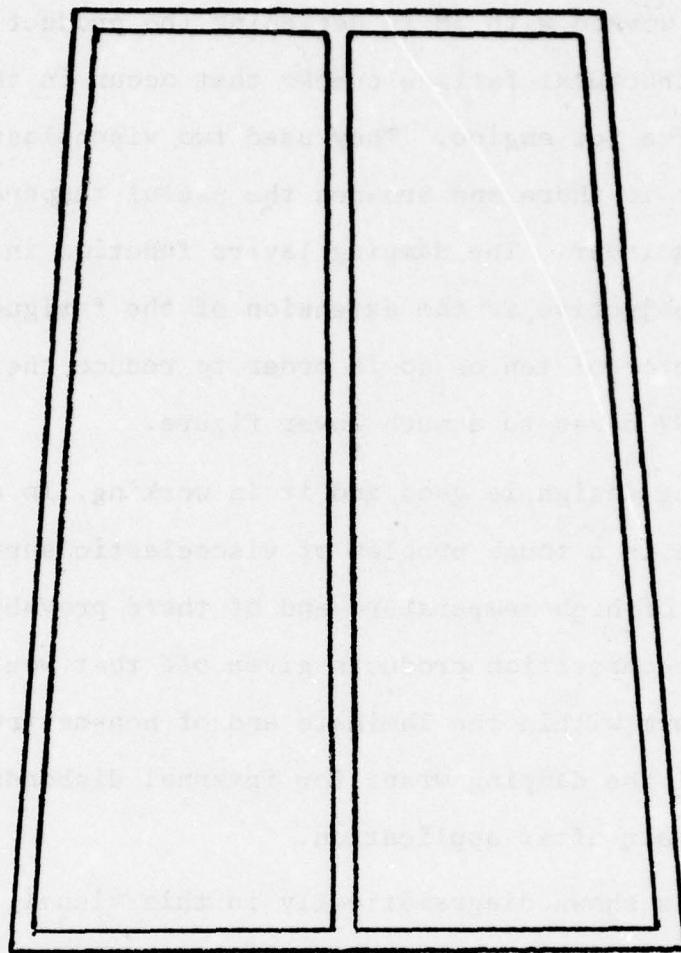
<u>VISCOELASTIC IDENTIFICATION</u>	<u>RANGE OF AVAILABLE THICKNESS T, MILS</u>	<u>USEFUL TEMP. RANGE OF DAMPING F, °F.</u>	<u>NATURAL AGING STABILITY AT USE TEMPERATURE</u>
ISD # 113	$1 \leq T \geq 1000$	$-20 < F < +30$	Excellent
ISD # 112	$1 \leq T \geq 1000$	$+50 < F < +100$	Excellent
ISD # 110	$1 \leq T \geq 1000$	$+75 < F < 125$	Excellent
NPE 1134	$1 \leq T \geq 10$	$+160 < F < 210$	Excellent
ISD # 830	$1 \leq T \geq 5$	$-30 < F < +20$	GOOD - Excellent

If I could show 100 men in this boat I would because everyone at this conference is together in the same boat -- that of solving problems with free and constrained layer damping. We're afloat on a sea of product acceptability due to public concern over noise and vibration, on an ocean of laws that are a result of this concern, and a flood of emerging appreciation of resonant damping in design of stable structures. The military has led the way in the past and they are leading the way today in calling this first ever conference on Viscoelastic Damping Technology of the 1980's.

3M is here to share openly with the intention of contributing to the building of "Community" among us.

As I understand the obligation of being a vendor of viscoelastic damping devices a prime obligation is to supply reliable data on the dynamic properties of viscoelastic materials and samples of those materials to designers. This we do. I've been asked to comment on the viscoelastics available from 3M. I've done this in this brochure. You are welcome to take a copy with you. The brochure contains a statement of our commercial policy, which I want to call to your attention, but which is not appropriate to discuss here. For now I'd like to discuss the major points summarized on this visual -- identify viscoelastics, thickness, stability, usual temperature of use.

I'll describe four applications that look really different from the outside but have the same blood in their veins -- like brothers. The common bond is energy absorption through shear displacement in a viscoelastic material. The differences in the applications are in mode shape, temperature, frequency, other features of the environment, the type of viscoelastic dictated by these features and the use of bending or axial movement to obtain the desired displacement in the viscoelastic. The first product is a lamination of three layers of aluminum foil with two different viscoelastics. (You will hear more about this application from Mike Parin).



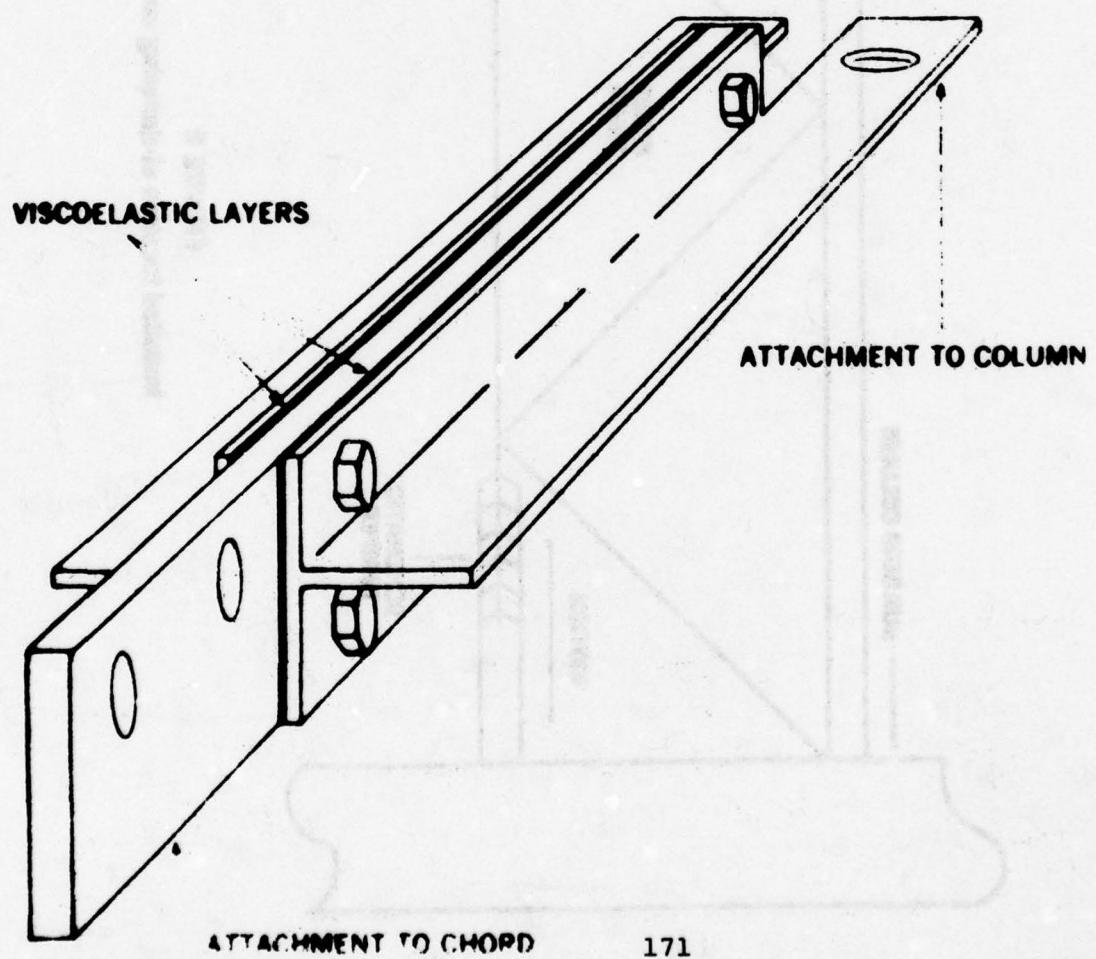
The Air Force worked with 3M in designing the product to reduce and control structural fatigue cracks that occur in the inlet guide vanes of a jet engine. They used two viscoelastics (ISD # 112 and ISD # 830) to share and broaden the useful temperature range of the damping layer. The damping layers function in bending. The specific objective is the extension of the fatigue life of the vanes by a factor of ten or so in order to reduce the annual repair cost of the IGV cases to a much lower figure.

The damping design is good and it is working. In addition to damping, there is a tough problem of viscoelastic survival during short periods of high temperature and of there provably being no volatile or decomposition products given off that would cause blisters to form within the laminate and of non-destructive examination of all the damping wraps for internal disbonds after manufacture and again after application.

The wrap is shown diagrammatically in this visual. Since integrity of all adhesive bonds is so vital the aluminum is phosphoric acid anodized and primed to present the best possible bonding surface. The viscoelastic is put through a devolatilizing heat cycle to insure that all possible volatile materials have been driven off. The lamination of the various layers is performed in such a way as to insure that there is no trapped air between the layers.

Non-destructive examination and approval of 100% of the wraps is obviously a vital point, for if only one out of 22 on an IGV case fails,

FIGURE 1
Sketch of A World Trade Center building damper.



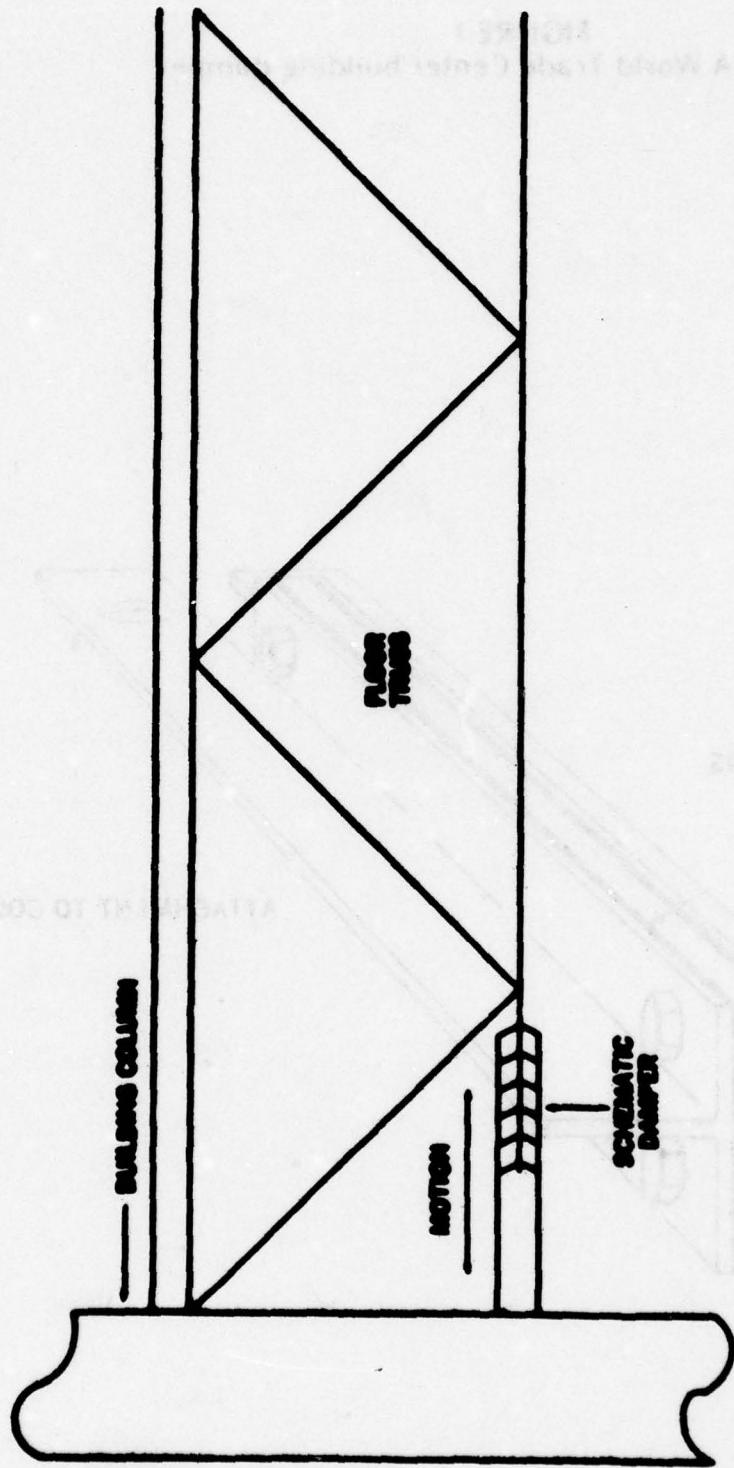


FIGURE II
Schematic drawing of counting unit

the case has to be taken out of service for repair or replacement of the wrap and the extended operation life objective is lost. We examine each wrap after manufacture by means of a ten minute exposure at 300°F. followed by charting of the blisters that might form on a transparent overlay sheet.

3M is challenged by the production and test requirements of this application. They require the most sophisticated and careful techniques we have ever employed. Their teaching will be important to future Air Force consideration of damping as a design rather than a temporary fix.

The World Trade Center damping application is interesting because the mechanism is viscoelastic shear produced by relative axial movement. Axial movement is especially appropriate where displacement is large such as wind or seismic excitation of structures. The W. T. C. engineers needed a device that would protect these tall buildings against the "punch" of a once-in-a-hundred-years wind and a device that would reduce and control day-to-day maintenance costs for broken waterpipes, windows and plaster that can result from building vibrations in average winds.

A damping unit is composed of three steel elements : 2 tees and 1 bar between whose broad faces is epoxy bonded two ISD # 110 viscoelastic layers. One end of the bar extends beyond the bonded area for attachment to the bottom chord of the floor truss while the ends of the 2 tees extend in the opposite direction and are bolted to a seat on the column.

NO

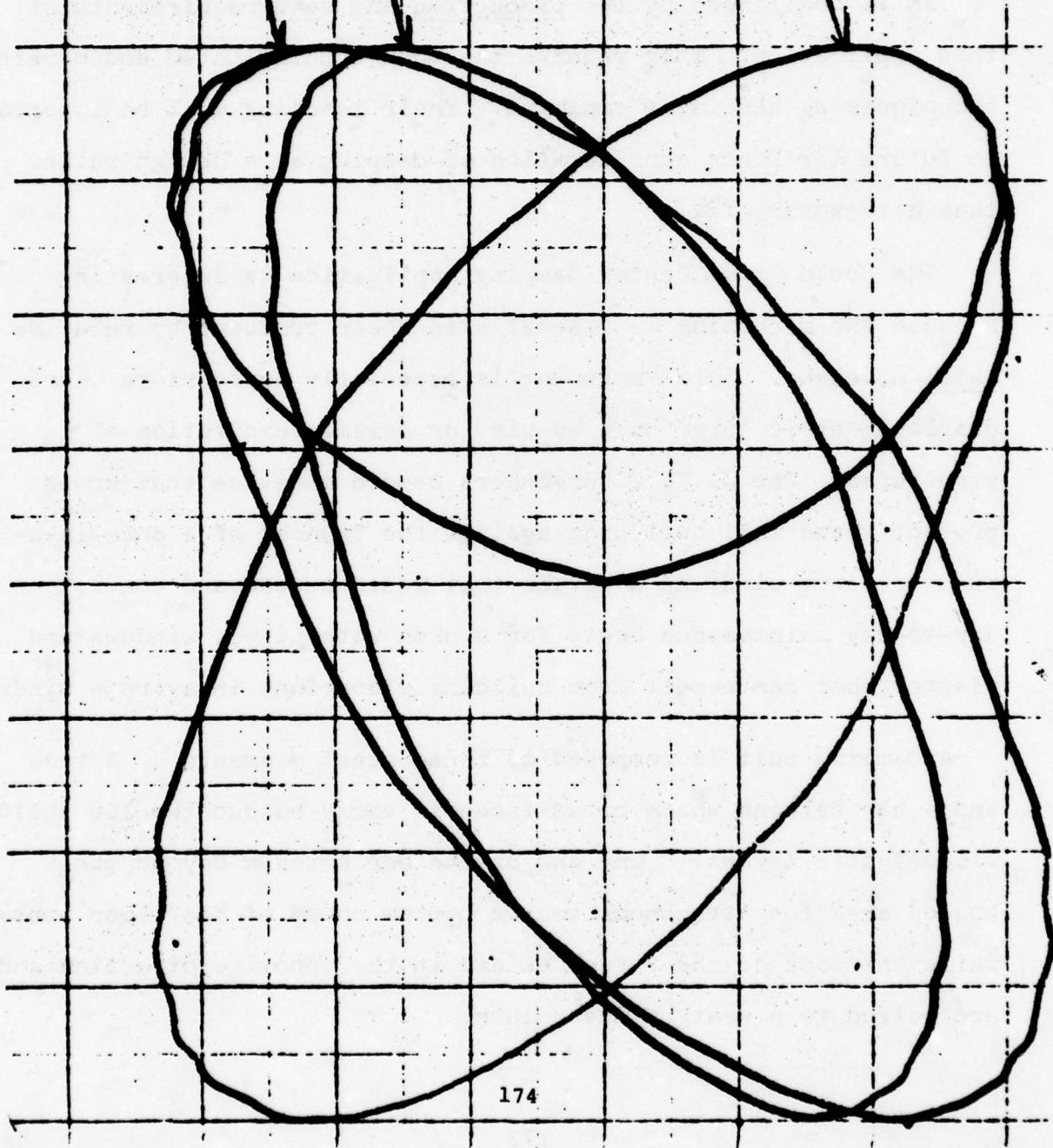
SUBJECT

3m

Two of the
frequencies
Loudness
Tone
Acoustics

0.75

0.25



NATURAL AGING STUDY OF ISD # 110 IN W. T. C. DAMPERS

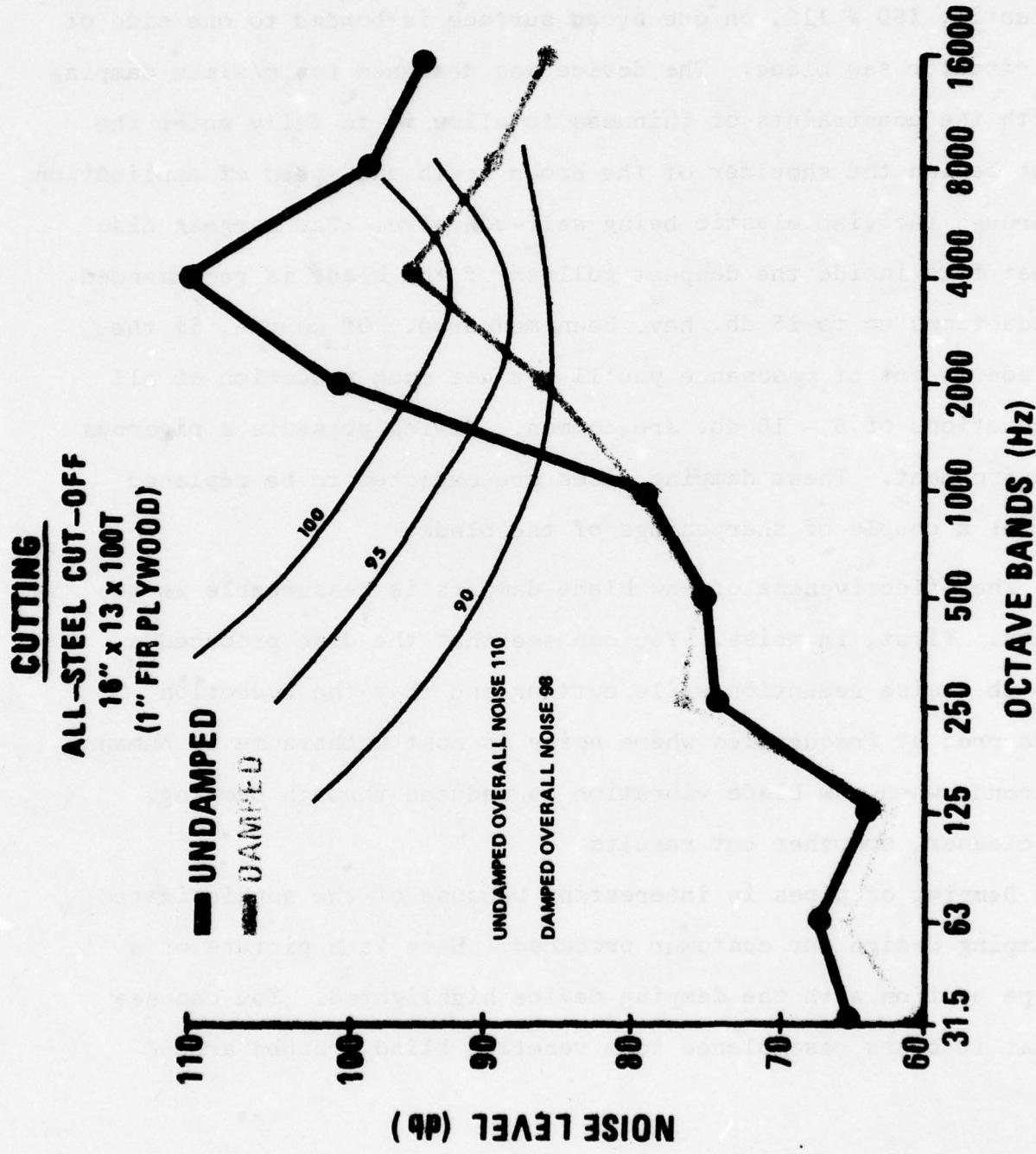
YRS.	ALLOWABLE USEFUL MINIMUM		ACTUAL AVE. VALUE		ALLOWABLE USEFUL MAXIMUM		LOSS FACTOR	STIFFNESS	STIFFNESS	LOSS FACTOR
	STIFFNESS	LOSS FACTOR	STIFFNESS	LOSS FACTOR	STIFFNESS	LOSS FACTOR				
0	6846	.738	11357	1.32				19154		---
6	6359	.655	11190	1.46				21042		---

When the building is excited at its natural frequency by a gust of wind the damper elements go in and out like a shock absorber. The elements move only a few thousandths of an inch. In so doing the viscoelastic material absorbs energy from the building and dissipates it as heat. The building comes rapidly to rest.

Dampers were tested for loss factor, stiffness, fatigue and ultimate strength. The loss factor and stiffness were calculated from hysteresis loops such as this and the change in these (their fatigue loss) was also calculated from a hysteresis loop but after 100 cycles of maximum deflection and return to original temperature. The rise in temperature during fatiguing was 3 - 4°F., enough, as you can see, to have a significant effect.

The loss factor and stiffness tests were repeated at the end of six years. No greater than a 10% reduction in loss factor nor a 10% spreading of the stiffness range from both ends was allowed. You can see that the provision was handily met.

This data is very significant because it is proof of the stability of polyacrylate viscoelastic materials. We have reams of data that shows this stability in other ways; for example, adhesion, but this is the first data that shows the materials are stable in their dynamic properties and safe to use in long term applications. With the exception of saw blade dampers everyone of the applications I will mention has a specific long term aging requirement. Your problems may share this requirement also.



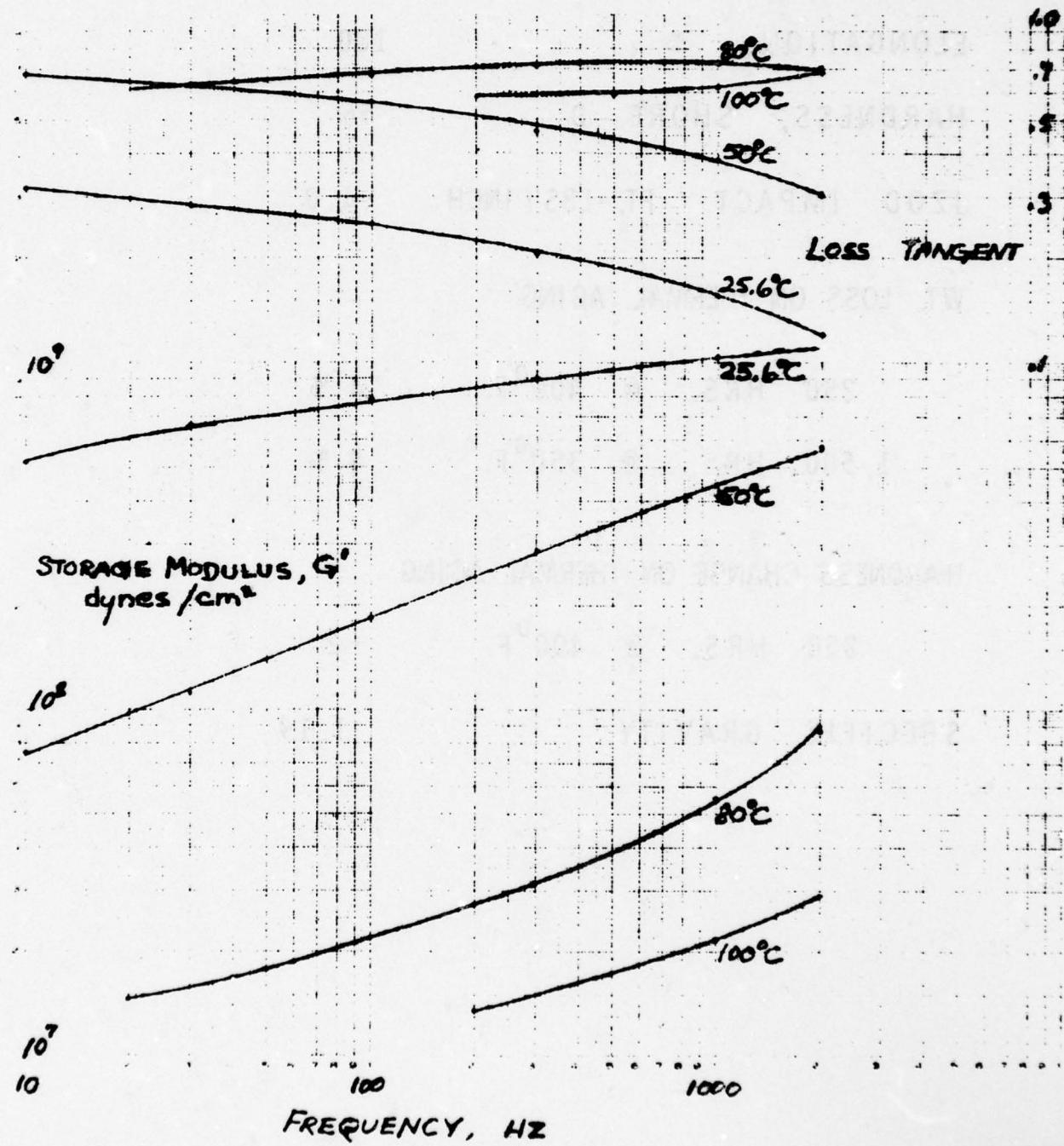
Saw Blade Dampers are worth mentioning briefly because they are a result of federal laws on hearing damage risk creating a market for constrained layer viscoelastic damping. In 3M's expression of such a damping device a 10 mil circular steel doughnut having 2 mils of a room temperature pressure sensitive viscoelastic, ISD # 112, on one broad surface is bonded to one side of a circular saw blade. The device was designed for maximum damping with the constraints of thinness to allow it to fully enter the cut behind the shoulder of the broad teeth and speed of application through the viscoelastic being self-adhesive. The largest disc that fits inside the deepest gullets of the blade is recommended. Reductions up to 15 db. have been measured. Of course, if the blade is not at resonance you'll not get much reduction at all. Reductions of 6 - 10 db. are common. Sawing presents a rigorous environment. These damping discs are expected to be replaced after a couple of sharpenings of the blade.

The effectiveness of saw blade dampers is measureable in two ways. First, in noise. You can see that the disc produced a 15 db. noise reduction while cutting and that the reduction occurred at frequencies where noise is most bothersome to humans. Second, when saw blade vibration is reduced through damping, a cleaner, smoother cut results.

Damping of pipes is interesting because of the sophisticated damping design our customer produced. Here is a picture of a pipe section with the damping device highlighted. You can see that it bears resemblance to a venetian blind wrapped around

POLY(1,4-PHENYLENE TEREPHTHALATE) 1134

DYNAMIC MECHANICAL PROPERTIES OF NPE 1134



PHYSICAL PROPERTIES NPE 1134

TENSILE, PSI 2,500
ELONGATION, % 100
HARDNESS, SHORE D 56
IZOD IMPACT, FT.-LBS / INCH 4.0

WT. LOSS ON THERMAL AGING

250 HRS. @ 400⁰F. 4 %
1,500 HRS. @ 350⁰F. 4 %

HARDNESS CHANGE ON THERMAL AGING

250 HRS. @ 400⁰F. +2

SPECIFIC GRAVITY 1.19

the pipe. The staves are square and rectangular sections that vary in size starting at about 1/8" square. The damping treatment is called a discontinuous constrained layer damper. It uses ISD # 112 viscoelastic material between each stave and the pipe. At the lowest frequencies the staves damp the bending vibrations of the pipe. At higher frequencies egg-shaped and twisting modes are significant. The unit mass of the end cross section of a stave is, in fact, a mass mounted on a viscoelastic spring. Each of these vibrates along a radius. Normal shear is introduced into the viscoelastic.

The last application reflects what 3M believes is one of the large markets opening up for engineered damping systems. The application is that of metal laminates for deep drawing and for damping at high temperatures for extended periods of time.

We laid the problem of high damping, long term, high temperature viscoelastic stability on 3 of the polymer labs in 3M. One of them came up with two good answers. This is the one we're going with. Not only is it a good damping material but it possesses excellent stability. We're not metallurgists but we've come to know that deep drawing a laminate will never be more successful than using the equivalent thickness steel in a single piece. As the draw gets more difficult the laminate has an increasingly tough time compared to a single sheet.

There's a great deal to be done in our laboratory and in the field. We've chosen to limit our field activity to a few accounts, primarily in the diesel engine industry. We expect that this viscoelastic will retain its good damping qualities for up to 10,000 hours at 200°F., the approximate major overhaul time for these engines.

Thank you for coming and thank you for giving 3M this opportunity to share briefly with you our technology, applications and excitement about the bright future for viscoelastic damping.

DEVELOPMENTS IN DAMPING TECHNOLOGY

**E. J. O'Keefe
Specialty Composites Corporation
Acoustics R&D
Newark, Delaware**

DEVELOPMENTS IN DAMPING TECHNOLOGY

Ed O'Keefe

Specialty Composites Corp.
Newark, DE
19713

Application methods and utilities for several types of damping systems currently in use are discussed. The basic molecular mechanisms for vibrational energy dissipation are described as well as some methods for improving performance over wider temperature and frequency ranges. Several new polymeric materials are introduced which show good potential for use as very wide temperature range dampers. Some new products which are an outgrowth of these technological advances are presented along with representative damping data.

DEVELOPMENTS IN DAMPING TECHNOLOGY

I. Background

Damping materials have been used in the control of noise for a number of years. The largest consumption of damping materials being used for public and private transportation vehicles. The materials usually used are of low quality, but very low cost.

Noise legislation has created a need for more effective damping systems for all types of industrial noise sources. The basic damping methods are compared in Fig. 1. Noise reductions are oftentimes easily obtained and can relate directly to the increase in composite loss factors. For instance, if the source is a vibrating plate, an increase in loss factor, z , from .01 to .1 will reduce the radiated noise level by 10dB.

Aerospace interest in damping resulted from the need to reduce vibrational stress in critical engine or structure members, thereby increasing component life, increasing reliability and decreasing maintenance costs. More emphasis is now being placed on damping for noise control, both in military and privately owned aircraft.

II. Standard Damping Systems

There are in current use, many varieties of materials and application designs. The following samples illustrate some of the commercial products which have proven to be most efficient. Choice of a particular material depends on many factors, some of which are cost, weight, loss factor, thickness, application technique, and temperature-frequency environment.

1. Extensional damper - usually are compounded from urethanes, vinyls, asphalts or rubbers. Some have an adhesive layer for quick application and some recommend epoxy adhesives. At the temperature of interest the material should have an elastic modulus of at least 1% of aluminum, and a material loss factor of 1 or greater. The damping thickness should be at least as thick as the base metal thickness. The composite loss factor of the combination plate and damper, Z_c , is proportional to these factors and in simplified form can be expressed as:

$$Z_c \approx \left(\frac{Z_2}{E_1} \frac{E_2}{E_1} \right) \left(\frac{T_2}{T_1} \right)^2$$

where Z_2 = Loss factor of damping material
 E_2 = Young's modulus of damping material
 E_1 = Young's modulus of base plate
 T_2 = Thickness of damping material
 T_1 = Thickness of base plate

These materials are sometimes available in a spray on solution which facilitates application on uneven surfaces.

2. Spaced Extensional - Advantage of spacer is in increasing strain of the outer damping layer. Helps to reduce both weight and cost.
3. Constrained Dampers - This construction places inner layer in shear. These systems are usually lighter and more efficient than extensional dampers, but tend to be more expensive (See Fig. 2).
4. MPM System - A premanufactured constrained damping laminate which will obtain very high z's. The inner layer is designed to optimize workability. It can be welded or drawn in similar fashion to conventional steel sheets. A preformed MPM system is often less expensive and easier to fabricate than trying to apply thick damping treatments. In addition, z can be much higher in the preformed system.
5. Tiger System - for thick plates, application of extensional damping treatments or prelamination of MPM layers is unfeasible. The best damping technique is to apply a thin adhesive damping material, then fasten a backup plate to the adhesive to form a constrained layer system. This technique can minimize added weight while maintaining adequate z's.

II. Design Criteria for Improved Damping Materials (see Fig. 3)

Until recently, the materials commonly used for damping were polymer compounds which had glass transition temperatures in the ranges of product application. In the glassy region, the molecules are not free to move and cannot dissipate mechanical stresses. In the rubbery region, the molecules move too easily and cannot absorb sufficient mechanical energy. In a relatively narrow transition region, both the material stiffness and dissipation factors are high enough to absorb

and reduce vibratory energy. The loss factor is a measure of the energy dissipation capacity of the material. It is defined as the ratio of loss modulus to storage modulus of the material. Storage and loss moduli for a broad temperature damping material are shown in Fig. 3.

The loss modulus is sensitive to frequency and strain as well as temperature. The frequency dependence arises from the time required for the polymer to "relax" from a cyclic strained condition. The strain level dependence results from increase molecular and filler interactions and softening due to polymer weakening. These factors must be considered when specifying material properties since standard test methods do not always correspond to actual acoustic environments.

The dissipation factor has been associated with several mechanisms. In the transition region the molecular groups can move with an additional degree of freedom, namely the rotational. If the applied stress occurs in a frequency region in which the molecular groups can couple with a moderate phase shift in strain response, then the vibrational energy will be dissipated. The loss factor in this region relates directly to the number of molecular groups able to absorb the applied stress, and the phase shift between stress and strain.

Beyond the frequency and temperature region of material transition, energy dissipation is explained in terms of molecular friction. The long chain molecules of the polymer backbone are coiled and intertwined. When the material is strained the molecules bend and slide, dissipating energy. This mechanism can be relatively temperature insensitive allowing for the possibility of temperature independent damping materials. The key is to start with a polymer backbone which is not temperature sensitive. The inorganic polymers seem to be best for this purpose.

Although some compounds have fairly constant ζ VS temperature characteristics, they usually do not show sufficiently high ζ by themselves. This is often true for the organic materials also. The ζ VS temperature characteristics can be altered through the addition of specific additives which can increase ζ and decrease temperature sensitivity. These fillers are thought to act in two ways. First, the fillers can increase the strain in the material, enabling the material to dissipate more energy. Secondly, the fillers can restrict the molecular motion of the molecules, increasing the phase lag between stress and strain and extending the temperature range of damping.

For specific damping problems where very high z and low weight are required, the standard viscoelastic materials may be the only suitable solutions. However, for general applications, where $z = .1$ is required, a broad band damping material would be ideal. Currently available materials can give $z = .1$ for MPM systems of near equal thickness. Some of the materials currently under development show good promise as add-on damping pads. The main advantages for these new materials will be ease of manufacturing, decreasing costs, and less weight. For instance a conventional three layer treatment could be replaced with a single, self adhering constrained layer damping pad.

IV. New Materials for Broad Temperature Range Damping (See Fig. 4)

Low temperature glass transition region rubbers (LT GTR's) exhibit some of the qualities required for good damping. They have sufficient low temperature z's to work well as extensional or constrained layer treatments. At the higher temperatures z plateaus at a reasonably high level, but not quite high enough to work well as an add-on damping treatment. Through the addition of special fillers and variations in the backbone polymer the overall z may be increased to more useful levels.

Inorganic rubbers also show good promise for use as broad temperature range materials. The systems under study have LT GTR's near -100°C , and also have slowly varying z's with temperature. Although this polymer can be used to temperatures exceeding 500°F , it has a loss factor which is decreasing compared with the rubber compound. However, the inorganic polymer has more potential for development due to the nature of its backbone polymer.

The fabrication technique for both the organic and inorganic materials is much more difficult than for conventional low cost dampers. The large mixing and calendering equipment required for these materials could make low volume quantities economically unattractive. However, there is no method which could attain such consistent z's unless multiple treatments were used, an alternative which is probably more expensive.

V. New and Developing Damping Systems (See Fig. 5)

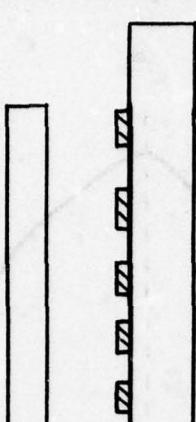
These curves illustrate the damping characteristics achievable with currently available materials. The top graph is data for current products. The room temperature

pad represents a breakthrough in cost more than technology. The high temperature composite is the first material exhibiting both high loss factor and broad temperature range in a single layer damping material, and has the added attraction of being a self adhering composite.

The middle curve is representative data for MPM type systems where moderate damping is satisfactory, but where a very broad temperature range is required. It is expected that the overall z 's of these composites will increase as optimum polymer formulations are developed.

The bottom curve shows the relatively poor performance of add-on treatments which have broad temperature characteristics. These systems will also show improvement as advances in polymer chemistry optimise their properties. Both extensional and constrained layer materials are under development for this class of add-on dampers.

BASIC SYSTEM TYPES

<u>Constrained, Extensional</u>	<u>Constrained MPM</u>	<u>Tiger System</u>
<p>Applied after component fabrication Used for thin metal Thicknesses .020" - .060"</p> 	<p>Preformed before component fabrication Used for moderate metal Thicknesses .050" - .250"</p> 	<p>Applied after component fabrication Used for thick plates Thicknesses .250" - 1.0"</p> 

191

Thickness Ratios 1/3:1 1.5:1 1:1 .5:1

Moderate Damping:
Low Cost
Low Weight

Thickness Ratios .08-.20 .1 - .5

Moderate Damping

Thickness Ratios .5:1

FIG. 1

Commercially Available Systems

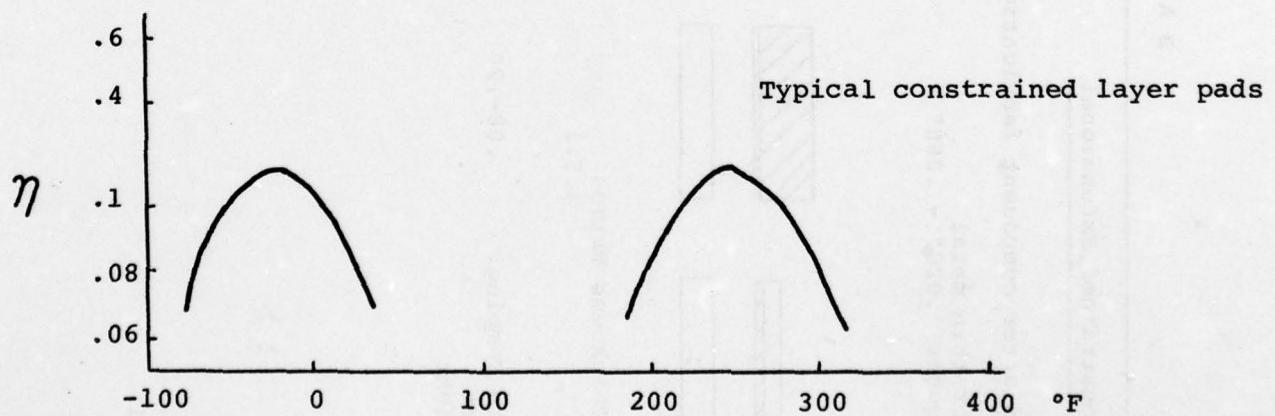
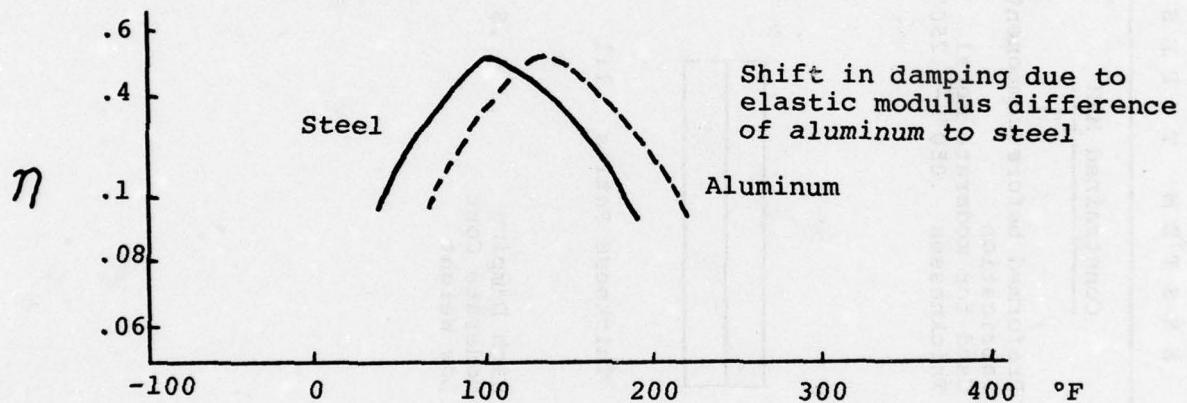
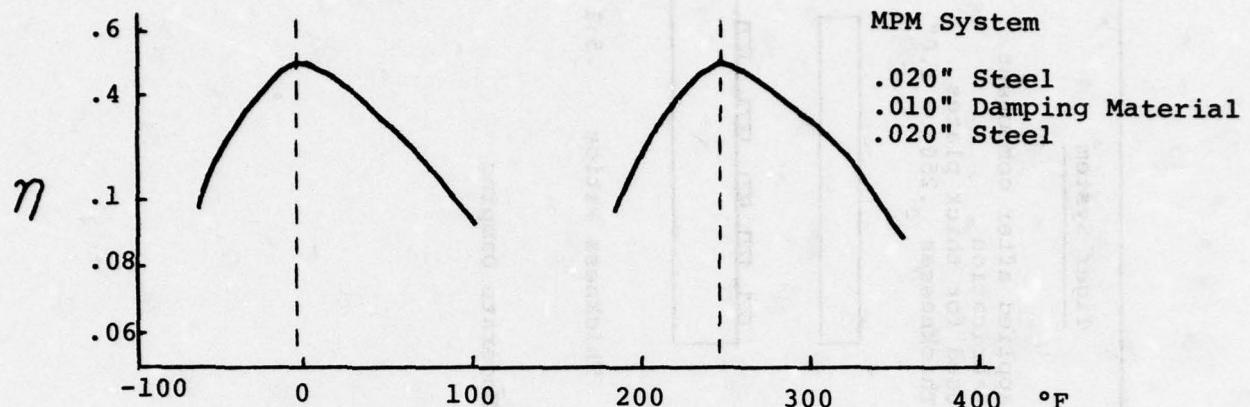


Fig. 2

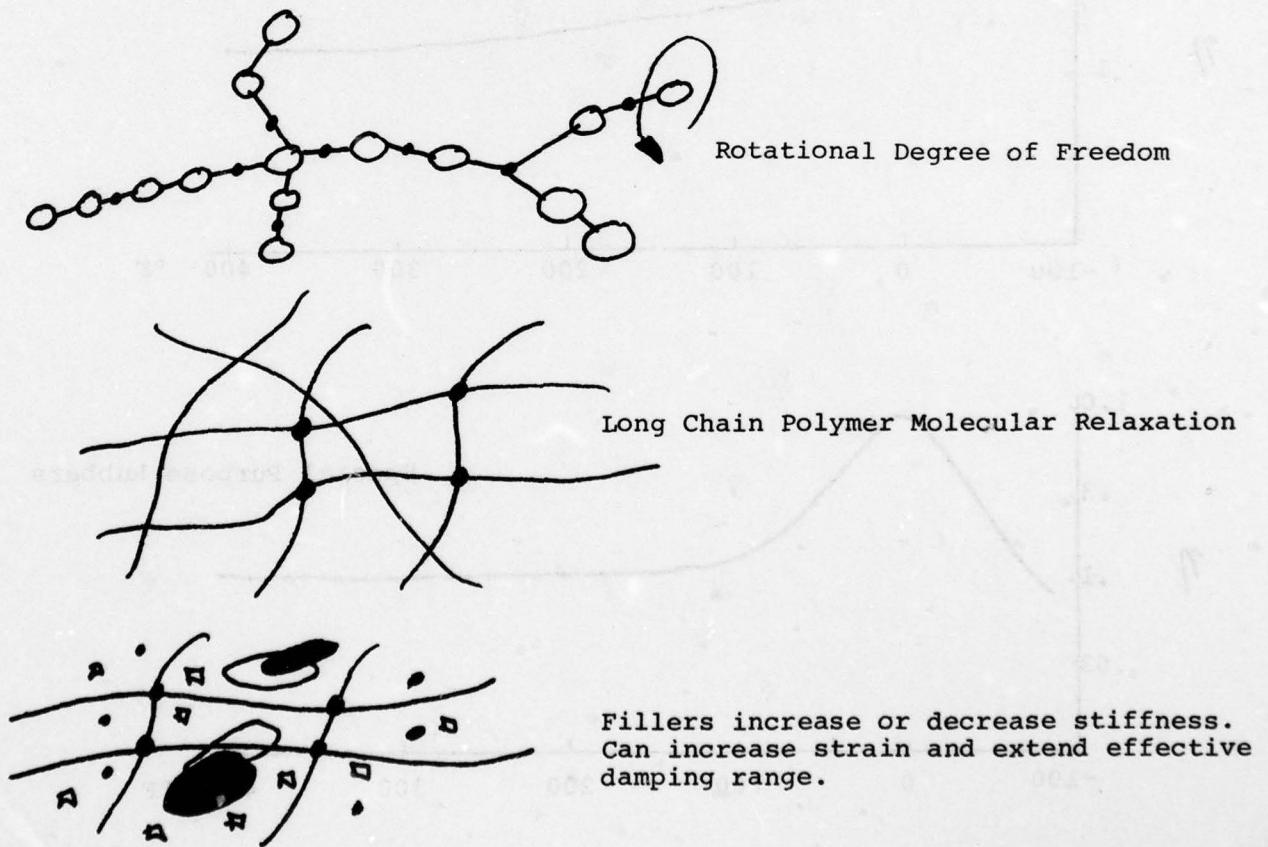
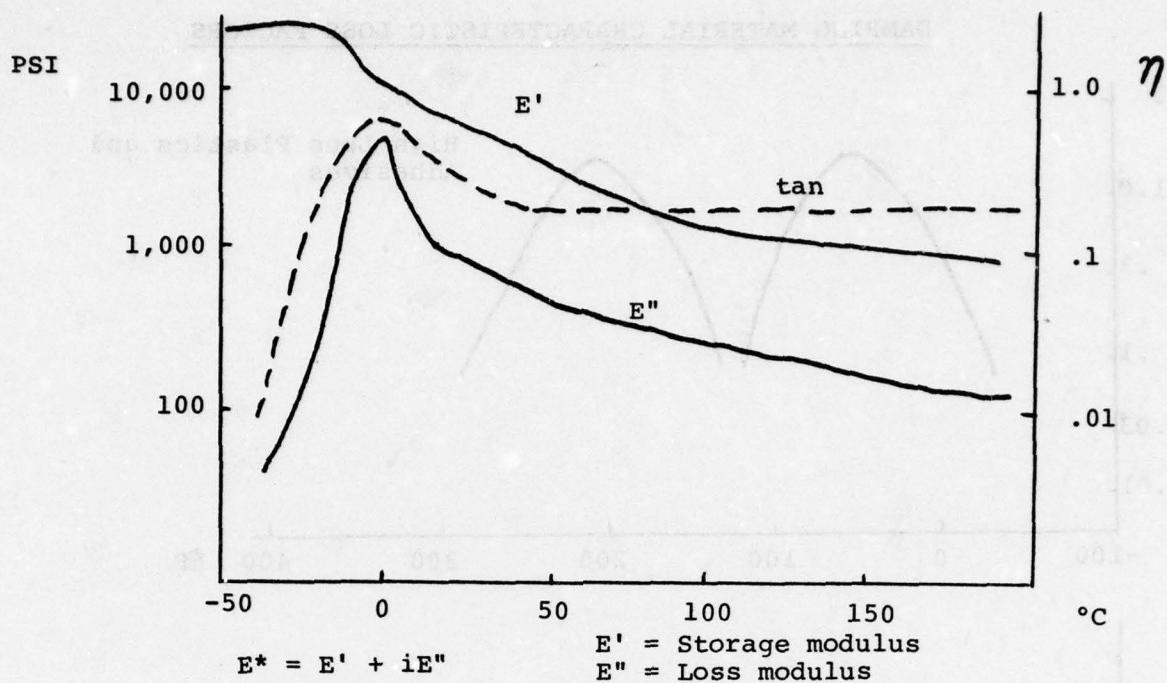


Fig. 3

DAMPING MATERIAL CHARACTERISTIC LOSS FACTORS

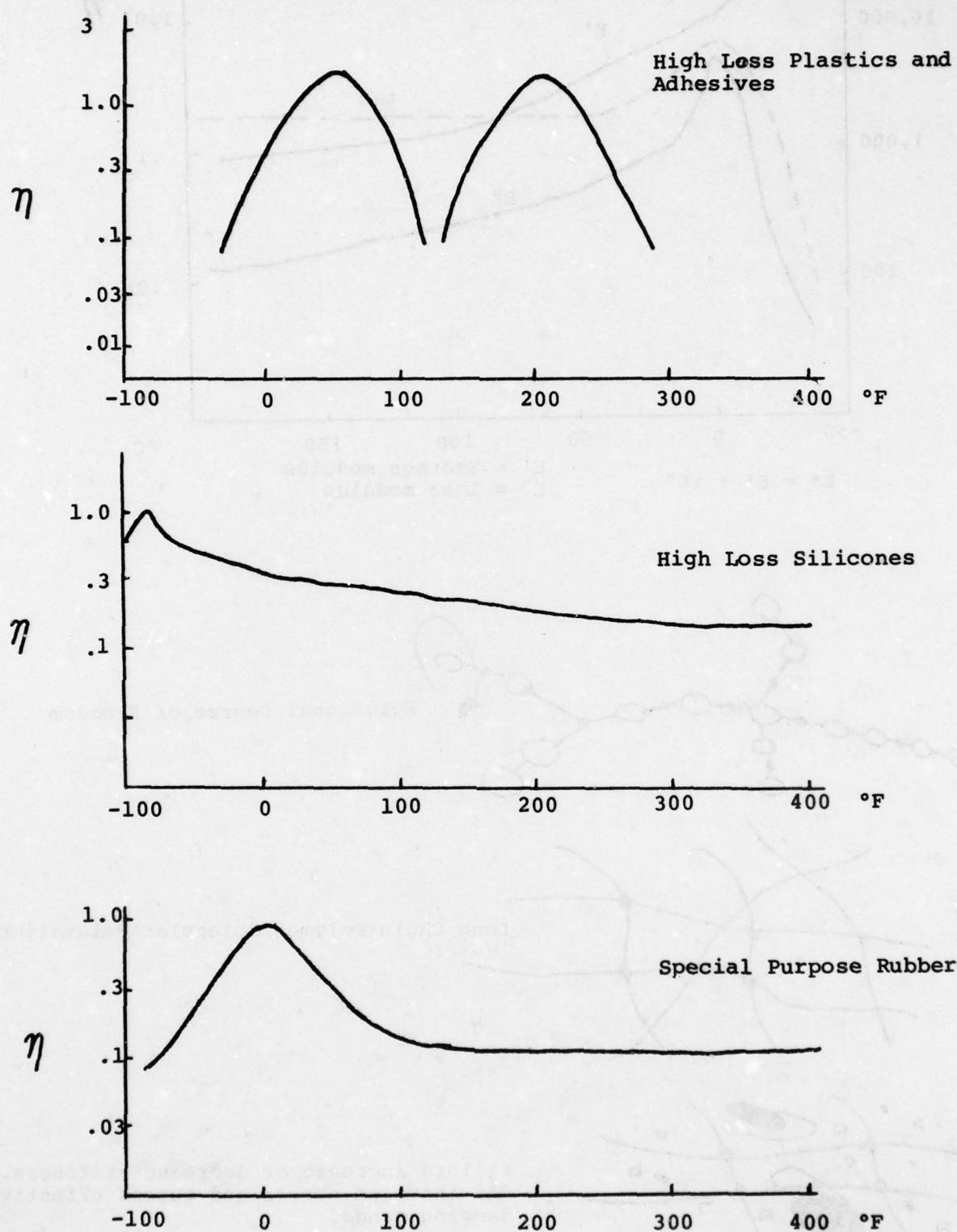


Fig. 4

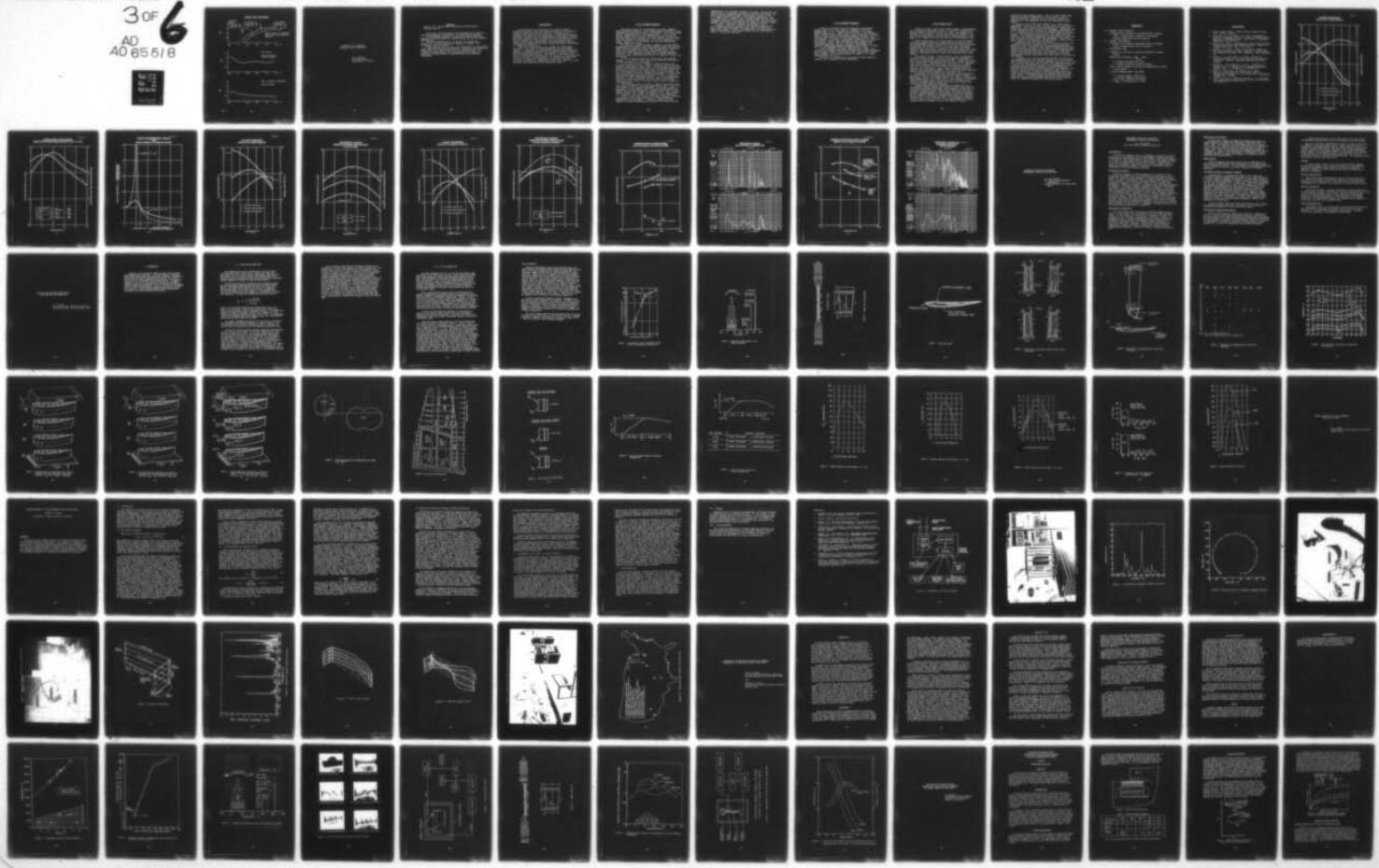
D-A065 518 AIR FORCE FLIGHT DYNAMICS LAB WRIGHT-PATTERSON AFB OHIO F/G 11/9
CONFERENCE ON AEROSPACE POLYMERIC VISCOELASTIC DAMPING TECHNOLO--ETC(U)
JUL 78 L ROGERS

NCLASSIFIED

AFFDL-TM-78-78-FBA

NL

3 OF 6
AD A0 65 518





SYSTEMS UNDER DEVELOPMENT

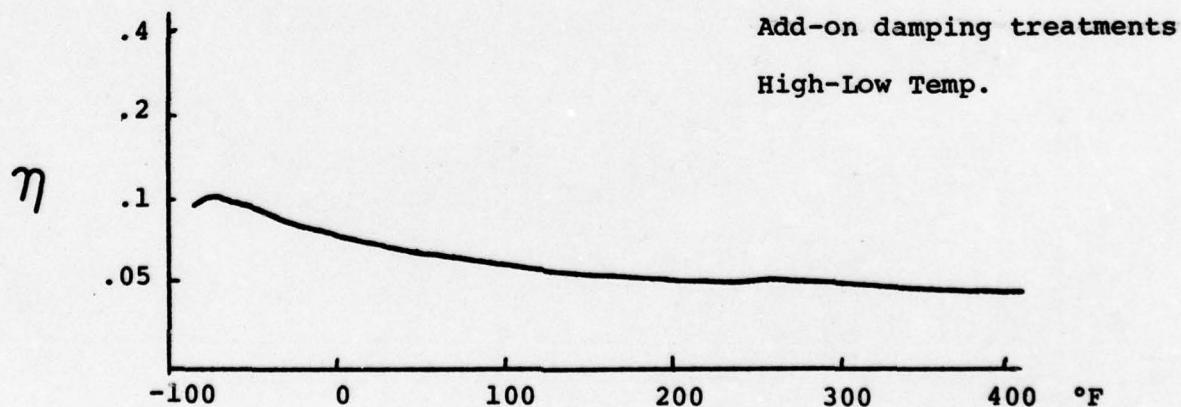
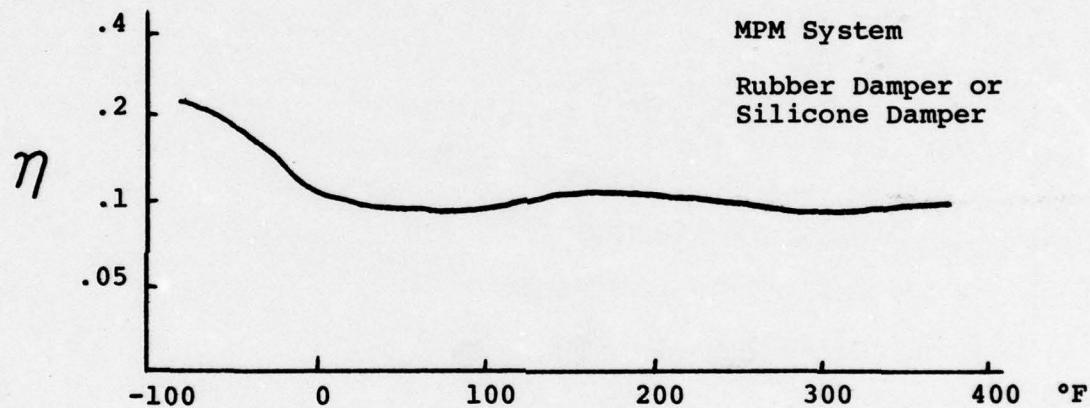
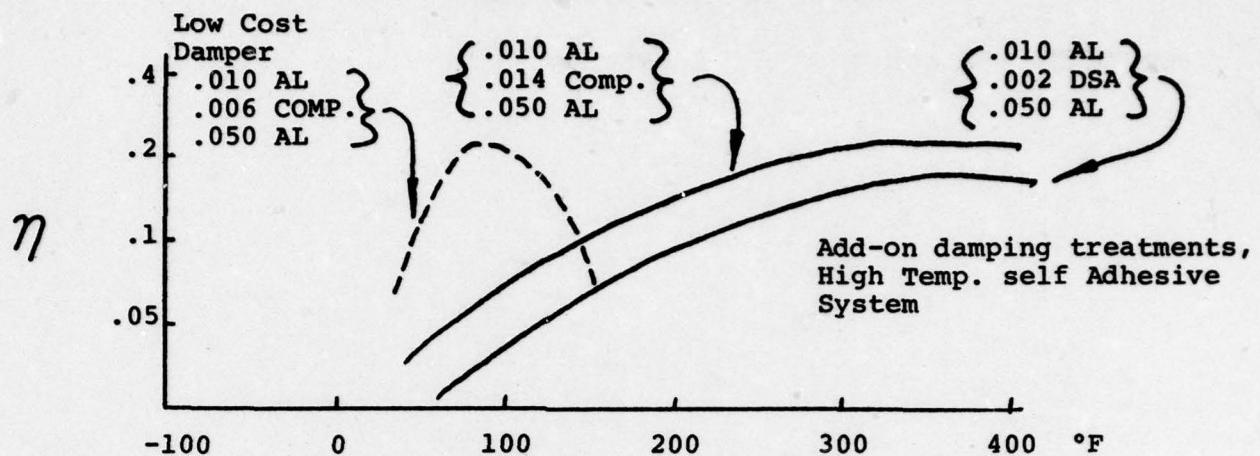


Fig. 5

**SELECTED E-A-R DAMPING
MATERIALS AND APPLICATIONS**

**E. H. Berger
EAR Corporation
Indianapolis, Indiana**

ABSTRACT

Berger, E.H. (E-A-R® Corp.) Selected E-A-R® Materials and Applications.

Three basic E-A-R® materials are discussed with regard to material properties, application, and experimental results.

C-1002 Isodamp® material is useful for constrained layer damping, vibration isolation, impact absorption, and low rebound applications.

C-2003 Exodamp™ material is useful for extensional damping and for constrained layer damping in thicker (1/8" or greater) steel structures.

C-3002 damping foam is useful for extensional or constrained layer damping of thin aluminum systems, especially when additional weight due to the damping material is a consideration. An interesting application is for constrained layer damping of electronic circuit boards to damp both board and component resonances.

INTRODUCTION

E-A-R® Corporation specializes in producing energy absorbing materials that find wide application in the related fields of noise and vibration control. Although we are probably best known for our E-A-R® Plug, a foam insert hearing protector, we would like to concentrate our discussion today on our other products which are designed for noise control at the source instead of at the receiver. We will consider only material properties, applications, and experimental results, since earlier speakers have amply covered the theory and effects of damping and isolation.

Today the E-A-R® product line consists of three basic materials - two types of polymer materials and one foamed version. Utilization of the materials extends from structural damping to occupant protection and includes vibration isolation and low rebound applications. Heretofore our energies have focused on industrial applications and thus much of our available data is relevant to such problems. We possess the technology to adjust our material compositions to optimize them for different frequency and temperature ranges and intend to do this through close cooperation with prospective users.

C-1002 ISODAMP® MATERIAL

The first material to be discussed is C-1002 Isodamp® energy absorbing material. This sheet polymer material is also available for injection molding or extruding. It is medium hard (Shore A durometer 60) at room temperature. C-1002 is non-burning (ASTM D 1692-59T) with excellent abrasion resistance and good resistance to water, oils and kerosene, and has a very high loss factor of approximately 1.5 at room temperature at 1 kHz. (See Fig. 1.) In Figure 1 we also see plotted the dynamic moduli for C-1002.

The material properties shown in Figure 1 and the others presented in this report, have been measured using the B&K 3930 Complex Modulus Apparatus and B&K MM 0002 Magnetic Transducers (B&K, 1964; De Matteo and Dudek, 1968; Dudek, 1970). By measuring properties over an approximate 2 decade frequency range and a 50°C temperature range, we have developed superposition graphs from which data such as is shown in Figure 1 can be derived.

C-1002 is ideally suited for constrained layer damping systems. It is easy to work with and can perform very well in systems for which it is optimized.

At E-A-R® we utilize a computer program based on the equations developed by Ross, Ungar, and Kerwin (1959) and more recently summarized by Ungar (1971). This program permits easy prediction of system loss factors given the dynamic properties of the constituents of the three layers of the structure. We have found good correlation between this program's predictions and the performance of real mechanical systems. In Figure 2 we have plotted some predictions for steel / C-1002 / steel and aluminum / C-1002 / aluminum systems. Over a wide temperature range the system loss factors are very high for these thin structures, with values of at least 20% of critical damping at room temperature.

The right hand scale of Figure 2 labeled "Estimated Large Panel Noise Reduction" (and also appearing on Figs. 5 and 7) is not germane to the present discussion. This scale refers to estimates of noise reductions for systems excited by multiple impacts and similar sources and is based on the work of Curtis Holmer (Holmer, 1971; Holmer and Lagace, 1972). These predictions are quite often useful in industrial noise situations.

C-1002 is also well suited for certain vibration isolation applications such as when excitation at system resonant frequencies is unavoidable. In Figure 3 classical single degree of freedom transmissibility curves for C-1002 (at room

temperature) and a neoprene isolator are shown. We see very low amplification at resonance afforded by the E-A-R® isolator, and also of course somewhat higher transmissibility than a less well damped isolator provides at the higher frequencies. But, it is important to remember that a highly damped isolator will circumvent standing wave resonance problems that can occur within undamped isolators at frequencies well above the system's fundamental natural frequency. (Muster and Plunkett, 1971).

Finally, C-1002 has excellent low rebound properties as can be demonstrated by dropping a ball made of C-1002 onto a very stiff, massive surface. Although the C-1002 maintains its shape after impact it will hardly bounce at all (less than 2" from a 6' drop onto concrete).

C-2003 EXODAMPTM MATERIAL

C-2003 is a highly filled and therefore considerably stiffer version of C-1002 (Shore A durometer 94 at room temperature). It is intended for extensional (free layer) damping applications. Like C-1002 it is easy to use and work with. C-2003 is self extinguishing (ASTM D 1692-68), with good abrasion resistance and very good resistance to water, oils and kerosene. In Figure 4, the dynamic properties of C-2003 are illustrated. We see that although the loss factor is lower than that of C-1002, that the Dynamic Young's Modulus is considerably higher, giving a resultant Loss Modulus (the important extensional damping parameter) that peaks at a value of 1.5×10^{10} dynes/cm² at room temperature at 1 kHz.

A well developed and amply verified theory (Ungar 1971) enables us to predict system loss factors for treated structures. As an example, Figure 5 illustrates these results for C-2003/steel systems, with thickness ratios of C-2003 - to - steel ranging from 0.5 to 2.0.

C-2003 is also suitable for constrained layer damping of thicker (1/8" or greater) steel structures.

C-3002 DAMPING FOAM

Finally we come to the E-A-R® damping foams. Our discussion will concern one such foam, C-3002, a 7 lb/ft³ (110 kg/m³) non-burning (ASTM D 1692-59T) closed cell foam. The dynamic properties of this foam at 1 kHz are illustrated in Figure 6. We see that the loss factor of this foam is greater than 0.3 over much of the temperature range and peaks at a value greater than 1.0.

Foams, quite often, on a weight basis, can provide better extensional damping than more dense materials such as C-2003. We have examined C-3002's performance on 50 mil aluminum systems and present the results in Fig. 7. We see that on an equal weight basis of .45 #/ft² (2.2 kg/m²) the foam is much more effective than the C-2003, although it will of course be 16 times thicker. Equal performances for the two materials occurs with about 1/2 the weight per unit area of the foam relative to the C-2003.

The C-3002 is also an ideal material to use in constraint on thin aluminum systems. In Fig. 8 we present experimental data for 8" long, 50 mil thick aluminum bars. We see that 1/4" foam used extensionally performs well giving a system loss factor of at least 0.04. Constraining the foam with a 5 mil aluminum cover plate improves the performance considerably to greater than 0.1, and as high as 0.4 at 200 Hz at room temperature. Covering the C-3002 with a light weight acoustical foam also improves the performance somewhat, thus providing both structural damping and acoustical absorption at the same time.

In Figure 9 we have shown the response of two different 50 mil aluminum bars as measured using the B&K Complex Modulus Apparatus. One bar is undamped whereas the other is constrained layer damped using 1/4" C-3002 with a 5 mil aluminum cover plate. Although the drive levels for the bars were the same in both cases, the graphic level recorder gain was 20 dB greater for recording of the damped bar response.

A particularly interesting vibration problem that was successfully treated using C-3002 foam, involved the protection of airborne electronic equipment from component failure due to vibration induced fatigue. Quite often vibration isolation of aircraft electronics may be insufficient and further measures such as internal damping of the equipment itself are necessary. Due to C-3002's low static stiffness (25% deflection after 60 seconds with 1.5 psi) combined with its high dynamic stiffness and loss factor (see Fig. 6) it is an ideal material to place between layers of printed circuit (PC) boards to form a

constrained layer damped system. The 1/2" thick C-3002 foam contours around the components on the PC board so that it contacts the board itself as well as tending to damp the resonances of the components as they are supported by their leads.

One-half inch C-3002 has a memory, i.e., after being compressed to as thin as .020", it will return to its original dimensions. This provides two easy methods for assembling these constrained layer circuit board systems. Compressed foam can be slipped between PC boards in a preassembled structure - or - a structure can be built by alternately stacking foam and boards. This completed structure will then need to be compressed in a direction perpendicular to the plane of the boards until the foam contours around the components. Using this latter method we constructed a system of board / foam / board / foam / board in the laboratory for testing.

The boards used for testing were 4" x 8 1/2" x 3/32" with integrated circuits, resistors, and a few small capacitors mounted on them. The boards were suspended edgewise with the longer dimension parallel to the ground. String supports were attached at the approximate nodal points of the first flexural mode of vibration of this free - free system. A vibration exciter was attached at one end and a B&K 4344 (2.7) gram accelerometer at the other end on the same side of the board as the exciter.

In Figure 10 we find the measured system loss factors at room temperature for this sandwich system, for a single board treated extensionally on the non-component side with C-3002, and for a single untreated circuit board. The untreated board has a fairly high loss factor to begin with, probably due to its laminated construction and multiply connected components. Nevertheless the treated boards show better loss factors by as much as a factor of ten for the sandwich system. This is further illustrated in Figure 11 where the responses for the single board and sandwich board are compared using the same drive levels. This demonstrates that significant advances in black box design may be possible through the use of damping foams for sandwich construction of PC board systems.

TERMINOLOGY

E' - Dynamic Young's Modulus

- A measure of the material's stiffness under varying load or equivalently a measure of the energy storage capabilities of the material.

E'' - Dynamic Loss Modulus

- A measure of the energy dissipated within the system (such as through heat due to friction).

n - Loss Factor = $\frac{E''}{E'}$

- A measure of the ratio of energy dissipated to energy stored.

- Equivalently defined as $\frac{D}{2\pi U_{\max}}$ where,

D = energy dissipated per cycle

U = maximum potential energy of system

- Thus n can be viewed as the energy dissipated per radian in the system.

z - Critical Damping Ratio = $\frac{C}{C_c}$ where,

C = viscous damping coefficient

C_c = critical damping coefficient

- $n = 2[\frac{C}{C_c}]$; this expression is exact.

BIBLIOGRAPHY

- 1) Brüel & Kjaer (1964). Complex Modulus Apparatus Type 3930. Naerum, Denmark.
- 2) De Matteo, J.A. and Dudek, T.J. (1968). Experimental Study of Measurement Reliability with the Complex Modulus Apparatus - Homogeneous Bars. Lord Mfg. Co., Technical Memorandum 1-68, Erie, PA.
- 3) Dudek, T.J. (1970). Determination of the Complex Modulus of Viscoelastic Two-Layer Composite Beams. *Journal of Composite Materials*, Vol. 4, p. 74-89.
- 4) Holmer, C.I. (1971). Effect of Structural Damping on the Sound Radiated from Impact Systems - A Field Study. Bolt Beranek and Neuman, Inc., Report No. 2106, Cambridge, MA.
- 5) Holmer, C.I., and Lagace, A. (1972). Effects of Structural Damping on the Sound Radiated from Impacted Structures. *American Industrial Hygiene Association Journal*.
- 6) Muster, D., and Plunkett, R. (1971). Isolation of Vibrations in L.L. Beranek (ed.), Noise and Vibration Control, Chap. 13, McGraw-Hill, New York, N.Y.
- 7) Ross, D. Ungar, E.E., and Kerwin, E.M. (1959). Damping of Plate Flexural Vibrations by Means of Viscoelastic Laminae, in J.E. Ruzicka (ed.), Structural Damping, Sec. 3, ASME.
- 8) Ungar, E.E. (1971). Damping of Panels, in L.L. Beranek (ed.), Noise and Vibration Control, chap. 14, McGraw-Hill, New York, N.Y.

Figure 1

**DYNAMIC PROPERTIES
FOR E-A-R® C-1002 (1000 Hz)**

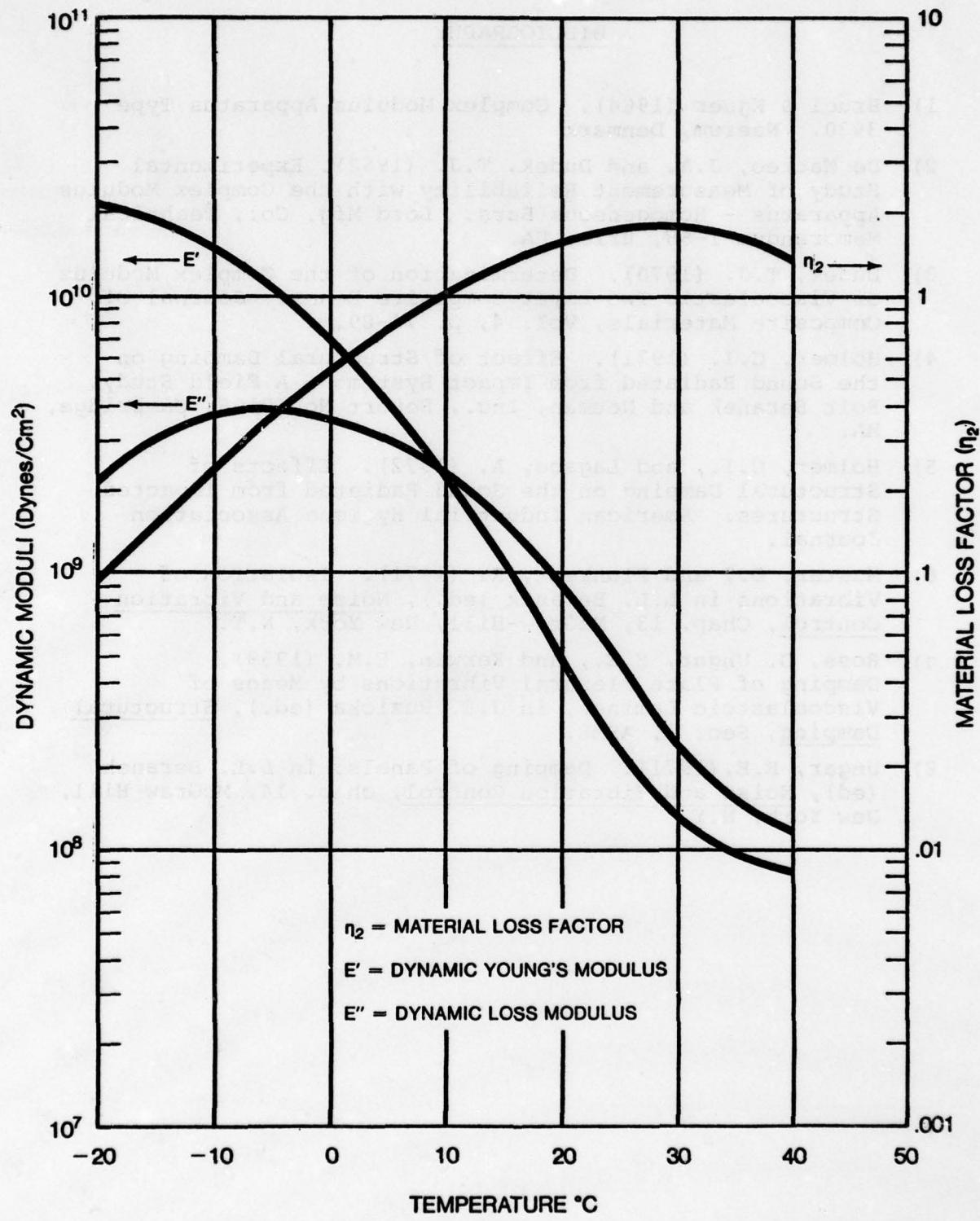


Figure 2

**CONSTRAINED LAYER DAMPING
PREDICTED SYSTEM LOSS FACTORS—E-A-R® C-1002**

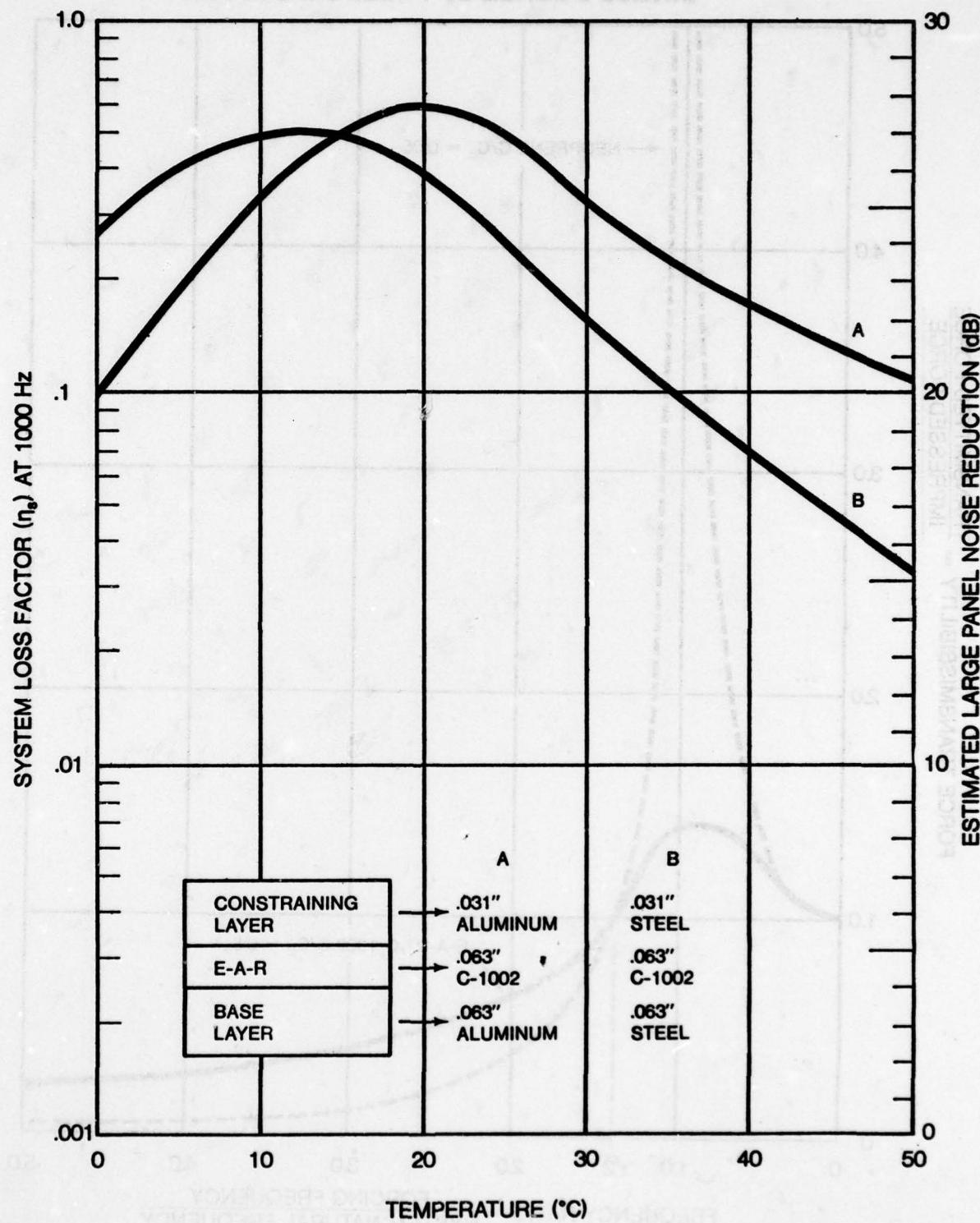


Figure 3

FORCE TRANSMISSIBILITY CURVES
FOR
SINGLE DEGREE OF FREEDOM SYSTEM

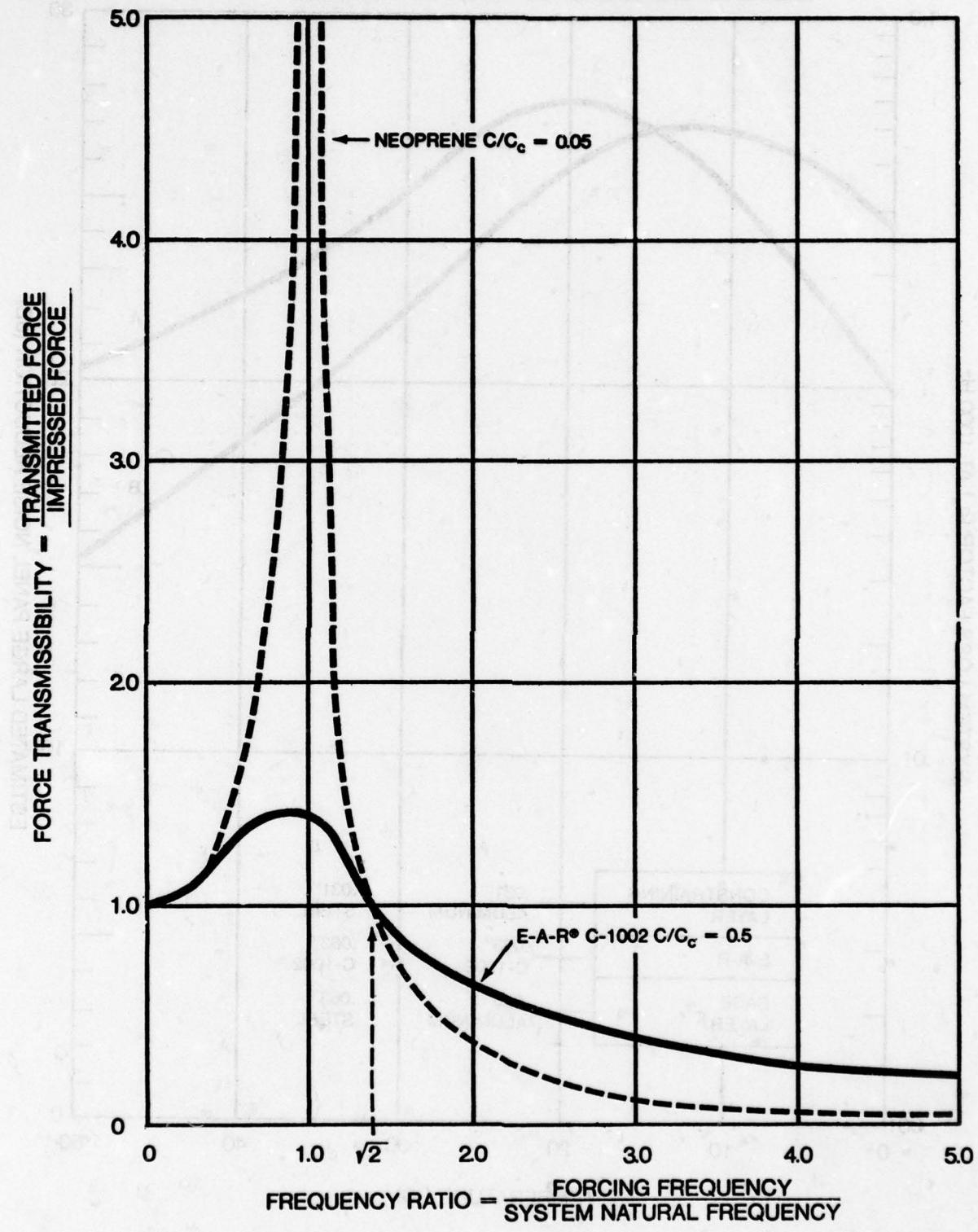


Figure 4

DYNAMIC PROPERTIES
FOR E-A-R® C-2003 (1000 Hz)

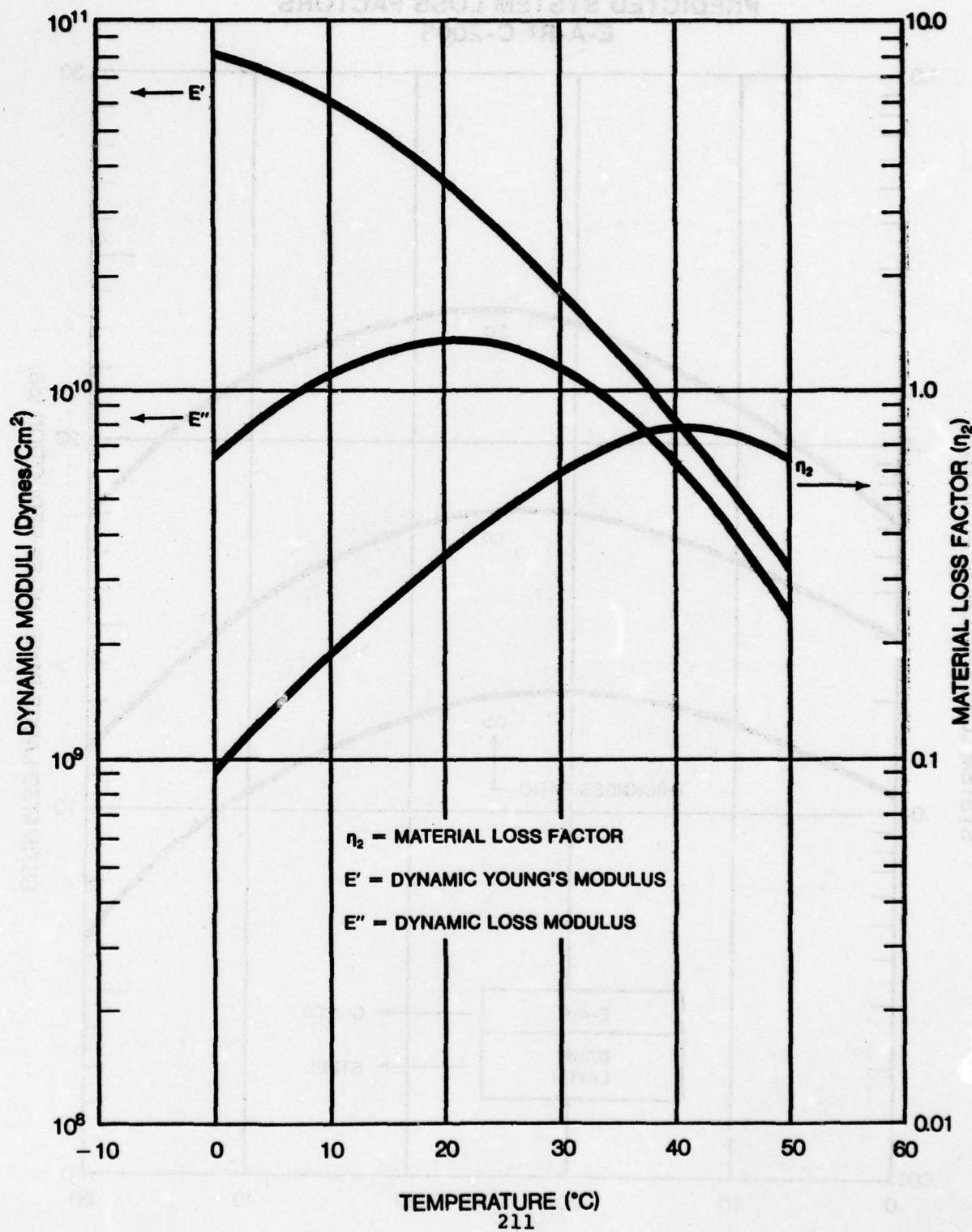


Figure 5

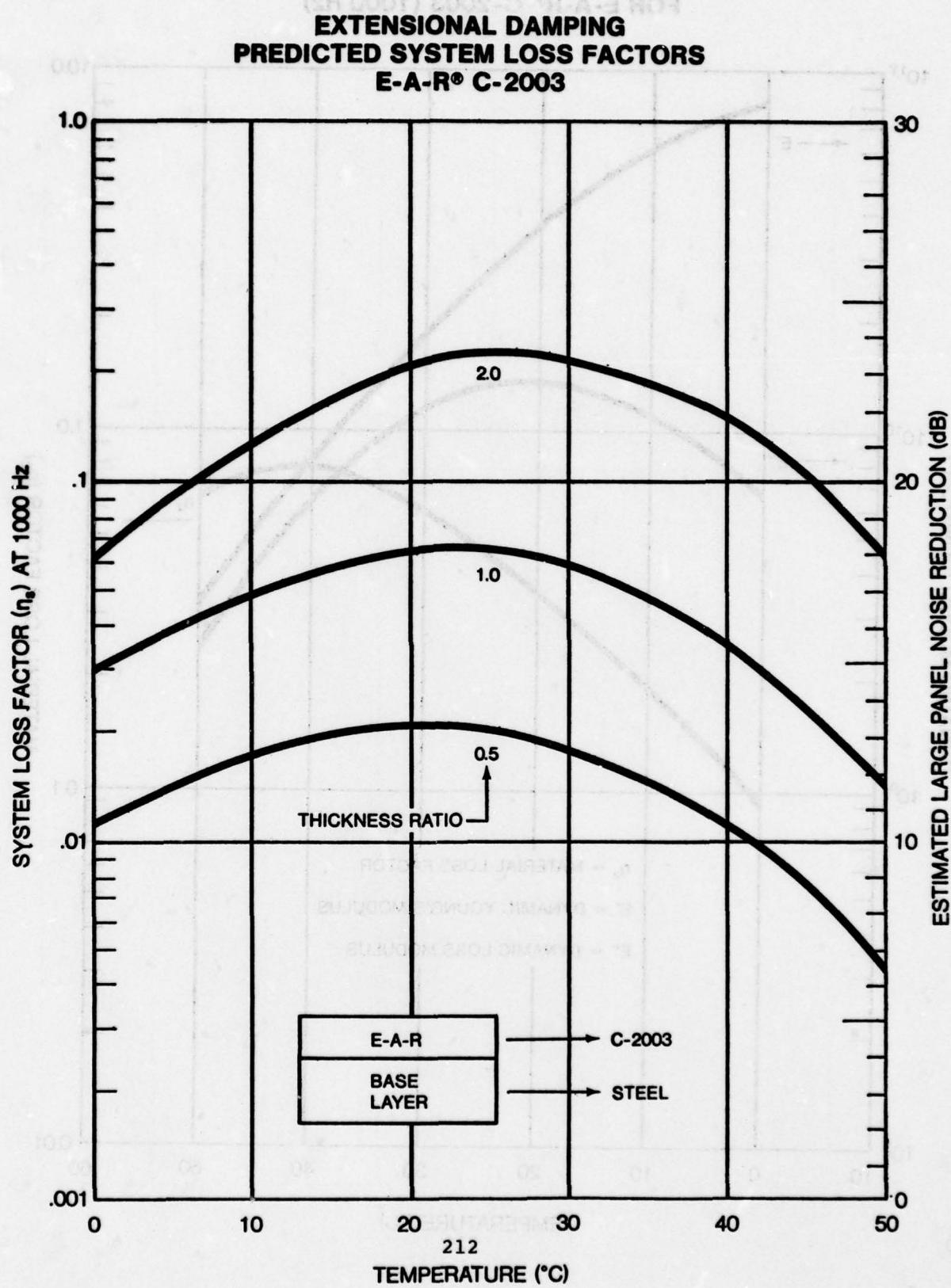


Figure 6

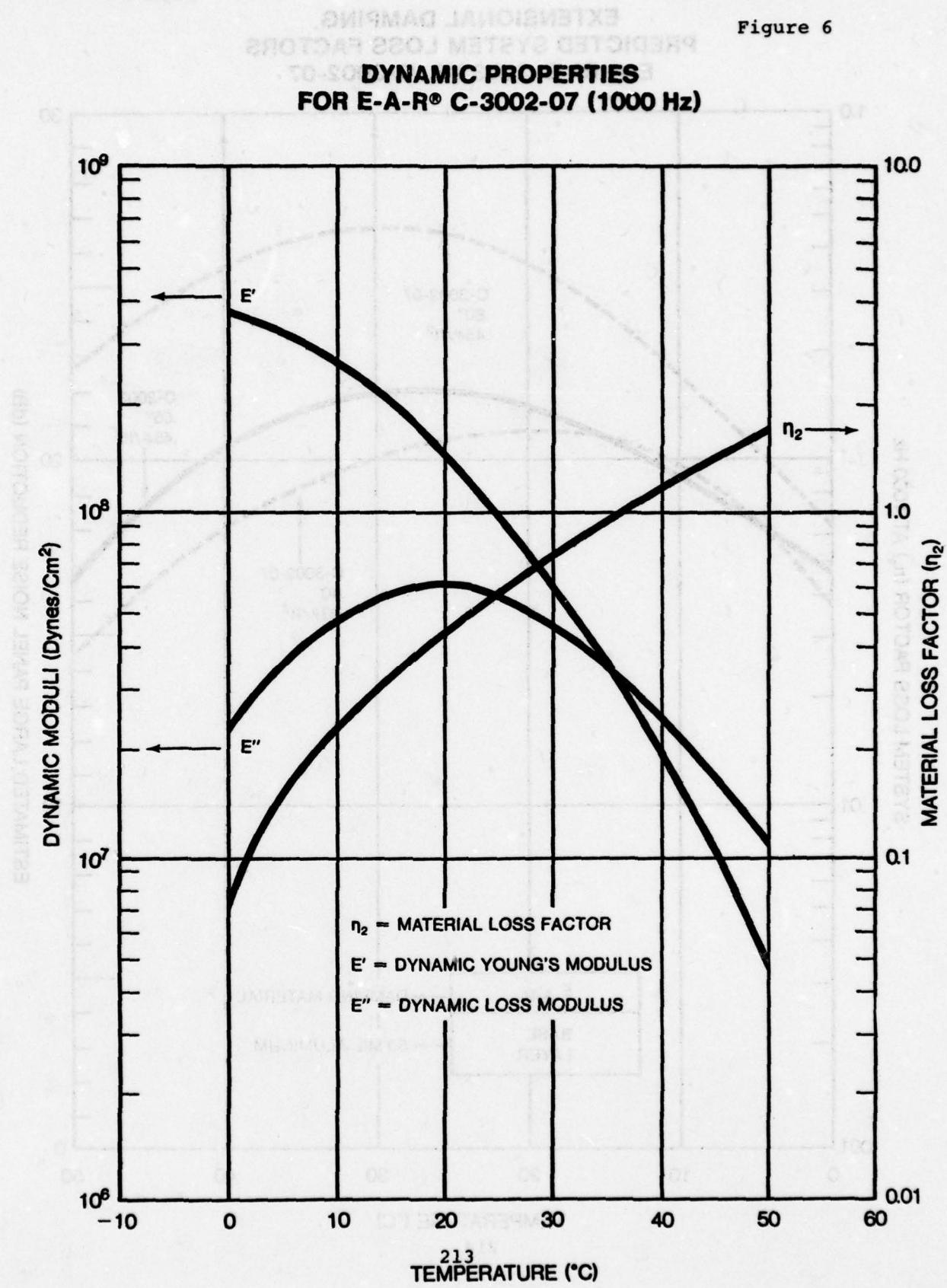


Figure 7

EXTENSIONAL DAMPING
PREDICTED SYSTEM LOSS FACTORS
E-A-R® C-2003 VS. C-3002-07

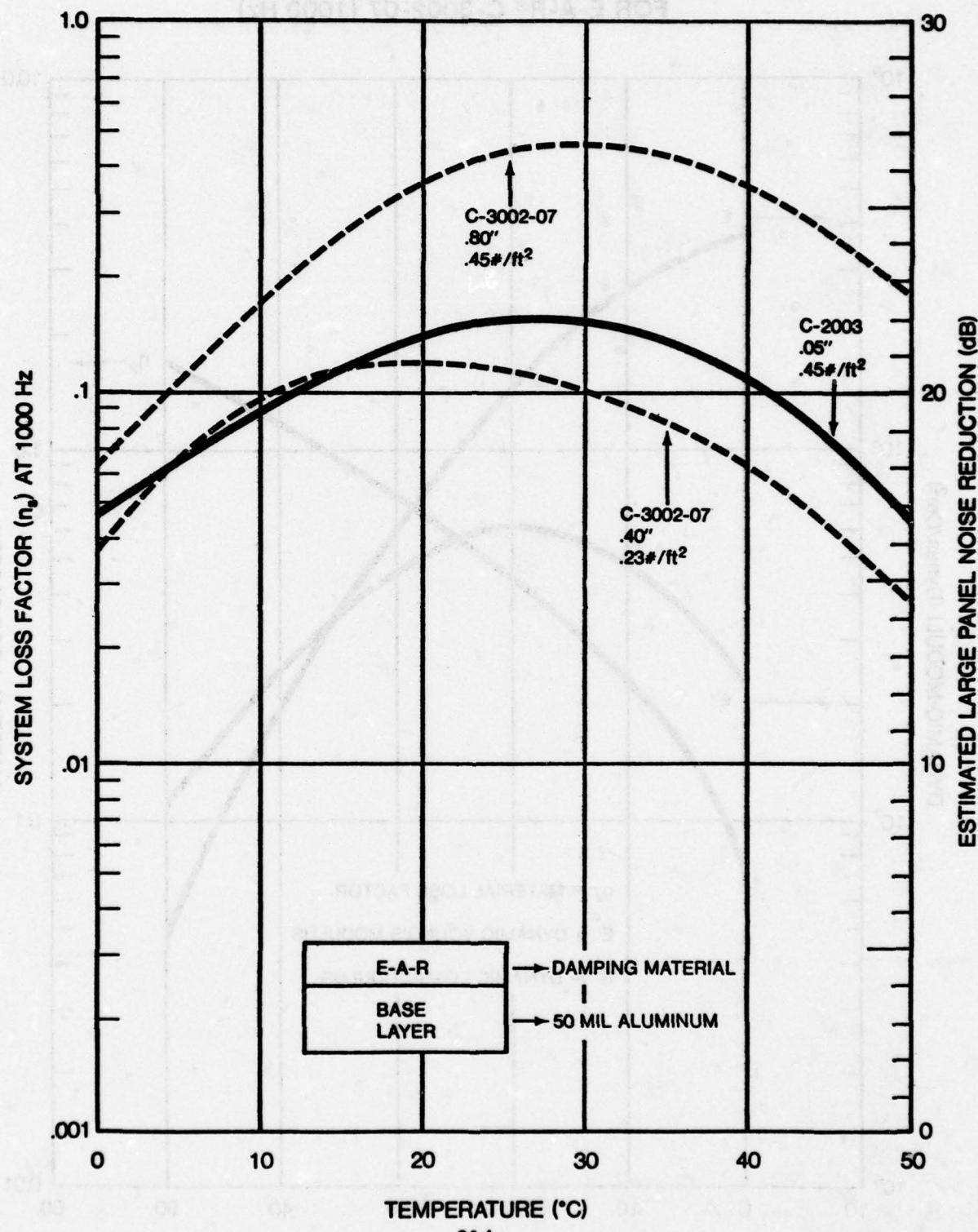


Figure 8

DAMPING 50 MIL ALUMINUM USING
E-A-R® C-3002-07-25 FOAM SYSTEMS

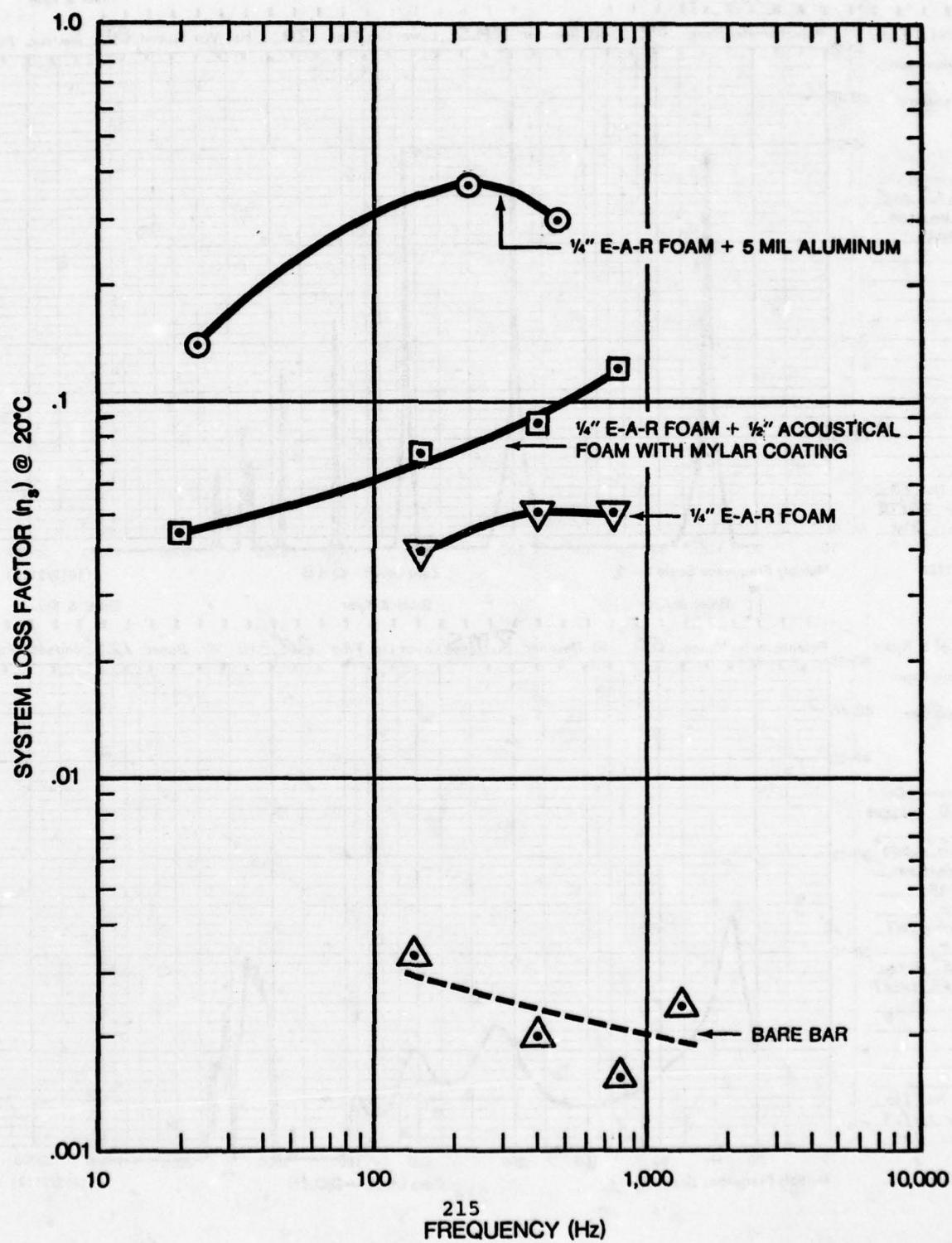


Figure 9

**RESPONSE OF DAMPED
AND UNDAMPED ALUMINUM BARS**

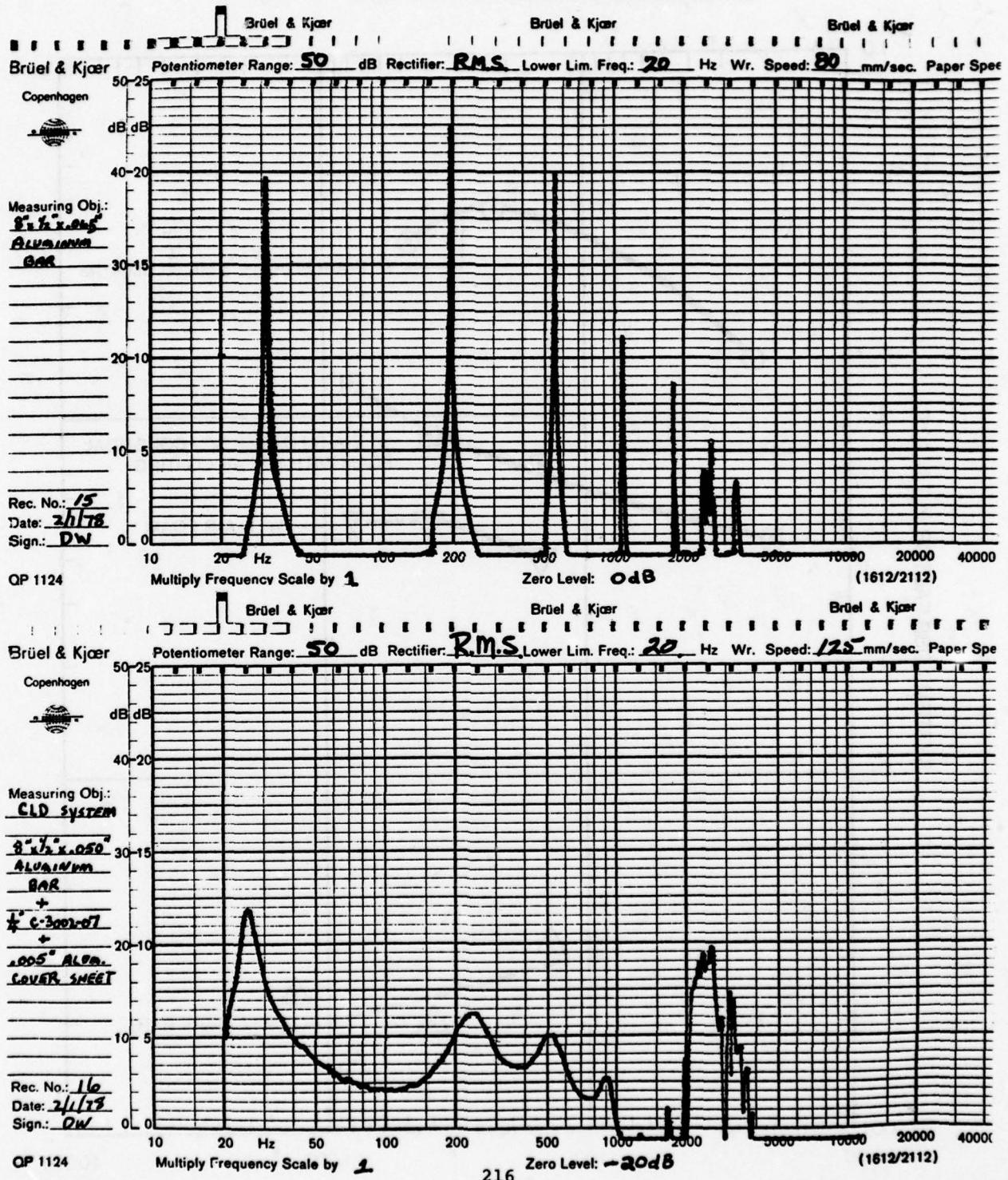
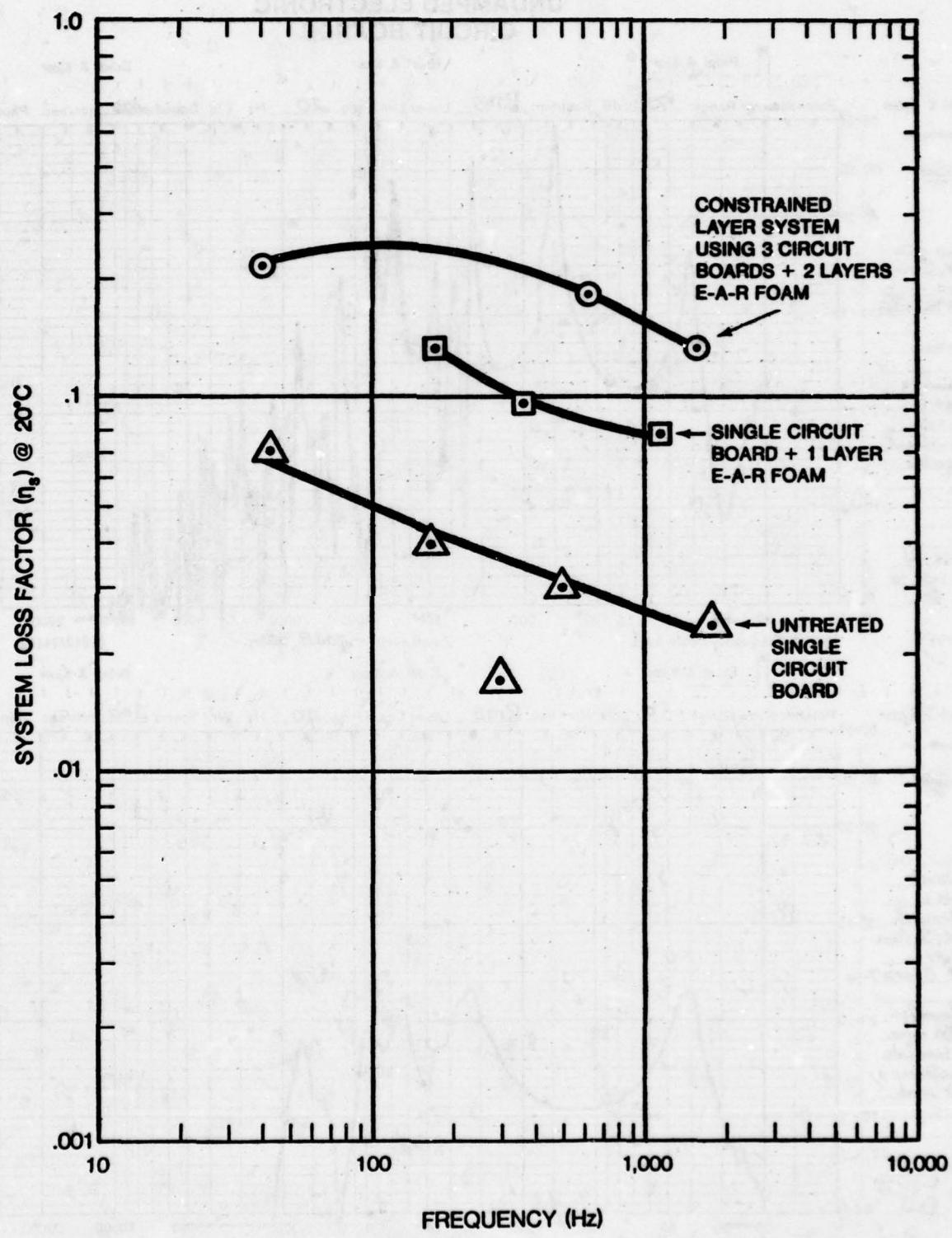


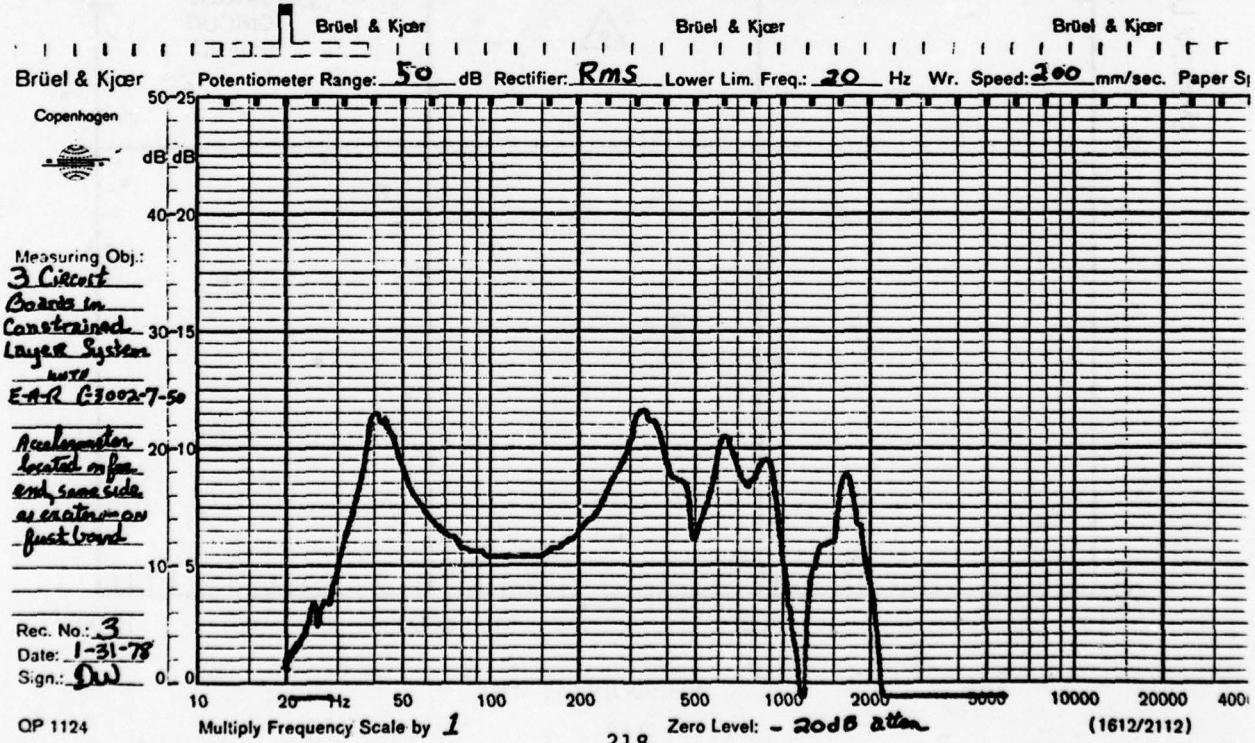
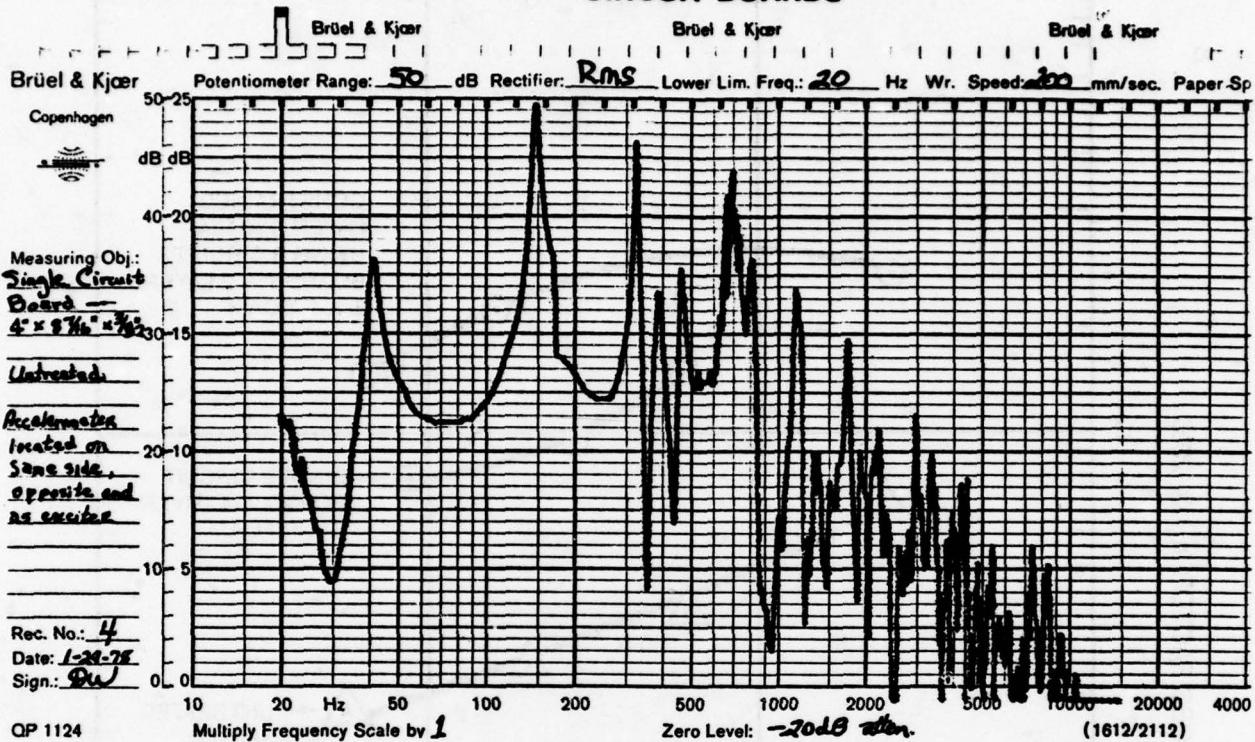
Figure 10

DAMPING ELECTRONIC CIRCUIT BOARDS
USING E-A-R® C-3002-07-50 FOAM



RESPONSE OF DAMPED AND UNDAMPED ELECTRONIC CIRCUIT BOARDS

Figure 11



**NECESSARY STEPS FOR SUCCESSFUL
VISCOELASTIC DAMPING APPLICATIONS**

**Dr. Lynn Rogers
Air Force Flight Dynamics
Laboratory
Wright-Patterson Air Force Base,
Ohio**

NECESSARY STEPS FOR SUCCESSFUL VISCOELASTIC DAMPING APPLICATIONS

Dr. Lynn Rogers
Air Force Flight Dynamics Laboratory

Introduction

As the title implies, this is intended to serve as an outline guide for the engineering of vibration damping, whether retrofit or designed-in type applications. Many times, viscoelastic damping is tried as a last minute shot-in-the-dark and fails miserably due to a lack of understanding of the basic facets. Hopefully as a result of this paper, the manager will allow sufficient time and resources, whether in-house or consultant, to properly design a viscoelastic vibration damping treatment.

Malfunction Analysis

Whenever hardware is malfunctioning (i.e., failing or not performing satisfactorily) or is predicted to malfunction due to mechanical vibration, the mechanism of malfunction must be understood. It must be somehow related to resonant response for damping to be effective. For example, the peak response to transient excitation consisting of a single impulse is not significantly dependent on damping, although the response decay is highly dependent on damping. As another example, response to periodic off-resonant excitation is not significantly dependent on damping. Of course, wide band random, periodic resonant excitation, and periodic excitation sweeping through resonance do cause high resonant response in lowly damped modes. Response to other types of dynamic excitation may or may not be affected by damping; e.g., shock spectra and transient loading. Consider sheet metal cracking: it could be due to high static stresses, low-cycle fatigue, off-resonant vibratory stresses, material or manufacturing defects, etc., as well as high-cycle fatigue caused by resonant response. The decision to increase damping should be the result of a considered rational process, with all assumptions recognized and justified.

Application Constraints

It often happens that introducing increased damping into a system is relatively easy, provided there are no other considerations. At the outset it is desirable to consider if there are stoppers in the peripheral disciplines, esthetics, schedule, or management bias. A formal program may be necessary to identify constraints and plan how to accommodate them in achieving a practical engineering solution. Some possible peripheral constraining areas are: adhesion, airflow, heat flow, survival temperature, temperature shock, temperature cycling, adverse chemical/fluid presence, corrosion, erosion, temperature cycling, etc.

Operational Environment

Because modal damping provided by viscoelastic material is highly dependent on operating temperature, mode shape, and, to a lesser extent on frequency, the environment must be defined in these terms. The temporal and spatial distribution of temperature in the presence of the installed viscoelastic material must be found. Most organizations consider only potential extremes in temperature. Here, the average operating temperature and range as a minimum are needed. Some combination of experimental data on undamped hardware, analysis, and judgment is required to obtain data defining problem mode(s).

Modal Survey

Often it happens that the previous step is experimental in nature and defines problem modal frequencies and not mode shapes for very practical reasons. In that event it is necessary to perform modal surveys on actual or accurately representative hardware specimens.

Preliminary Design of Damping Treatment

Conceptually, it is deceptively easy to state that any mechanical vibration system may be thought of as a super position of single degree of freedom oscillators; and the design problem is to place a proper viscoelastic element in parallel with the spring in each of the problem modes. In practice, considerable ingenuity and art may be required. In the most basic terms, the geometry of the damping treatment must be such that any deformation of the system in a problem mode must cause strain in the viscoelastic material; simultaneously, the viscoelastic material must be selected such that its modulus and loss factor result in peak damping for the operating environment. For a clamped or simply supported skin panel using a constrained layer treatment, design guidelines are well established. For modes where a significant amount of energy is in stringers or frames, more ingenuity may be required to find an efficient damping treatment. There is no substitute for experience.

In the PD phase, there are other considerations also; namely, the constraints mentioned above. Obviously, the installation/manufacture procedures is one which must be worked.

Experimental Damping Measurements

While at this juncture, theoretical analysis is adequate to serve as a guide during preliminary design and as a sufficiently accurate indication of small incremental extrapolations; no methods are established to the point that experimental damping measurements are not required to establish accurate damping levels as a function of temperature. Therefore, experimental measurements of modal damping as a function of temperature are probably necessary.

A complicating factor is that there may not be a one-to-one correspondence between modes of the untreated and treated system.

One very important consideration to bear in mind is the source of damping in the experimental setup. Many times novices and experienced experimentalists alike are badly fooled in this regard. In fact, in most applications, the first task in the experiment should probably be to minimize damping in the specimen and experimental setup. The mechanical joints in the specimen, the mounting of the specimen, and instrumentation lead wires can all be a significant source of damping and mask effects. All experimentalists have horror stories they could tell.

Iterate

It goes without saying that if the measured modal damping of the problem modes is not sufficiently high over the expected operating environment that a design iteration is necessary. Analysis, judgment, or experience can be used and retest may or may not be necessary.

Service Verification

Some form of data gathering for initial actual operation in the service environment is probably required to verify that malfunctions are actually abated. This could range from extensive instrumentation, recording, and analysis to a very cursory inquiry.

Service Evaluation

It may be necessary or highly desirable to gather sufficient in-service data to fully quantify and evaluate the beneficial effects of the damping treatment. This phase could also discover some unknown or unanticipated aspect of the operational environment which could seriously degrade the effectiveness of the damping treatment. All operational aspects are covered and the design is fully qualified for fleet implementation.

Fleet Implementation

This phase refers to incorporating fully-qualified procedures for implementing the damping treatment into the entire fleet, whether it is a retrofit or production application. Standard facilities, personnel, and equipment are utilized.

**SPATIAL AND TEMPORAL TEMPERATURE
DISTRIBUTION CONSIDERATIONS**

**D. B. Paul
Air Force Flight Dynamics Laboratory
Wright-Patterson Air Force Base, Ohio**

I. INTRODUCTION

Generally in any viscoelastic damping project there are three major thermal design conditions. First and foremost, the damping system operational thermal environment must be defined. Knowledge of the variation of time at temperature when damage is occurring is necessary for the optimization of the damping system. The damping system must also survive the temperature extremes of the damped component, where, these temperatures may be significantly different than the operational temperatures. Also, the influence of the damping system on overall system thermal performance must also be assessed. This paper will illustrate damping thermal design methodology by discussion of two recent damping design projects.

II. TF30P100 INLET GUIDE VANE

The TF30P100 engine has been experiencing a very high rate of inlet guide vane (IGV) cracking, due to resonant vibration, with nearly 50% of in-service vanes showing severe damage. Although there were several short and long term "fixes" under investigation, the approach involving vane damping through the application of a viscoelastic damping treatment has proven to be the most cost effective.

Crucial to the successful application of the viscoelastic treatment was knowledge of temperature when the most significant damage occurs. This knowledge was obtained from the F-111 "Service Life Monitoring Program" in the form of total outside air temperature (T_T) and mach number (M) vs time (Figure 1). The assumption was made that the damping operational temperature was essentially adiabatic wall temperature. The data was reduced by the following equation:

$$T_{aw} = T_T \left(\frac{1 + R \left(\frac{\gamma - 1}{2} M^2 \right)}{1 + \frac{\gamma - 1}{2} M^2} \right)$$

where R is the turbulent boundary layer recovery factor and γ the ratio of specific heats. The resulting distribution of time at temperature for operational design is presented in Figure 2. The operational thermal environment was defined to be 95% of the operational flight time and the resulting temperature range is 0°F to 125°F. The temperature distribution throughout the vane and damping material for the operational design condition was assumed to be uniform.

The damping configuration chosen for this application, considering both the dynamic and thermal environments, is shown in Figure 3. The configuration consists of three constraining layers of aluminum foil, two (2) layers of viscoelastic and a high temperature epoxy bond layer.

The survival condition for this design is created by the application of anti-icing air to the interior of the inlet guide vane with a total outside air temperature of 40°F. Heat diffuses through the titanium vane and generates high bond line and damping material temperatures. The vanes nearest the bleed air ports on the inlet case are subjected to 607°F bleed air in the anti-icing channels in a fully developed turbulent channel flow condition and a 40°F external turbulent boundary layer (see Figure 4). The most extreme temperatures occur at the damper-vane interface on channels aft from the leading edge. The leading edge temperatures are much lower due to stagnation point cooling. The nonuniformity in the temperature distribution is illustrated in Figures 5 through 8 which are examples of the data taken in the development program.

A most interesting side effect of the damper treatment was the improvement of the anti-icing capability of the inlet guide vane. The leading edge is critical for icing due to the high stagnation point cooling. Aft channel skin areas are warmer since there is a decrease in external boundary layer cooling. In the bare vane configuration (Figures 9 and 10) the separate anti-icing channels are almost thermally independent of each other due to the low conductivity of the titanium vane, however, in the wrapped configuration (Figure 10) the leading edge receives conduction heating from the aft anti-icing channels through the aluminum foil. The improvement in anti-icing capability was verified through a 3-D thermal analysis performed by Pratt & Whitney, East Hartford, CT. Presented in Figure 10 is the predicted temperature distribution for a damped vane under moderate icing conditions with the lowest leading edge temperature greater than 32°F. In Figure 9 are the bare vane temperature predictions under the same moderate icing condition with the leading edge equal to 32°F, and in Figure 8 the prediction of the bare vane under the severe icing condition are shown which indicates icing at the leading edge.

III. B-1 Aft Equipment Bay

The engine placement on the B-1 is such that the exhaust plumes are parallel to and near the aft fuselage. During after burning (AB), these plumes produce an intense noise and thermal radiation environment. This environment is most severe during AB takeoff and during ground AB operation. This is due to the higher density and size of the plume and the low level of aerodynamic cooling. The resulting acoustic environment in the aft avionics bay was much higher than the avionics bay equipment design levels and a viscoelastic damping treatment was proposed as a method of reducing the noise level into the acceptable range.

Since a purely analytic study would not provide the desired accuracy in temperature distributions needed for optimization of the damping treatment, an experimental program was undertaken in conjunction with the B-1 Division of Rockwell International. Figures 12 and 13 indicate the placement of nine fuselage skin thermocouples in relationship to the engine exhaust plume. While these thermocouples provided basic data on the transient thermal response of the aft structure they could not produce sufficient information to allow a complete thermal distribution map to be drawn. Therefore, thermal patches and temperature indicating paint were utilized to extend the instrumentation coverage.

In order to perform design calculations, it was necessary to obtain from the data (1) plume radiation heat flux distributions absorbed at the fuselage surface (Q_{pr}), (2) ground level cooling flux distributions (Q_{cg}) and (3) takeoff aerodynamic convective cooling flux distributions (Q_{ct}).

These distributions were obtained by utilizing one dimensional heat conduction models as depicted in Figure 14. Shown in Figure 15 is a typical response of the fuselage skin to ground after burning where ΔT_s is defined to be the difference between the skin temperature and ambient temperature ($\Delta T_s = T_s - T_A$). The ground thin skin ΔT_s maximum is directly proportional to total AB time and inversely proportional to skin heat capacity. The ground level cooling flux Q_{cg} distribution was assumed approximately constant with time and thus could be obtained by matching the one dimensional heat conduction model to the thermocouple response during the cool down portion of the ground AB run. The plume radiation heat flux distribution Q_{pr} was obtained by matching analysis to data during the heating portion of the ground AB run and utilizing the previously obtained Q_{ct} . Shown in Figure 16 is the typical thin skin thermal response during takeoff. Plume radiation heat flux levels are basically unchanged from the ground level since the change in altitude is small. However, the convection cooling is proportional to Mach Number (M) raised to the .8.power. Reduction of the takeoff thermal data was made by using the third data reduction model in Figure 15 and the

above assumptions.

Once the distributions of Q_{pr} , Q_{cg} and Q_{ct} were known, the establishment of the damping thermal design conditions were possible. Due to the aircraft limitation on AB ground time operation, the operational temperature distribution was determined by the takeoff condition. Shown in Figures 17 through 19 are the total range of operational temperatures vs waterplane stations at several different fuselage locations. The curves in Figures 17 and 18 and the top curve in Figure 19 indicates the maximum change in temperature from ambient, while the range of operational temperature is the distance between the curves and the horizontal axis. These ΔT_s maximum curves are only a mild function of skin heat capacity, since, in the time region $\Delta\theta_2$ (Figure 16) $Q_{pr} \approx Q_{ct}$ and thus the skin temperature is quasi-steady. Therefore, these ΔT_s maximum curves would apply to different materials and skin thickness as long as they exhibit the Figure 16 type response (i.e., thin skin). The mean ΔT_s is a function of material, total AB time and skin thickness. Shown in Figure 19 are examples of the influence of total AB time on mean ΔT_s .

In order to optimize the damping treatment, knowledge of the percentage of time at temperature is necessary. An example of such data is presented in Figure 20. These predictions are a function of both AB time and damper configuration but not greatly influenced by location. Obviously, in order to complete the operational design temperature requirements, aircraft usage information is needed. For example, aircraft basing information is utilized for the definition of ambient temperatures.

The survival design condition was determined by the a one minute AB ground run (aircraft limit) on a MIL-210-B 1% "hot day". Maximum viscoelastic temperature distribution is presented in Figure 21 for a .096 inch skin and a .025 inch damping treatment.

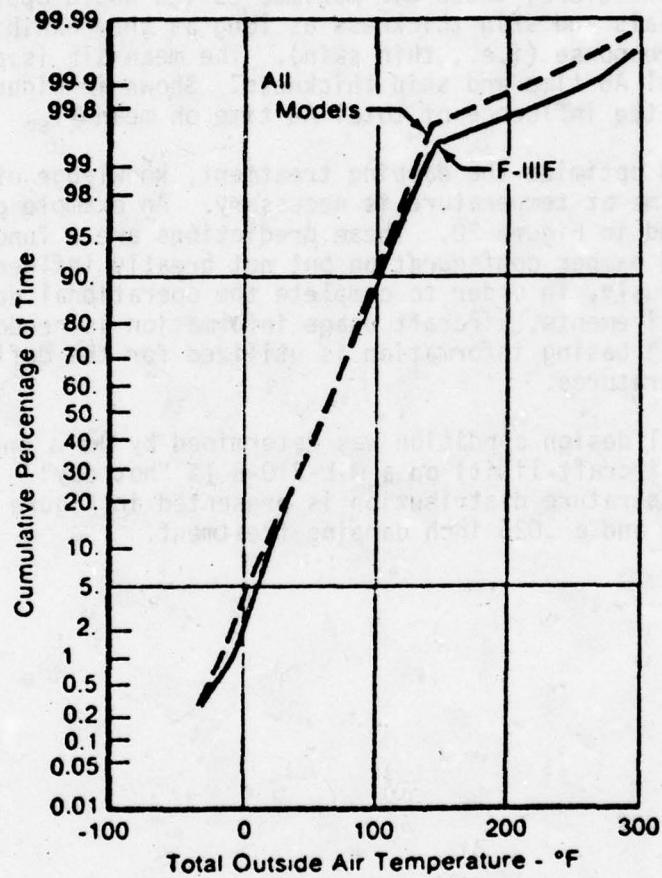


FIGURE 1 Percentage of Time at Temperature from Service Life Monitoring Program Data

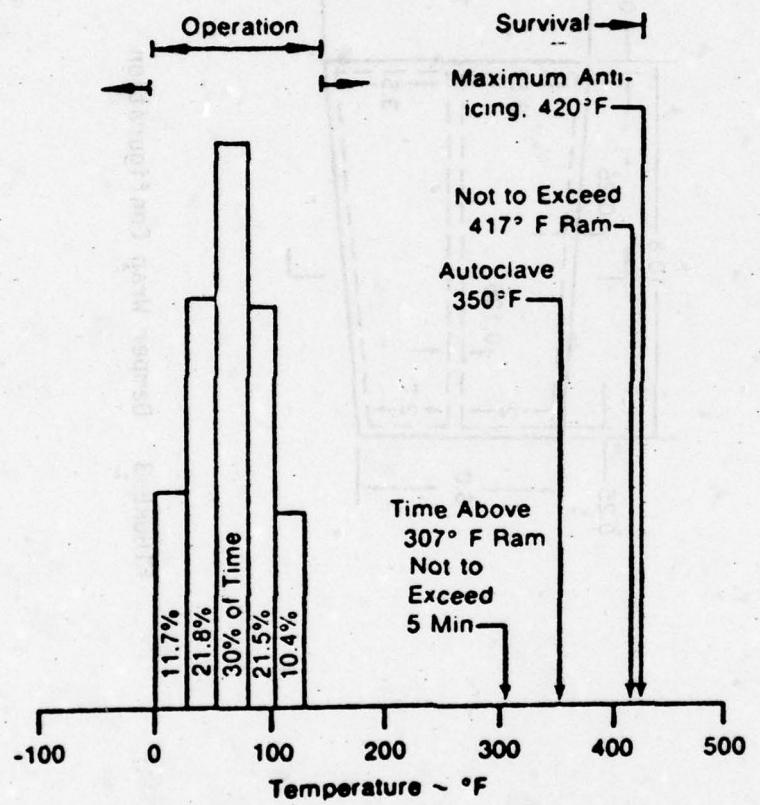
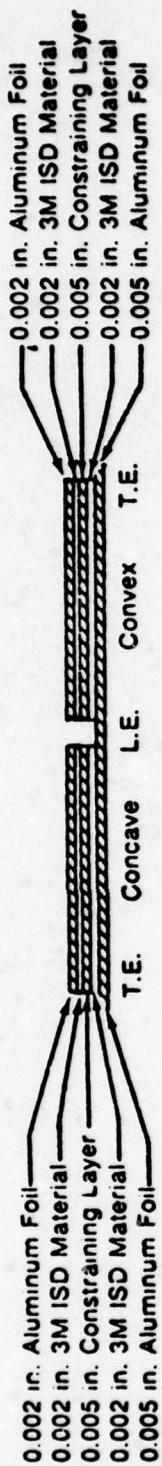


FIGURE 2 Temperature Requirements of IGV Damping Treatment



All Dimensions in inches

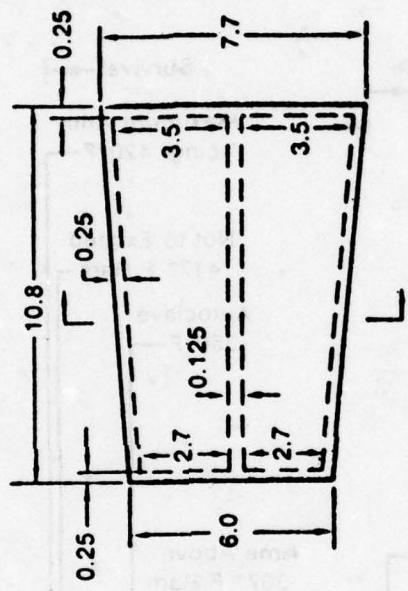


FIGURE 3 Damper Wrap Configuration

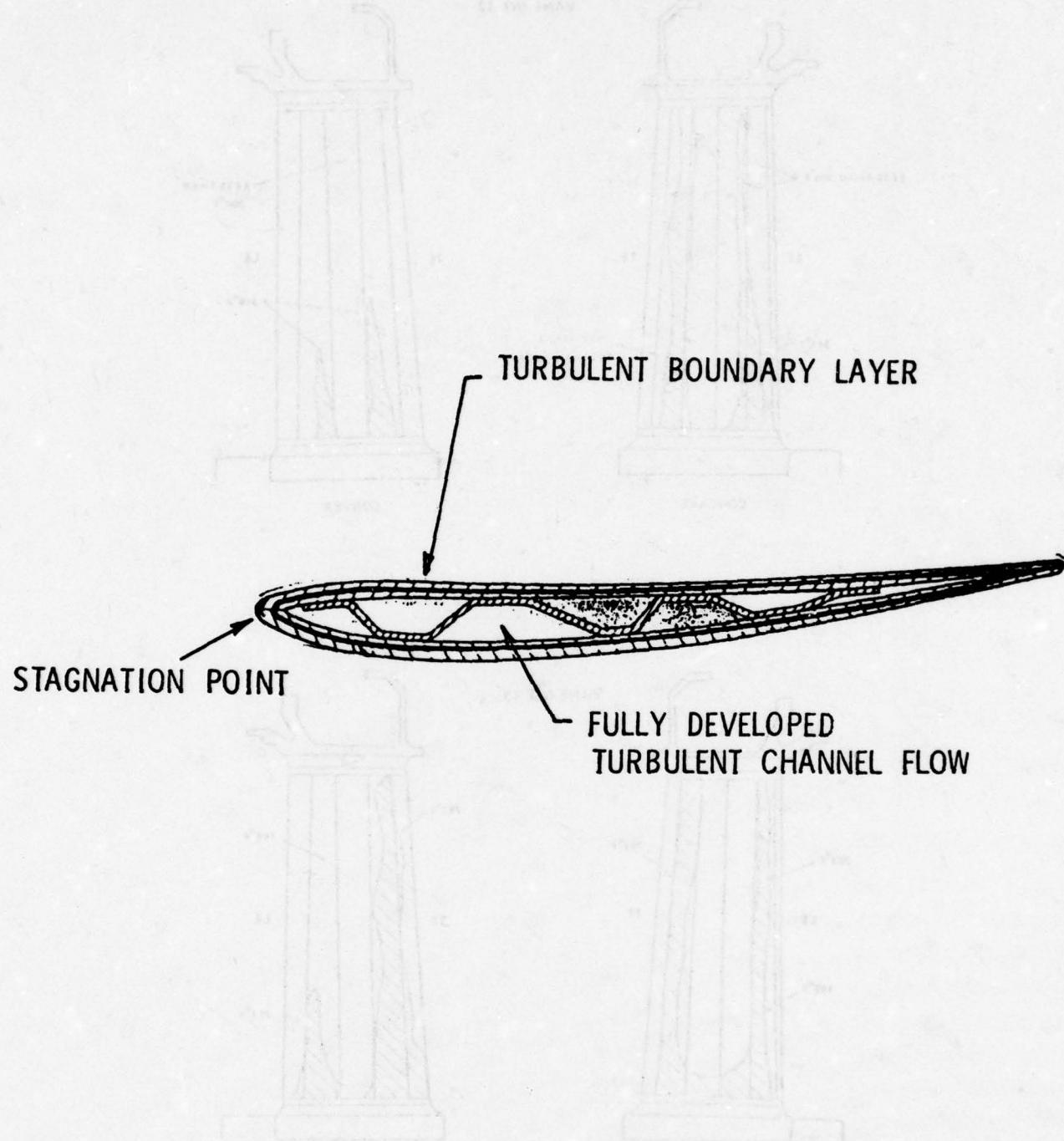
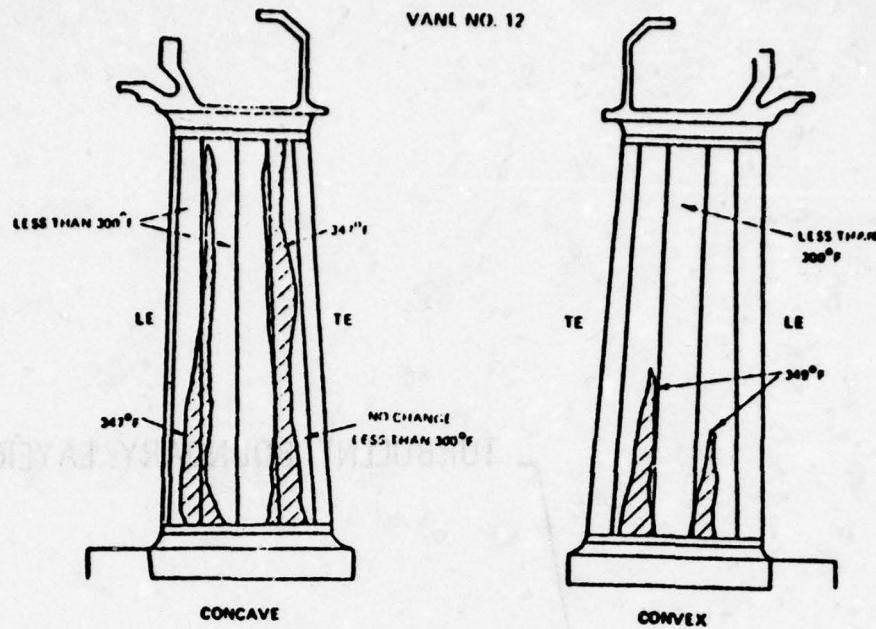


FIGURE 4 IGV Thermal Model

VANE NO. 12



VANE NO. 13

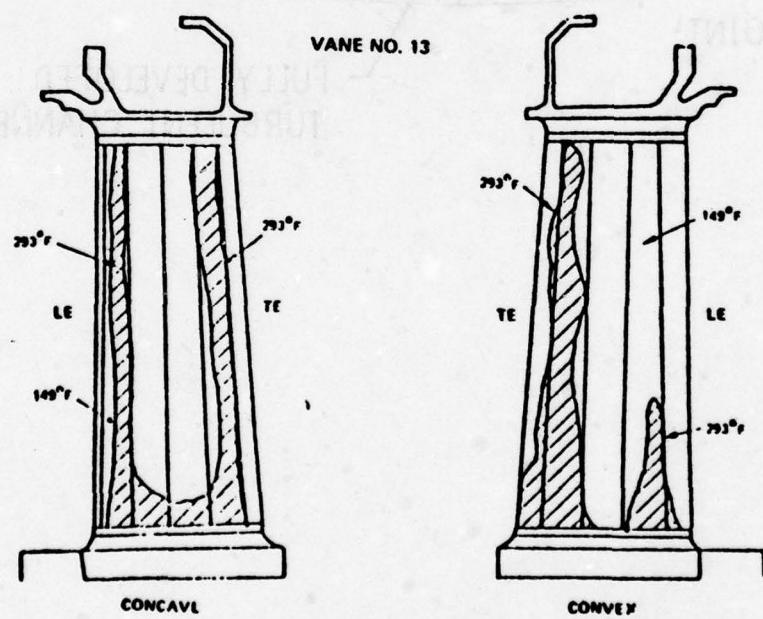


FIGURE 5 Temperatures Indicated by Thermal Paint on Inlet Guide Vanes

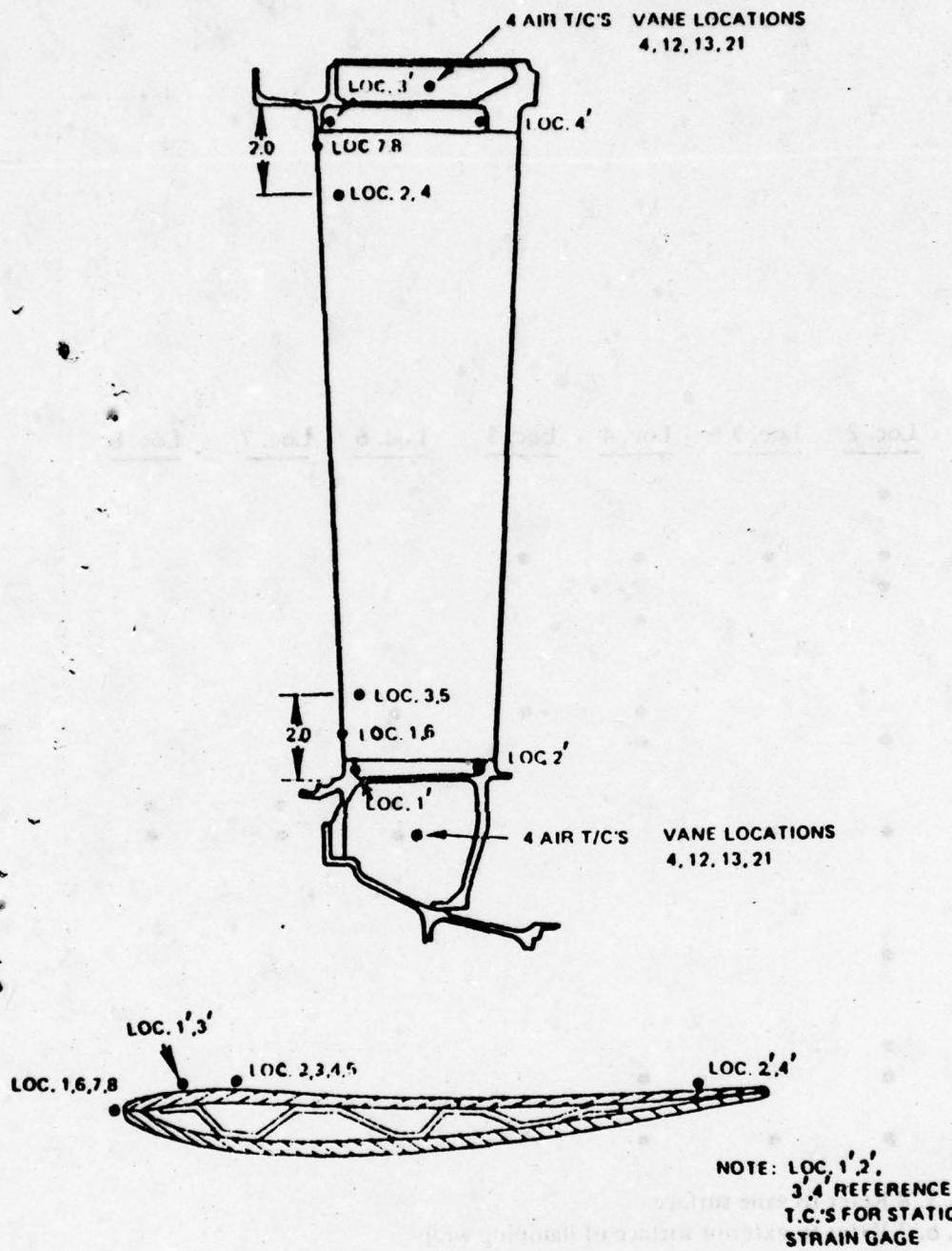


FIGURE 6 Thermocouple Instrumentation for TF30-P-100 Inlet Case

<u>Vane No.</u>	<u>Loc. 1</u>	<u>Loc. 2</u>	<u>Loc. 3</u>	<u>Loc. 4</u>	<u>Loc. 5</u>	<u>Loc. 6</u>	<u>Loc. 7</u>	<u>Loc. 8</u>
2		•						
3								
4		•	•	•	•			
5		•						
6				•				
7								
8								
9				•	•	•		
10		•		•				
11								
12	•					•	•	•
13	•	•	•			•	•	•
14								
15								
16								
17		•						
18								
19								
20		•						
21		•			•			
22								
23		•	•	•				

NOTE: Loc. 1, 2, 3, 8 Refer to vane surface
 Loc. 4, 5, 6, 7 Refer to exterior surface of damping wrap

FIGURE 7 Thermocouple Instrumentation for TF30-P-100
 Inlet Case

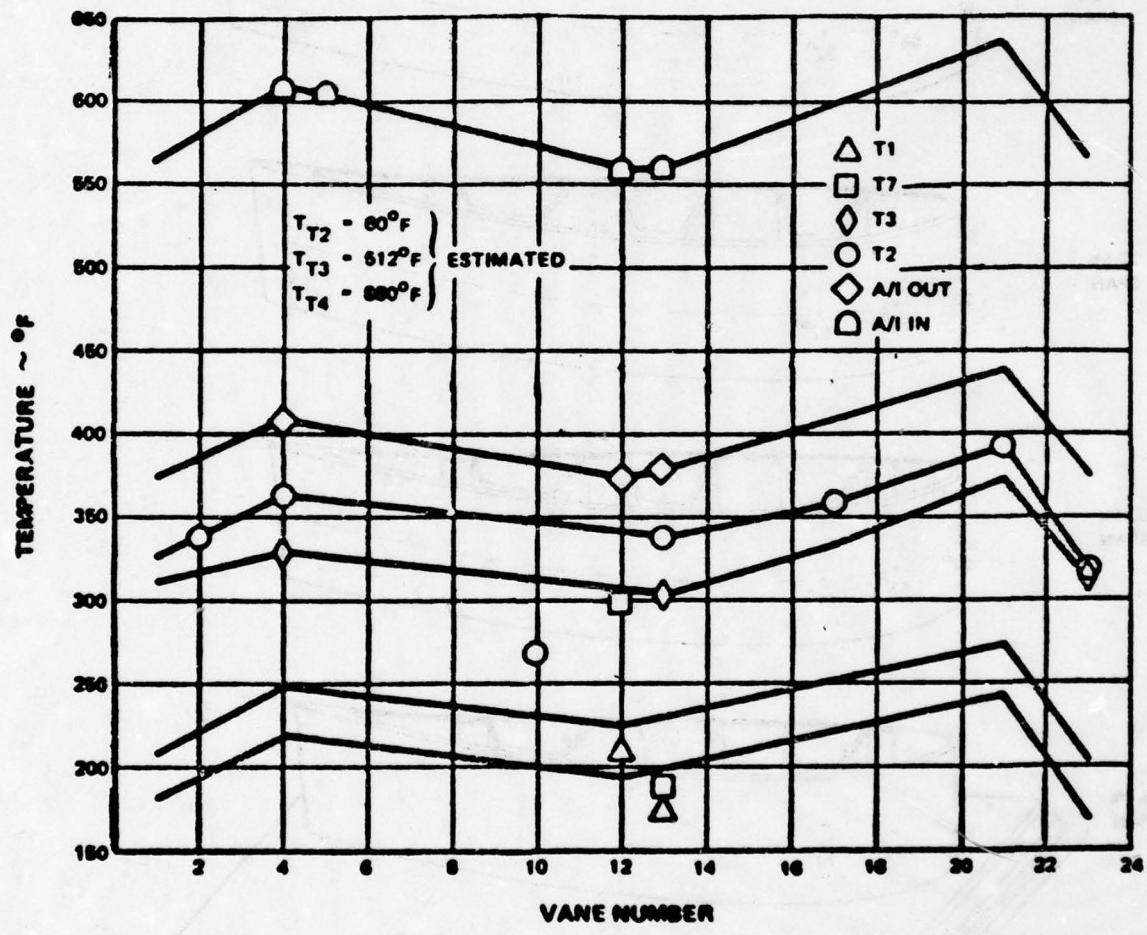


FIGURE 8 Inlet Guide Vane Thermocouples at Wrap-Vane Interface Data

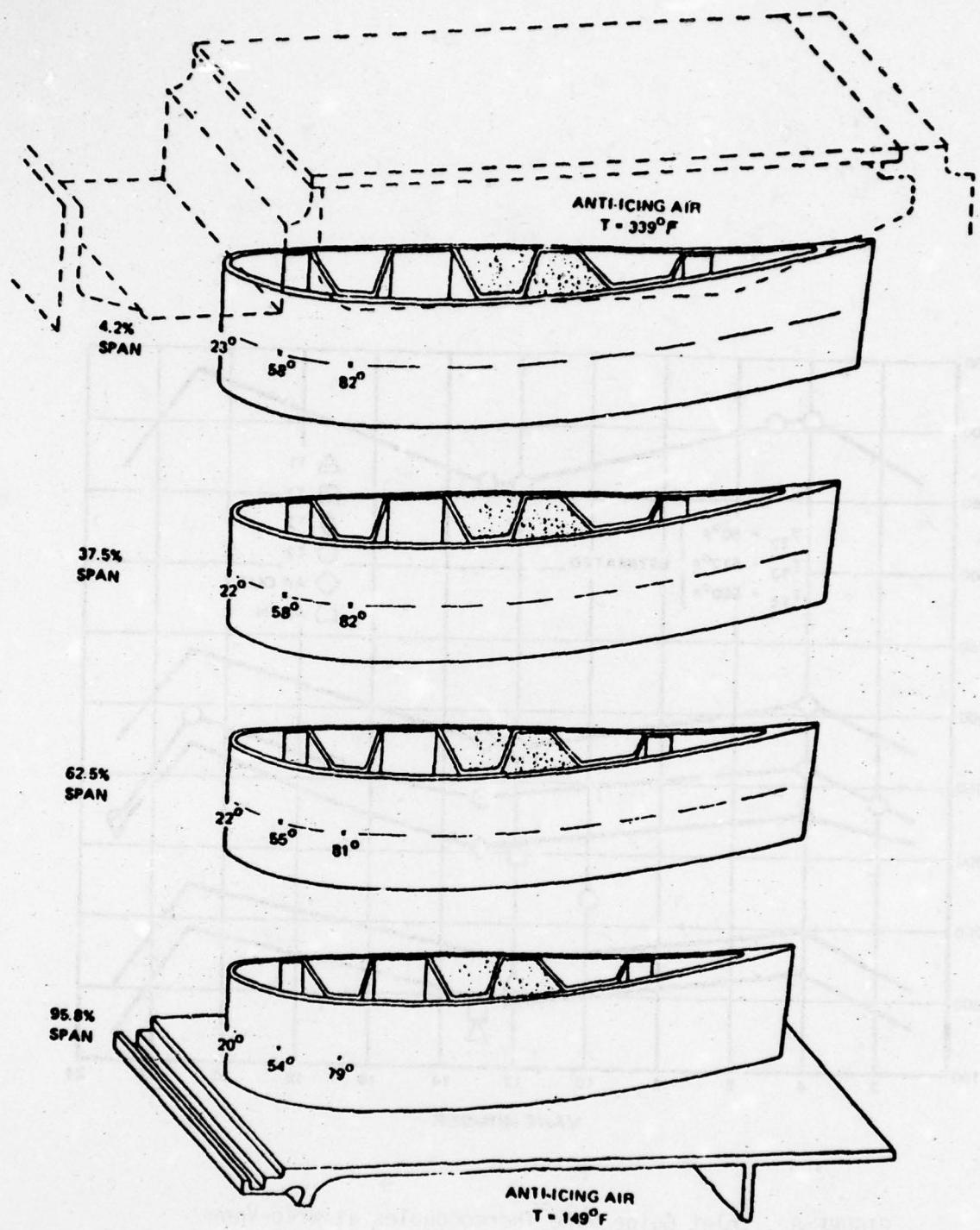


FIGURE 9 Predicted Analytical Temperatures on Surfaces of Unwrapped Inlet Guide Vane Under Severe Icing Conditions ($T_{amb} = 40°F$, 50% Power, $1 \text{ gm/m}^3 H_2O$)

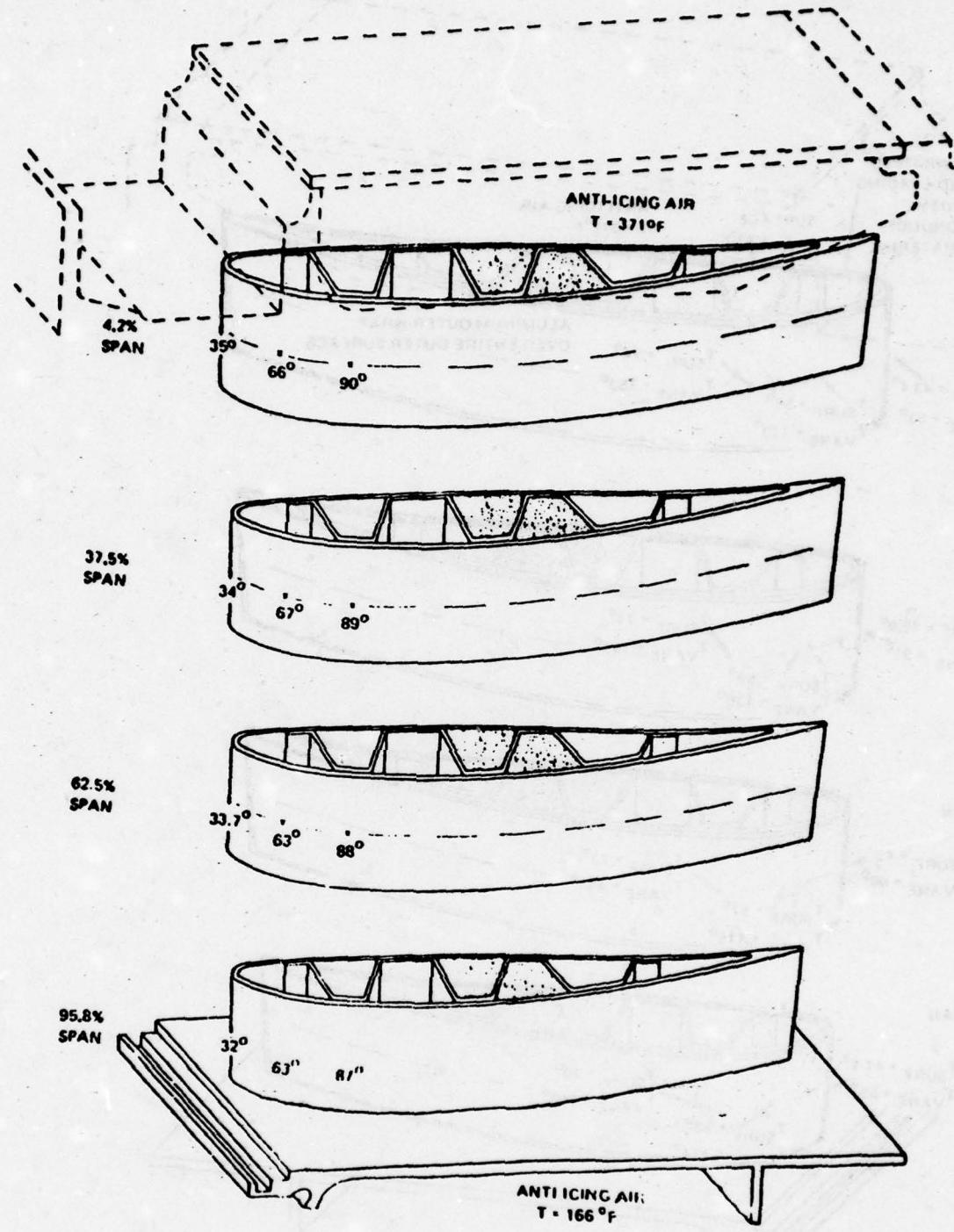


FIGURE 10 Predicted Analytical Temperatures on Surfaces of Unwrapped Inlet Guide Vane Under Moderate Icing Conditions ($T_{amb} = 100^{\circ}\text{F}$, 50% Power, 1 gm/m H_2O)

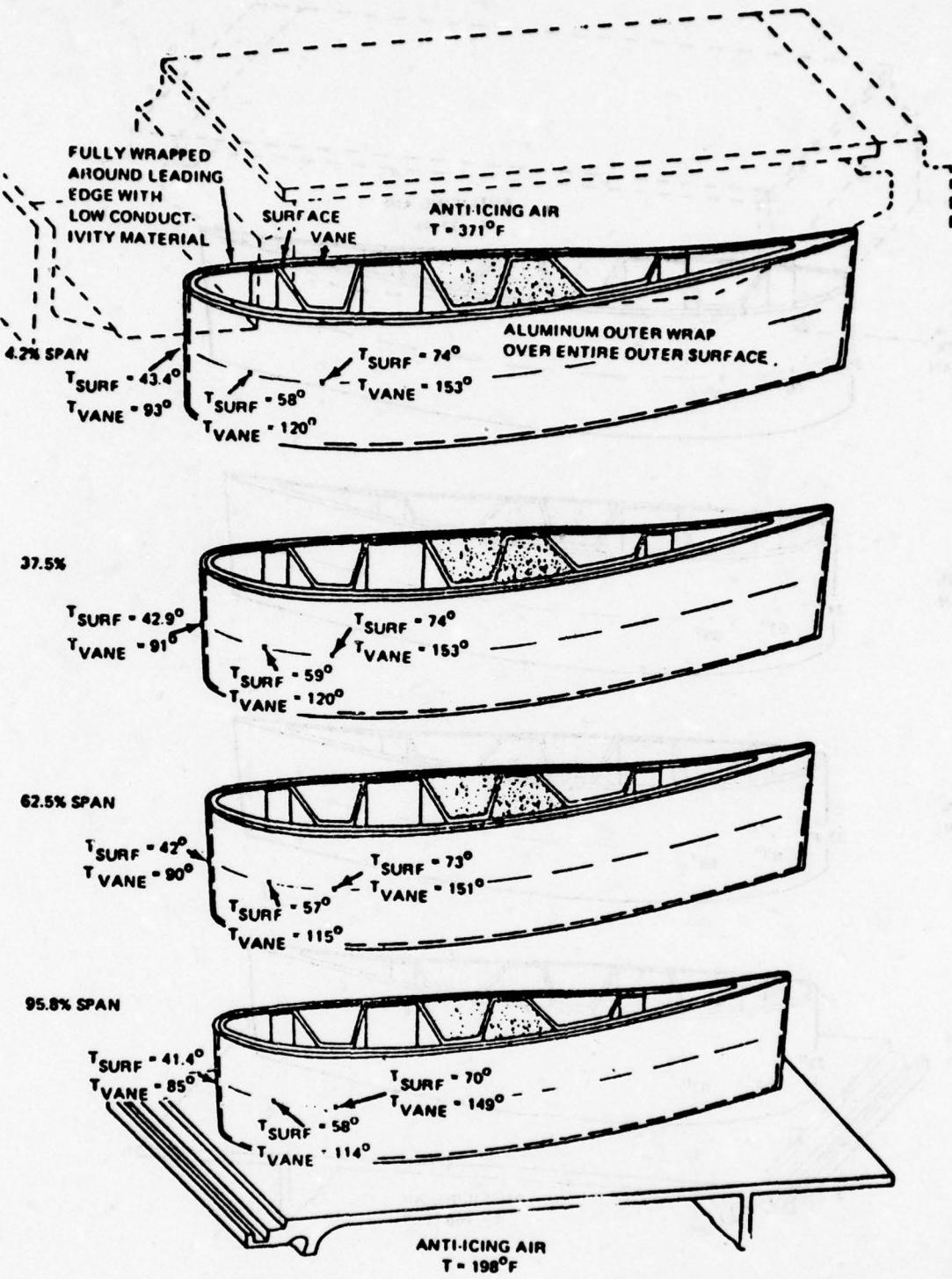


FIGURE 11 Predicted Analytical Temperatures on Surfaces of Wrapped Inlet Guide Vane Under Moderate Icing Conditions ($T_{amb} = 10^\circ F$, 50% Power, $1 \text{ gm/m}^3 H_2O$)

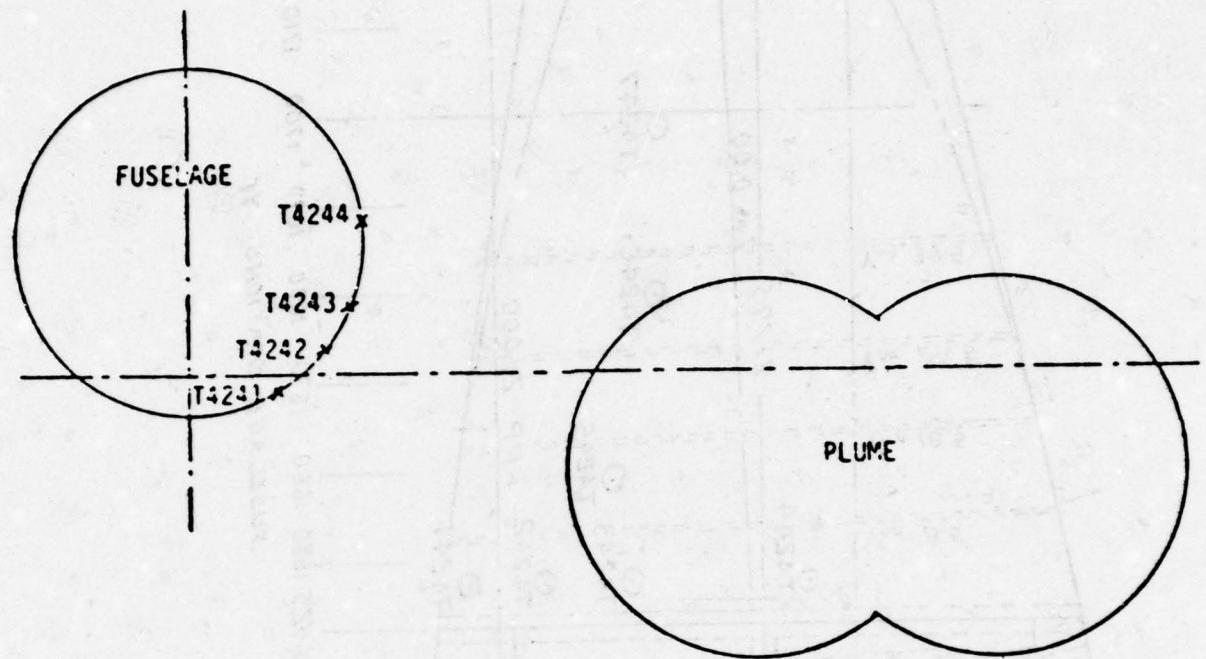


FIGURE 12 Relative Orientation of Thermocouples and Plume
at Y_f 1648.5

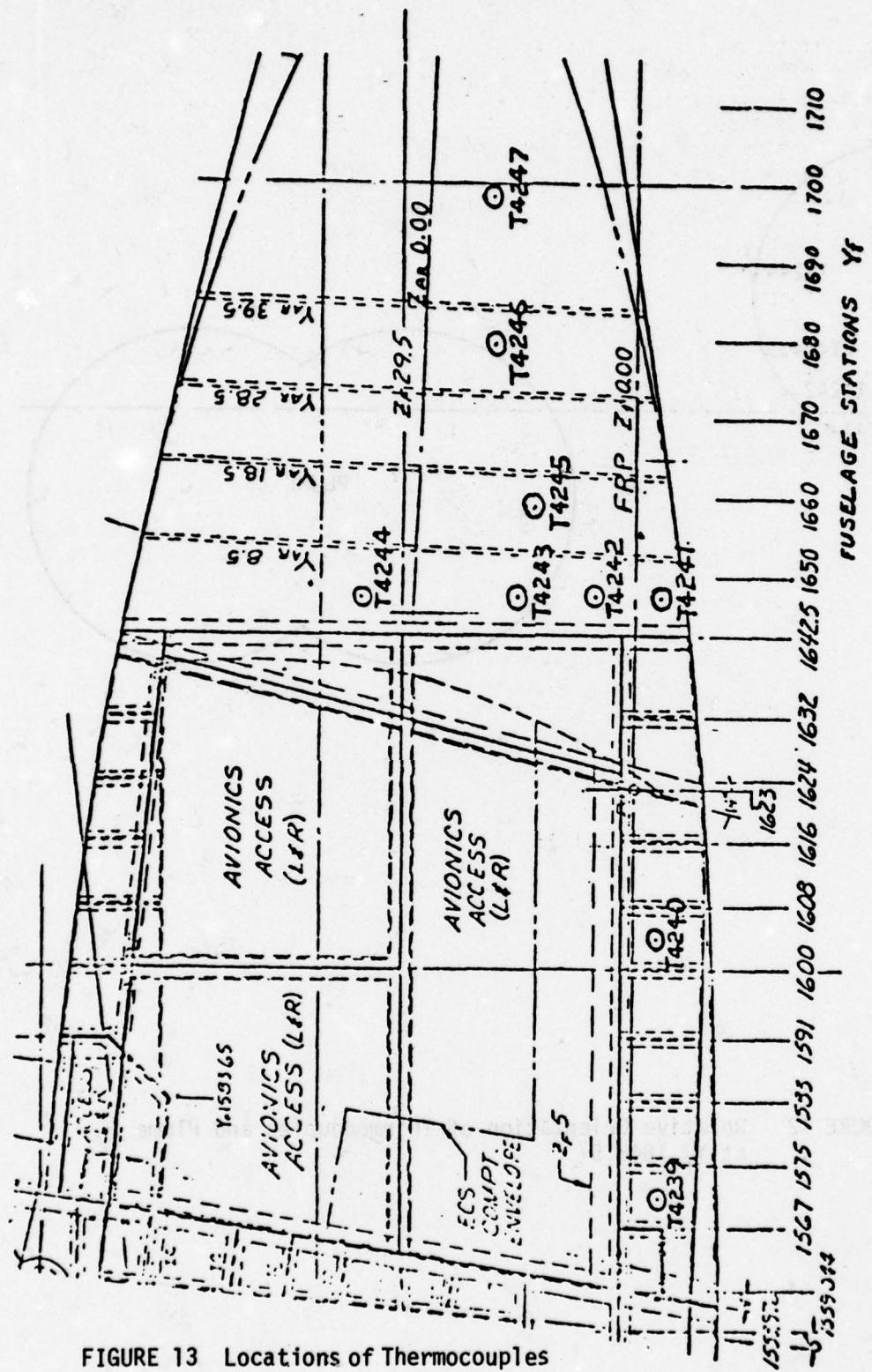
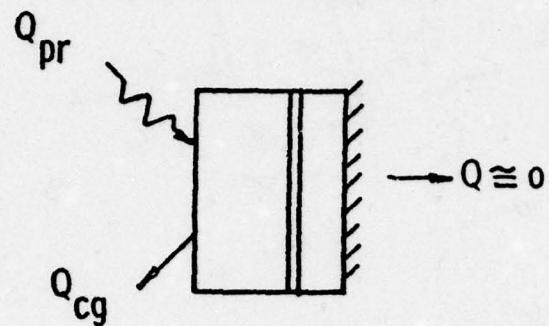
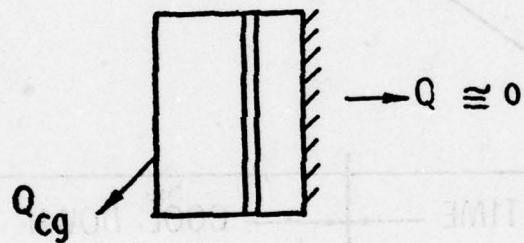


FIGURE 13 Locations of Thermocouples

GROUND RUN (AB HEATING)



GROUND RUN (COOL DOWN)



TAKEOFF

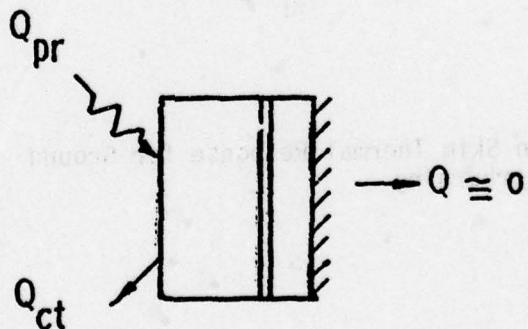


FIGURE 14 Data Reduction Thermal Models

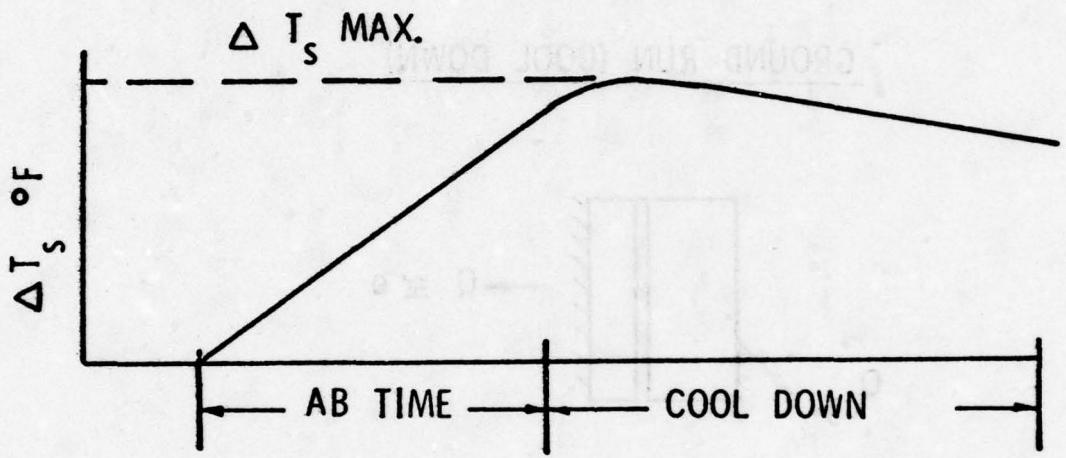
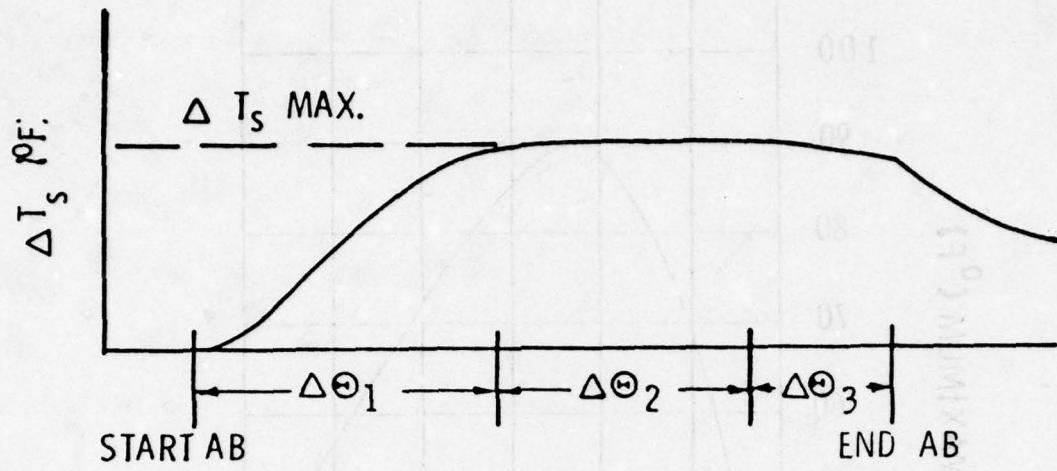


FIGURE 15 Thin Skin Thermal Response for Ground Afterburning



TIME REGION	THERMAL CONDITION	
$\Delta \Theta_1$	PLUME RADIATION	$>$ CONVECTION COOLING
$\Delta \Theta_2$	PLUME RADIATION	\approx CONVECTION COOLING
$\Delta \Theta_3$	PLUME RADIATION	$<$ CONVECTION COOLING

FIGURE 16 Thin Skin Thermal Response for Takeoff Afterburning

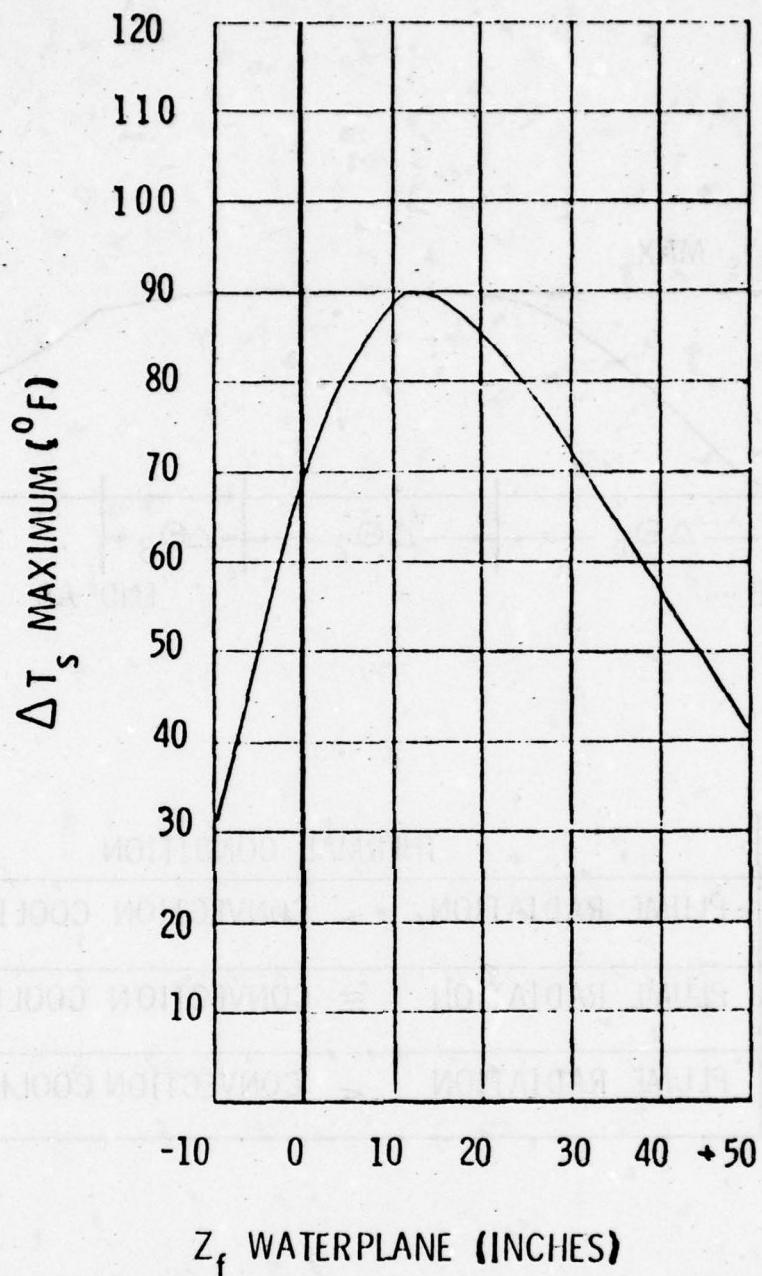


FIGURE 17 Damping Temperature Design Range: $Y_f = 1571$

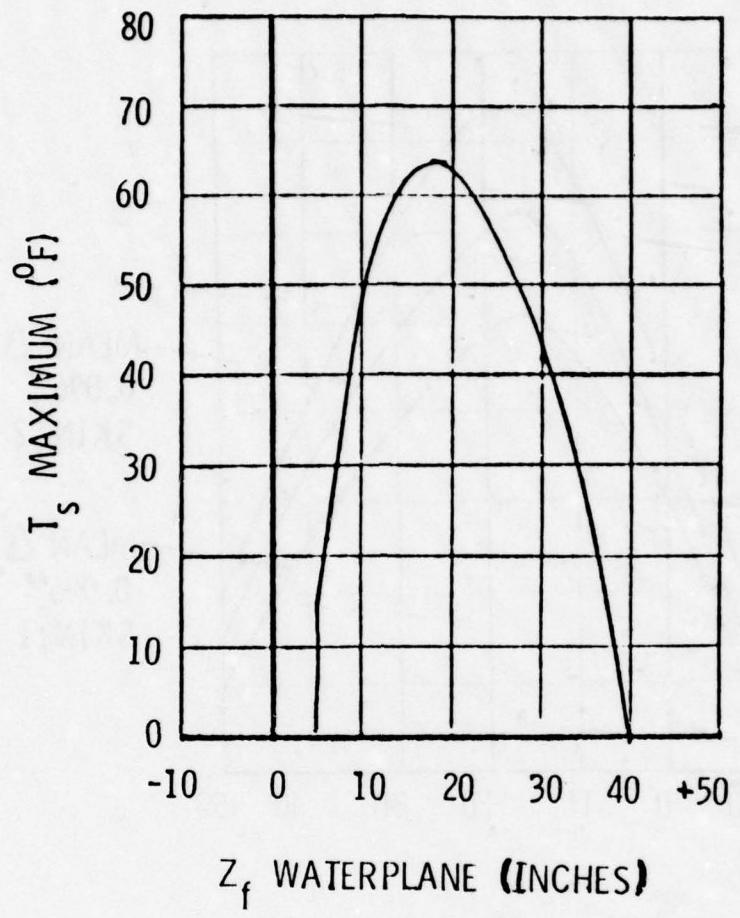
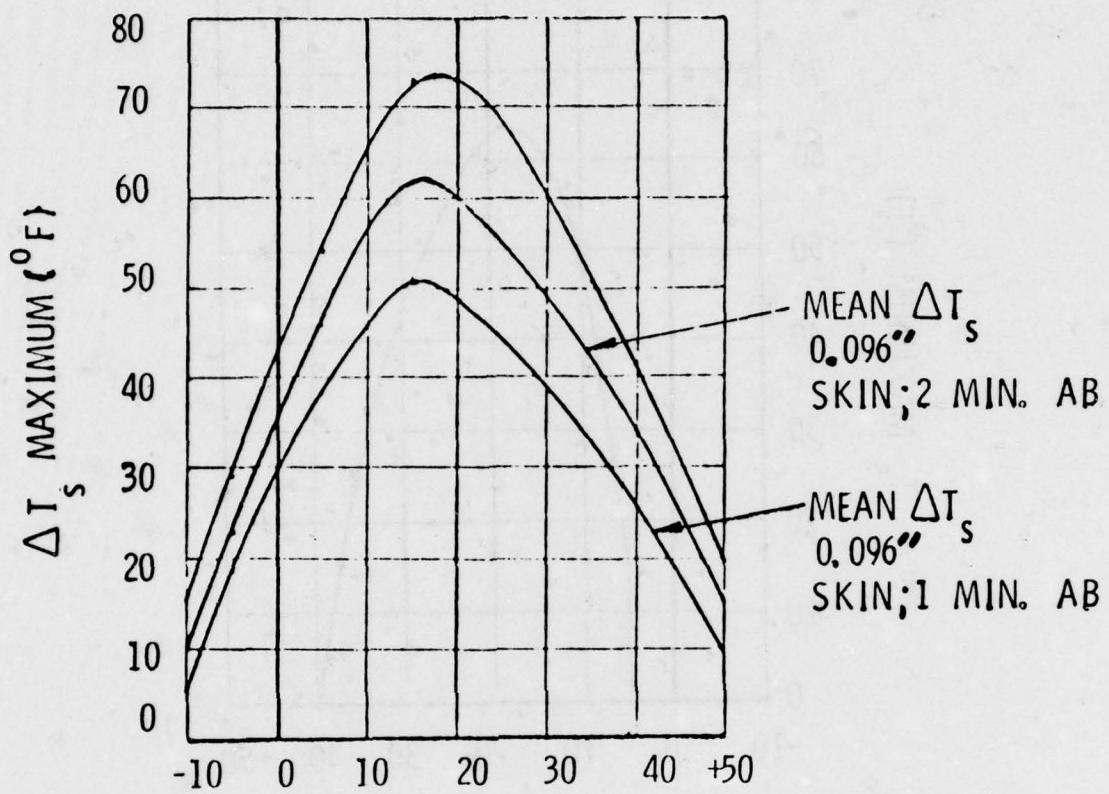


FIGURE 18 Damping Temperature Design Range: $\gamma_f = 1700$



Z_f WATERPLANE (INCHES)

FIGURE 19 Damping Temperature Design Range: $Y_f = 1648$

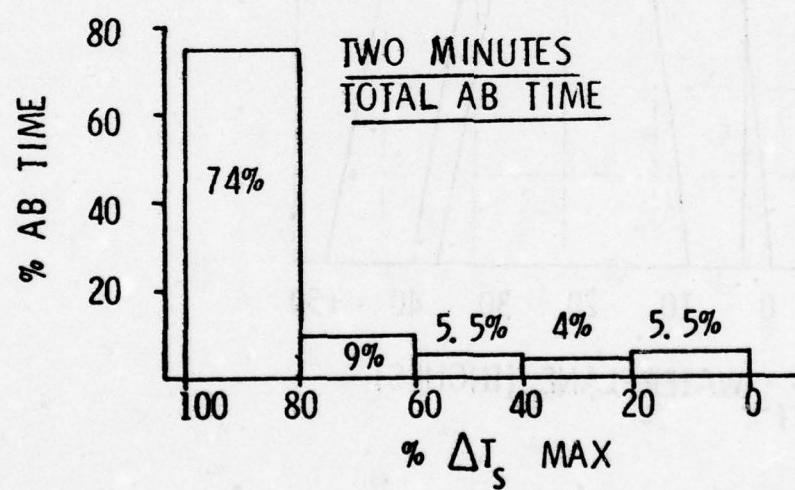
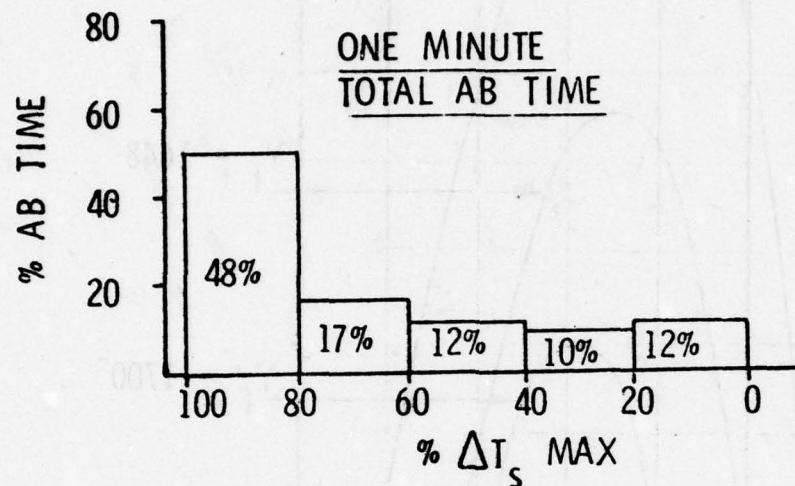


FIGURE 20 Percentage of Time at Temperature
(.096 Inch Skin: .025 Damper)

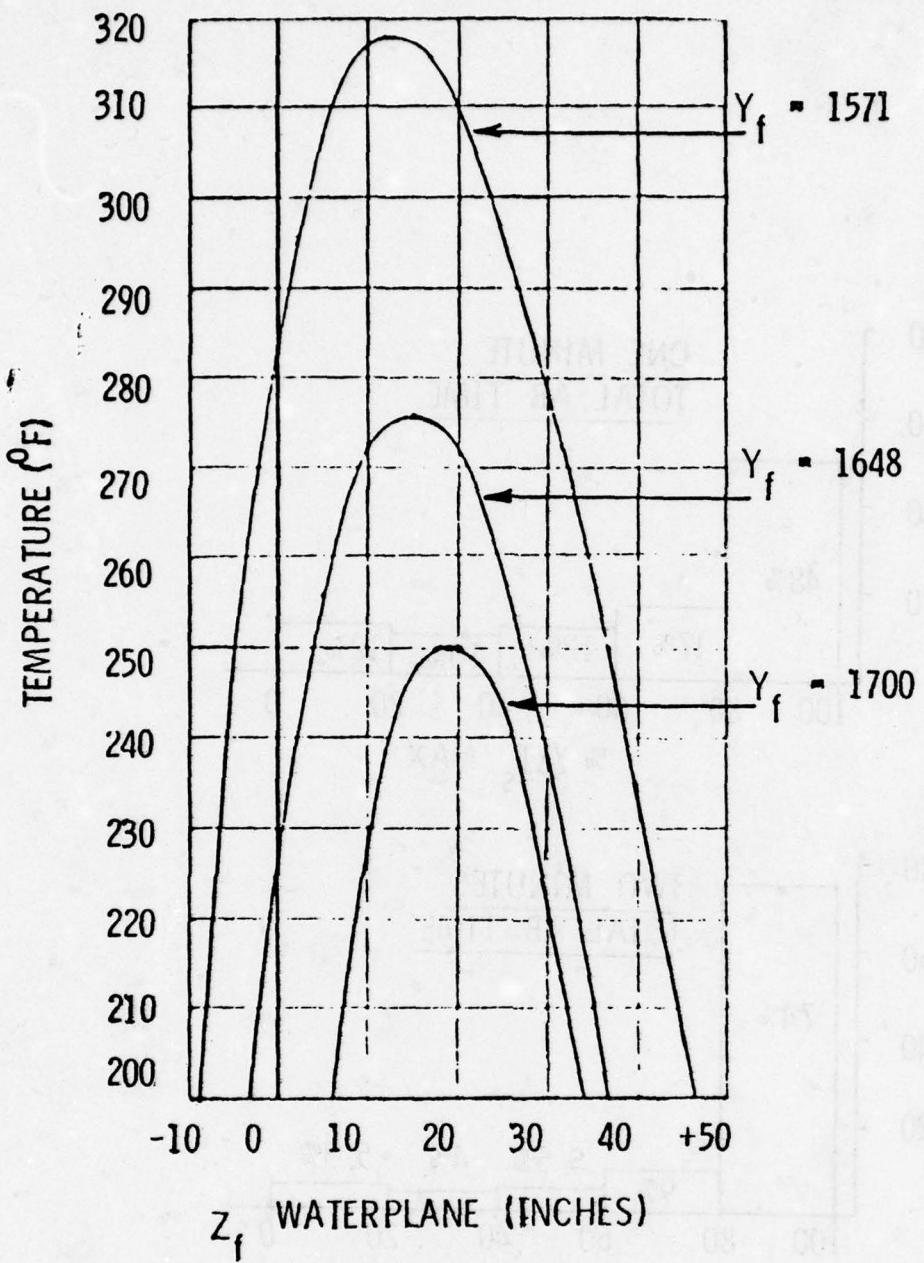


FIGURE 21 Maximum Temperature Condition

**FOURIER ANALYSIS IN THE LABORATORY
AND IN THE FIELD**

M. L. Drake
University of Dayton Research Institute
Dayton, Ohio

FOURIER ANALYSIS IN THE LABORATORY AND IN THE FIELD

Michael L. Drake

University of Dayton Research Institute

ABSTRACT

The digital fast Fourier analyzer is quickly changing the look of vibration analysis laboratories. This paper will discuss the use of this equipment in the design and evaluation of damping applications. Sufficient general discussion of the Fourier analyzer will be included so that the reader will be able to understand the equipments functional use. Several testing methods for obtaining frequency response functions will be discussed and an example of the data collected for a damping fix design will be given.

I. Introduction

The advent of the digital fast Fourier analyzer has opened many new avenues to the test engineer in the world of experimental vibration measurements. This paper addresses the use of this equipment in experimental testing both in the laboratory environment and as field test instrumentation. Several testing methods will be discussed. Emphasis will be placed on the use of the analyzer as a tool used in the design of damping treatments. The paper will describe the basic Fourier analyzer system currently in use at the University of Dayton and the pertinent data which this system can produce. An illustration of the use of the systems through a specific example will be given.

II. The Fourier Analyzer

The Fourier transform equation is defined by

$$F(S) = \int_{-\infty}^{\infty} f(x) e^{-i2\pi xs} dx. \quad (1)$$

This equation is useful in many disciplines ranging from pure mathematics to waveform analysis [1].¹ Of particular interest is the use of the Fourier transform to transform an electrical waveform in the time domain generated by a transducer measuring the response of a vibrating structure, into spectral data in the frequency domain. Although this ability has existed for some time, the cumbersome and time consuming work necessary to accomplish this task limited its use.

It was the advances made in computer technology, along with growth in micro-electronics, that led to the development of a mini-computer which could perform Fourier transforms. The result of these developments is the digital fast Fourier transform analyzer. In forming a Fourier transform, the analyzer actually uses a discrete Fourier transform [2]. This transform, as it's name implies, does not give amplitude and phase (or real and imaginary) data for a continuum of frequencies, but does give amplitude and phase information at evenly spaced (discrete) frequency points within a frequency range. The frequency resolution (frequency spacing where data is taken) and maximum value of frequency are controlled by the Analog to Digital Converter (ADC) settings used when the data was sampled [2]. Further details of the mathematics involved in obtaining a Fourier transform is beyond the scope of this paper. However, a definition of two types of Fourier transforms is necessary for later reference. Generally, a Fourier transform has a frequency range from zero Hertz (or D.C.) to some maximum frequency (Fmax). This is called a baseband transform. It is obvious that, with a given data storage area, the higher in frequency the transform goes, the larger frequency between data points, lending to (poorer) frequency resolution. This means that high frequency analysis of closely spaced resonances is impossible because of resulting poor frequency resolution. To overcome this problem, software and hard-

1. Indicates reference number in reference list

ware have been developed to allow the formation of a band - selectable Fourier transform [3]. Here, the test engineer can set the lower frequency limit at a value other than zero. For a fixed data storage area, the frequency band of interest can be reduced, which reduces the frequency interval between data points and hence results in better frequency resolution.

Figure 1 shows a schematic of the Fourier analyzer currently being used by the University of Dayton. The basic system consists of a central C.P.U. with 32K memory, a Fourier system control unit, an analog to digital converter and an oscilloscope for viewing data. This basic system contains all the necessary ingredients to do Fourier analysis; however, several essential "luxuries" were added. A small teleprinter, a high speed paper tape reader and an interactive graphics terminal with a head copy unit for report-quality copies of data, all proved to be very useful. The final addition to the system is a mass data storage device in the form of a moving head disc. The mass storage capability is vital for the analysis of large structural systems, where large quantities of data are collected and stored for post processing. Figure 2 shows a rack-mounted system in the laboratory.

III. Data Necessary for Damping Design

With a small amount of theory and the analyzer system explained, the definition of what data is necessary for damping treatment design and methods of obtaining such data is now necessary. The primary data output from a Fourier analyzer needed for damping design is the frequency response function [4]. The frequency response function is obtained by simultaneously measuring and digitally storing the time histories of the structure excitation force and the acceleration response. These time-domain signals are then analyzed, using the Fourier analyzer, which calculates, in the frequency domain, the acceleration auto power spectrum G_{yy} , the force auto power spectrum G_{xx} , the cross power spectrum G_{yx} , and the frequency response function $H(i\omega)$ where:

$$H(i\omega) = \frac{\overline{G_{yy}} *}{\overline{G_{xx}}} \quad (2)$$

The analyzer also calculates the coherence function S^2 where

$$S^2(i\omega) = \frac{|G_{yx}|^2}{|G_{xx}| |G_{yy}|} , \quad 0 \leq \delta^2 \leq 1. \quad (3)$$

The coherence function used here is a measure of the "quality" of the data, since a coherence value of unity indicates that the output (acceleration) is completely causally related to the input (force) [5]. A coherence value other than unit alerts one that

* \overline{G} indicates average over several samples.

something could be wrong in the test set-up. Problems such as bad cables, ground loops, spurious excitation by ambient acoustic noise, nonlinearities in the test structure or problems in the signal conditioning system all tend to reduce coherence values. These low values of coherence lend to early detection of bad experimental data, resulting in less lost testing time due to retesting otherwise needed to replace unnoticed "bad" data.

The structural data that is needed for optionally designed damping applications are: 1) Resonant frequencies; 2) Resonant mode shapes; 3) Resonant modal damping. The resonant frequencies are necessary because damping materials have frequency dependent properties; ie modulus, E_D and loss factor η_D . The resonant mode shapes define the characteristic wave length of the structure which, in turn, affect the geometric configuration of the damping design. Finally the inherent modal damping (approximately equal to the inverse of the resonant amplification factor) indicates to the designer the amount of added damping needed. It also gives the test engineer a method of comparing various damping applications from which the most effective design can be chosen.

All three of these structural parameters can be derived from frequency response functions. A typical acceleration-frequency response function is shown in Figure 3. The resonant frequencies are easily obtained by direct inspection of the frequency response function. From the magnitude and phase information available in a frequency response function, mode shapes can be derived for a test structure from a collection of frequency response functions taken at many points across the test structure [6] [7]. Modal damping can be obtained any of several ways. First direct half power bandwidth measurements can be made from the magnitude of the frequency response function. Second, a "Nyquist" curve fit around a particular resonance can be used, providing the resonant frequencies are widely separated [6] [8]. Finally, a Laplace Curve fit routine can be used to fit the entire frequency response function, which would result in the determination of the modal damping for all the major modes [4]. We usually obtain modal damping by the Nyquist curve fit approach. Figure 4 shows a typical Nyquist plot of a frequency response function in the neighborhood of a resonance. The modal damping is determined from

$$\eta_s = \frac{4R\Delta F}{F_r DS} \quad [8] \quad (4)$$

where R is the radius of the circle fitted to the data, ΔF is the frequency resolution, F_r is the resonant frequency, and DS is the maximum arc length along the circle between any two frequency points. This maximum arc length occurs at the point of resonance [8]. The process of determining structural loss factor by this method has been programmed so that the analyzer can compute the loss factor. It must be noted that this method is invalid for closely spaced modes.

IV. Methods for Obtaining Frequency Response Functions

The basics for forming a frequency response function is to excite the test specimen at a point and measure the input force while measuring the structural response at the same point (driving point frequency response function) or some other point (cross frequency response function). Generally speaking, the structural response is measured with an accelerometer; however, strain gages, velocity transducers, etc., can also be used. Force input to the structure is usually one of the following: 1) Impact; 2) Electromagnetic shaker excitation, or 3) Non-contacting magnetic transducer excitation. Our work is done primarily with the impact method or magnetic transducer excitation.

Perhaps the most widely used method for force input to a structure in Fourier analysis is the impact method. Figure 5 shows an impact test in progress. In this figure you see the basic ingredient for impact testing; ie, a hammer with a force gage mounted on it. In this case the striking part of the force gage was made of hard plastic. The striking tip of the force gage plays an important role in determining the effect of the impact. The stiffness of the tip controls the upper frequency limit of the impact if you ignore the effects of the structural stiffness at the point of impact. As the stiffness of the force tip increases, the upper limit of the frequency content of the input force increases. Using this knowledge, the test engineer can tailor the energy content of the impact to a desired maximum frequency limit. Another consideration in impact testing is the local stiffness of the structure to be hit. The same logic applies here as with the hammer tip; therefore, the stiffer the structure at the point of impact the higher the frequency content of the input force. If the point of impact is sufficiently less stiff than the impact tip of the hammer, local nonlinear structural deformations will occur in the test structure causing erroneous force readings to be made. An example of "bad" impact testing would be impacting a skin-stringer type structure in the center of the skin panel.

The advantages of the impact method are the quickness and ease of set-up, and the ease of collecting large numbers of frequency response functions by moving the impact point while leaving the pick-up point constant. The main disadvantage is the limited frequency content of the force input. This reveals itself any time the test engineer works with a light weight flexible structure or at any frequencies above 2000 Hz. Another disadvantage, particularly in the damping design business, is the difficulty in conducting impact testing in an environmental chamber.

In the design of a damping application, a very prominent method of structural excitation is the non-contacting magnetic transducer. Figure 6 shows the experimental set-up for driving a structure with a magnetic transducer. Note that the set-up includes a massive transducer holder to avoid fixture resonants

which may interfere with the measurements.

The magnetic transducer consists of a permanent magnet with an electro-magnet wrapped around the permanent magnet. By varying the current into the electro-magnet, the magnetic field is varied which in turn varies the force on a small magnetic disc attached to the structure. This method of testing has many advantages. Since the excitation is coming from a non-contacting source, there are no structural resonances induced or modified by mechanical connections. It is also very adaptable to environmental chamber testing, and can produce excitation to very high frequency levels. The major disadvantage in the increased complexity of set-up over that of the impact test method. Current testing includes usage of a specially designed transducer to temperatures as high as 2000°F.

Several methods of excitation using the magnetic transducer as the force driver are available [9]. Presently the use of periodic random and pure random noise as force inputs are predominant.

Periodic random noise has the advantage that it is analyzer generated thereby making the entire test controlled and measured by the analyzer. The basic need for pure random excitation is the band selectable Fourier transform. The analyzer currently cannot produce periodic random signals such that a band selectable transform can be calculated.

V. An Example of the use of a Fourier Analyzer

Perhaps the best way to tie all this together is through an illustration of a specific problem. Currently a high cycle fatigue cracking problem exists on the low pressure support of the TF-41 jet engine. To determine if a damping application could be used to control this problem, frequency response functions were taken to determine the resonant frequencies, mode shapes and modal damping of the structure. These response functions were taken using periodic random noise excitation with a magnetic transducer as the driver. An accelerometer measured the structural response. An entire low pressure support was the test specimen.

The low pressure support is the first set of static waves in the TF-41. It is located between the first and second stage fans. The blade passage frequencies over the R.P.M. range of this engine ranged from 1042 to 4650 Hz. Assuming that the main driving forces causing the high cycle fatigue problem were coming from blade passage frequencies, the upper frequency limit of analysis was set at 5000 Hz. The low pressure support is a ring of stator vanes contained by an inner and outer shroud. The vanes are approximately 10.5 inches long. To do a proper modal analysis, define all the resonant frequencies and determine the modal damping inherent in the structure a matrix of frequency response functions were obtained. The matrix of functions obtained consisted of fifty frequency response functions on the vane (five rows of ten points per row) and fifteen frequency response

functions on the outer shroud (three rows of five points per row). This is shown in Figure 7. The outer shroud was modeled to determine if there was coupling between the vane and the shroud. A typical frequency response function from this set is shown in Figure 8.

The major resonant frequencies defined by survey was 1) 530 Hz, 2) 1300 Hz, 3) 1410 Hz, 4) 2350 Hz, 5) 2950 Hz, 6) 3630 Hz, 7) 3960 Hz, 8) 4170 Hz, 9) 4640 Hz. Using the matrix of frequency response functions and available software for Fourier analyzers, mode shapes for these frequencies were determined. Of these modes six were easily identifiable as typical clamped-clamped plate modes, e.g., 530 Hz first bending (see Figure 9), 1300 Hz - first torsion, 1410 Hz - second bending, 2350 Hz - second torsion (see Figure 10), 4170 Hz - third bending, 4640 Hz fourth torsion. The other three modes were more complicated modes which contained cord-wise node lines. It can easily be seen from Figure 8 that there are several resonant frequencies which exist in the engine operating speed. By studying the mode shapes of the resonances in the speed range of the engine, and knowing the location of the crack initiation, the modes of major concern were narrowed to four. They occurred at 1410 Hz, 2350 Hz, 4170 Hz, and 4640 Hz. The modal damping (η) was found to range from .01 to .008 (resonant amplification factor of 100 to 125) for these modes. This low inherent modal damping coupled with the bending moment distribution which could be seen from the mode shapes, led to the conclusion that a constrained layer damping treatment could reasonably be expected to control the resonant high cycle fatigue problem. This conclusion was based on information obtained from the Fourier analyzer. From here, the only data necessary to complete the design of a damping application would be the operational temperature requirements. All other data necessary is available from the analyzer data, ie, resonant frequency, mode shape (wave length), and structural damping.

VI. Field Capability

At this point the advantages of working with the Fourier analyzer in the laboratory is obvious. One can also readily see the powerfulness this equipment would have if it could be obtained in a field data acquisition package. At the University, we developed such a package under an Air Force P.R.A.M. contract. The system is shown in Figure 11 in the engine repair shop at Nellis Air Force Base, Nevada. The system was basically the one shown in Figure 1 except the inter-active graphics terminal and hardcopy unit was eliminated. The analyzer was packaged in three air shippable containers which weigh approximately 300 pounds each. During the past year of operating this system, it has traveled over 16,000 miles. See Figure 12 for locations where system has been used. This system has proved very valuable for obtaining large quantities of high quality data necessary for damping design.

VII. Summary

Through the use of proper test techniques, the Fourier analyzer is a powerful tool in vibration analysis. It can provide all the necessary dynamic data to evaluate whether or not a damping application is appropriate and if it is, can also provide dynamic data needed in the design effort for the damping fix. The analyzer has the demonstrated ability to accomplish this task both in the laboratory environment and in the field.

VIII. Acknowledgments

This work was sponsored by the Metals Behavior Branch of the Air Force Materials Laboratory, in part under Contract F33615-76-C-5137 with the University of Dayton Research Institute. The author wishes to acknowledge Dr. D.I.G. Jones for assisting with editing and Judy Mills for typing the manuscript.

References

1. Bracewell, Ron, *The Fourier Transform and Its Application's*, McGraw - Hill Book Company, New York, 1965.
2. Hewlett Packard - Application Note 140-0.
3. Ramsey, K.A. "Effective Measurements for Structural Dynamics Testing, Part II" *Sound and Vibration*, December 1975.
4. Brown, Dave - Short Course - "Modal Analysis Theory and Measurement Techniques" Sponsored by University of Cincinnati and Hewlett Packard.
5. Bendat, J.A., and Piersol, A.G., Measurement and Analysis of Random Data, John Wiley and Sons, New York, 1966.
6. Drake, M.L. and Henderson, J.P., "An Investigation of the Response of a Damped Structure Using Digital Techniques", Shock and Vibration Bulletin 45, Part 5, 1975.
7. Richardson, M., and Knishan, J., "Identifying Modes of Large Structures from Multiple Input and Response Measurements" Aerospace Engineering and Manufacturing Meeting, November 29 - December 2, 1976.
8. Klusterman, A.L., "On The Experimental Determination and Use of Modal Representations of Dynamic Characteristic" Ph. D. dissertation, University of Cincinnati, 1971.
9. Brown, D., Carbon, G., Ramsey, K. "Survey of Excitation Techniques Applicable to the Testing of Automotive Structures" International Automotive Engineering Congress and Exposition, February 28- March 4, 1977.

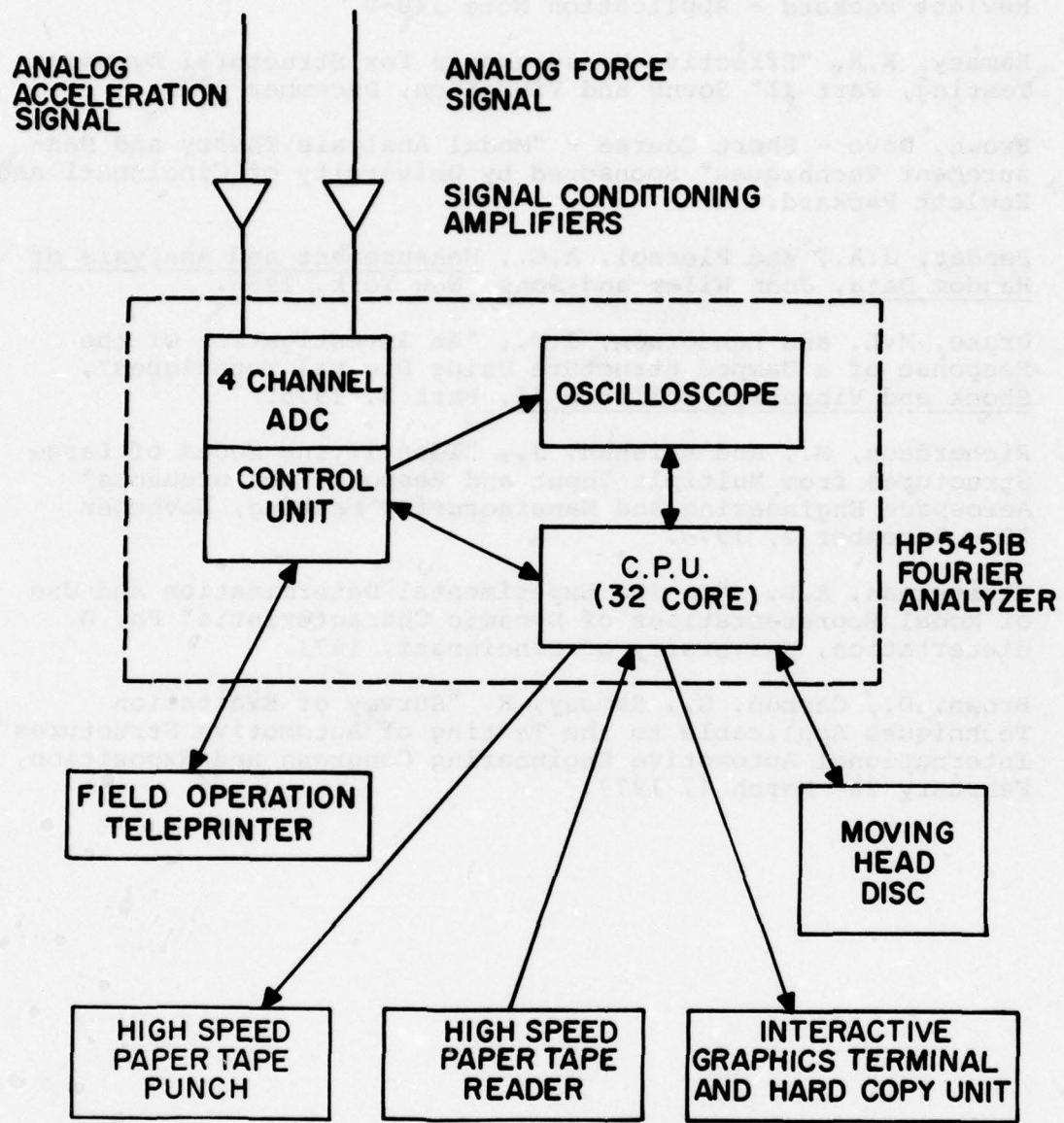
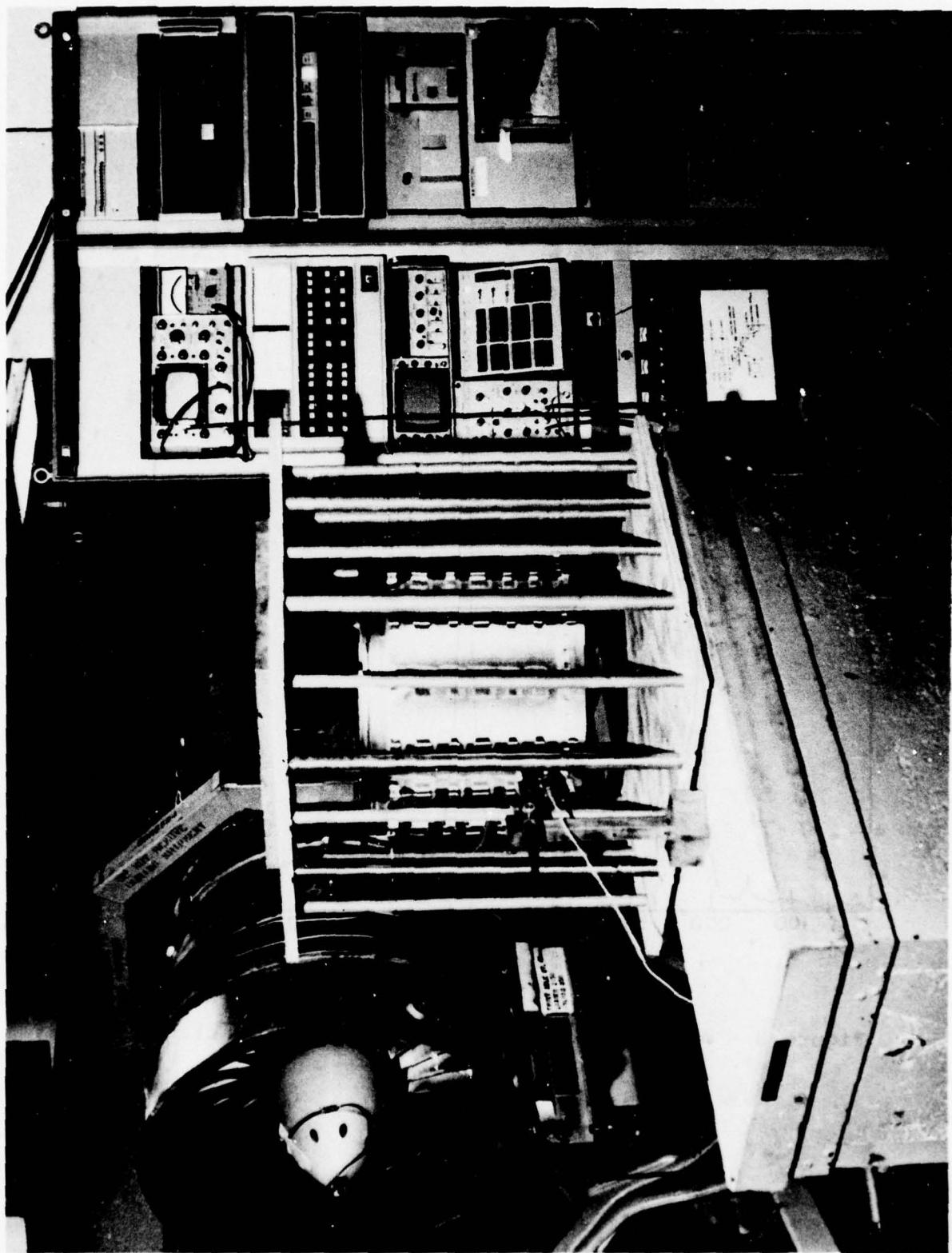


Figure 1 - Schematic of Fourier Analyzer

Figure 2 - Rack-mounted system



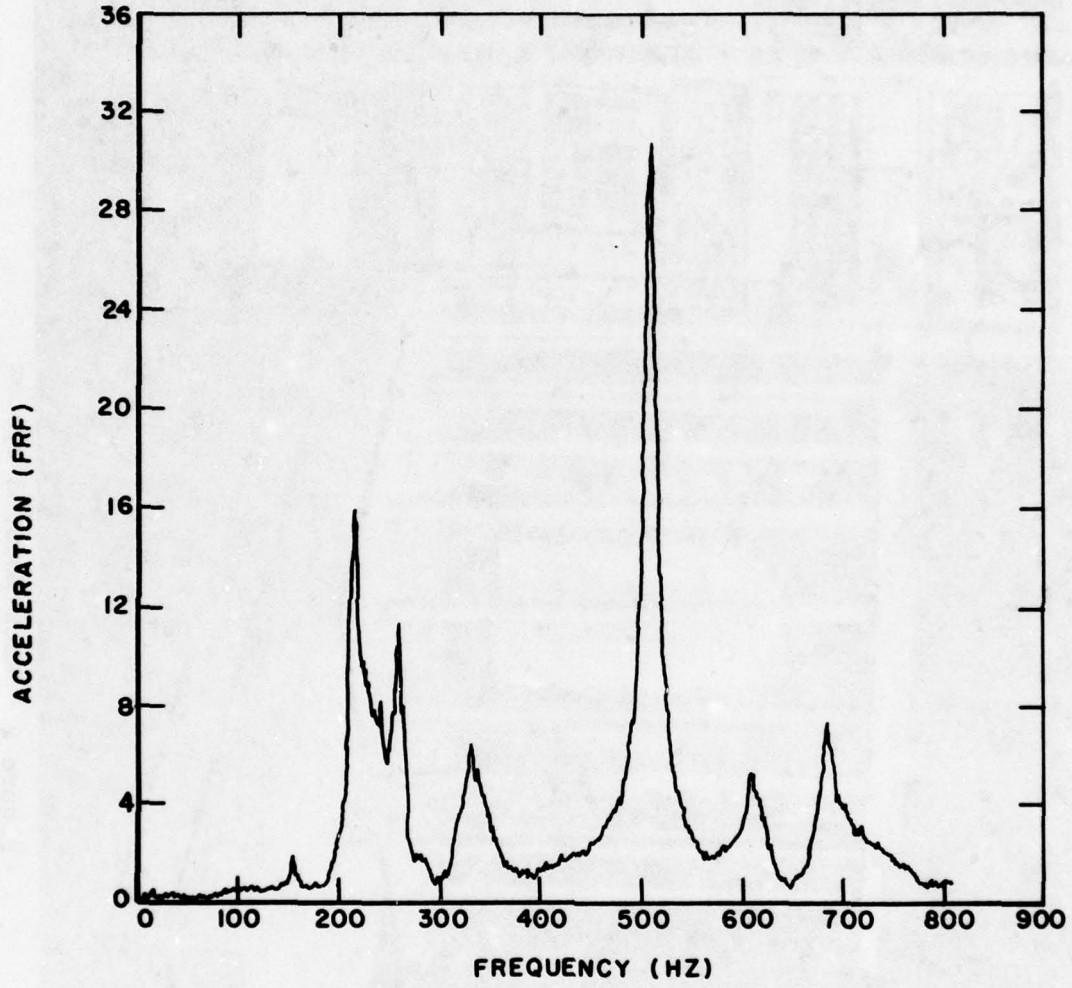


Figure 3 - Acceleration-frequency response function

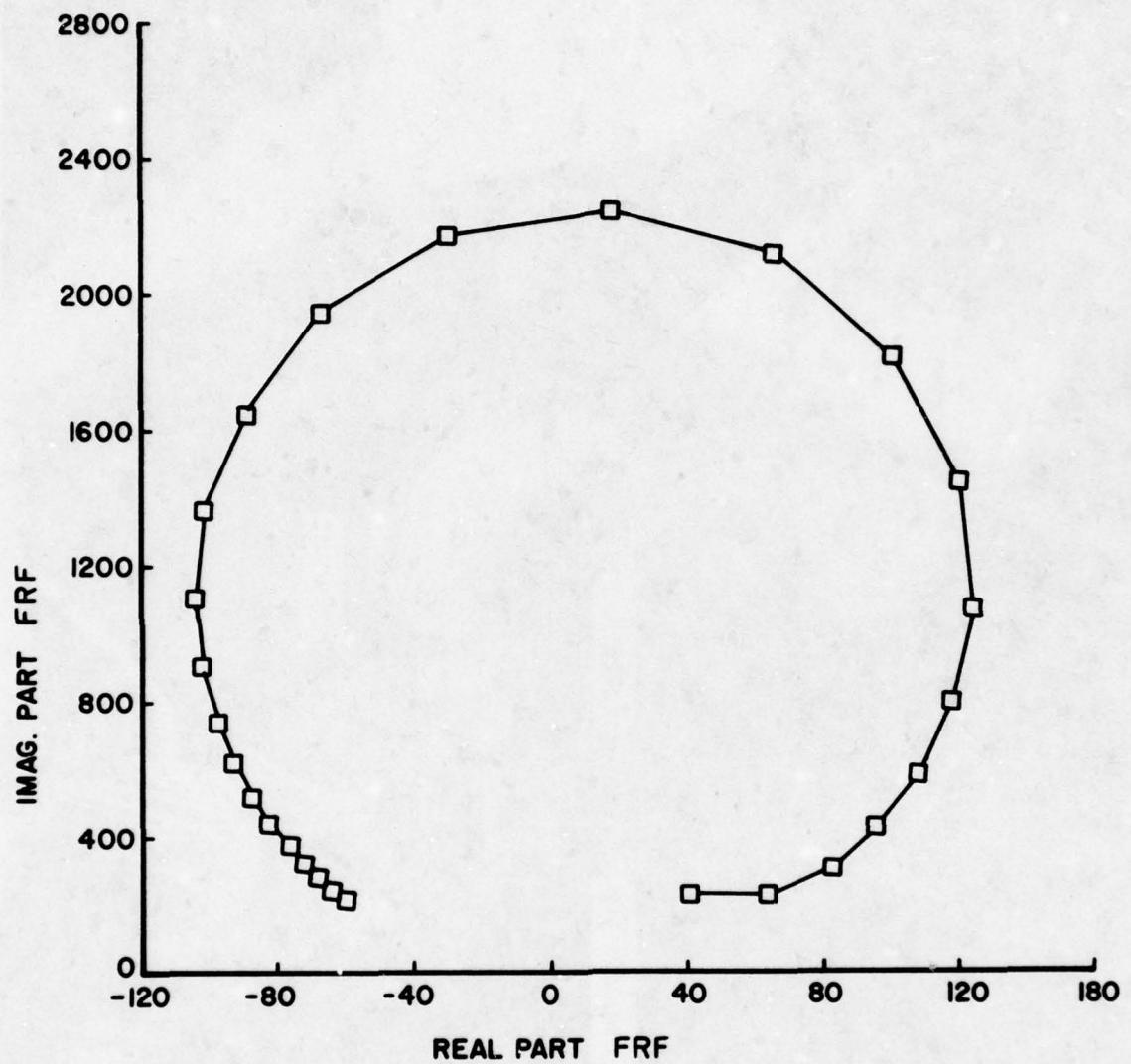


Figure 4 - Nyquist plot of a frequency response function

Figure 5 - Impact test in progress

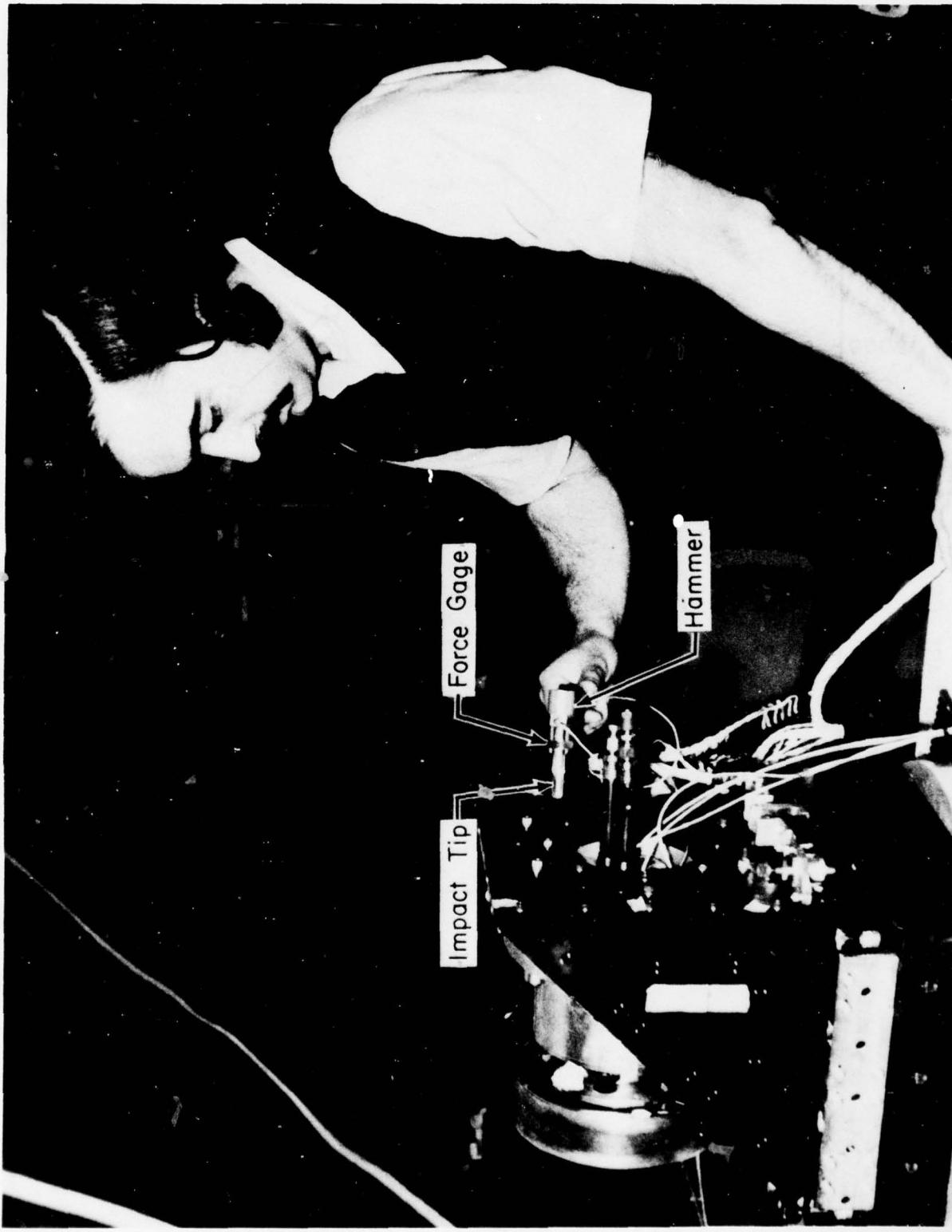
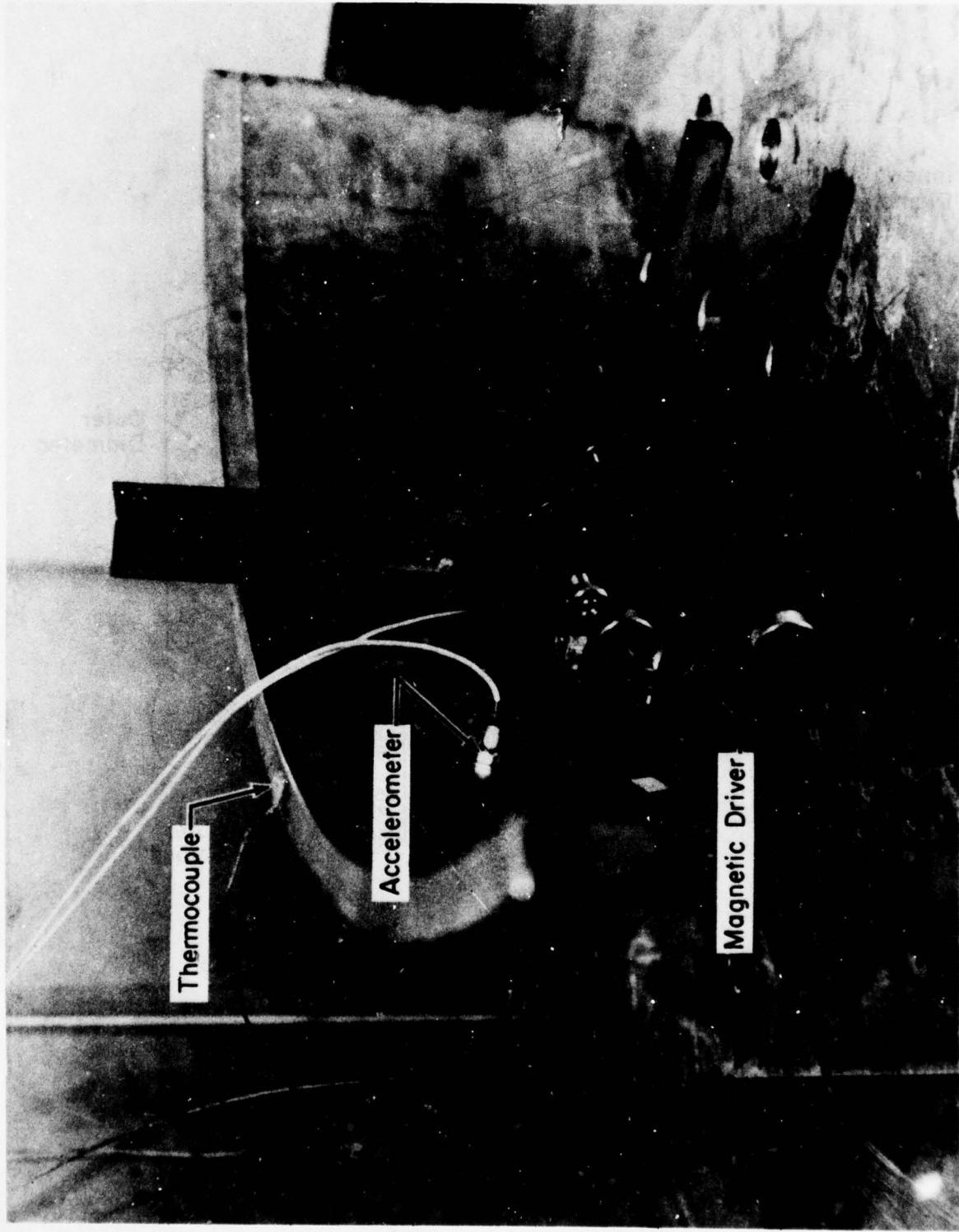


Figure 6 - Experimental set-up for driving a structure with a magnetic transducer



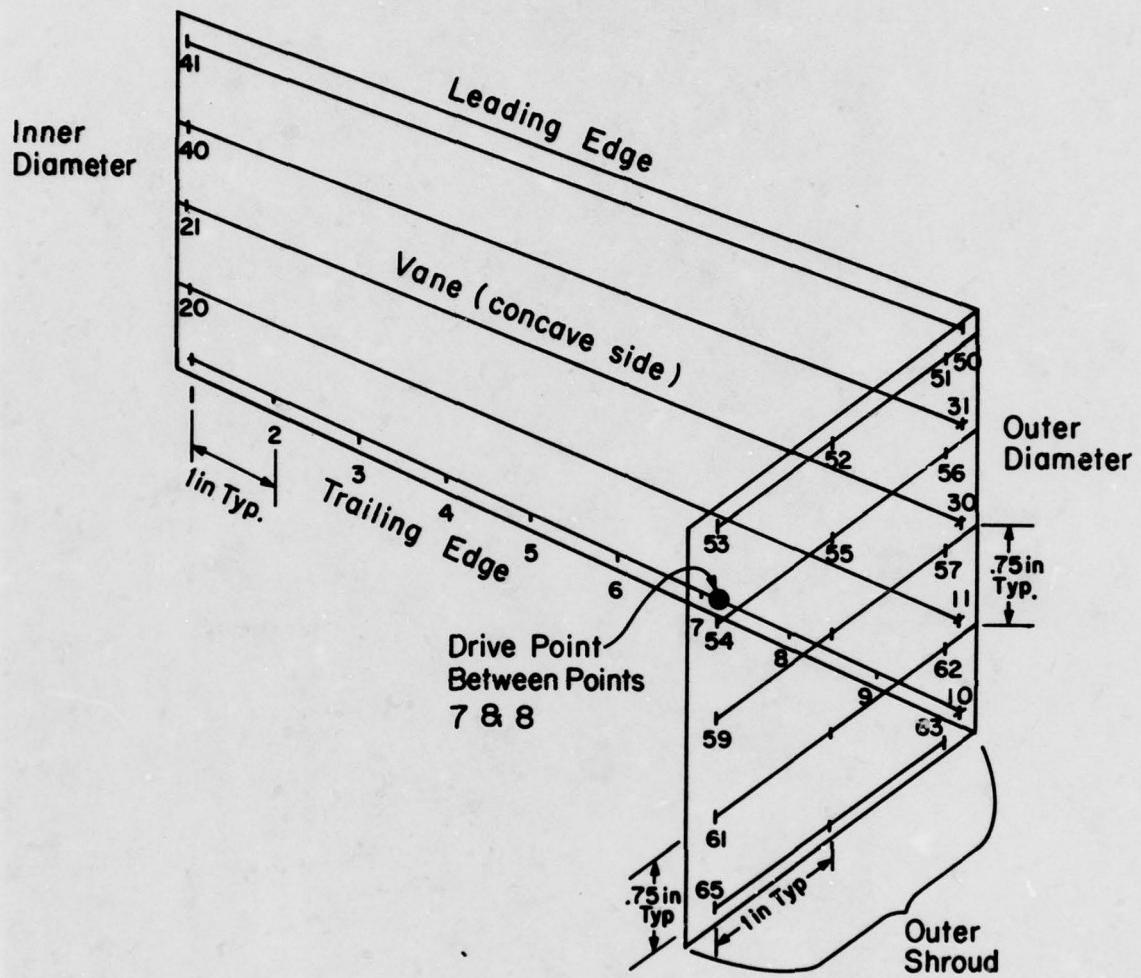


Figure 7 - Matrix of functions

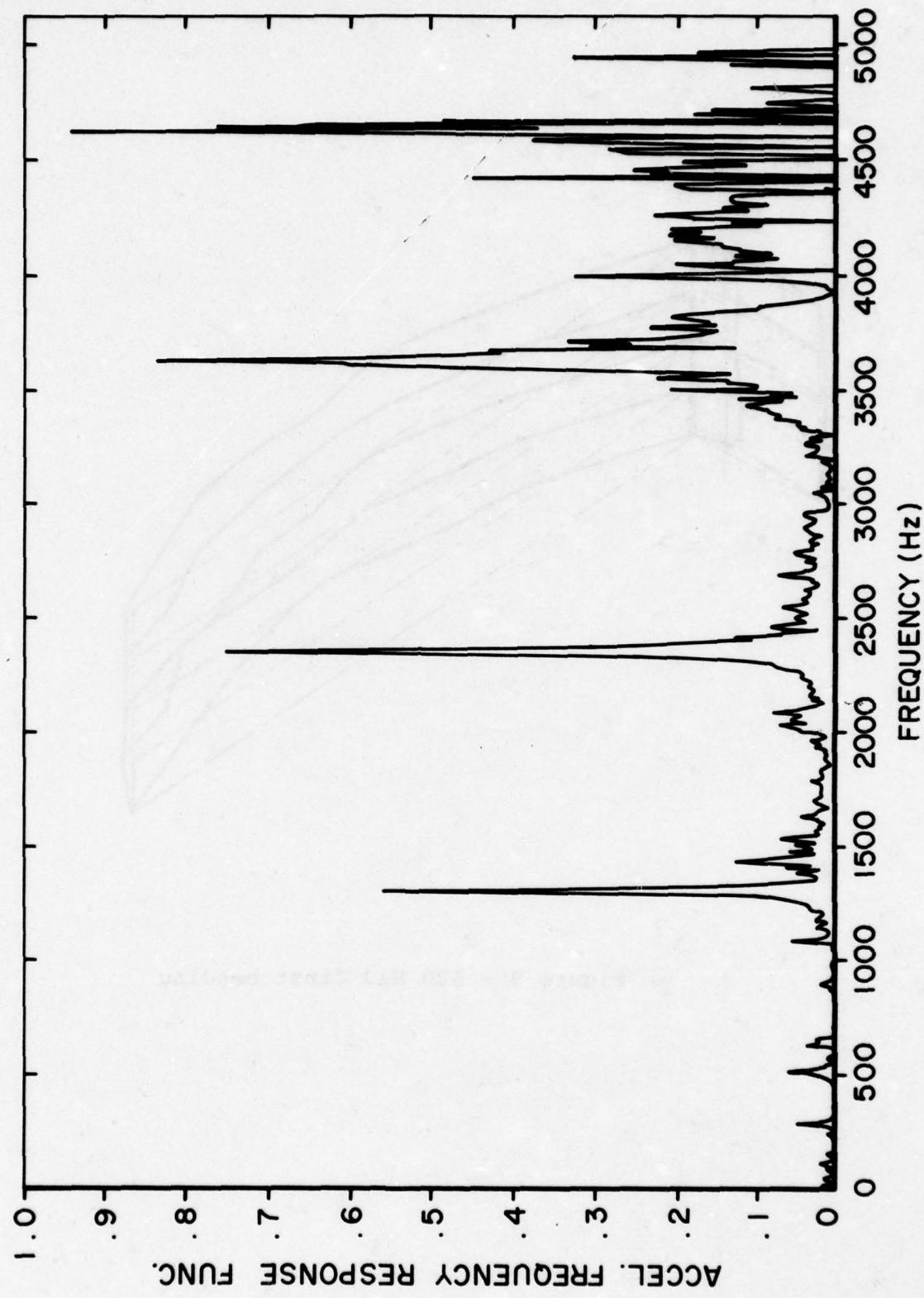


Figure 8 - Typical frequency response function

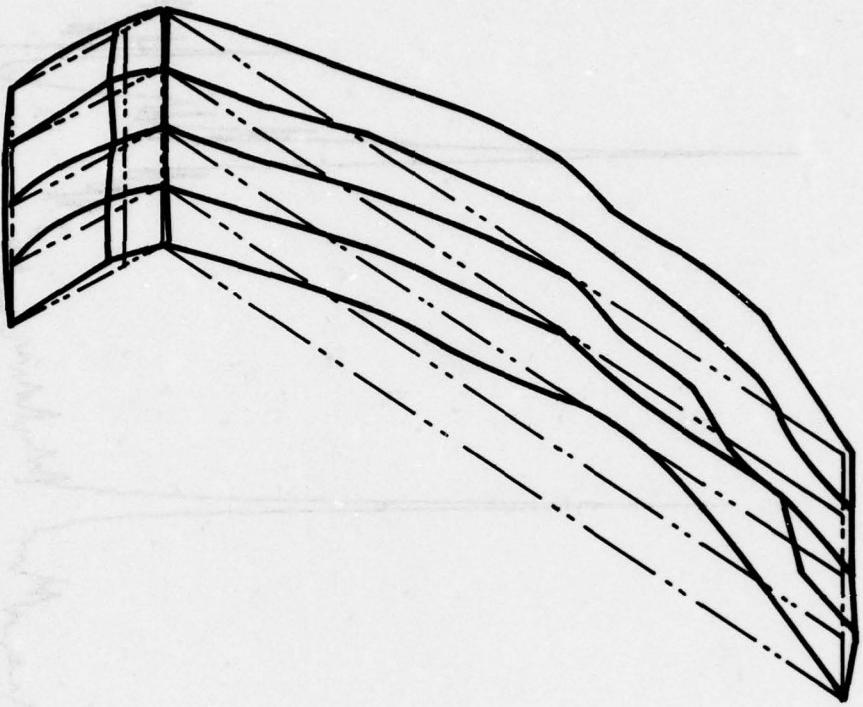


Figure 9 - 530 Hz, first bending

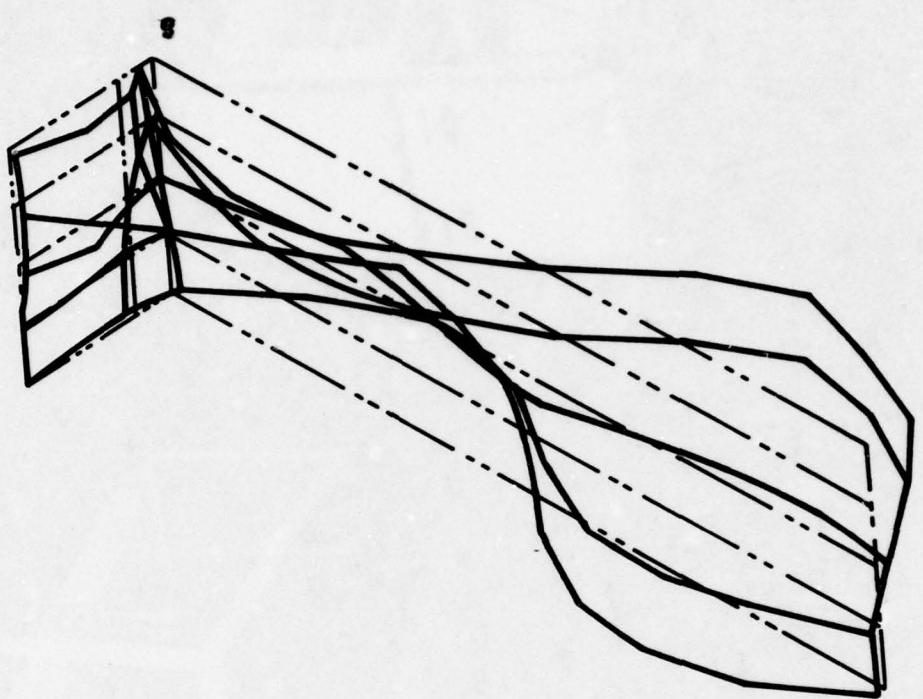
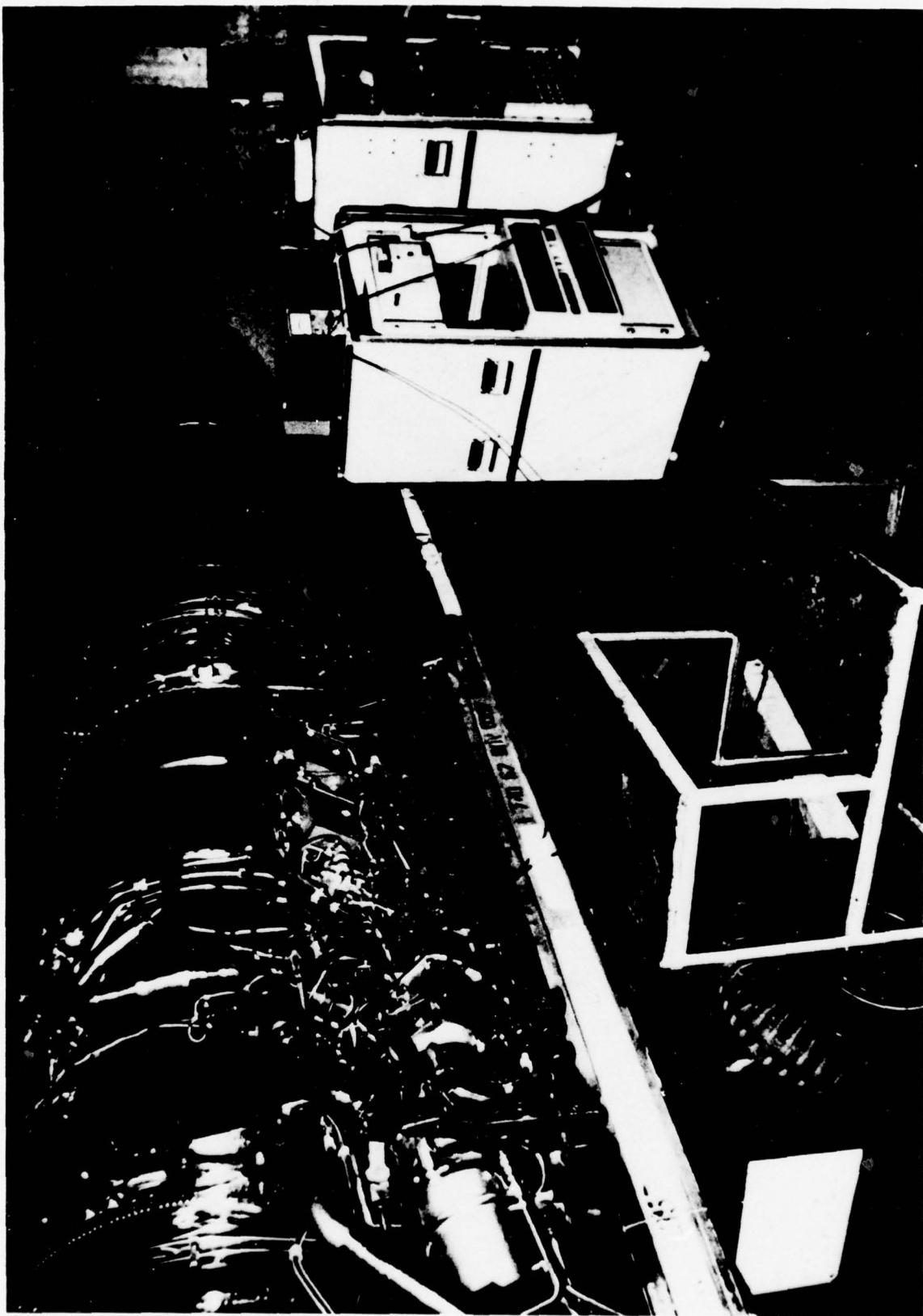


Figure 10 - 2350 Hz, second torsion

Figure 11 - System of the field data acquisition package



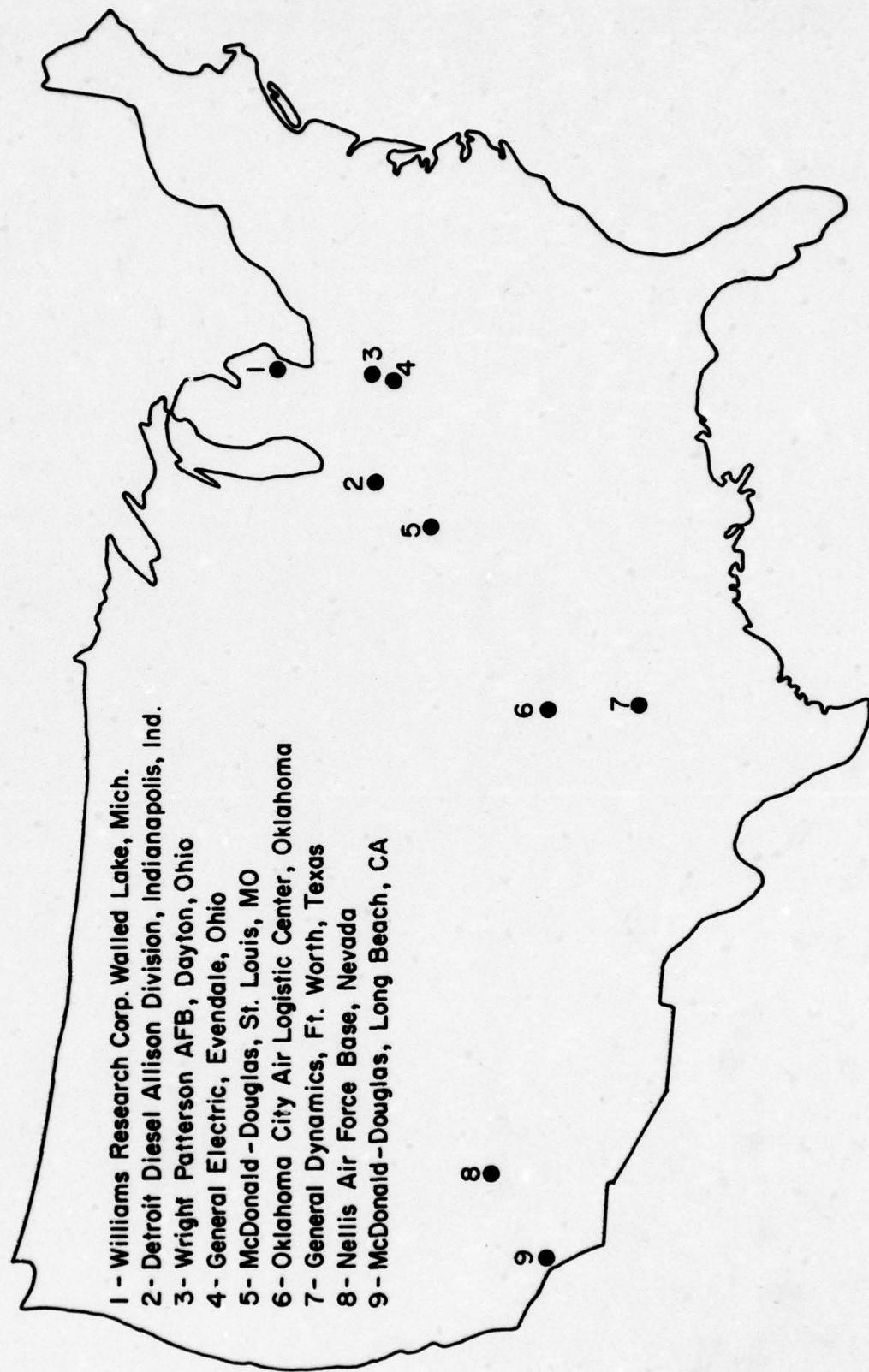


Figure 12 - Locations where system has been used

A THOROUGHLY ENGINEERED APPLICATION OF DAMPING
TECHNOLOGY TO JET ENGINE INLET GUIDE VANES

Lynn C. Rogers
Air Force Flight Dynamics Laboratory
Wright-Patterson Air Force Base, Ohio

and

Michael L. Parin
University of Dayton Research Institute
Dayton, Ohio

INTRODUCTION

The TF-30-P100 Jet Engine is employed in the U. S. Air Force F-111F Fighter Aircraft. It is a modern, highly sophisticated, high thrust-to-weight ratio jet engine. Inlet air first encounters the inlet guide vanes (IGV). These stationary air foils slightly turn the air for entry into the first stage fan blades, which pass near the trailing edge of the IGV's. The IGV's are titanium weldments which are in turn welded to inner and outer shrouds (cylindrical sections) to form the IGV case assembly. Hot bleed air passes through the IGV during climatic icing conditions. In the past few years, cracks have been discovered in the IGV's prior to the completion of the required lifetime. The cracks have been of such size and number that maintenance/refurbishment has become a high cost item.

An examination of cracked surfaces proved that they were due to high cycle fatigue. Test cell and flight test measurements have shown that vibratory stresses are very high while static stresses from thermal gradients and residual manufacturing strains are contributory. Spectrum analysis has shown that excitation is predominantly discrete at engine order and blade passage frequencies with some wide band excitation from inlet air turbulence. Some results (from one third octave band analysis) are presented in Figure 1 where the vibratory frequency of peak stresses in test cell operation is plotted versus the corresponding engine speed. Secondary peaks within 15% of the maximum amplitude are also shown.

Individual blade passage frequency (at 28 times engine speed represented by the 28E line in Figure 1) excites the fourth torsion mode at 4000Hz, fifth bending at 3600 Hz, and third torsion at 3000 Hz. These are nominal frequencies as they vary with temperature and other engine conditions. The first torsion mode at 850 Hz and first bending at 350Hz are excited at lower engine orders. Analysis revealed that the highest vibratory stresses were occurring in the 3000 and 4000 Hz modes. An analysis of service operations indicates that engine speeds which excite these modes occur throughout the entire flight envelope. An attractive approach to vibratory stress reduction and consequent crack abatement and life extension was judged to be an additive, multiple constrained layer, broad temperature range, viscoelastic damping treatment.

REQUIREMENTS

In the application of viscoelastic damping material, an essential requirement is the knowledge of the temperature at which vibratory damage occurs in service. Figure 2 shows cumulative percent of time versus total outside air temperature for service operation of the F-111 aircraft. Based on this data it was decided to design the damping treatment for the average temperature of 62°F. (Note that this compares closely to the 59°F standard

day temperature). Figure 3 shows a summary of the temperature requirements of the IGV damping treatment. The operating range is between 0° and 125°F and accounts for 98% of engine operation and, presumably, damage. The values in the individual bars are the percent of operating time for that particular temperature increment. In addition to the operating temperature, the survival temperature is an over-riding consideration. During operation of the F-111 aircraft, the ram temperature is not to exceed 307°F for greater than five minutes during any excursion and is not to exceed 417°F at any time. The autoclave temperature for curing the structural adhesive used to bond the damping treatment to the vane is 350°F. The heat transfer analysis for normal anti-icing operation shows that the maximum bond line temperature is 420°F. It follows that 420°F is the maximum temperature for survival.

In addition to temperature, there are other requirements which are crucial considerations in the design of the damping treatment. One of the major issues is adhesion. Obviously, the damping treatment must adhere to the existing structure and remain in place during service operation for it to be effective. A major factor in adhesion and bonding technology is surface preparation of the aluminum foil in the damping wrap and of the titanium of the existing IGV structure.

Another factor is airflow as it affects engine performance and turbine inlet temperature, where an increase of even 5°F will significantly reduce life of turbine components. The inlet area between the vanes is partially blocked from the thickness of the damping wrap on the vane surface. Obviously, the blocked area consideration alone would result in degraded performance; however, it happens that the smoothing effect of the damping wrap over the protruding spanwise welds (of fabrication) completely offsets the blockage effect, and there is no measurable net effect on performance.

Another factor was distortion tolerance of the engine which the damping wrap does influence beneficially. Formability of the damping wrap to the vane surface was also a major consideration. Another factor was foreign object damage (FOD), and the aluminum foil, backed up by the soft viscoelastic adhesive, is susceptible. Erosion is another factor. The effectiveness of the anti-icing was a rather major concern. The channels between the interior stiffeners of the vane contain anti-icing air during appropriate climatic conditions. Thus, the damping wrap must not provide an insulating effect. It must provide heat transfer to the vane leading edge surface to prevent the formation of ice. The survival temperature of 420°F, which results from the most severe anti-icing conditions, has already been mentioned. This 420°F temperature approaches the upper limits of the material used. The handling of anti-icing effectiveness and of maximum bondline temperature required extensive heat transfer analyses. Overhaul is another major item. When service time accumulates on the engine such that it needs to be overhauled, the IGV case itself must be overhauled. If the damping wrap is sufficiently damaged, from FOD and so forth, it must be replaced; then this must be relatively easily performed operation.

LABORATORY TESTS

Due to the high cost of engine test cell experimental programs, a laboratory test program was devised to design an additive damping treatment and investigate the effect it could be expected to have on the vibratory stress levels of the IGV's.

The initial phase of the work focused on selecting a suitable experimental setup that would give sufficiently accurate modal damping measurements of additive damping treatments. A number of support configurations for the IGV's were devised and analyzed. Finally, a vane welded between two (2) large titanium blocks was chosen. This arrangement adequately simulated the actual boundary condition the vanes were subjected to in the engine and the inherent specimen baseline modal damping insured a reliable comparison between the vane damping levels before and after damping treatment.

A modal survey of the specimen, using holographic techniques, revealed several vibration modes. These included the first through fifth bending modes and the first through fourth torsional modes. Figure 4 illustrates the most damaging of these modes along with their respective frequencies. These mode shapes and frequencies compare quite favorably with those identified by the engine manufacturer in independent tests.

Tests were conducted on the vane specimen over a wide temperature range to determine the effect of additive damping wraps on the modal damping of the vane as a function of temperature. The vane was excited by using a magnetic transducer driving an iron disc bonded onto the vane. The response was picked up by an accelerometer. Both the transducer and accelerometer were located to insure excitation and response of the third and fourth torsional modes. Figure 5 is a schematic of the test system used.

Four (4) damping wrap designs were evaluated. Each had the same geometry but varied as to viscoelastic and constraining layer materials. By varying the material composition of the wraps, both the level of damping and the effective temperature range of the wrap could be changed as desired. The basic wrap design is illustrated in Figure 6.

Figure 7 is the plot of modal loss factor versus temperature for the four (4) damping wrap designs. Each curve is designated as to its inner constraining layer and damping material used. As can be seen, the wrap can be designed to be effective over different temperature ranges by changing its composition. Figure 7 includes a bar graph depicting percent time at temperature increments which the vanes experience during their service life. This bar graph, in conjunction with the loss factor curves, indicate that the ISD-830-110 and aluminum configuration is less suitable for the desired temperature range. The other three (3) configurations all provide acceptable damping levels over the temperature range of interest.

The final choice of wrap configuration was made on the basis of factors other than composite loss factor versus temperature curves. Difficulties and tight process control requirements with the viscoelastic materials

adhering to the Ultra-High Modulus (UHM) Graphite eliminated the ISD/112/113-U.H.M. graphite design. The ISD-113/830-aluminum configuration provided damping over the temperature range. In the final analysis, however, a wider margin in the effective damping level for the temperature region above 125°F dictated the use of the ISD 112/830-aluminum wrap design. This margin also provided significant damping of the lower modes at the service operating temperatures.

During the course of the testing it was necessary to establish the damping properties of 3M's ISD-113 viscoelastic material as a function of temperature and frequency. The complex modulus properties of ISD-113 were measured using a vibrating beam technique. A schematic of the example system used is shown in Figure 8. Curves of shear modulus and loss factor versus temperature for various frequencies are shown in Figure 9.

DESCRIPTION OF THE DAMPING TREATMENT

The damping treatment, illustrated in Figure 6, consists of aluminum foil constraining layers and viscoelastic damping material. The viscoelastic material used was the 3M Company ISD-830 on the concave surface (two layers), and ISD-112 on the convex surface (again, two layers). Each constraining layer was five mils of aluminum foil. Under the viscoelastic was two mils of aluminum foil, necessary to prevent air entrapment, which would severely degrade the durability. The two mils of aluminum foil were bonded to the titanium surface with a structural adhesive (AF 126 epoxy, nominally five mils thick). The total thickness was about 20 mils. The circumference (i.e., picture frame) of the damping treatment, including the leading edge, was bonded to the titanium surface.

ENGINE TEST CELL OPERATION

During a series of engine operations in the test cell the vibratory stresses were investigated for the IGV case with and without damping treatment. Numerous strain gages and thermocouples were located to give data on temperature distribution and stress reduction. Performance tests were also made. Parameters were measured which would permit calculation of turbine inlet temperature which significantly affects the life of turbine components. Distortion tolerance was also measured and it was found that the additive damping treatment enhanced the distortion tolerance. Durability was also investigated, that is, the tolerance of the damping wrap to the anti-icing temperature cycles, and steady state temperature distributions were investigated. The main durability test consisted of 50 cycles of anti-icing air. This is representative of 1200 hours of engine service operation. In addition, modal damping of the significant modes was measured in the test cell with and without damping treatment. In all instances modal damping was significantly increased with the damping treatment in place.

FIELD EVALUATION TEST

Prior to fully qualifying the wrap design, but at such a time that its development was considered adequate for service confirmation, a set of damping wraps was installed on an IGV case that was mounted on an engine in service. These wraps were instrumented with temperature indicating paints and patches for the purpose of acquiring additional information on the in-service thermal environment. The aircraft on which this case was installed was equipped with a service life monitoring program recorder which allowed a review of the aircraft flight usage in the event any change in the wrap was detected. Pilot debriefings were to include the number of times the anti-icing system was activated during flight and the time duration. Pre-flight inspection of the wraps was requested. In the event damage to a wrap was found, a quick and simple repair procedure was outlined, which consisted of trimming away any disbonded region of foil and applying a quick setting, two part epoxy to the exposed edges. This procedure circumvented any need to perform lengthy maintenance on the aircraft because of the wraps.

At this writing the field service evaluation wraps have accumulated in excess of 185 hours on the engine. During this time no cracks have been detected. The wraps have successfully withstood the thermal environment with no loss of damping effectiveness. Minor F.O.D. damage has occurred on a few wraps. These wraps were repaired using the procedure outlined above without impact to the aircraft flight schedule or operational readiness. These wraps have continued to provide adequate dynamic stress reduction for the vanes as evidenced by the notable absence of vane cracks.

Visual inspection and coin tap tests reveal the excellent condition of the field service wraps, and the absence of vane cracks indicate the wraps are effectively reducing dynamic vane stresses. The temperature indicating paints and patches confirm the upper temperature bound used for the wrap design.

The field evaluation test has shown that a wrapped inlet guide vane does abate in-service cracking of the vanes and that the wraps can withstand the severe service environment to make them a practical, low-cost easily implemented remedy to the high maintenance cost vibration induced cracking.

SUMMARY

The additive damping wrap provides significant vibratory stress reduction sufficient to prolong the service life of inlet guide vanes to the design life. The field service wraps provide data showing the wraps are sufficiently durable to withstand the service environment and abate vane cracks. The damping treatment is a practical, low-cost, attractive means of greatly abating the occurrence of cracks in the inlet guide vanes.

ACKNOWLEDGEMENTS

This work was performed under the sponsorship of the Air Force Materials Laboratory and Aeronautical Systems Division. Of the many organizations and individuals who supported this effort, Pratt and Whitney Aircraft, The 3M Company, Dr. J. P. Henderson, Mr. D. Paul, Mr. M. A. Stibich, and Mr. W. P. Dunn should be mentioned.

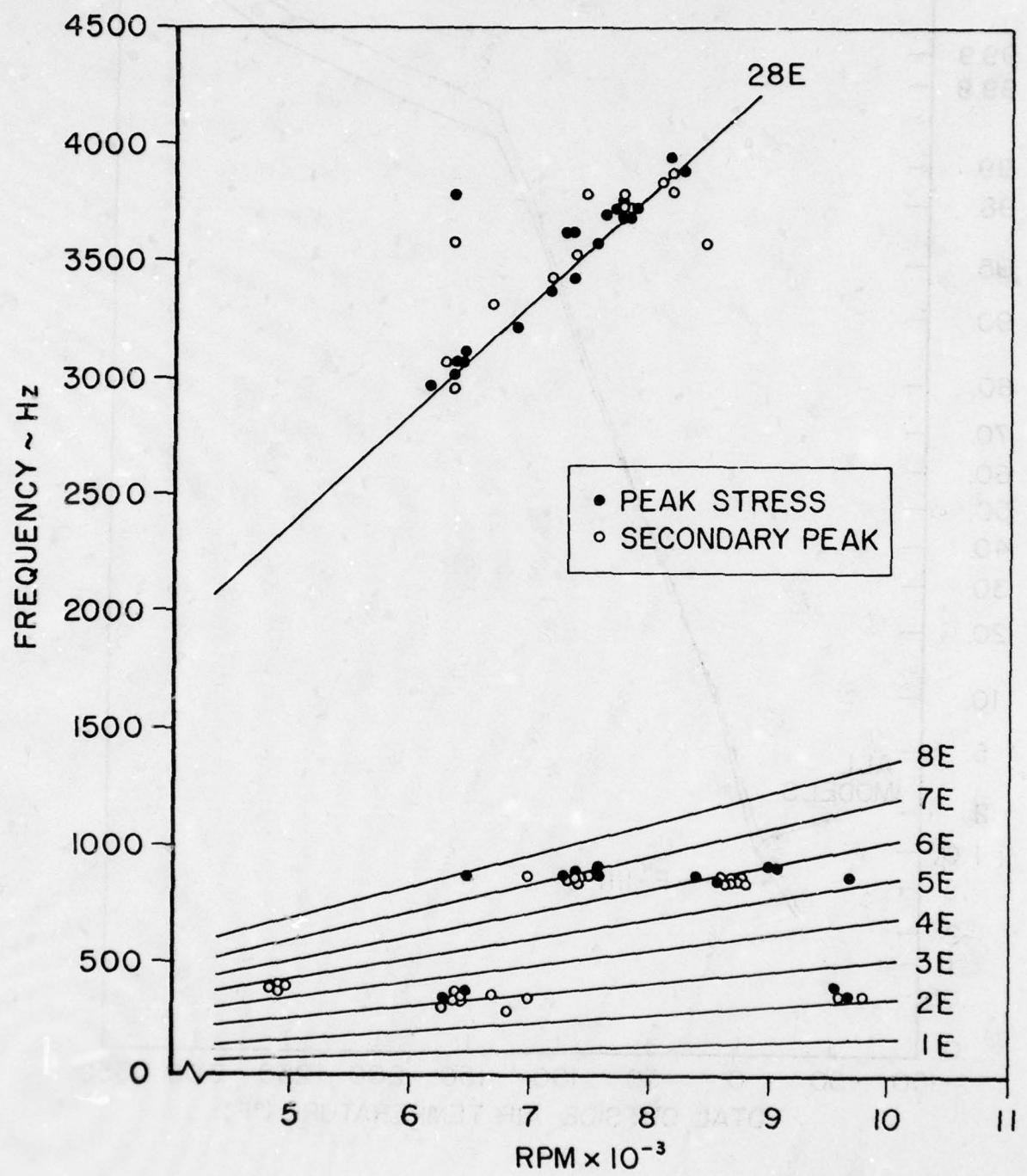


Figure 1. Frequency and RPM of Peak Stresses.

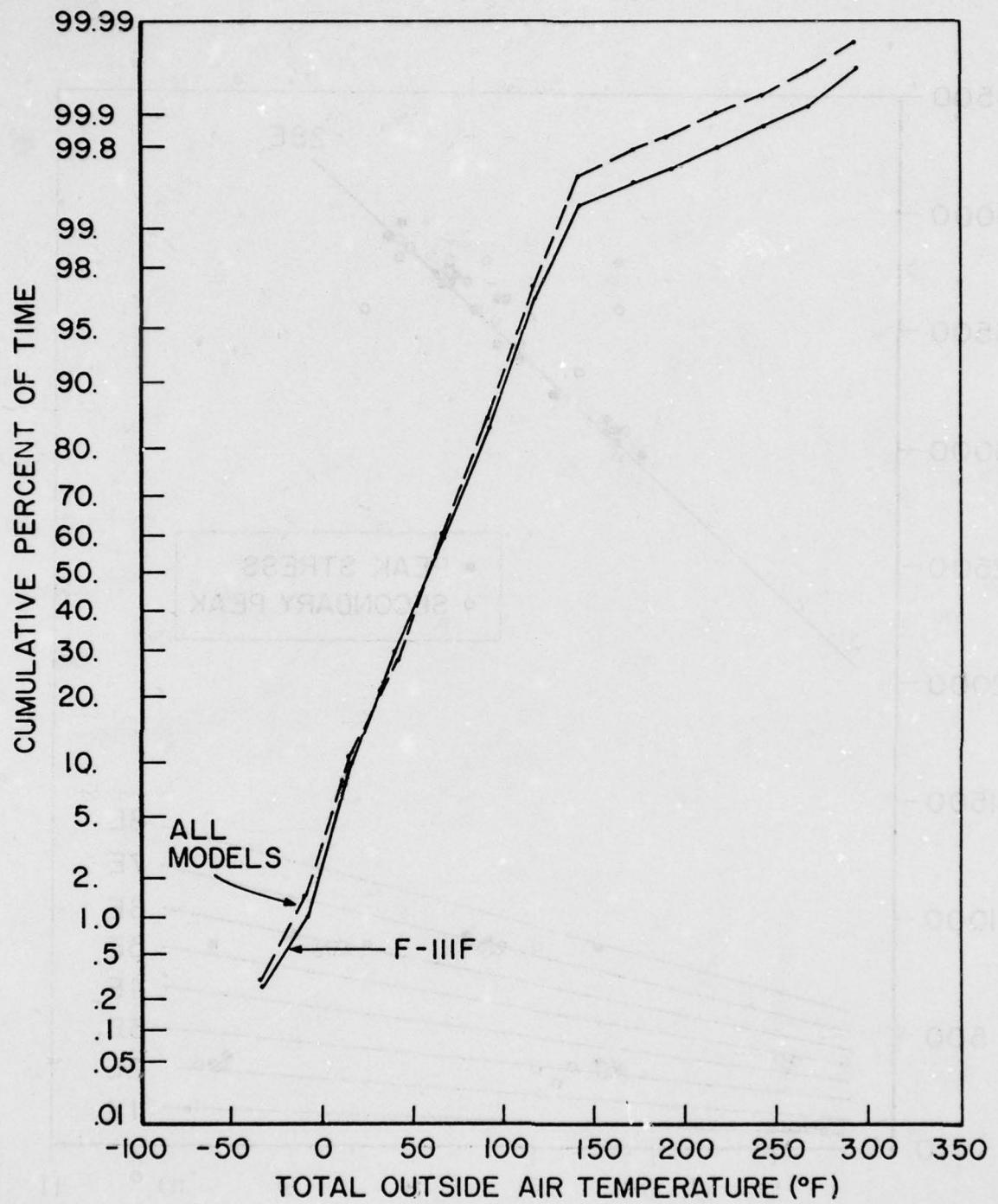


Figure 2. Percent of Time at Temperature From Service Life Monitoring Program Data.

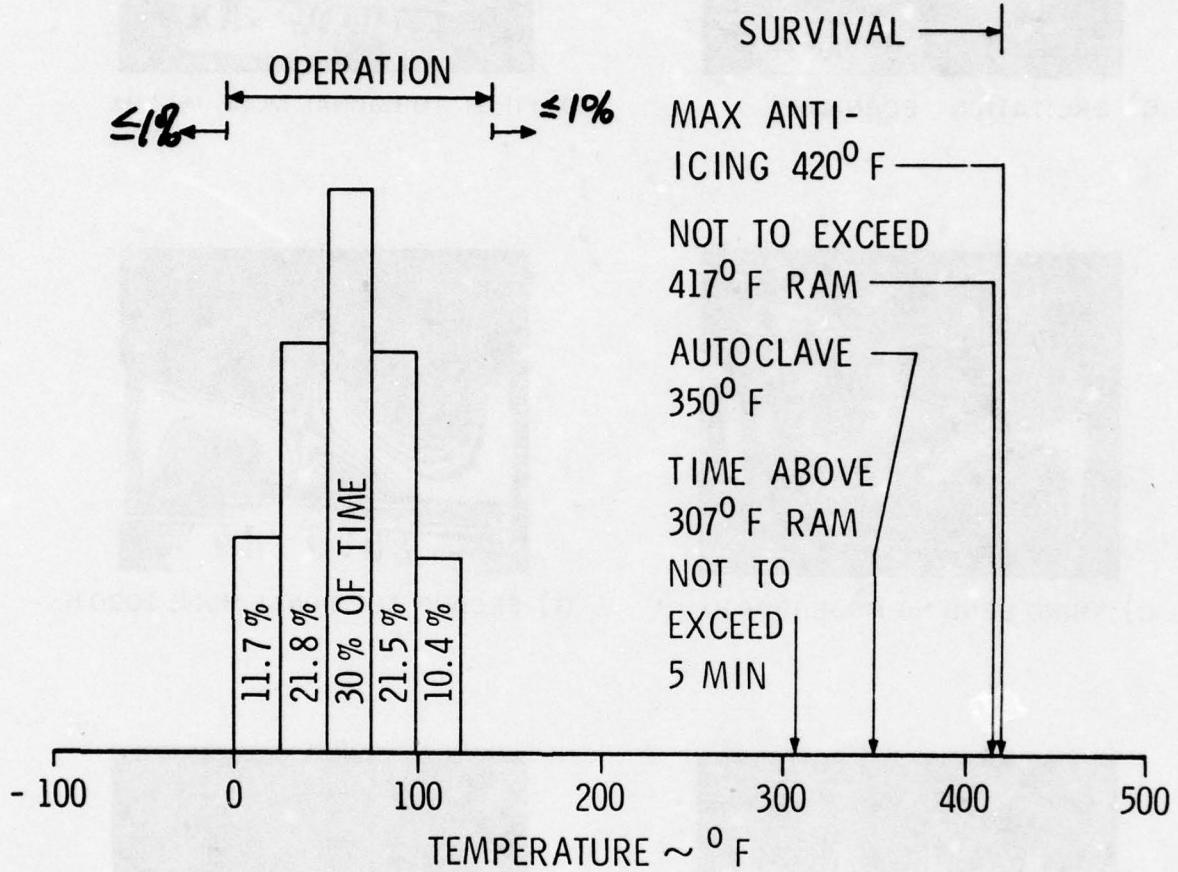
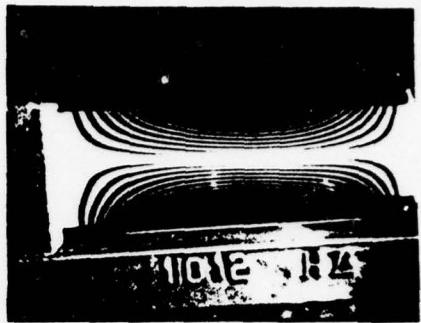


Figure 3. Temperature Requirements of IGV Damping Treatment.



a) EXCITATION TECHNIQUE



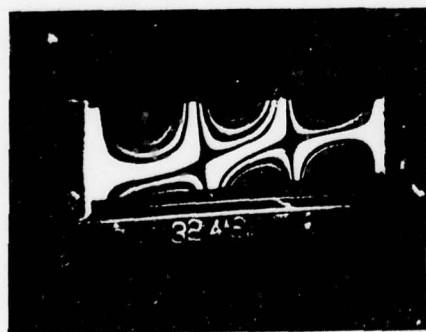
b) FIRST TORSIONAL MODE 1012 Hz



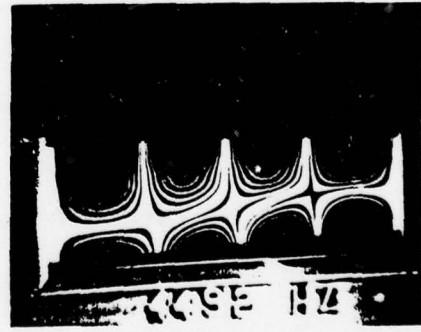
c) THIRD BENDING MODE 1994 Hz



d) SECOND TORSIONAL MODE 2090 Hz



e) THIRD TORSIONAL MODE 3242 Hz



f) FOURTH TORSIONAL MODE 4492 Hz

Figure 4. TF-30-P-100 Inlet Guide Vane Shapes.

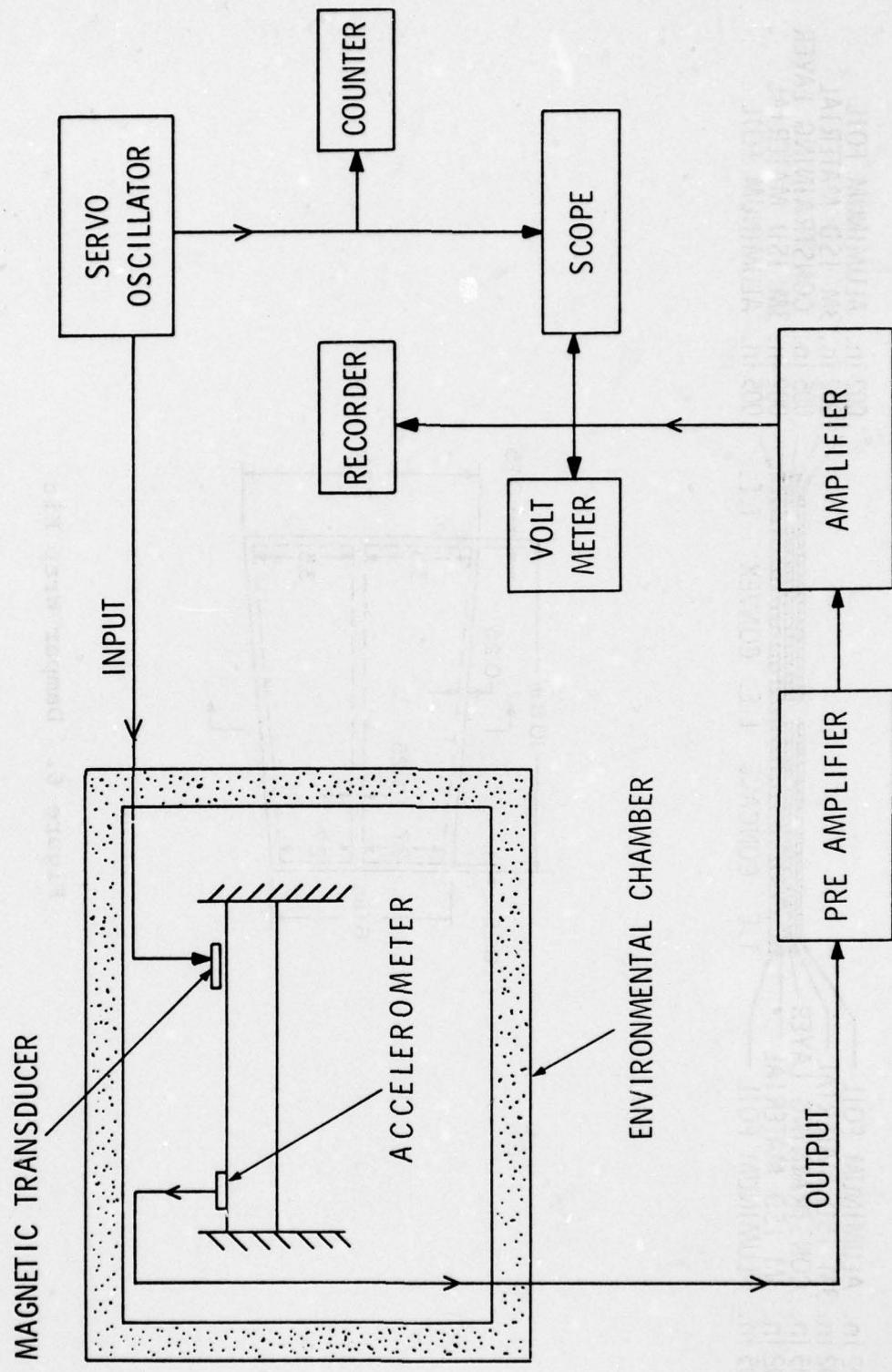


Figure 5. Laboratory Test Set-up.

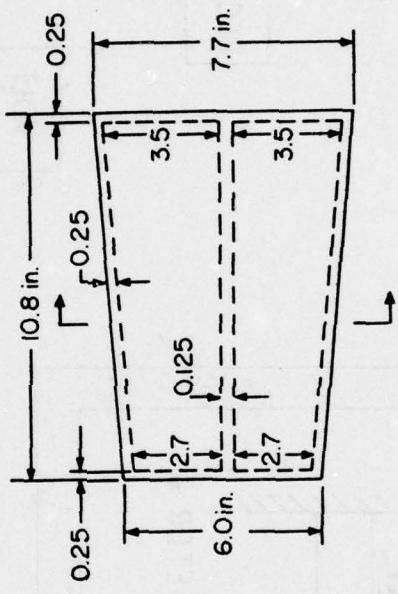
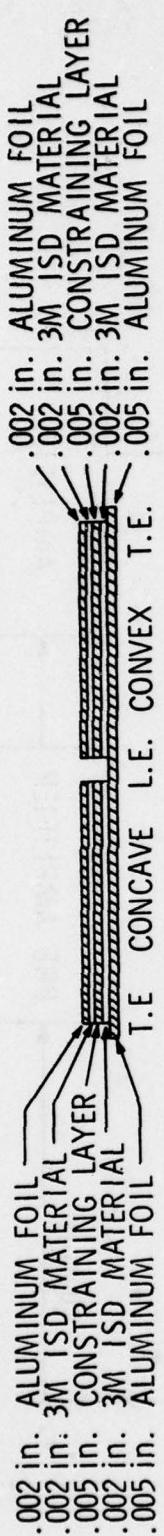


Figure 6. Damper Wrap Kit

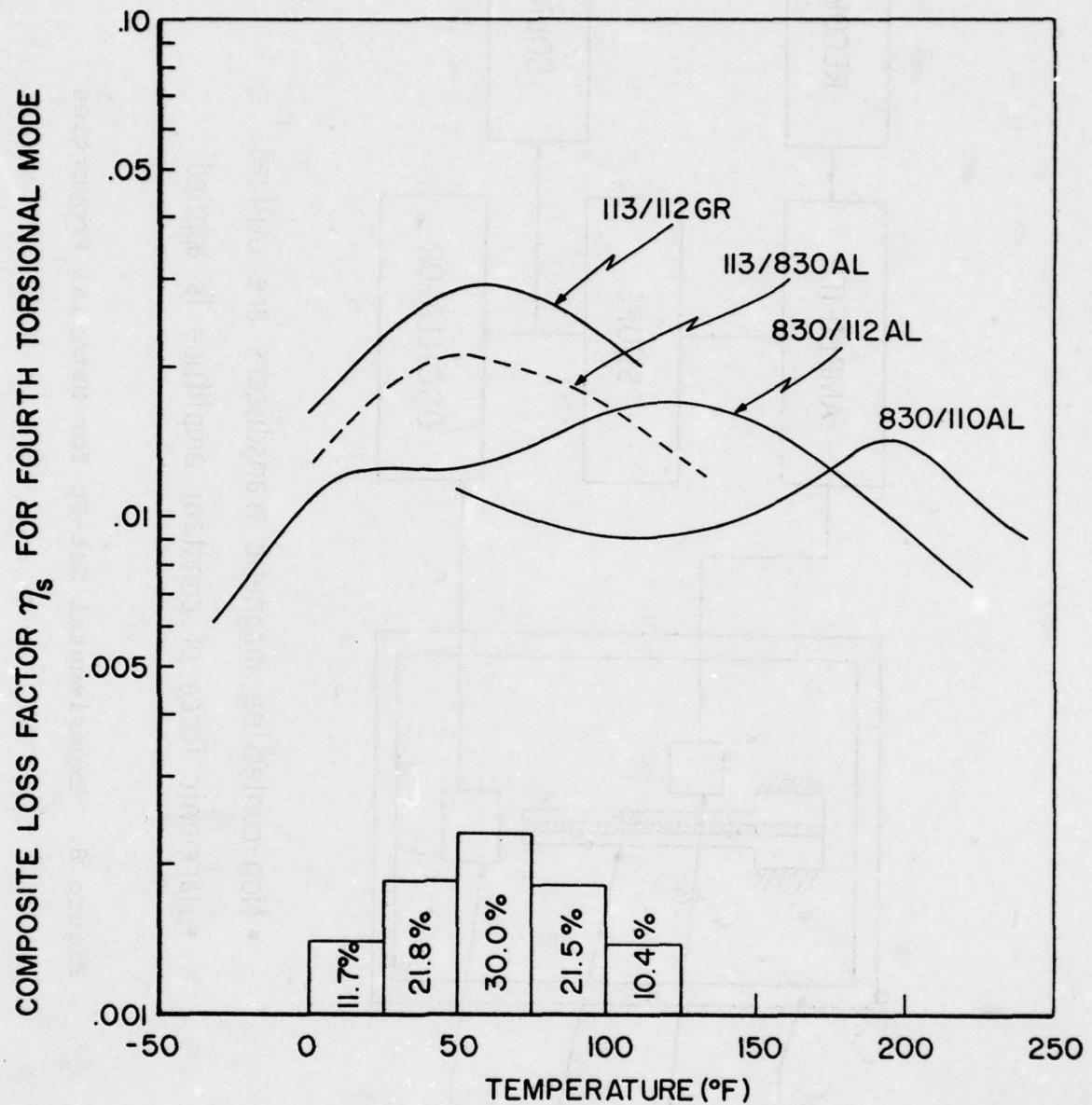
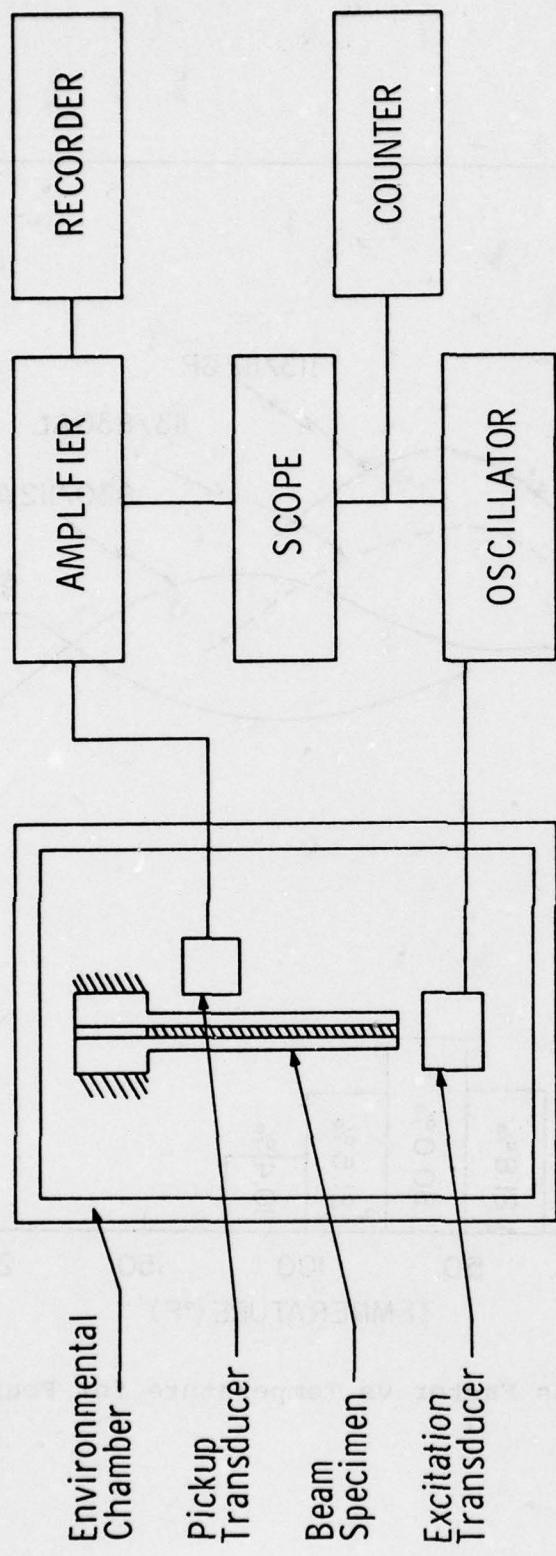


Figure 7. Composite Loss Factor vs Temperature for Four Damping Treatments.



- Non-contacting magnetic transducers are utilized
- Harmonic force of constant amplitude is applied

Figure 8. Experimental Set-Up for Material Properties

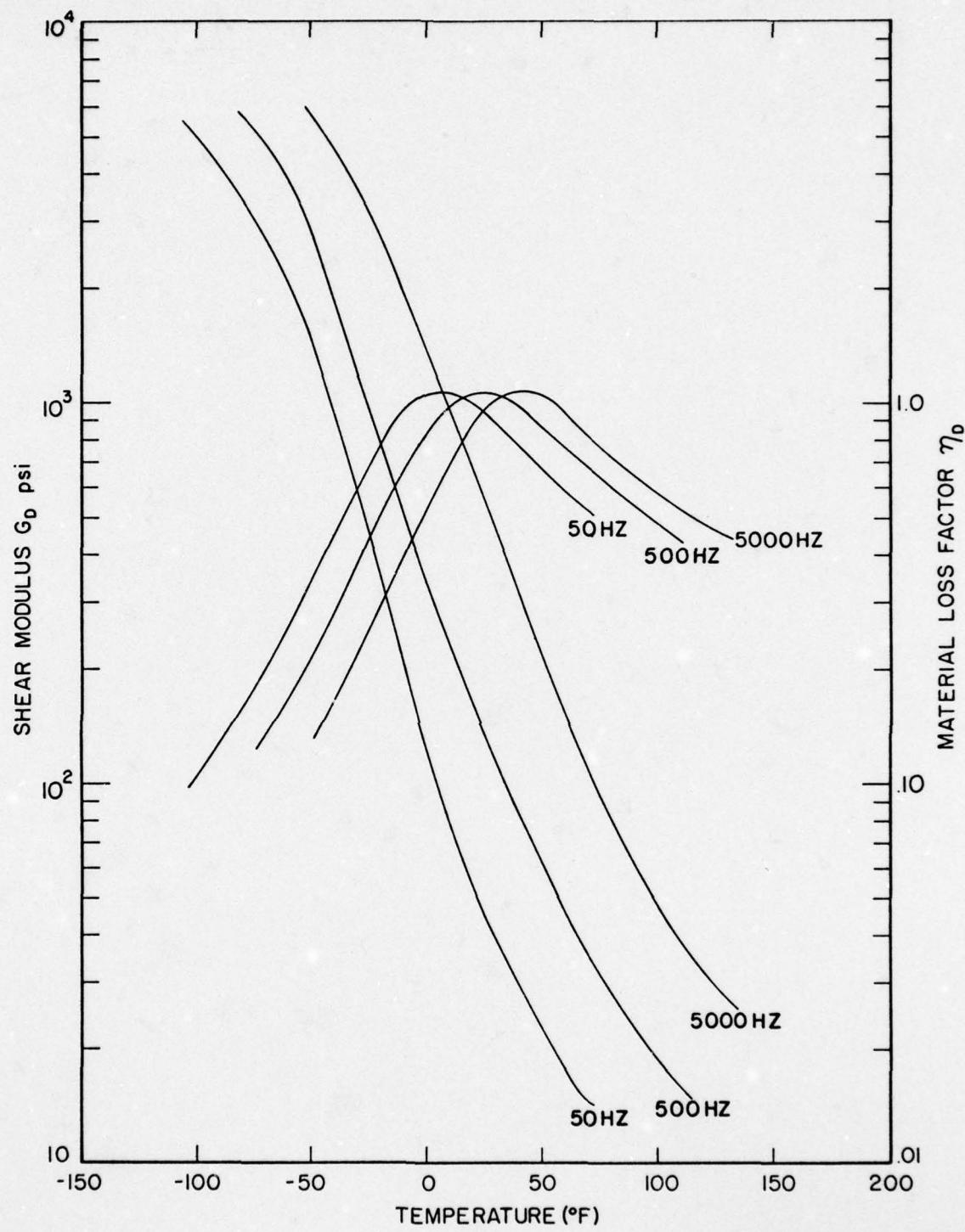


Figure 9. Graph of Shear Modulus (G_D) and Loss Factor (η_D) vs Temperature of 3M's ISD-113 for Various Frequencies.

HIGH MODULUS GRAPHITE FIBER
CONSTRAINED LAYER DAMPING TREATMENT
FOR HEAVY AEROSPACE STRUCTURES

J. Soovere
Lockheed-California Company
Aeromechanics Department
Burbank, California

**HIGH MODULUS GRAPHITE FIBER
CONSTRAINED LAYER DAMPING TREATMENT
FOR HEAVY AEROSPACE STRUCTURES**

J. Soovere

Lockheed-California Company

ABSTRACT

A program for the development of damping treatment applicable to stringers and frames on a wide-bodied transport airplane is summarized. The program involved the complete engineering of the constrained layer damping treatment from material selection and characterization to application on a wide-bodied transport aircraft. Sylgard 188 was used as the damping compound and Hitco 1900 ultrahigh modulus uniaxial composite as the constraining layer. The effect of modal coupling on the loss factor is demonstrated.

INTRODUCTION

A research program was conducted in 1972 to investigate the use of damping treatment, applicable to stringers and frames on a large transport airplane, for purposes of low-frequency cabin noise control. The problem was caused by multiple pure-tone noise in the center engine intake duct penetrating into the aft cabin. The frequency region of interest was close to 200 Hz, with lower frequencies also considered. The structural response in this frequency region was expected to involve the overall modes of the stiffened shell. The study was confined to the aft fuselage section of the airplane.

The program involved the complete engineering of the constrained layer damping treatment. This included the material selection, material characterization, adhesive and surface treatment development, fabrication, damping treatment optimization by analysis, performance verification, airplane shell modal response studies, installation and, finally, flight tests. Additional requirements imposed on the program included the installation time limited to the typical airplane service down time including the removal and replacement of the trim panels, good durability, minimum effect on the stiffener load distribution, and low weight. This paper presents a summary of the program.

AIRPLANE STRUCTURE

The airplane fuselage (Figure 1), in the region of the damping treatment, follows conventional aluminum construction consisting of single skin stiffened by built-up open section rings and "z" stringers. Typical range of dimensions are summarized in Table 1. The rings taper down to a smaller depth around the windows where a thicker, bonded double-skin construction is used.

The typical stringer cross-sectional area (A) and the second moment of area-to-area ratio (I/A) are considerably less than for the rings. The rings, therefore, represented the most critical design condition for the damping treatment. Consequently, the ring dimensions formed the basis for selecting the channel section beam for use in the subsequent damping treatment performance verification tests. The test beam dimensions are also summarized in Table 1.

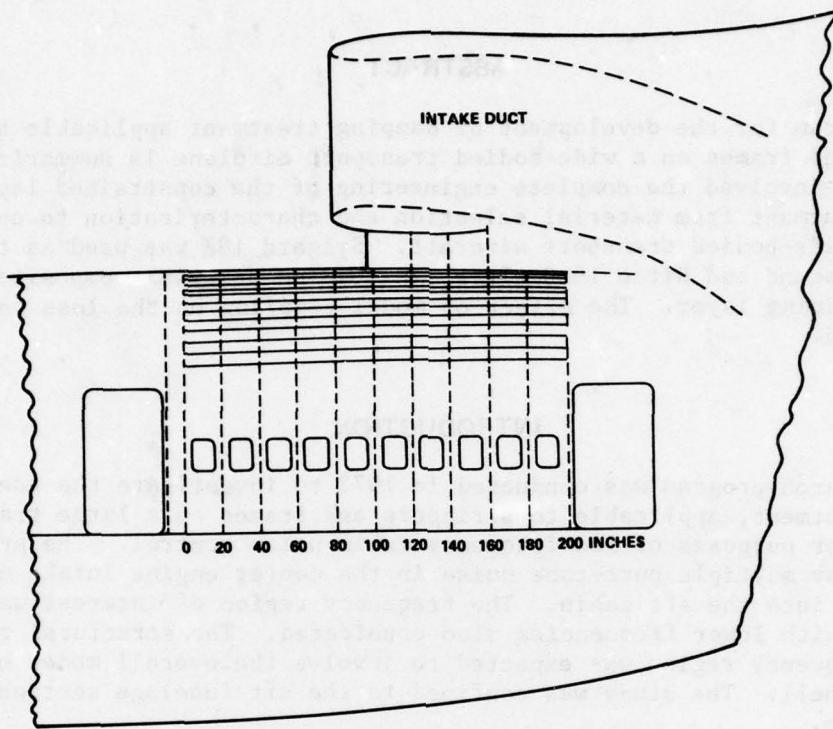


Figure 1. Airplane Rear fuselage Area

TABLE 1. TYPICAL STIFFENER PARAMETERS

Identification	Length Ins.	Width Ins.	Height Ins.	Area_2 $A \text{ In.}^2$	I/A_2 In.
Test Beam	65	1	6	0.982	4.78
Airplane Rings	-	1	6	0.55 to 1.2	5.3 to 4.6
Airplane Stringers	20 Between Rings	1	1.35	0.23 to 0.38	0.26 to 0.48

NOTE: Ring and stringer A and I/A include an effective skin width.

MATERIAL SELECTION

The dimensions of the structure dictated the use of the most efficient damping treatment--namely, the constrained layer damping. Preliminary analysis (Reference 1) confirmed that a substantial increase in both the stringer and frame damping could be obtained by means of the constrained layer damping treatment. For minimum weight, however, the modulus of the constraining layer must be considerably greater than the parent material and its density considerably less. Uniaxial ultrahigh modulus graphite fiber composite is highly suited for this purpose. Figure 2 illustrates the benefits to be gained for an optimally damped, simply supported aluminum beam, when compared with the more conventional airplane metals. Hitco HG 1900-8 graphite fiber preimpregnated with U.S. Polymeric E715 resin was selected on the basis of high modulus and favorable price for the uniaxial tape.

The skin, stringer, and frame temperature of a trimmed airplane is close to the ram air temperature which is around 0°F at cruise. For an untrimmed airplane, the temperature for the ring flange could be as high as 50°F at cruise. Thus, the damping compound was required to have a high damping value over a wide temperature range. Studies carried out on various damping compounds in Reference 2, indicated that a silicone-based damping compound would meet these requirements. None of the compounds studied in References 2 and 3 were commercially available. Sylgard 188 resin from Dow Corning was the only commercially available silicone-based damping compound and, therefore, was adopted for the program.

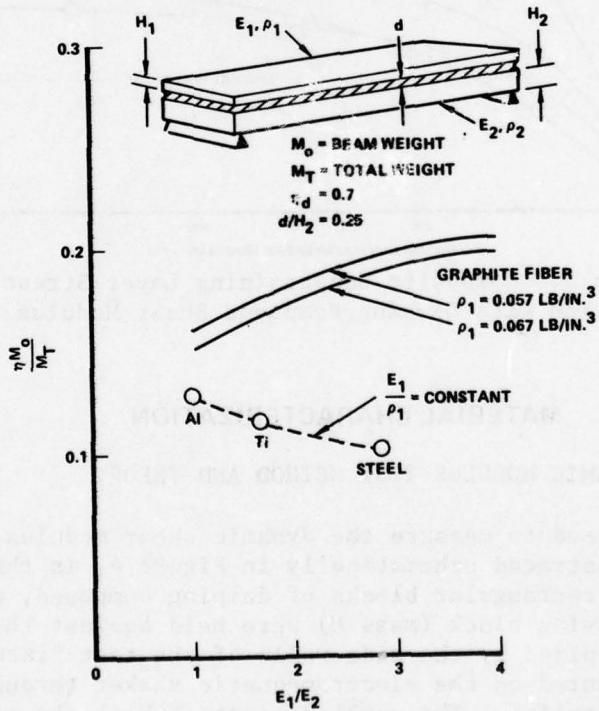


Figure 2. Modified Optimum Loss Factor as a Function of Young's Modulus Ratio

In addition to the need for a high loss factor over a wide temperature range, the damping compound had to have a relatively low static shear modulus. This requirement arose from the relatively low ultimate strength (approximately 70 ksi) of the ultrahigh modulus composite constraining layer. Calculations were performed to determine the stress in the composite constraining layer as a function of both the airplane frame stress and the damping compound shear modulus. Typical results illustrated in Figure 3, indicate that the damping compound maximum allowable shear modulus should be below 75 to 150 psi, depending on the frame stress, to meet the limit load criteria. Control over the load transfer could be exercised by varying the damping layer thickness for a given constraining layer length. Sylgard 188 damping compound appeared favorably suited in view of its relatively low static shear modulus.

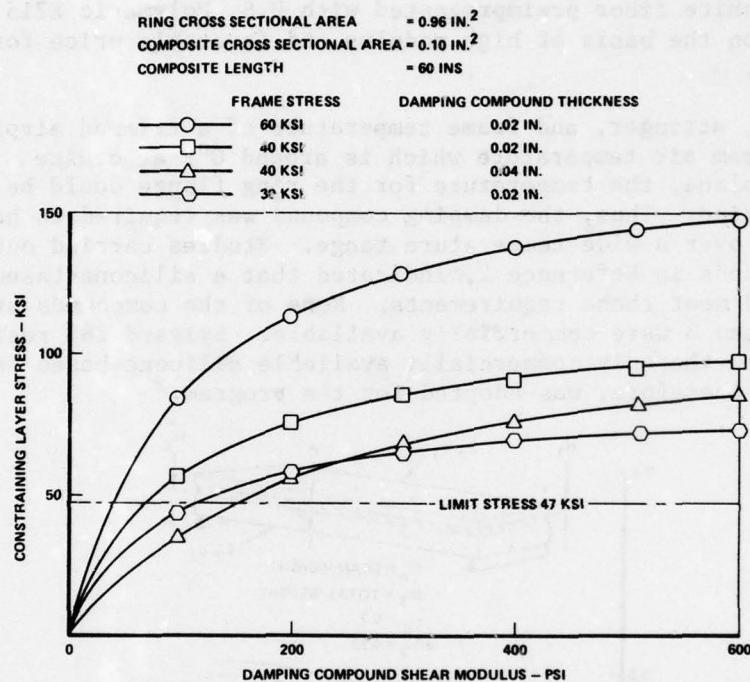


Figure 3. Composite Constraining Layer Stress Variation with Damping Compound Shear Modulus

MATERIAL CHARACTERIZATION

DAMPING COMPOUND DYNAMIC MODULUS TEST METHOD AND THEORY

The test setup used to measure the dynamic shear modulus and loss factor, which is illustrated schematically in Figure 4, is the same as used in Reference 2. Two rectangular blocks of damping compound, one on each side of the center moving block (mass M) were held against the moving block by slight pressure applied by the side walls of the test fixture. The test fixture itself is mounted on the electromagnetic shaker through which the sinusoidal force is applied. The accelerations of both the moving block (\ddot{x}) and the shaker table (\ddot{a}), and the relative phase angle (ϕ) between the two accelerations were recorded.

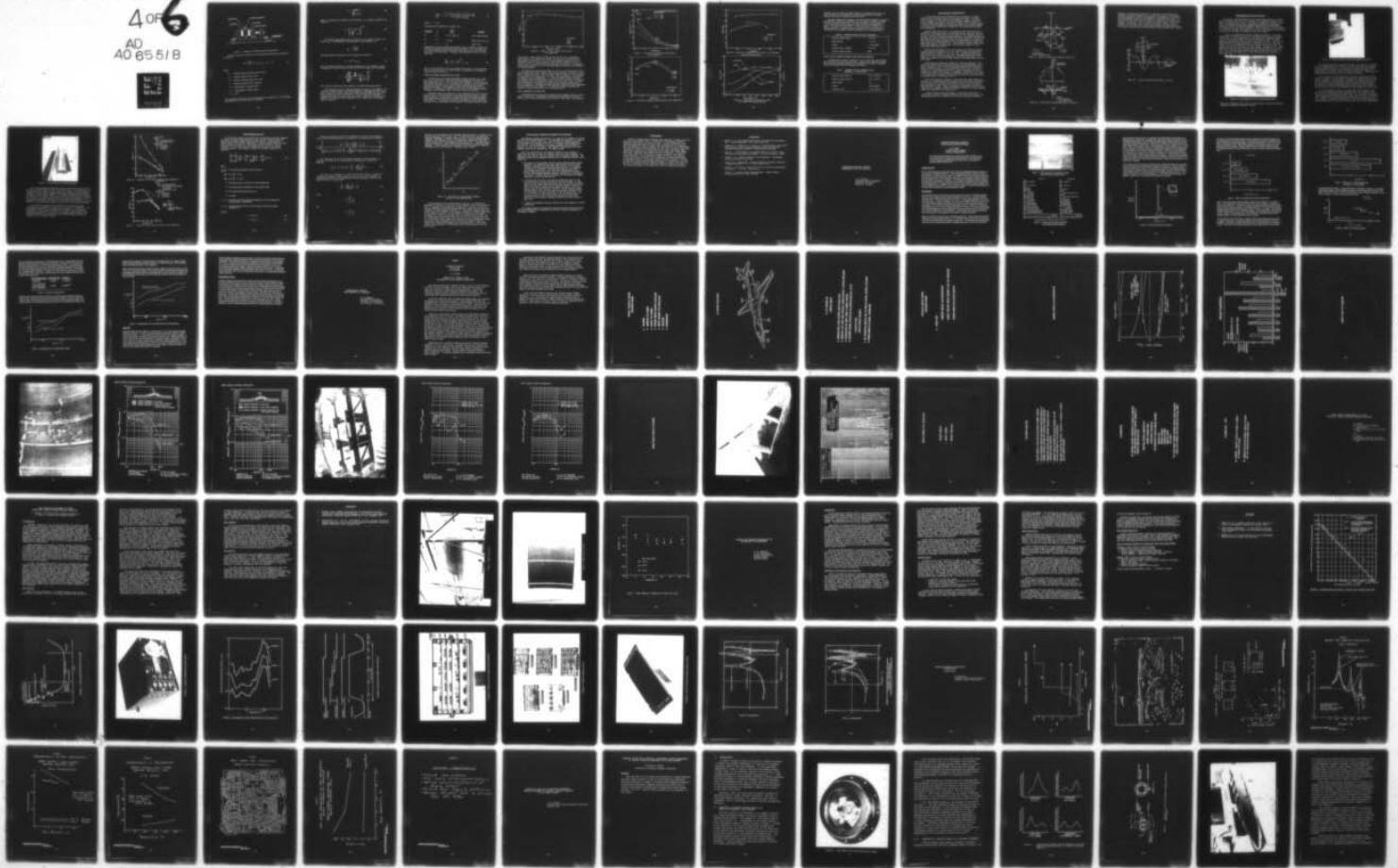
D-A065 518 AIR FORCE FLIGHT DYNAMICS LAB WRIGHT-PATTERSON AFB OHIO F/G 11/9
CONFERENCE ON AEROSPACE POLYMERIC VISCOELASTIC DAMPING TECHNOLOGY--ETC(U)
JUL 78 L ROGERS

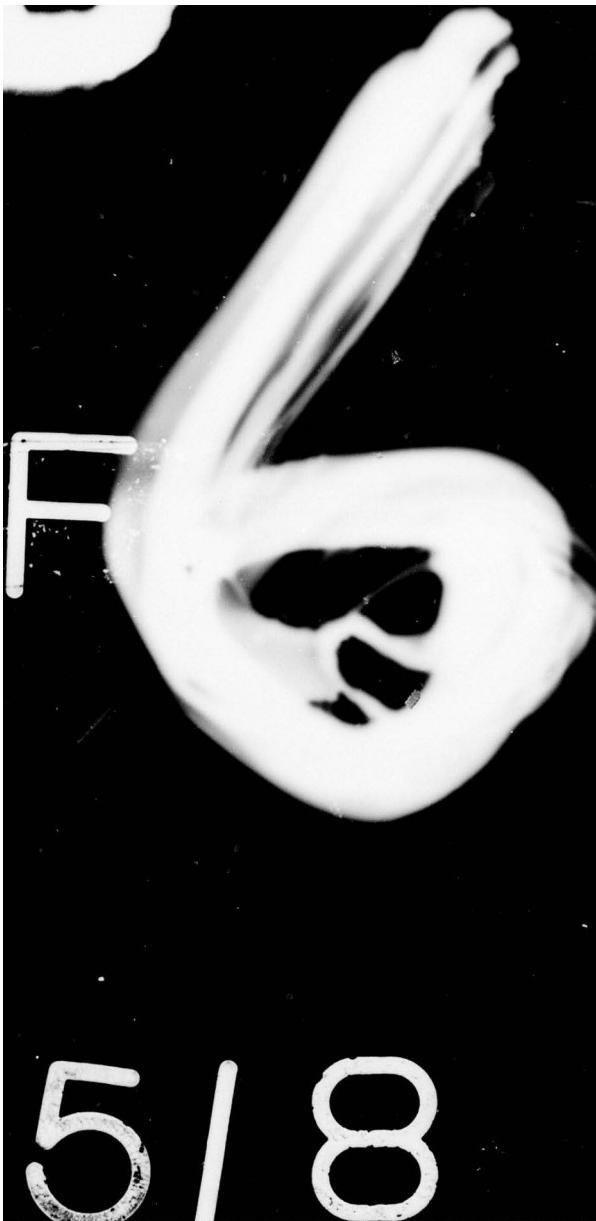
UNCLASSIFIED

AFFDL-TM-78-78-FBA

NL

4 OF 6
AD
A065518





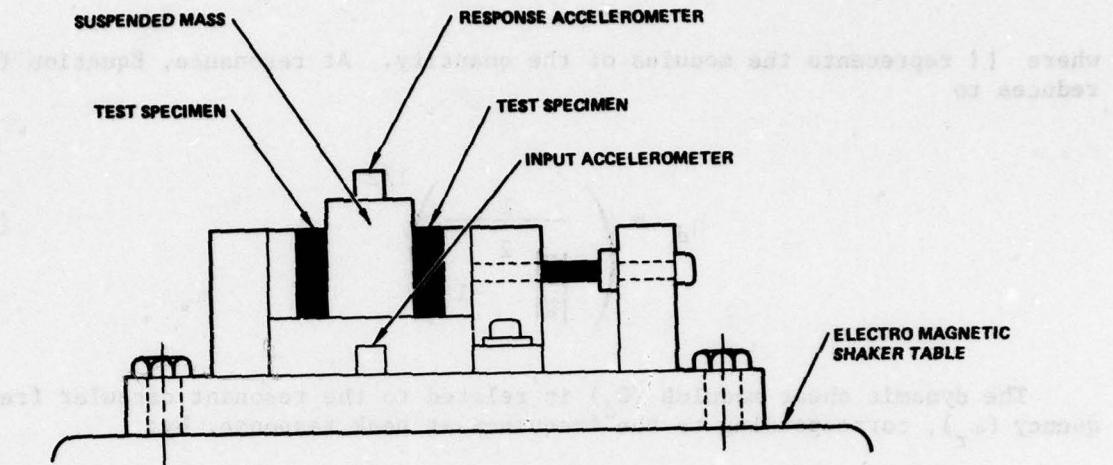


Figure 4. Schematic of Dynamic Modulus Test Fixture

The basic equation of motion for the moving block excited by the shaker, is given by

$$M\ddot{x} + \frac{2G_d A}{d} (1 + i\eta_d) (x - a) = 0 \quad (1)$$

where:

G_d = damping compound dynamic shear modulus

η_d = damping compound loss factor

A = damping compound single face area

d = damping compound block thickness

x = displacement of moving block

a = displacement of shaker table

$i = \sqrt{-1}$

With sinusoidal excitation and some manipulation of Equation 1, the following relationship for the loss factor is obtained:

$$\eta_d = \frac{\sin \phi}{\left| \frac{\ddot{x}}{a} \right| - \cos \phi} \quad (2)$$

where $\left| \cdot \right|$ represents the modulus of the quantity. At resonance, Equation (2) reduces to

$$\eta_d = \left(\frac{\frac{1}{2}}{\left| \frac{\ddot{x}}{a} \right|^2 - 1} \right)^{1/2} \quad (3)$$

The dynamic shear modulus (G_d) is related to the resonant circular frequency (ω_r), corresponding to the frequency at peak response, by:

$$G_d = \frac{\omega^2 r M d}{2A} \quad (4)$$

The phase angle at resonance is not 90 degrees but given by

$$\phi = \tan^{-1} (1/\eta_d) \quad (5)$$

For off-resonance testing at a circular frequency (ω) the resonant circular frequency must first be extracted from the test data using the relationship

$$\omega_r = \omega \left(\frac{\left| \frac{\ddot{x}}{a} \right|^2 - \left| \frac{\ddot{x}}{a} \right| \cos \phi}{\left| \frac{\ddot{x}}{a} \right|^2 + 1 - 2 \left| \frac{\ddot{x}}{a} \right| \cos \phi} \right)^{1/2} \quad (6)$$

and thereafter substituted into Equation 4 to obtain the shear modulus.

Both resonance and off-resonance testing were used in this program. Off-resonance testing provides a convenient method for measuring the loss factor over a wide range of shear angle by progressively increasing the input level without having to adjust the frequency. Error analysis was performed to establish the range of accuracy for the testing. Using error analyses, the sensitivity of the loss factor (Equation 2) to a small error in the phase angle, is given by

$$\frac{\partial \eta_d}{\partial \phi} = - \frac{r^4 - r^2 (1 - 0.5 \eta_d^2) - 0.5 \eta_d^2 (1 + \eta_d^2)}{r^4 + \eta_d^2 r^2 + 0.25 \eta_d^4} \quad (7)$$

where: $r = \omega/\omega_r$

The three basic conditions to consider are:

<u>Condition</u>	<u>r</u>	<u>$\frac{\partial \eta_d}{\partial \phi}$</u>	<u>Comments</u>
1)	$\rightarrow 0$	$\rightarrow 2(1 + \eta_d^2)/\eta_d^2$	error amplification
2)	$\rightarrow 1$	$\rightarrow 0.5\eta_d^4$	small error for $\eta_d < 1$
3)	$\rightarrow \infty$	$\rightarrow 1$	equal error

Consequently, the best results are obtained close to resonance, whereas the frequency range well below resonance must be avoided. For a loss factor of 0.5, r must be above 0.68 for the error in the loss factor to be less than the error in the shear angle. Similarly, from Equations 4 and 6, it can be shown that

$$\frac{\delta G_d}{G_d} \leq \left(1 + \eta_d^2 \right)^{1/2} \eta_d \delta \phi \quad (8)$$

That is, the fractional error in the dynamic shear modulus is less than the error in the phase angle (in radians) which is acceptable for the measured range of values for ϕ and η_d .

SYLGARD 188 DYNAMIC MODULUS AND LOSS FACTOR

An initial batch of Sylgard 188 damping compound was made into a sheet just over 0.1 inch thick. Rectangular test specimens were cut from the sheet measuring 0.5 by 1.25 by 0.1 inches when installed in the test fixture under slight compression. As in Reference 2, no bonding was used between the specimens and the test fixture, with slippage prevented by test fixture surface indentations. Low-temperature tests used the same apparatus as in Reference 2, consisting of a small enclosure cooled by air passed through an air/methane heat exchanger which in turn was cooled by liquid CO_2 .

Preliminary tests were conducted at room temperature with an 0.118 pound moving block to obtain variations of loss factor with shear angle as illustrated in Figure 5. Near-resonance testing was employed covering a range of shear angles between 0.001 and 0.05 radians with the loss factor calculated from Equation 2. Off-resonance testing at frequencies of 60 and 120 Hz provided poor data as indicated by error analysis. The sudden fall-off in loss

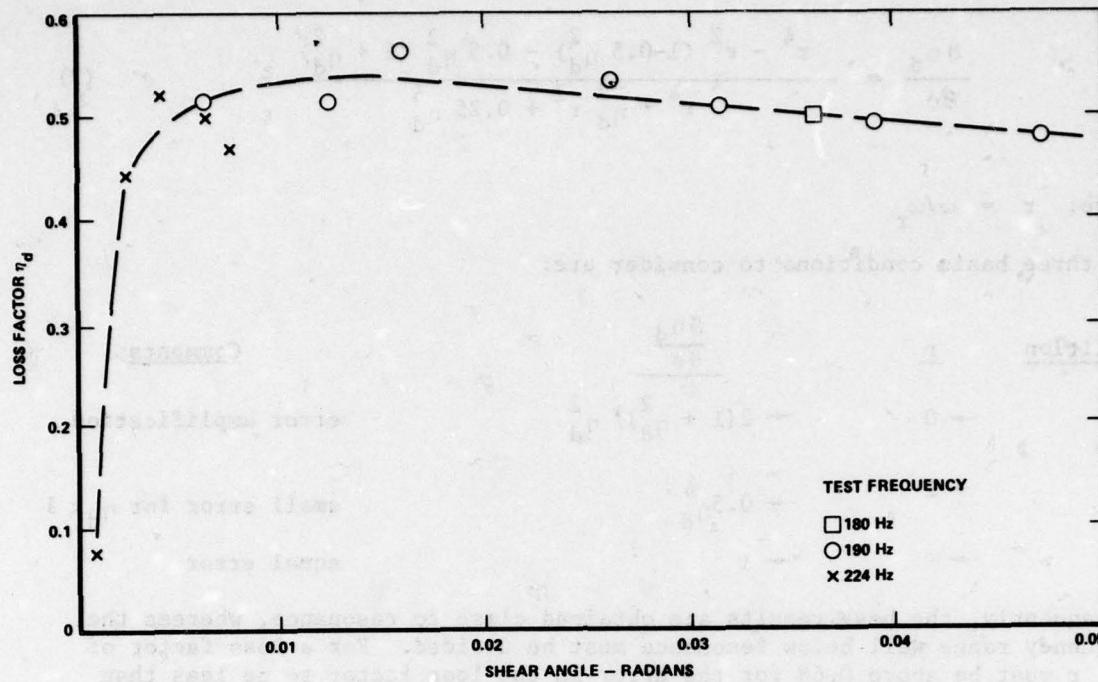


Figure 5. Effect of Shear Angle on Loss Factor for Sylgard 188

factor below a shear angle of 0.002 radians could be due to measurement inaccuracies at low acceleration levels. No fall-off in loss factor with shear angle was observed for the silicon-based damping compounds tested (Reference 3) down to shear angles of 0.001 radians. However, some of the earliest work on silicon-based damping compounds (Reference 4) did indicate a shear-angle sensitivity at very low shear angles, producing a stiffening of the damping compound.

Two additional moving block weights of 0.85 and 1.56 pounds were used in the low-temperature tests together with resonance testing. Equations 2 and 3, used to obtain loss factor, produced nearly identical results. The variation of the dynamic shear modulus and loss factor with temperature is illustrated in Figures 6 and 7, respectively. The lines represent constant frequency data obtained through interpolation of the test data when plotted as function of frequency such as illustrated in Figure 8 for the loss factor. The test data were reduced to standard form using the same reduction parameters as used in Reference 5 for Sylgard 188 and presented together with the comparable data from Reference 5 in Figure 9. The relatively large differences may possibly be due to differences in the curing procedure.

STATIC PROPERTIES OF SYLGARD 188

The dynamic modulus test results indicated that Sylgard 188 had a useful level of loss factor. Thereafter, procedures were developed for its production in 0.04 inch thick sheets 8 feet long and 1 foot wide. The 0.04-inch

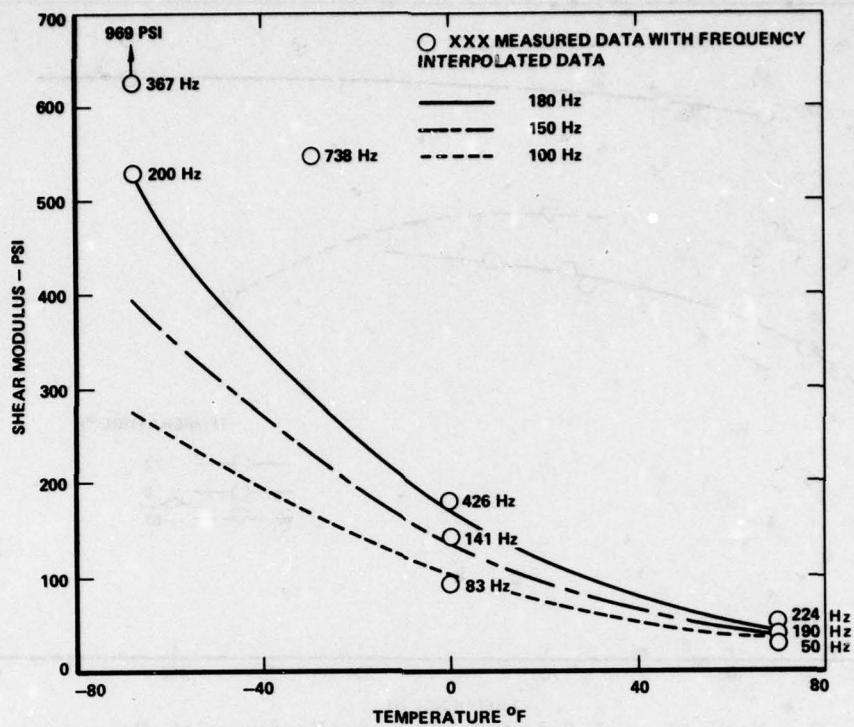


Figure 6. Variation of Sylgard 188 Shear Modulus with Temperature

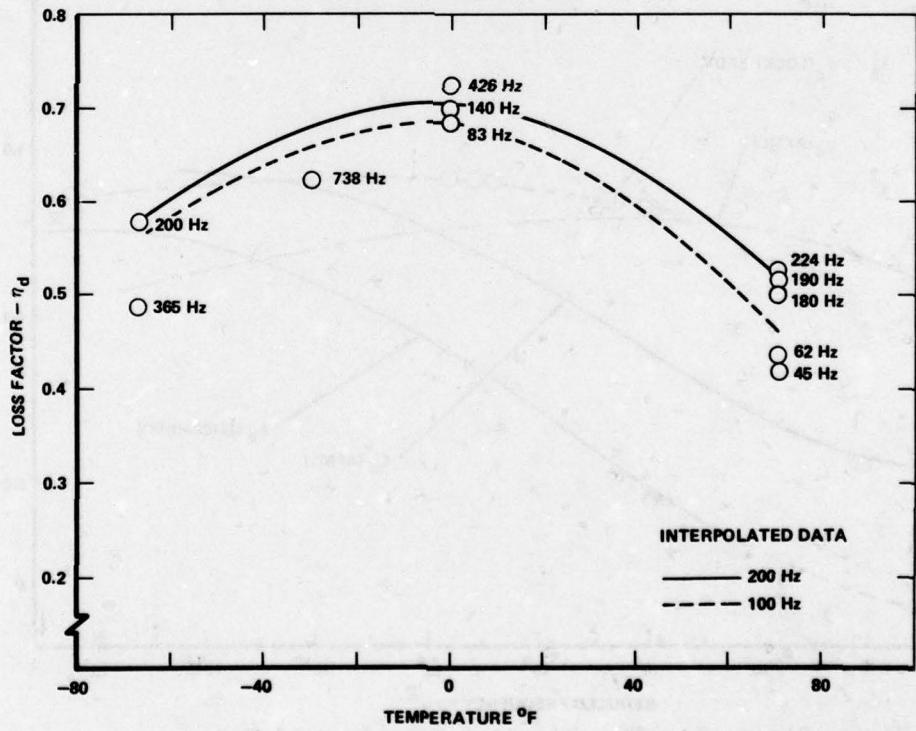


Figure 7. Variation of Sylgard 188 Loss Factor with Temperature

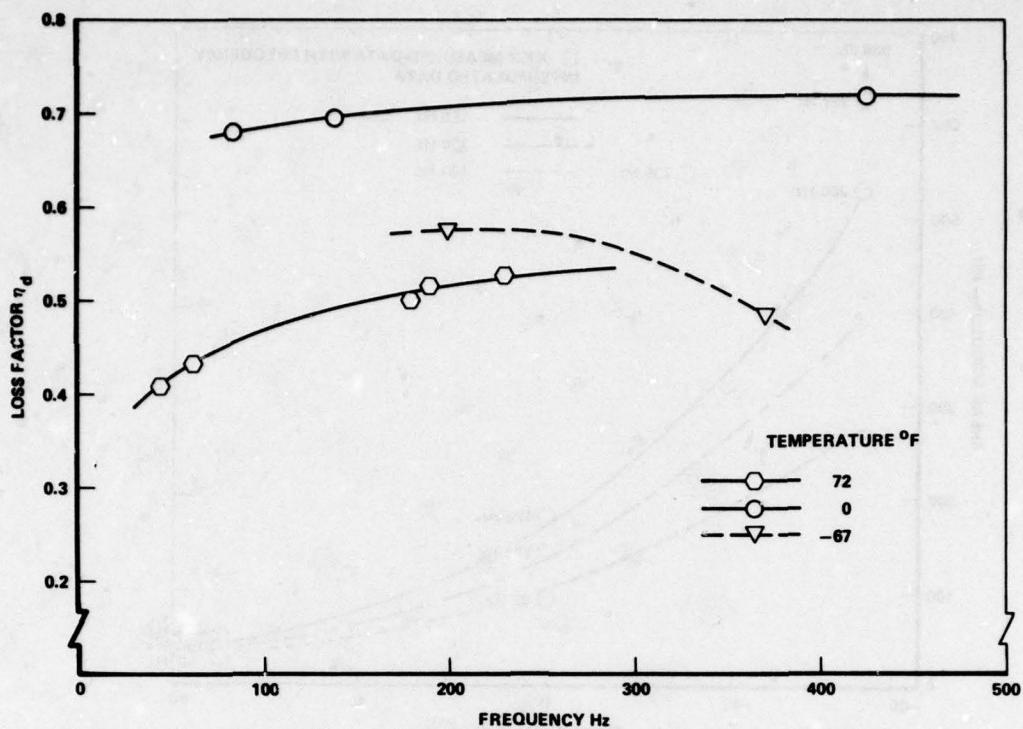


Figure 8. Variation of Sylgard 188 Loss Factor with Frequency

AFML REF J.S.&V. (1974) 33 (4), 451-470

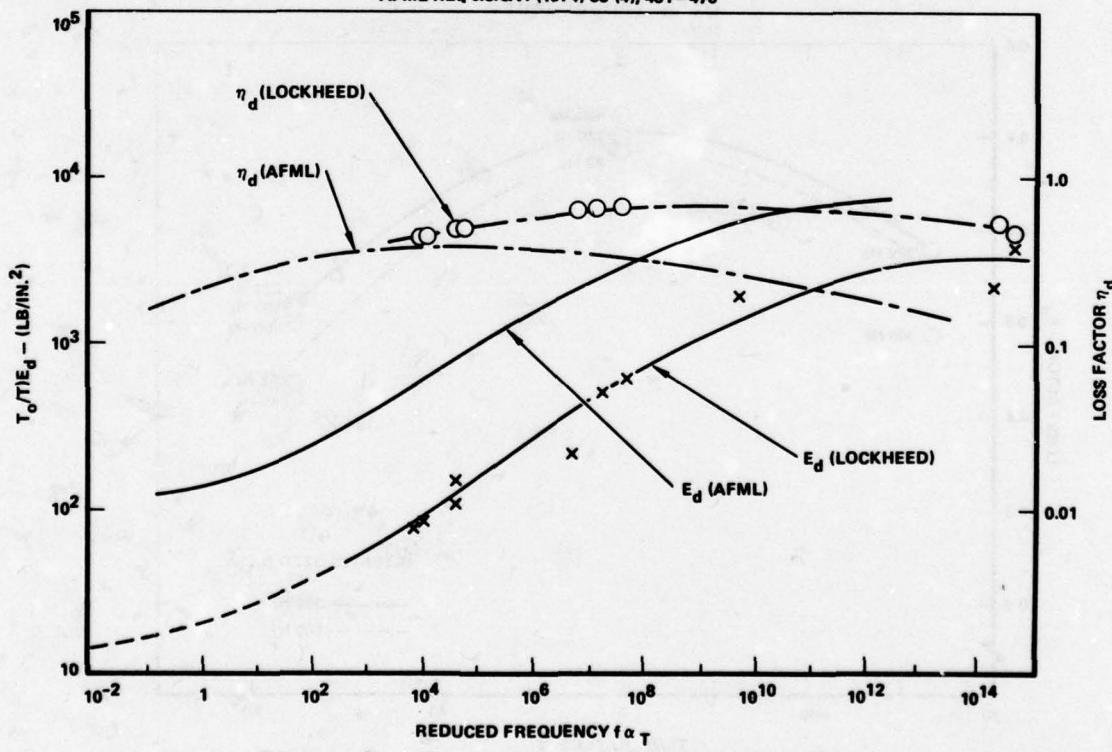


Figure 9. Comparison of Experimental Data for Sylgard 188 Damping Material

thickness could be readily achieved without too much development work, and also coincided with the theoretically predicted thickness for optimum damping at the ram air temperature during cruise.

Adhesive systems were developed to bond the damping compound to both the graphite fiber composite and aluminum, and the degree of adhesion verified by double-lap shear coupon tests. Tensile tests were also conducted on a 1-inch wide 0.04-inch thick specimen. These results are summarized in Table 2. Analyses were conducted to ensure that stresses produced in the damping layer due to thermal expansion, pressurization, and mismatched curvatures did not exceed the static allowables for the damping material.

TABLE 2. MEASURED SYLGARD 188 STATIC PROPERTIES

Tensile Young's Modulus	15.0 PSI
Shear Modulus	5.6 PSI
Density	0.04 LB/IN ³
Ultimate Shear Strength	32.8 PSI
Ultimate Tensile Strain	> 300%

HITCO HG 1900-8 UNIAXIAL GRAPHITE FIBER COMPOSITE PROPERTIES

A unidirectional composite beam with a 0.15 by 0.92 inch cross section was fabricated and cured in an autoclave. Tensile test, cantilever flexural tests, and resin content analysis were conducted on a section of the beam. The data from these tests are summarized in Table 3.

TABLE 3. MEASURED UNIAXIAL COMPOSITE STATIC PROPERTIES - HG 1900-8/E715

Tensile Young's Modulus	29.9×10^6 PSI
Flexural Young's Modulus	27.9×10^6 PSI
Fiber Volume	45%
Density	0.056 LB/IN ³
Ultimate Stress	70 KSI (approx)

AIRPLANE SHELL VIBRATION TEST

A ground vibration test was conducted on the airplane aft fuselage shell in which sinusoidal excitation was applied vertically to a frame flange by means of a 100-pound force electromagnetic shaker. The purpose was to determine the nature of the shell vibration, whether resonant or forced; to measure the damping in the shell structure in the overall modes; to identify the mode shapes of the shell vibration; and to obtain a measure of the axial and circumferential wavelengths. The airplane was untrimmed and unpressurized.

Baseline flight tests without the treatment, were flown with the untrimmed but pressurized airplane to establish the shell vibration levels and the interior noise levels within the aft cabin over the frequency range of interest. The use of the unpressurized airplane in the ground vibration test was dictated by limited airplane availability time. Because of the expected high modal density in the aircraft shell, the pressurization was expected to shift some of the pressure-sensitive lower frequency modes into higher frequency regions such as around 180 Hz. These shifted frequency modes around 180 Hz were expected to exhibit modal characteristics similar to the unpressurized modes around 180 Hz.

Nine fixed accelerometers were used to measure the vibration response, of which seven were attached to selected locations along one ring and the remaining two were attached to the intake duct. One fixed microphone was used to measure the internal noise level. These measurements were supplemented by a roving probe accelerometer and a hand-held noise meter. The shaker was attached to the ring flange through a force gage positioned close to the ring.

Preliminary sine sweeps were conducted to identify resonances. Fine-tuning onto resonance was accomplished by means of the Kennedy-Pancu vector plots (Reference 6) constructed from phase and amplitude data measured at stepped frequency points. A typical multimodal vector plot is illustrated in Figure 10. The resonance is located at the position where the rate of change of arc length with frequency is a maximum. The loss factor can also be extracted from the vector plots as illustrated in Figure 10. The line AB is the modal vector and passes from the resonance point B through the center of the modal circle to the modal origin A.

After fine tuning onto resonance, force-level sweeps were conducted to establish the relationship between the shaker force and internal noise level. The criterion used to establish the shaker excitation level for vibration survey was based on reproducing noise levels in the aft cabin identical to those measured in flight. After a preliminary acceleration probe survey six rings and four stringers, exhibiting the highest response in a given frequency region, were selected for the modal survey.

A typical fuselage shell mode shape at a frequency of 180.3 Hz is illustrated in Figure 11, measured radially along a ring and stringer. The corresponding axial and circumferential intake duct mode shape, measured

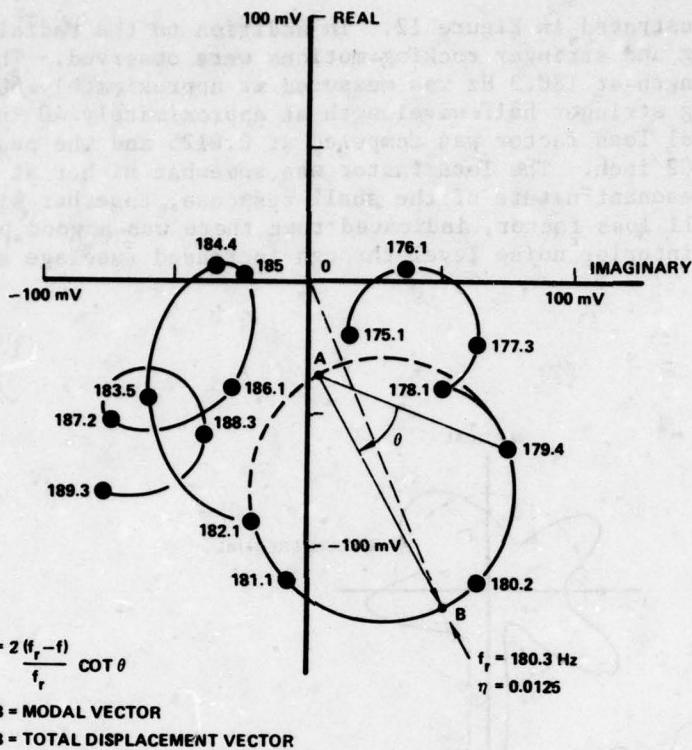


Figure 10. Typical Airplane Ring Response Vector Plot

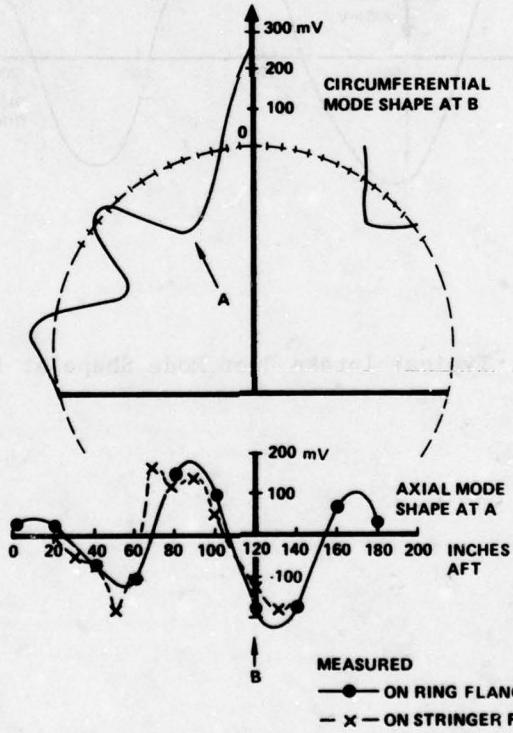


Figure 11. Typical Rear Fuselage Mode Shape at 180.3 Hz

radially, is illustrated in Figure 12. In addition to the radial motion, considerable ring and stringer rocking motions were observed. The average ring half wavelength at 180.3 Hz was measured at approximately 60 inches and the corresponding stringer half wavelength at approximately 40 inches. At 180.3 Hz the modal loss factor was computed at 0.0125 and the peak ring displacement at 0.002 inch. The loss factor was somewhat higher at lower frequencies. The resonant nature of the shell response, together with the relative low shell loss factor, indicated that there was a good possibility of reducing the interior noise level through increased fuselage shell damping.

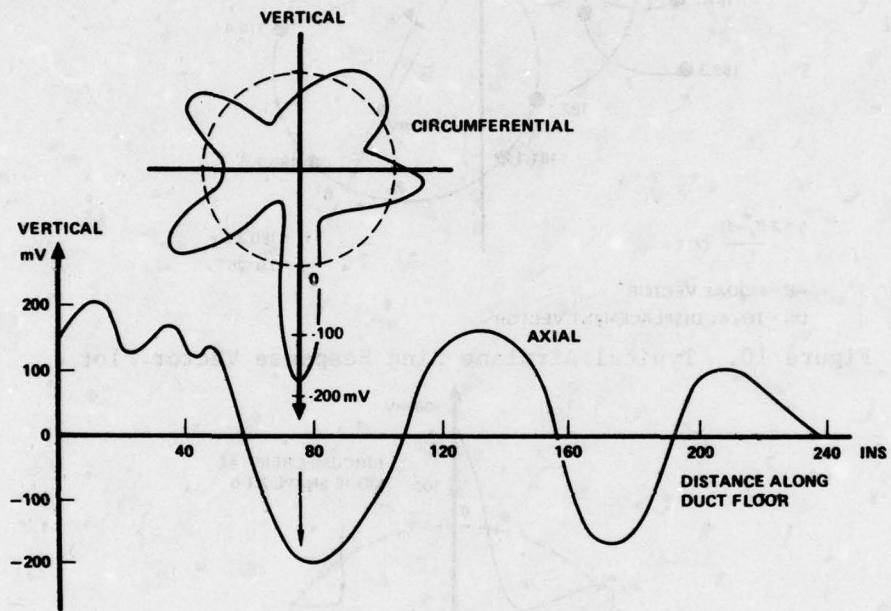


Figure 12. Typical Intake Duct Mode Shape at 180.3 Hz

PERFORMANCE VERIFICATION TESTS

The material characterization and the airplane shell vibration response test provided the basic data for the design of the damping treatment. The theory in Reference 1 is, however, applicable to single-mode uncoupled vibration. The airplane modal survey indicated the presence of considerable stiffener rotation, for which the damping treatment would not be effective, in conjunction with the radial vibration. Thus, the amount of energy absorbed by the damping treatment in relation to the total energy present in the vibration would be less than that predicted by the above theory.

To assist in assessing the effect of modal coupling, and at the same time provide a difficult test case for the damping treatment, a performance verification test was conducted* on a simply supported, straight, channel section aluminum beam (Figure 13) used to simulate the rings. The beam dimensions and sectional properties are summarized in Table 1. The beam was simply supported on flexures attached to the upper half of the frame web (Figure 14), thereby permitting the lower flange of the beam to roll. The damping treatment was applied to the lower flange. The beam was also simply supported laterally as the flexures permitted rotation about the vertical axis. Thus a complex modal coupling was possible which was expected to be more severe than that experienced in the airplane and thus to provide a worst case test.

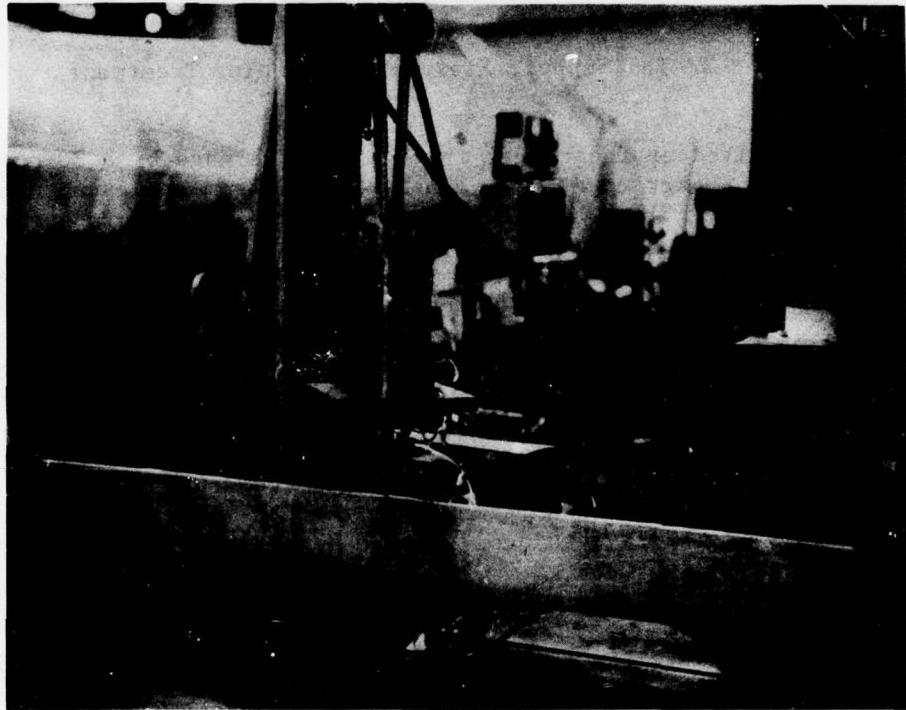


Figure 13, Experimental Set Up for Beam Damping Test

*Tests were conducted by the author at the Institute of Sound and Vibration Research, Southampton University, England.

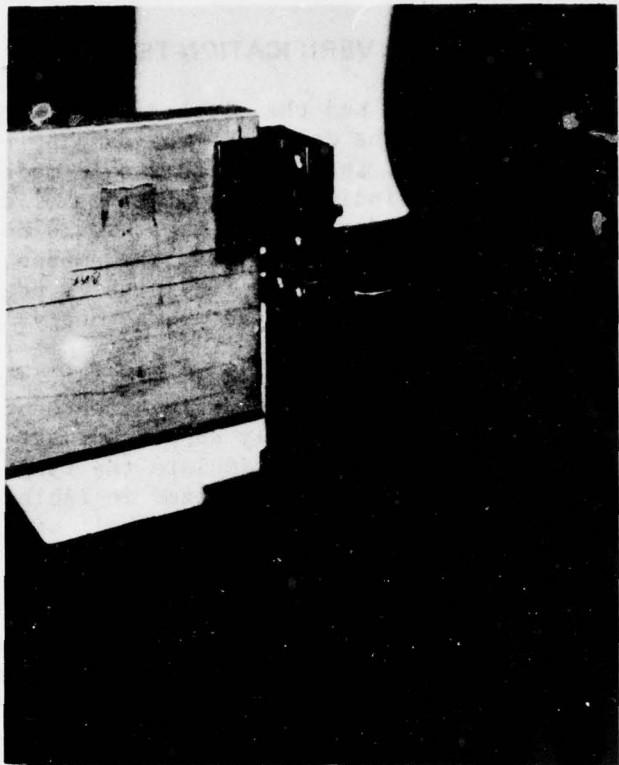


Figure 14. Beam End Support Flexure and Damping Treatment

The beam was excited at the center through a force gage by a 30-pound force electromagnetic shaker mounted in a heavy steel frame and suspended by bungee rubber (Figure 13). The response was measured by strain gages placed axially on the upper and lower frame flange and the composite constraining layer center lines at the center of the beam. This arrangement emphasized the strain due primarily to vertical bending.

Static tests were first conducted by centrally loading the beam with weights, by means of a pulley system, to measure the static strains in each of the components. With the shaker connected, sine sweeps were first conducted to identify the resonances and thereafter the inphase and out-of-phase dynamic strains were measured with a resolved components indicator in response to a constant amplitude harmonic excitation. The resonant frequency and loss factor were obtained from the Kennedy-Pancu vector plots.

In the low-temperature tests, the whole beam and its supports were enclosed in a thermally insulated box (Figure 15) with a groove cut into the top cover to accommodate the shaker drive rod. The beam was cooled by evaporating liquid nitrogen poured into a tray below the beam. The temperature, measured with two thermometers protruding into the enclosure, was first allowed to stabilize, and thereafter, the beam vibration response was measured periodically during the slow temperature rise to room temperature.

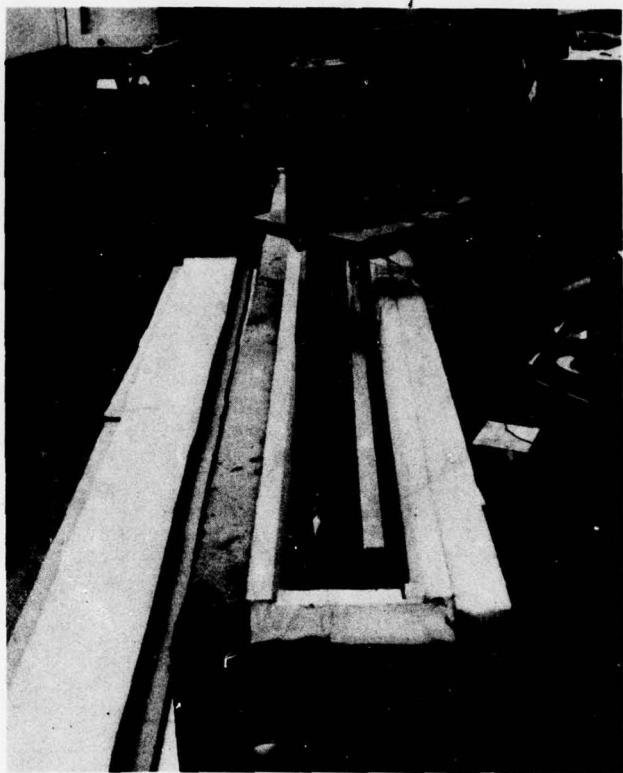


Figure 15. Beam Mounted in Thermal Enclosure

The damping compound maximum shear angle varied between 0.016 radians at -20°F and 0.024 radians at 70°F during these tests. On completion of the temperature tests, further response tests were conducted with the damping treatment first partially removed from both ends leaving approximately 60% coverage, and then finally removed. The damping treatment on the stringers was limited to 19 inches by the frames out of a half wavelength of 40 inches. Thus effects of partial coverage on the loss factor were important. The measured untreated beam loss factor of 0.004 indicated that almost all of the damping in the predominantly bending mode was due to the damping treatment.

The measured and theoretically (Reference 1) predicted resonant frequencies are illustrated in Figure 16 as a function of temperature. The corresponding loss factors are summarized in Figure 17 as a function of temperature. Also included in Figure 17 is the theoretically predicted optimum damping which is a function of the damping layer thickness. The discrepancy between the measured and the predicted damping and resonant frequency is due to modal coupling.

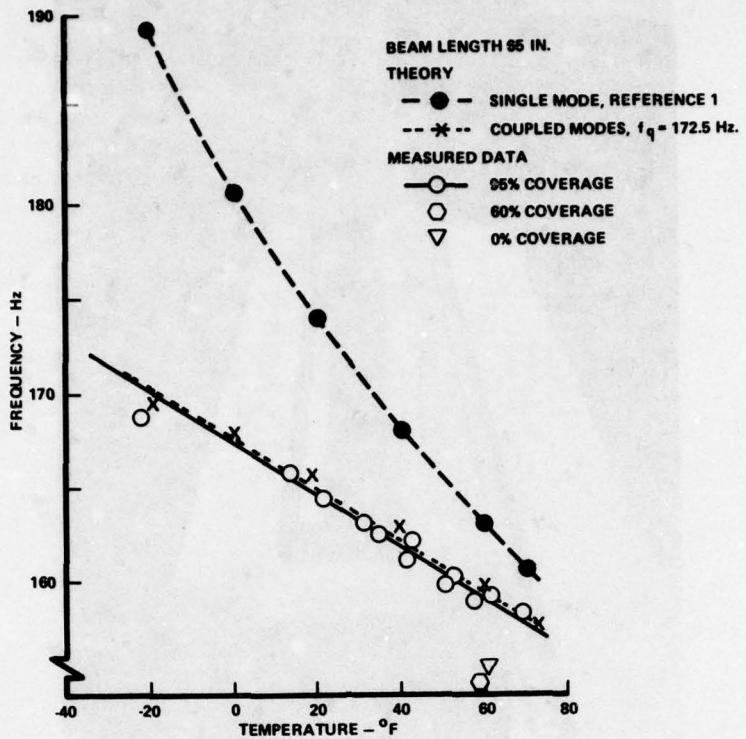


Figure 16. Variation of Test Beam Frequency with Temperature
BEAM LENGTH 65 IN.

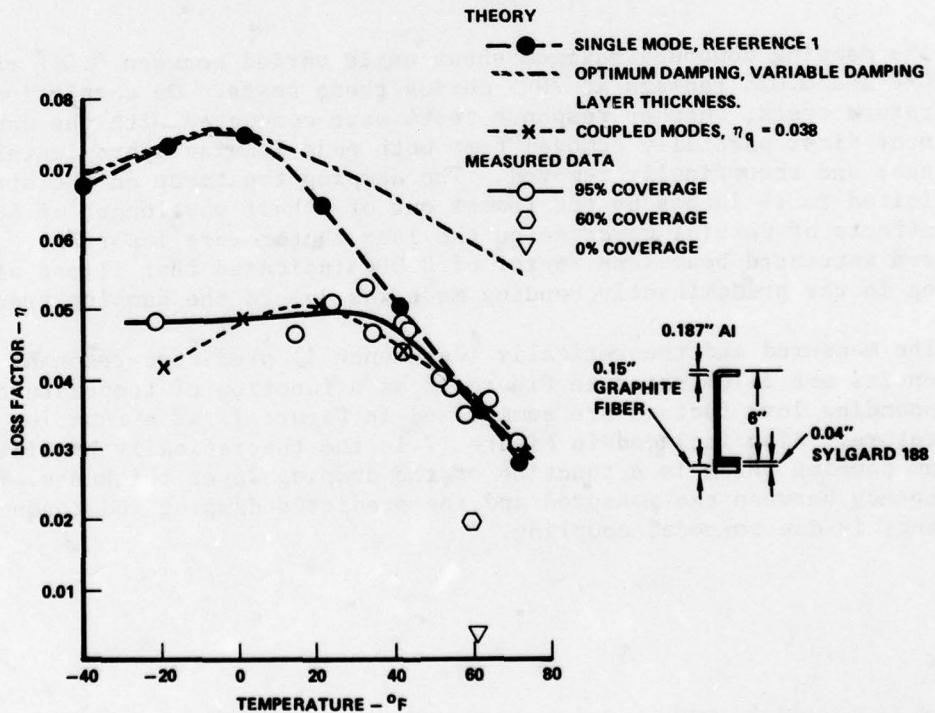


Figure 17. Variation of Test Beam Loss Factor with Temperature

COUPLED MODE ANALYSIS

The difference between the measured and theoretically predicted frequency is typical of coupled mode behavior in which one mode assumes a lower frequency and the other a higher frequency when coupled. A two-degree-of-freedom system was therefore assumed with a complex diagonal stiffness matrix and a coupled inertia matrix. The analysis follows the theory used in Reference 7 for two modes coupled through both the inertia and complex stiffness matrices. The equation of motion for harmonic excitation is given by:

$$\begin{bmatrix} A_{11} & A_{12} \\ A_{21} & A_{22} \end{bmatrix} \begin{Bmatrix} \ddot{w} \\ \ddot{v} \end{Bmatrix} + \begin{bmatrix} K_{11}^* & 0 \\ 0 & K_{22}^* \end{bmatrix} \begin{Bmatrix} w \\ v \end{Bmatrix} = \begin{Bmatrix} \bar{P} \\ a\bar{P} \end{Bmatrix} \sin \omega t. \quad (9)$$

where:

$[A_{jk}]$ = the coupled generalized inertia matrix

$$K_{11}^* = A_{11} \omega_r^2 (1 + i\eta_r)$$

$$K_{22}^* = A_{22} \omega_q^2 (1 + i\eta_q)$$

w = the generalized coordinate for the bending mode

v = the generalized coordinate for the lateral mode

\bar{P} = the generalized excitation force

a = constant

ω_r, ω_q = uncoupled circular resonant frequencies for the bending and lateral modes, respectively

η_r, η_q = uncoupled loss factors for the bending and lateral modes, respectively

writing:

$$w = \bar{w} \sin \omega t \quad (10)$$

$$v = \bar{v} \sin \omega t \quad (11)$$

Substituting Equations 10 and 11 in Equation 9, and after some manipulation, the following expression is obtained for the bending modal intensity \bar{w}

$$\frac{\bar{w}}{P} = \frac{1}{A_{11}} \left[\frac{\omega_q^2 - \omega^2 \left(1 + a \frac{A_{12}}{A_{22}} \right) + i\eta_q \omega_q^2}{\omega_q^2 \omega_r^2 (1 - \eta_q \eta_r) - \omega^2 (\omega_q^2 + \omega_r^2) + \left(1 - \frac{A_{12}^2}{A_{11} A_{22}} \right) \omega^4 + i\omega_r^2 \omega_q^2 (\eta_r + \eta_q) - i\omega (\omega_q^2 \eta_q + \omega_r^2 \eta_r)} \right] \quad (12)$$

The expression for the lateral modal intensity \bar{v} was not required. At resonance, the real part of the denominator in Equation 12 becomes zero. Therefore:

$$\omega_q^2 \omega_r^2 - \omega^2 (\omega_q^2 + \omega_r^2) + \left(1 - \frac{A_{12}^2}{A_{11} A_{22}} \right) \omega^4 = 0 \quad (13)$$

The term $\eta_q \eta_r$ is assumed to be small and therefore omitted. Equation 12 represents the coupled frequency equation for the case of zero damping. On rearranging Equation 13 and replacing the circular frequency ω with the frequency f in Hz, it follows that:

$$y = \left\{ 1 - \frac{A_{12}^2}{A_{11} A_{22}} \right\} x + f_q^2 \quad (14)$$

where:

$$y = \frac{f_r^2 f_r^2}{f_r^2 - f^2} \quad (15)$$

and

$$x = \frac{f^4}{f_r^2 - f^2} \quad (16)$$

Equation 14 is the equation for a straight line with slope, $1 - (A_{12}^2/A_{11} A_{22})$, and the intercept, f_q^2 , on the y axis. On substituting the theoretically predicted (Reference 1) resonant frequency for f_r and the averaged measured frequency, from Figure 16 for f , at corresponding temperatures into Equations 15 and 16 and then plotting the values for x and y , a straight line is obtained (Figure 18). This validates the assumption of a coupled two-mode response. A least-squares fit was applied to the data points in Figure 18 resulting in $f_q = 172.5$ Hz and $1 - (A_{12}^2/A_{11} A_{22}) = 0.992$.

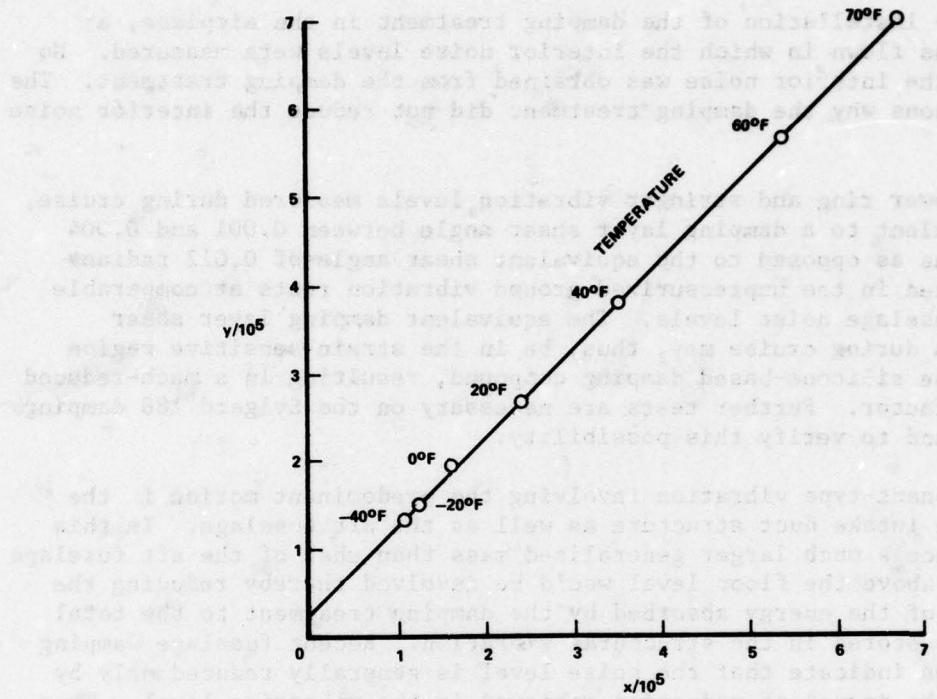


Figure 18. Correlation of Coupled-Mode Frequency Equation 14 with Measured Data

The extraction of the uncoupled modal loss factor η_q involved the separation of Equation 12 into its real and imaginary parts; the computation for $1 + a(A_{12}/A_{22})$ in the numerator of Equation 12; and lots of data processing to match the predicted coupled modal loss factor with the test data in Figure 17, using assumed values for η_q . The uncoupled lateral mode loss factor should be a constant if the damping treatment was totally ineffective in the lateral vibration. The loss factor η_q , extracted in the manner described, did in fact vary between 0.035 at 70°F and 0.045 at -20°F, with an average value around 0.038. Even with the use of the average value for η_q , the predicted lower coupled mode frequency and the corresponding coupled loss factor, when superimposed on the test data in Figures 16 and 17, respectively, showed good agreement with the measured data. The results indicate the importance of incorporating modal coupling effects into the basic theory.

APPLICATION OF DAMPING TREATMENT TO AN AIRPLANE

The damping treatment was applied to 11 rings and 25 stringers in the aft section of the airplane (Figure 1). The treatment was applied on the rings in five sections, each 60 inches long, with the composite constraining layer cross-sectional area ranging from 0.115 to 0.16 square inches depending on the ring I/A. On the stringers, the damping treatment was restricted in length to 19 inches by the frames. The composite constraining layer cross-sectional area on the stringers was 0.04 square inches.

After the installation of the damping treatment in the airplane, a flight test was flown in which the interior noise levels were measured. No reduction in the interior noise was obtained from the damping treatment. The potential reasons why the damping treatment did not reduce the interior noise levels are:

- The lower ring and stringer vibration levels measured during cruise, equivalent to a damping layer shear angle between 0.001 and 0.004 radians as opposed to the equivalent shear angle of 0.012 radians obtained in the unpressurized ground vibration tests at comparable aft fuselage noise levels. The equivalent damping layer shear angles during cruise may, thus, be in the strain-sensitive region for the silicone-based damping compound, resulting in a much-reduced loss factor. Further tests are necessary on the Sylgard 188 damping compound to verify this possibility.
- A resonant-type vibration involving the predominant motion in the entire intake duct structure as well as the aft fuselage. In this instance a much larger generalized mass than that of the aft fuselage shell above the floor level would be involved thereby reducing the ratio of the energy absorbed by the damping treatment to the total energy stored in the structural vibration. Recent fuselage damping studies indicate that the noise level is generally reduced only by half the amount of reduction achieved in the vibration level. Thus a ratio of the total generalized mass to the aft fuselage shell generalized mass of 3 to 1 would bring the amount of the noise reduction from the damping treatment to within the band of measurement error.
- A forced, non-resonant fuselage vibration for which damping is totally ineffective.

An alternate method for reducing the multiple pure-tone noise in the aft cabin was developed which eliminated the need for further investigation of the damping treatment.

CONCLUSIONS

Uniaxial ultrahigh modulus graphite fiber composite is highly suited for use as the constraining layer of a constrained layer damping treatment, especially when applied to heavy structures. For good correlation to be achieved between test data and theory, modal coupling must be considered when the possibility exists, otherwise the loss factor will be overestimated. The relatively good correlation between the test data and theory, when modal coupling was included, also vindicated the loss factor and dynamic shear modulus data measured by the moving-block test method over a wide temperature range. Additional work needs to be done to establish the region of stress sensitivity for silicone-based damping compounds. More emphasis should be placed on the acquisition and analysis of flight-measured data to identify the nature of the noise problems and shell vibration problems. Ground shaker tests on unpressurized shells could be misleading. Care must be taken in the application of damping treatments to complex structures for which it is difficult to define the total weight of structure involved in the vibration and which is too complex for accurate theoretical analysis.

REFERENCES

1. Ruzicka, J. E. et al, "Damping of Structural Composites with Viscoelastic Shear - Damping Mechanisms." NASA CR-742, March 1967.
2. Lamoree, M. D., LaBarge, W. L., Prydz, R.A., "The Development, Fabrication and Evaluation of Sonic Fatigue Resistance of Aerospace Structures Utilizing Viscoelastic Materials." AFML-TR-69-140, June 1969
3. Coote, C. T., "Measurement of the Damping Properties of Silicon - Based Elastomers Over Wide Temperature Ranges." J.S. & V, 1972 21(2), 133-147.
4. Painter, G. H., "Dynamic Properties of BTR Elastomers." SAE National Aeronautics Meeting, October 1958.
5. Jones, D.I.G., "Temperature - Frequency Dependence of Dynamic Properties of Damping Materials." J.S. & V, 1974 33(4), 451-470.
6. Kennedy, C. C. and Pancu, C.B.P., "Use of Vectors in Vibration Measurement and Analysis." J. Ac. Soc., November 1947.
7. Soovere, J., "Control Surface Impedance Theory." Hawker Siddeley Aviation Research Report #844, June 1968.

**AIRFRAME STRUCTURAL DAMPING
EVALUATIONS AND APPLICATIONS**

**H. W. Bartel
Lockheed-Georgia Company
Advanced Structures
Marietta, Georgia**

AIRFRAME STRUCTURAL DAMPING EVALUATIONS AND APPLICATIONS

H. W. Bartel
Lockheed-Georgia Company
Marietta, Georgia 30063

This article documents the text and visual aids used in a fifteen minute oral presentation at the beginning of the second day of the Conference. The article presents generalized experimental data, and examples of damping material effectiveness.

INTRODUCTION

This is a brief sampling of experimental work done at the Lockheed-Georgia Company, on the application of damping materials. Most of Lockheed-Georgia's analytical work has been tailored to specific structural cases, and therefore does not have general application. The experimental work however has been more generic, and might be of greater interest to those concerned with structural damping. This presentation therefore excludes theoretical and analytical developments, and presents only samples of experimental work on damping material applications. The applications have been mostly for light-weight secondary structure on transport aircraft, either to control resonant response to prevent flexural fatigue, or to control sound transmission to provide passenger comfort.

DISCUSSION

An interesting series of early tests were conducted to rank some of the damping concepts either in use, or thought to have potential application at that time. The nine damping materials tested in that series are pictured in Figure 1 as they were applied; in full coverage, sheet form. In order of thickness, they were: a foil-adhesive tape about 8 mils thick; a foil-backed fabric adhesive tape about 16 mils thick; a mastic type elastic sealant compound about 3/16" thick; a foil-backed foam adhesive tape 1/4" thick; a vinyl-backed foam adhesive tape 1/4" thick; a closed-cell elastic vinyl foam 1/2" thick; insulating type vinyl-backed fiberglass on a dual-faced adhesive tape; and closed cell cast styrene foam 2" and 4" thick bonded with a viscous adhesive. These materials were ranked according to their effectiveness in reducing stress at the edge of a resonant skin panel.

Figure 2 summarizes the results for one particular panel case. The test panel was aluminum (flat) and had clamped edge conditions. The rms flexural stress with and without damping treatment was monitored with strain gages in each case. The treatments are ranked according to the ratio of treated panel stress to untreated panel stress, for the first and second

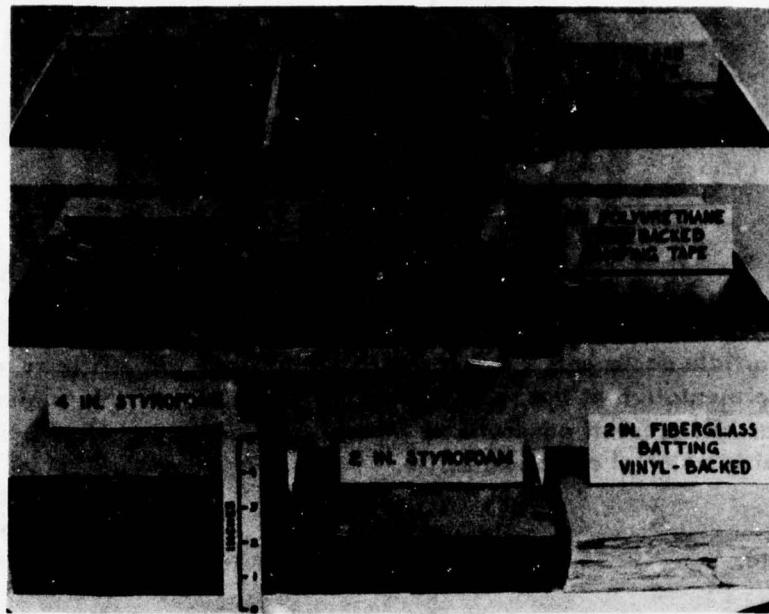


**Figure 1. Some Materials And Damping Concepts
Tested For Relative Effectiveness**

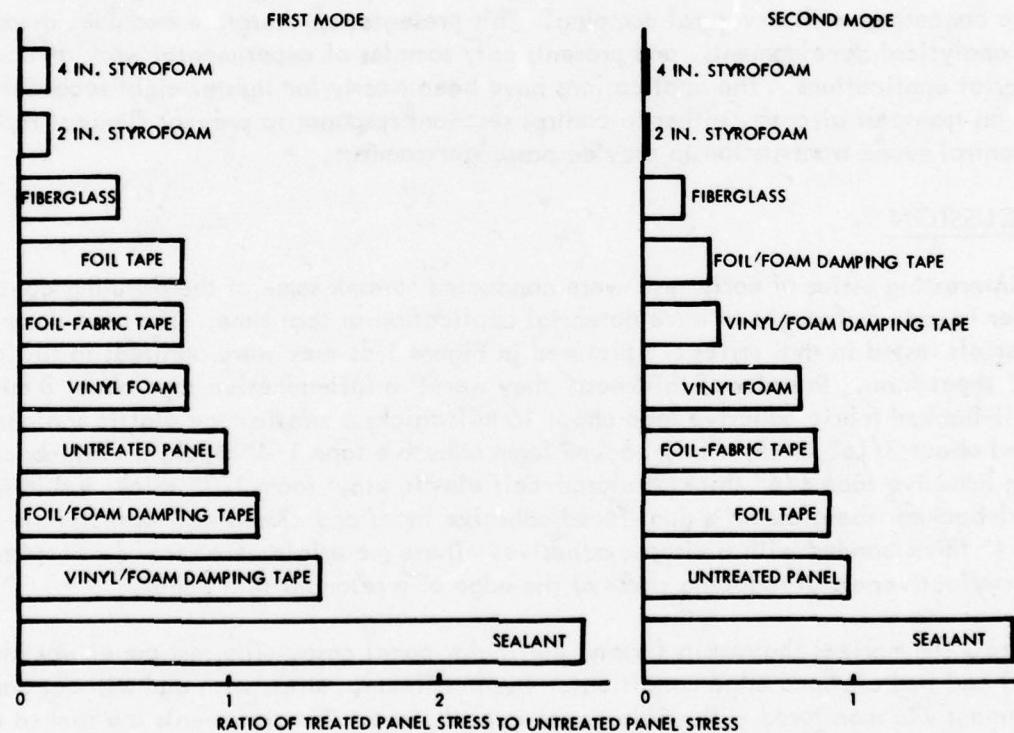


**Figure 2. Ranking Of Damping Concepts For
Controlling Resonance Response**

resonant modes in the same panel. As expected, the materials become more effective on higher order panel resonances. The rigid foam is particularly effective probably due more to stiffening than damping. The foil-back tapes offered slight improvements; the non-hardening elastic sealant was detrimental. There is wide variation in the mechanism by which these materials affect the skin stress. The materials are not always "dampers" in the correct sense. Some act as stiffeners, some act as tuned absorbers, some as friction dampers, some as viscous dampers, some simply add mass, some possess a combination of these properties. Thus the behavior of the treatment will depend strongly on the skin panel characteristics, e.g. thickness, span, aspect ratio, frequency, amplitude, etc. The ranking of the materials will be altered if the skin panel parameters are changed. These early data established clearly that properly applied damping could be used effectively to reduce flexural strain in aircraft panel structures. The data also demonstrated that uncertainties are attendant in the application of damping.

Silicon-based polymeric composite materials became available in recent years, and preliminary evaluations showed these damping compounds to be attractive. Figure 3 shows the resonance response at the center of a flat aluminum skin panel, having clamped edges, excited through the frequency range of the fundamental mode, with and without the silicon based damping material. The dramatic effect of the damping material is obvious. In this case the damping material was applied in sheet form, at 1.25 times panel thickness; full coverage.

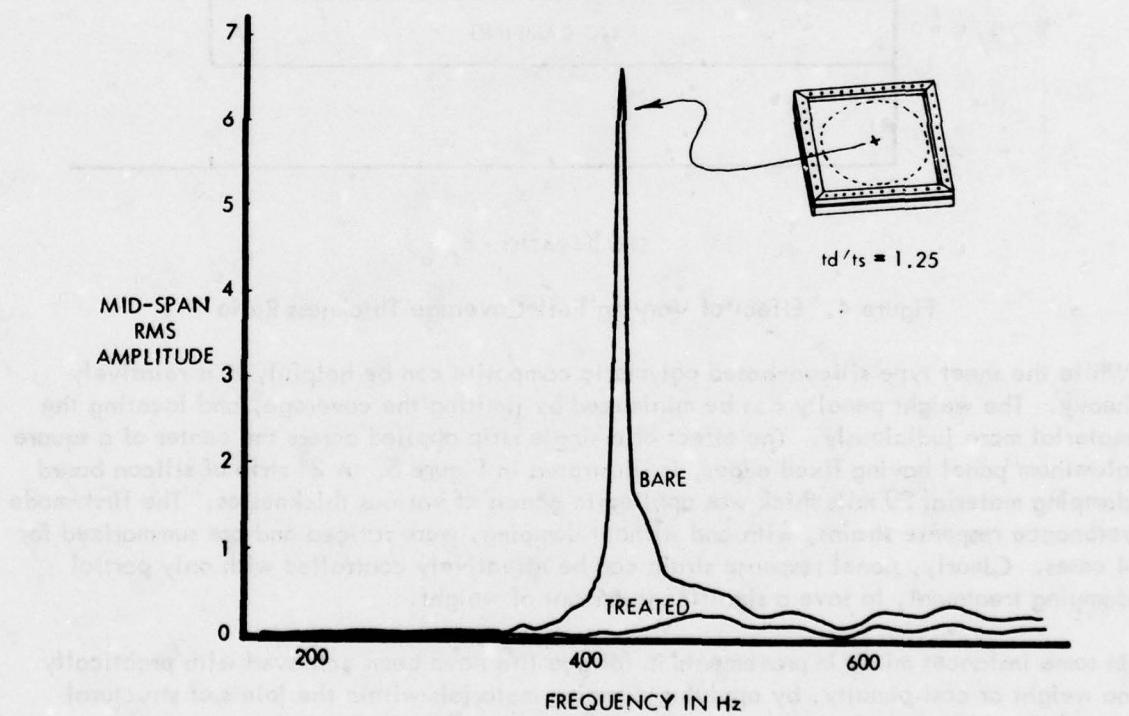


Figure 3. Silicon Base Polymeric Composite

The effect of varying the silicon-based polymeric composite full coverage thickness ratio was investigated in a later series of tests. In these tests flexural strain was obtained at the edge of a flat aluminum panel responding at its fundamental resonance. The ratio of strain level with damping, to strain level without damping, is summarized in Figure 4 for three damping material thicknesses. Damping material thickness is ratioed to panel thickness. With damping material at 110% of skin thickness, strain is reduced to 42% of the undamped level.

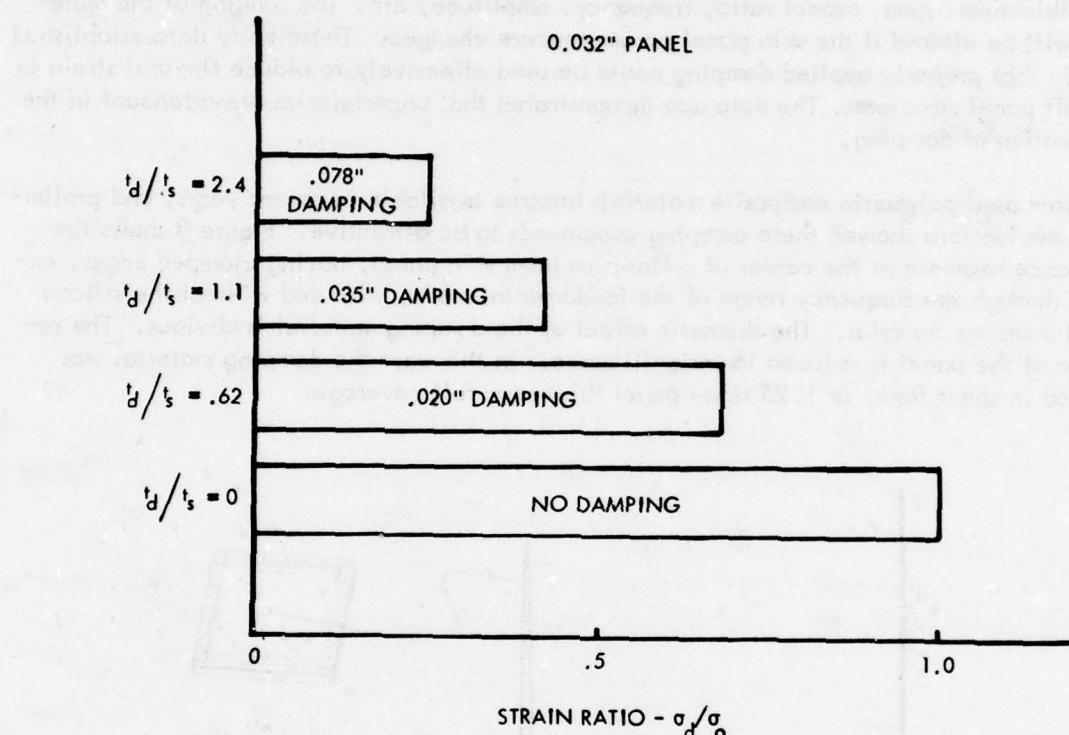


Figure 4. Effect of Varying Full-Coverage Thickness Ratio

While the sheet type silicon-based polymeric composite can be helpful, it is relatively heavy. The weight penalty can be minimized by limiting the coverage, and locating the material more judiciously. The effect of a single strip applied across the center of a square aluminum panel having fixed edges, is illustrated in Figure 5. A 2" strip of silicon based damping material 20 mils thick was applied to panels of various thicknesses. The first-mode resonance response strains, with and without damping, were ratioed and are summarized for 4 cases. Clearly, panel response strain can be effectively controlled with only partial damping treatment, to save a significant amount of weight.

In some instances minor improvements in fatigue life have been achieved with practically no weight or cost penalty, by applying damping materials within the joints of structural assemblies. The benefit is thought to be due as much to wear prevention as to response reduction. Multi-bay skin-rib panel assemblies have been fatigue tested with and without

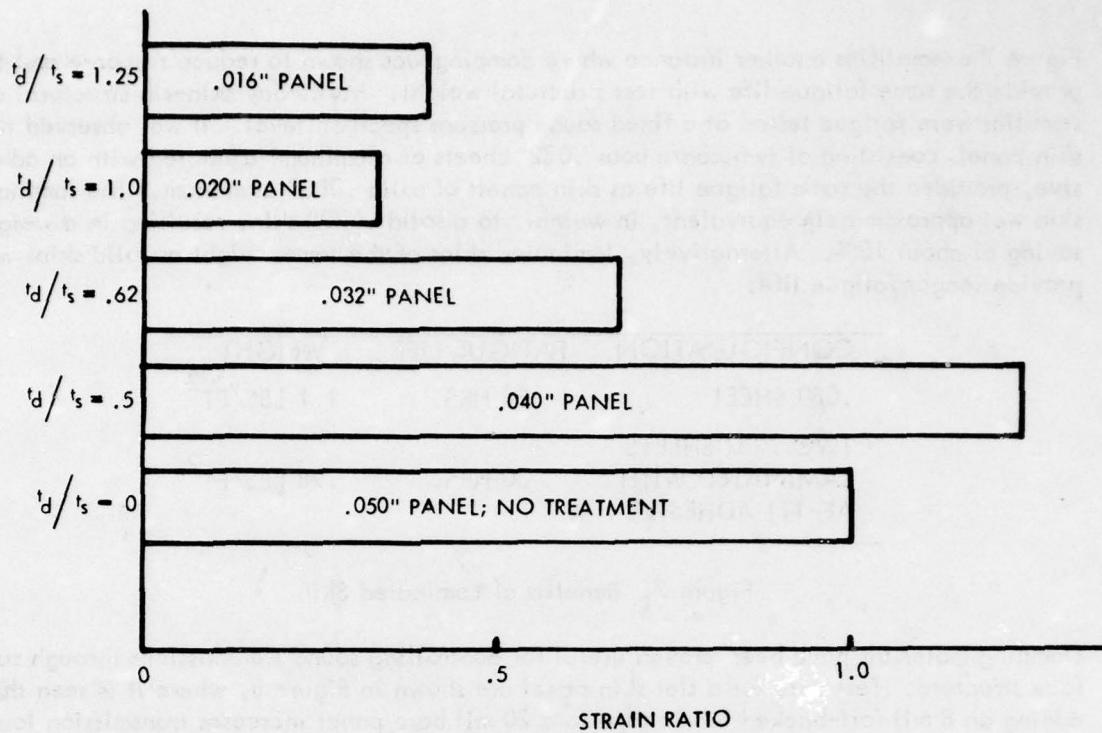


Figure 5. Effect of 2" x .020" Damping Strip
on Response of Various Panels

fay surface sealants applied, to reveal the effects on life shown in Figure 6. The benefits revealed are nominal, although additional benefits would be expected if life were on the order of 10^9 or 10^{10} cycles. At 10^9 cycles of flexure, wear of the faying surfaces can contribute to fatigue, and fay surface sealants reduce wear.

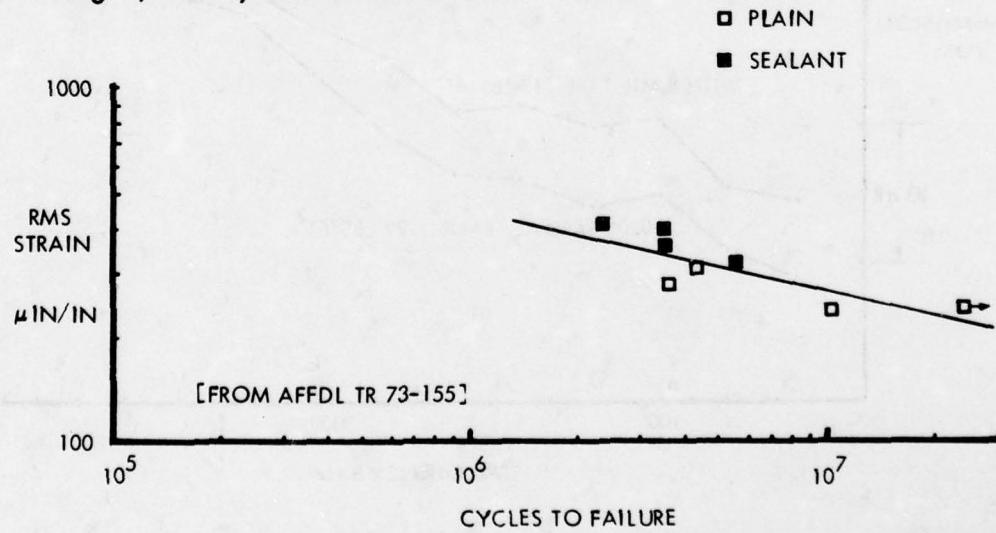


Figure 6. Effect of Fay Surface Sealant

Figure 7 exemplifies another instance where damping was shown to reduce response and thus provide the same fatigue life with less structural weight. Multi-bay skin-rib structural assemblies were fatigue tested at a fixed sound pressure spectrum level. It was observed that skin panels consisting of two continuous .032" sheets of aluminum laminated with an adhesive, provided the same fatigue life as skin panels of solid .080" aluminum. The laminated skin was approximately equivalent, in weight, to a solid .070" skin, resulting in a weight saving of about 10%. Alternatively, laminated skins of the same weight as solid skins would provide longer fatigue life.

CONFIGURATION	FATIGUE LIFE	WEIGHT
.080 SHEET	30 HRS.	1.1 LBS/FT ²
TWO .032 SHEETS LAMINATED WITH AF-111 ADHESIVE	30 HRS.	.98 LBS/FT ²

Figure 7. Benefits of Laminated Skin

Damping materials have been proven useful for controlling sound transmissions through surface structure. Test data for a flat skin panel are shown in Figure 8, where it is seen that adding an 8 mil foil-backed fabric tape to a 20 mil bare panel increases transmission loss by as much as 6dB. In this case the foil-backed tape acts as a "constrained layer" damper, and

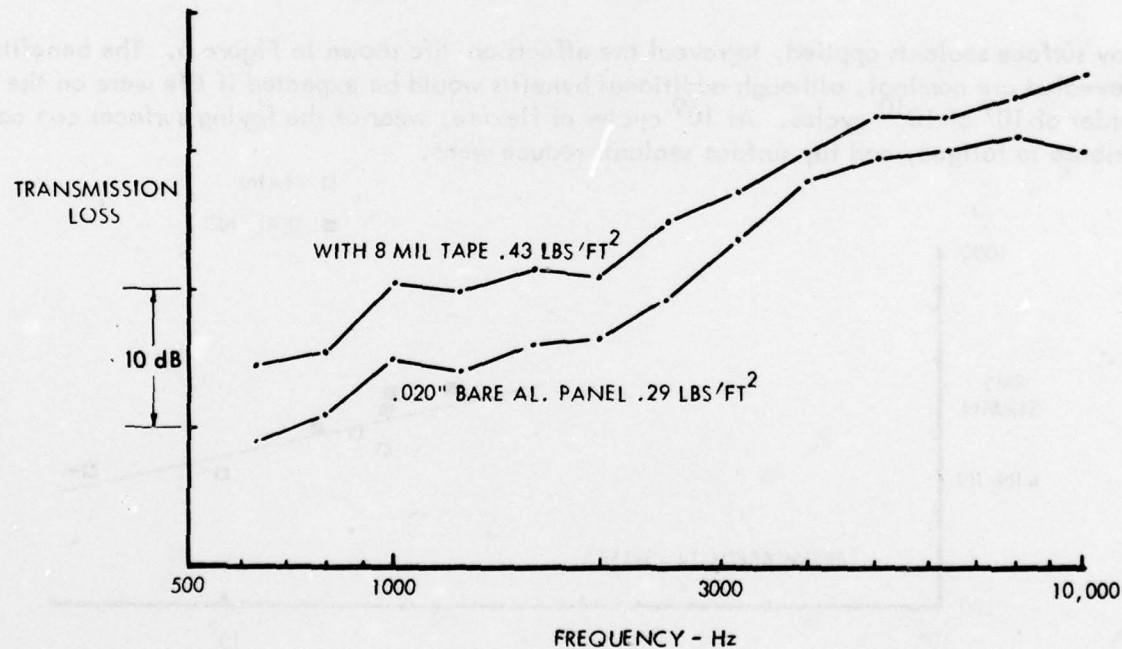


Figure 8. Soundproofing with Foil-Back Fabric Tapes

reduces resonant response. The improvement in transmission loss is, on average, slightly better than would be expected from the addition of .14 lbs/ft² of mass. Thus the damped panel is behaving more like a "limp" membrane.

When a silicon based polymeric composite material is added to a bare skin panel, the material acts as a "free-layer" damper. The resonant response of the skin panel is reduced, and the damped panel behaves more like a limp membrane. The test data shown in Figure 9 indicate increases in transmission loss of 8 to 10dB, obtained from a 62 mil sheet applied to a 20 mil flat panel.

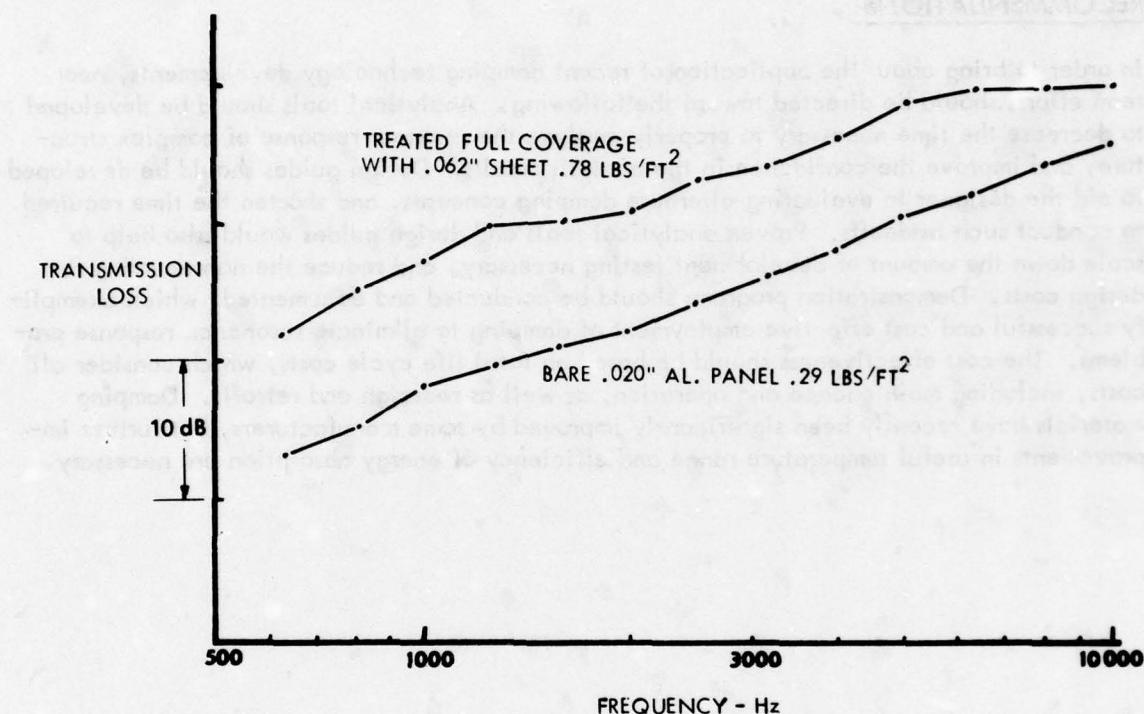


Figure 9. Soundproofing with Silicon Base Polymeric Sheet Damping

SUMMARY

Damping material has been applied, to a limited extent, in all major Lockheed-Georgia production airframes. It is used in soundproofing most versions of the JetStar, a general aviation jet transport. It is also used in the C-130 and the C-141 transport airplanes, to control cabin noise in local areas of high-intensity external noise. Damping materials are used to control noise in the environmental air distribution systems in the JetStar, C-130, C-141, and C-5. In order to enhance sonic fatigue life, damping compounds are used in certain mechanically fastened joints of C-130, C-141 and C-5 secondary structure. Laminated skins are used to improve fatigue life or reduce weight in certain secondary structures in the C-5 nacelles and the L-1011 empennage.

While viscoelastic damping has been evaluated in a variety of material variations and structural applications, and has been proven to be a useful structural material, it has not been widely used. This limited use arises from a combination of factors that can be summarized as: a lack of confidence that the damping application will be successful; a lack of time and resources to perform the analyses, tests, and evaluations required to insure success; lack of authorized funding to design or redesign for minimum life cycle cost. In most cases of structural response problems that develop after product entry into service, the aforementioned confidence, time, and cost considerations usually result in a simple beef-up being the chosen alternative.

RECOMMENDATIONS

In order to bring about the application of recent damping technology developments, near term efforts should be directed toward the following. Analytical tools should be developed to decrease the time necessary to properly analyze the resonant response of complex structure, and improve the confidence in the analysis results. Design guides should be developed to aid the designer in evaluating alternate damping concepts, and shorten the time required to conduct such tradeoffs. Proven analytical tools and design guides would also help to scale down the amount of development testing necessary, and reduce the nonrecurring redesign costs. Demonstration programs should be conducted and documented, which exemplify successful and cost effective employment of damping to eliminate resonance response problems. The cost effectiveness should be based on total life cycle costs, which consider all costs, including maintenance and operation, as well as redesign and retrofit. Damping materials have recently been significantly improved by some manufacturers, but further improvements in useful temperature range and efficiency of energy absorption are necessary.

VISCOELASTIC DAMPING
APPLICATIONS B-1 AIRCRAFT

A. G. Tipton
Los Angeles Division
Rockwell International
Los Angeles, California

SUMMARY

VISCOELASTIC DAMPING

APPLICATIONS

B-1 AIRCRAFT

A. G. TIPTON

MEMBER OF THE TECHNICAL STAFF
LOS ANGELES DIVISION, ROCKWELL INTERNATIONAL

The vibration environment induced by acoustic noise in the aft fuselage of the B-1 aircraft was higher than initial predictions and a series of tasks were initiated to reduce the vibration amplitude. Conventional isolation systems and structural damping concepts were evaluated. The viscoelastic damping concepts consisted of faying surface applications and constrained layer treatments added to existing structural designs.

A series of laboratory tests on damped and undamped beams were conducted to evaluate the relative effectiveness of various damping materials and configurations as a function of temperature and frequency. The most effective damping treatment configuration was selected for aircraft installation and evaluation. Faying surface treatments were evaluated but cold flow of the damping material resulted in loose structural joints and therefore could not be utilized without further study.

Flight test evaluations of selected constrained layer damping treatments were conducted on two B-1 aircraft. The damping treatments were installed on the thin skin-frame tail cone fairing on one aircraft, and in a tail cone section modified to simulate the heavier gage construction of aft fuselage equipment bays with installed equipment mass supported on simulated shelves, on the other aircraft. The aircraft structural vibration level was recorded during take off operations at maximum afterburner power prior to installation of damping treatments to obtain baseline data. Successive vibration measurements were recorded on both aircraft with various damping treatment configurations. The vibration responses of the damped aircraft structure were normalized to the undamped responses to illustrate the effectiveness of the damping treatments. The vibration reduction achieved by structural damping approached an order of magnitude at high frequencies above 1000 Hz but was less effective in the lower frequency ranges.

Constrained layer viscoelastic damping was applied to several antennas, subsequent to initial test failures, to reduce the structural response and induced stress level imposed during laboratory vibration qualification tests. Laboratory tests were conducted with and without damping treatments to determine damping effectiveness. Maximum response reduction exceeded an order of magnitude. The damping treatments were incorporated into the aircraft antenna designs.

Constrained layer damping treatment application to existing aircraft structure impose practical installation problems. The stiffness of the constraining layer makes application over irregular structural surfaces difficult and adversely affects the adhesion of the damping treatment. Damping treatment application to aircraft structure subjected to normal operating environments which includes hydraulic fluid, petroleum residues, etc. require meticulous surface cleaning to insure proper adhesion.

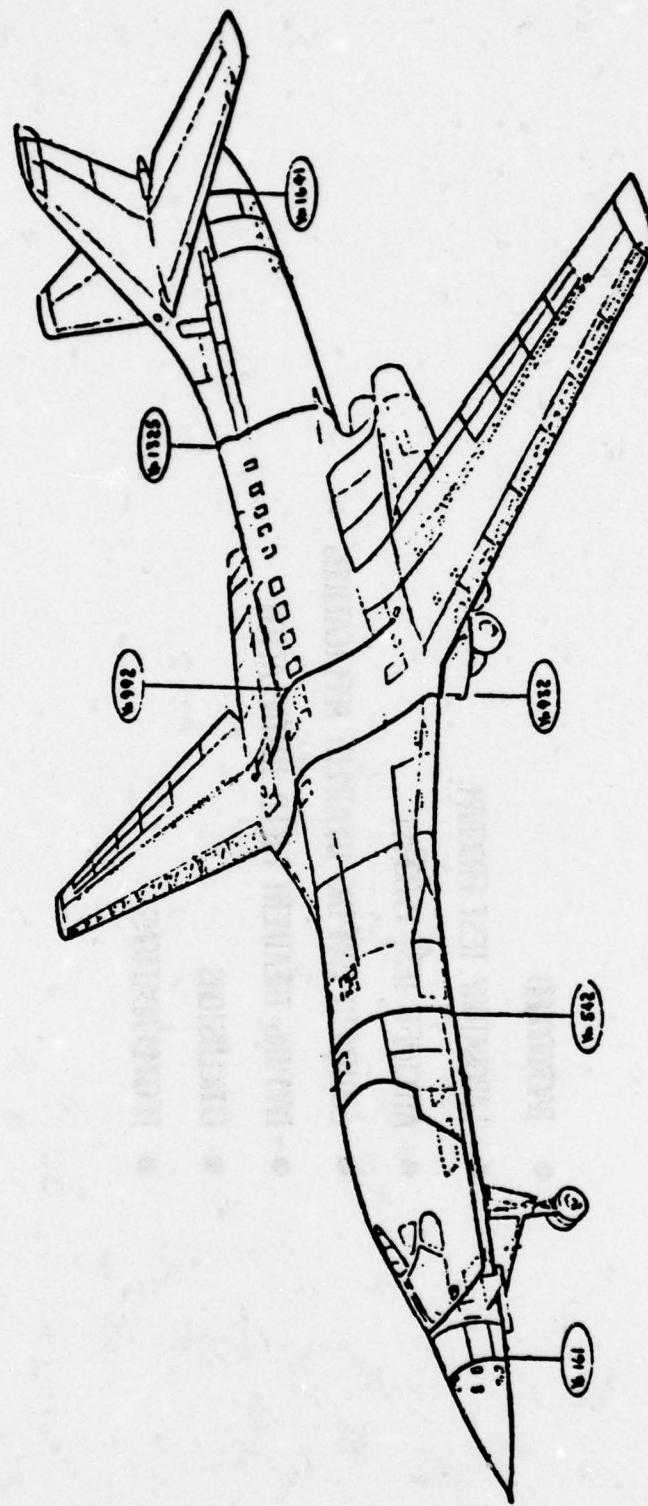
Constrained layer viscoelastic damping properly applied to aircraft structure can reduce structural vibration. The additive damping treatments, however, are not as effective as conventional isolators in reducing vibration to equipment installed on aircraft structure. Conventional isolation systems require greater installation volume and perhaps an optimum relationship exists between airframe structural damping and equipment damping techniques that would preclude the use conventional isolators and result in more effective usage of available equipment bay volume.

The B-1 aircraft damping evaluation was conducted under schedule constraints that did not permit optimization and was limited to additive treatments. It is anticipated that application of optimized additive damping treatments and designed in damping concepts utilizing sandwich construction would result in greater structural vibration reduction than was obtained in the initial B-1 aircraft damping evaluations.

**ROCKWELL VISCOELASTIC DAMPING
DEVELOPMENT PROGRAM**

- BACKGROUND
- LABORATORY TEST PROGRAM
- AIRCRAFT TEST PROGRAM
- EQUIPMENT DAMPING TREATMENT APPLICATIONS
- DAMPING TREATMENT FIELD INSTALLATION
- CONCLUSIONS
- RECOMMENDATIONS

B-1 DAMPING APPLICATIONS



B-1 AFT EQUIPMENT BAY
VIBRATION PROBLEM

- VIBRATION LEVELS EXCEED EQUIPMENT QUALIFICATION LEVELS
- SCHEDULING & COST IMPACT MAKES REDESIGN & REQUALIFICATION OF EQUIPMENT UNDESIRABLE
- SCHEDULING DOES NOT PERMIT CHANGE TO PRIMARY STRUCTURE
- DEVELOPMENT PROGRAM INITIATED FOR TWO VIBRATION REDUCTION SYSTEMS
 - ISOLATION SYSTEMS
 - ADDITIVE DAMPING TREATMENTS
- THIS PRESENTATION ADDRESSES ONLY THE ADDITIVE DAMPING TREATMENT DEVELOPMENT
- PROGRAM CONDUCTED BY ROCKWELL INTERNATIONAL

**VISCOELASTIC ADDITIVE DAMPING
DEVELOPMENT PROGRAM**

- **LIMITED SCOPE**
 - LABORATORY MATERIAL SELECTION/EVALUATION
 - AIRCRAFT STRUCTURE DAMPING TREATMENT FLIGHT TEST EVALUATIONS
 - EQUIPMENT DAMPING APPLICATION EVALUATION

LITERATURE

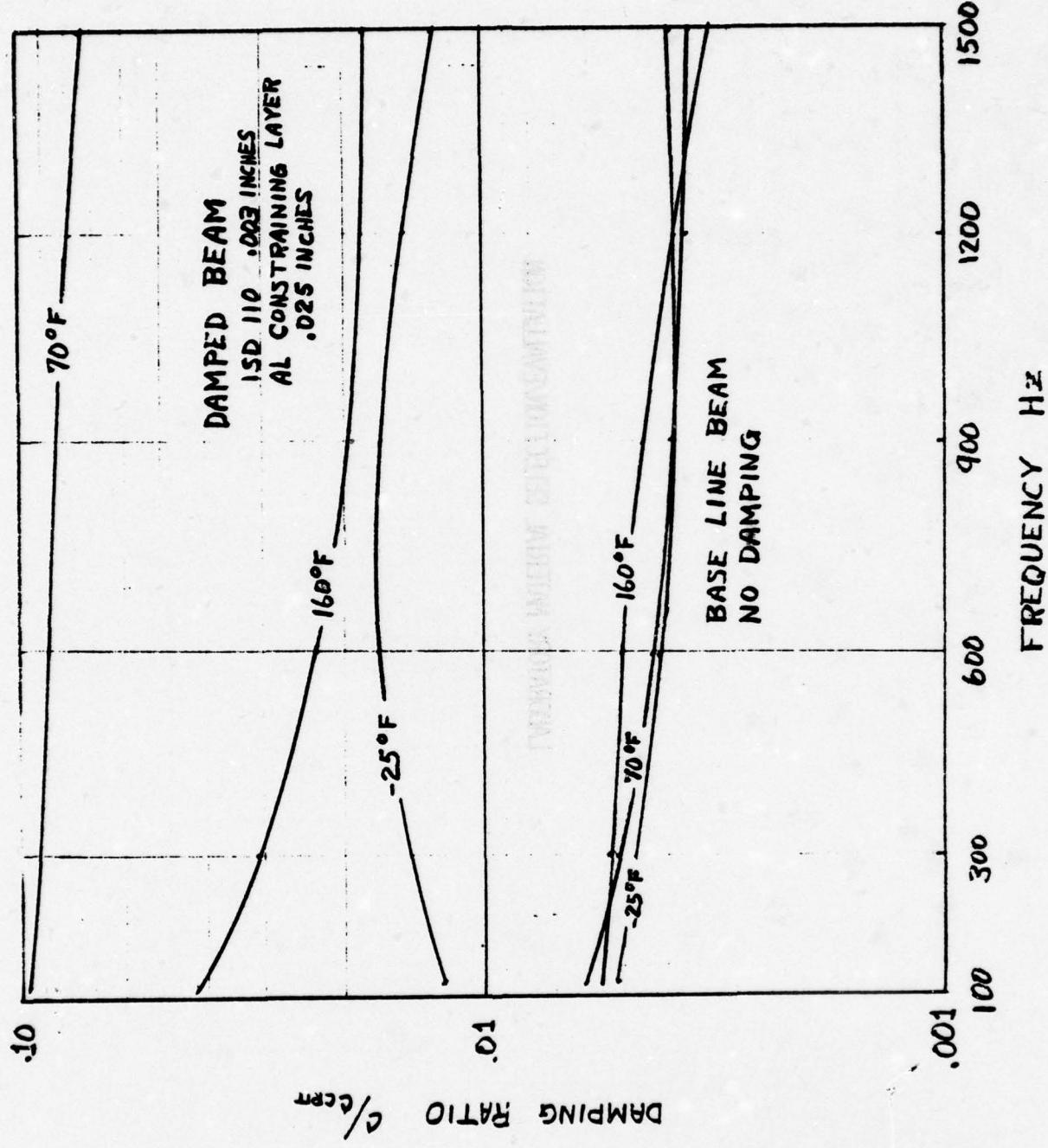
100	300	400	500	600	700	800	900	1000
-----	-----	-----	-----	-----	-----	-----	-----	------

NO PUBLICATIONS
SIZE TYPE INDEX

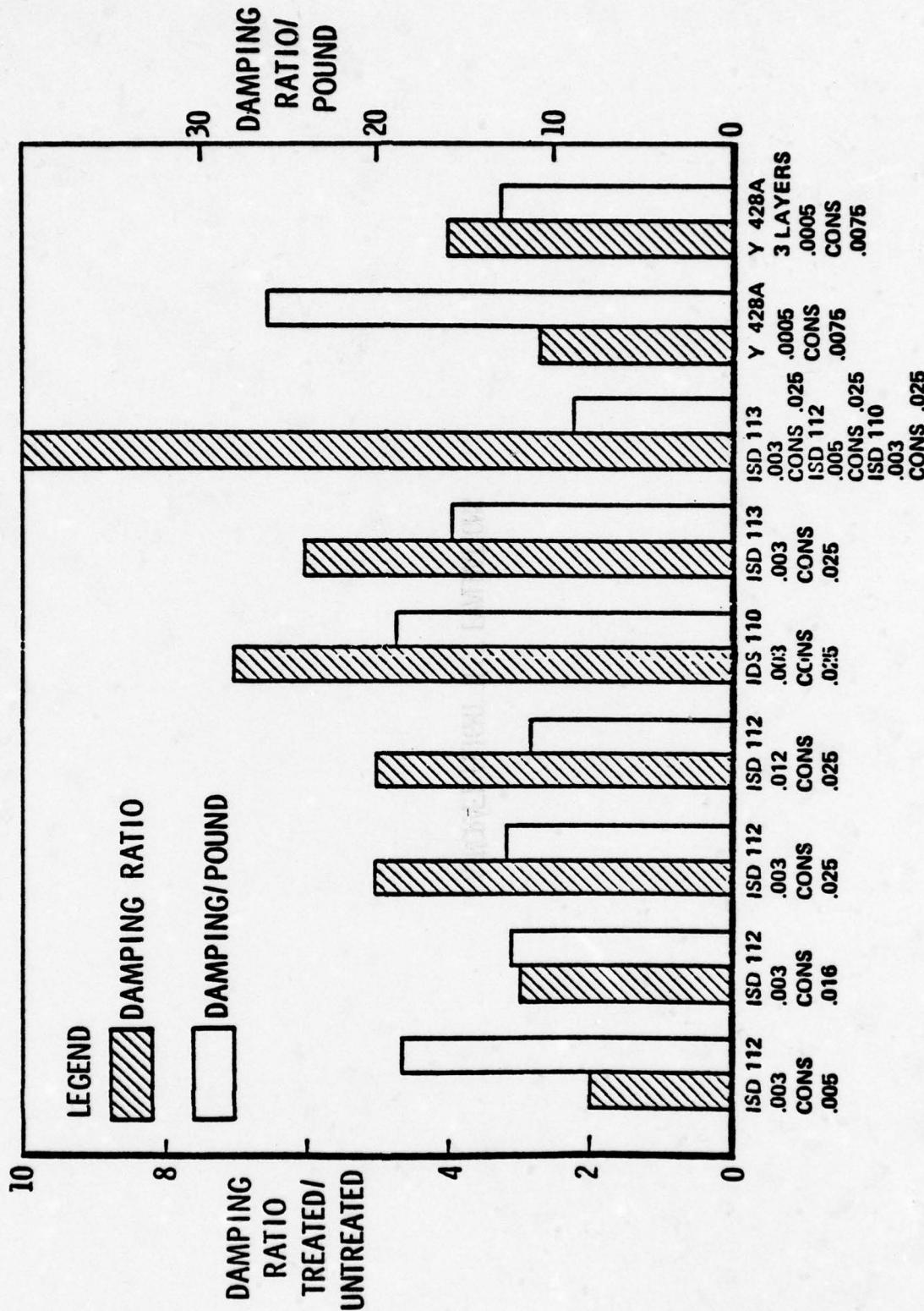
DETAILED OUTLINE

LABORATORY MATERIAL SELECTION/EVALUATION

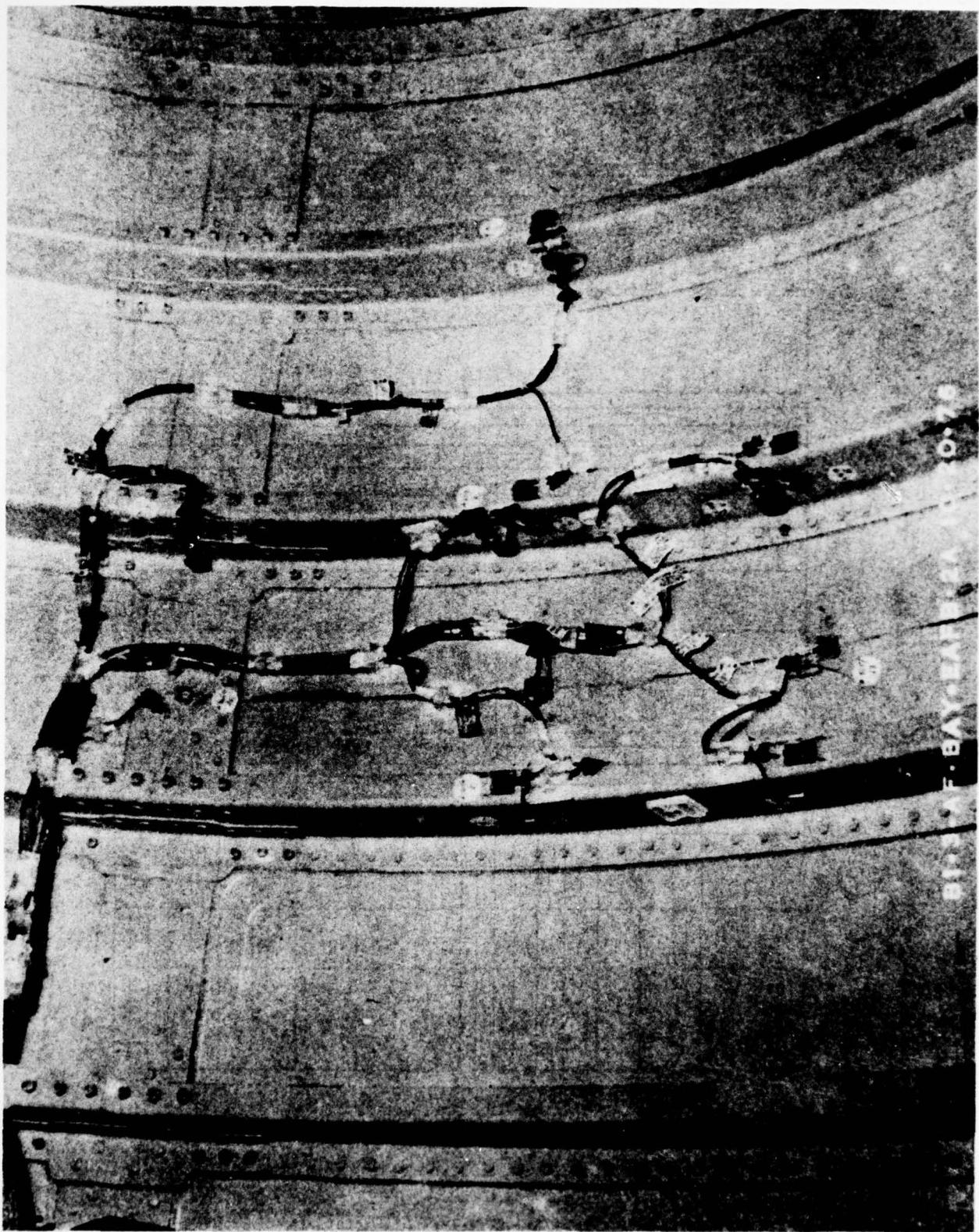
BEAM DAMPING



BEAM DAMPING

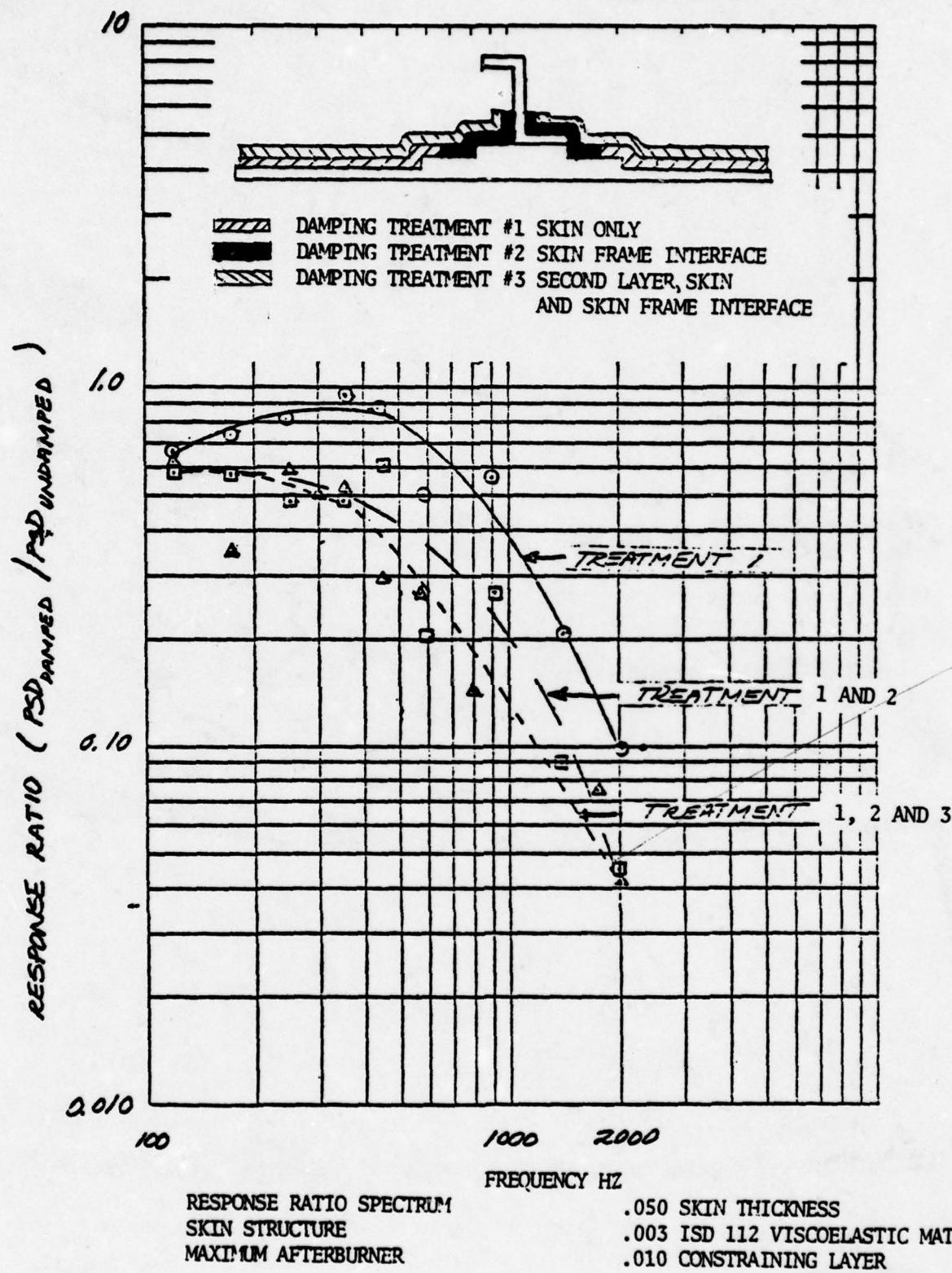


AIRCRAFT FLIGHT TEST EVALUATIONS

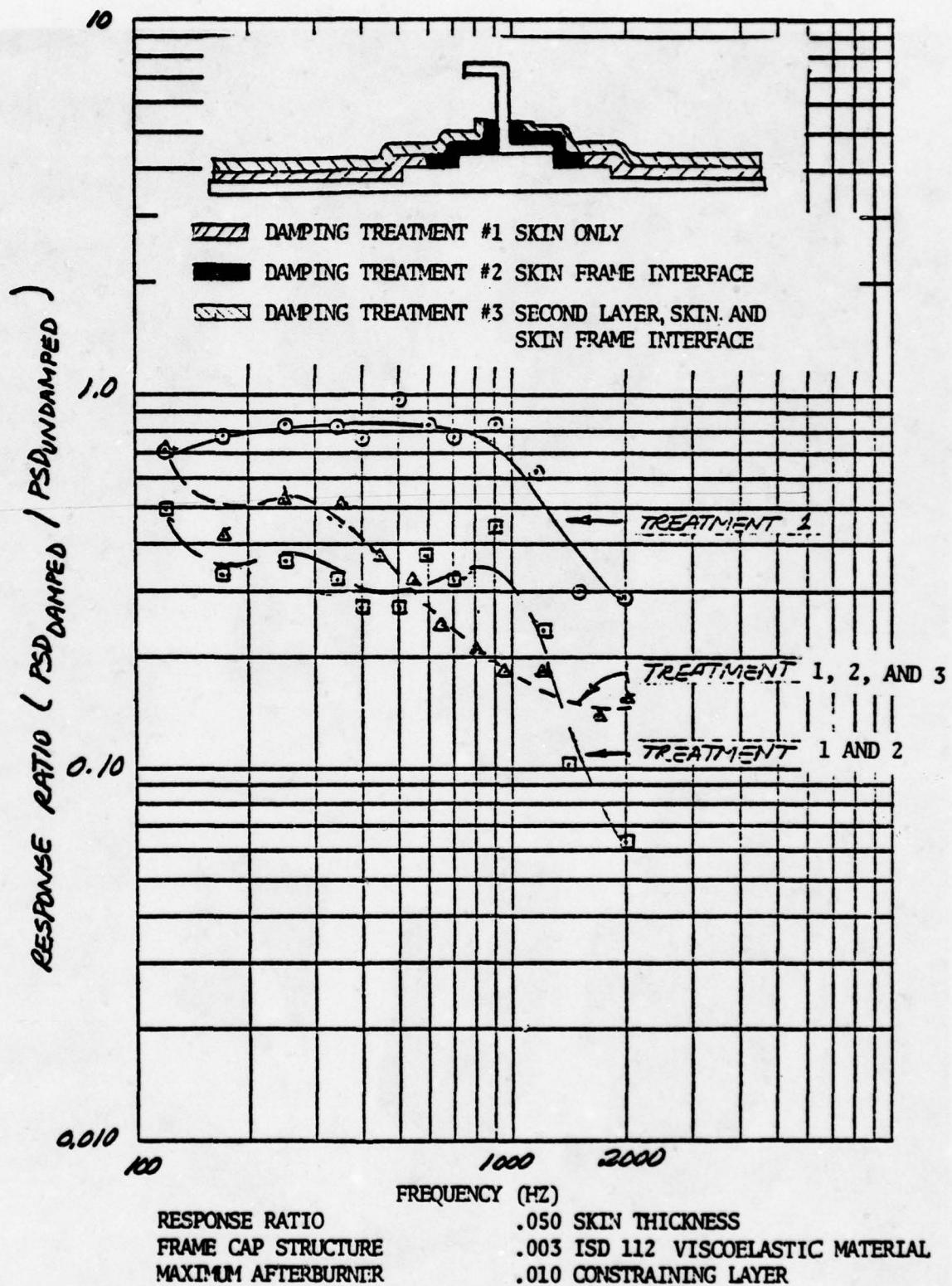


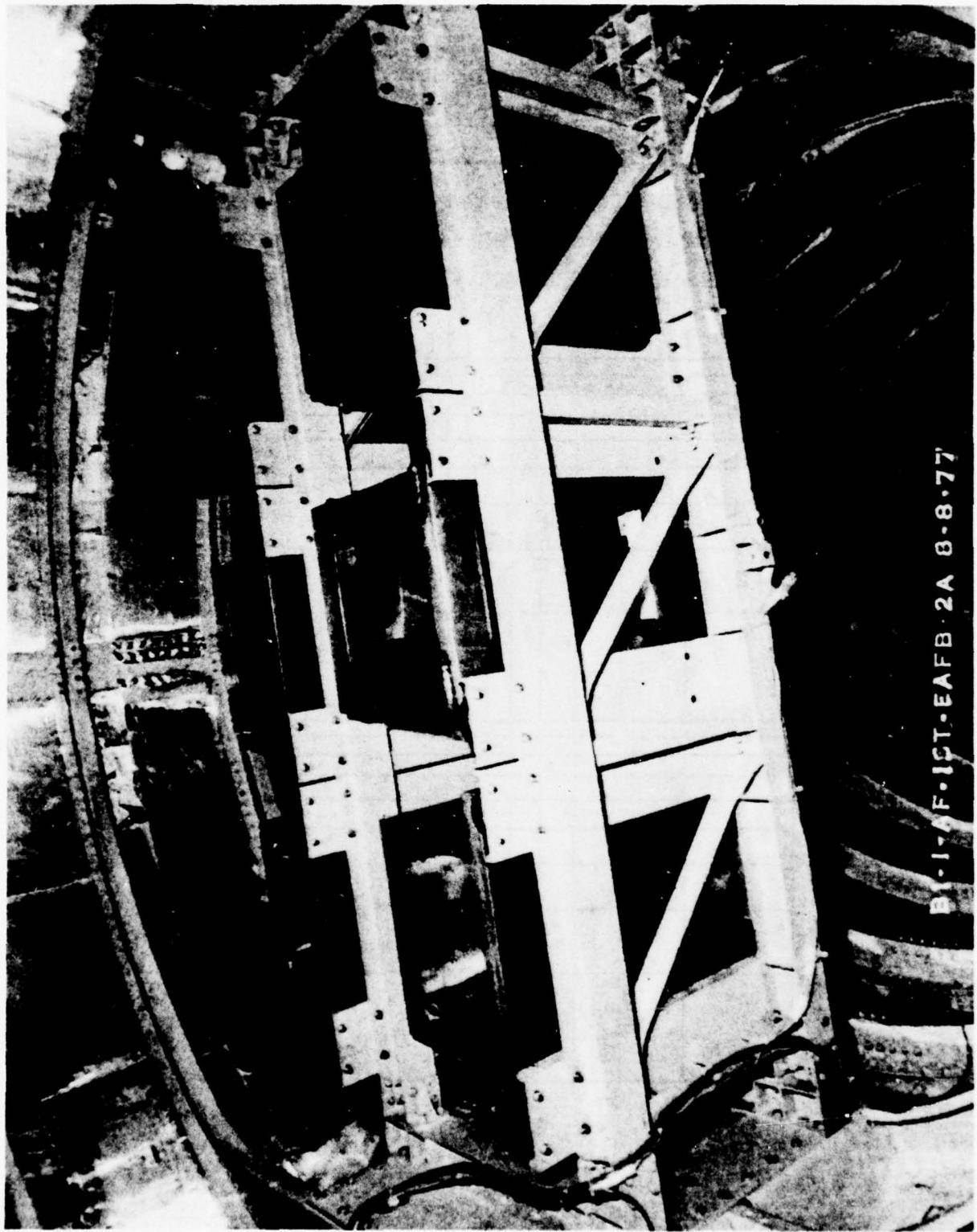
343

NORTH AMERICAN ROCKWELL CORPORATION



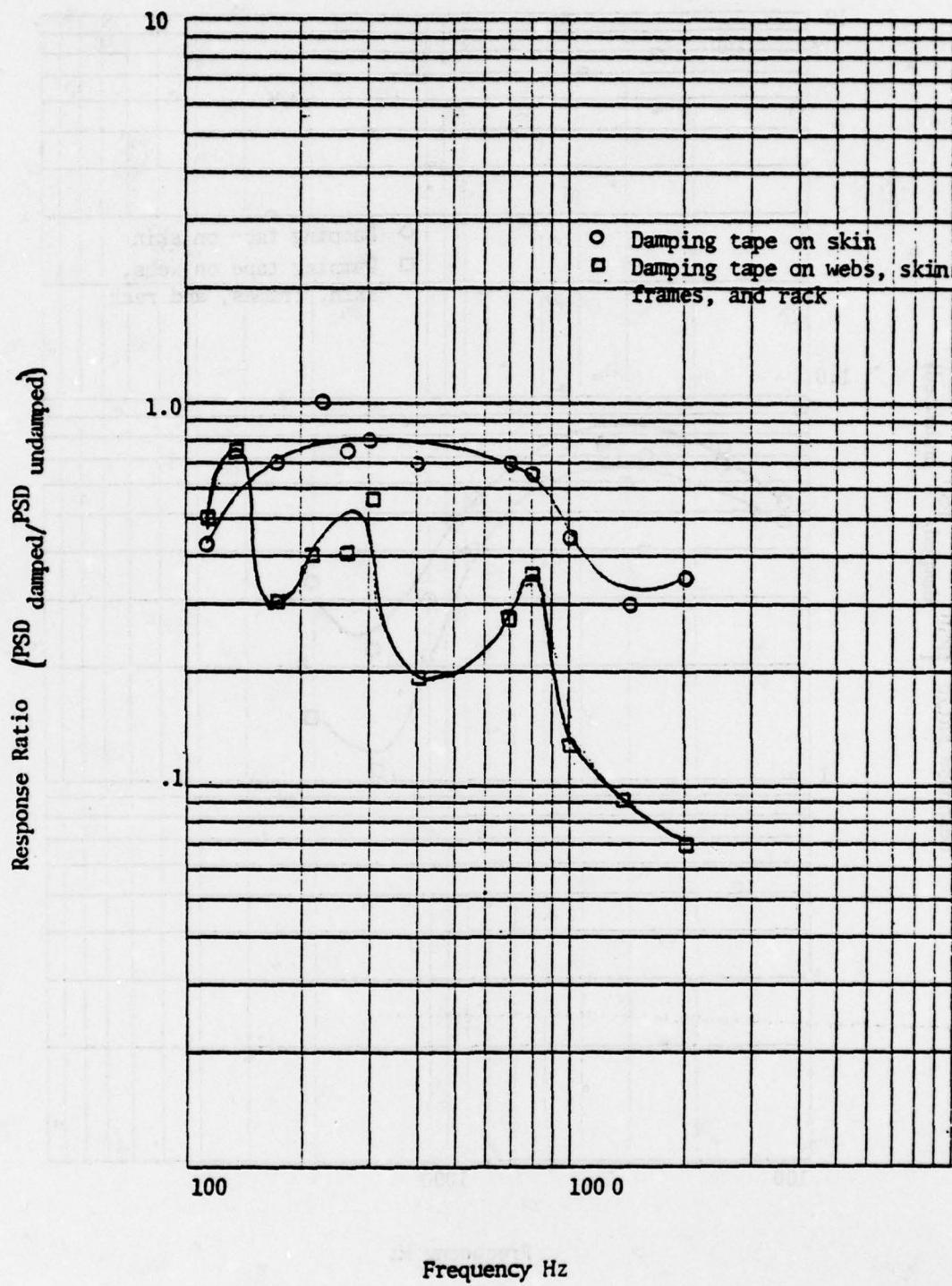
NORTH AMERICAN ROCKWELL CORPORATION





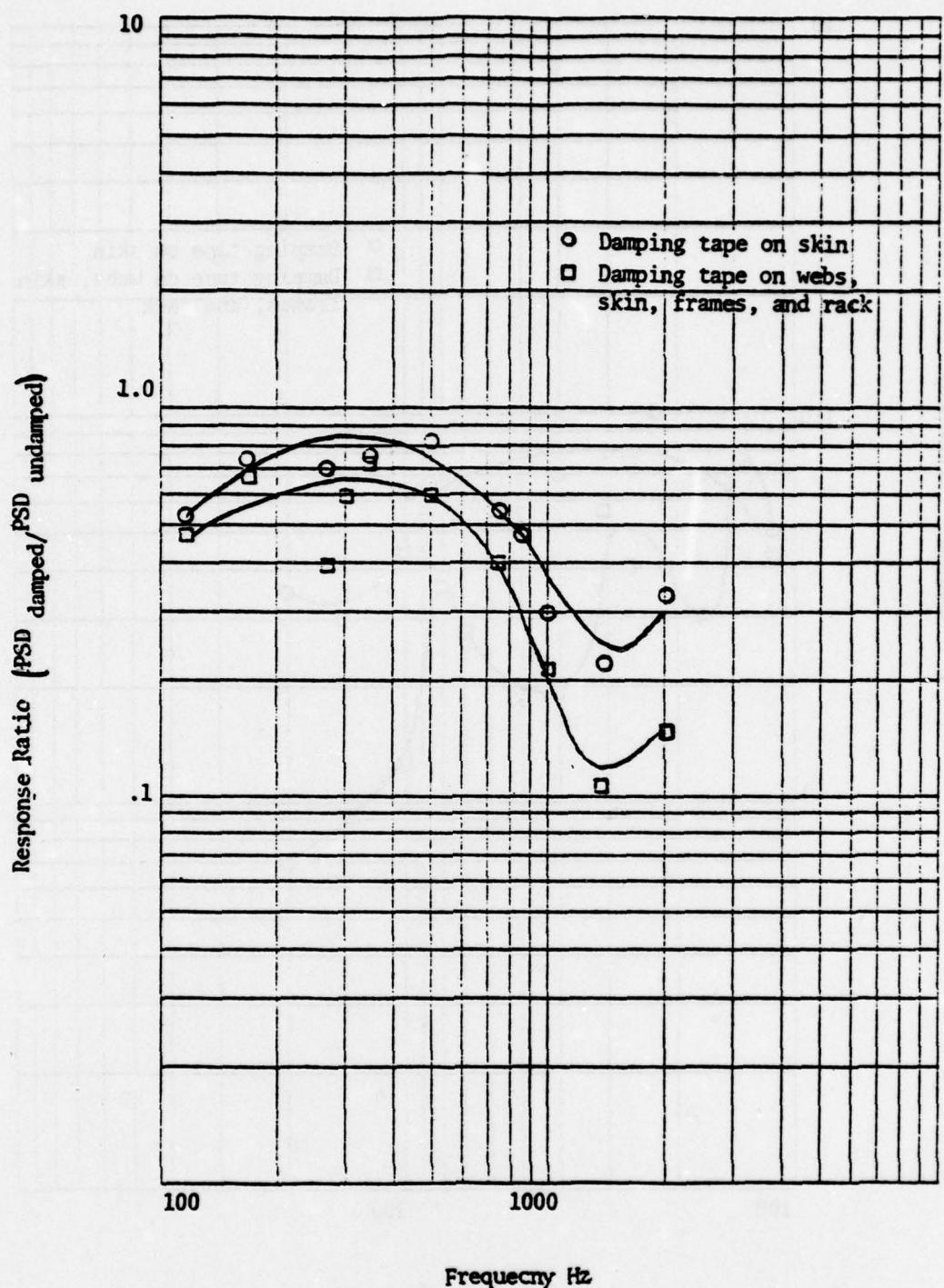
B-1-AF-1ST-EAFB-2A 8-8-77

NORTH AMERICAN ROCKWELL CORPORATION



Aft avionics bay
Rack mid span locations
Vertical response ratio

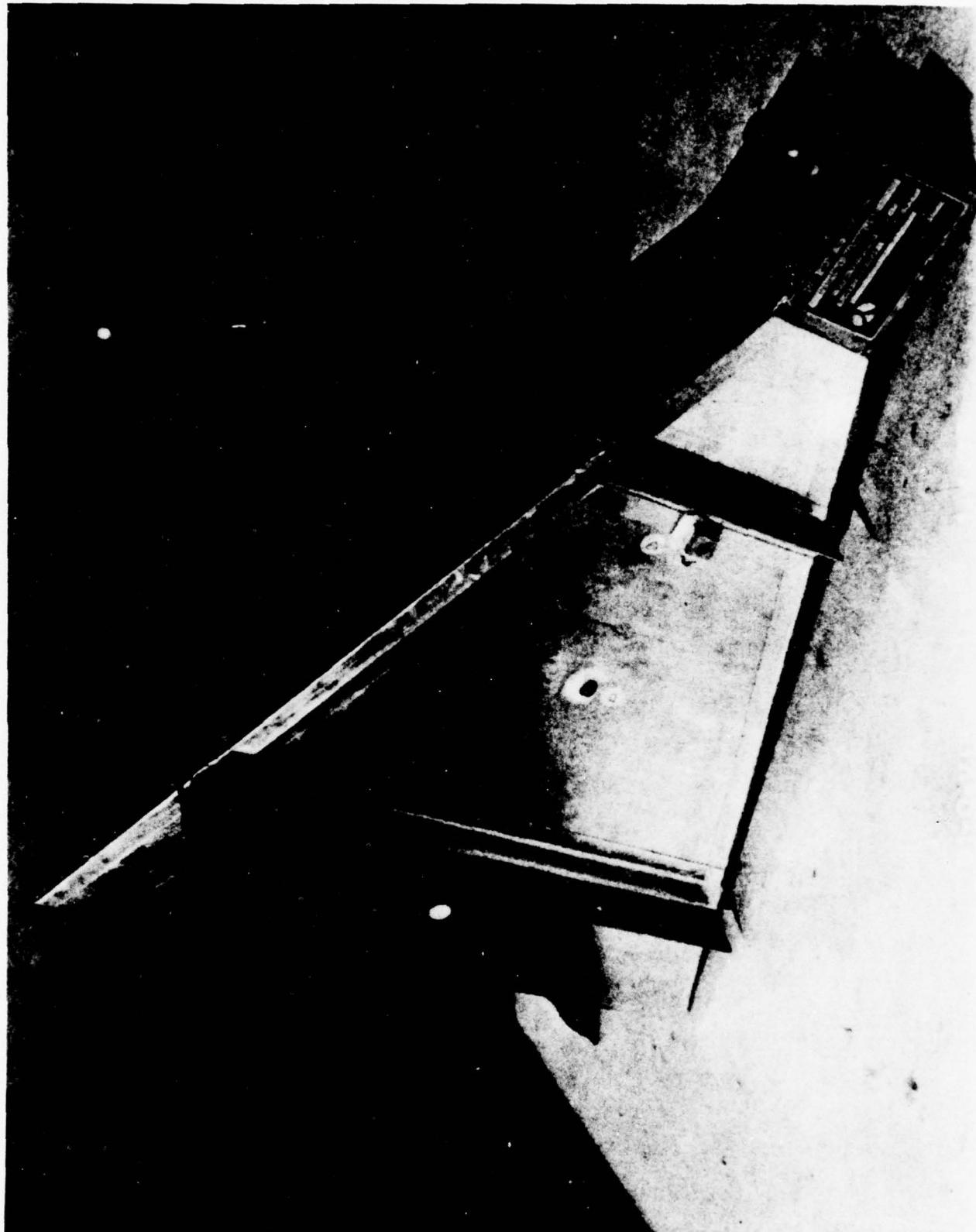
.10 AL. SKIN THICKNESS
.003 ISD 112 VISCOELASTIC MATERIAL
.020 AL. CONSTRAINING LAYER

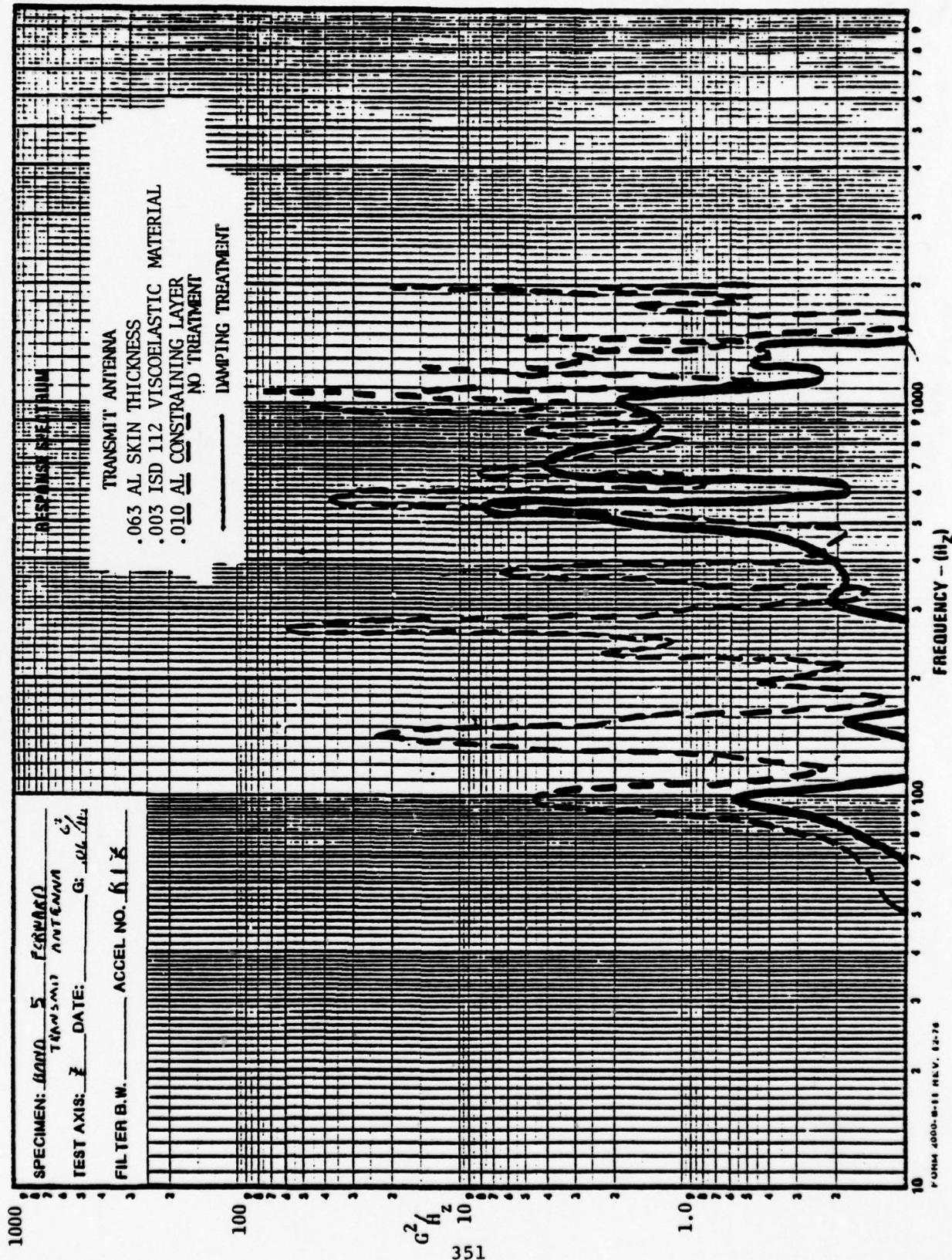


Aft avionics bay
Rack support locations
Vertical response ratio

.100 AL. SKIN THICKNESS
.003 ISD 112 VISCOELASTIC MATERIAL
.020 AL. CONSTRAINING LAYER

DAMPING DIRECTLY APPLIED TO EQUIPMENT





DAMPING TREATMENT FIELD INSTALLATION

- IRREGULAR SURFACES
- SURFACE CLEANING
- MATERIAL SPRING BACK

PRELIMINARY CONCLUSIONS

- ADDITIVE DAMPING IS MOST EFFECTIVE ON HIGHLY RESONANT STRUCTURE
- INITIAL EVALUATIONS INDICATE GOOD RESPONSE REDUCTION POTENTIAL OF AIRFRAME STRUCTURE WITH ADDITIVE VISCOELASTIC DAMPING MATERIALS
- ANTENNA HORN STRUCTURE DAMPING TREATMENT EVALUATION INDICATES SIGNIFICANT RESPONSE REDUCTION
- LABORATORY DAMPING TREATMENT APPLICATION TECHNIQUES ARE MORE DIFFICULT WHEN ADAPTED TO FIELD APPLICATION
- ADDITIONAL EVALUATION (ANALYTICAL & EMPIRICAL) IS REQUIRED TO OPTIMIZE ADDITIVE DAMPING TREATMENTS

RECOMMENDATIONS

- STRUCTURAL RESPONSE CHARACTERISTICS SHOULD BE CORRELATED WITH CONFIGURATIONS OF ADDITIVE DAMPING TREATMENTS TO MAXIMIZE VIBRATION REDUCTION.
 - STRUCTURAL RESPONSE CHARACTERISTICS
 - DOMINATE FREQUENCY MODES
 - STRAIN ENERGY DISTRIBUTION
 - CONFIGURATIONS OF ADDITIVE DAMPING TREATMENTS
 - MATERIAL TYPE
 - MATERIAL THICKNESS
 - MATERIAL PLACEMENT
 - NUMBER OF LAYERS
 - TILE LENGTH
- FAYING SURFACE DAMPING TREATMENTS REQUIRE FURTHER EVALUATION. INITIAL TESTS INDICATE COLD FLOW RESULTING IN LOOSE JOINTS.

RECOMMENDATIONS (CONT.)

- RECOMMEND PROGRAM TO EVALUATE DESIGNED IN SANDWICH TYPE DAMPING APPLICATIONS
- LABORATORY APPLICATION TECHNIQUES SHOULD BE DEVELOPED THAT FIELD INSTALLATION PERSONNEL CAN FOLLOW

MODAL DAMPING MEASUREMENTS ON PABST
ADHESIVELY BONDED AIRFRAME FUSELAGE STRUCTURE

R. Gordon
Air Force Flight Dynamics
Laboratory
Wright-Patterson Air Force Base,
Ohio

and

J. Sharp
Aeronautical Systems Division
Wright-Patterson Air Force Base,
Ohio

**MODAL DAMPING MEASUREMENTS ON PABST
ADHESIVELY BONDED AIRFRAME FUSELAGE STRUCTURE**

R. Gordon - Air Force Flight Dynamics Laboratory
J. Sharp - Aeronautical Systems Division

Introduction

Resonant vibration in an aircraft airframe can cause both high interior noise levels for crew or equipment and reduced structural life through sonic fatigue. The structural damping is a major factor in the resonant response of airframe structures and, therefore, is a key element in controlling interior noise and sonic fatigue. The damping of conventional mechanically-joined structures is generated by friction and air pumping in mechanically-fastened joints, acoustic radiation from the panels, and other minor sources. The inherent damping of all aircraft structural materials, e.g., aluminum, titanium and advanced composites, is very low and is insignificant in the damping of all structures.

Recent advances in structural adhesive bonding technology for airframes have shown this technology to be an attractive alternative to mechanical fastening in many applications. The dynamic properties of adhesively-bonded joints in built-up structures is an important area which must be investigated before this technology can be applied in areas where sonic fatigue or interior noise are critical. Specifically, the damping properties of adhesively bonded joints and built-up structures with many such joints must be determined. The nature of a bonded joint is to eliminate the friction and air pumping as sources of damping.

In 1975, the Advanced Metallic Structures Advanced Development Program Office (AMS/ADP) of the Air Force Flight Dynamics Laboratory (AFFDL) initiated a large-scale program to design, fabricate, and test a full-scale fuselage section using adhesive bonding as the primary structural joining method. This program, entitled Primary Adhesively Bonded Structural Technology (PABST), has also fabricated several small adhesively bonded test panels. The AMS/ADP recognized the PABST program as an opportunity to conduct damping measurements on bonded fuselage structure. Dynamic tests to measure resonant frequencies, mode shapes, and modal damping of portions of the PABST fuselage test article and a small test panel were conducted. Modal damping versus temperature of the small test panel is presented. Mode shape and damping data measured from the PABST fuselage are not yet available.

Test Program

Test Article Description - The PABST fuselage test article represents a section of the YC-15 forward fuselage from the nose to

just aft of the wing box. The majority of skin-to-substructure joints are adhesively bonded with mechanical fasteners in a few locations. Substructural joints are all mechanically fastened. Figure 1 shows the PABST test article during fabrication. The small adhesively bonded test panel was singly curved, with both stringers and frames dividing it into four bays. The stringers were bonded to the outside of the curved skin with frames bonded to the inner surface. The panel had no mechanical fasteners. The panel measured approximately 4' x 5'. Figure 2 shows the panel being tested in the temperature-controlled chamber.

Test Method - A digital impact test technique was used to determine the dynamic properties of the small test panel and two areas of the PABST fuselage. The technique uses a miniature instrumented hammer to excite the article with a measured input pulse. The structural response is measured at a desired location with a miniature accelerometer. The input force pulse and response acceleration signal are then digitally processed by a fourier analyzer system to calculate the transfer function between the points. Transfer functions are measured at each point of a grid covering the surface of the structure. The resonant frequencies, mode shapes, and modal damping of the test article are then calculated by the fourier analyzer. Reference 1 presents detailed description of the digital impact test technique.

Test Description - Two areas of the PABST fuselage were tested for room temperature modal properties. One area was located just below the floor level between fuselage stations 583 and 607. This area was very similar in configuration to the small test panel with internal ring frames and external longerons. The test grid used on the small test panel was also used on this area. The second test area was located on the fuselage sidewall between fuselage stations 751 and 775. The area was roughly two feet square and covered two ring frame bays. This area of the PABST fuselage had no longerons. A grid of 63 transfer functions was measured on this area.

The small test panel was suspended in a vertical plane by nylon cords attached to its four corners. This configuration was chosen to minimize the damping introduced into the panel by its mounting. The panel was located in a large environmental chamber for the purpose of measuring model damping versus temperature. The panel was tested over a frequency range of 0 to 500 Hz. The range was limited to a 500 Hz upper limit by resolution requirements of the fourier analyzer. This range was considered representative of frequencies where resonant vibration and sonic fatigue are observed in airframes. Room temperature transfer functions measured at a few selected locations on the panel were looked at first to ensure that fictitious high levels of damping from boundary conditions or other sources were not present. Panel resonant frequencies were recorded from these transfer functions. Next,

transfer functions were measured at 149 grid locations on the panel at room temperature. These transfer functions would be used to generate the panel mode shapes. Finally, a single location on the panel surface was chosen for measuring modal damping versus temperature. Transfer functions were measured for this point at temperatures of 0°, 28°, 49°, 65°, 80°, and 106°F.

Test Results

Of the data measured during this program, only modal damping versus temperature for the small test panel has been analyzed. The remaining data will be analyzed in the near future. The small test panel exhibited resonant frequencies from 42 Hz to beyond the 500 Hz upper limit of measurement. Modal damping data from three modes of the panel at 397, 407, and 425 Hz are plotted in Figure 3. The figure shows average values of loss factor, η , near .002 ($Q = 500$) for all three modes with no noticeable dependence on temperature. Although analysis of the PABST fuselage data has not yet been accomplished, preliminary indications from transfer function half power bandwidth damping estimates indicate that modal damping of the fuselage was much higher than that measured on the panel. Values of loss factor, η , were in the range of .01 to .02, which is on the order of built-up, mechanically-fastened structure.

Conclusions

The data presented here show damping values of an adhesively-bonded panel tested with minimal damping added by boundary conditions of approximately $\eta = .002$. This is nearly an order of magnitude less than values generally accepted for built-up structure with mechanical fasteners (1,2). A direct comparison of these data is not valid, however, because of differences in modal frequencies, boundary conditions, and test methods

The only valid comparison of the modal damping of the test panel would be with a panel identical in configuration and boundary conditions but with riveted joints replacing the adhesive bonding. Unfortunately, no such data is available at present. The data reported herein tentatively shows that adhesively-bonded structure has lower modal damping, but this can only be proven by more testing of built-up adhesively-bonded structures.

REFERENCES

1. Gordon, R.W., "Modal Investigation of Lightweight Aircraft Structures Using Digital Techniques," Air Force Flight Dynamics Laboratory, Technical Report AFFDL-TR-77-124, December 1977.
2. Ballentine, J.R., et al., "Refinement of Sonic Fatigue Structural Design Criteria," Air Force Flight Dynamics Laboratory, Technical Report AFFDL-TR-67-156, January 1968.

Figure 1 - PABST Test Article

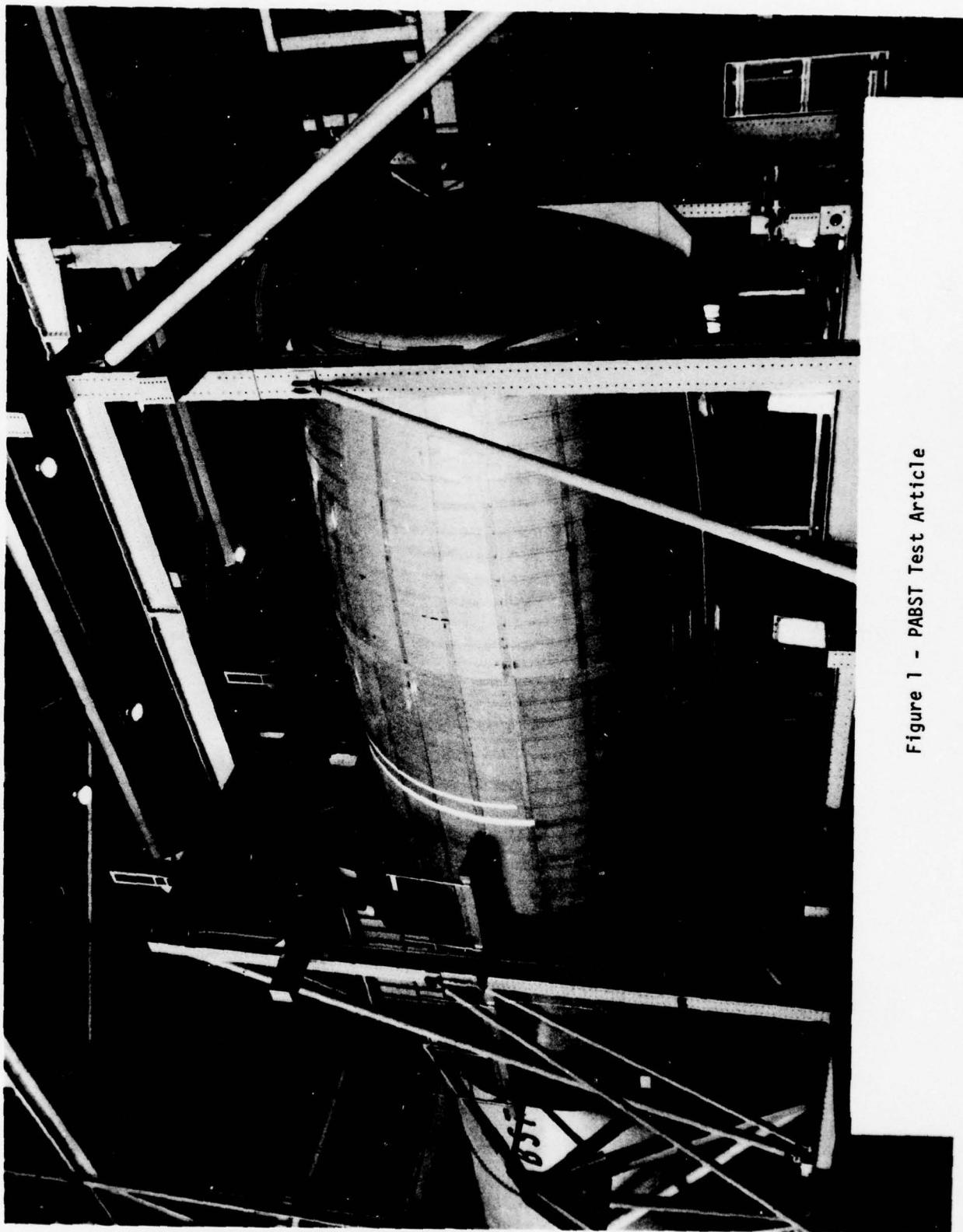
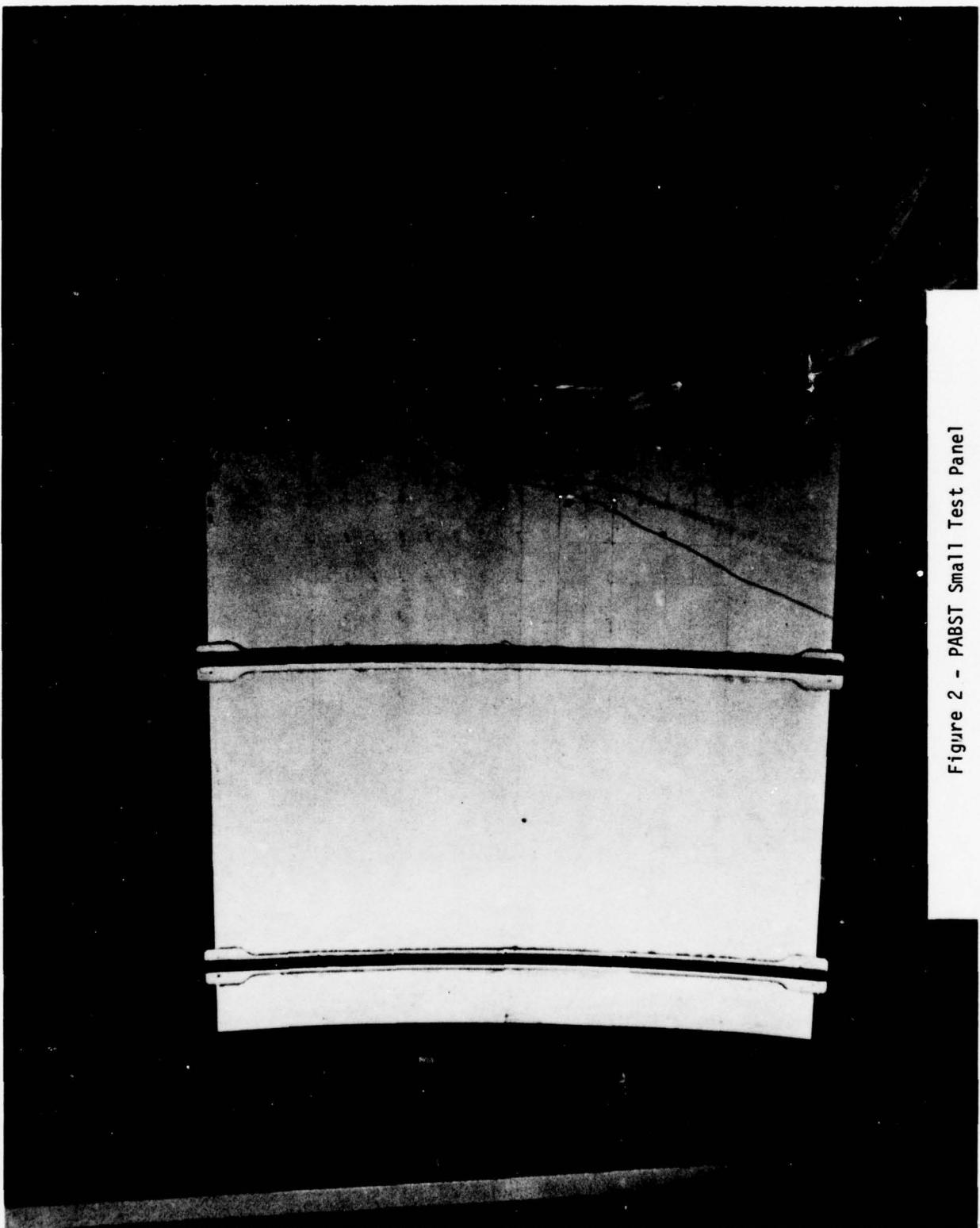


Figure 2 - PABST Small Test Panel



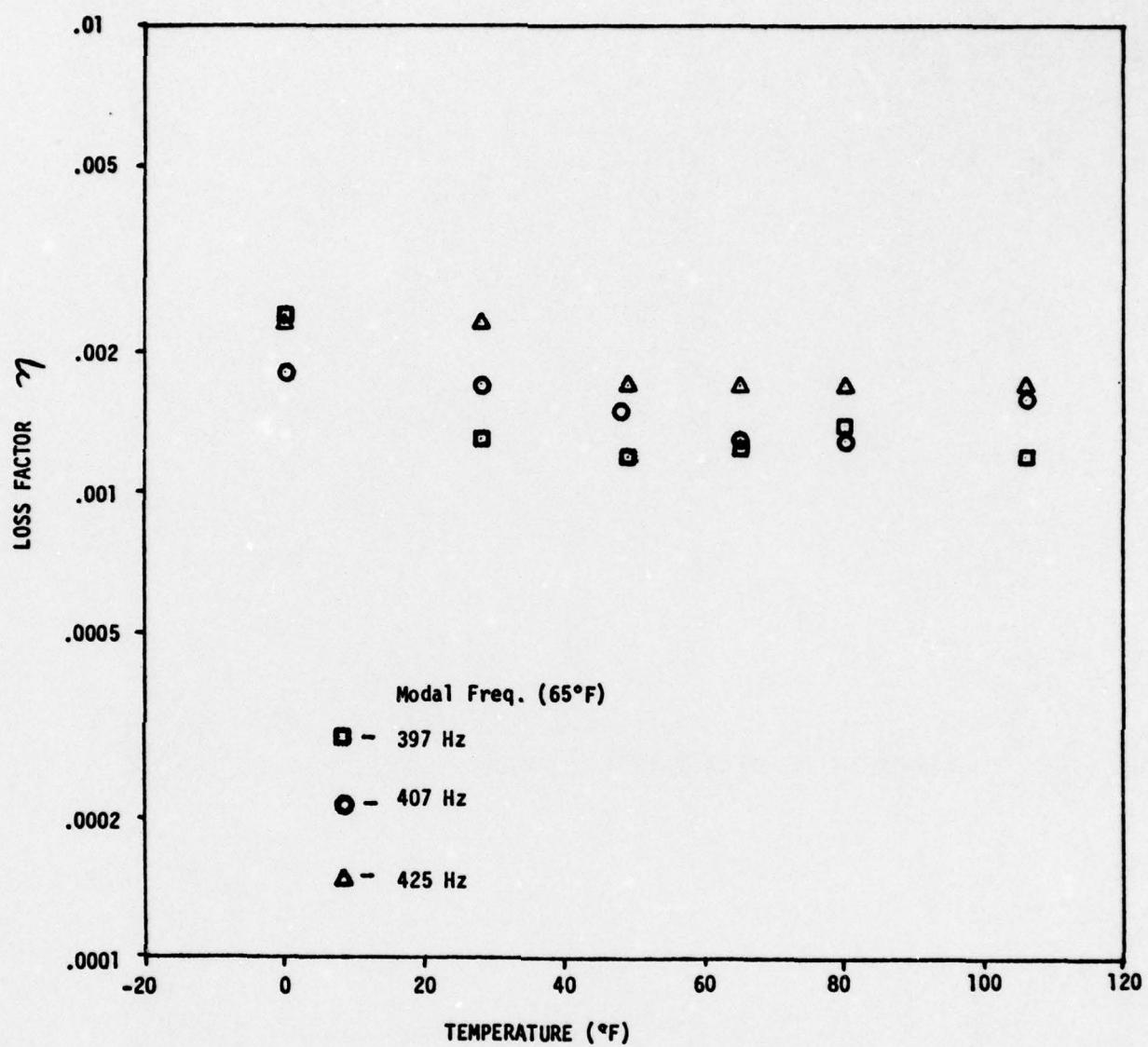


Figure 3 - Modal Damping vs Temperature of Small Test Panel

DAMPING FOR ENHANCED RELIABILITY IN
VIBROACOUSTIC ENVIRONMENTS

R. N. Hancock
J. A. Hutchinson
Vought Corporation
Vibroacoustics
Dallas, Texas

Introduction

Recent Department of Defense emphasis on improved equipment reliability, both to increase systems readiness and to reduce maintenance costs, is adding emphasis to the techniques for achieving equipment and systems reliability. Application of viscoelastic damping materials to control response to vibroacoustic forces is one of the techniques that will surely receive increased attention over the next few years.

Requirements for hardware testing are being revised to provide better integration of test results into the program design phase. Or said differently, the desire is to extend the product design phase to incorporate Test Analyze And Fix (TAAF) procedures with a thorough evaluation of design technique. Thus, a product reliability growth, TAAF, cycle has been defined during which opportunities are presented to the engineer to design, test, evaluate, and retest damping materials and other control techniques. Vought has had the opportunity to exercise the new procedures during a recent product development, an avionics "black box", including application of viscoelastic damping to control PC card response. This paper briefly summarizes the project, pointing out some of the constraints and considerations which led to the decision to use card damping, and results of response control finally achieved.

With any new procedure there is a learning curve with which to be reckoned. In the case of the new reliability growth testing procedures, one of the most difficult hurdles to overcome is the concept that the purpose of the test is to exercise the hardware so as to cause weak points to fail in the lab so that they can be corrected to prevent field failures. It takes a while for most program managers to accept the idea that test failures mean success. To alert the reader to some of the problems likely to be encountered, the authors have taken some literary license by overstating the design constraints which applied to the particular "black box" for which damping was used. The interest is to typify the problems which confront the Dynamics Engineer and limit his choice of control alternatives.

DOD Emphasis on Reliability and Vibrations

Failure to properly account for environments during product design and testing phases has been stated by Department of Defense spokesmen as the most probable cause of poor equipment field reliability(1). Thermal and vibration stresses have been identified as the two most offensive environments. Both are important in selecting damping treatment. The DOD has three separate programs for reliability improvement in engines, systems and structures - all candidates for damping technology. Changes are being made in DOD procurement methods, testing methods and in the system of specs and standards, tailored for particular installations, in an attempt to improve systems.

Over the past 4-5 years, several meetings have been held and publications issued describing the new DOD requirements. Typical of these was the Joint Logistics Commanders Reliability Workshop Final Report, which contained Fig. 1 in a paper presented by Gates.⁽²⁾ The trend of the data here shows as equipment becomes more expensive, and more complex, the time between failures becomes less. Two points of particular interest on this figure are these marked "R" and "WF". The latter illustrating almost one-hundred times more reliable performance than the former. The significance attached to the difference was that the WF point was generated by equipment which the contractor was required to maintain in field service; thus, continuing his design and fixes into field deployment as a condition of profit. The point has been made that it is possible to generate more reliable equipment if the manufacturer pursues his design and can be motivated to sell reliable equipment rather than mere replacement spares for less reliable equipment. If procurement methods and testing methods do indeed fulfill this idea, then more requirement for damping as a response control technology will have been generated.

Growth testing (test, analyze and fix) is a procedure for simulating some aspects (environments for one) of field service in the laboratory, so that failures can be experienced and design fixes made. This test cycle is shown in relation to the overall equipment life cycle in Fig. 2.⁽³⁾ Literary liberties have been taken with this curve, since in actuality the dotted portion of the curve applies to equipment type rather than an individual item, whereas the bathtub curve applies to a single item. But the point is that rate of failure can be reduced by proper testing and correction of equipment deficiencies during the test cycle.

Hardware Design

An external view of the "black box" is shown in Fig. 3. Measurements are about 10 x 10 x 8 inches, and the box weighs a few pounds. Between initial exposure to the design, in the proposal stage or early in the design stage, and the hardware stage, the dynamics engineer is apt to witness several changes and should be wary. For example, at initial contact the box design may be of well damped riveted construction with relatively loose tracks for PC boards - the installation being on an isolated, damped avionics bay shelf. The hardware will reflect design conditions imposed by other organizations - design, producibility, reliability, avionics, maintainability, cost effectiveness, etc., so that the final design may be

- a hard cast box with tight boards
- located in a spot that couples to the speed broke hinge
- placed with no room for isolators
- in the midst of a growth test with failures and production design almost approved for final production.

In which case the dynamics engineer's options are severely limited. Examination of failures which occurred early in growth testing showed redesign of several of the piece part mounts (capacitors) necessary for strength. Motion of the PC cards was deemed too severe in combination with

the thermal environment. The vibration test spectrum is shown in Fig. 4 by the curve marked MEAN + T. It was combined with temperature in the test cycle shown in Fig. 5. Late in the test program the data which served as a base for the vibration and temperature profiles were re-examined and the vibration cycle was split into 4 spectra to more nearly represent the flight profile major events and the temperature profile was more realistically modified to eliminate the temperature extremes which could never occur in service in combination with vibration. Three temperature profiles were used. Both temperature and vibration were applied such that the same combination repeated rarely.

Damping Application

Figure 6 gives an edge view of the five PC cards located in the box. All cards were examined for response in the box and individually during application of various damping materials. Curves are shown later for the number 2 card. As can be seen here, the space available for material is limited. The limit was set at .080 inches to allow for card removal and manufacturing tolerances to prevent interference with adjacent cards.

Figure 7 shows the variety of card arrangements. Damping was eventually applied to all except number 5, to reduce response in the fundamental modes. Response was maximum at the edge opposite the connectors; zero at the sides and still significant at the connector. Additional edge constraints were added at the maximum response edge. Damping reduced the terminal motion sufficiently.

After studying dynamic characteristics of the boards, a set of dynamic characteristics was derived for damping material - both free and constrained. Other constraints, mostly imposed by maintainability considerations limited these. The material needed to be clear in order to see the wire feedthroughs, removable and reusable to allow circuit repair, be no more than .080 thick and be previously qualified for use to avoid a qualification procedure costing \$80 - 100K. The configuration selected after testing several materials and talking to several vendors, is shown in Fig. 8. The material used was 3M - 15D 112, .060 thick with an .020 scotch ply glass constraining layer applied to the back of the board. It is peelable at -40°F.

Response of the typical board (No. 2) is shown in Fig. 9 with and without the damping treatment, at room temperature. It had previously been decided that a reduction in amplitude of from 2-3:1 would be satisfactory on the first mode. As seen here, the reduction was about 4:1 on the first, over 2:1 on the second and less on the higher modes at room temperature.

The response for the final material is shown in Fig. 10 for four different temperatures. The curves depict about what would be expected for a viscoelastic optimized for operating temperatures between about 60 and 120°F. Reduced performance at both cold and hot temperatures extremes was deemed acceptable since maximum vibration cannot occur at these temperature extremes. The extremes should only occur at ground conditions with the

aircraft environmental control system off.

Reliability growth tests, as they have recently been defined to include "realistic" environments, provide excellent means for the vibroacoustics engineer to analyze design difficulties and to empirically evaluate results of his recommended design changes. For the next few years a few growing pains should be expected with the new procedures, since time constraint will normally be severe for defining the cause of a test failure and implementing a fix so that the test can continue.

Other Damping Application

Within an Aerospace company, especially an airframe manufacturing company, opportunities exist in numerous areas to make application of damping technology. The following table names a few of these possible applications from the standpoint of extending the life of structures and systems. The last item listed emphasizes the need to validate analysis with tests.

Uses of Viscoelastic Materials to Extend the Life of Structures/Systems

Structure - apply locally to existing hardware

- o Stripes, clips, straps, splices, & patches
- o Apply to fatigue or fracture-sensitive structures
- o Increase damping in composite & bonded structures - especially integral damping -- improve overall dynamic responses

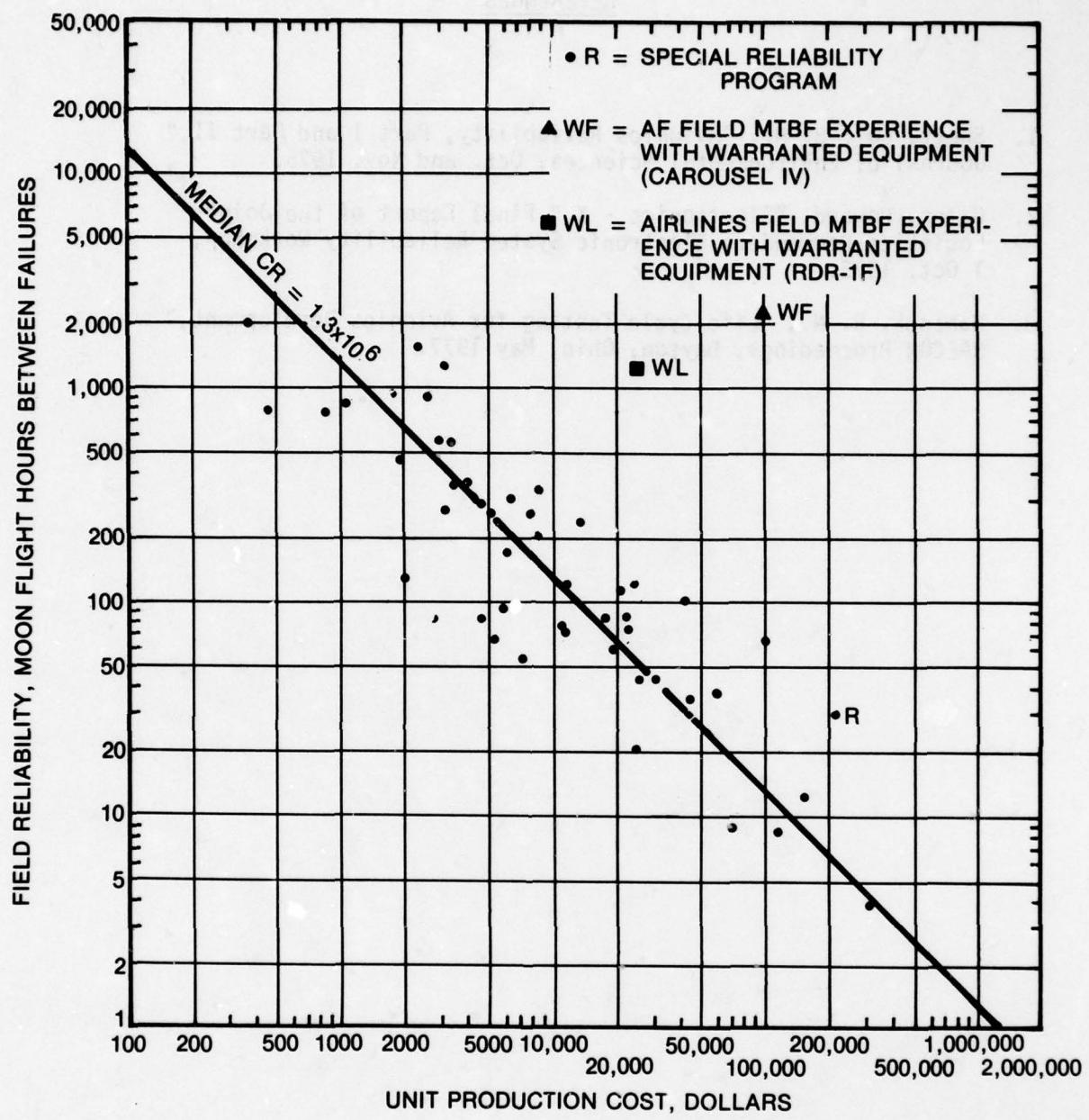
Systems - apply to new or existing hardware

- o Coatings, constrained layers, sandwich, joints
- o Apply to tailpipes, inlets, avionics shelves & components, instrument panels, radar mounts
- o Improve local dynamic responses
- o Stabilize guidance & weapons delivery platform

Validate application methodology by tests ... structures & systems.

REFERENCES

1. Swett, Col. B. H., "Avionics Reliability, Part I and Part II," Journal of Environmental Sciences, Oct. and Nov. 1975.
2. Gates, Howard, "Electronics - X," Final Report of the Joint Logistics Commanders Electronic System Reliability Workshop, 1 Oct. 1975.
3. Hancock, R. N., "Life Cycle Testing for Avionics Development," NAECON Proceedings, Dayton, Ohio, May 1977.



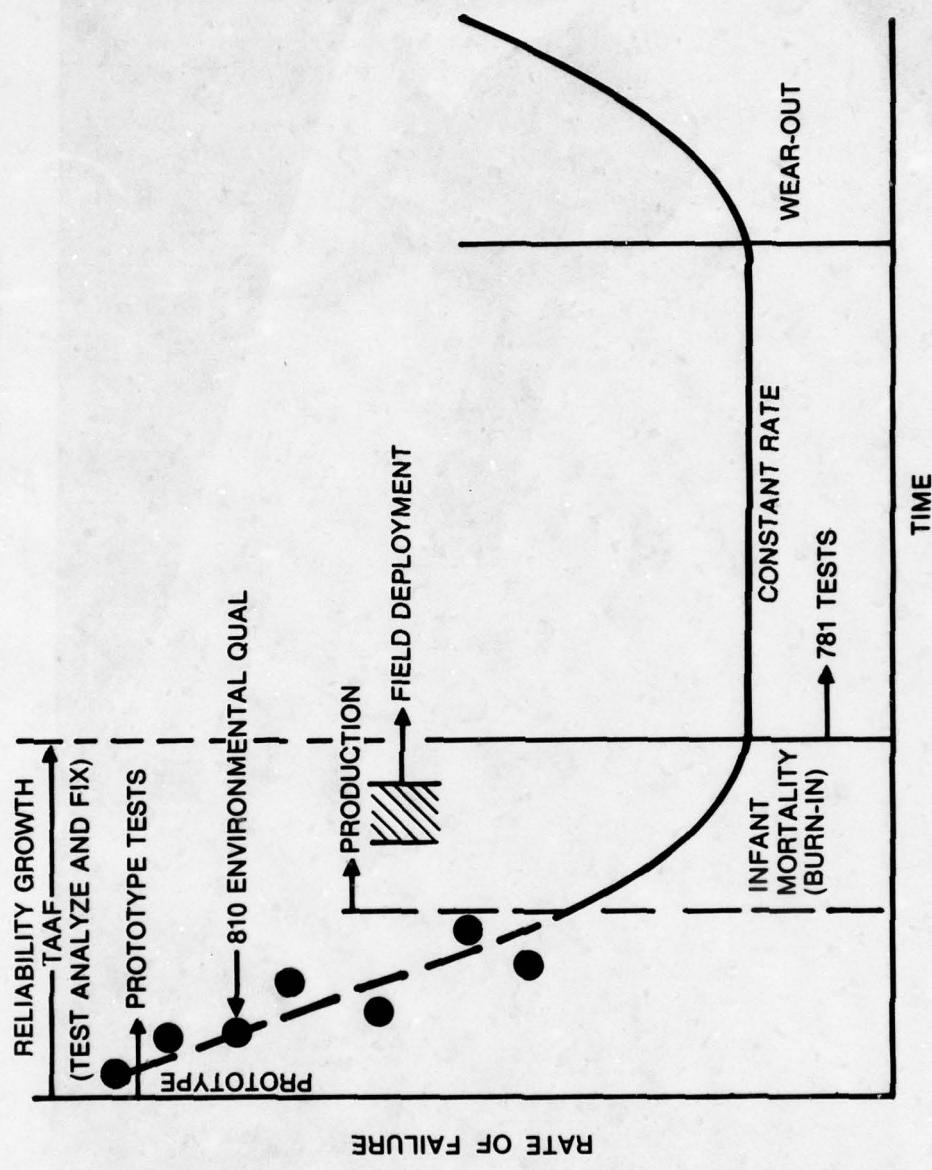


FIGURE 2: TYPICAL BATHTUB RATE OF FAILURE

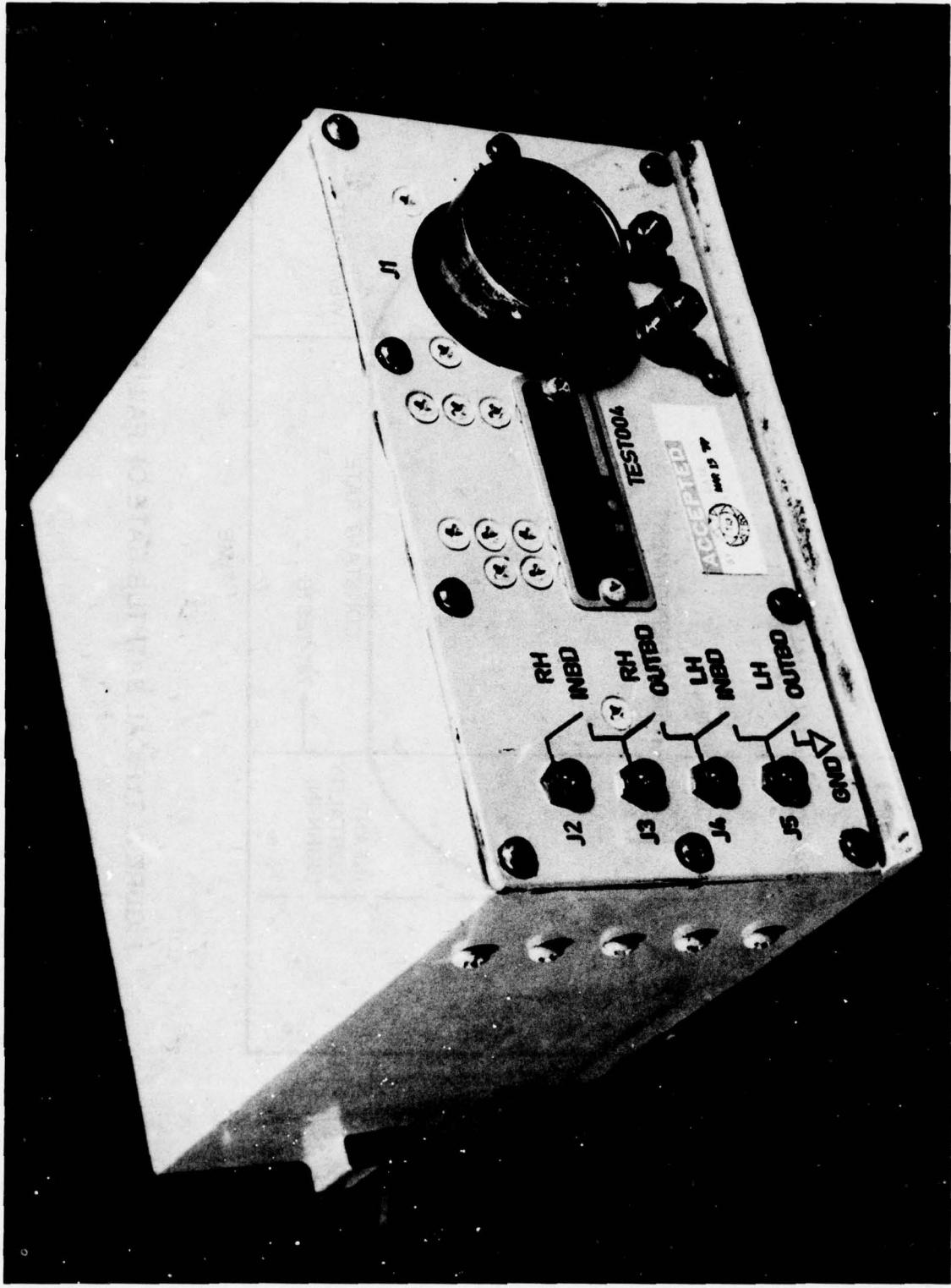


FIGURE 3: AVIONIC COMPONENT (BLACK BOX)

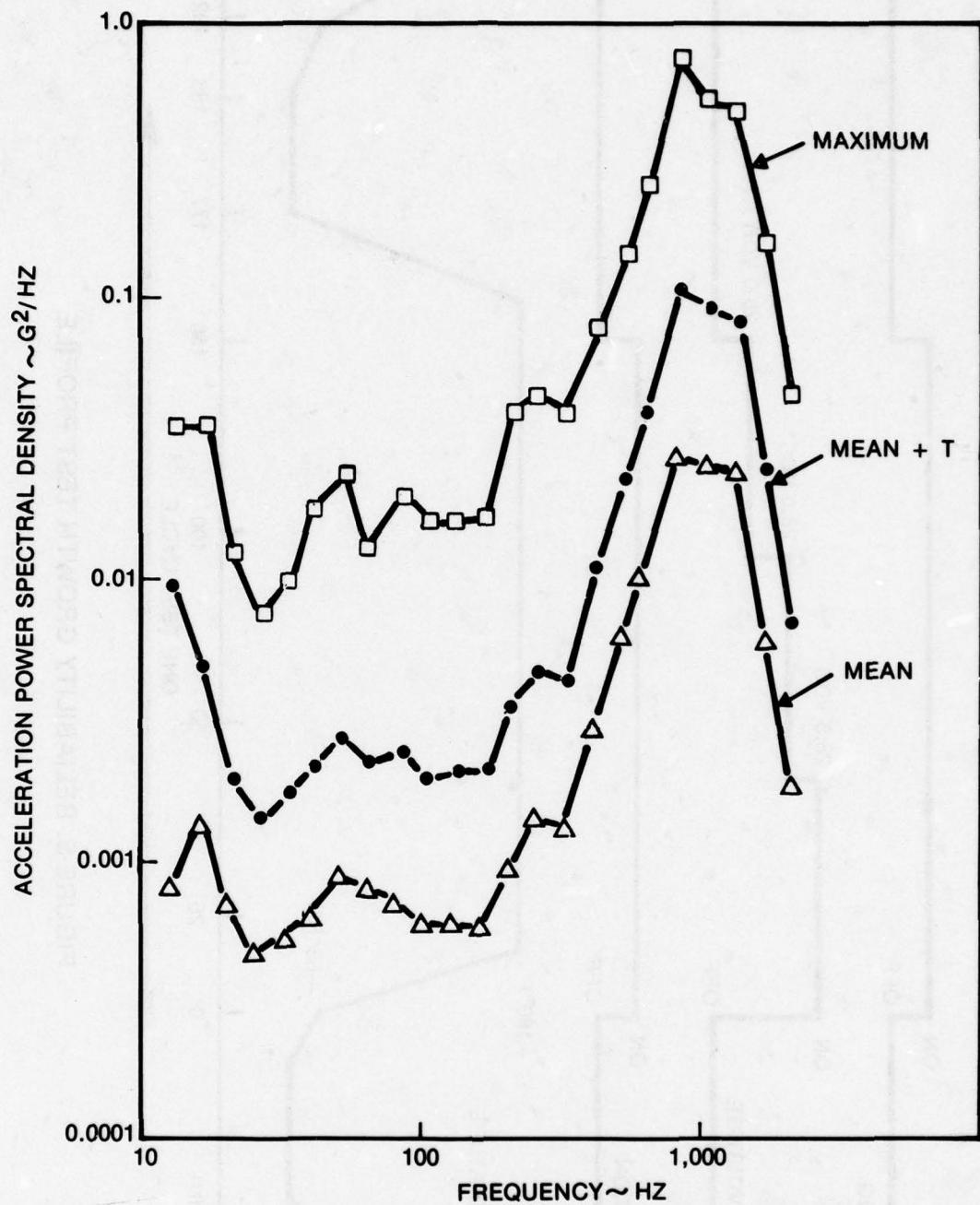


FIGURE 4: MEASURED FLIGHT VIBRATION DATA (LOCATION 1)

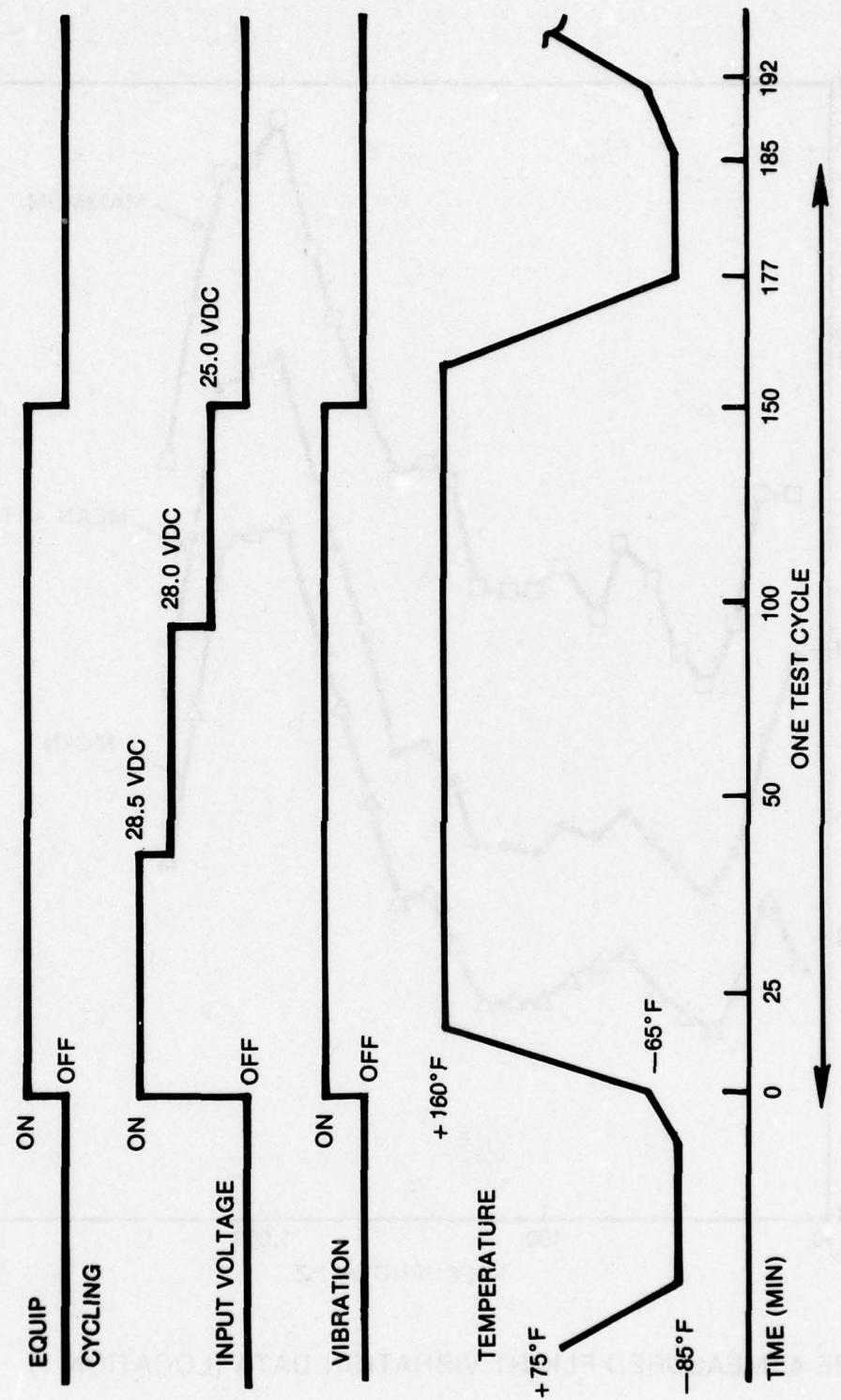


FIGURE 5: RELIABILITY GROWTH TEST PROFILE

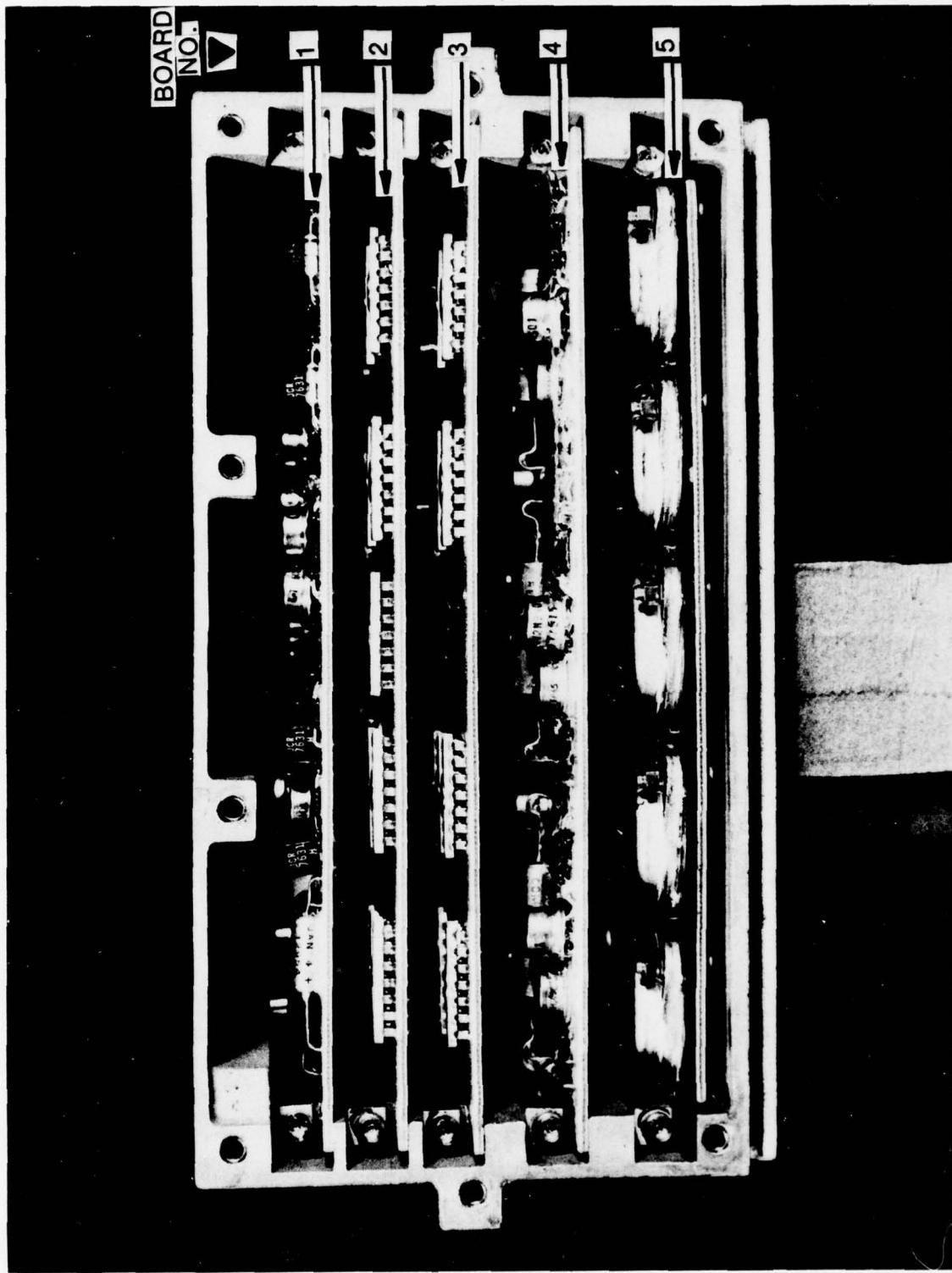


FIGURE 6: PRINTED CIRCUIT BOARD ARRANGEMENT

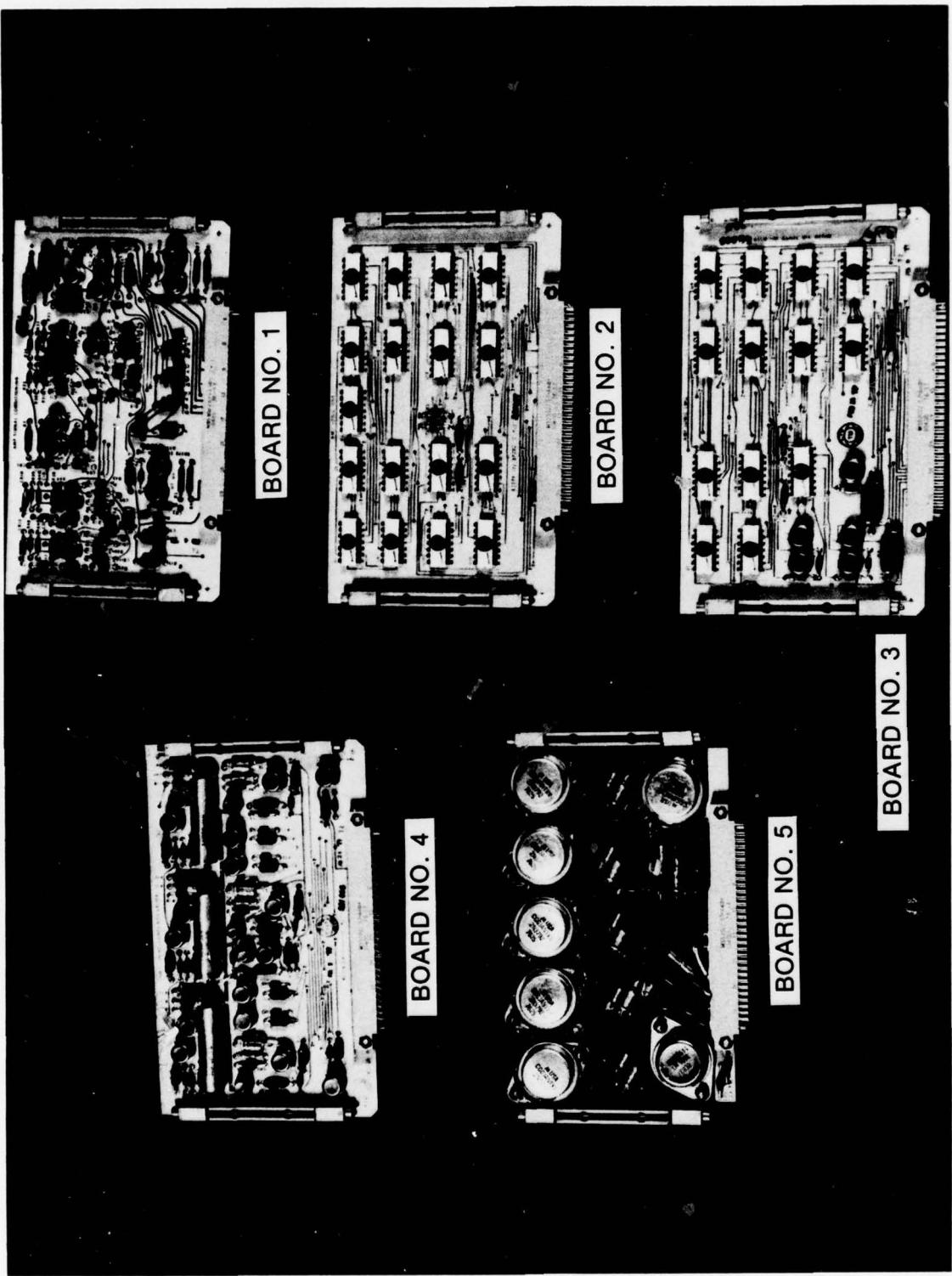


FIGURE 7: CIRCUIT BOARD LAYOUT

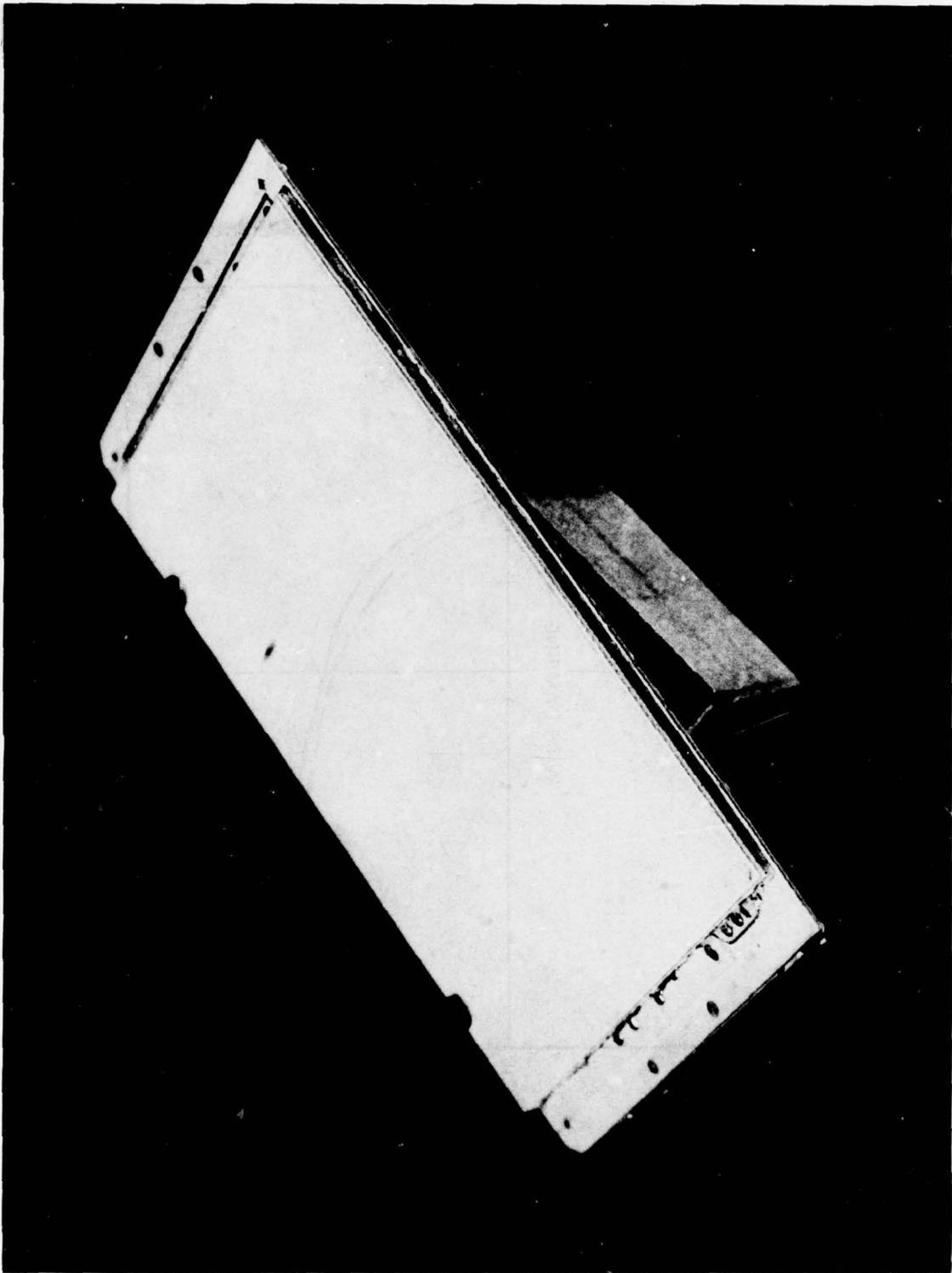


FIGURE 8: CIRCUIT BOARD DAMPER INSTALLATION

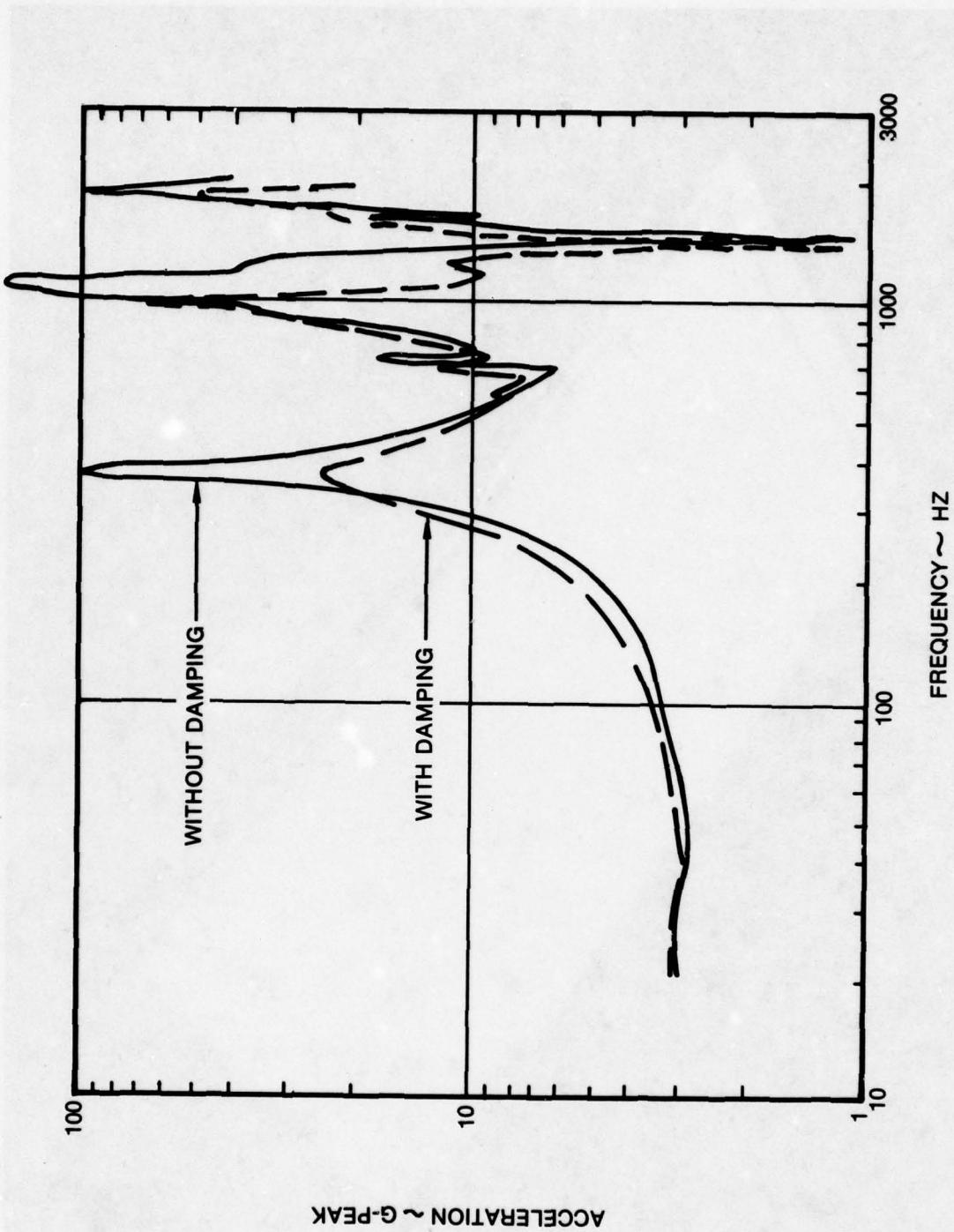


FIGURE 9: PC BOARD RESPONSE WITH AND WITHOUT DAMPING MATERIAL

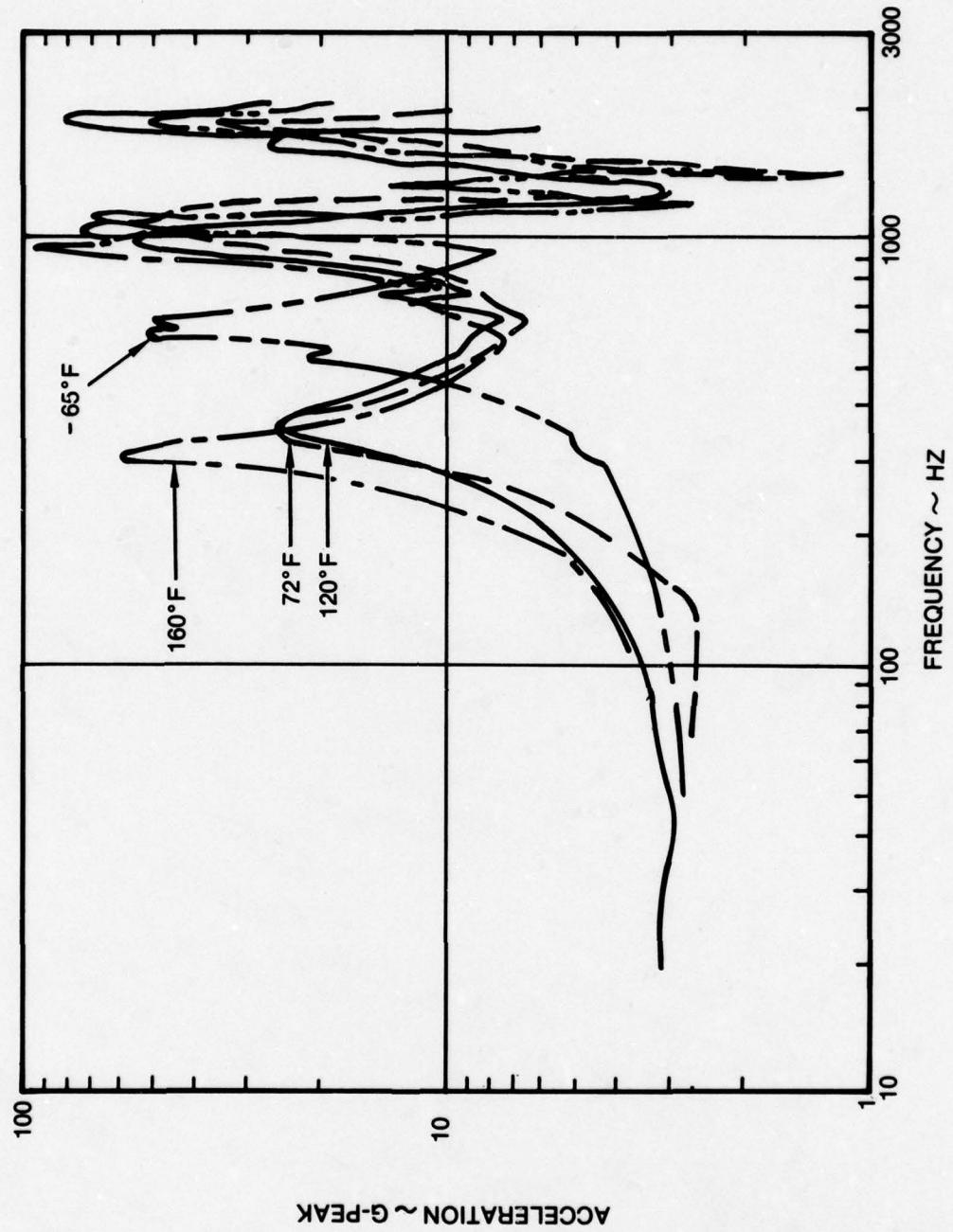


FIGURE 10: PC BOARD RESPONSE WITH .060 IN DAMP MATERIAL & .020 FIBERGLASS CONSTRAINING LAYER VS. TEMPERATURE

HAMILTON STANDARD ELECTRONICS
PRESENTATION
SLIDES ONLY

W. Ammerman
Hamilton Standard Electronics
Windsor Locks, Connecticut

FIGURE 1

VIBRATION SPECIFICATION TRENDS

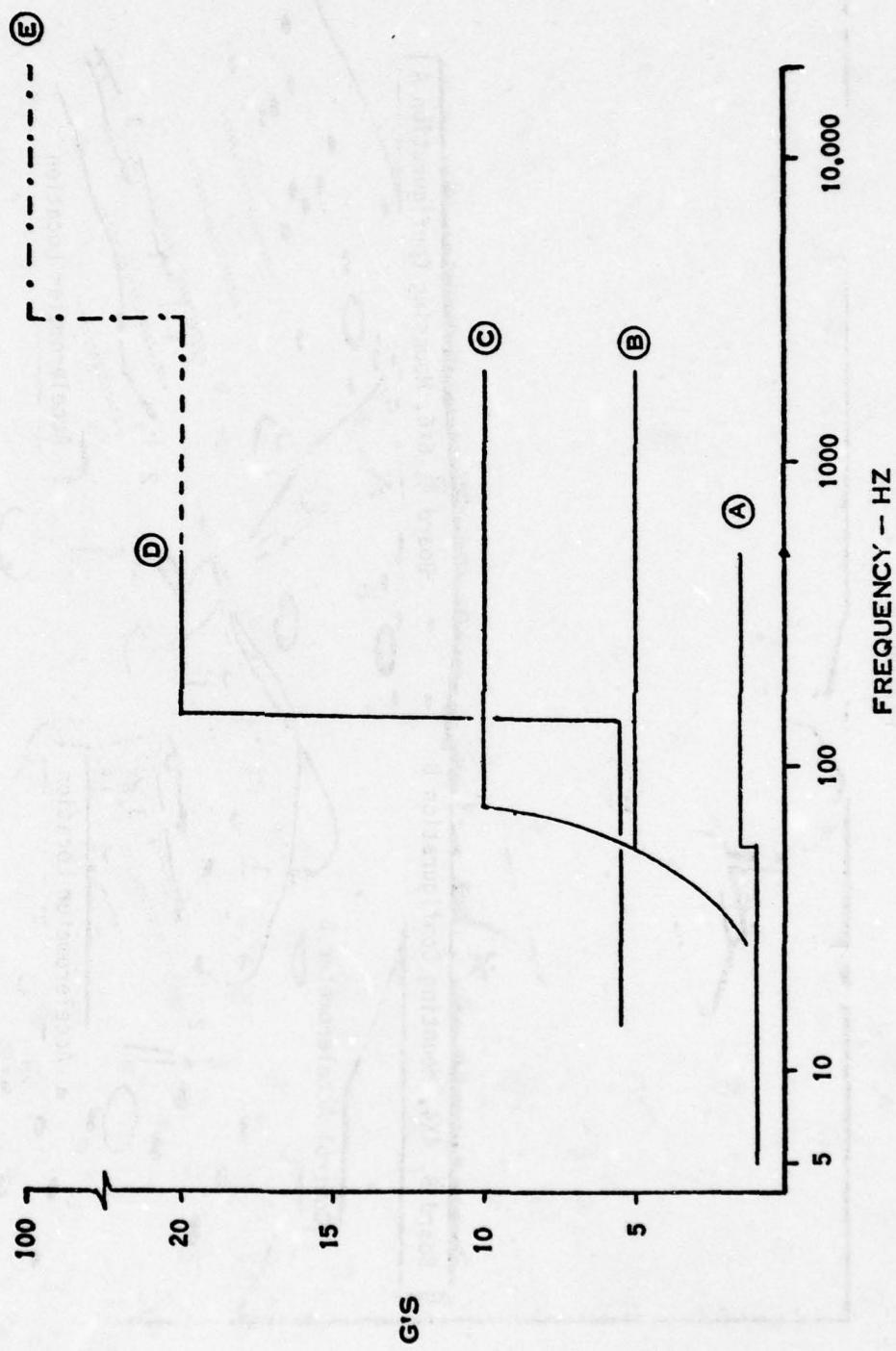
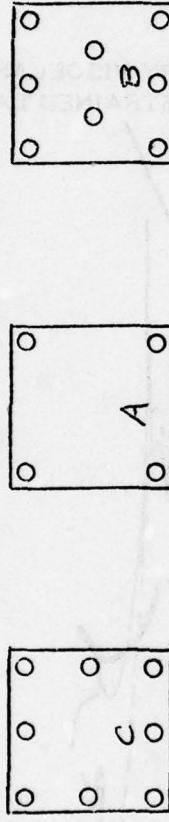


FIGURE 2



CONSTRAINED LAYER DAMPING MATERIAL EVALUATION
BARE BOARD SURVEY
ROOM TEMPERATURE



Test Board Configurations

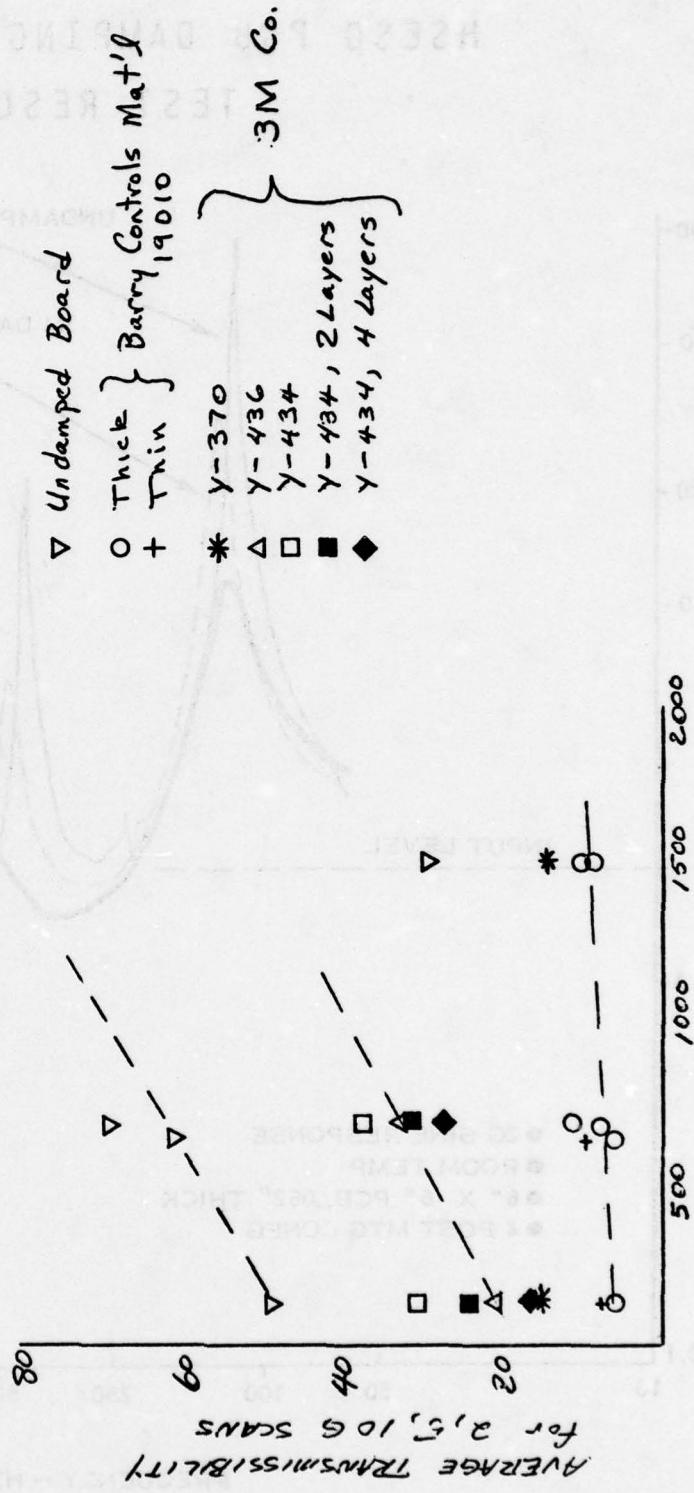


FIGURE 4
HSESD PCB DAMPING EVALUATION
TEST RESULTS

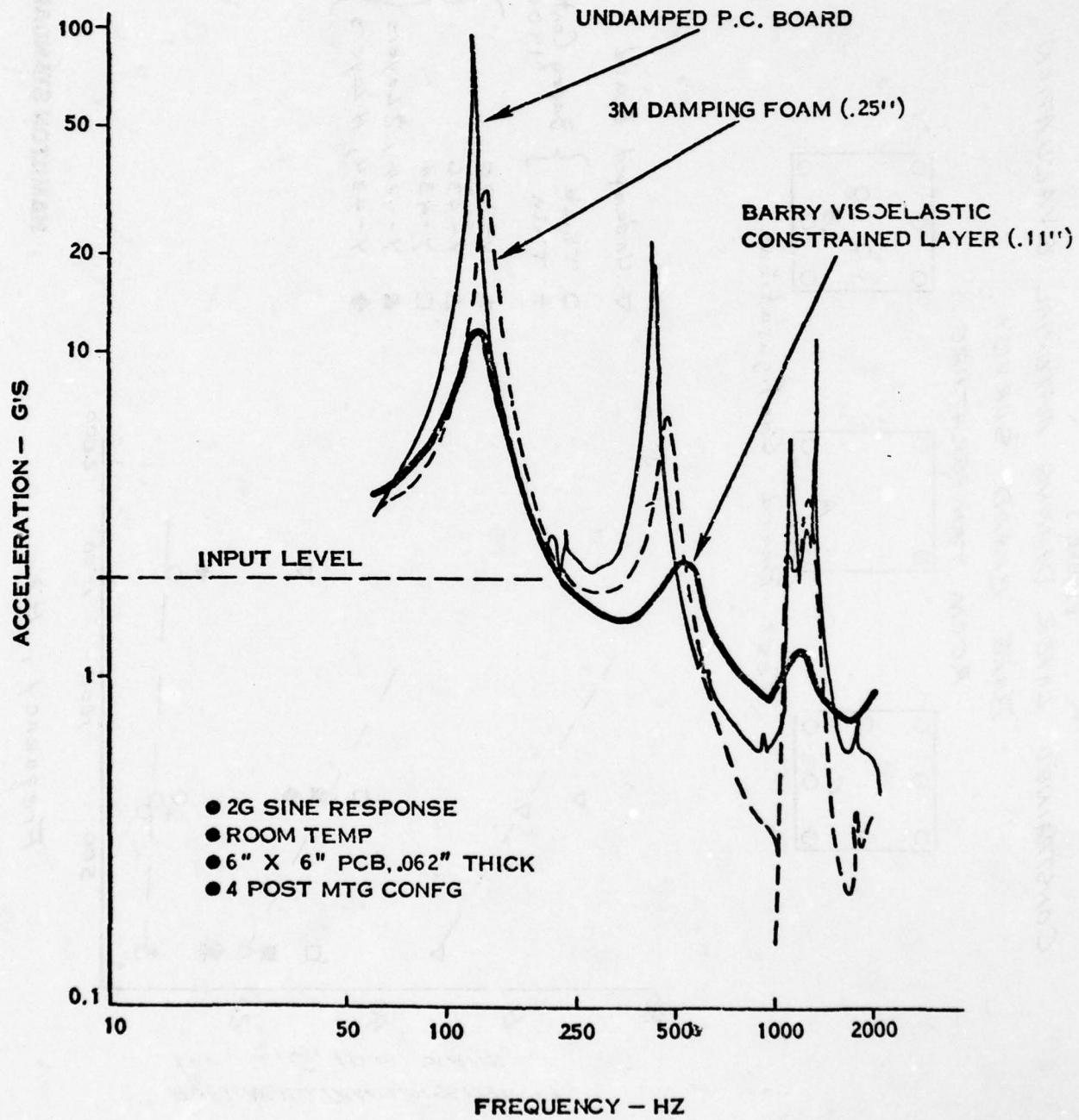


FIGURE 5
TRANSMISSIBILITY VS INPUT ACCELERATION

BARRY CONTROLS CIRCUIT BOARD
DAMPING MATERIAL 19010

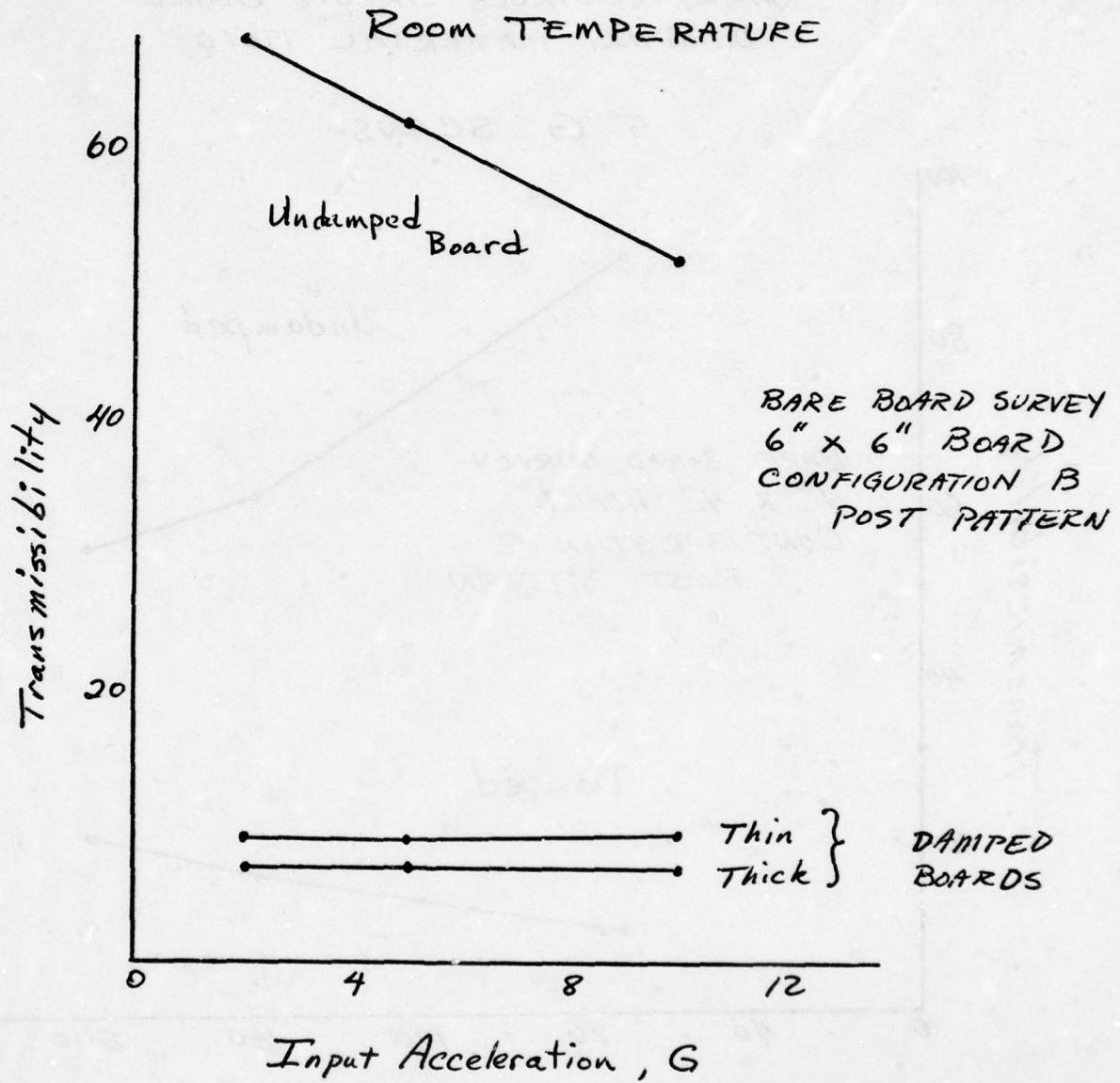


FIGURE 6

TRANSMISSIBILITY VS TEMPERATURE

BARRY CONTROLS CIRCUIT BOARD
DAMPING MATERIAL 19010

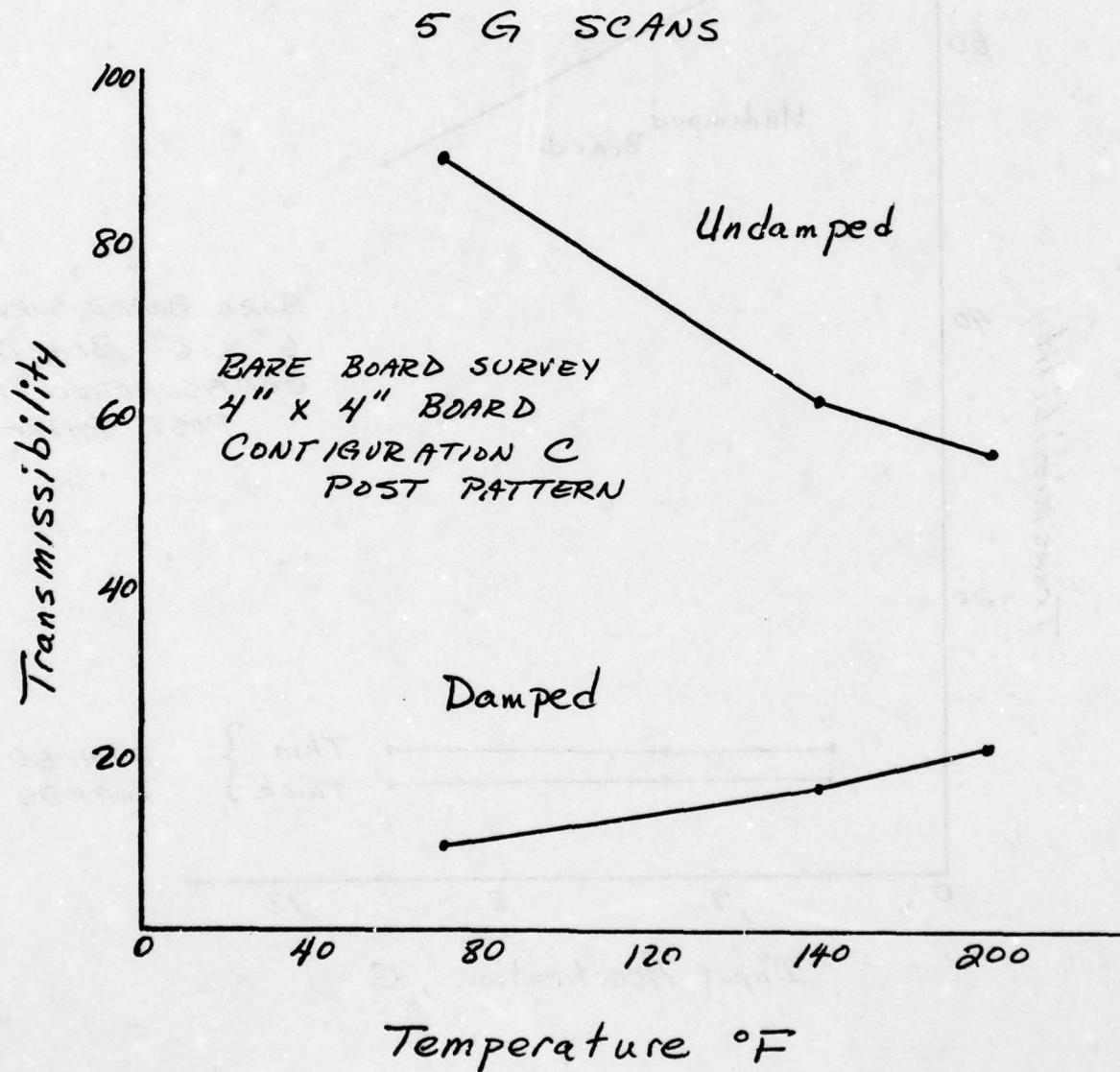


FIGURE 7

TEST BOARD FOR CONSTRAINED
LAYER DAMPING MATERIAL

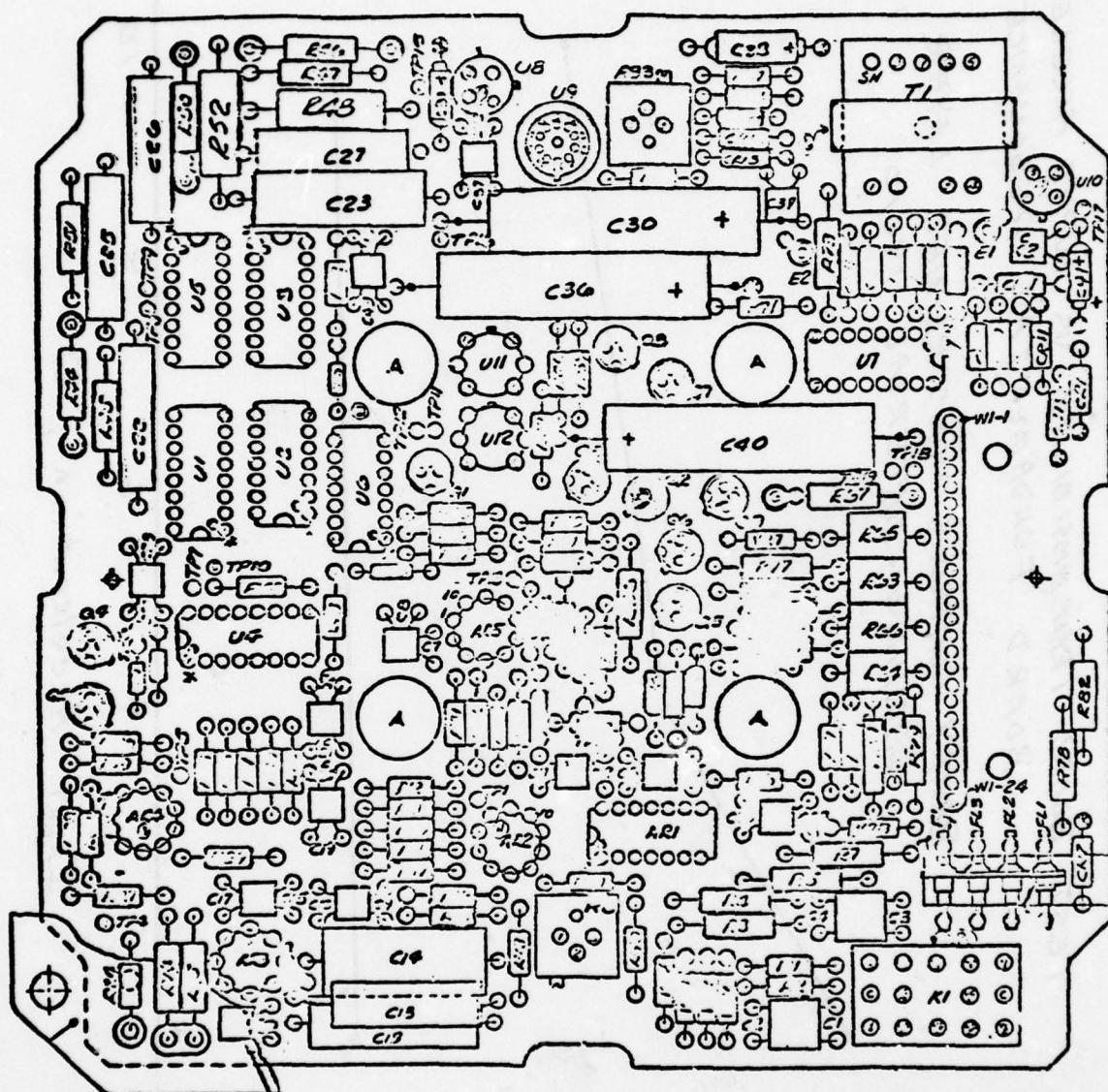
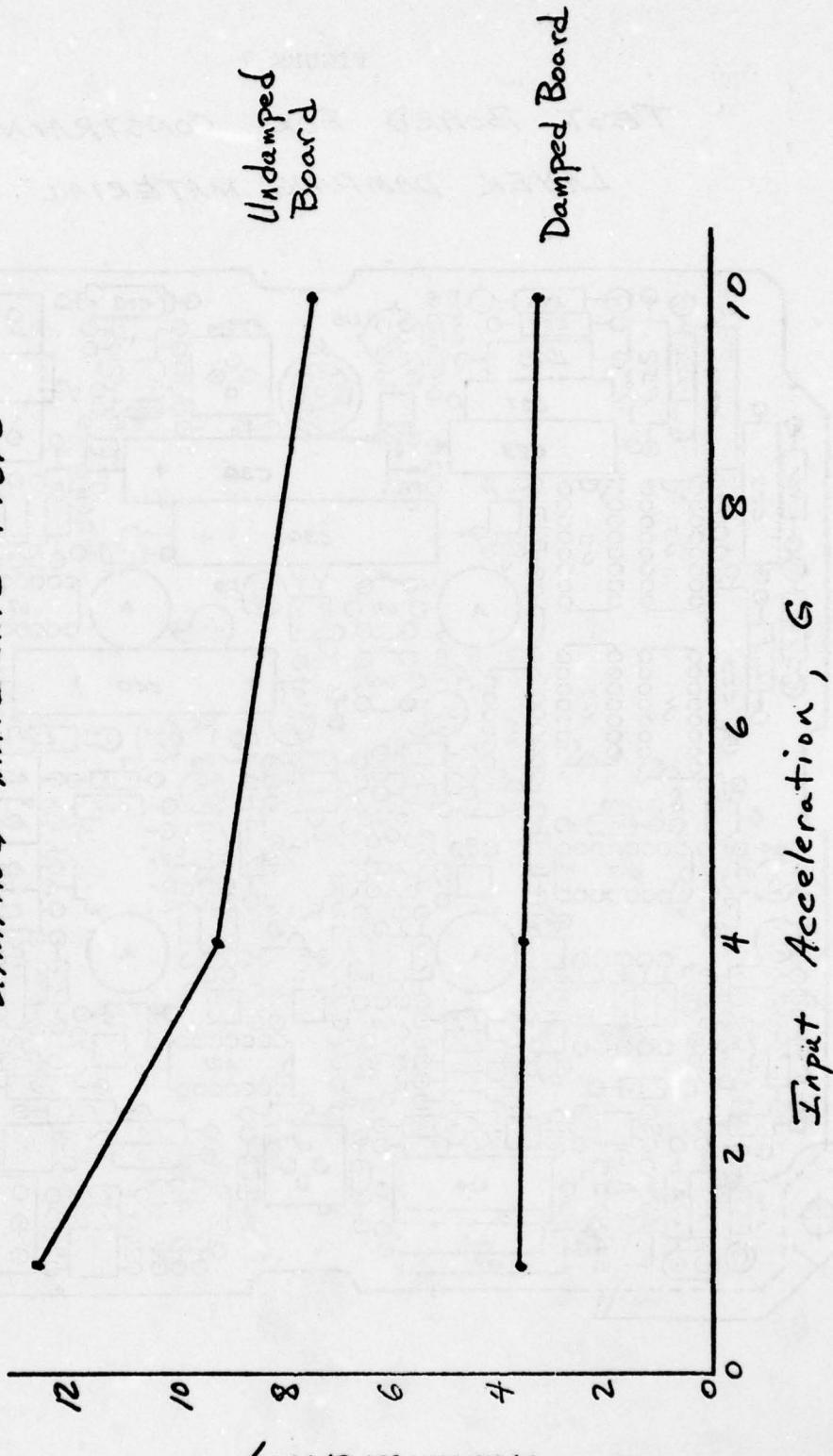


FIGURE 8

TEST BOARD TRANSMISSION VS INPUT ACCELERATION
BOARD FUNDAMENTAL RESONANCE

BARRY CONTROLS CONSTRAINED LAYER
DAMPING MATERIAL 19010



4/1/91 SJS/MSR/L

FIGURE 9

FUTURE INVESTIGATIONS

- Evaluate more materials
- More testing at environmental extremes
- Optimize amount and placement of damping material
- Evaluate high frequency performance
- Develop theoretical tools to minimize high cost testing

EXAMPLES OF THE USE OF ADDITIVE ELASTOMERIC
DAMPING TREATMENTS TO CONTROL VIBRATION PROBLEMS
IN AIR FORCE SYSTEMS

C. M. Cannon
University of Dayton Research Institute
Dayton, Ohio

EXAMPLES OF THE USE OF ADDITIVE ELASTOMERIC DAMPING TREATMENTS
TO CONTROL VIBRATION PROBLEMS IN AIR FORCE SYSTEMS

Charles M. Cannon

University of Dayton Research Institute

Abstract

Over the past 15 to 20 years the University of Dayton Research Institute under contract to the Air Force Materials Laboratory has been involved in a number of projects where damping treatments incorporating elastomeric damping materials have been used to control acoustically or mechanically induced high cycle fatigue failures [1,2,4,5]. Some of these projects will be discussed in this paper.

I. INTRODUCTION

In order to properly design and optimize a damping treatment to control the resonant vibrations of a structure or component, a designer needs to know the following: (1) the operational temperature in order to select a material with maximum damping in that range, (2) the frequency response of the system so that a damping application can be selected appropriately; i.e., tuned devices for single or closely-spaced resonances, surface treatments for many resonances, or surface treatments for many resonances over a wide frequency range, and (3) mode shapes of vibration so that the location of the damping treatment can be determined. As the various projects are discussed, reference will be made to the above three points.

Basically, there are three types of damping treatments or techniques used to control resonant vibrations. They are: (1) free layer damping treatments, (2) constrained layer damping treatments, and (3) tuned damping devices utilizing viscoelastic materials.

II. REDUCTION OF VIBRATION INDUCED DAMAGE IN AN ULTRA HIGH FREQUENCY (UHF) ANTENNA

The first project to be discussed is an example of the use of a tuned viscoelastic damper to control a resonant vibration induced fatigue failure. The example is a UHF antenna used in the F-100 aircraft [1]. A photograph of the antenna showing a tuned viscoelastic damper in place is shown in Figure 1. A study of the response of the antenna indicated the resonant mode causing the failure was such that the motion of the center part of the antenna (the electrical connector and adjacent disk) was up and down, almost as a single degree-of-freedom system. The resulting surface strains in this mode were concentrated in the bend radius which eliminated the use of surface damping treatments. The mode shape did lend itself ideally to the use of a tuned viscoelastic damper.

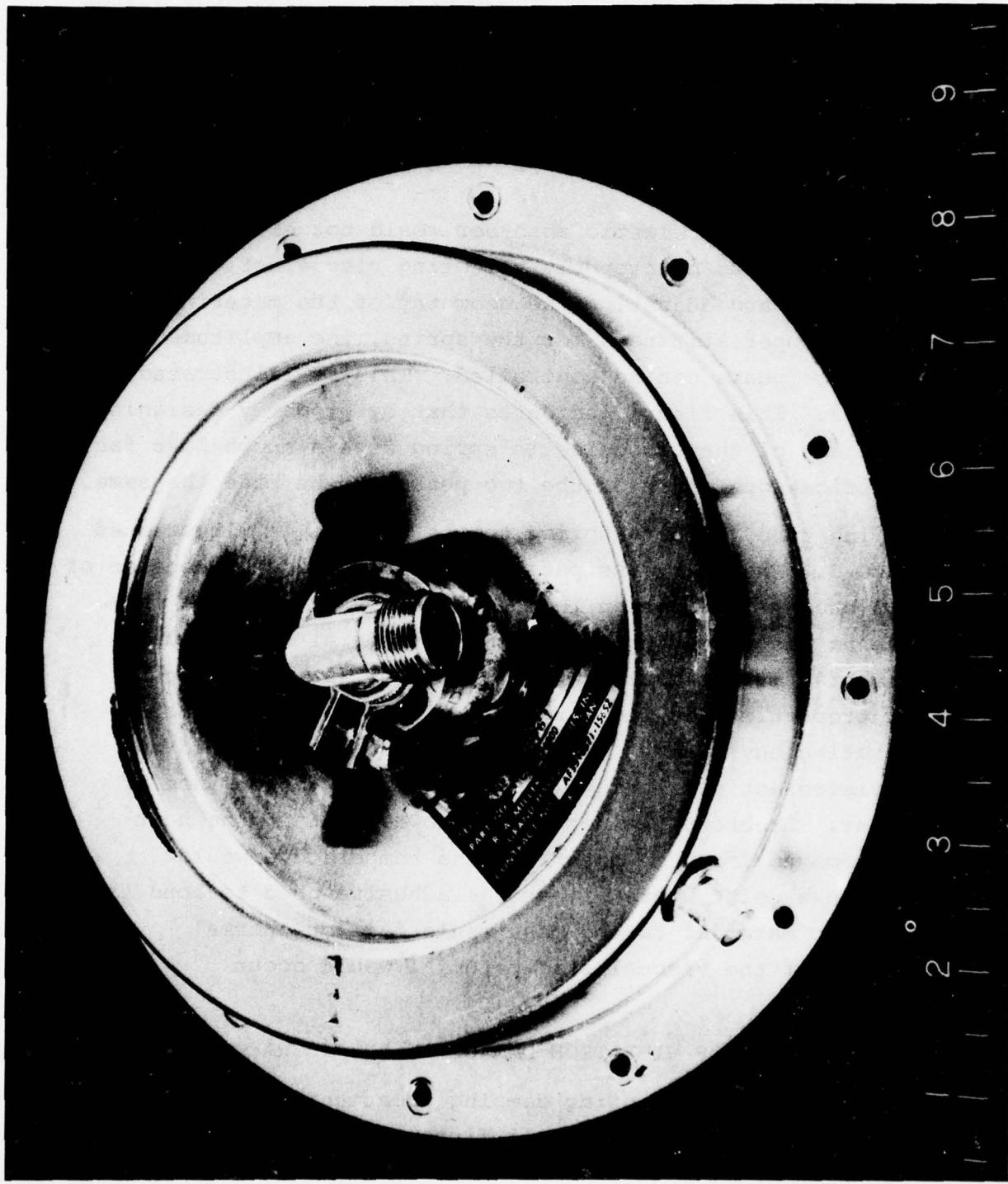


Figure 1 UHF Antenna with Tuned Viscoelastic Damper.

The excitation force was essentially a broad-band random input which eliminated the use of an undamped tuned absorber. The application of an undamped absorber would change the system to a two degree-of-freedom system; eliminating the original resonance but introducing two other resonances very possibly as damaging as the original resonance. Since the excitation force was broad-band random, the other two resonances would be excited.

A tuned viscoelastic absorber would not eliminate the new resonances, but by properly selecting viscoelastic materials for the spring and adjusting the geometry of the material to obtain the proper stiffness for the spring, the amplitude of the resonance peaks can be controlled. This is illustrated in Figure 2. This figure indicates that by properly designing the stiffness of the viscoelastic spring with a known loss factor, the amplification factor of the two peaks can be made the same.

The tuned damper applied to the antenna is illustrated in Figure 3. The heat dissipation gaps are necessary because of the high energy dissipation in the viscoelastic material when the antenna was vibrating, causing the material to heat up. The viscoelastic material eventually chosen was one whose damping properties did not vary strongly with temperature in the operating environment of interest so that heat build-up in the viscoelastic material would not affect performance of the damper. Laboratory experiments showed that if the heat was not removed from the material, the temperature would increase to a point where either the adhesive used to bond the viscoelastic material to the mass would fail or thermal degradation of the viscoelastic material would occur.

III. REDUCTION OF VIBRATION DAMAGE IN AN AIRCRAFT DISPENSER

Another example using damping treatments to control vibration problems was the SUU-41 dispenser shown in Figure 4 [3].

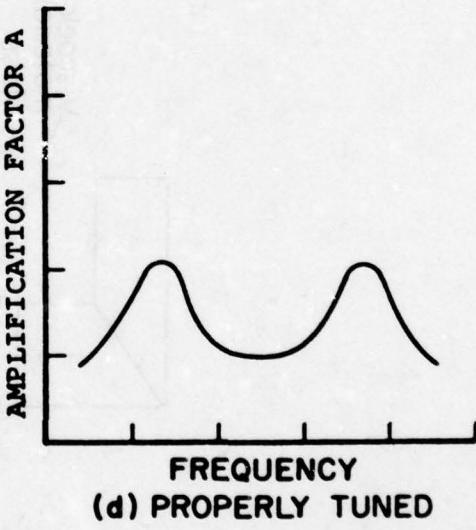
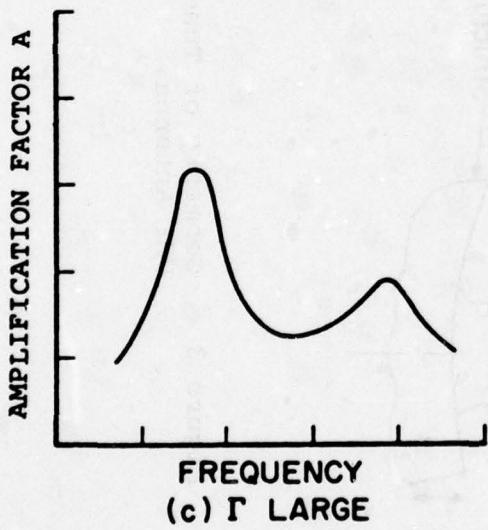
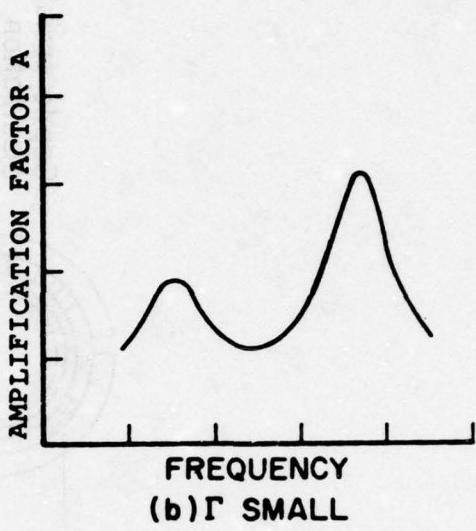
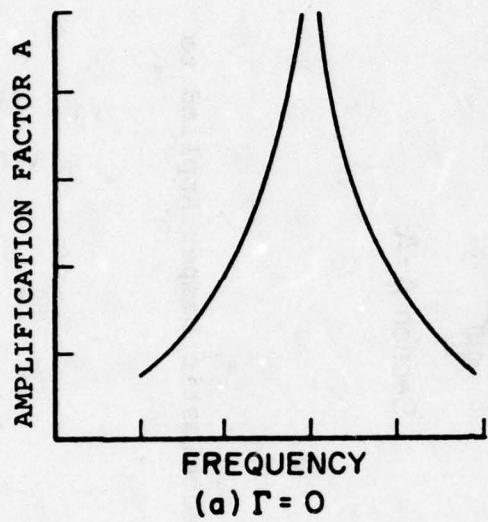


Figure 2 Amplification Factor versus Frequency for a Two Degree-of-Freedom System for Various Stiffness Ratios, γ .

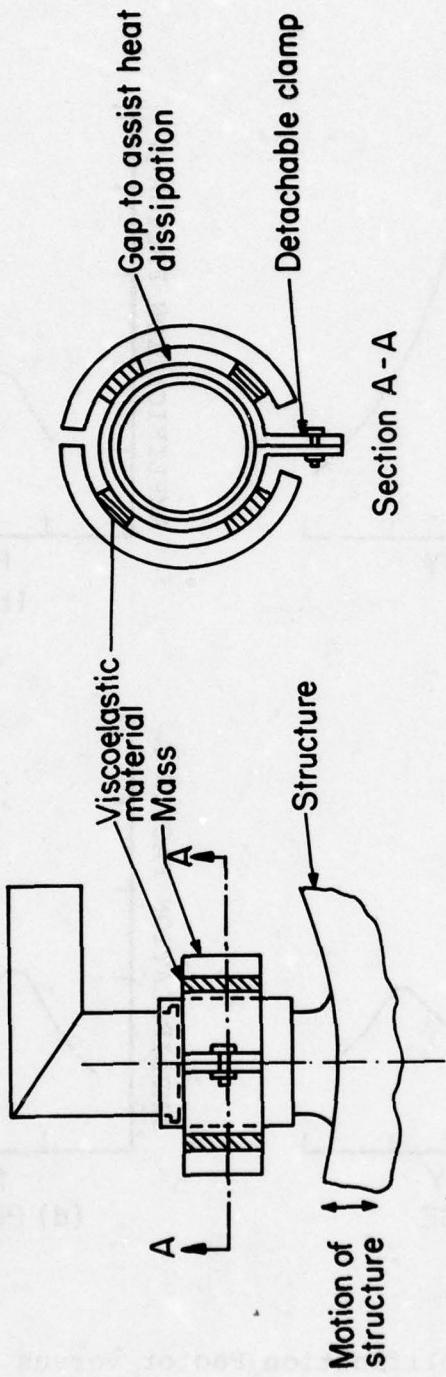
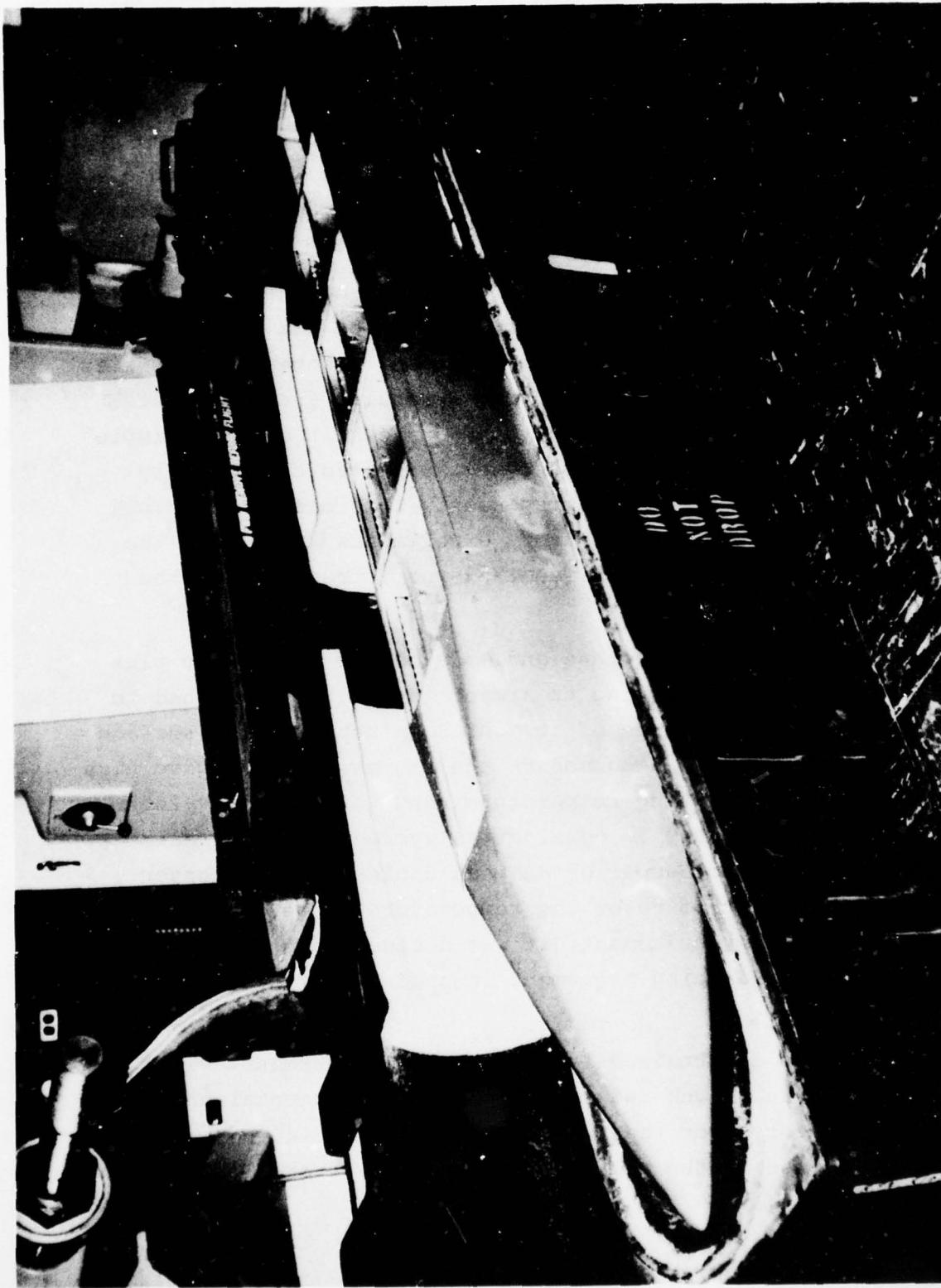


Figure 3 Geometry of Tuned Viscoelastic Damper Applied to
UHF Antenna.

Figure 4 Photograph of SUU-41 Dispenser Showing Cavities and Webs.



The dispensers were attached under the wings and fuselage of the F-4 aircraft and the stores were held in the box-like cavities of the dispensers, serving to maintain a smooth aerodynamic surface, prior to release. Upon release of the stores, cavity resonances were set up in the SUU-41. As the aircraft returned from its mission, these cavity resonances caused excessive vibration of the center webs. The failure rate was so high a dispenser barely lasted a single mission with cracks appearing at a stress raiser in the web as shown in Figure 5.

Mode shapes and resonant frequencies of the web in the dispenser and a web removed from the dispenser and mounted in a fixture were obtained. The mode shapes and resonant frequencies compared very favorably. Some typical results are illustrated in Figure 6. This indicated the boundary condition of a simple web mounted in the fixture closely approximated the boundary conditions of the web in the dispenser. This made it possible to use a single web for laboratory experiments to evaluate the effects of damping treatments on the dynamic response of the webs in the dispenser.

The frequency response and mode shapes of the web plus the criteria for the damping treatment is that: (1) it had to operate within a clearance of at most 0.1-inch from the surface of the web in order to accommodate the stores, and (2) give high damping over an operating temperature range of -30°F to +200°F which made it necessary to consider a layered damping treatment. A tuned viscoelastic damper or dampers could not meet these criteria. In order to cover the temperature range of interest and the thickness requirement, it was decided to use a constrained layered damping treatment instead of a free layered treatment.

Various constrained layered damping treatments were applied to a single web and tested in an environmental chamber in the laboratory over the temperature range of interest. Typical response of the undamped and damped web are illustrated

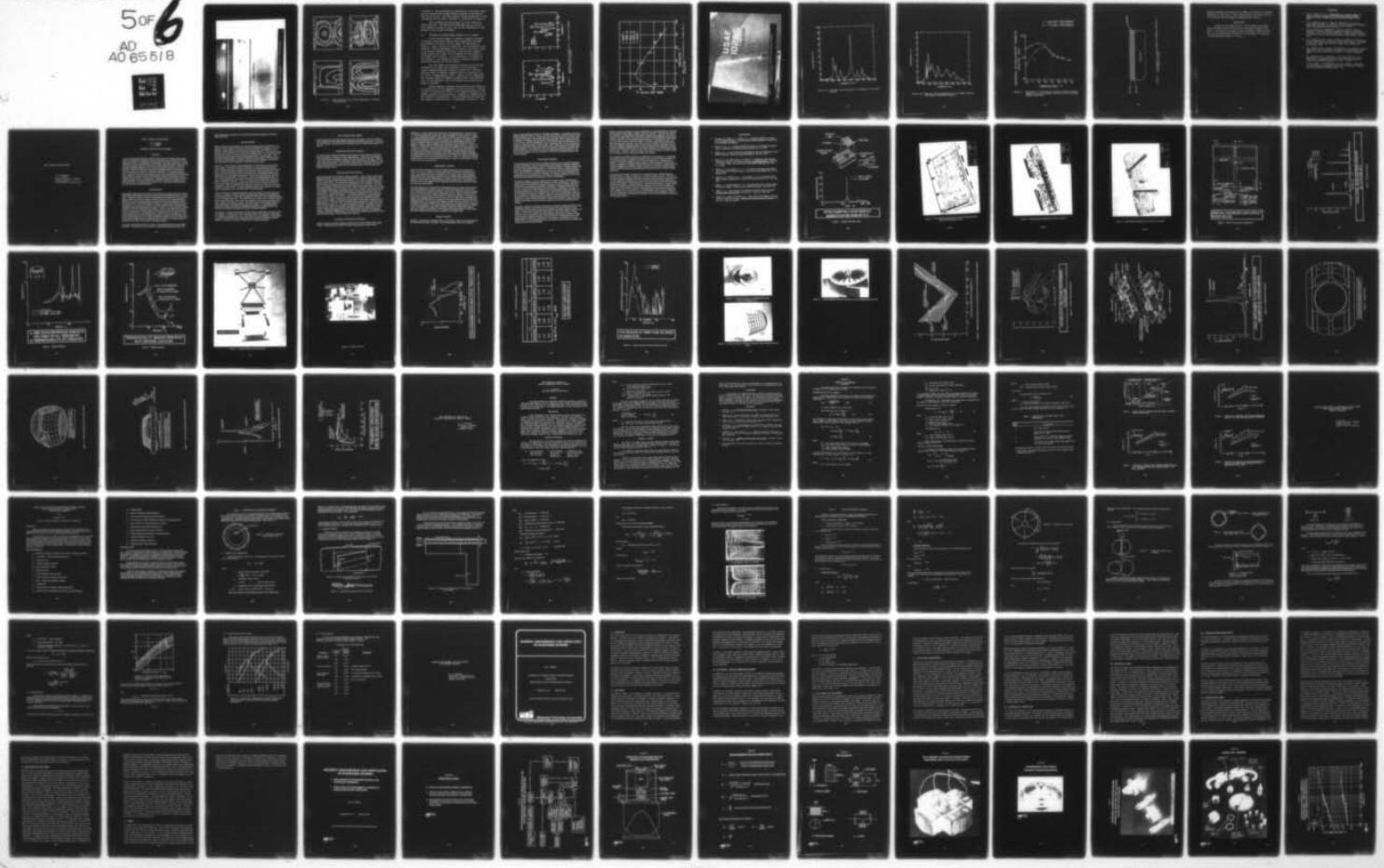
D-A065 518 AIR FORCE FLIGHT DYNAMICS LAB WRIGHT-PATTERSON AFB OHIO F/G 11/9
CONFERENCE ON AEROSPACE POLYMERIC VISCOELASTIC DAMPING TECHNOLO--ETC(U)
JUL 78 L ROGERS

UNCLASSIFIED

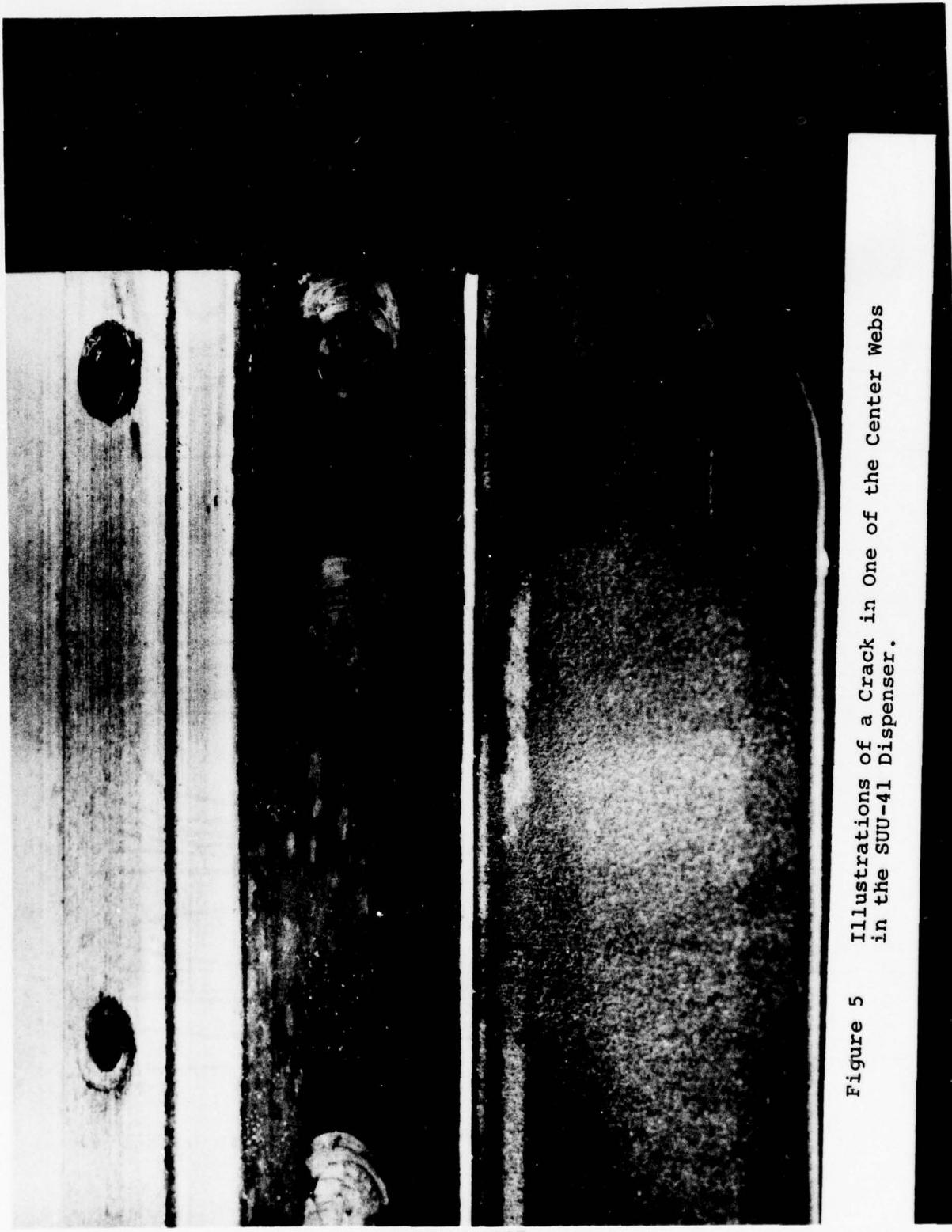
AFFDL-TM-78-78-FBA

NL

5 OF 6
AD 65518







407

Figure 5 Illustrations of a Crack in One of the Center Webs
in the SUU-41 Dispenser.

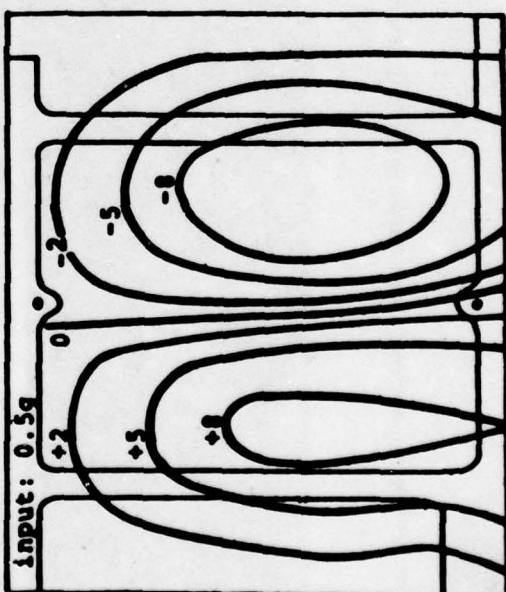
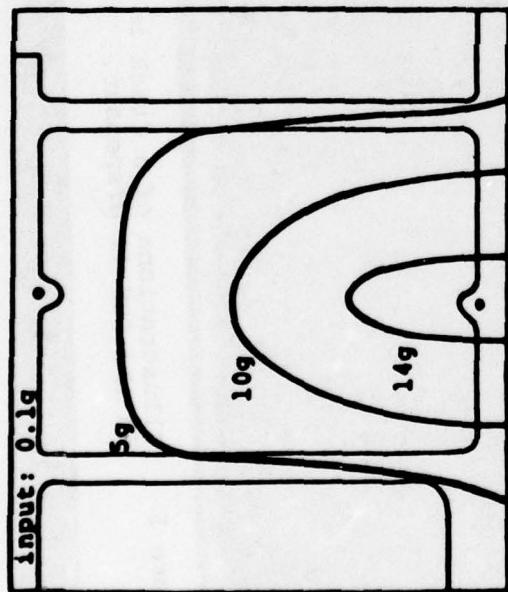
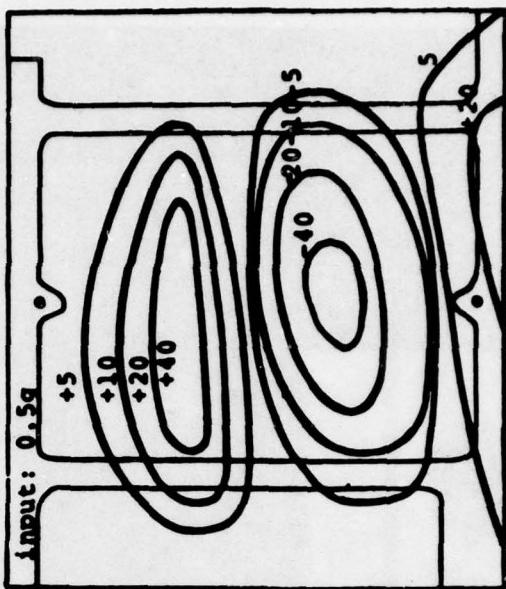
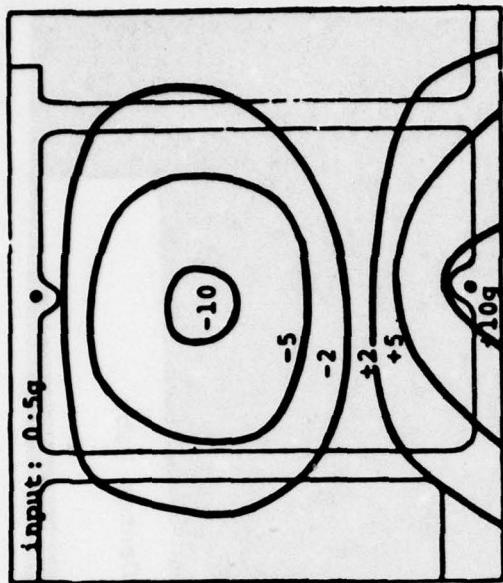


Figure 6 Mode Shapes of First Four Resonances of SUU-41 Dispenser Web.

in Figure 7. The configuration selected was a five-layer treatment of aluminum and 34-428A adhesive applied to the central portion of the web. The modal damping versus temperature of the web damped with the above treatment is illustrated in Figure 8.

This configuration was forward for field testing in operational use. The tests were successful and give a five-fold increase in service life. The fix was implemented in the production and retrofit programs.

IV. CRACKING OF LEADING EDGE FAIRINGS OF F-15 RUDDER

A more recent example of applying a damping treatment to control a high cycle fatigue crack formed along the bond line between the fairing and the rudder is illustrated in Figure 9. After 100 hours of operation, the fairings had to be replaced. During replacement of the fairing, the rudder -which is an advanced composite structure- incurred severe damage (often causing the rudder to be scrapped) and this damage to the rudder was of concern. As an alternative to redesign of the fairing, it was decided to design a damping treatment to extend the fatigue life of the fairing.

The mode shapes and frequency response of the fairing attached to the rudder was determined in the laboratory. A typical undamped response is shown in Figure 10a. The temperature range the damping treatment had to be effective over was -25°F to approximately +100°F. Because of the temperature and frequency range the damping treatment had to be effective over, it was decided to use a two-layered constrained layered damping treatment.

Several damping treatment configurations were tested in the laboratory over the temperature range of interest. Figures 10 and 11 illustrate the effect of the damping treatment on the dynamic response of the fairing as a function of temperature for two different configurations. The configuration that gave the best damping characteristics is illustrated in Figure 12. The

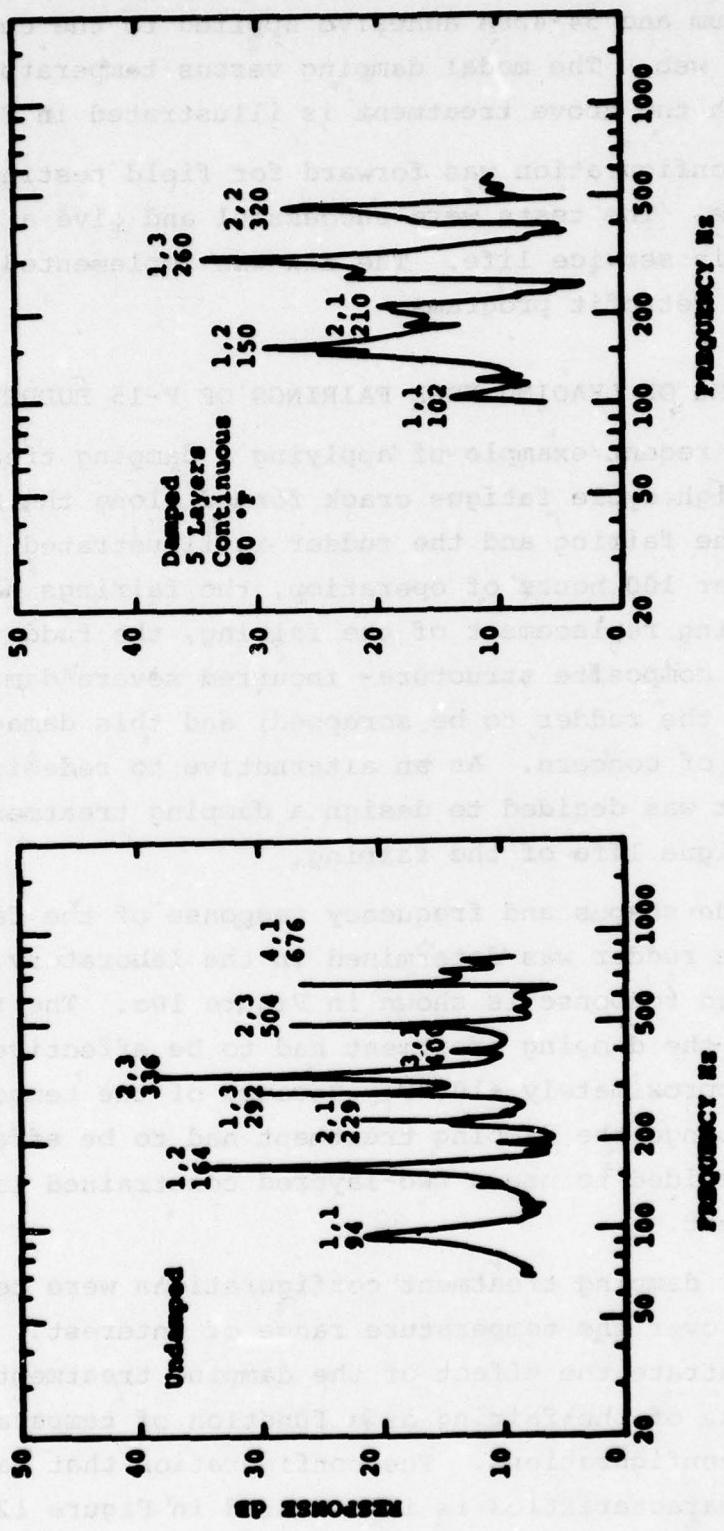


Figure 7 Response versus Frequency for a Damped and Undamped Web of SUU-41 Dispenser.

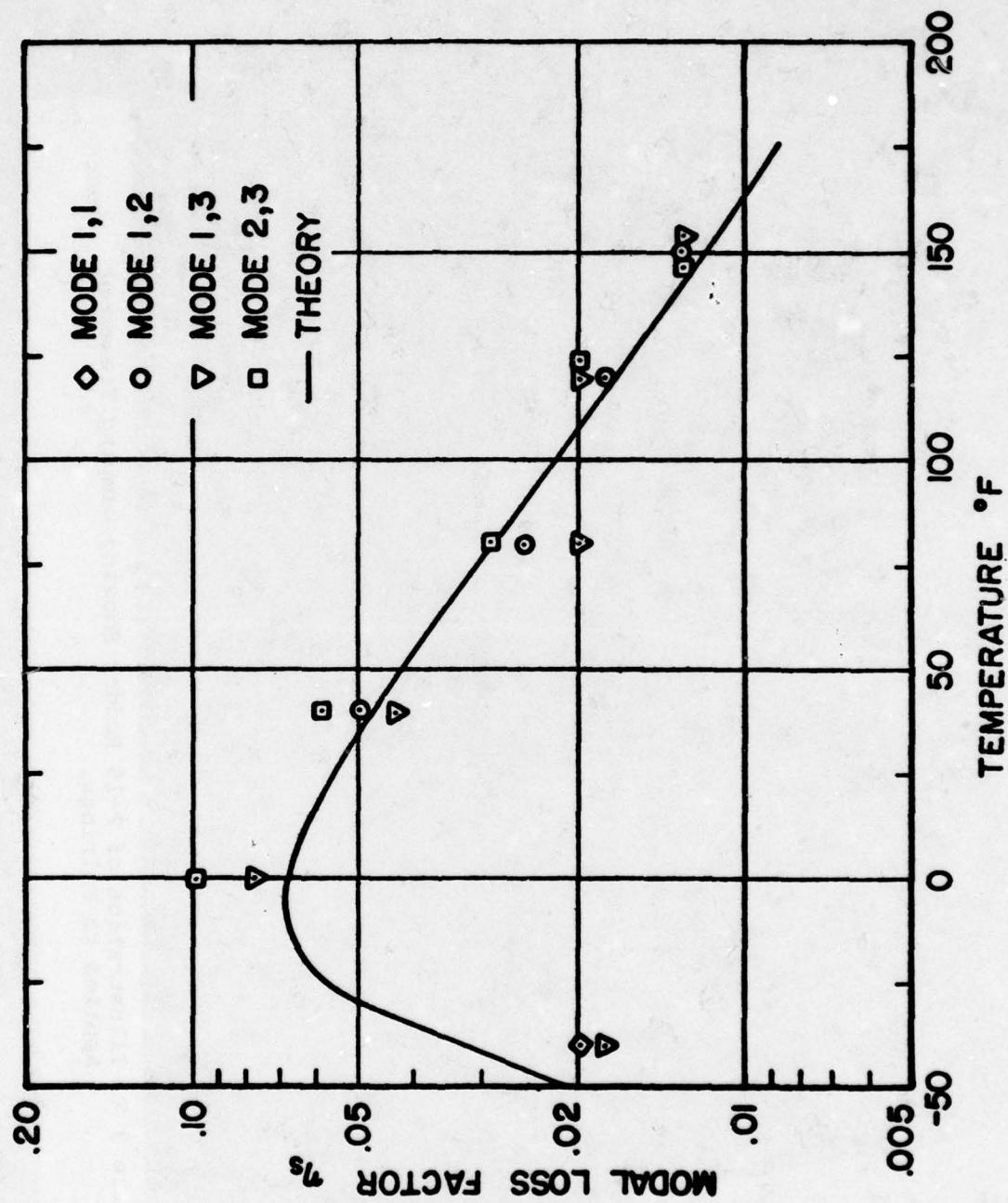


Figure 8
Modal Damping versus Temperature of Damped sut-41
Dispenser Web.

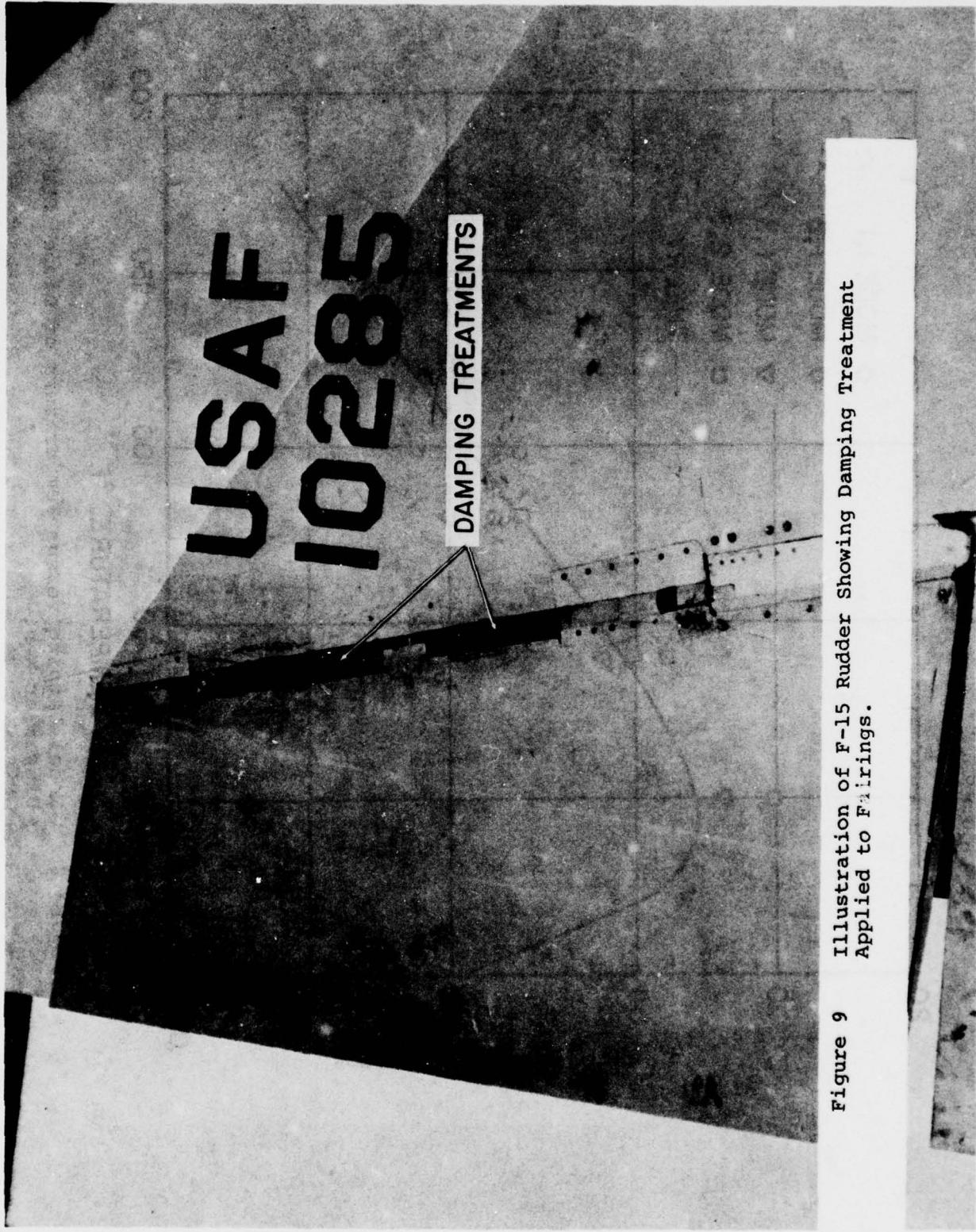


Figure 9 Illustration of F-15 Rudder Showing Damping Treatment Applied to Fairings.

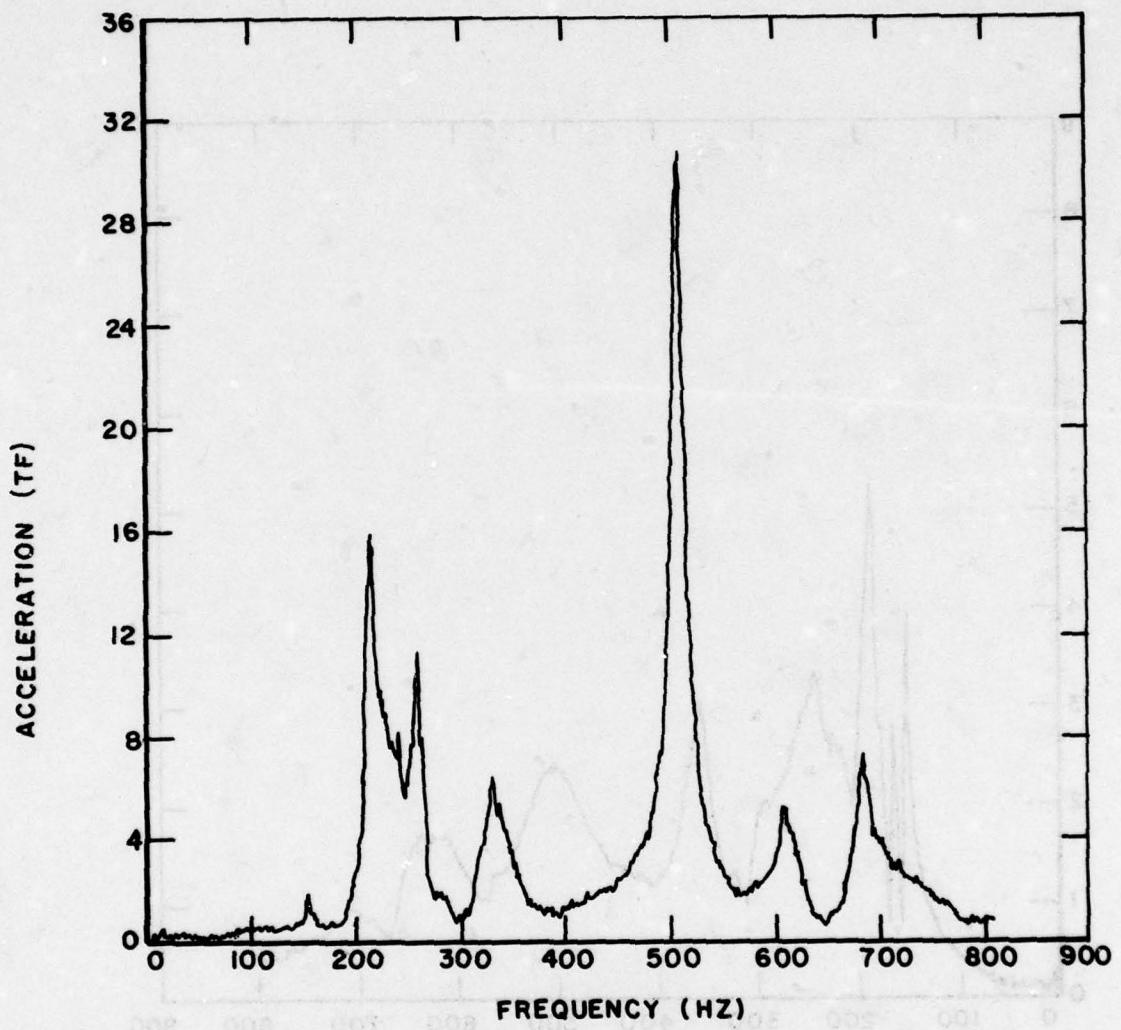


Figure 10a Response versus Frequency of Undamped F-15 Rudder Fairing.

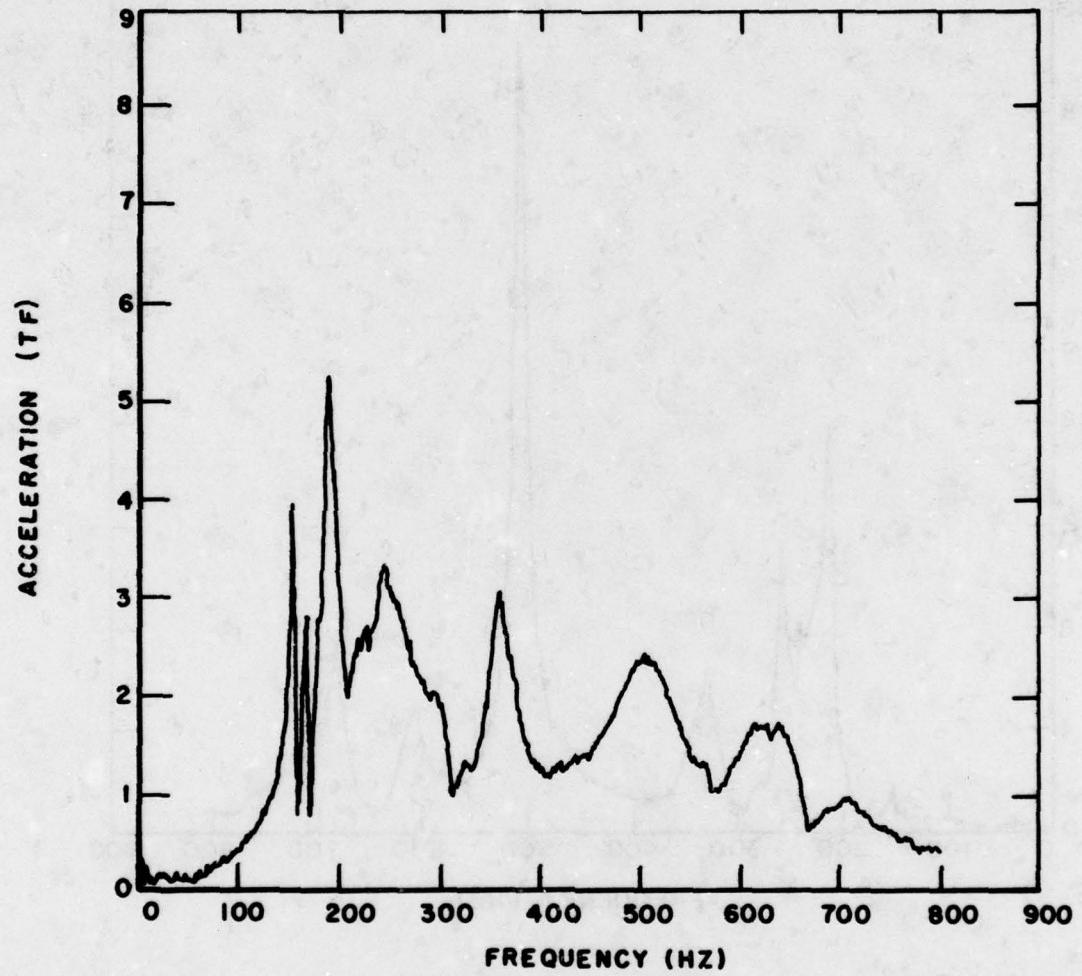


Figure 10b Response versus Frequency of F-15 Rudder Fairing with Damping Treatment Applied.

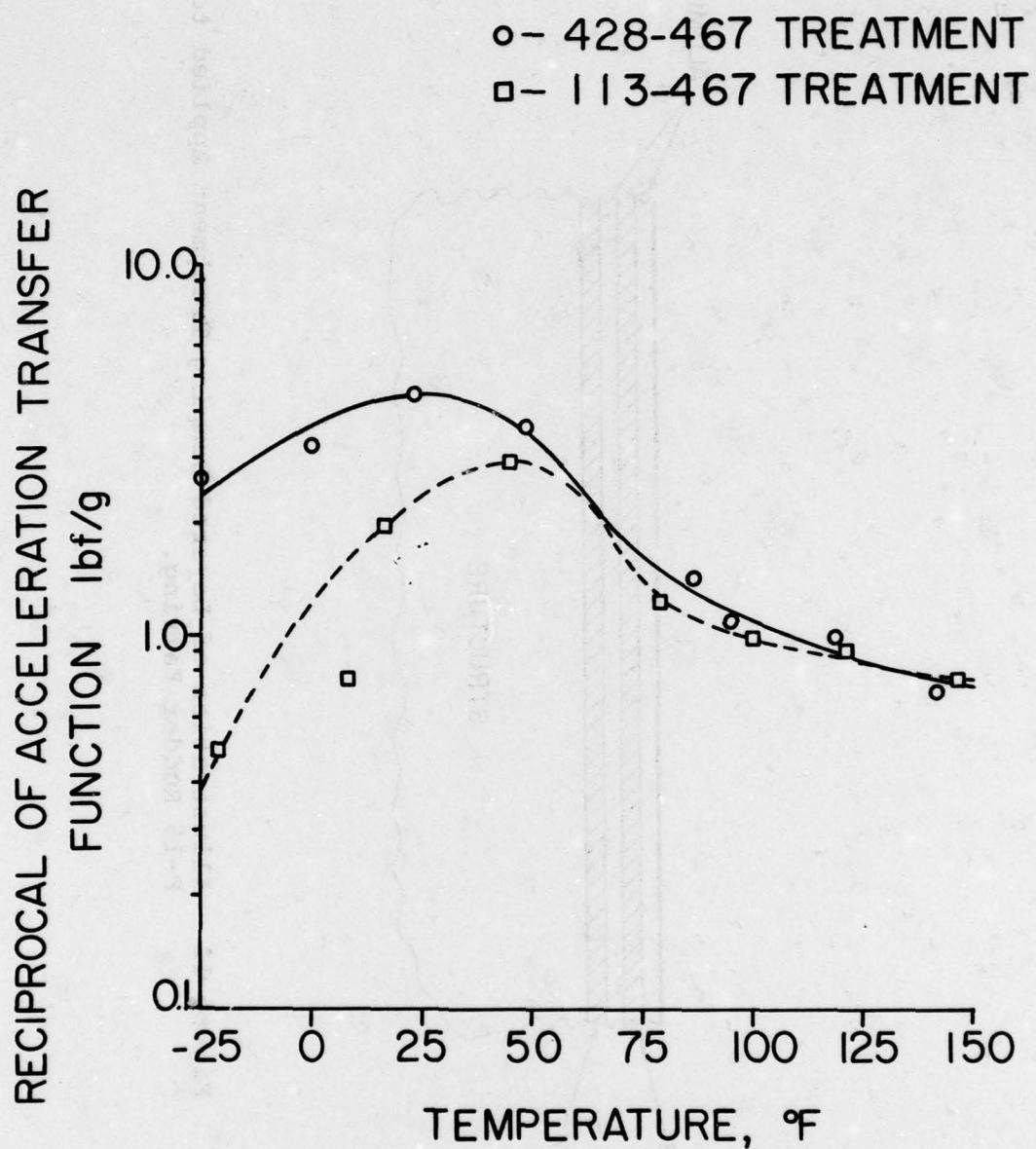


Figure 11 Reciprocal of Acceleration Transfer Function versus Temperature of F-15 Rudder Fairing for Two Different Damping Treatments.

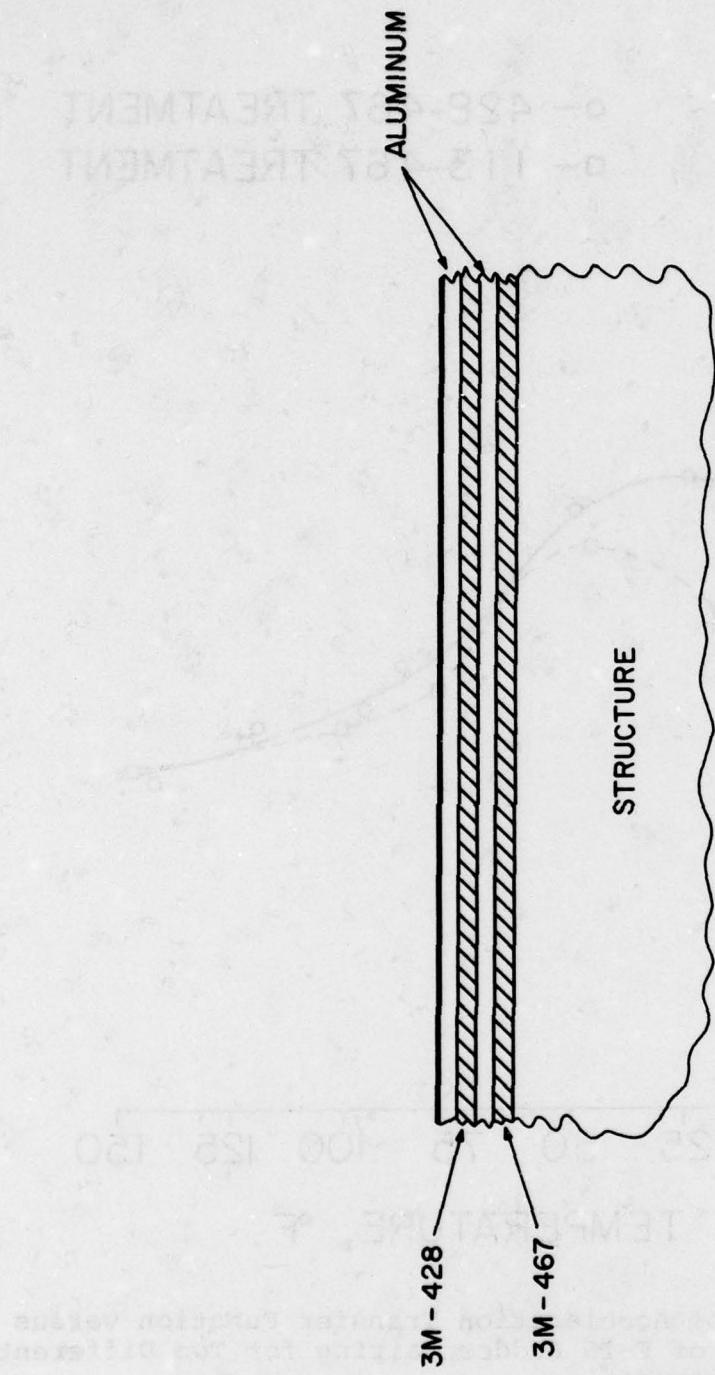


Figure 12 Illustration of Layered Damping Treatment Applied to
F-15 Rudder Fairing.

damping treatment was applied to a number of aircraft for service evaluation of the crack. After approximately 300 hours, none of the fairings with the damping treatments have failed.

CONCLUSIONS

These are an example of but a few vibration problems that have been solved with additive elastomeric damping treatments. The point to be made is that an additive damping treatment can be successfully designed if the designer is cognizant of the parameters noted in the text.

REFERENCES

1. D.I.G. Jones, et. al., Development of a Tuned Damper to Reduce Vibration Damage in an Aircraft Radar Antenna, AFML-TR-67-307, Wright-Patterson Air Force Base, Ohio, 1967.
2. J.P. Henderson and A.D. Nashif, "Reduction of Interior Cabin Noise Levels in a Helicopter through Additive Damping," Shock and Vibration Bulletin 44, Part 5, 1974.
3. D.I.G. Jones, J.P. Henderson, and A.D. Nashif, "Use of Damping to Reduce Vibration Induced Failure in Aerospace Systems," Proc. Air Force Conference on Fatigue and Fracture of Aircraft Structures and Materials, Miami Beach, Florida, 1969.
4. L.C. Rogers and M.L. Parin, "Additive Damping for Vibratory Stress Reduction of Jet Engine Inlet Guide Vanes," Presented at the 47th Shock and Vibration Symposium, Albuquerque, New Mexico, 1976.
5. J.D. Sharp and M.L. Drake, "Elimination of a Resonant Fatigue Problem for Major Maintenance Benefits," Presented at the ASME Vibrations Conference, Chicago, Illinois, September 1977.
6. M.L. Drake and J.P. Henderson, "An Investigation of the Response of a Damped Structure Using Digital Techniques," Shock and Vibration Bulletin 45, Part 5, 1975.
7. D.I.G. Jones, J.P. Henderson, and A.D. Nashif, "Reduction of Vibrations in Aerospace Structures by Additive Damping," Shock and Vibration Bulletin 40, 1970.

SMRD DAMPING APPLICATIONS

J. M. Medaglia
C. V. Stahle
General Electric Company
Space Division
Philadelphia, Pennsylvania

SMRD DAMPING APPLICATIONS

**J. M. Medaglia
C. V. Stahle**

GENERAL ELECTRIC-SPACE DIVISION

ABSTRACT

A survey of Spacecraft Materials Research and Development (SMRD) damping applications is presented. The damping materials utilized are from a family of GE-SD developed epoxy base, low outgassing, space qualified viscoelastic compounds. Various applications are described including circuit boards, equipment support structures, an acoustic attenuating enclosure, and primary subassembly structures. Design approaches to additive treatments are discussed. Integrally damped designs are emphasized. Typically the swept sine resonant magnifications of the viscoelastically damped structures are reduced to between two and eight. For candidate configurations, parametric variations using design aid numerical analysis and three dimensional finite element analysis are shown to be an effective means of optimization using appropriate design criteria. The philosophy of adequate treatment and system design is emphasized where possible in preference to simply striving for the maximum composite loss factor. The applications presented are a combination of flight hardware and research and development projects.

INTRODUCTION

The General Electric Space Division has been pursuing viscoelastic damping material development, applications and practical engineering design approaches for over eight years. Initially, control of vibration in spacecraft circuit boards and relay panels to enhance spacecraft reliability required the development of low outgassing damping materials by the Spacecraft Materials Research and Development (SMRD) section in the Space Division. The SMRD damping materials are epoxy based polymers and have been applied to a variety of structures. Computer codes have been developed which adequately predict the damping and stiffness of composite structures using viscoelastic materials in free and constrained layer designs. Today, many analytic tools exist to design for damping in not only flat plate-like structures but also in singly and doubly curved shell structures, rib-stiffened panels, bracketry and truss-works but refinement is needed for truly precise analytic predictions. Systems considerations in integrally damped designs such as strength and stiffness supplement the goal of high damping to produce designs which are weight effective and which meet overall needs in a satisfactory way without over-design or excessive margins.

This paper presents the results of a variety of damping applications using the SMRD materials. The applications are presented in essentially chronological order with

initial applications to printed circuit boards and subsequent applications involving larger structures.

CIRCUIT BOARDS

Figure 1 describes an application to control the resonant response amplitude of a relay panel. The mechanical relays were known to be sensitive to vibration. As a consequence, design criteria were imposed to limit the dynamic amplification of the panel to 6 while providing a 150 Hz minimum resonant frequency. The original design consisted of a 0.090 inch aluminum plate with a stiffening rib. The rib was removed and low density foam was bonded to the plate with holes to evade the relays. This maintained enough stiffness to minimize deflections and provided an offset distance to maximize stretching of the viscoelastic material which was applied as a free layer. The damping and resonant frequency satisfied the design criteria.

Figures 2, 3, and 4 illustrate typical applications of constrained layer treatment to circuit boards. The frame in Figure 2 supports two similar boards which are so densely packed with electronic parts that no path was available to install damping material. The board boundary conditions were altered to accomplish damping. A mid-span support was removed from both ends of the frame. The damping material was bonded on the now free edges using one board as the constraining layer for the other. The strip was approximately 1/4 inch wide. Figure 3 illustrates the placement of narrow constrained strips so that they are deformed by the fundamental mode in the region of maximum curvature. Figure 4 illustrates that as long as the constraining layer is continuous some damping material may be removed to clear lead wires or components. Figures 2 through 4 show applications which were optimum in the sense that they solved the problem. Greater damping could have been achieved with reduced weight if damping had been considered early in the design phase.

Figure 5 illustrates an integrally damped circuit board design for a high vibration environment. Connector rocking, which could break glass bodied parts or fatigue lead wires mounted nearby, is controlled by bonding the connector to the constraining layer of strips of damping material. Free edge modes are controlled by the damped sandwich finger and the edge strip. Other modes are controlled by the center constrained layer strip. Figure 5 is not drawn to scale. The relative sizes of the damping materials, constraining layers, and board are determined by analysis. This integral design approach includes provisions for the damping treatment from design inception permitting a more effective treatment and greatly enhancing reliability.

On boards in a moderate environment, often one strip is sufficient to control its vibration response. A strip which is 5% of the board width is often adequate. Epoxy-glass is a suitable constraining layer (CL). The strips can be more effective with aluminum or high modulus graphite epoxy constraining layers permitting a smaller width and thickness. However, care must be taken to avoid excessive stiffening.

HEAVY GAUGE STEEL BEAMS

Figure 6 shows that even heavy gauge steel can be well damped. The test configuration consisted of 36-inch long steel bars supported and excited at the center. All modes were well damped. The performance was predicted using a straight beam analysis design aid.

EQUIPMENT SUPPORT BULKHEAD

In systems design, extensive treatment of the avionics or other sensitive equipment may not be possible, adequate or most weight effective. Treatment of the equipment can be minimized when equipment support structure vibration is controlled. Figures 7 and 8 show what can be done by replacing a heavy gauge aluminum bulkhead by a integrally damped design (IDD). Since the IDD response is low, the gauges can be further reduced so that the IDD weighs less than the undamped design while maintaining an adequate strength margin.

DAMPED SUPPORT BRACKETRY

Equipment may also be protected by damped bracketry. Figures 9 and 10 show such a damped bracket for a camera which was developed for the NASA Goddard Space Flight Center for the International Ultraviolet Explorer. The camera is bolted to the inner frame at three points. The inner frame is supported by metal "dog-legs" which eliminate hysteretic misalignment while providing flexibility in all directions. The inner frame is redundantly connected to the channel shaped constraining shells via six blocks of damping material which is strained by any of the six rigid body modes of the camera. The redundant path through the damping material also provides a large fraction of the total stiffness. This design protects the camera from high frequencies (to which an internal part is sensitive) by isolation. The bracket resonances are well damped as can be seen in Figure 11 and Table 1, which show results of hard mounted bracket/camera testing. Figure 12 shows the camera response when installed on the deck (which was not treated). This design was analyzed by finite element methods with adequate success. The fourth mode of vibration analytic prediction is compared to test measurements in Figure 11. The natural frequency was within 10 percent of the prediction and the isolation characteristic satisfactorily matched. Beginning at 650 Hz, camera elastic modes were isolated well enough to protect the internal parts of the camera. Response magnification was also satisfactorily predicted. The undamped bracket had response magnifications of 10 to 20 at various frequencies and had no clear isolation characteristic. This is evidenced in Figure 12.

ACOUSTIC ATTENUATING ENCLOSURE

Figure 13 shows an acoustic container developed for the NASA Goddard Space Flight Center to demonstrate the feasibility of space shuttle payload acoustic covers,

Reference 1. It has a double wall construction. The cylinder body is composed of two 0.020-inch thick aluminum sheets with a core of damping material as shown in Figure 14. The end bulkheads consist of a flat disk and a shallow cone of aluminum connected by wedges of damping material as shown in Figure 15. Parametric variations were made to determine the amount of area coverage by the SMRD damping material, the thickness needed to obtain a suitably stiff composite crosssection and a low surface density. The high composite stiffness allowed the light weight cylinder (0.75 psf) to be effective in reducing the noise transmission into the container at the lower frequencies as shown in Figure 16. Overall the noise reduction was 20 dB with a fiberglass reverberent liner blanket and 12 dB without the blanket. The high damping controlled noise transmission in the mid-frequency range when the enclosure began resonating. At higher frequencies the noise transmission was reduced by the "mass law" primarily, but damping is of value at the high frequencies, also. Figure 17 compares the internal Sound Pressure Level of the viscoelastic enclosure with that of other designs, all with respect to the same external SPL.

SUBASSEMBLY DAMPING

Figure 18 shows the Japanese Broadcast Satellite Experiment (BSE) Transponder which is 25 x 54 x 10 inches in size and weighs about 200 pounds including the equipment. The undamped structure responded at a level which would exceed component qualification levels. Parametric variations led to a graphite epoxy constrained layer treatment (two pound total weight) placed as strips in a grid-like pattern between components. Figure 19 shows a typical before and after response plot. The damped response of 15 was low enough so that the expected launch environment would not exceed the component specifications.

The BSE spacecraft also included other damping applications. During vehicle vibration testing the response of a reaction wheel and of the S-band antenna and K-band feed were controlled by the addition of damping. The reaction wheel had a response magnification of 34 and the S-band response magnification was 44. These levels were discovered early in the vibration test and would have seriously threatened the structural integrity of the equipment and structure if not corrected. In both cases, treatments were designed and installed before the completion of the test avoiding damage and expensive additional testing. The reaction wheel response magnification was reduced to 4.5 by the introduction of a strut composed of two metal angle bars connected by a pad of damping material in direct shear. The S-band/antenna feed response magnification was reduced to 10.9 by the addition of a plate-like connection between the three S-band support tubes and a flange in the feed horns. This placed the damping material in direct shear between the flange plate and the plates connected to the support rods.

GIMBAL DAMPING

Recently, the feasibility of damping doubly curved gimbal "rings" was demonstrated for the Charles Stark Draper Laboratory. The standard gimbal, Figure 20, had heavy

rings and extra material thickness for strength and stiffness. In Figures 21 and 22 the damping approach is shown. Excess material was removed so that the structure could be more easily damped. The constrained layer treatment restored much of the original stiffness, but weighed 20% less than the standard gimbal. With a natural frequency of 124 Hz and a response magnification of 8, the damped design was satisfactory. This response is shown in Figure 23 which is from a subsystem test. Work is continuing to complete the feasibility study on three gimbal rings in the presence of the flight temperature gradients. This treatment is used in combination with Draper developed interfacial damping and a viscoelastic device in the intergimbal bearing assemblies. The plot shown in Figure 23 is for an orientation in which only the gimbal damping treatment is effective.

CONCLUDING REMARKS

The preceding examples show that viscoelastic damping can be successfully applied in a variety of situations. Much has been alluded to with respect to adequate predictions, systems design and parametric variation. Accurate predictions, complete analysis and the number of parametric variations are, on the whole, areas for continued development. The establishment of design criteria is also an area for continued development. In the case of avionics circuit board damping, the minimum amount of damping, the appropriate first natural frequency, the maximum response acceleration level and the maximum allowable deflection response all need to be quantified.

The optimum design is one which satisfies all the design criteria. Maximizing the composite structural damping is not necessarily the only consideration. Several parameters must be considered in the design of structures using viscoelastic materials. Perhaps the most important parameter is temperature. Although the materials may survive a wide range of temperature they will effectively dissipate strain energy in resonant vibrations only over a relatively narrow temperature range. Typically, relatively high loss factors can be expected over a 10°C to 40°C temperature range for any one polymeric formulation. Polymer blends and multimaterial designs can extend the high loss factor range but often the maximum composite loss factor is reduced in comparison to single material treatments. Clearly the temperature range over which effective performance is desired must be defined as well as the required amount of damping.

Parametric variations of damping treatments are needed for design optimization using established criteria. Figure 24 shows an isothermal carpet plot which is one of a series of similar optimization parametric variation plots which should be made for any design. It can be seen in Figure 24, which was one of the plots made for a large structure, that it is possible to exceed the stiffness and damping criteria by increasing the amount of damping material or the thickness of the constraining layer. Even though maximum damping and stiffness are not achieved, a treatment of 1/2-inch SMRD with a 1/4-inch constraining layer is the optimum design because it satisfies the design criteria at minimum weight.

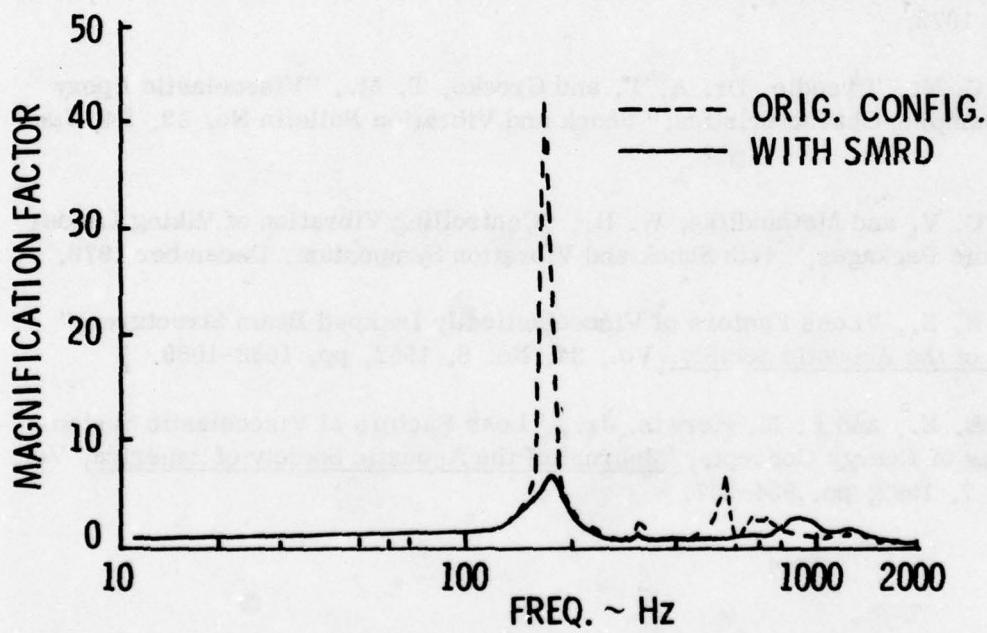
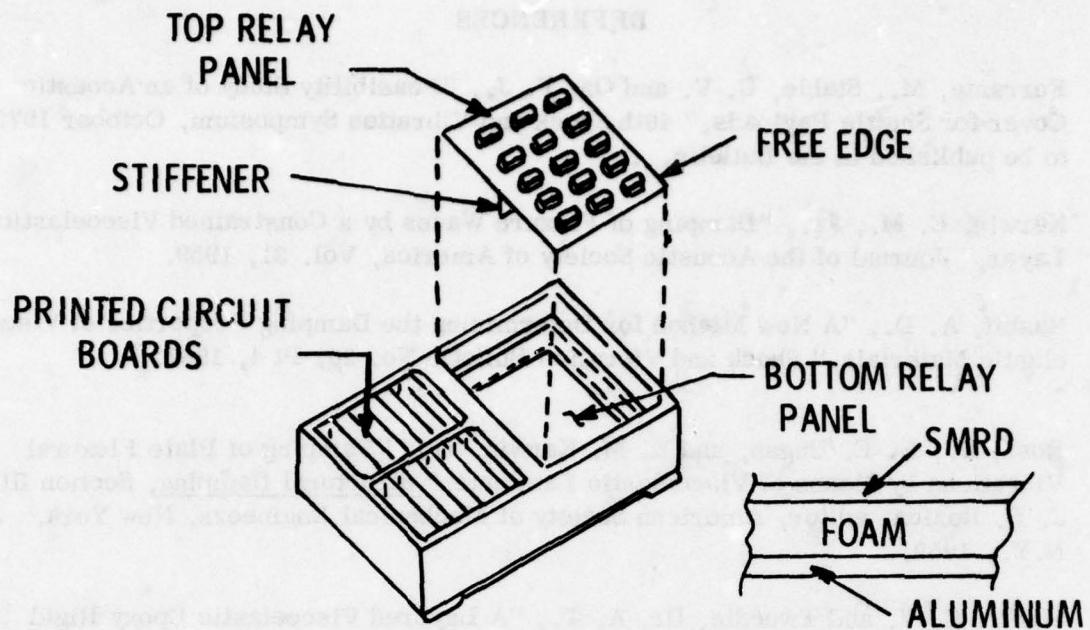
Stiffness as well as damping is a major consideration in many applications. In systems where protection from random vibration response is desired, the greater the first natural frequency, the higher the overall random vibration G_{rms} response. For random vibration, the design should be as flexible as possible while maintaining suitably small deflection response to avoid impacting adjacent parts or damaging parts on the vibrating structure by excessive bending curvature. Similarly, some designs require isolation from harmonic stimulus. Conversely, acoustic enclosures or barriers benefit from high stiffness and damping when low surface mass density is desired as in air or spaceborne designs. Stiffness also has obvious importance in the alignment of optical systems where load paths through the viscoelastic materials must be redundant rather than primary. Stiffness, modal decoupling, and frequency separation as well as damping are often governing considerations rather than strength.

The strength of viscoelastic polymers is relatively low in comparison to conventional structural materials. The primary load path should not pass through viscoelastic materials because of their weakness and cold flow characteristics. In designs where strength is needed to withstand resonant response, highly damped structures can be lighter in weight than conventional structures because less strength is needed when the resonant amplitude is controlled. Analytic methods are available to predict damping using viscoelastic polymers enabling strength considerations to be included in design trade-offs.

Having determined design criteria such as temperature range, adequate damping, resonant tuning, strength and alignment, viscoelastic damping analysis can be used to optimize the design. Design aid (flat plate and beam theory) parametric evaluations can be widely applied. In designs which are not flat and for which accurate analyses are needed, finite element modeling and strain energy calculations can provide reasonable estimates of damping. A systems approach, accounting for stiffness, strength, weight, alignment and thermal distortion as well as damping over the service temperature range can be used. Finally, it must be remembered that the temperature range over which vibration control is needed (e.g., the temperature range in which the most life cycle vibration time is spent) may be much narrower than the temperature range for survival or operation in the absence of vibration. This must be considered in establishing the design criteria.

REFERENCES

1. Ferrante, M., Stahle, C. V. and On, F. J., "Feasibility Study of an Acoustic Cover for Shuttle Payloads," 46th Shock and Vibration Symposium, October 1975, to be published in the Bulletin.
2. Kerwin, E. M., Jr., "Damping of Flexure Waves by a Constrained Viscoelastic Layer," Journal of the Acoustic Society of America, Vol. 31, 1959.
3. Nashif, A. D., "A New Method for Determining the Damping Properties of Viscoelastic Materials," Shock and Vibration Bulletin No. 36, Pt 4, 1967.
4. Ross, D., E. E. Ungan, and E. M. Kerwin, Jr., "Damping of Plate Flexural Vibrations by Means of Viscoelastic Laminate," Structural Damping, Section III, J. E. Ruzica, editor, American Society of Mechanical Engineers, New York, N.Y., 1959.
5. Stahle, C. V. and Tweedie, Dr. A. T., "A Layered Viscoelastic Epoxy Rigid Foam Material for Vibration Control," Shock and Vibration Bulletin No. 42, P4, January 1972.
6. Stahle, C. V., Tweedie, Dr. A. T. and Gresko, T. M., "Viscoelastic Epoxy Shear Damping Characteristics," Shock and Vibration Bulletin No. 43, P4, June 1973.
7. Stahle, C. V. and McCandliss, W. H., "Controlling Vibration of Viking Lander Electronic Packages," 44th Shock and Vibration Symposium, December 1973.
8. Ungar, E. E., "Loss Factors of Viscoelastically Damped Beam Structures," Journal of the Acoustic Society, Vol. 34, No. 8, 1962, pp. 1082-1089.
9. Ungar, E. E., and E. M. Kerwin, Jr., "Loss Factors of Viscoelastic Systems in Terms of Energy Concepts," Journal of the Acoustic Society of America, Vol. 34, No. 7, 1962, pp. 954-957.



OFFSET DAMPING LAYER REDUCES MAGNIFICATION FROM 44 TO 6

Figure 1. Landsat PSM Relay Panel

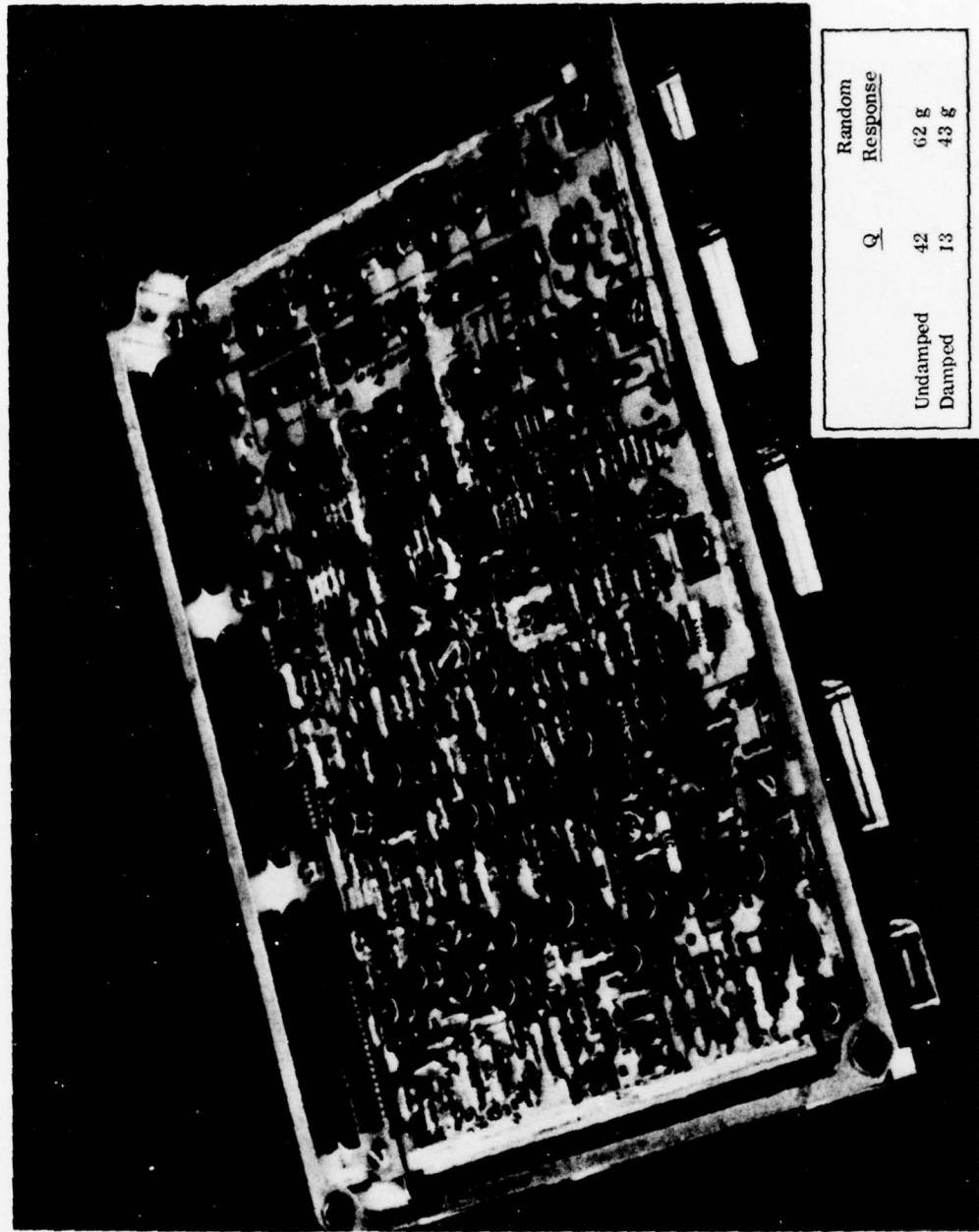


Figure 2. Final Damping Configuration of DAPU Double Board with Strips Between Boards at Ends

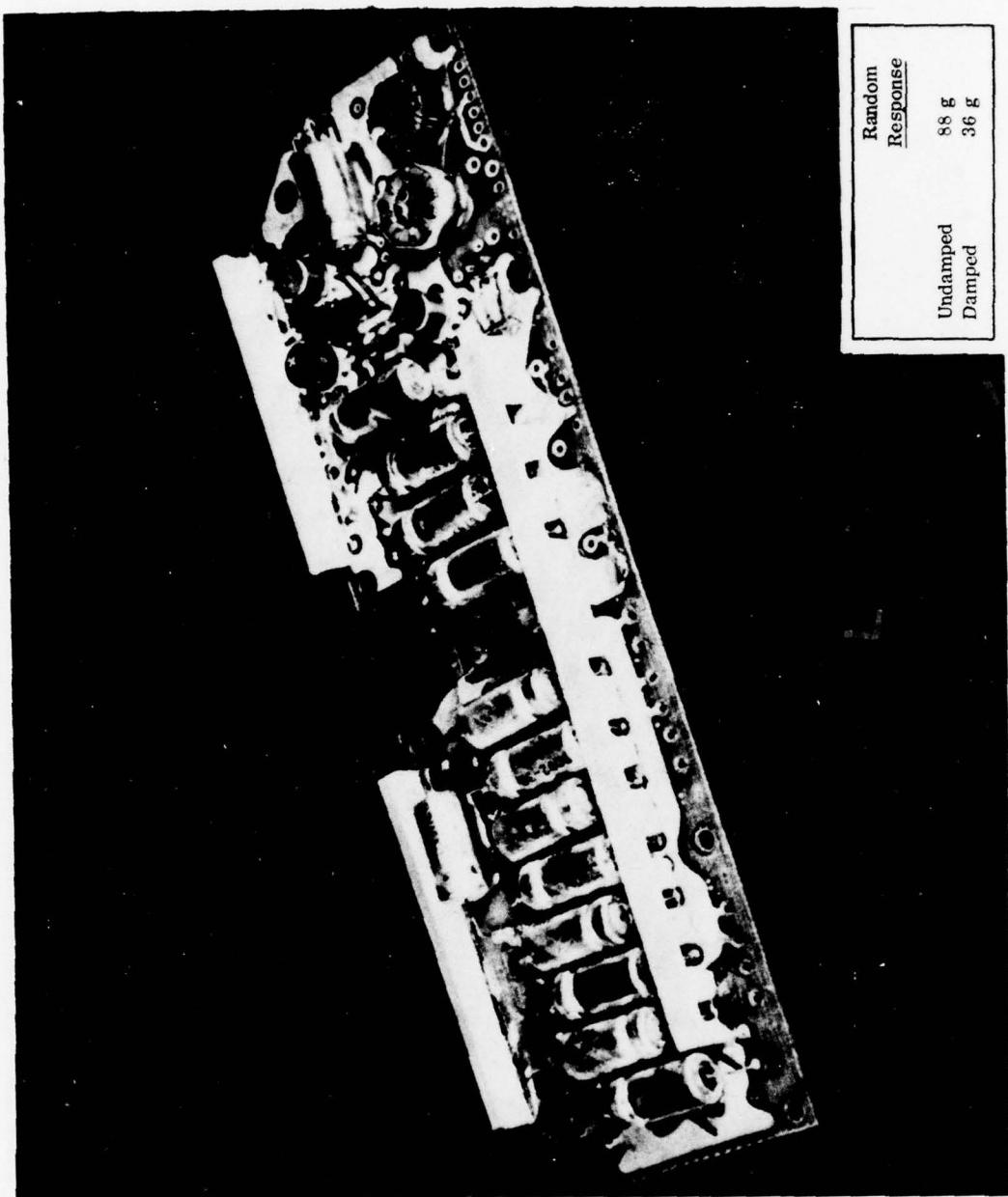


Figure 3. Final Damping Configuration of SSCA 130 Board

429a

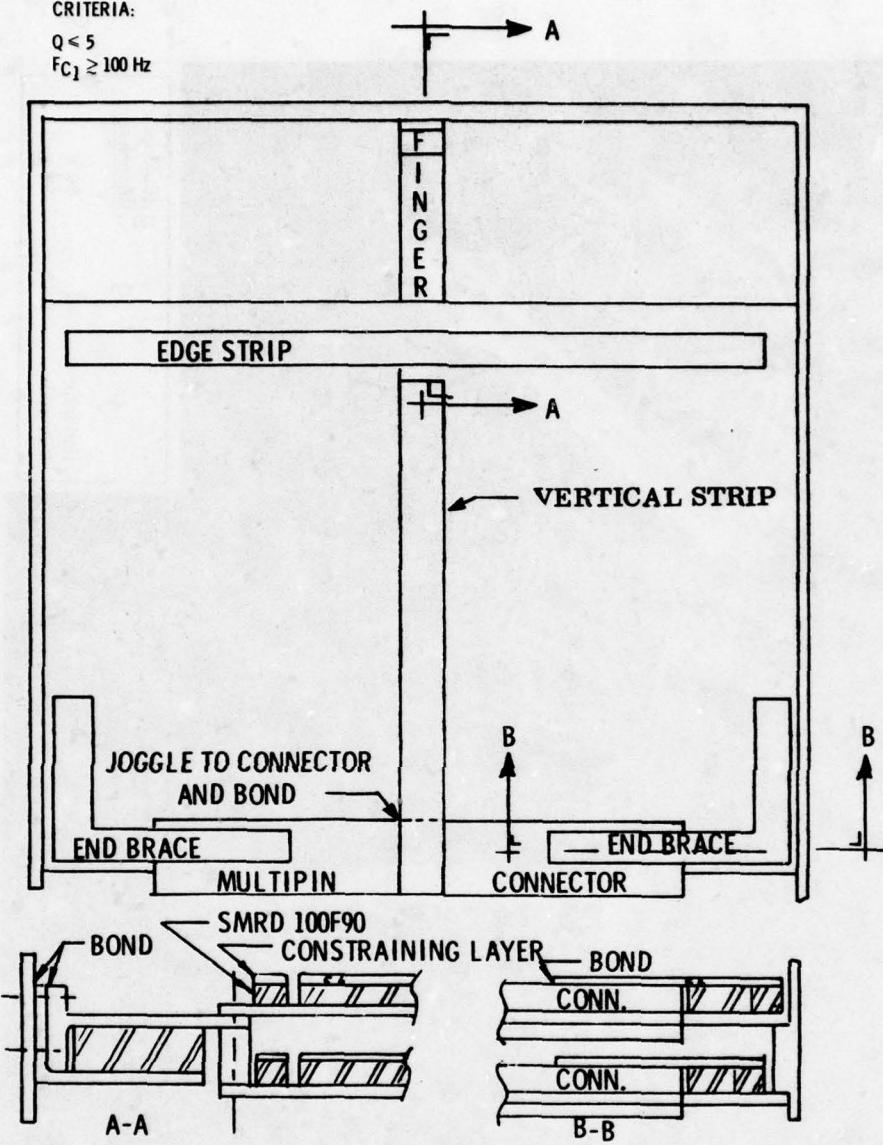


Figure 4. Final Damping Configuration of BPA 1100-010 Board

4296

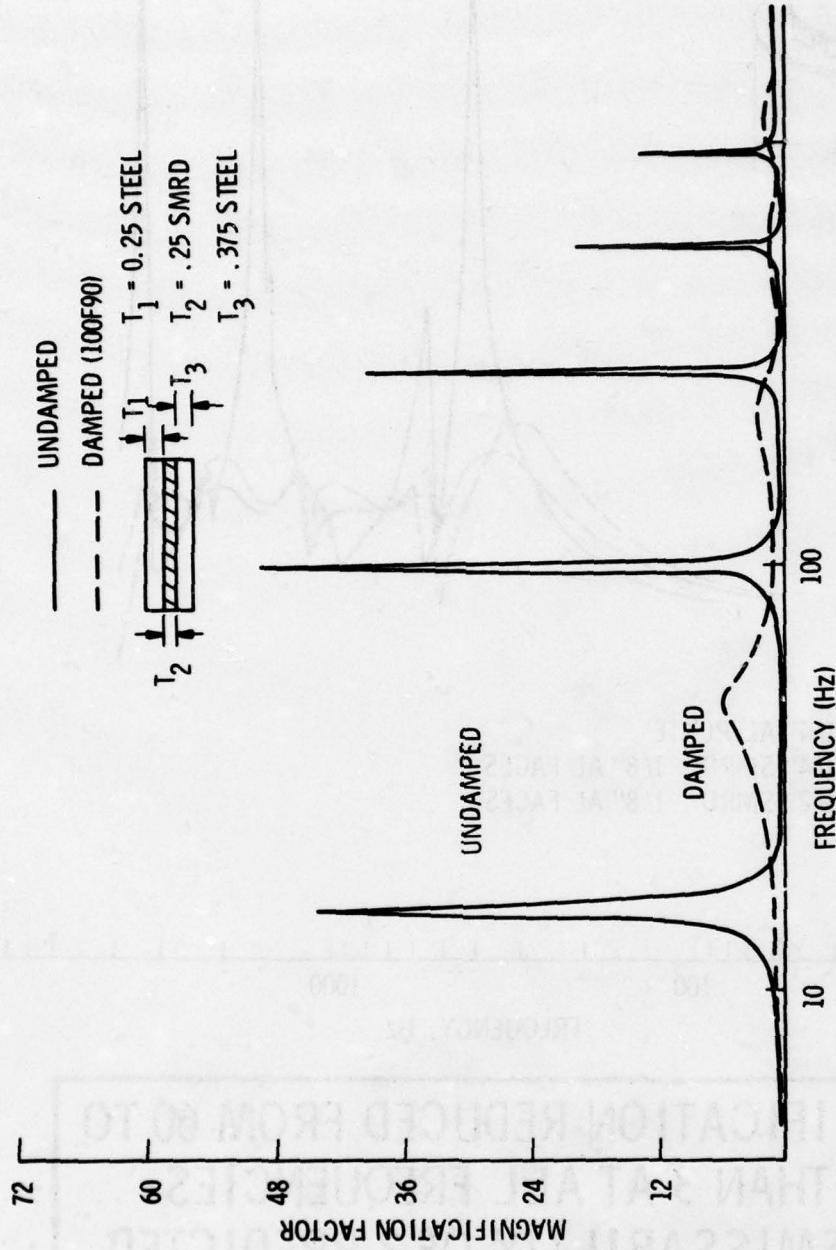
CRITERIA:

$Q < 5$
 $f_{C_1} \geq 100 \text{ Hz}$



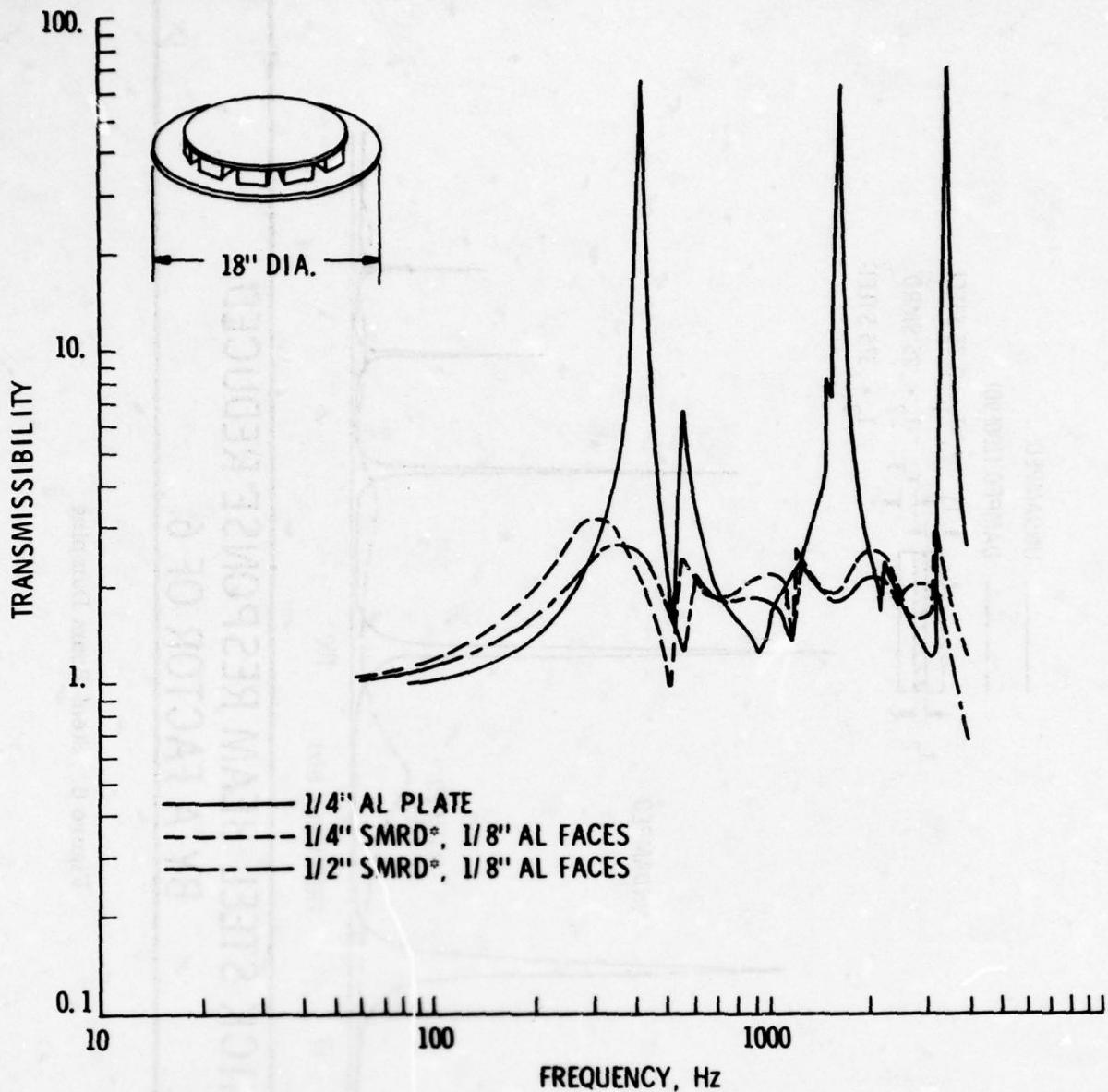
DAMPING INTEGRATED INTO CIRCUIT BOARD DESIGN

Figure 5. Typical Circuit Board Configuration



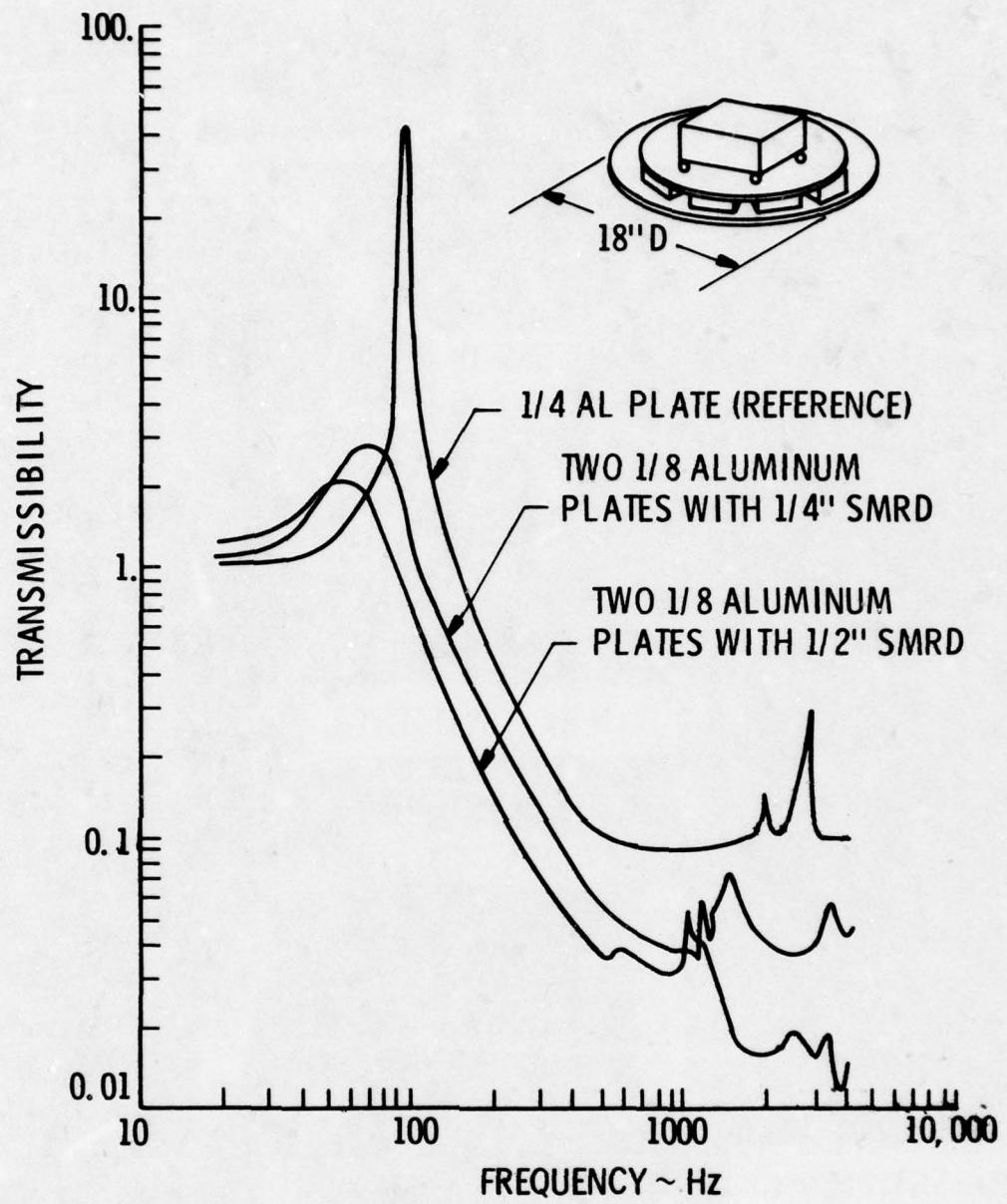
**THICK STEEL BEAM RESPONSE REDUCED
BY A FACTOR OF 6**

Figure 6. Steel Beam Damping



- AMPLIFICATION REDUCED FROM 60 TO LESS THAN 3 AT ALL FREQUENCIES
- TRANSMISSIBILITY OF 2 PREDICTED

Figure 7. Bulkhead Damping



**TRANSMISSIBILITY REDUCED FROM 45 to 2
WITH IMPROVED ISOLATION**

Figure 8. Bulkhead Isolation

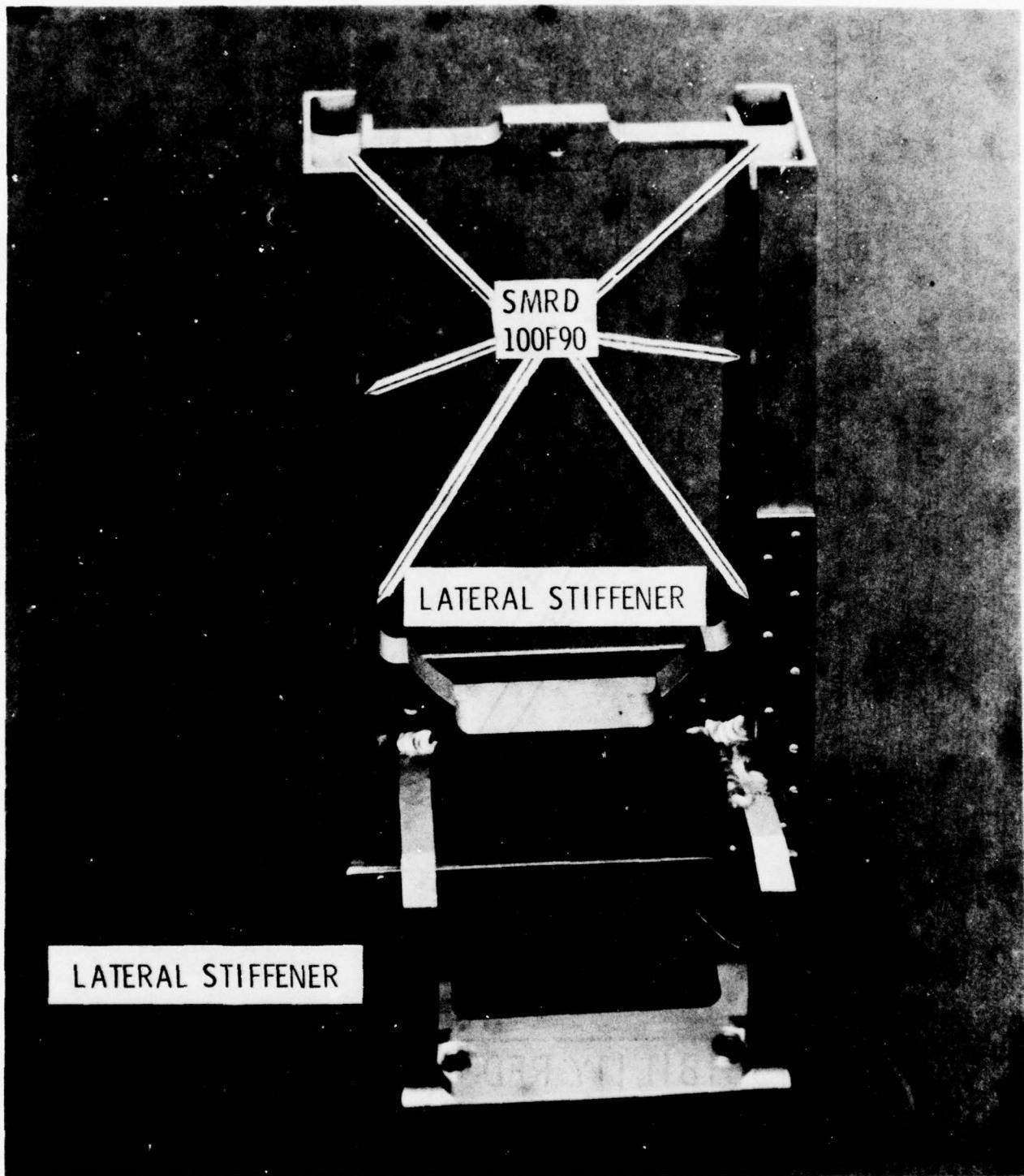


Figure 9. Damped Secondary Camera Bracket

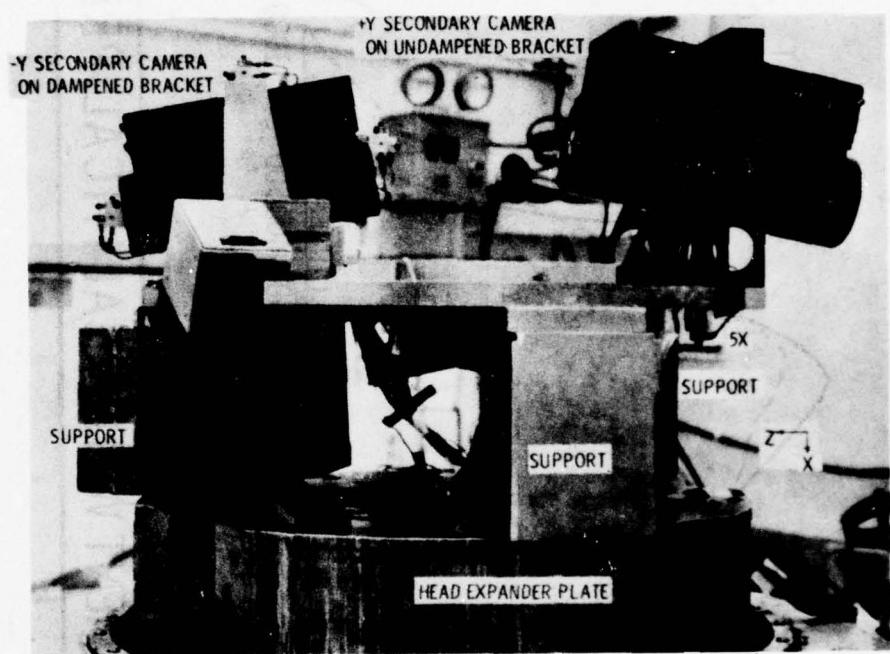
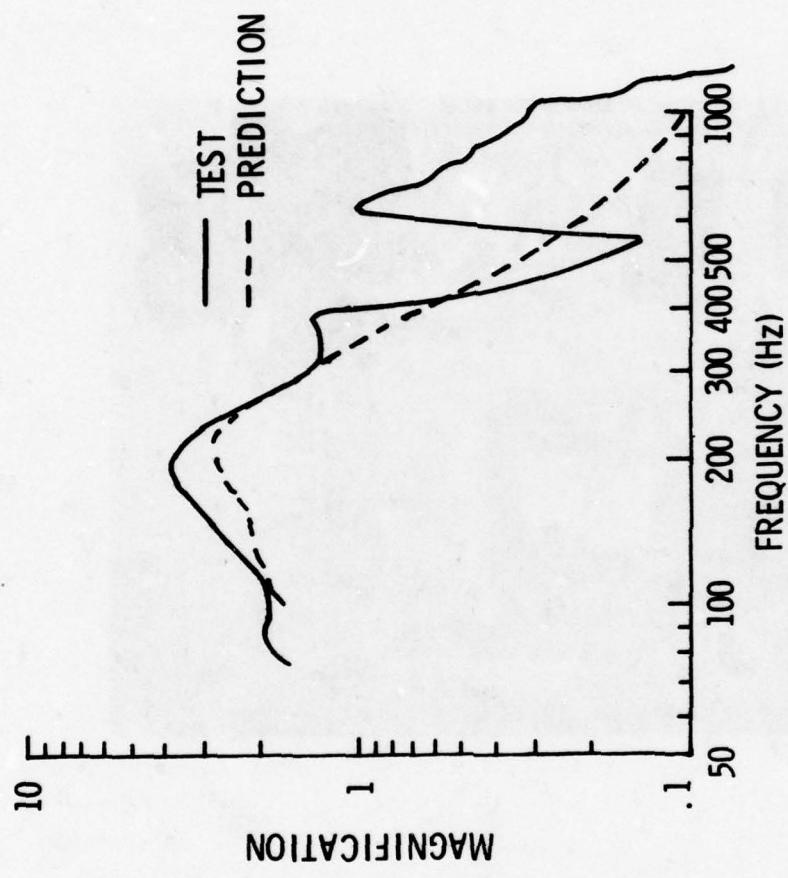


Figure 10. Deck Test Set Up



GOOD AGREEMENT WITH ANALYTICAL PREDICTIONS

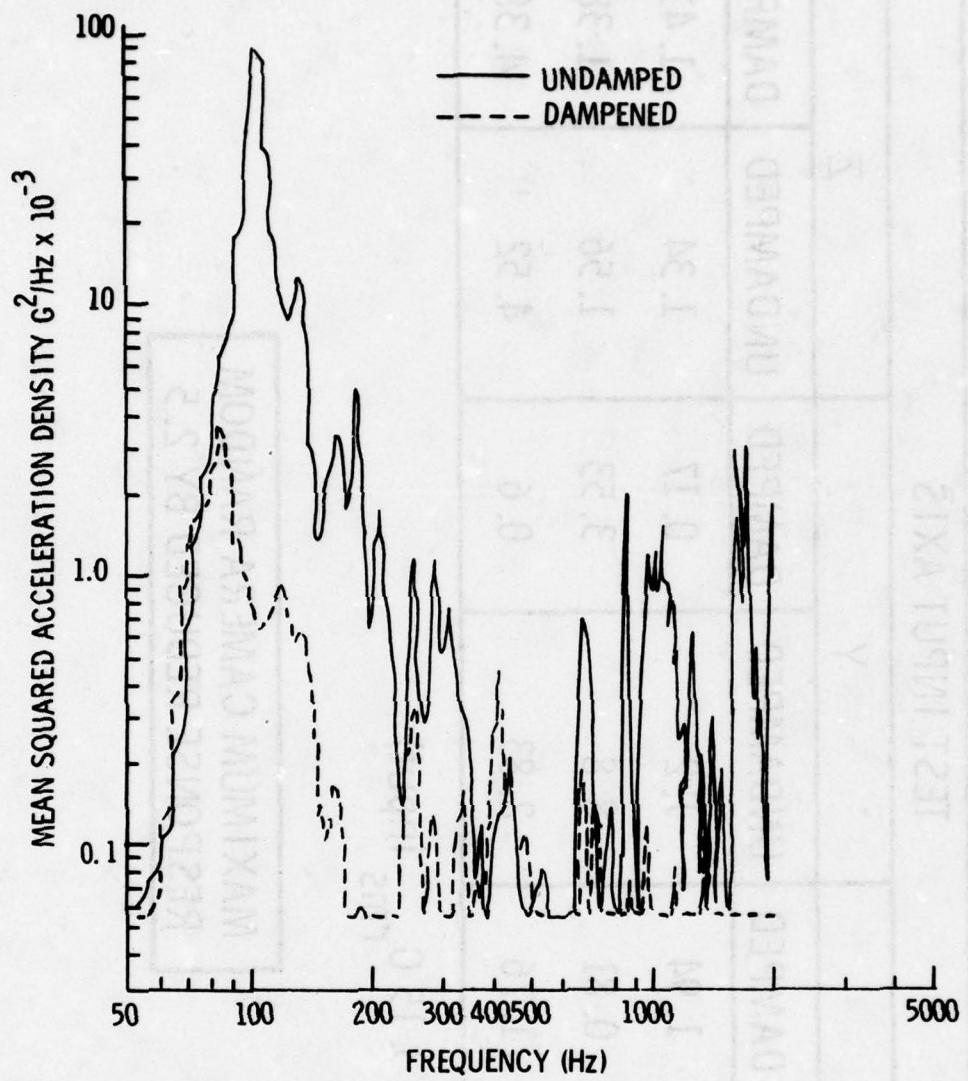
Figure 11. Camera Response on Hard-Mounted Damper Bracket

Table 1. Camera Bracket G_{rms} Response

		TEST INPUT AXIS				
		X	Y	Z		
UNDAMPED	DAMPED	UNDAMPED	DAMPED	UNDAMPED	DAMPED	
4.1	1.94	1.2	0.17	1.34	1.41	
4.2	0.81	8.8	3.53	1.56	1.38	
8.8	1.76	2.83	0.6	4.52	4.38	

(0.005 G^2/Hz ; 3.15 G_{rms} input)

**MAXIMUM CAMERA RANDOM
RESPONSE REDUCED BY 2.5**



PSD REDUCED BY MORE THAN AN ORDER OF MAGNITUDE

Figure 12. Camera Random Vibration Response on Deck

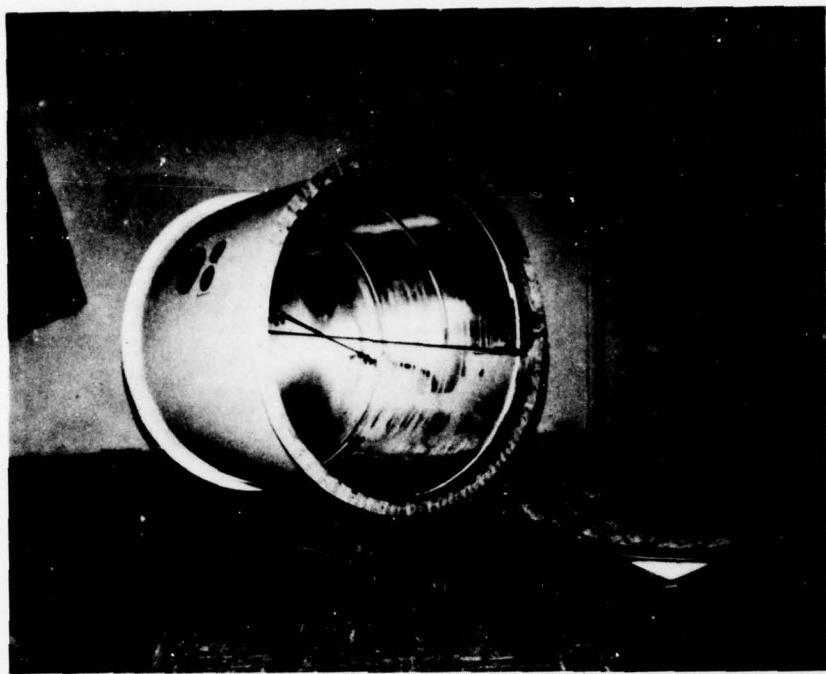


Figure 13. Acoustic Enclosure, One Bulkhead Removed
with the Fiberglass Liner

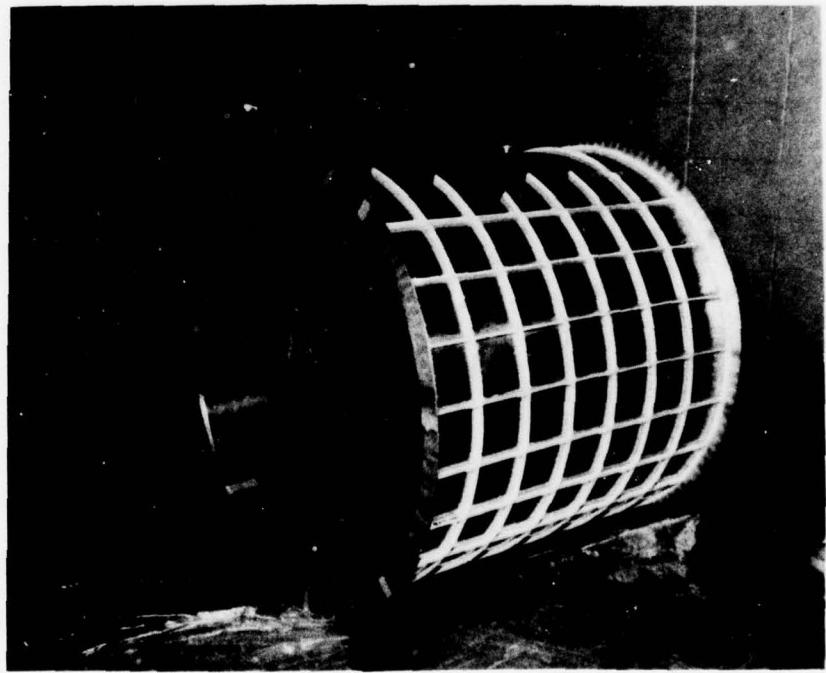


Figure 14. Acoustic Enclosure Cylinder Viscoelastic Epoxy Damping Material Layout

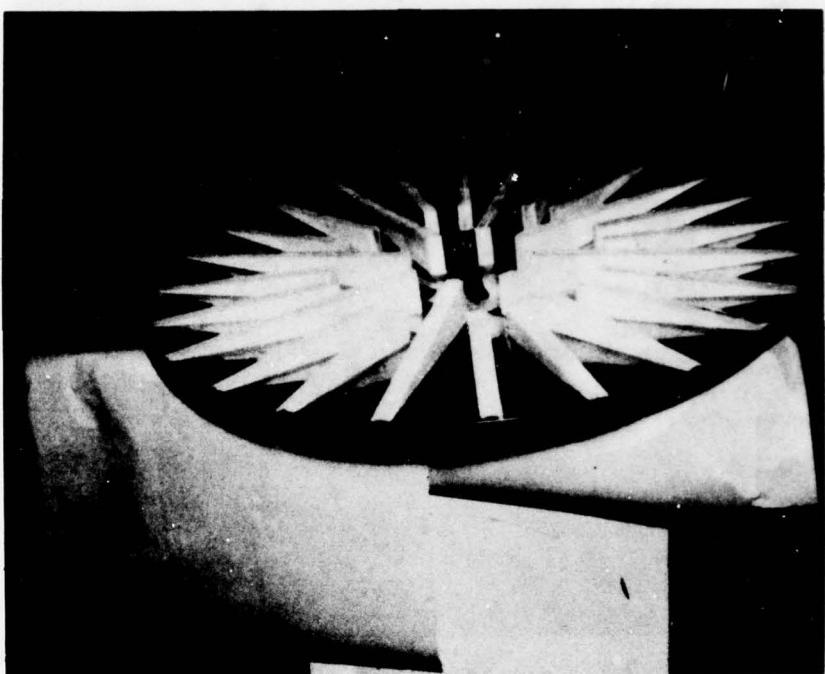


Figure 15. Acoustic Bulkhead Internal Viscoelastic Epoxy Damping Material Layout

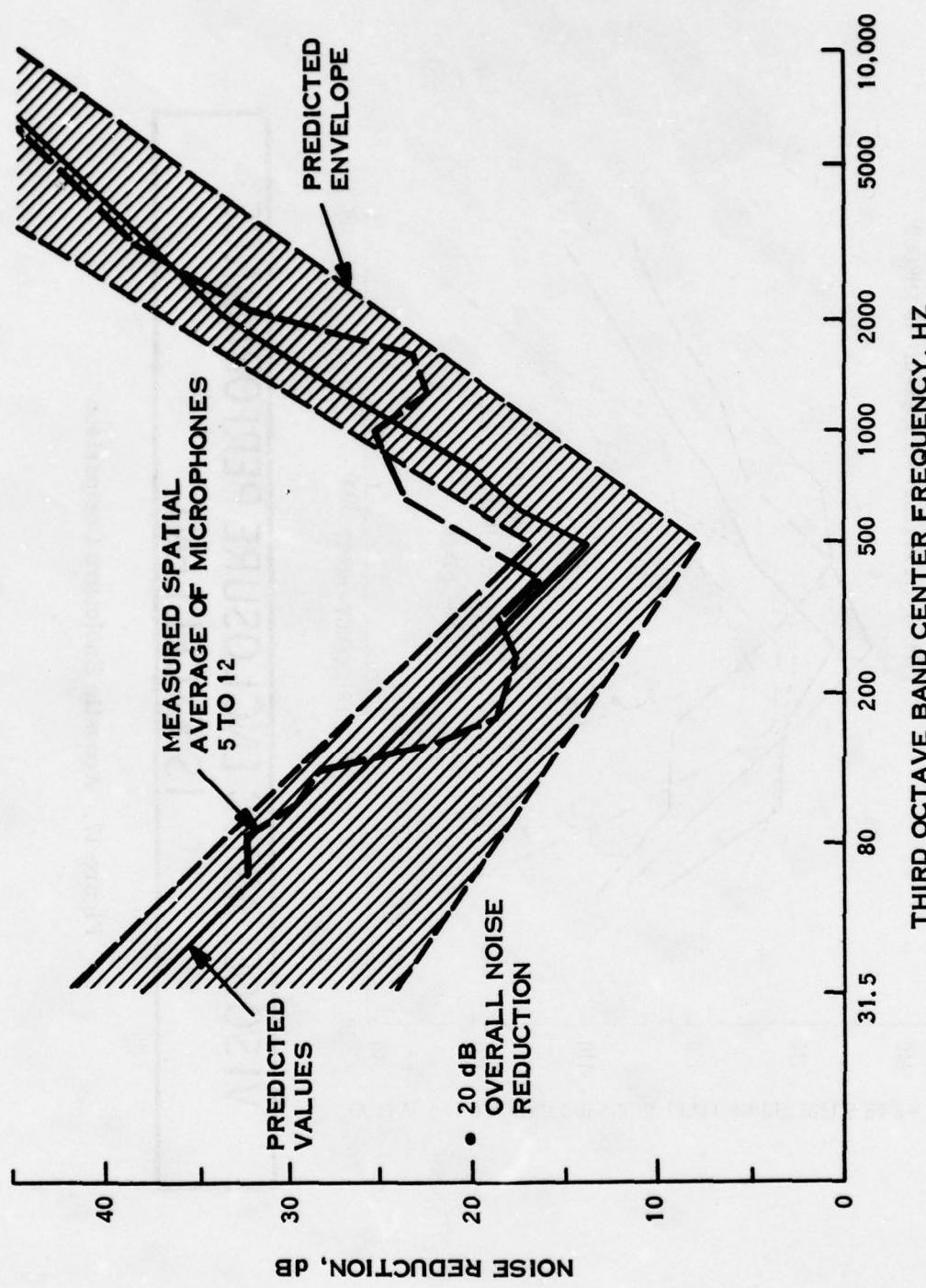
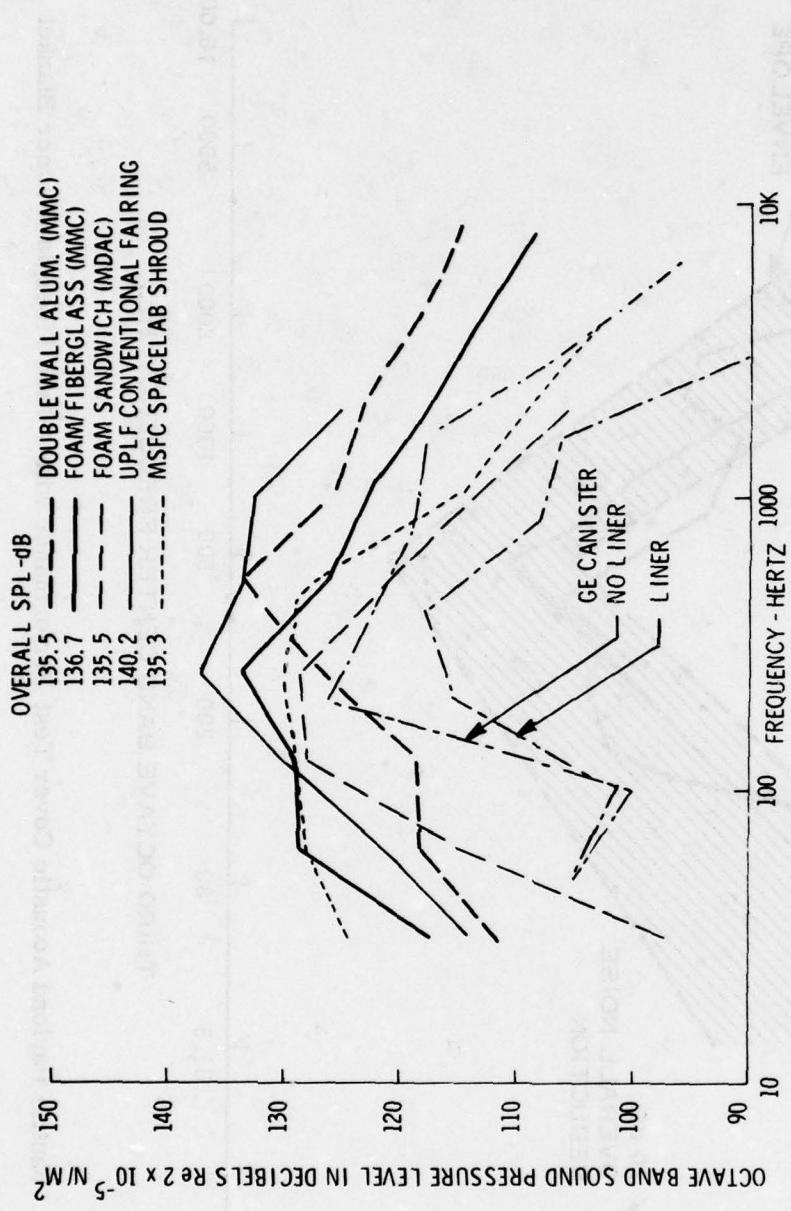


Figure 16. Shuttle Payload Acoustic Cover Test Performance with 1-Inch Fiberglass Liner Blanket



**VISCOELASTIC ENCLOSURE PERFORMANCE
IS EXCELLENT**

Figure 17. Acoustic Enclosure Comparison

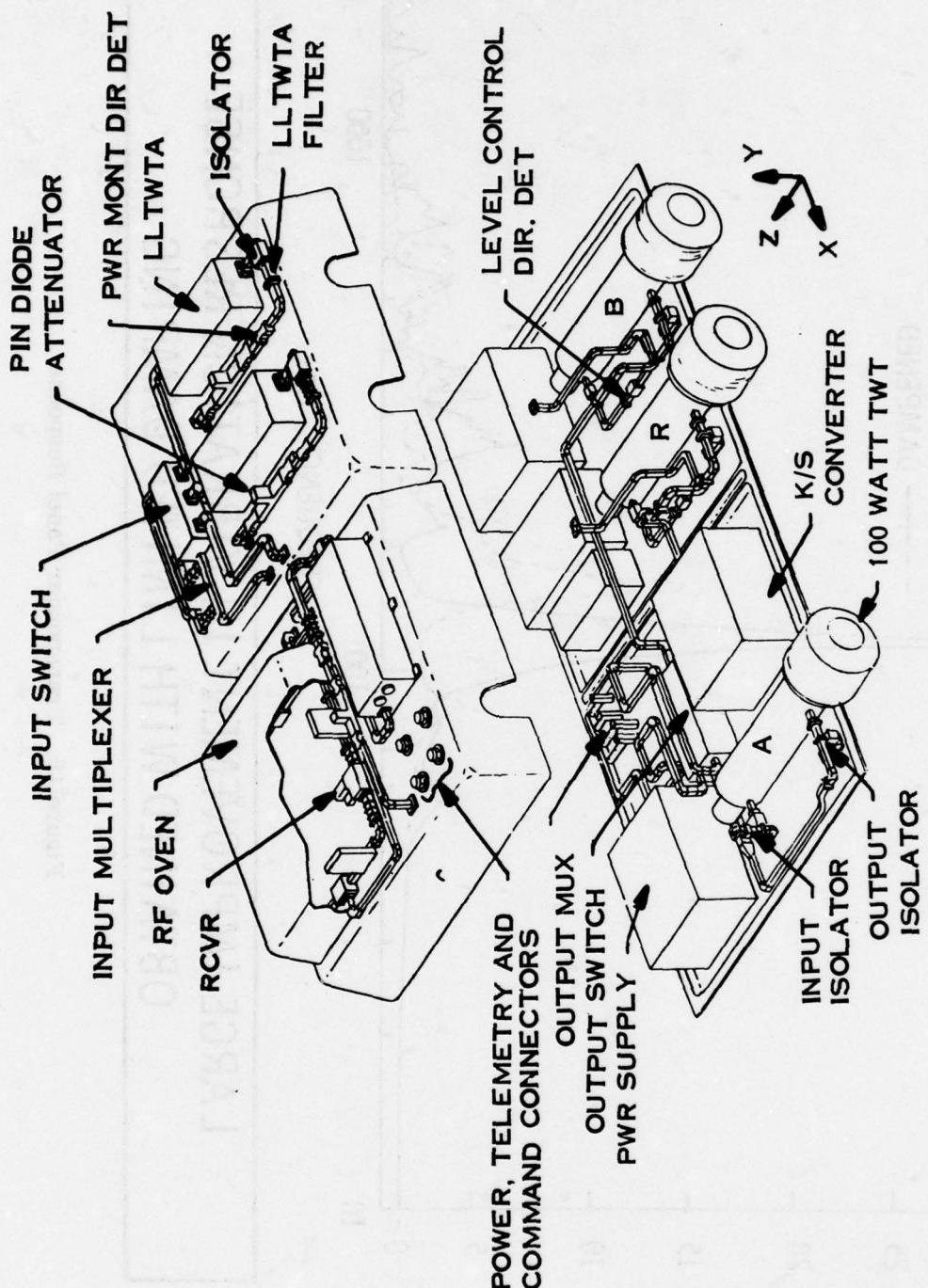
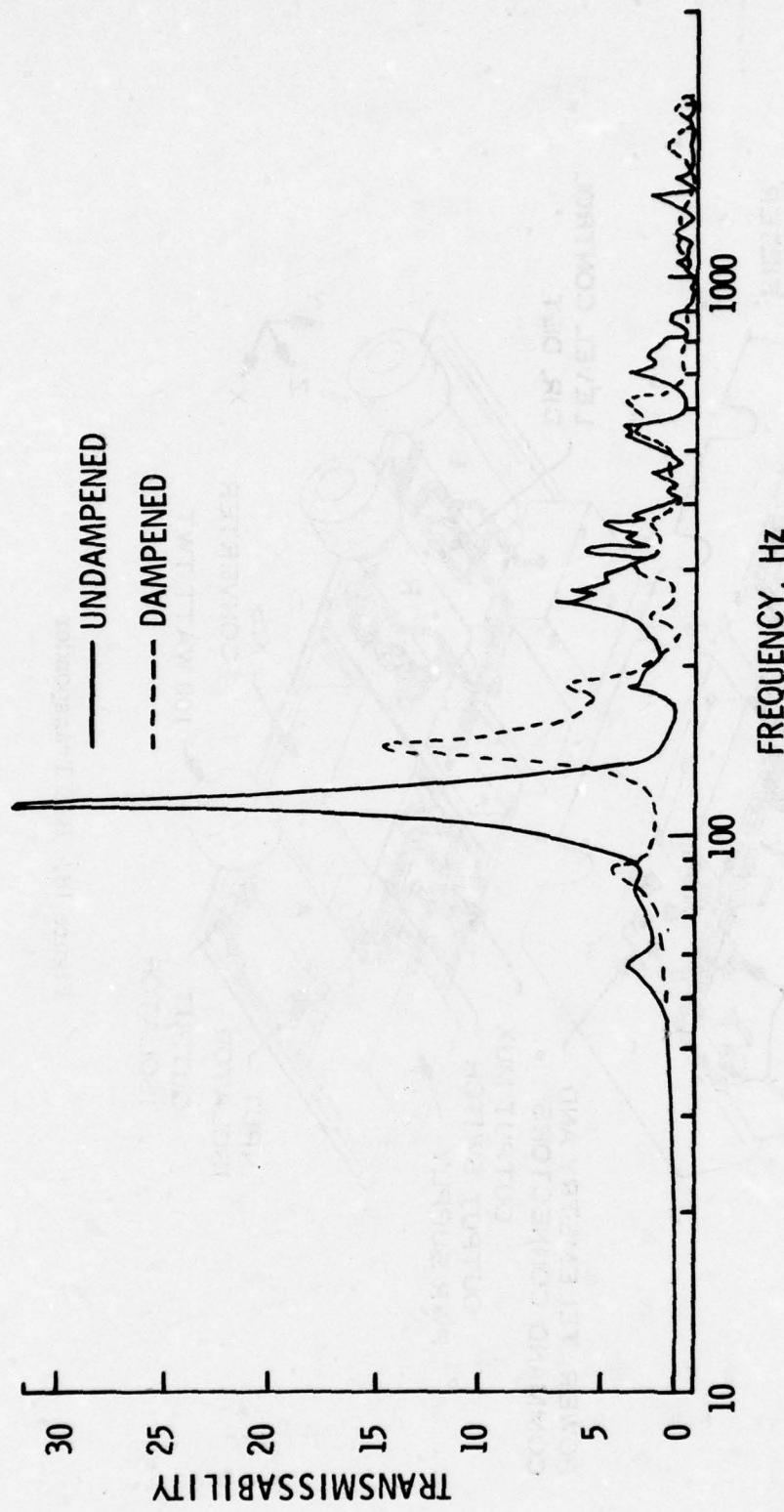
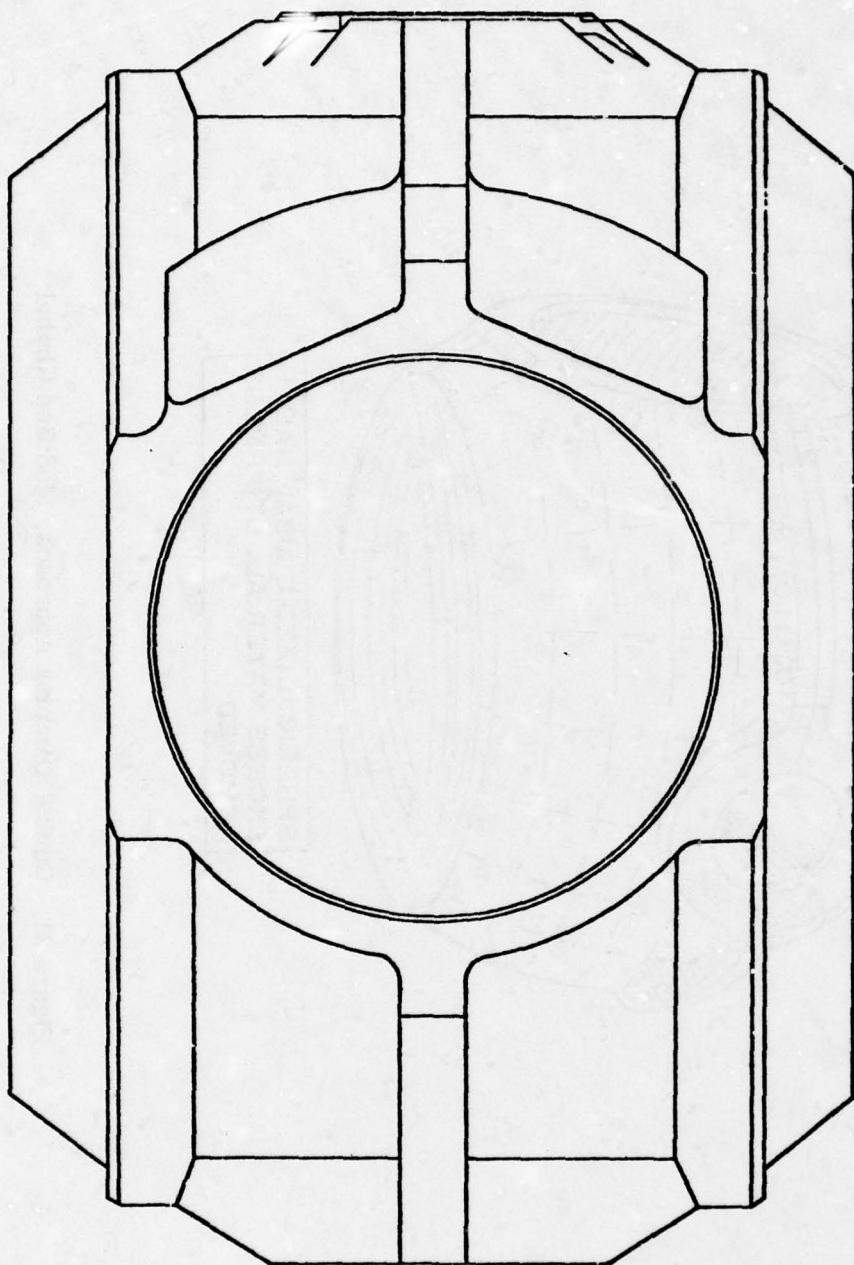


Figure 18. BSE Transponder



LARGE IMPROVEMENT IN VIBRATION RESPONSE
OBTAINED WITH LIMITED DAMPING

Figure 19. Transponder Panel Response



STANDARD DESIGN REQUIRES THICK MATERIAL
AND RINGS FOR STIFFNESS AND STRENGTH

Figure 20. Standard Gimbal

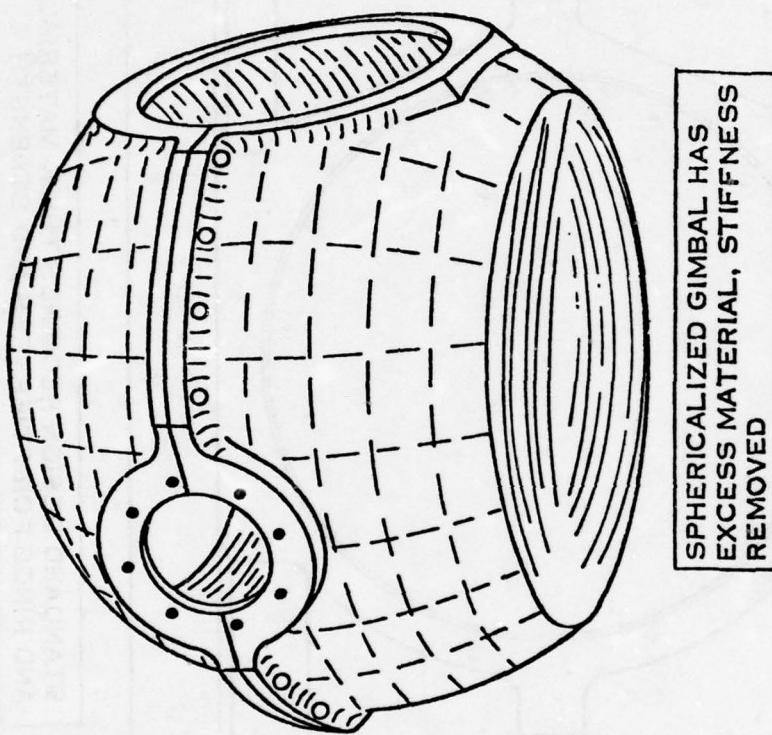


Figure 21. Gimbal Damping Approach, Modified Gimbal

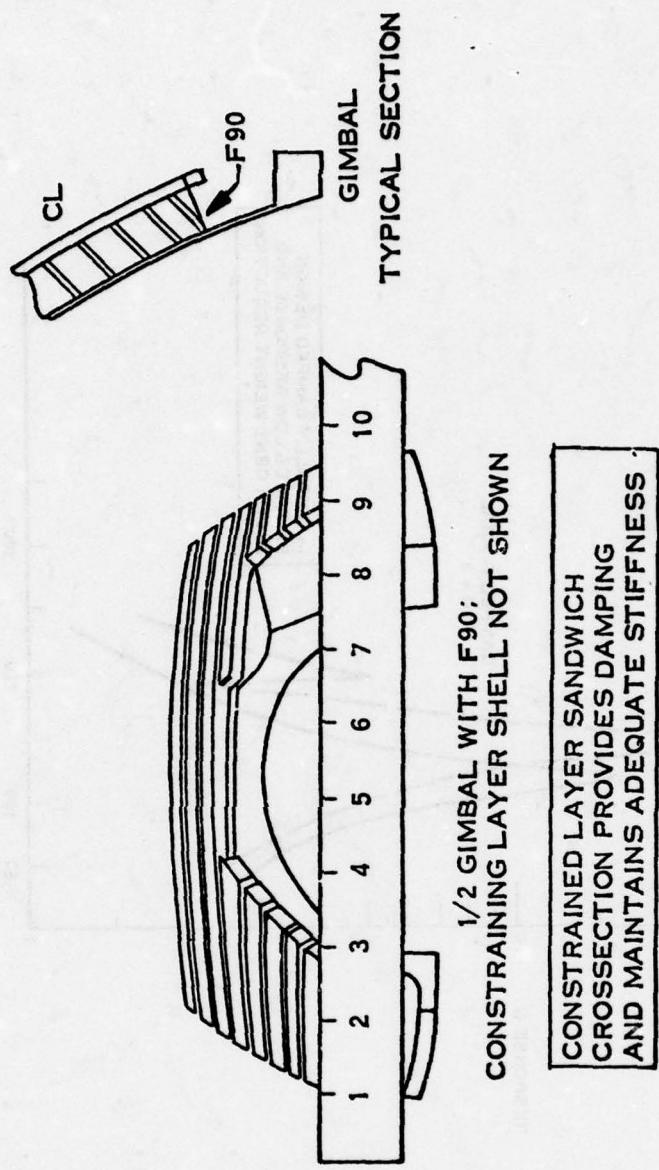


Figure 22. Gimbal Damping Approach Damping Material Layout

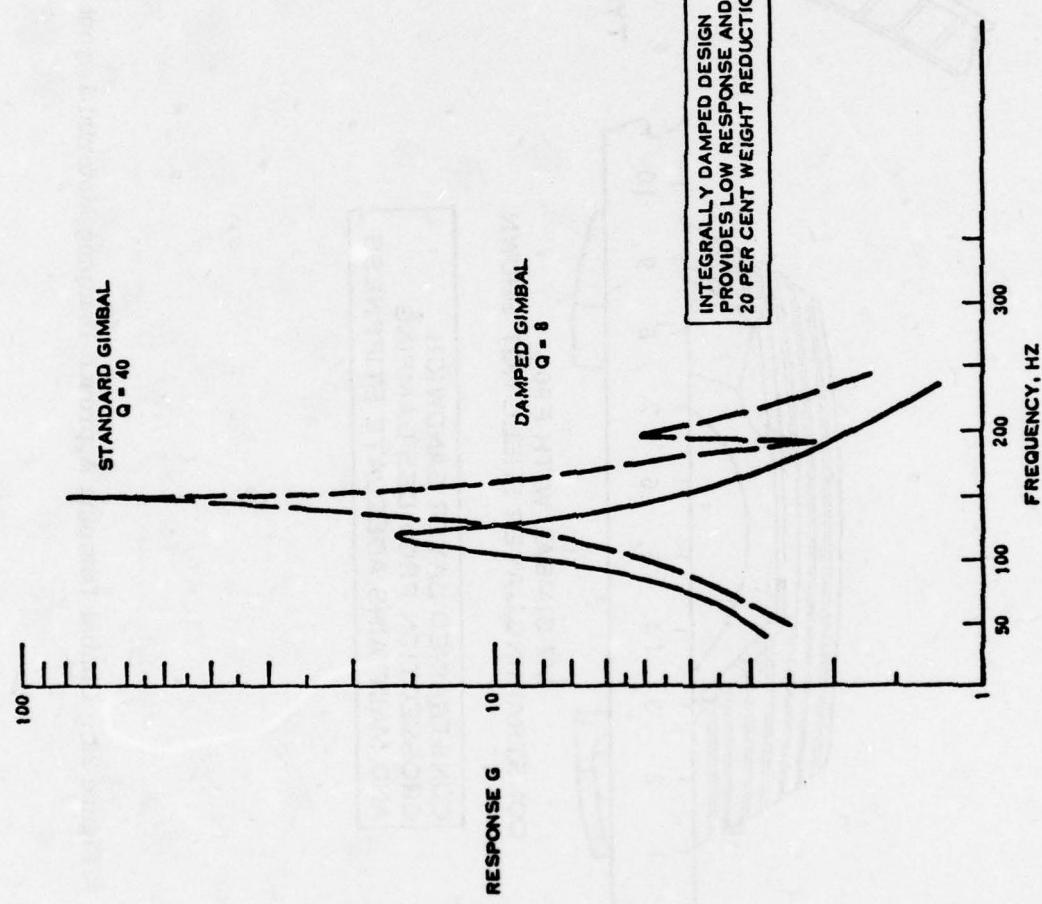
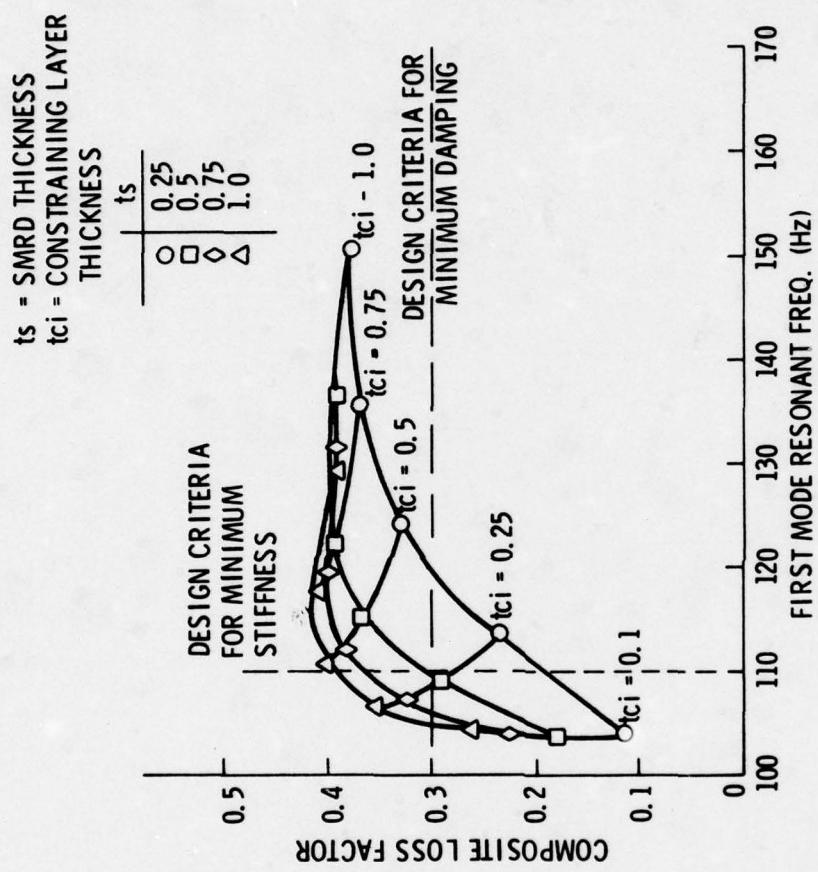


Figure 23. Gimbal Vibration Response for 2G Input



PARAMETRIC VARIATIONS DEFINE DESIGN CONFIGURATION

Figure 24. Design Optimization

THE INFLUENCE OF DAMPING ON
ACOUSTIC TRANSMISSION LOSS OF PANELS

L. L. Faulkner
Battelle, Columbus
Laboratories
Columbus, Ohio

THE INFLUENCE OF DAMPING ON ACOUSTIC TRANSMISSION LOSS OF PANELS

L. L. Faulkner
Battelle, Columbus Laboratories

ABSTRACT

This paper presents an analytical prediction procedure, verified by laboratory measurements, for the prediction of the acoustic transmission loss of panels due to the addition of damping materials. The prediction procedure accounts for the added mass of the damping material and the loss factor of the added damping material.

INTRODUCTION

Sound transmission loss through panels has been traditionally described as being controlled by the stiffness of the panel, the stiffness region, the mass of the panel, the mass region, and the coincident frequency of the panel as illustrated in Figure 1. The addition of damping to a panel is normally considered to influence the transmission loss in the regions of the fundamental panel resonances and the coincident frequency, see Figure 1. Since an added damping material acts as an energy dissipation element in the panel system, an energy analysis will show that the damping material will influence the acoustic transmission loss at frequencies other than the fundamental panel resonances and the coincident frequency. The purpose of this paper is to present the influence of added damping materials in the mass controlled frequency region on the so-called mass-law transmission loss.

TECHNICAL DISCUSSION

The objective is to be able to separate the effect of damping properties of an added material on the transmission loss of a panel from that of the effect of added mass. This means that if the damping loss factor for the added material is available, the transmission loss-versus-frequency curve can be constructed. This can be done using the following equation:

$$\text{T.L.} = \text{field-incidence mass law due to mass of panel} + \text{field-incidence mass law due to mass of damping mat'1.} + \text{transmission loss due to the damping effect of the damping mat'1.}$$

or in the mathematical form:²

$$\begin{aligned} \text{T.L.} = 10 \log_{10} & [1 + \frac{\rho_w}{2 \rho_c}] - 5 + 10 \log_{10} (\frac{\rho_{st}}{\rho_s})^2 \\ & + A \log_{10} (B \omega^2) \end{aligned} \quad (1)$$

where:

- T.L. = field incidence acoustic transmission loss of a panel
in the mass-law region, dB²
 ρ_s = panel surface density, Kg/m²
 ρ = density of air, Kg/m³
 ρ_{st} = panel plus damping material surface density, Kg/m²
 c = speed of sound in air, m/sec
A, B = properties of a particular damping material that
depend on frequency.

The first two terms in Equation (1) are easily found once the masses of the panel and of the damping material are known. The third term can be found from a transmission chamber test by subtracting the first two terms from the so-obtained transmission loss, or this term can be determined from the loss factors of the panel and the loss factor of the panel plus added damping material as follows:

$$\text{transmission loss due to damping added to the panel} = 10 \log_{10} \left(\frac{\eta_c}{\eta_s} \right) \quad (2)$$

where:

- η_c = combined loss factor of the panel plus added material
 η_s = loss factor of panel without added material.

The loss factors may be determined from calculations or from decay rate methods. If the form of Equation (1) is utilized, the constants A and B can be determined for a specific type of added damping material in a specific damping system and then this form becomes a design equation for that particular system. The form of Equation (2) allows the determination of transmission loss from fundamental properties of the panel and damping material.

SUMMARY OF RESULTS

The results for three types of add-on damping systems; unconstrained damping, foam with a self-adhesive damping layer and glass fiber attached to the panel with adhesive, are summarized in Figures 2 through 4. Descriptions of the systems studied are given in Table 1.

The computed transmission loss values were from measured values of loss factor for the base panel and the panel plus damping material using the decay method.

Figure 4 for the panel with a glass-fiber material needs some discussion. Due to the presence of a thin layer (septum) to protect the glass fiber on one side away from the panel, a sandwich-type arrangement was formed which resulted in a constrained layer-type damping system. For this case, the transmission loss expression of Equation (8) results in that an additional noise reduction of 25-30 percent of the field-incidence mass law of the panel was used [1]. This additional transmission loss gave good agreement for the

total noise reduction term that was attributable to the damping effect, the added mass of the damping material, and the additional transmission loss due to the constrained layer system.

CONCLUSIONS

The addition of a damping material to reduce the sound transmitted to the receiving space may result in an increase of the transmission loss of about 2 - 21 dB in the mass law region. The transmission loss can be obtained from a knowledge of the mass per unit area of the panel and of the added damping material in addition to the loss factor due to the added damping material. The effect of the damping loss factor can be determined from a sound transmission chamber or from loss-factor measurements.

REFERENCES

1. Beranek, L. L., Noise and Vibration Control, McGraw-Hill Book Company, New York, 1971.
2. Rajab, M. D., "An Investigation of the Effect of Damping Materials on Noise Transmission", M. Sc. Thesis, The Ohio State University, 1978.
3. DeBoer, S. E., "The Effect of Steel Covers on Impulse Noise Attenuation", M. Sc. Thesis, The Ohio State University, 1972.
4. Klausing, T. A., "An Investigation of Various Design Parameters Relating to the Noise Attenuation of Metal Covers", M. Sc. Thesis, The Ohio State University, 1969.
5. Faulkner, L. L. and Hamilton, J. F., "Vibration and Noise Reduction of Beams and Plates by Use of Boundary Damping and Stiffness", An ASME Paper No. 77-DET-155.
6. Faulkner, L. L., Handbook of Industrial Noise Control, Industrial Press, Inc., New York, 1976.
7. American Society for Testing and Materials, E90-70, Standard Recommended Practice.

APPENDIX A

SUMMARY OF THE PERTINENT EQUATIONS

The equations utilized to develop the transmission loss form given by Equation (1) are summarized as follows:

Transmission Loss Due to Damping

The sound radiated by one side of a continuous system excited by a point force for bending waves in the structure is given by the following (Reference 1)

$$\pi_{rad} = \frac{F^2_{rms} \rho c \sigma_{rad}}{Z \rho w \eta_s} f \quad \text{watts,} \quad (3)$$

Z = input impedance for a point force.

The sound power level is given by

$$L_w = 10 \log_{10} \frac{\pi_{rad}}{\pi_{ref}} \quad \text{dB.} \quad (4)$$

The difference in sound power level (which, in most cases, can be considered a change in sound pressure level) for the case of damping uniformly applied over a panel is given by the following relation:

$$\begin{aligned} \Delta L_w &= \Delta L_p = L_{wc} - L_{ws} \\ &= 10 \log_{10} \frac{\pi_c}{\pi_{ref}} - 10 \log_{10} \frac{\pi_s}{\pi_{ref}} \\ &= 10 \log_{10} \frac{\pi_c}{\pi_s}, \end{aligned} \quad (5)$$

where:

- L_{wc} = the sound pressure level for the case of no damping
- L_{ws} = the sound pressure level for the case of added damping
- π_c = power radiated with damping
- π_s = power radiated without damping.

By substituting Equation (3) into Equation (5), the difference in sound pressure level or noise reduction is found to be:

$$T.L. = \Delta L_w = \Delta L_p = 10 \log_{10} \frac{\eta_c}{\eta_s} = 10 \log_{10} \frac{2\xi}{\eta_s} \quad (6)$$

where:

T.L. = noise reduction due to damping

η_c = loss factor for a damped panel

η_s = internal loss factor for steel panel where

$$10^{-4} < \eta_s < 10^{-2}$$

ξ = damping ratio (note $2\xi = \eta$).

In the foregoing result, the small shift in maximum response due to change in damped natural frequency has been neglected which is valid, provided acoustic information is desired in octave bands or one-third octave bands.

From Equation (6), a knowledge of the loss factor or damping ratio the change in sound pressure level can be determined.

Relation of Field Incidence to Normal Incidence

From Reference [1]:

$$R_o = 10 \log_{10} \left[1 + \left(\frac{\omega p}{2\rho_s} \right)^2 \right] \text{ dB}, \quad (7)$$

where:

R_o = normal incidence mass law, dB

ρ_s = panel surface density, Kg/m^2

ρ = density of air, Kg/m^3

c = speed of sound in air m/sec

$\rho c = Z_a$ = acoustic impedance of air, $\text{Kg/m}^2 \text{ sec.}$

From Reference [1]:

$$R_f = R_o - 5 \text{ dB}, \quad (8)$$

where:

R_f = field incidence mass law, dB

R_o = normal incidence mass law, dB

This is used for $R_o \geq 15$ dB and gives a diffuse field with a limiting angle of about 78° .

Influence of Added Damping Mass

If a material is added to a panel, then the additional noise reduction due to the mass of the added material is given by

$$\delta R_f = [R_f]_{\text{total}} - [R_f]_{\text{original}}$$

$$\delta R_f = 10 \log \frac{\left[1 + \left(\frac{\omega p}{2\rho_s} st / 2\rho c \right)^2 \right]}{\left[1 + \left(\frac{\omega p}{2\rho_s} / 2\rho c \right)^2 \right]} \quad (9)$$

$$\delta R_f = 20 \log \left(\frac{\rho_s st}{\rho} \right),$$

where:

$$\rho_{st} = \text{total surface density, Kg/M}^2$$
$$\rho_s = \text{original panel surface density, Kg/m}^2.$$

Loss Factor

Determination of the loss factor (η):

$$\eta = \frac{d}{27.3 \times f_n} \quad (10)$$

where:

d = decay rate (dB/sec)

f_n = natural frequency at the desired frequency range (Hz).

This form was utilized to measure the loss factor for the plate and the plate plus added damping material for use in Equation (1).

TABLE 1: DESCRIPTION OF THE PANELS USED IN THIS INVESTIGATION

Panel Number	Description
1	Bare steel plate.*
2	Plate with an added unconstrained material applied to one side
3	Plate with a 1-in. foam-type damping material applied to one side by a self-adhesive layer
4	Plate with a 1-in. glass fiber layer applied to one side with adhesive

(*) Steel panel .031 inches thick with a 4 sq. ft. area treated in the damping experiments.

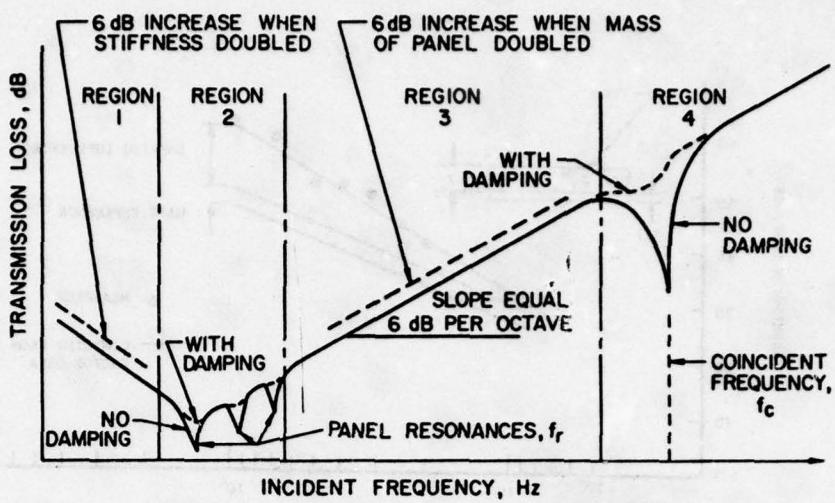


FIGURE 1. TYPICAL ACOUSTIC TRANSMISSION-LOSS VERSUS FREQUENCY RELATION FOR A PANEL

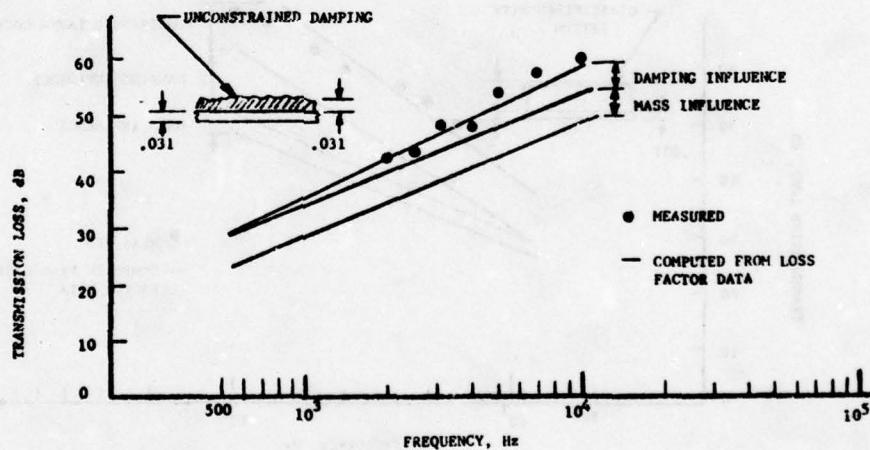


FIGURE 2. COMPARISON OF MEASURED AND COMPUTED TRANSMISSION LOSS OF AN UNCONSTRAINED DAMPING TREATMENT EQUAL TO THE PANEL THICKNESS

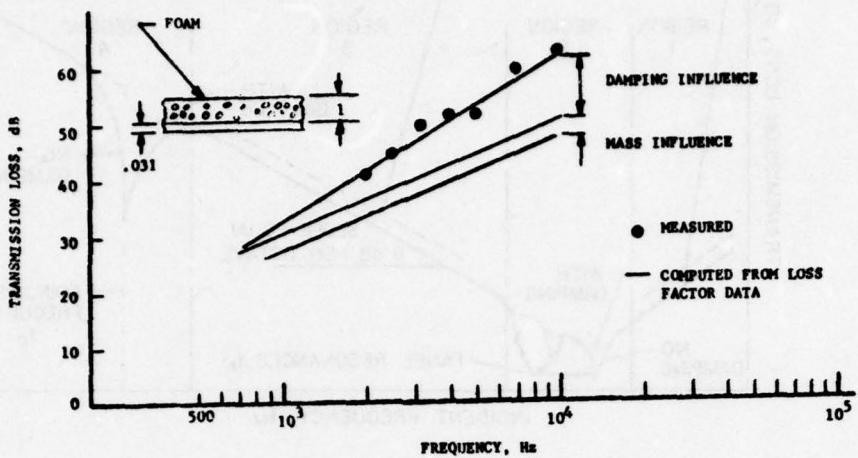


FIGURE 3. COMPARISON OF MEASURED AND COMPUTED TRANSMISSION LOSS OF A ONE-INCH FOAM-DAMPED DAMPING TREATMENT

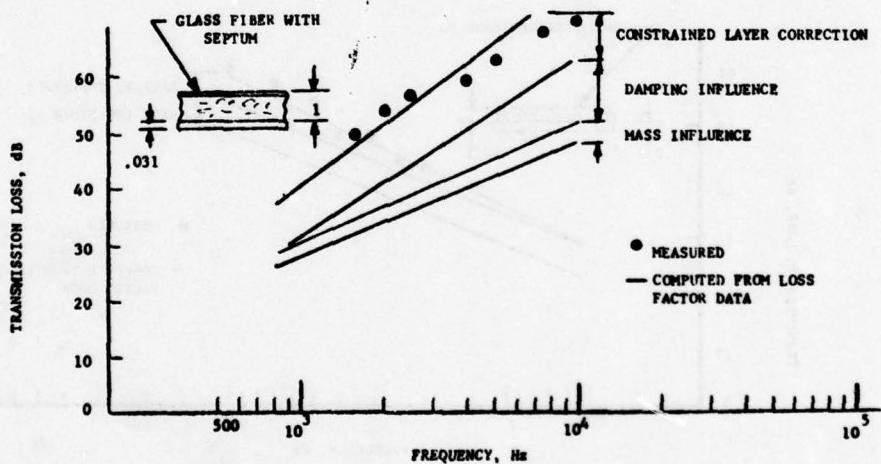


FIGURE 4. COMPARISON OF MEASURED AND COMPUTED TRANSMISSION LOSS OF A ONE-INCH GLASS FIBER DAMPING WITH A CONSTRAINING SEPTUM LAYER

VIBRATION REDUCTION OF AIRBORNE OPTICAL SYSTEM
USING LIGHT WEIGHT CONSTRAINING
DAMPING TECHNIQUE

C. P. Lui
Hughes Aircraft Company
Laser Division
Culver City, California

VIBRATION REDUCTION OF AIRBORNE OPTICAL SYSTEM
USING LIGHT WEIGHT CONSTRAINING
DAMPING TECHNIQUE

By

Chang P. Liu

Hughes Aircraft Company, Culver City, California

ABSTRACT

Structural vibrations in the range of 150 to 500 Hz caused by servo systems had introduced an unacceptable degradation in the pointing of a laser beam from a precision airborne pointing and tracking system.

These problems were greatly relieved by the application of constrained layer viscoelastic damping to the housing structure as well as to its critical autoalignment mechanism of this optical system. It had been observed that the overall damping characteristics of the treated structure was close to the theoretical prediction of the design analysis. Improvement in damping efficiency of more than an order of magnitude for the primary mode of vibration has been confirmed.

LIST OF SYMBOLS

A = Maximum Angular Displacement of Mirror Support (radian)

B = $1/12 EH^3$ = Flexural Stiffness (lb-in)

d = Diameter (in)

E = Young's Modulus (lb/in²)

G = Shear Modulus (lb/in²)

H = Thickness (in)

I = Area Moment of Inertia (in⁴)

J = Mass Moment of Inertia (lb-in-sec²)

K = EH = Extensional Stiffness (lb/in)

l = Length (in)

p = Wave Number of Elastic Deformation (in⁻¹)

Q = Quality Factor (Amplification Factor) (Dimensionless)

V = Volume (in^3)

X = Shear Parameter (Dimensionless)

Y = Geometrical Parameter (Dimensionless)

β = Loss Factor of Shear Modulus of Material (Dimensionless)

η = Loss Factor of Composite Plate or System

δ = Deflection of Structural Element (in)

μ = Mass Density/Unit Area ($\text{lb}\cdot\text{sec}^2/\text{in}^3$)

γ = Shear Deformation (Radian or Dimensionless)

λ = Length of Elastic Wave (in)

ω = Angular Frequency (rad/sec)

ζ = Damping Ratio (Dimensionless)

INTRODUCTION

For optical pointing/tracking systems built for high resolution and fast response, materials with high stiffness are usually used. Before damping materials were added to the system, damping was entirely due to structural damping. Vibrational energy was dissipated at structural joints and interfaces. Component damping such as internal friction or hysteretic damping had very little overall contribution to the dissipation process.

During initial servo test, it was found that the optical beam oscillation caused by structural vibration excited by the servo motors was excessive. The need for vibration attenuation became apparent in order to achieve functional requirement for this precision pointing and tracking system.

Because of the number of degrees of freedom involved in the mechanical structure, it was decided that the use of viscoelastic material would be the most practical method for this application. It was believed that a passive damping technique would be least risky since in general energy dissipation tends to stabilize the mechanical motion.

PART 1. VIBRATION OF REFERENCE MIRROR

The reference mirror is presently bonded on 12 flexible finger supports. Any rotational disturbance about either the azimuth axis or elevation axis can excite this annulus mirror in such a way that the mirror cell will respond in a warping mode. Bending stiffness of this mode for the ring is less than the stiffness with respect to its in-plane bending mode. (See Figure 1.)

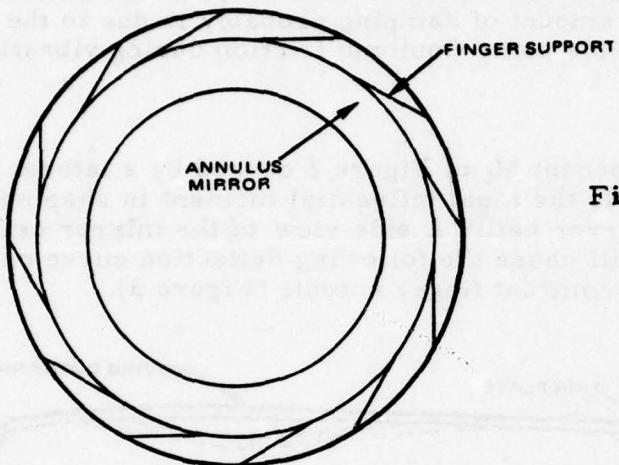


Figure 1. Schematic of annulus mirror and its cell.

1.1 ENERGY OF VIBRATION

Maximum kinetic energy of the vibrating annulus reference mirror can be expressed as

$$K.E. = \frac{1}{2} J \omega_n^2 A^2$$

where

$$J = \text{mass moment of inertia} = \frac{1}{2} m \bar{R}^2$$

$$= \frac{1}{2} \frac{40}{386} (13)^2 = 8.75 \text{ in-\#-s}^2$$

$$\omega_n = \text{resonance freq. of cell}$$

$$= 140 \text{ Hz} \quad (\text{Direct Observation})$$

$$A = \text{Amplitude} = 10^{-3} \text{ rad} \quad (\text{Direct Observation})$$

$$\therefore K.E. = \frac{1}{2} (8.75) (2\pi \times 140)^2 (10^{-3})^2 = 3.38 \text{ in-\#}$$

The actual amount of vibrational energy is not really large.

However, in the absence of adequate damping, the kinetic energy will increase continuously under a resonance condition when the support structure keeps on feeding energy into the mirror cell. During a previous autoalignment test a Q of about 160 was reported. This means that

$$\zeta_{eq.} = \frac{1}{2Q} = \frac{1}{2(160)} = 0.0031$$

which appears to be the case since this mirror cell is made of aluminum with rigidly bonded interfaces. The amount of damping probably is due to the three mounting studs which provide some Coulomb friction during vibration.

1.2 DAMPER DESIGN

We believe that the component M_t of Figure 2 caused by a lateral motion of the reference mirror is the most influential moment in shaping the mode of vibration of this mirror cell. A side view of the mirror cell flange shows that this loading will cause the following deflection curve on the side of the mirror cell with intermittent finger cutouts (Figure 3).

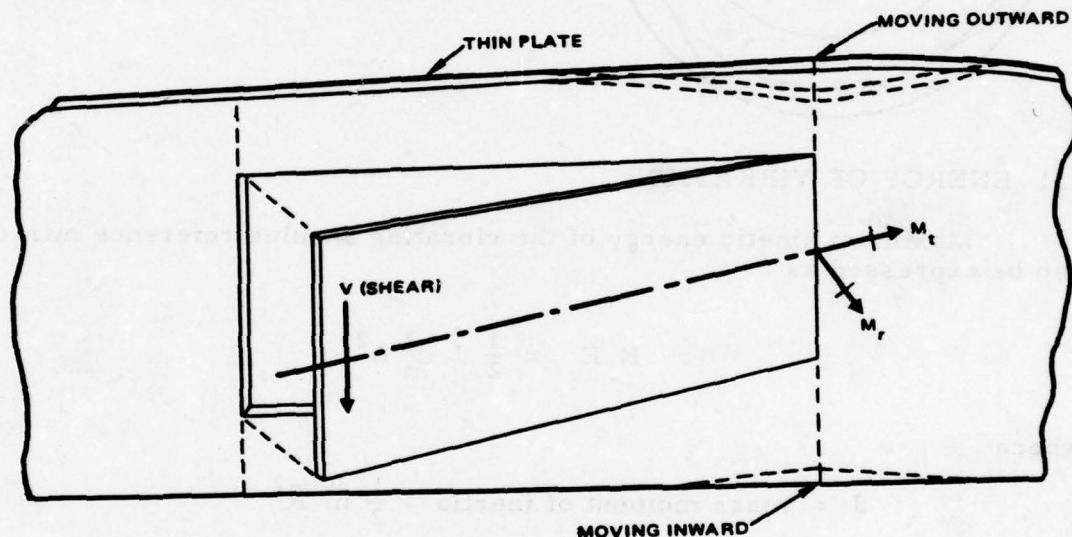


Figure 2. Moments transmitted to cell due to inertial load of reference mirror.

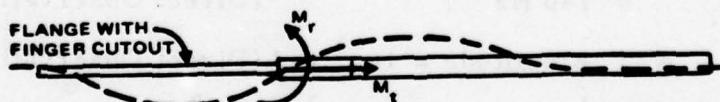


Figure 3. Vibrational deformation of cell flange.

For the reference ring modification, it was suggested that the mounting flange of the cell first be stiffened by an added structural ring. The damper spacer should be designed to transmit mostly shear forces by using "T" shaped cross sections, so that the overall flexibility of the mirror cell will be modified to raise both its natural frequency and damping.

Overall thickness of the damper ring is limited to about 0.110 inch due to the availability of installation space. A reasonable thickness of bonding material must be provided between the mirror cell and the spacer. Thus the different layers of the damper ring will be designed according to Figure 4.

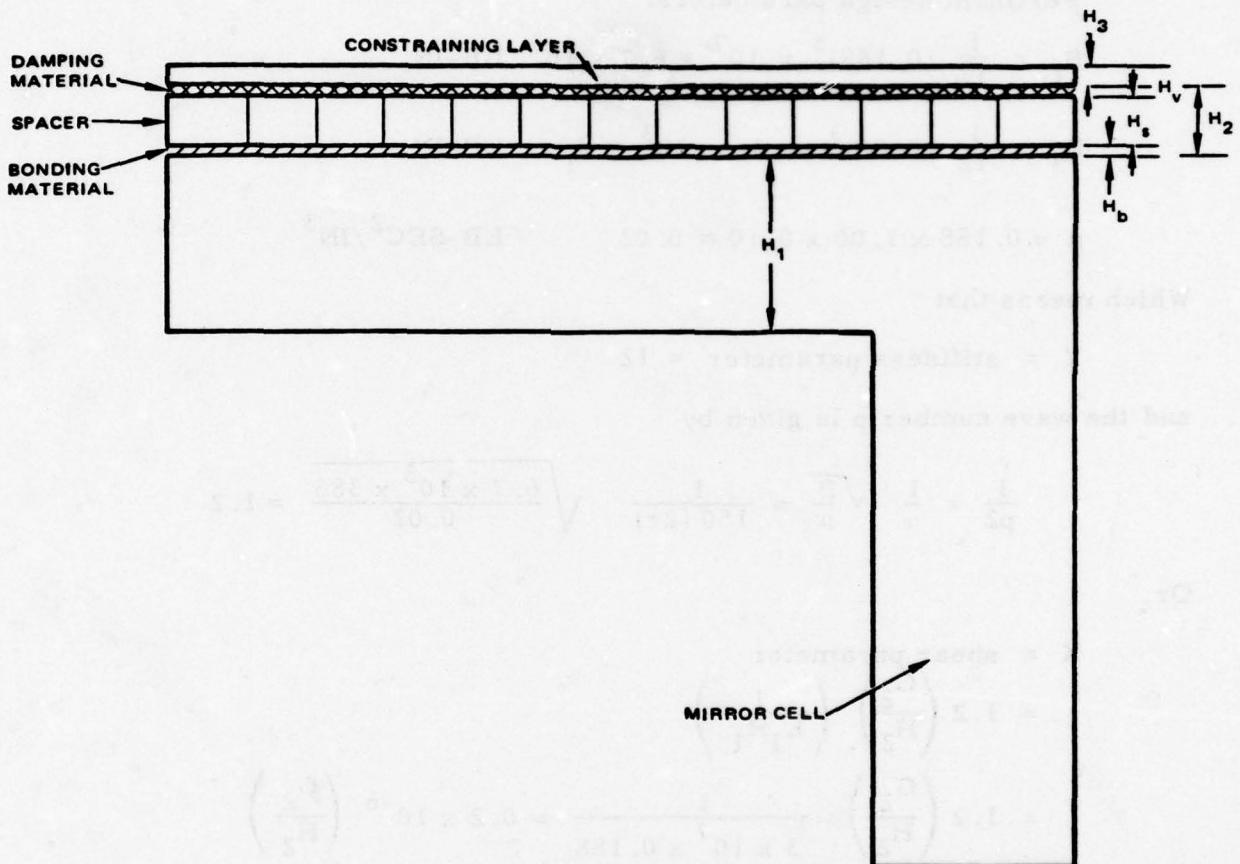


Figure 4. Schematic representation of the damper ring design.

with

$$H_1 = \text{cell thickness} = 0.188 \text{ inch}$$

$$H_b = \text{bond thickness} = 0.005 \text{ inch}$$

$$H_s = \text{spacer height} = 0.080 \text{ inch}$$

$$H_v = \text{thickness of visco-elastic layer} = 0.005 \text{ inch}$$

$$H_2 = t_b + t_s + t_v = 0.090 \text{ inch}$$

$$H_3 = \text{thickness of constraining layer} = 0.020 \text{ inch}$$

Pertinent design parameters:

$$B_1 = \frac{1}{12} (0.188)^3 \times 10^7 \approx 6.7 \times 10^3 \text{ LB-IN}$$

$$B_3 = \frac{1}{12} (0.02)^3 \times 3 \times 10^3 \ll B_1 \text{ LB-IN}$$

$$\mu \approx 0.188 \times 1.00 \times 0.10 \approx 0.02 \text{ LB-SEC}^2/\text{IN}^3$$

Which means that

$$Y = \text{stiffness parameter} \approx 12$$

and the wave number p is given by

$$\frac{1}{p^2} = \frac{1}{\omega} \sqrt{\frac{B}{\mu}} \approx \frac{1}{150(2\pi)} \sqrt{\frac{6.7 \times 10^3 \times 386}{0.02}} \approx 1.2$$

Or,

$$X = \text{shear parameter}$$

$$= 1.2 \left(\frac{G_2}{H_2} \right) \left(\frac{1}{E_1 H_1} \right)$$

$$= 1.2 \left(\frac{G_2}{H_2} \right) \frac{1}{3 \times 10^7 \times 0.188} \approx 0.2 \times 10^{-6} \left(\frac{G_2}{H_2} \right)$$

By using Lord LR3-606 urethane material, we have chosen

$$G_2 \approx 12,500 \text{ psi}$$

and

$$H_2 = 0.010 \text{ inch}$$

This gave us $X \approx 0.25$ for optimal damping.

And the best loss factor can be obtained would be

$$\eta_{\max} = \frac{\beta_2 Y}{2 + Y + \frac{2}{X_{\text{opt}}}} \approx \frac{12 \beta_2}{2 + 12 + \frac{2}{0.25}} \approx 0.545 \beta_2$$

Assuming that

$$\beta_2 = \text{Damping material loss factor} \approx 0.50$$

it gives

$$\eta_{\max} = 0.27$$

Consequently

$$Q_{\text{Damped}} = \frac{1}{\eta} = 3.70$$

Thus an amplitude reduction of

$$\frac{Q_{\text{Undamped}}}{Q_{\text{Damped}}} = \frac{160}{3.70} \approx 43$$

times can be achieved.

1.3 TEST RESULT

Based on this analysis, the mirror cell was bonded at 12 places to the damping material and spacer. It covered about 30 percent of the surface area of the cell. Typical results showed that

$$Q_{\text{Damped}} \approx 16.8$$

$$\zeta \approx 0.029$$

Figures 5 and 6 are oscilloscope photographs which represent the unmodified and modified assembly respectively, and clearly demonstrate the benefit of constraining layer damping for position stabilization.

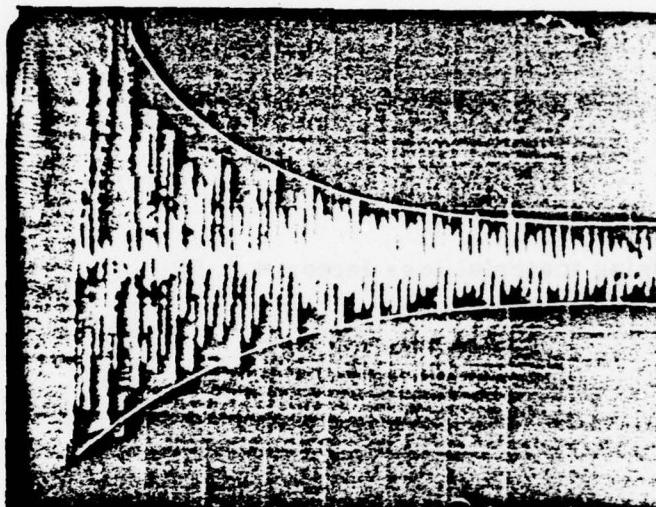


Figure 5. Vibration of mirror in cell before treatment $Q = 140$, $\zeta = 0.0036$.

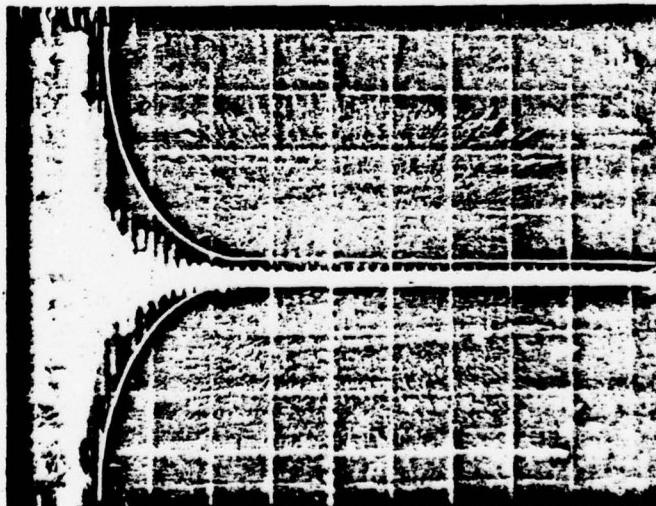


Figure 6. Damped vibration after treatment $Q = 16.8$, $\zeta = 0.029$.

PART 2. BEAM EXPANDER DAMPING

Because of the aperture size, acoustic excitation on the order of 200 Hz seems to become a source of sustaining disturbance.

Under operational conditions:

1. Vibrational frequency range of 150 ~ 250 Hz
2. Temperature range of 40°F ~ 140°F.

Results calculated in this report are based on optimum conditions. It is expected that:

1. $Q_{Front} \approx 4.0$
2. $Q_{Back} \approx 3.0$
3. $Q_{Mid-section} \approx 9.0$

Since vibrational energy induced at any source will be transmitted to all parts of the entire structure and attachments, overall damping efficiency may be estimated to be

$$Q_{overall} \sim 5.0$$

As temperature drops or as vibrational frequency of some part is increased due to local stiffeners, the damping efficiency will be reduced. It is estimated that the overall efficiency of energy dissipation may be represented by the following range of quality factor.

$$5.0 \leq Q_{overall} \leq 8$$

2.1 FRONT RING

Design Parameters:

$$\frac{1}{Y} = \frac{B_1 + B_3}{H_{31}^2} \left(\frac{1}{k_1} + \frac{1}{k_3} \right)$$

with,

$$B_1 = \frac{1}{12} EH_1^3 , \quad k_1 = EH_1$$

$$B_3 = \frac{1}{12} EH_3^3 , \quad k_3 = EH_3$$

$$\frac{H_3}{H_1} = \frac{1.1}{0.75} = 1.47$$

$$H_{31} = \frac{1}{2}(H_1 + H_3) + 0.10 = 0.93$$

thus,

$$\begin{aligned}\frac{1}{Y} &= \frac{(1 + 1.47^3)H_1^3}{12(1.03)^2} \left(\frac{1}{H_1} + \frac{1}{H_1} \frac{H_1}{H_3} \right) \\ &= \frac{1}{12} \frac{1 + 1.47^3}{(1.03)^2} (0.75)^2 (1 + 0.68) = 0.31\end{aligned}$$

or,

$$Y = 3.23$$

Material Selection

Using Dyad 606 of the Souncoat Company, with damping properties

$$\beta_{\min} \approx 0.50$$

$$\beta_{\max} \approx 0.67$$

This means that

$$X_{\text{optimal}} = 0.45$$

and

$$X_{\text{optimal}} = 0.40$$

The construction of the front ring (Figure 7) most likely will result in one complete wave between each two adjacent strut supports, which lead us to assume

$$\lambda = \frac{1}{3}(\text{circumference}) = \frac{1}{3}\pi d \approx 25 \text{ inches}$$

consequently,

$$\frac{1}{P} \approx \frac{25}{2\pi} = 4.17$$

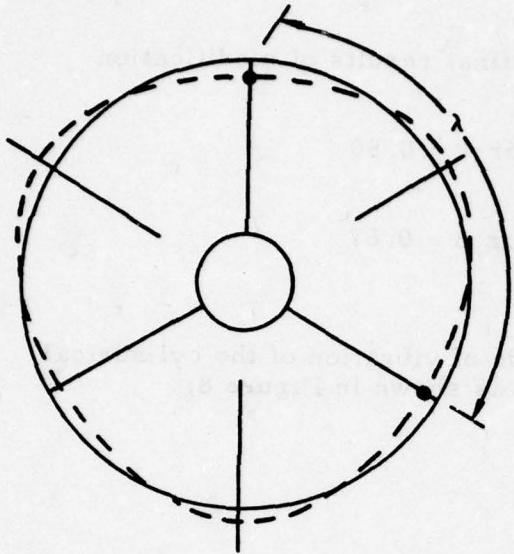


Figure 7. Bending of front ring.

By taking an average value of $X \approx 0.42$, we obtain

$$\begin{aligned}
 X &= \frac{1}{\left(\frac{1}{p}\right)^2} \frac{G_2}{H_2} \left(\frac{1}{E_1 H_1} + \frac{1}{E_3 H_3} \right) \\
 &\approx 17.4 \left(\frac{G_2}{H_2} \right) \left(\frac{1}{10^7} \right) \left(\frac{1}{0.75} + \frac{1}{1.10} \right) \\
 &= 3.90 \times 10^{-6} \left(\frac{G_2}{H_2} \right) \approx 0.42
 \end{aligned}$$

which means that it requires

$$\frac{G_2}{H_2} = 108,000 \text{ lb/in}^2/\text{in}$$

The choice of Soundcoat Dyad 606 with

$$G_2 \approx 10,000 \text{ psi}$$

and

$$H_2 = 0.10 \text{ in}$$

appears to be in good order. From these the final results of modification will be:

$$Y \approx 3.23 \text{ and } \left\{ \begin{array}{l} \eta = 0.20 \text{ for } \beta = 0.50 \\ \eta = 0.28 \text{ for } \beta = 0.67 \end{array} \right.$$

2.2 BACK RING

It is believed that the fundamental mode of vibration of the cylindrical beam expander under torquing is of the shape as shown in Figure 8.

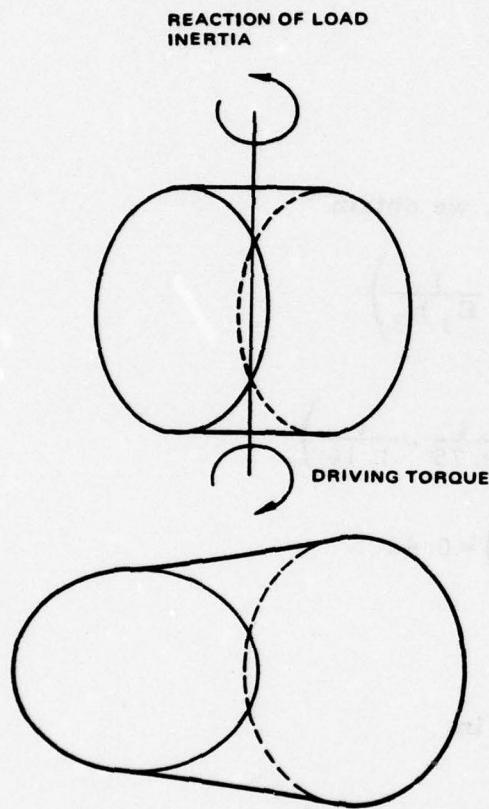


Figure 8. Warping of cylinder when torqued.

Figure 9 shows how the back ring structure with four local stiffeners deforms in its first mode of bending vibration. While Figure 10 shows this back ring vibrates in its second modal shape.

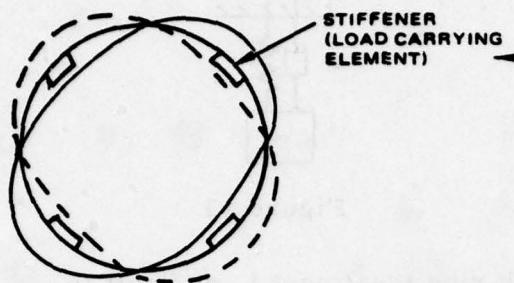
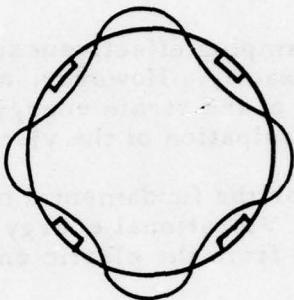


Figure 9. Back ring in its first vibrational mode.

Figure 10. Back ring in its second vibrational mode.



Damping of the back ring is achieved by incorporating a shear layer between the back ring and the stiffer constraining ring element (Figure 11).

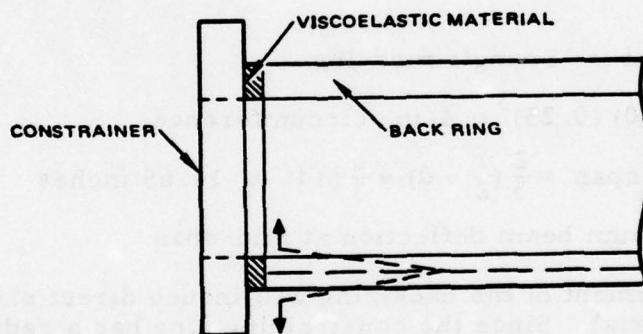


Figure 11. Decoupled shear motion between back ring and constrainer.

Nature of vibrational motion of a portion of the back ring between its two nodal sections can be considered as equivalent to the D. C. F. system as shown in Figure 12 or after another step of reduction, it is equivalent to the drawing shown in Figure 13.

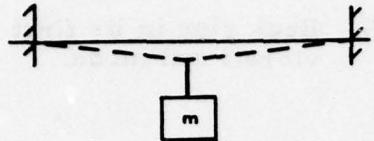


Figure 12

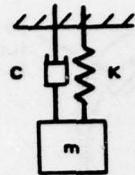


Figure 13

Damping effectiveness of this back ring treatment is difficult to analyze exactly. However, a reasonably good estimate can be made by the balancing of the strain energy of the mechanical system to the capacity of energy dissipation of the visco-elastic damping material.

For the fundamental mode of vibration, the rear ring will deform into ellipses. Vibrational energy of $1/2$ of the ring between nodal points can be estimated from the elastic energy of a beam under simple supports. That is

$$E_{vib} = \frac{EI\pi^4\delta^2}{4l^3}$$

where

$$E = 10^7 \text{ psi} = \text{Young's modulus}$$

$$I = \frac{1}{12}(8.0)(0.25)^3 \approx 4/\text{in. circumference}$$

$$l = \text{beam span} = \frac{2}{3}\left(\frac{1}{2}\pi d\right) = \frac{\pi}{3}(14) = 14.65 \text{ inches}$$

δ = maximum beam deflection at mid-span

The radial displacement of the back ring will induce direct shear strain in the visco-elastic material. Since the constraining ring has a radial thickness of about twice that of the original back ring of the beam expander, this constraining element is nearly 8 times as stiff as the back ring structure.

The strain energy of the damping layer can be obtained from:

$$E_{vis} = \frac{Gy^2}{2}V$$

where

$$G \approx 10,000 \text{ psi} = \text{shear modulus}$$

$$\gamma = \text{shear deformation} = \frac{\delta'}{t} = \frac{\delta}{2t}$$

$$V = \text{Volume of damping material} \approx 5 \times 0.85 \times 0.10 = 0.43 \text{ in}^3$$

(effective volume)

From the relation of the viscoelastic material's composite modulus of elasticity

$$\tilde{G} = G(1 + j\beta)$$

where for the present case

$$\beta = \text{loss factor of material} \approx 0.70$$

We can estimate the composite loss factor of the back ring structure as given by

$$\eta \approx \frac{E_{\text{damp}}}{E_{\text{vib}} + E_{\text{vis}}} = \frac{\beta \left(\frac{GV}{2} \frac{\delta^2}{4H^2} \right)}{\left(\frac{EI\pi^4}{4l^3} + \frac{GV}{8H^2} \right) \delta^2}$$
$$= \frac{\beta GV}{\frac{2EI\pi^4 H^2}{l^3} + GV} \approx 0.47$$

2.3 MID-SECTION

Due to actual structural complexities of this section, it is difficult to modify it based on an optimum damping treatment. Under this circumstance, the best damping result can be achieved by incorporating damping tiles in the form of a damping sheet of 0.05 in. thickness with a constraining layer of 0.40 in. thickness.

Following similar mathematical derivation, it can be shown in this section that the geometrical parameter

$$Y \approx 3.0$$

So that from the following design curves, as shown in Figure 14 it can be said

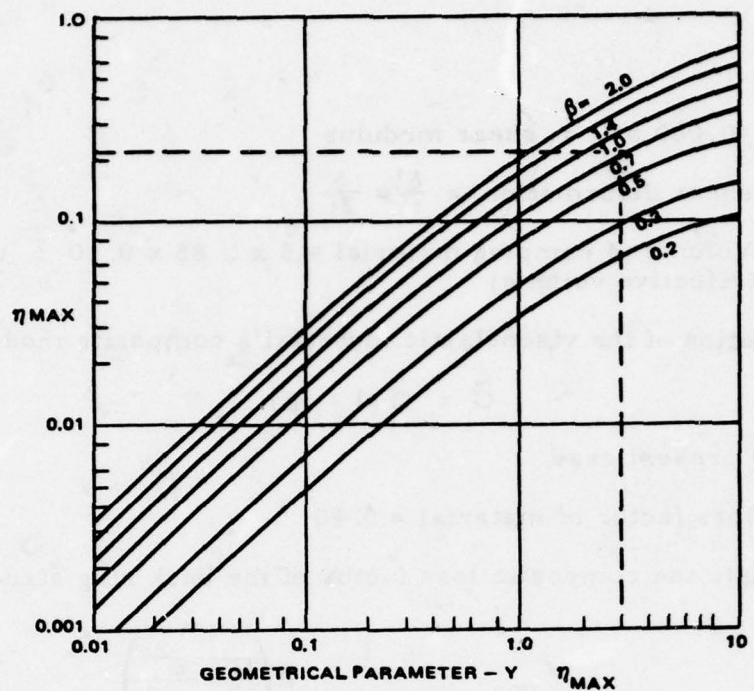


Figure 14. Maximum shear damping as a function of geometrical parameter and loss factor of material.

that for Dyad 606 damping material, in the temperature range of 40°F to 140°F and a frequency range of 150 Hz to 250 Hz, we have

$$\beta \approx 0.70$$

and

$$\eta_{\max} = \text{composite damping loss factor} \approx 0.22$$

Since the damping tiles cannot cover the entire mid-section, the overall damping efficiency may be reduced by a factor of 2. Thus a judicial estimate of this portion of the beam expander is

$$\eta \approx 0.11$$

2.4 DAMPING MATERIAL DATA

This data sheet presents the nominal values of the visco-elastic material supplied by Soundcoat Company, Inc. of New York. Since it is impractical to consider uniformness of the physical properties of different sheets of similar visco-elastic material, some variation from the values of these design curves should be acknowledged (see Figure 15).

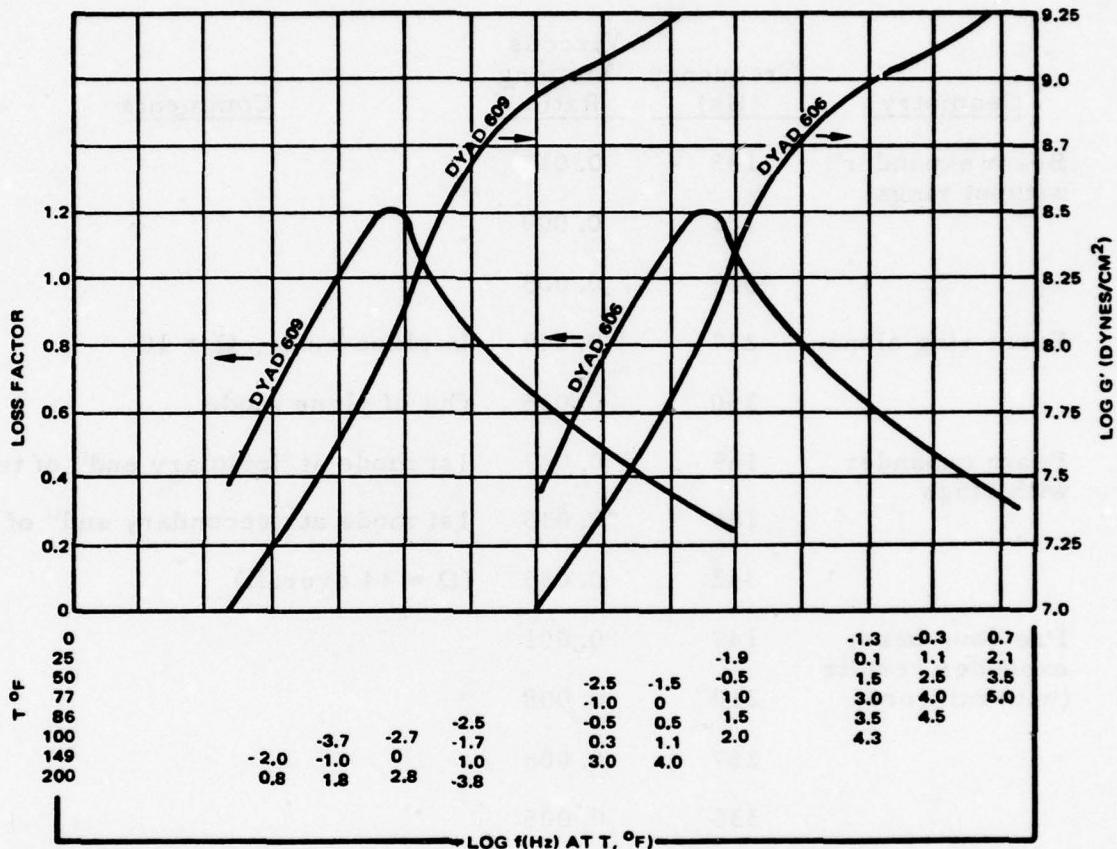


Figure 15. Loss factor, temperature in degrees Fahrenheit versus frequency for Soundcoat Dyad vibration damping elastomers.

2.5 TEST RESULT

To determine the effectiveness of the damping treatment, the beam expander was tested using the Modal Analysis System. The following summary of results is from Lanny J. Larson.

SUMMARY OF TEST RESULTS

<u>Geometry</u>	<u>Frequency (Hz)</u>	<u>Viscous Damping Ratio</u>	<u>Comments</u>
Beam expander without rings	135	0.013	
	181	0.009	
	322	0.005	
Front ring alone	217	0.049	In plane mode, $Q \approx 10$
	350	0.035	Out of plane mode
Beam expander with rings	169	0.027	1st mode at "primary end" of tube
	186	0.035	1st mode at "secondary end" of tube
	342	0.035	($Q \approx 14$ overall)
Previous beam expander results (with mirrors)	147	0.001	
	210	0.008	
	257	0.006	
	336	0.005	

**PROPERTY MEASUREMENT AND APPLICATION
OF ELASTOMER DAMPERS**

A. J. Smalley
Mechanical Technology Inc.
Machinery Dynamics Section
Latham, New York

PROPERTY MEASUREMENT AND APPLICATION OF ELASTOMER DAMPERS

by A. J. Smalley

Conference on Aerospace Polymeric Viscoelastic Damping

Dayton, Ohio

Sponsored by the Air Force Flight Dynamics Laboratory

Presentation: 7/8

February 1978

(Program funded and administered by NASA-Lewis Research Center)



Mechanical Technology Incorporated

968 ALBANY SHAKER ROAD LATHAM, NEW YORK 12110 TEL: 518/785-2211

I. INTRODUCTION

For several years MTI has been involved in a program of investigation into elastomer damping. The objectives of this program are summarized in Figure 2. The emphasis of the program is on learning, by test of materials and components, sufficient information to design and demonstrate effective elastomer dampers for control of forced and self-excited vibrations. The area of application chosen for this design and demonstration is that of high speed rotating machinery, where both types of vibration are prevalent. The common approach followed in rotordynamics design and analysis is to identify desirable bearing support properties in terms of stiffness and damping parameters, and then to synthesize a mechanical component which provides these properties or provides the best compromise thereto. Such a design approach creates a need for effective component property predictions and this need provided the basic impetus for this program.

In Figure 3 are shown the idealized components of a broad based program to provide and verify the required information. Shown are material property tests, component property tests, development of empirical factors, simplified and detailed analytical procedures, development of a data base of material properties and geometry factors for specific components, verification of predictions, and application of the technology in a design mode. As discussed below, the program to this point has been following predominantly along the empirical and simple analytical paths of this program, and more recently, into the verification and application areas.

II. TEST METHOD

An important element of the program is a powerful test method - the Base Excitation Resonant Mass Test Method. As implemented at MTI, this test method employs a large shaker upon which are mounted test elements in which the elastomer component of interest forms the connection between shaker and a supported mass. Accelerometers mounted on the table and on the supported mass, provide information on transmissibility and phase relationships between base and mass vibrations. The shaker imparts sinusoidal motion to the base and, in the region of resonance of supported mass on the elastomer spring, accurate figures for stiffness and damping of the elastomer component can be extracted. Figure 5 shows the relationships employed to extract stiffness and damping values and, in the case of shear test specimens, the relationships used to determine effective storage and loss moduli in shear. Test data acquisition

and reduction are all computerized. The operating procedure is to set shaker frequency and displacement across elastomer at desired values, check for satisfactory temperature distributions, and then to instruct the computer to acquire data for acceleration, displacement, temperature, and frequency. An immediate printout of raw data and calculated stiffness and damping values are presented to the operator, who reviews this summary and, if it is satisfactory, instructs the computer to store it permanently on a disk file. At the end of a test series, a neat tabulation of test results is presented.

In Figure 6, the various components tested under the program are shown. These include: thin rectangular sheets which are loaded in shear, cylindrical buttons which are loaded in compression, rings of rectangular cross-section which are loaded in radial direction, and O-rings which are also loaded in a radial direction. In Figures 7, 8, 9, and 10, are shown photographs of test fixtures for the shear, compression, ring cartridge and O-ring components.

III. TEST RESULTS - SHEAR AND COMPRESSION SPECIMENS

In Figures 11 & 12, are shown typical results for the shear and compression specimens. The individual test data points are shown together with a power-law line which provides minimum RMS deviation from the test data points. Both stiffness and damping data is shown for these two specimens. As may be seen, the data tends to fall in the range from 50 Hz to 1500 Hz, for which this test method is best suited, and into which the requirements of rotating machinery applications most commonly fall.

In Figure 13, are shown a typical set of material property results. Here storage shear modulus is plotted against frequency for four different temperature values. In Figure 14, the result of applying the WLF law to these material properties is shown. The universal line which best fits all of the individual test data points is shown as reduced modulus versus reduced frequency, and superimposed are the individual test data points which show the closeness of adherence to this line.

For the cylindrical compression specimens, an effort has been made to establish an effective prediction method which employs the shear modulus results from shear specimen tests together with a factor which accounts for the particular geometrical shape of the compression specimen. Elasticity theory has shown that a quadratic dependence of cyl-

indrical specimen stiffness on shape factor exists (where shape factor is the ratio of stressed area to unstressed area), and the present effort has assumed the same basic dependence on shape factor applies for frequency dependent stiffness and damping properties. The parameter which has been empirically determined is the coefficient of shape factor squared in the expression:

$$K = \frac{3GA}{h} (1 + \beta S^2)$$

where: G is the shear modulus
A is the stressed area
h is the height
S is the shape factor
 β is the coefficient to be determined empirically.

The majority of elasticity based analyses show β to have a value of 2. In some cases, the value obtained empirically for β was also close to 2. In other cases, it fell significantly below 2. An effort to obtain test data from other workers in the field was made, but limited comparable data was found. The work of Cannon, Nashif, and Jones provided the best basis for a similar empirical investigation. In this case, data covering a diameter-to-height ratio from 1 to 5 was available, and the shape factor coefficient, β , at both 250 and 500 Hz was found to be in the region of 1.485, which agrees surprisingly closely with the value obtained in our investigation for a diameter-to-height ratio in the range 1 to 4.

IV. RING CARTRIDGE TEST AND ANALYSIS

Having performed empirical investigations on shear and compression specimens, an investigation into the ring cartridge of rectangular cross-section was mounted. Available predictive methods for this particular geometry were sought. The work of Göbel provided the only published analysis of this component and includes some confidently stated, but unsubstantiated, correction factors to account for the shape factor of the ring. We also developed a very simple "beam-column" predictive method which assumes the ring to be made up of a series of non-interacting beams and columns, and takes no account of shape factor effects. Using these two predictive methods and the material properties previously obtained from shear specimen tests, predictions of stiffness and damping as a function of frequency were made. Measurements of stiffness and damping using the test assembly shown in Figure 9, were also made, and comparisons between predictions

and tests obtained a typical result as shown in Figure 18. This comparison illustrates, as was generally the case, that measured component values fall between the two sets of predictions. Rings of two different rectangular cross-sections were tested with length-to-thickness ratios of 1 and 2 respectively. In general, the shorter ring gave measured properties closer to the beam column predictions, and the longer ring gave measured properties closer to the Göbel predictions. Since the Göbel predictions attempt to account for the length of the ring, this trend is probably to be expected.

V. O-RING DYNAMIC CHARACTERISTICS

The base excitation resonant mass test method has been employed in a predominantly empirical investigation of O-ring stiffness and damping properties. O-rings are used as seals for squeeze film dampers for rotating machinery and the contributed stiffness and damping properties are of considerable interest. As will be shown later, we are also planning to use O-ring dampers without a squeeze film for a power transmission shaft application. In this investigation, the influence of 8 parameters was sought: material, temperature, strain, squeeze, O-ring cross-sectional diameter, stretch, groove width, and of course, frequency. For all tests, data was obtained as a function of frequency and frequency was, indeed, a significant parameter. Of the other seven parameters, those having the most pronounced effect were material, temperature, dynamic strain, and squeeze; and results illustrating these pronounced trends are shown in Figures 19, 20, 21, and 22. Three different materials were investigated: Viton 70, Viton 90, and Buna Nitrile. The highest loss coefficient and strongest frequency dependence was exhibited by the Viton 70, for which loss coefficients as high as 1.1 were measured. Viton 90 exhibited almost a factor of 4 increase in stiffness over Viton 70 but loss coefficients were about 1/2 those of the Viton 70. The Buna N, which was also a 70 durometer material, had similar stiffness levels to the Viton 70 but showed less variation in stiffness with frequency, and loss coefficients in the range of .3. The Viton results are representative of a material in its' transition zone.

The effects of temperature on O-ring properties are shown in Figure 20 (in this case, for Viton 70) and the very strong influence of temperature is shown. A sharp reduction in stiffness and loss coefficient results from relatively small increases in temperature above the 70°F. nominal value used in these tests. Stiffness fails by a factor of about

3 for a relatively modest increase in temperature and, above about 150° F., there is in fact, very little further reduction in stiffness even to temperature values as high as 420° F for which a limited amount of data was obtained. Loss coefficient falls by a factor of 10 in the range of temperature investigated.

Dynamic strain was an important governing parameter, as is shown in Figure 21. In general, both stiffness and loss coefficient were reduced by increasing strain in the frequency range tested but, at frequencies below 50 Hz., there is a suggestion that increasing strain could, in fact, have a reverse effect. A maximum dynamic strain of 5 mils double amplitude was imposed at frequencies up to 600 Hz. Beyond this, the peak amplitude was decreased in inverse proportion to frequency up to 1000 Hz. Such amplitudes are approaching the limit of the capabilities of the present test method and required approximately 100 G's of table acceleration. Based on these results, it is clear that strain is a very important parameter and must be accounted for in design.

In order to positively locate an O-ring, it is necessary to impose a certain degree of static compression of its' cross-section, and the measure of this static compression is termed "squeeze". Squeeze is defined as the ratio of interference to nominal cross-section diameter and is expressed as a percentage. Recommended values for O-ring design applications are in the region of 15%. Investigations were carried out in the present study from 5% to 30% and it was shown, as illustrated in Figure 22, that squeeze is a very important parameter in determining both stiffness and damping of the O-rings. The reason for this effect is that squeezing increases the area of contact between elastomer and metal parts. Thus, as a particular stress is generated due to dynamic strain of the O-ring, the transmitted force is increased as a result of the increased contact area. Thus, stiffness increases strongly with increasing squeeze. Loss coefficient, however, is reduced, indicating that dissipation effects do not increase with squeeze so rapidly as energy storage effect.

VI. THE EFFECTS OF A ROTATING LOAD

In a recent investigation, a first step towards application of elastomer dampers in rotating machinery was undertaken. The objective of the investigation was to determine if similar component properties were observed when the elastomer damper was configured as a cartridge for multi-directional load capacity and subjected to a rotating load. A

rotating load analog to the base excitation resonant mass test method was built. This test rig included a high speed rotor driven by an integral turbine which was capable of running to 60,000 RPM. The rotor ran vertically and, at its' upper end, the test element was mounted on the outside of a rolling element bearing. Rotating unbalance in the rotor transmitted a rotating force to the test element. Similar data extraction methods were used based on accelerometer signals on the input and output side of the elastomer test element. Severe problems of noise, coupled conical and translatory motion, and reduced controllability of the excitation force were encountered, but after substantial development effort, usable results were obtained and a typical set is shown in Figure 23 for a rectangular cross-section ring cartridge. Although significant scatter is apparent, the general level of the results corresponds well to the predictions.

VII. THE EFFECTS OF STRAIN

The effects of dynamic strain obviously have been so important in our investigations that significant effort has been devoted to trying to establish an effective means of accounting for strain in a design procedure. The results are by no means conclusive since they have as yet been directed only at Polybutadiene, a material whose transition frequency lies significantly above those tested. The results we do have tend to indicate that strain is, in fact, a much more consistent governing parameter than frequency. In Figure 24, stiffness and damping are plotted versus frequency for a cylindrical button loaded in compression, subjected to excitations over a wide range of strains. The vertical scatter in the stiffness and damping results at a particular frequency represents the effects of the different strain values. Clearly this scatter is high. In Figure 25, loss coefficient is plotted against frequency for the same conditions and strain ranges, and again, the scatter is wide throughout the frequency range. In Figure 26, the same set of data has been re-plotted versus strain. Vertical scatter now represents the effect of different frequencies. What is clear is that the scatter is now much reduced and that a line fitted through the data to minimize RMS deviation does provide a reasonably satisfactory representation of all the data. In Figure 27, a similar plot of loss coefficient versus strain is presented and, again, encouraging consistency results. Based on these results, the thesis to be pursued is that, for materials not in their transition zone, design analysis is best served by considering strain as the parameter which will most consistently govern stiffness and damper performance. This thesis needs to be pursued further and demonstrated by application, and attention should be directed at the development of a comprehensive material and component data base for use in design.

VIII. CURRENT AND FUTURE PROGRAM EFFORTS

The results discussed to this point highlight the significant elements of our elastomer program to this point. In order to partially streamline the presentation, some interesting measurements and analysis of thermo-viscoelastic effects have not been covered.

In Figure 28, are summarized the current efforts underway in this program. We are endeavoring to broaden the data base of material properties, and to verify that similar component behavior occurs with other materials. We also have two rotating machinery application tests at various stages of development. These efforts will be discussed below.

The range of materials which could be investigated is wide, and a partial list is shown in Figure 29. Above the dotted line, are shown the materials for which we are now acquiring test specimens and for which we will be undertaking tests over the next six or eight months. We feel there is a limitation in available data on elastomer materials in these frequency ranges, and that there is a need to develop such properties for a range of materials and to present them on a reasonably uniform basis.

MTI has a number of test rigs available which have the common characteristic of running above bending critical speeds (that is critical speeds where a significant amount of modal energy is in the shaft). Two of these rigs have been chosen for investigation of elastomer damping capabilities. In both cases, the rigs were originally designed to run on squeeze film dampers and we are now seeking to replace the squeeze film dampers with dry elastomeric dampers.

IX. TURBOSHAFT ENGINE DAMPER

The first test rotor I shall discuss is a dynamic simulator of a front drive turbo-shaft engine power turbine. For the front drive application, the inner spool must pass all the way through the gas generator spool and have power taken off at the compressor end of the engine. This imposes tendencies towards a long, thin, shaft running at high speed with bending critical speeds in its' operating range. To control vibrations at critical speeds, bearings must be located at points where there is some dynamic motion and the properties of the bearing supports must be optimized to best match up with the dynamic properties of the rotor itself. An effective approach to this optimization process is to seek those support properties which optimize the system log decrement at cri-

tical speeds of interest. To calculate the log decrement, damped natural frequencies or complex eigenvalues of the system must be determined accounting for both rotor and its' supports. The log decrement is then a non-dimensional measure of the system damping. It is desirable to have as high a value as possible for log decrement. In applying this optimization approach to the turbo-shaft engine of interest, log decrement was calculated as a function of damping, having established a good value for support stiffness. In Figure 31, log decrement is plotted against damping and it is seen that, for each of the two critical speeds of interest, there exists an optimum value of damping. It was then necessary to find out what compromises are imposed by the use of elastomer materials. It turns out that, for the desired value of support stiffness, loss coefficients tends to limit the obtainable damping to values significantly below the optimum. This is illustrated in tabular form in Figure 32. For Polybutadiene with loss coefficient set at .2, and for Viton 70 with a loss coefficient set at .8, effective damping values at the two critical speeds of interest have been calculated and these are compared with the optimum values and the log decrement values for the two elastomers are compared with the optimum log decrement value. These results clearly indicate that a significant sacrifice in damping and log decrement results from use of elastomers but out experience shows that none of these log decrement values would prohibit effective balancing and operation through such critical speeds.

Having identified desirable damping properties and the compromises necessary in an elastomer damper, we have done the mechanical design work needed to realize elastomer dampers of the desired stiffness (of order 100,000 lbs.-in) and damping. Figure shows the test rig with the elastomer dampers. The design selected consists of three individual rows of cylindrical buttons located every 120° around each bearing, giving nine buttons in all for each bearing. The elastomer buttons are bonded between thin metal platens which are inserted in appropriate slots to support the bearing housing and which can be preloaded by means of backing screws. The elastomer component design is clearly very modular and rapid changes of the elastomer dampers can be implemented. It is planned to test two different materials -- Viton 70 and Polybutadiene, as well as configurations providing different values of stiffness to allow some empirical optimization of stiffness and damper properties. The rig is now in the advanced stages of assembly and it is expected to start testing within the next few weeks. The test procedure will be started by a careful balancing of the test rotor to run with minimum vibration through its' speed range. Then response, with the various damper designs, to controlled levels of unbalance, will be measured and resultant vibration character-

stics will be compared over the speed range. As a point of reference, a set of data will be obtained where the elastomer damper is replaced by a solid metallic hard mount for which very low system damping levels are to be expected.

X. POWER TRANSMISSION SHAFT DAMPER

The second test rig which has been selected for application testing of elastomer dampers is a large test facility intended for the general development of advanced technology power transmission components including engines, gearboxes, couplings, bearings, dampers, and shafting. Figure 33 shows an isometric view of the test rig. Major components are a 300 hp, 3600 RPM drive motor, a magnetic clutch which allows continual speed variation from essentially zero to 3600 RPM, and a gearbox with a gear ratio of approximately 5.7 to 1 with two output shafts, the first corresponding to input speed, the second providing up to 20,000 RPM. The high speed output is connected to a high speed spindle from which is suspended a 12' long hollow shaft, 3" in outer diameter with an 1/8" wall thickness. There is a second, similar, spindle at the other end of the shaft. Such a shaft is representative of what would be used in an advanced technology helicopter tail rotor drive shaft. Almost all helicopter tail rotor drive shafts employ short, sub-critical, shaft sections with many bearings and couplings, and the long shaft offers advantages of simplicity, reduced weight, reduced number of bearings and couplings, improved maintainability, etc. The major problem with a long, flexible shaft is that it must traverse flexural critical speeds to attain desired operating speeds and sometimes its' range of operating speed must encompass a critical speed. Initial tests of this shaft were carried out with no damping. The shaft as directly connected to hard mounted spindles. The results was a shaft which exhibited extreme sensitivity to unbalance and a potential for severe self-excited vibrations. The resultant problems are illustrated in Figures 34 and 35. On each figure, four frequency spectrum plots are presented at different stages in the acceleration of the shaft. Figure 34 corresponds to operation below the first critical speed. The first plot indicates some excitation of the first critical speed when running at half the first critical speed. The second and third plots show relatively low amplitudes both at running speed and at the frequency corresponding to the first critical speed. The fourth plot shows some increased amplitude at the first critical speed as running speed starts to approach it. In Figure 36, plots corresponding to negotiation of the first critical speed and operation above the first critical speed are shown. When running speed is close to the first critical speed, very pronounced amplitudes occur as unbalance exci-

tation drives the first critical speed. Previous balancing efforts had, however, reached a condition where the first critical speed could be negotiated. What occurs after the first critical speed is negotiated is interesting in that vibrations at the first critical speed are sustained and indeed, remain higher than any vibrations at running frequency. Sub-synchronous excitation of a critical speed such as illustrated here is indicative of some form of destabilizing mechanism, and it is speculated that internal friction in the shaft or the couplings is the cause of this self-excited vibration. Whatever its' cause, it can be concluded that effective operation of a supercritical power transmission shaft can not be performed without more damping than the configuration initially investigated.

Based on this conclusion, a damper was designed for the supercritical shaft. Figure 36 shows schematically how this was accomplished; an extension shaft was added to the flexible shaft, connected to it via a coupling and connected at its' other end to the down stream spindle. The spindle was shifted some 18" further from the drive end. A damper was provided as close as possible to the end of the original shaft and vibration forces were transmitted to the damper via a rolling element bearing, in which the shaft extention was mounted. The first damper was a squeeze film damper, and Figure 37 shows the results which were obtained with this damper. Here we see the negotiation of three flexural critical speeds and stable operation to over 10,000 RPM, which is some eleven times the first critical speed. We are now about to start work on designing an elastomer damper for this supercritical shaft test rig. In basic terms, this means getting rid of the oil and selecting a damper configuration which provides optimum control of vibrations within the constraints imposed by elastomer materials. It is expected that we will start testing this elastomer damper during the second half of this calendar year.

XI. SUMMARY

In summary then, MTI's program employs a powerful computerized test method to establish material and component property data. We are now in the position of being able to apply this test method in a production mode and hope to establish libraries of material property data for use in design. We are, further, seeking to establish credibility and demonstrated performance for elastomer dampers in a very critical area of forced and self-excited machinery vibrations. The simplicity of the elastomer damper offers significant advantages over squeeze film dampers, and we hope to identify those areas of application where the attendant constraints on damping performance are toler-

able and to identify how best to exploit the damping capability available in elastomer materials for this application. If effective performance for elastomers in this application can be demonstrated, we believe there will be motivation for expanded investigation of basic elastomer properties, and the further generation of information which will allow the designer to confidently apply elastomers in control of forced and self-excited vibrations.

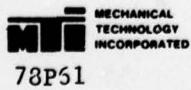
PROPERTY MEASUREMENT AND APPLICATION OF ELASTOMER DAMPERS

- **MEASUREMENT OF ELASTOMER MATERIAL AND
COMPONENT PROPERTIES**
- **APPLICATION OF ELASTOMERS IN CONTROL OF
FORCED/SELF-EXCITED VIBRATIONS**

by A. J. Smalley

Presentation: 7/8 February 1978

(Program funded and administered by NASA-Lewis Research Center)



78P51

FIGURE 2

PROGRAM GOALS

- DEVELOP ELASTOMER MATERIAL PROPERTIES
- DEVELOP AND VERIFY PREDICTIVE METHODS FOR ELASTOMER COMPONENT GEOMETRIES
- DEMONSTRATE EFFECTIVENESS OF ELASTOMER DAMPERS IN CONTROL OF FORCED/SELF-EXCITED VIBRATIONS



78P61

FIGURE 3
**BLOCK DIAGRAM ILLUSTRATING THE INTERACTION OF TEST,
 DATA REDUCTION, ANALYSES AND PREDICTION**

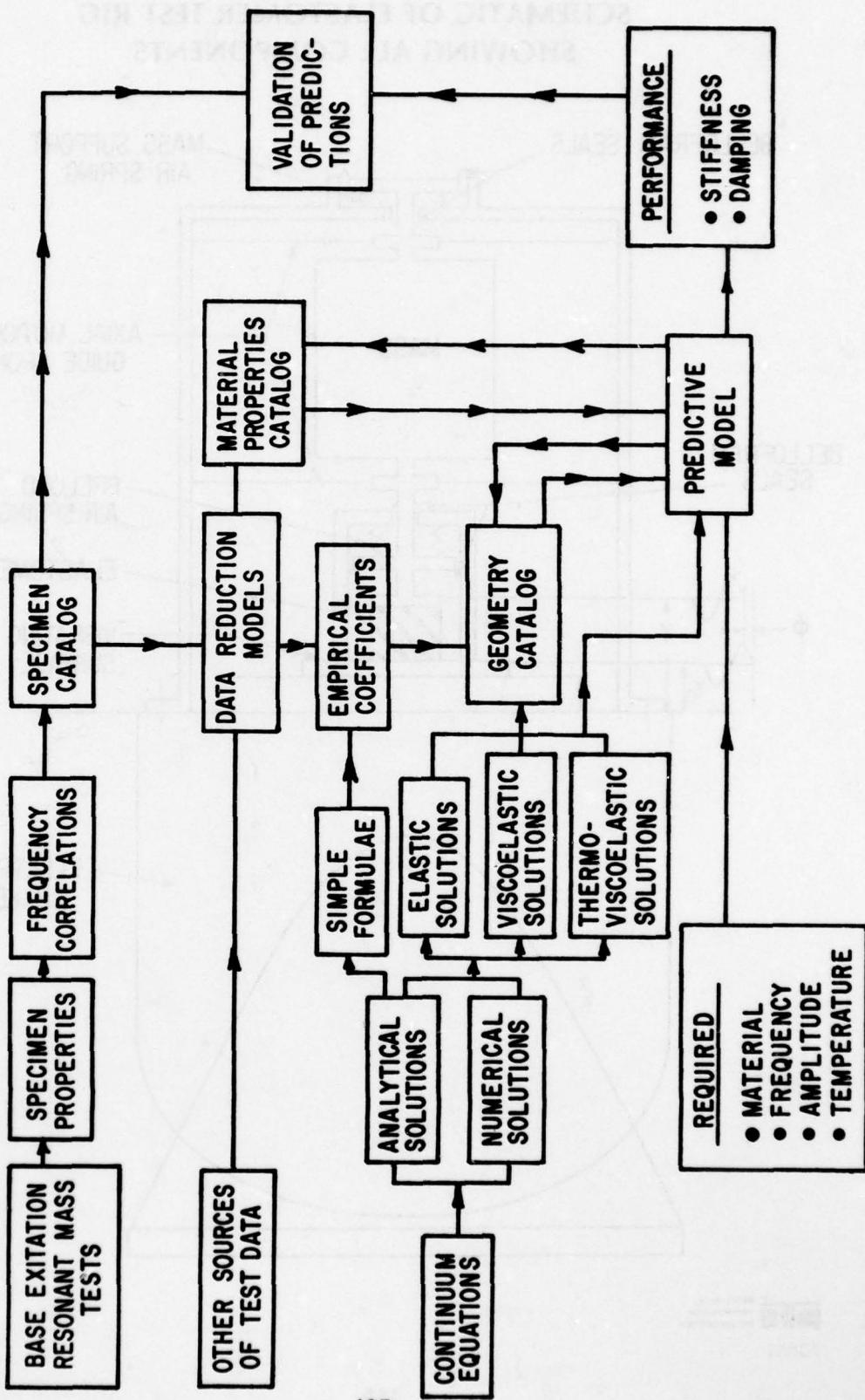


FIGURE 4

**SCHEMATIC OF ELASTOMER TEST RIG
SHOWING ALL COMPONENTS**

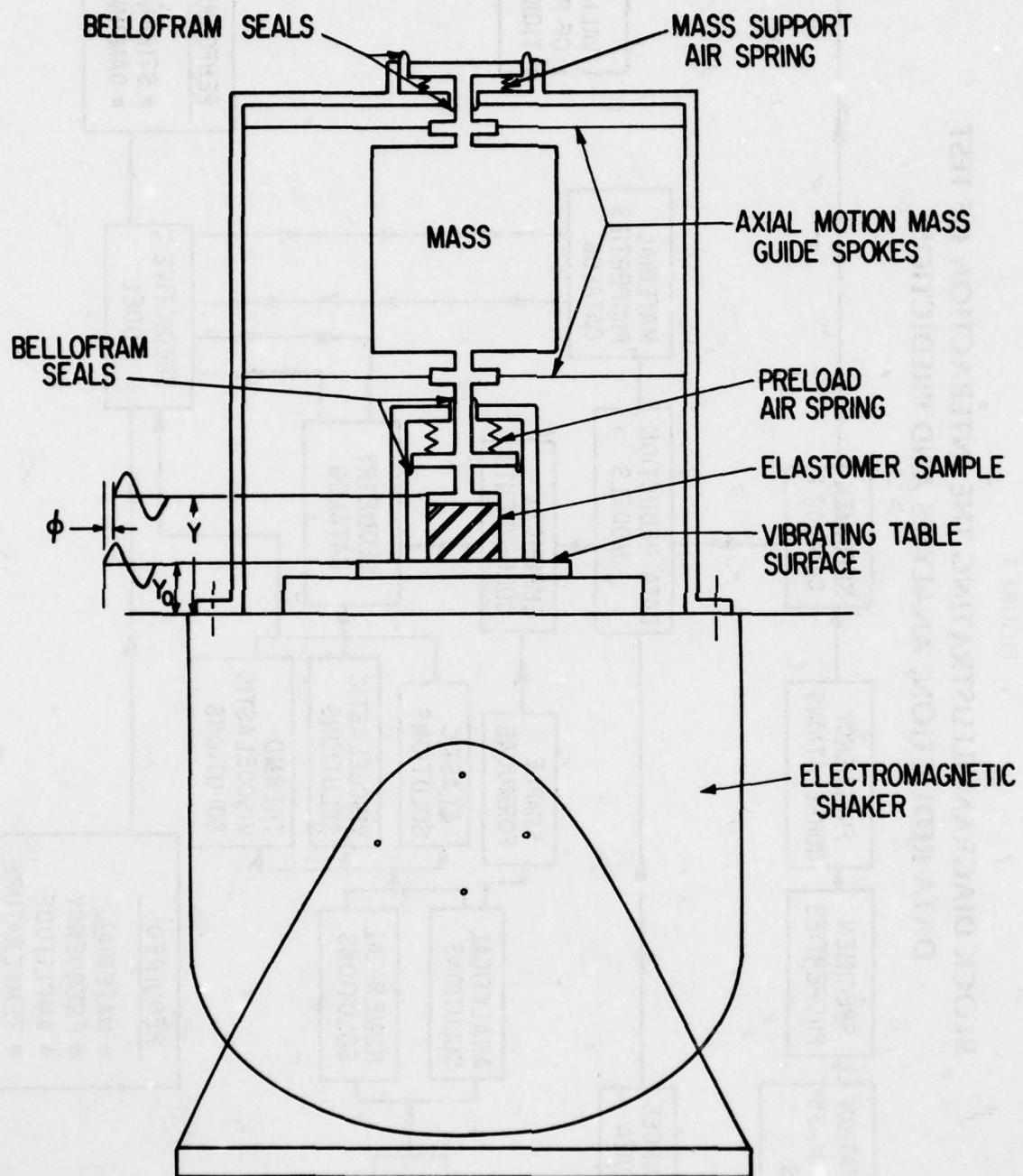


FIGURE 5

RELATIONSHIPS FOR DATA REDUCTION

$$\alpha = \frac{|A_{OUT}|}{|A_{IN}|} = \frac{\text{OUTPUT ACCELERATION AMPLITUDE}}{\text{INPUT ACCELERATION AMPLITUDE}}$$

ϕ = PHASE ANGLE BETWEEN INPUT AND OUTPUT ACCELERATION

$$K_1 = \frac{\omega^2 M [a^2 - \alpha \cos \phi]}{a^2 - 2\alpha \cos \phi + 1} \quad (\text{STIFFNESS}) \text{ LB/IN}$$

$$K_2 = \frac{\omega^2 M \alpha \sin \phi}{a^2 - 2\alpha \cos \phi + 1} \quad (\text{DAMPING}) \text{ LB/IN}$$

$$\eta = \frac{K_2}{K_1} \quad (\text{LOSS FACTOR, OR LOSS COEFFICIENT})$$

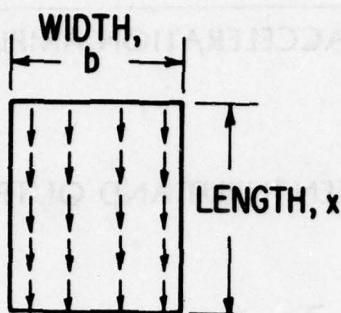
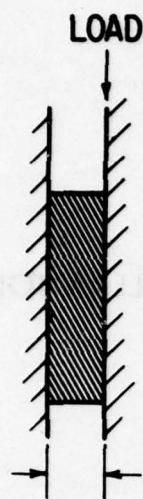
FOR SHEAR SPECIMENS, WE OBTAIN

$$G' = \frac{K_1 h}{\text{AREA}} \quad \text{LB/IN}^2 \qquad G'' = \frac{K_2 h}{\text{AREA}} \quad \text{LB/IN}^2$$

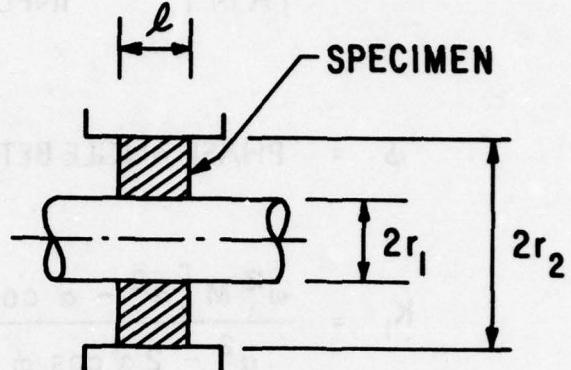
$$\eta = \frac{G''}{G'}$$

FIGURE 6

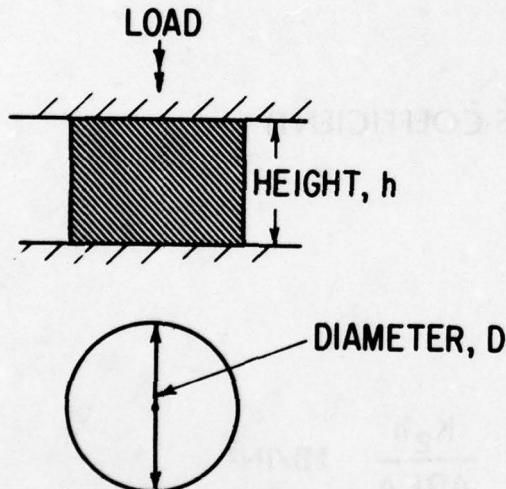
TEST ELEMENTS



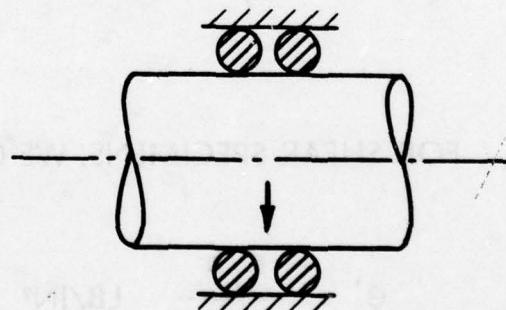
A. SHEAR ELEMENT



C. CARTRIDGE



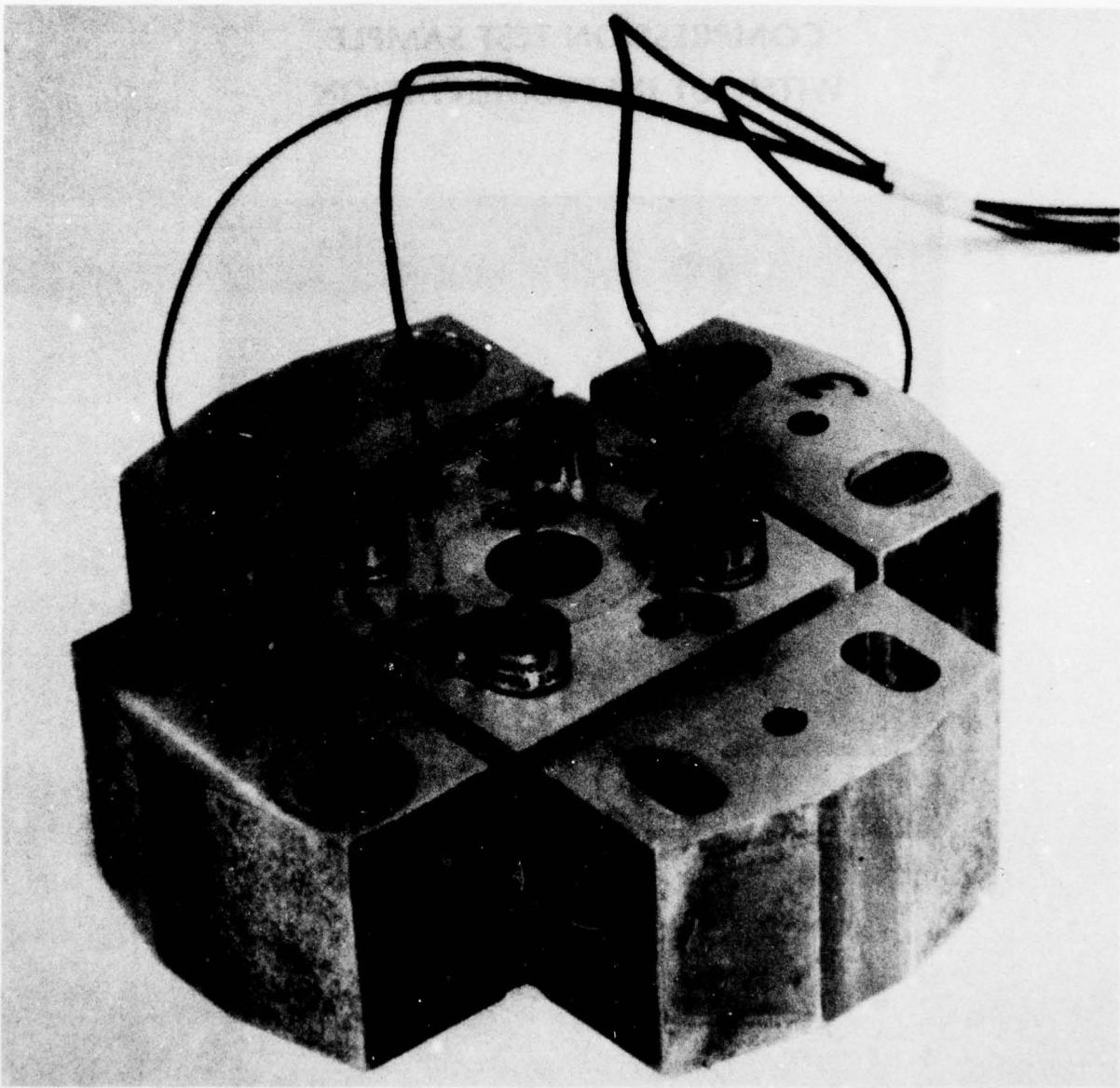
B. COMPRESSION ELEMENT



D. O-RING

FIGURE 7

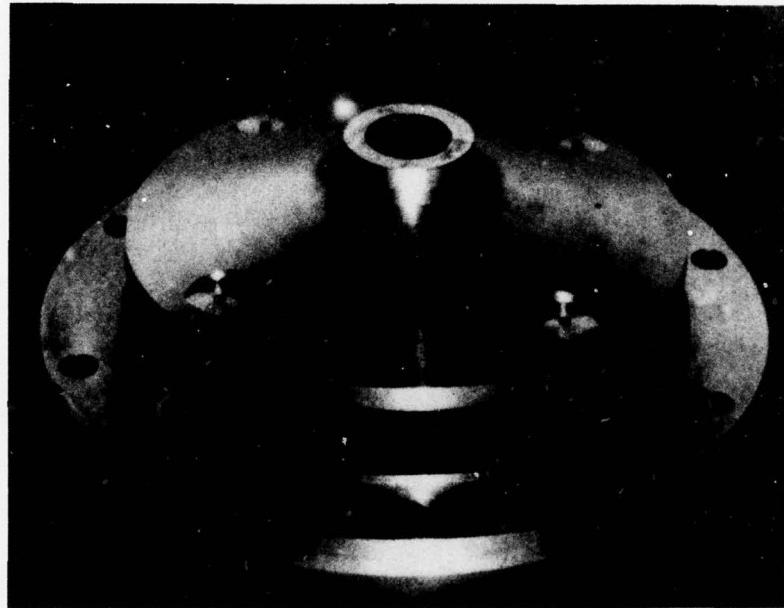
**TEST ASSEMBLY OF FOUR ELASTOMER SHEAR
SPECIMENS, EACH 2.54 CM (1.0 IN.) HIGH**



MTI
MECHANICAL
TECHNOLOGY
INCORPORATED
78P61

FIGURE 8

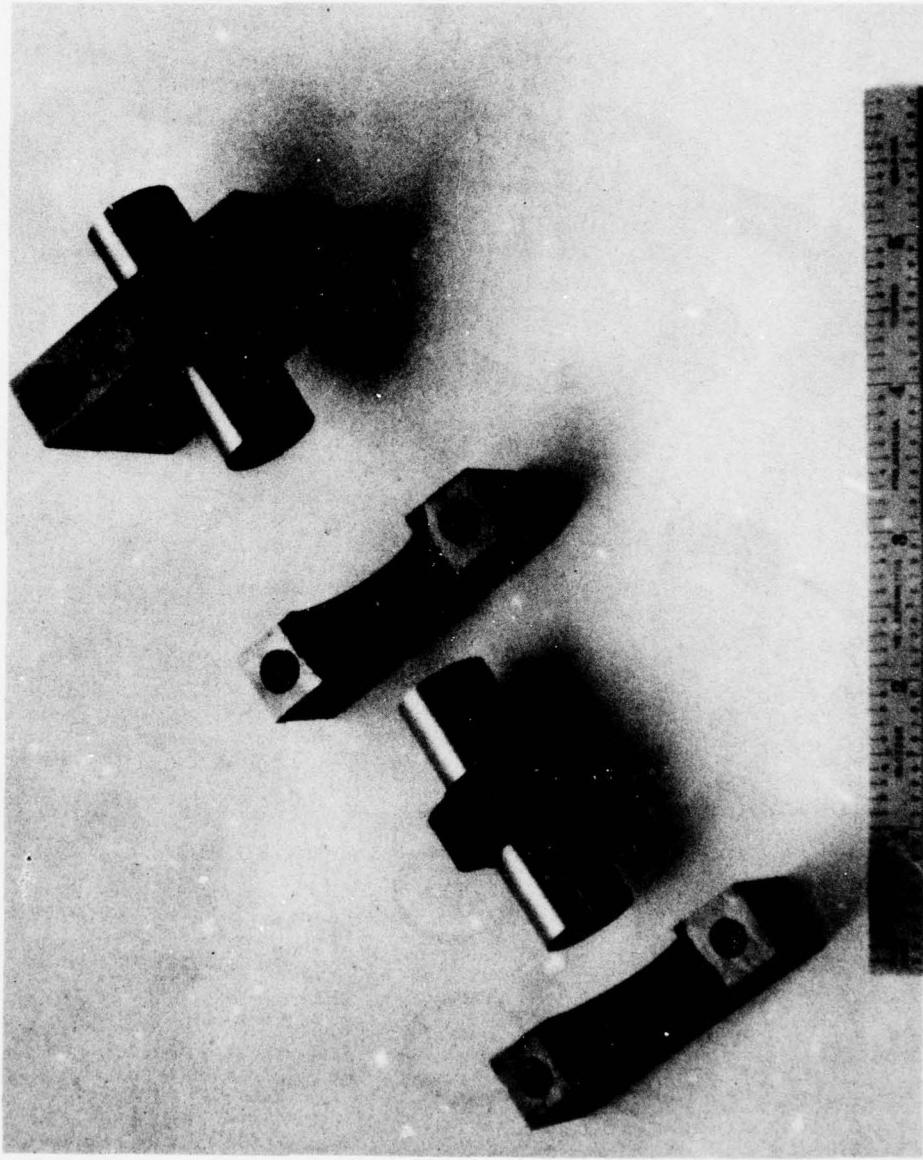
**COMPRESSION TEST SAMPLE
WITHOUT INSTRUMENTATION**



MTI MECHANICAL
TECHNOLOGY
INCORPORATED

78P61

FIGURE 9
ELASTOMER CARTRIDGE SPECIMEN BEFORE
BONDING OF OUTER SHELL (LEFT) AND WITH
OUTER SHELL IN PLACE (RIGHT)



MECHANICAL
TECHNOLOGY
INCORPORATED
78P61

FIGURE 10
O-RING TEST ASSEMBLY

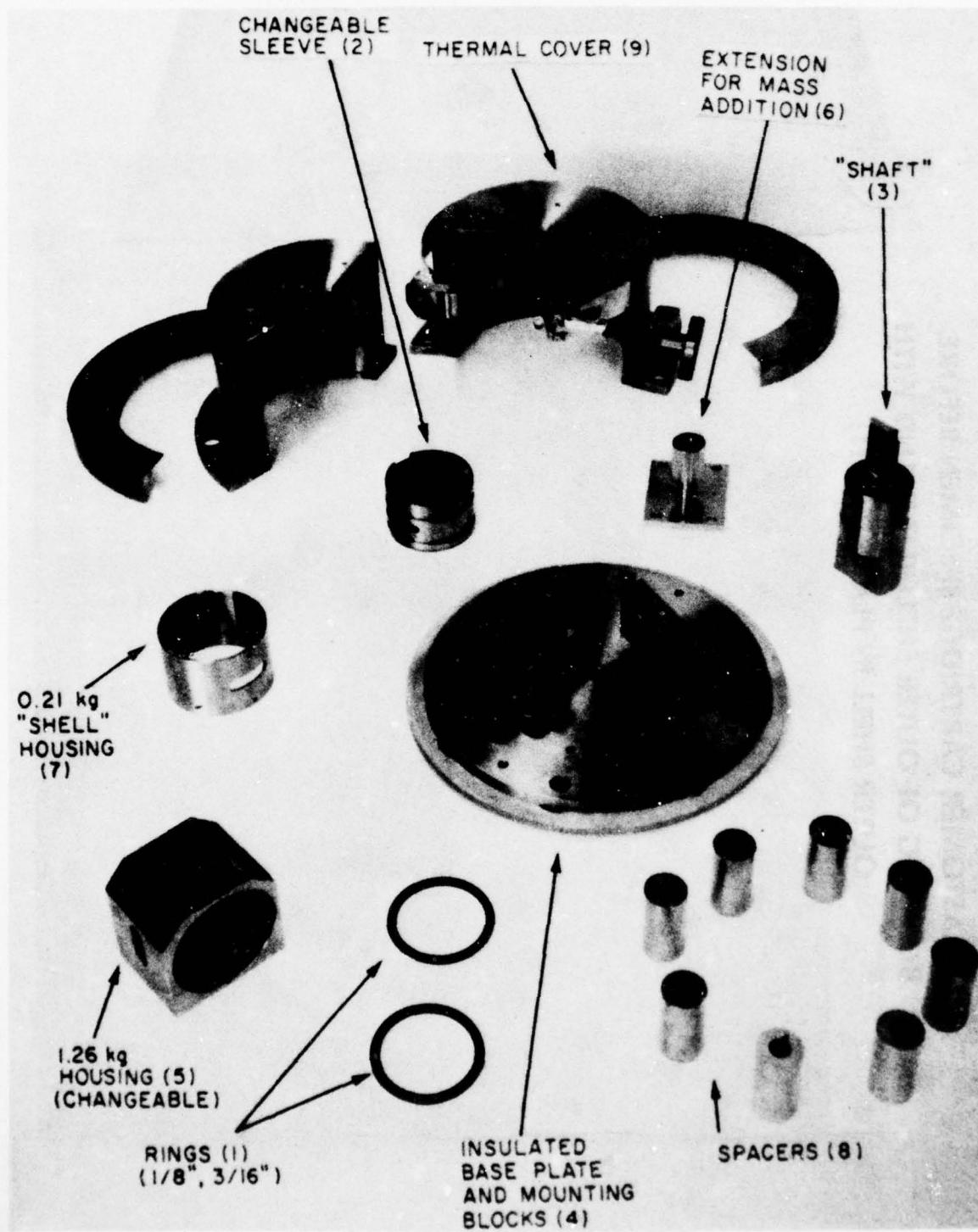
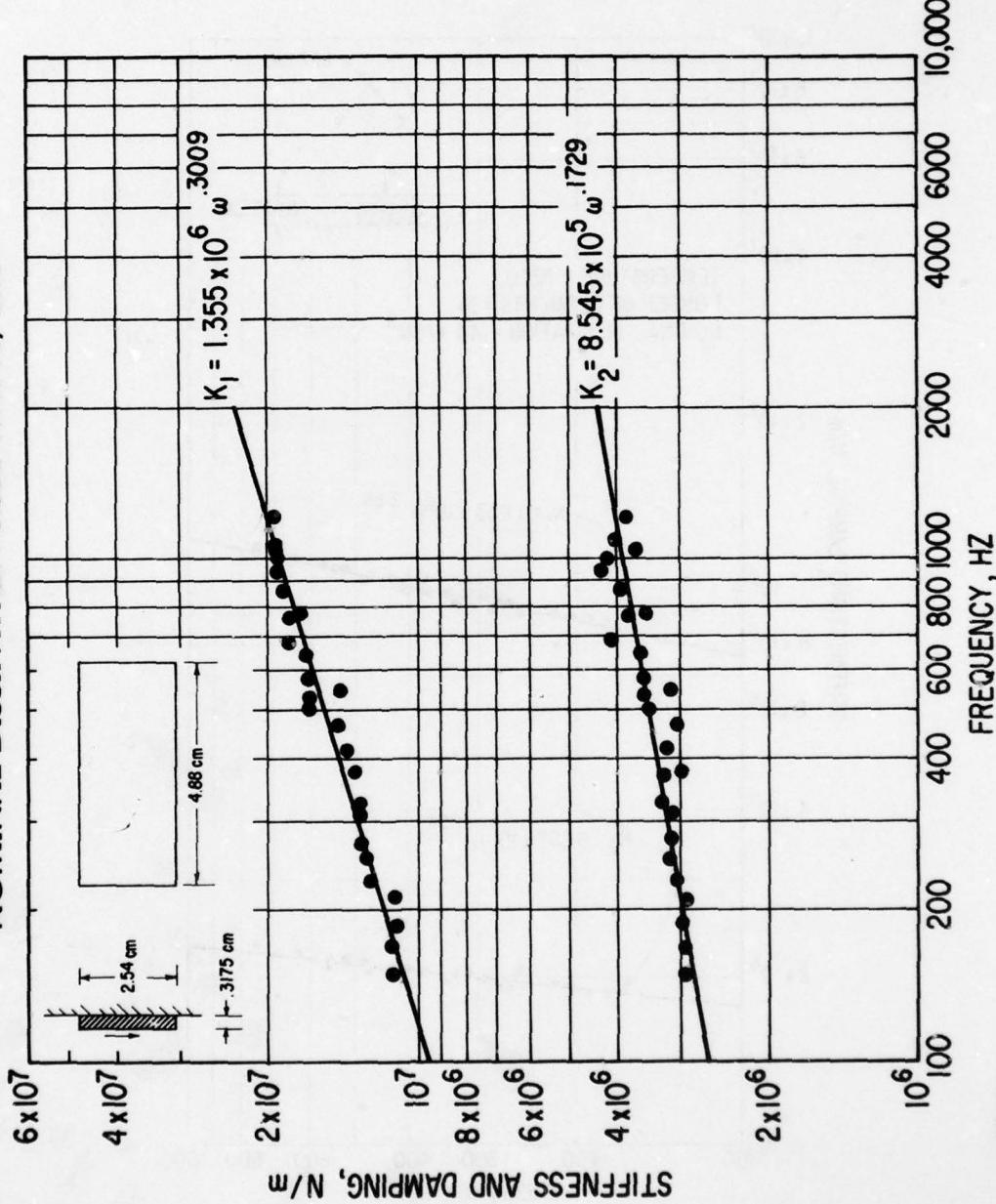


FIGURE 11
**STIFFNESS AND DAMPING VS. FREQUENCY —
 SHEAR SPECIMENS — ZERO PRELOAD, 32 C —
 NOMINAL DISSIPATION 0.352 WATTS/CM³**



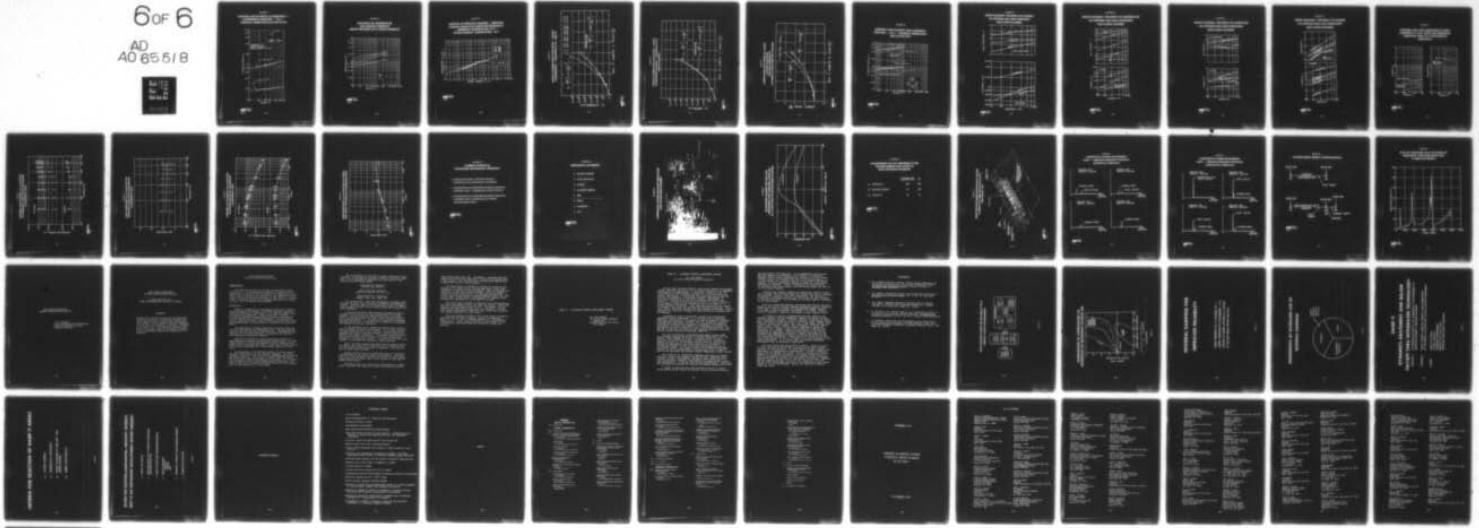
D-A065 518 AIR FORCE FLIGHT DYNAMICS LAB WRIGHT-PATTERSON AFB OHIO F/G 11/9
CONFERENCE ON AEROSPACE POLYMERIC VISCOELASTIC DAMPING TECHNOLOGY--ETC(U)
JUL 78 L ROGERS

UNCLASSIFIED

AFFDL-TM-78-78-FBA

NL

6 OF 6
AD
AO 65518



END
DATE
FILED
5-79
DDC

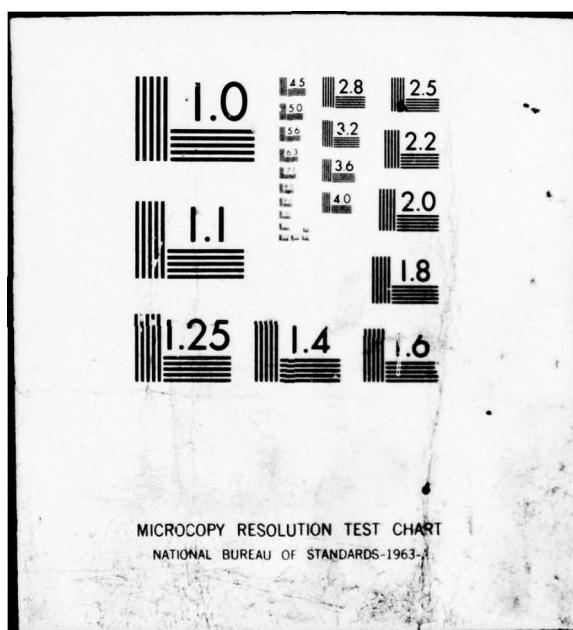


FIGURE 12
**STIFFNESS AND DAMPING VS FREQUENCY —
 COMPRESSION SPECIMEN — 32 C —
 NOMINAL DISSIPATION 0.44 WATT/CM³**

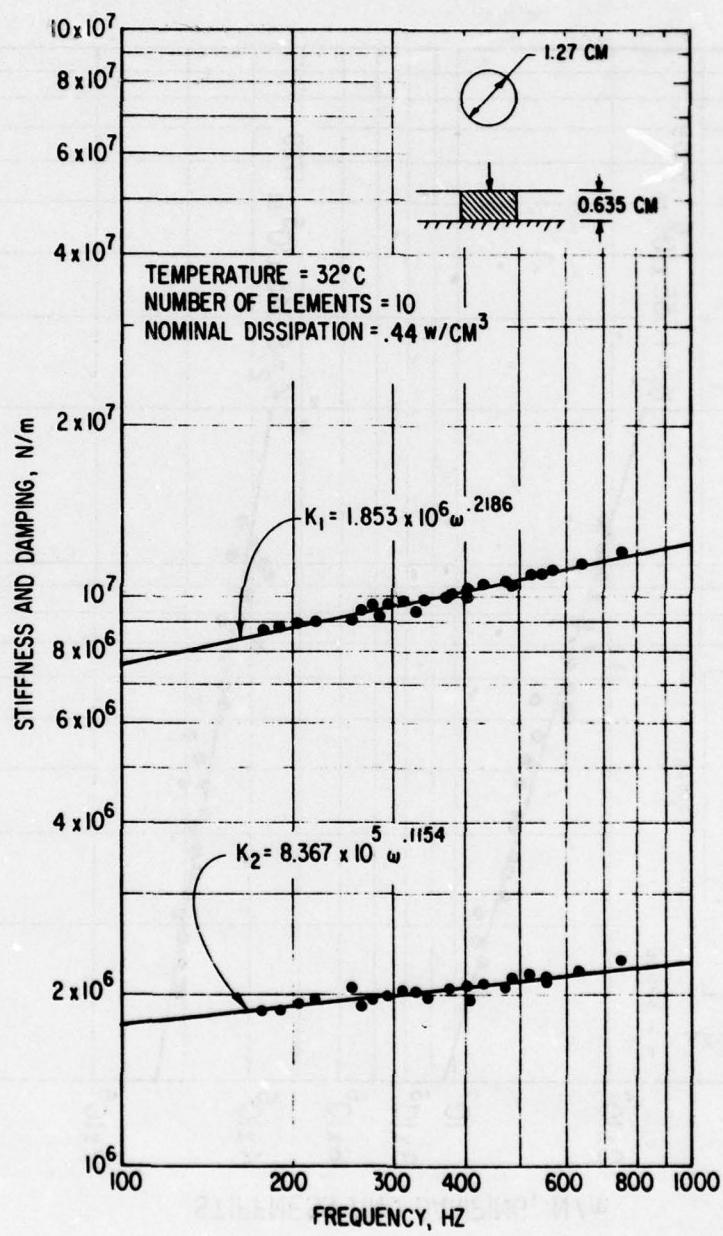
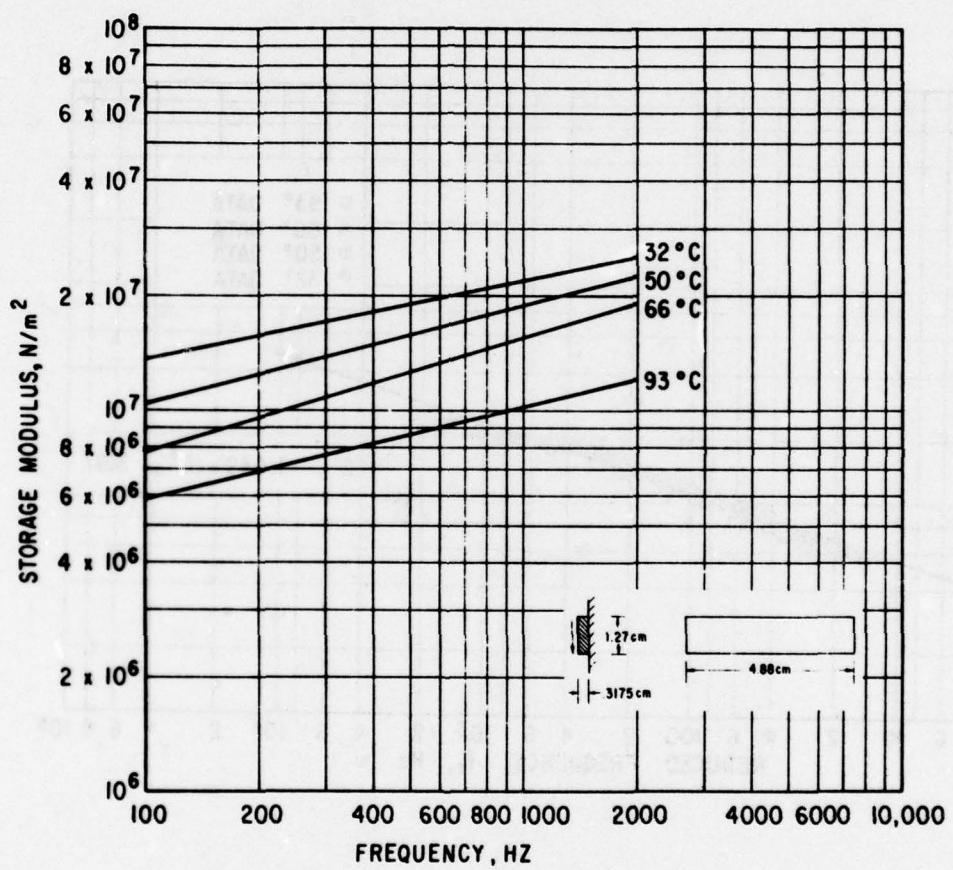


FIGURE 13

**INFLUENCE OF TEMPERATURE
ON STORAGE MODULUS
(SHEAR SPECIMEN DATA, EIGHT ELEMENTS)**

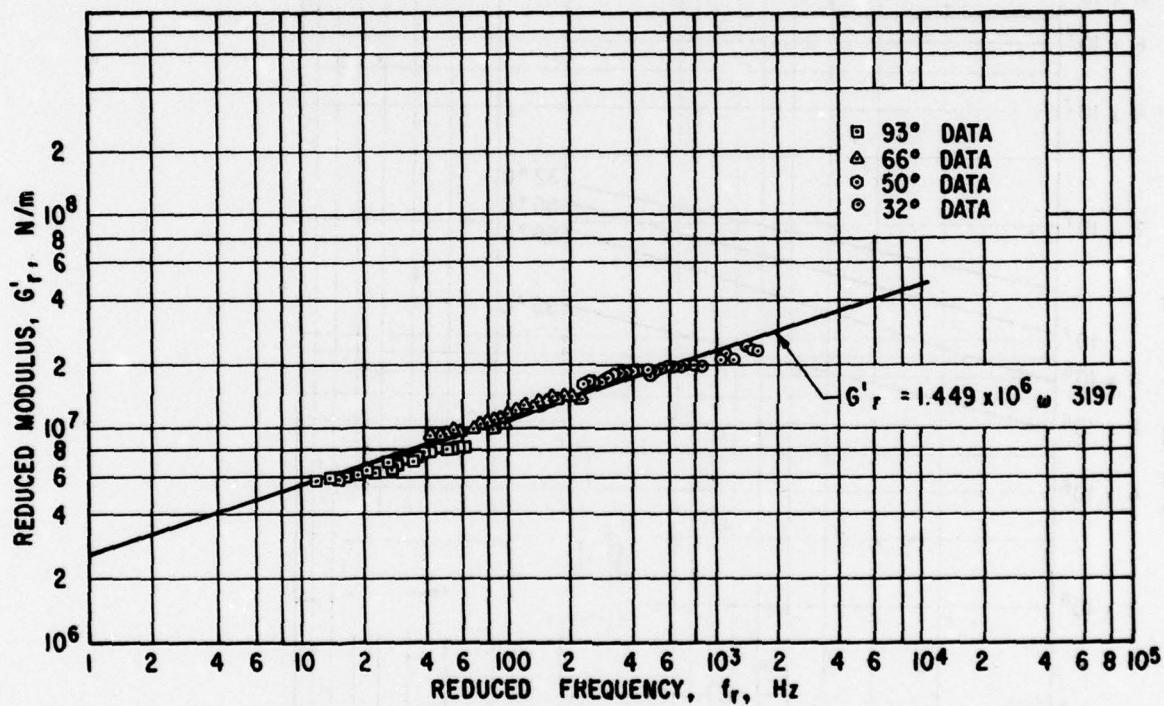


MTI MECHANICAL
TECHNOLOGY
INCORPORATED

78P61

FIGURE 14

**METHOD OF REDUCED VARIABLE — REDUCED
STORAGE MODULUS VS REDUCED FREQUENCY
— REFERENCE TEMPERATURE, 32 C —
CHARACTERISTIC TEMPERATURE; -50 C**



MECHANICAL
TECHNOLOGY
INCORPORATED
78P61

FIGURE 15

**PHASE II CORRELATION FOR SHAPE — SINGLE
COMPRESSION — DIAMETER 0.5 IN., 1000 Hz**

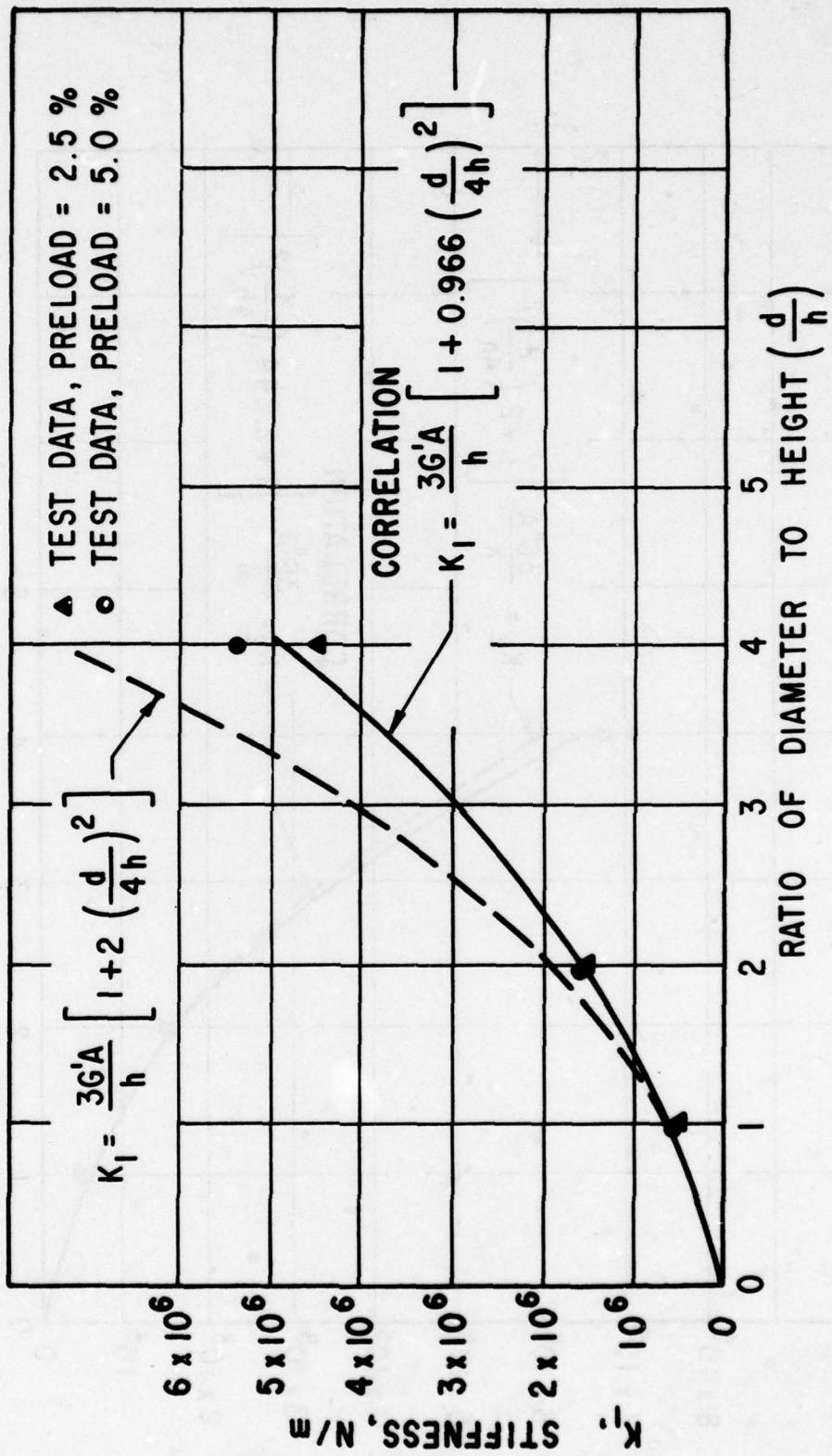


FIGURE 16

PHASE II CORRELATION FOR SHAPE — SINGLE
COMPRESSION ELEMENT — DIAMETER 0.5 IN.,
1000 Hz DAMPING

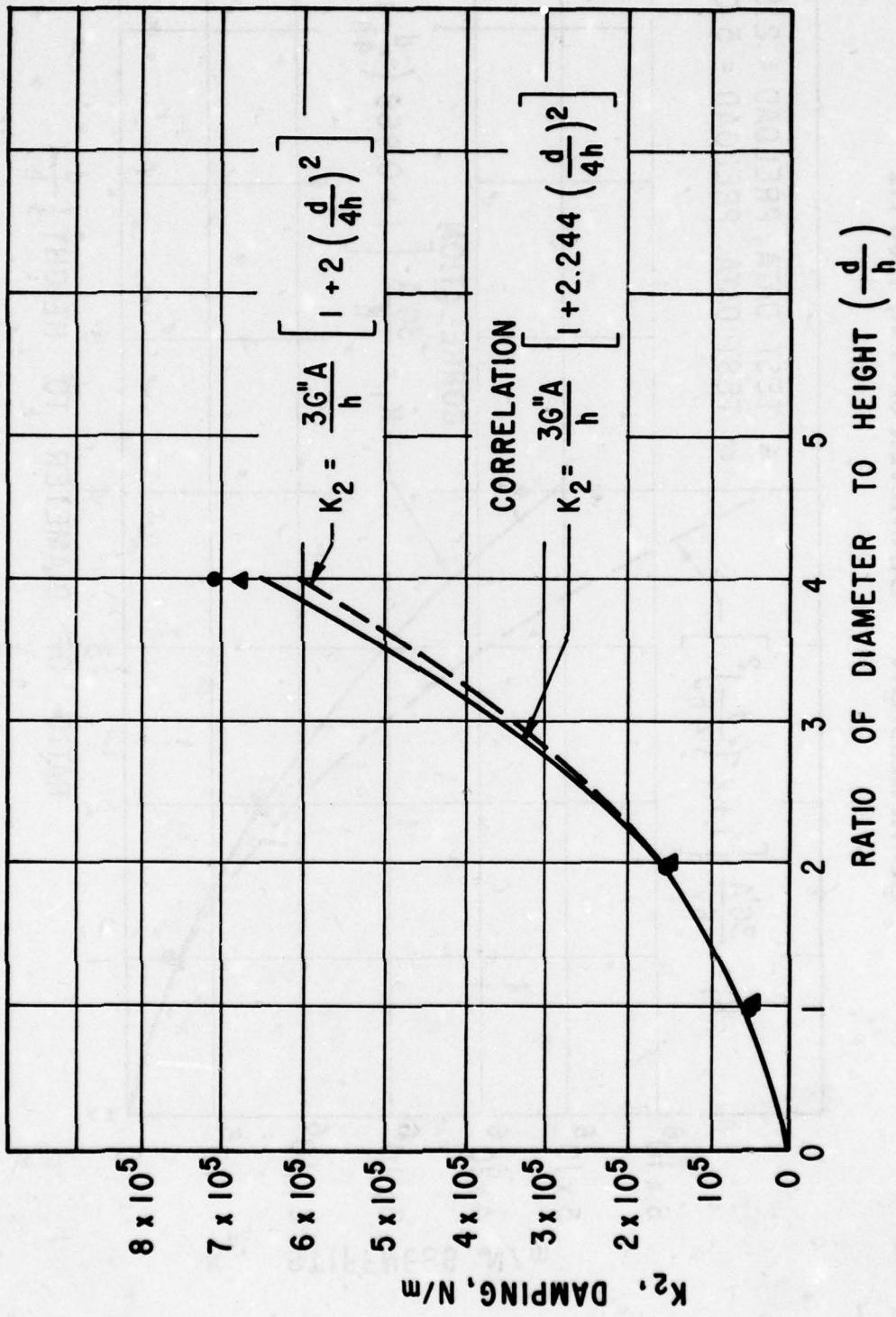
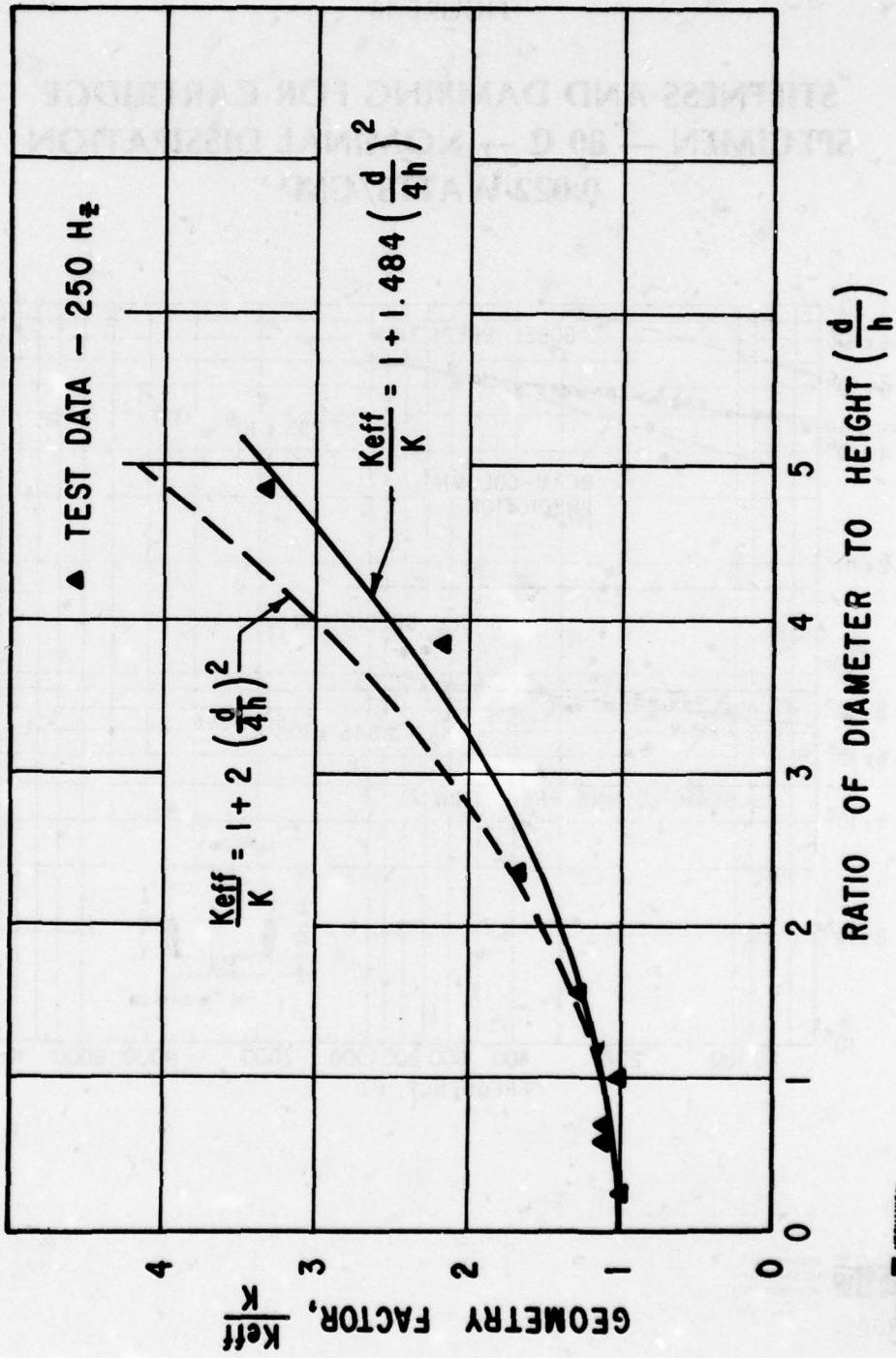


FIGURE 17
CORRELATION WITH WORK OF NASHIF,
CANNON AND JONES
DYNAMIC STIFFNESS OF
CYLINDRICAL ELASTOMER TEST SPECIMEN

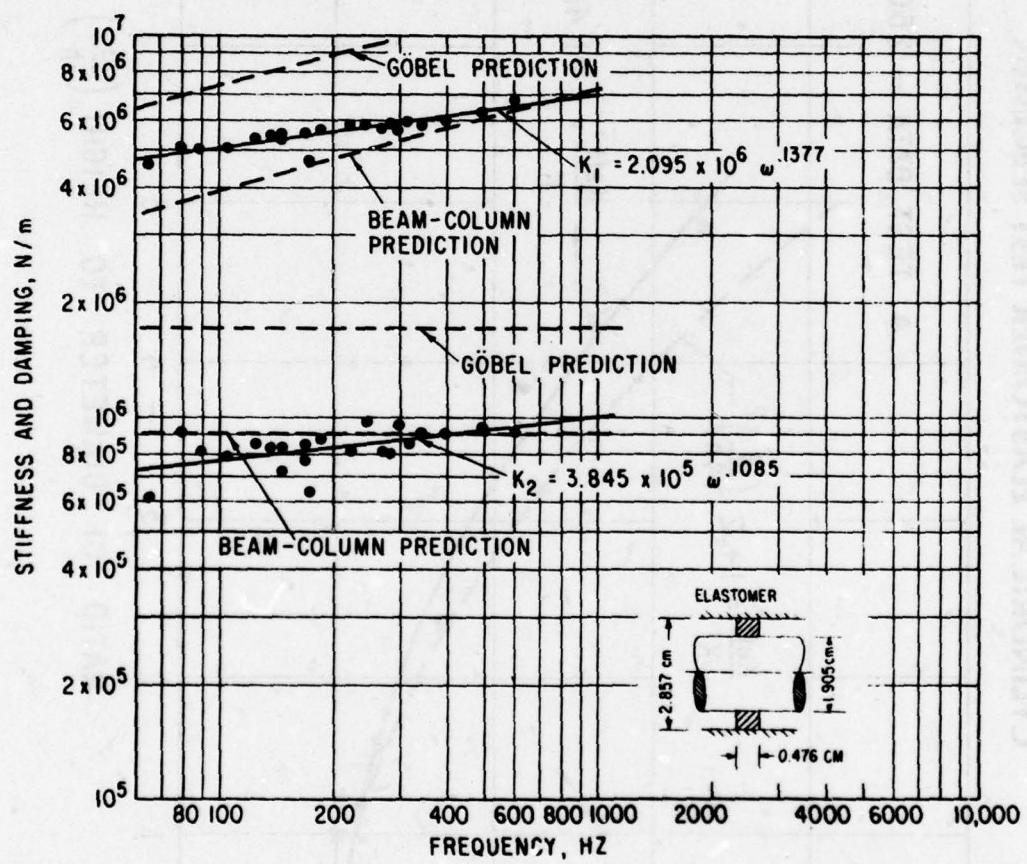


MITSUBISHI
TECHNOLOGY
INCORPORATED

78P61

FIGURE 18

**STIFFNESS AND DAMPING FOR CARTRIDGE
SPECIMEN — 80 C — NOMINAL DISSIPATION
0.022 WATTS/CM³**



MTI MECHANICAL
TECHNOLOGY
INCORPORATED

7SP61

FIGURE 19

**TREND SUMMARY: THE EFFECT OF MATERIAL
ON STIFFNESS AND LOSS COEFFICIENT
FOR O-RING DAMPERS**

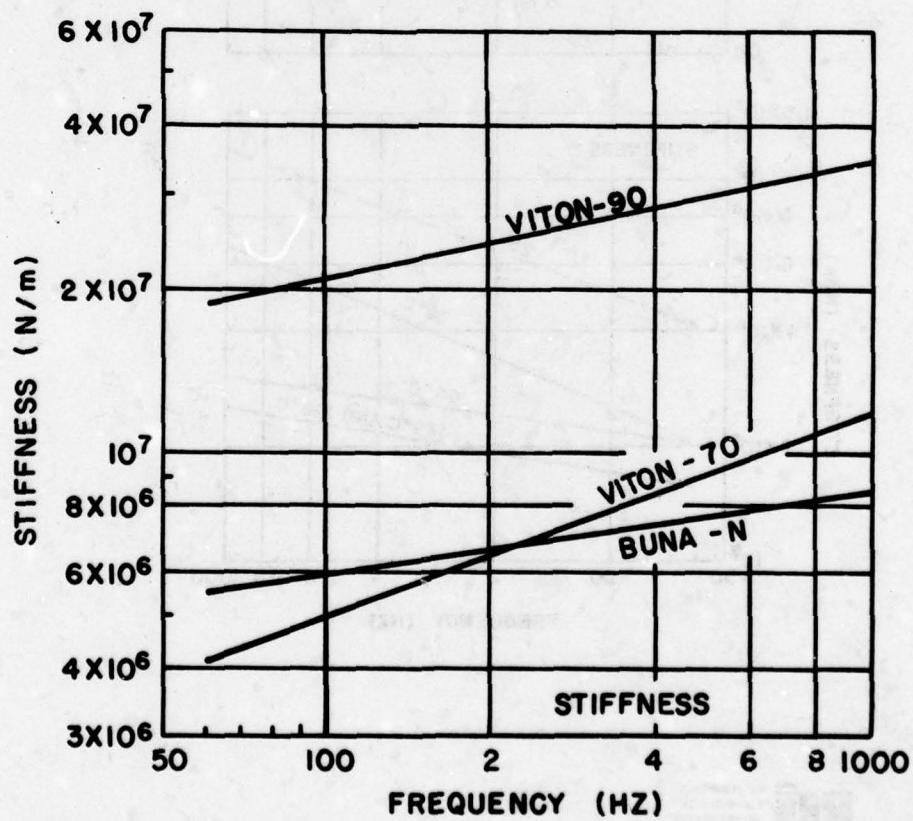
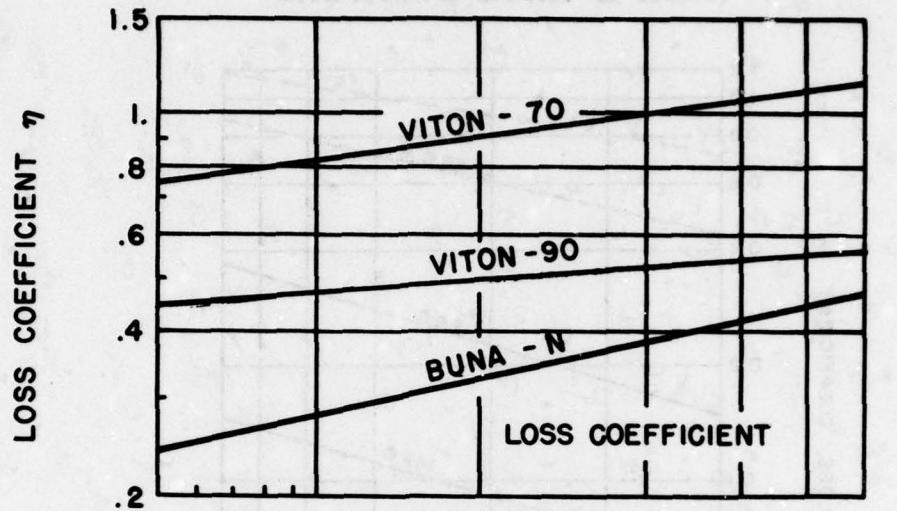


FIGURE 20

TREND SUMMARY: THE EFFECT OF TEMPERATURE
ON STIFFNESS AND LOSS COEFFICIENT
FOR O-RING DAMPERS

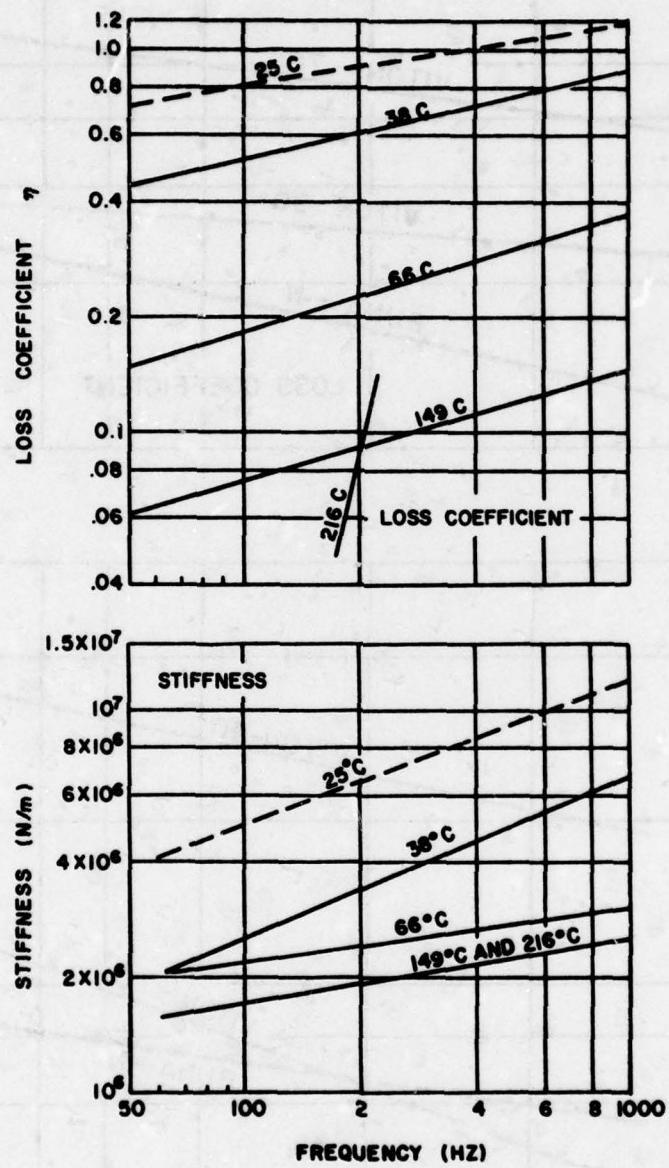


FIGURE 21

TREND SUMMARY: THE EFFECT OF AMPLITUDE
ON STIFFNESS AND LOSS COEFFICIENT
FOR O-RING DAMPERS

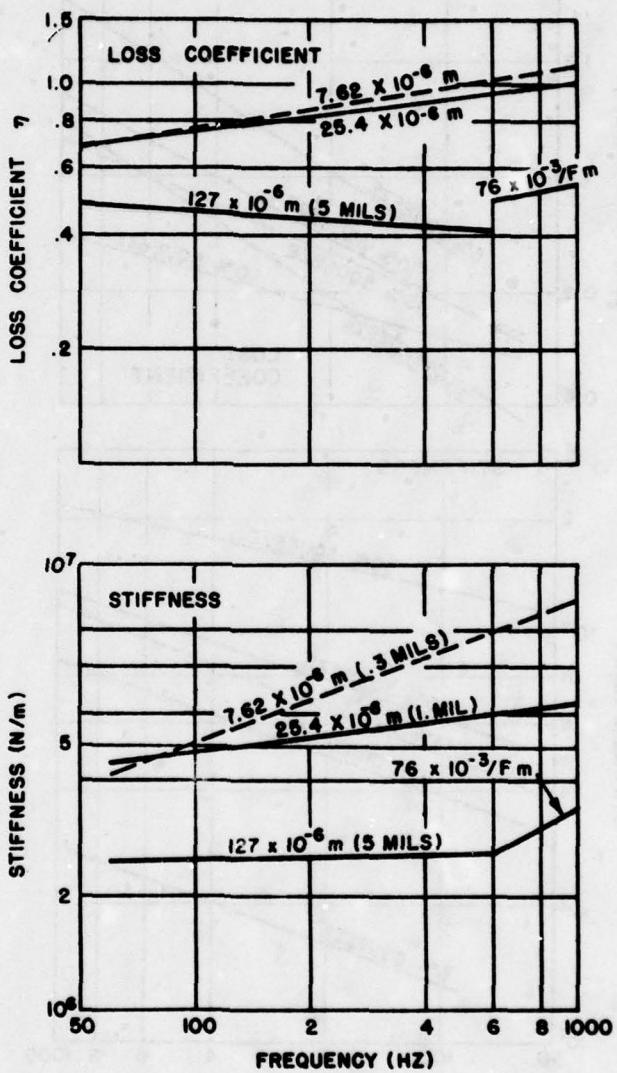


FIGURE 22

**TREND SUMMARY: THE EFFECT OF SQUEEZE
ON STIFFNESS AND LOSS COEFFICIENT
FOR O-RING DAMPERS**

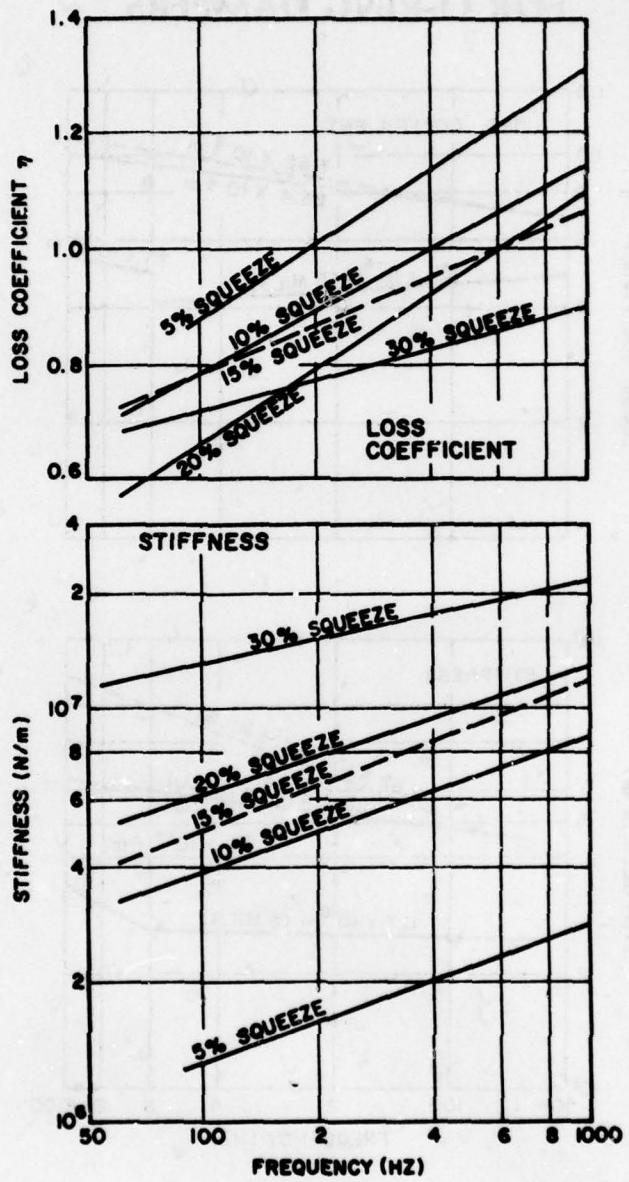
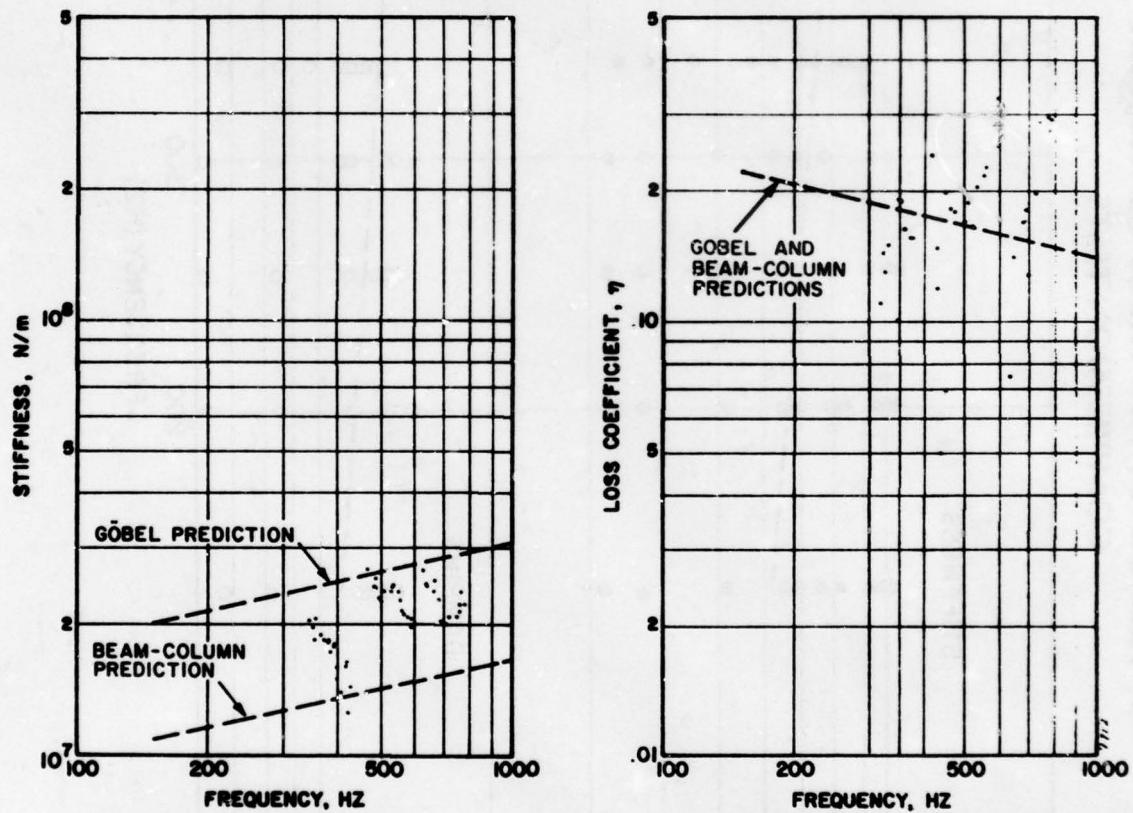


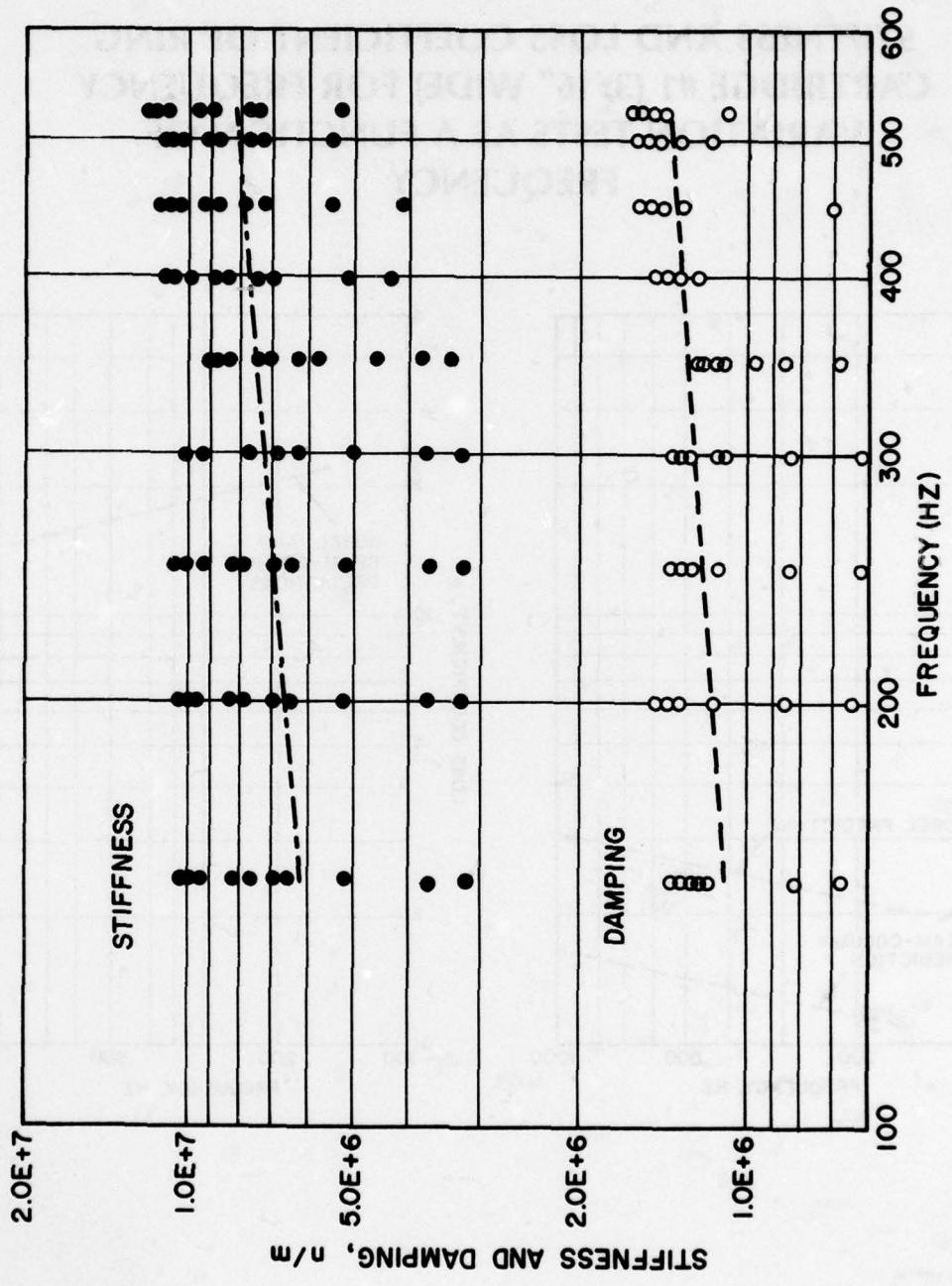
FIGURE 23

**STIFFNESS AND LOSS COEFFICIENT OF RING
CARTRIDGE #1 (3/16" WIDE) FOR FREQUENCY
VARIATION TESTS AS A FUNCTION OF
FREQUENCY**



M MECHANICAL
TECHNOLOGY
INCORPORATED
78P61

FIGURE 24
STIFFNESS AND DAMPING AS A FUNCTION
OF FREQUENCY FOR THE 66°CENTIGRADE
COMPRESSION TESTS



MECHANICAL
TECHNOLOGY
INCORPORATED
78P61

FIGURE 25
LOSS COEFFICIENT AS A FUNCTION OF
FREQUENCY FOR THE 66° CENTIGRADE
COMPRESSION TESTS

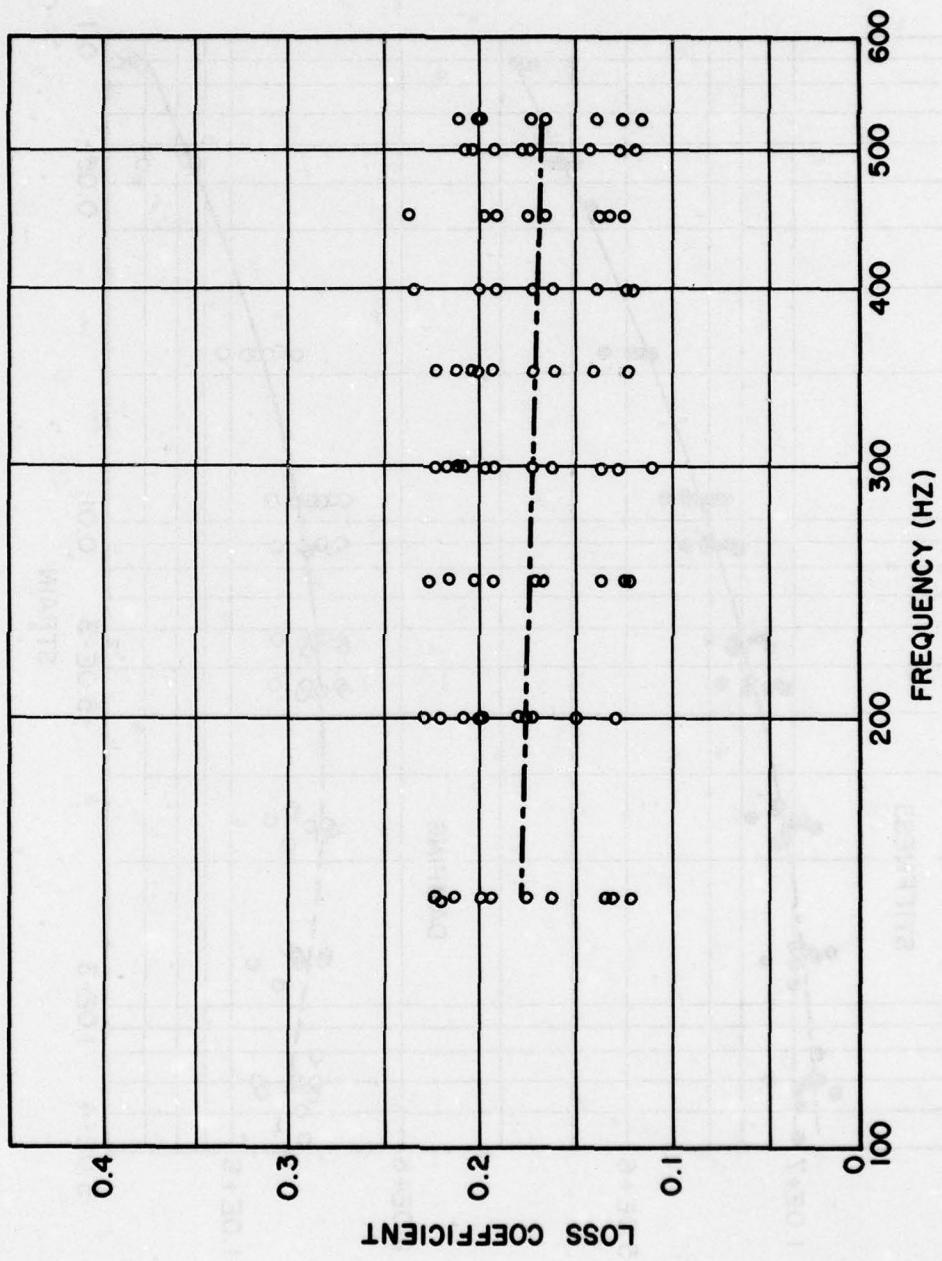
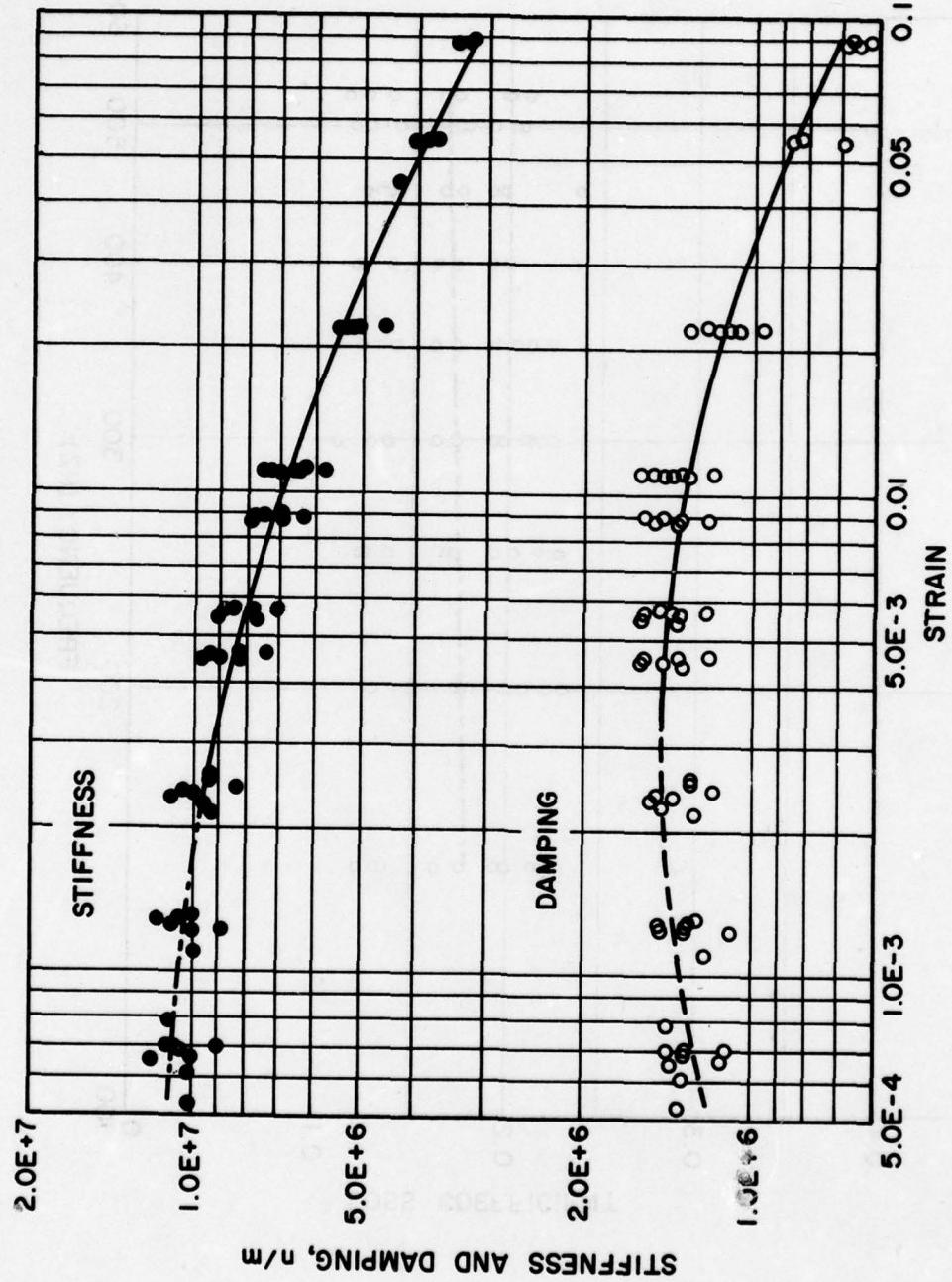


FIGURE 26

STIFFNESS AND DAMPING AS A FUNCTION
OF STRAIN FOR THE 66° CENTIGRADE
COMPRESSION TESTS



Mechanical
Technologies
Incorporated
78E61

FIGURE 27

LOSS COEFFICIENT AS A FUNCTION OF STRAIN
FOR THE 66° CENTIGRADE COMPRESSION TESTS

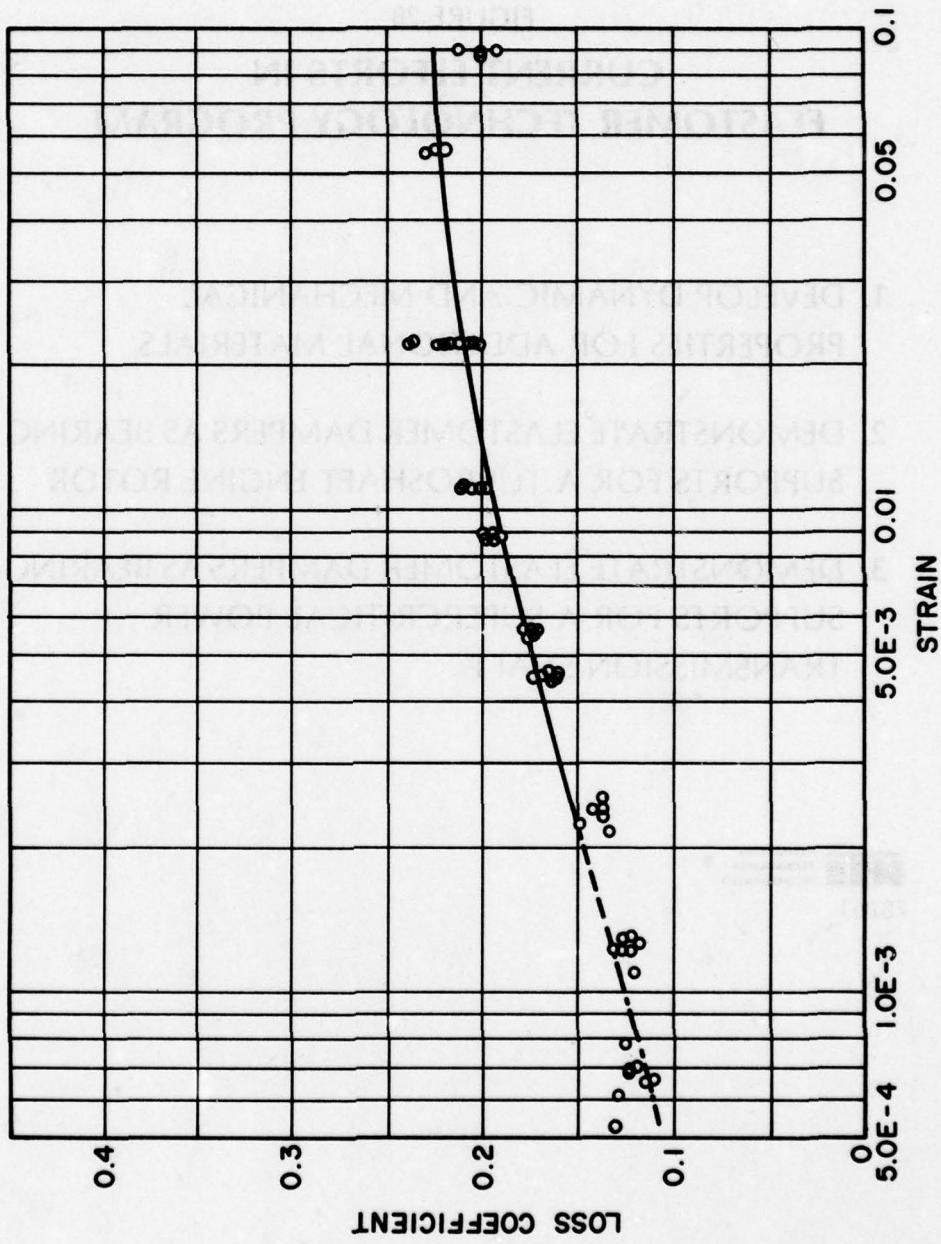


FIGURE 28

CURRENT EFFORTS IN ELASTOMER TECHNOLOGY PROGRAM

1. DEVELOP DYNAMIC AND MECHANICAL PROPERTIES FOR ADDITIONAL MATERIALS
2. DEMONSTRATE ELASTOMER DAMPERS AS BEARING SUPPORTS FOR A TURBOSHAFT ENGINE ROTOR
3. DEMONSTRATE ELASTOMER DAMPERS AS BEARING SUPPORTS FOR A SUPERCRITICAL POWER TRANSMISSION SHAFT



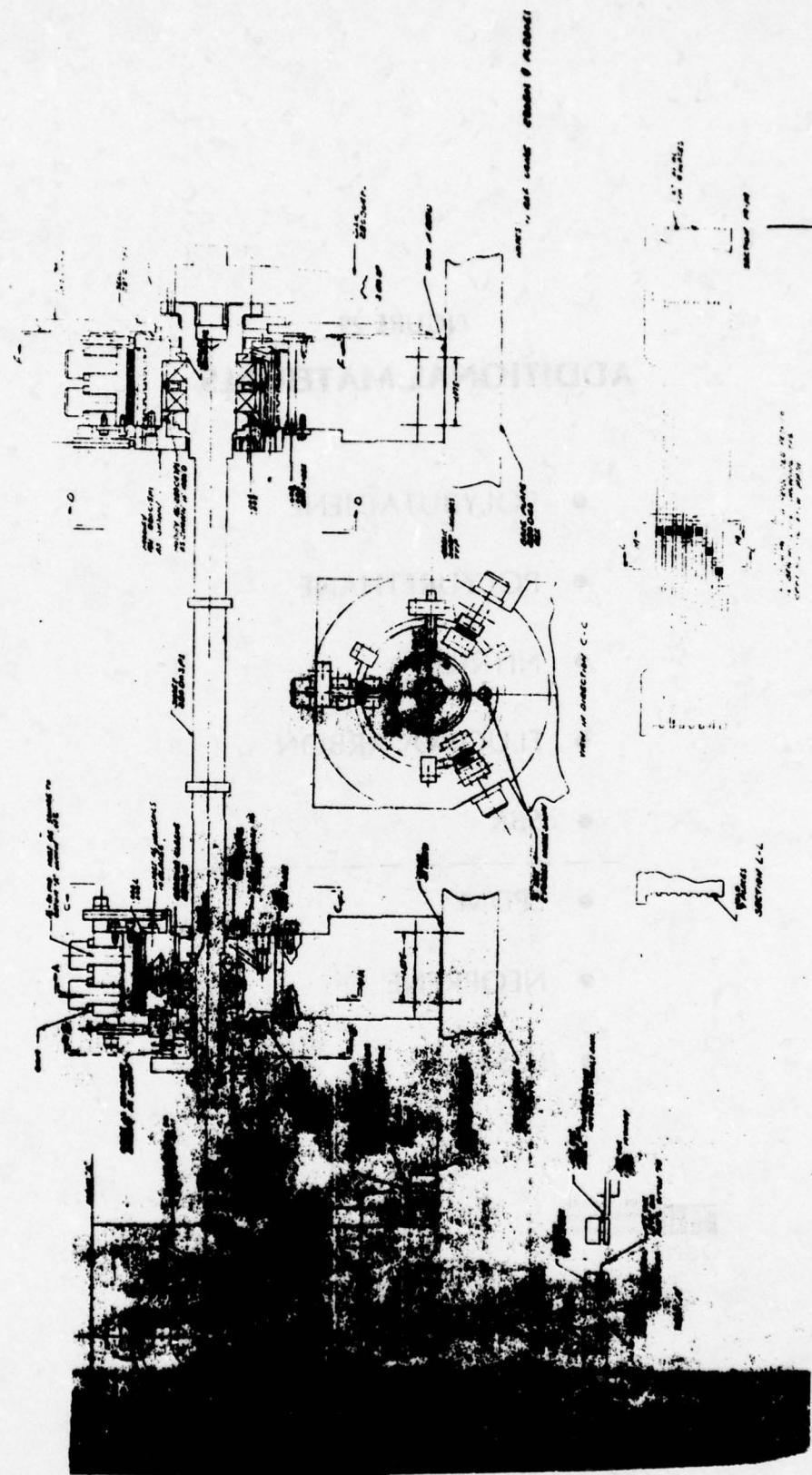
FIGURE 29
ADDITIONAL MATERIALS

- POLYBUTADIENE
- POLYURETHANE
- NITRILE
- FLUOROCARBON
- SBR
-
- EPDM
- NEOPRENE
- LCS



FIGURE 30

TURBOSHAFT ENGINE DYNAMIC SIMULATOR
WITH ELASTOMER DAMPERS



MECHANICAL
TECHNOLOGY
INCORPORATED
78P61

FIGURE 31
**ELASTOMER DAMPER TEST RIG LOG
DECREMENT FOR FORWARD CRITICALS
AS A FUNCTION OF ELASTOMER DAMPING**

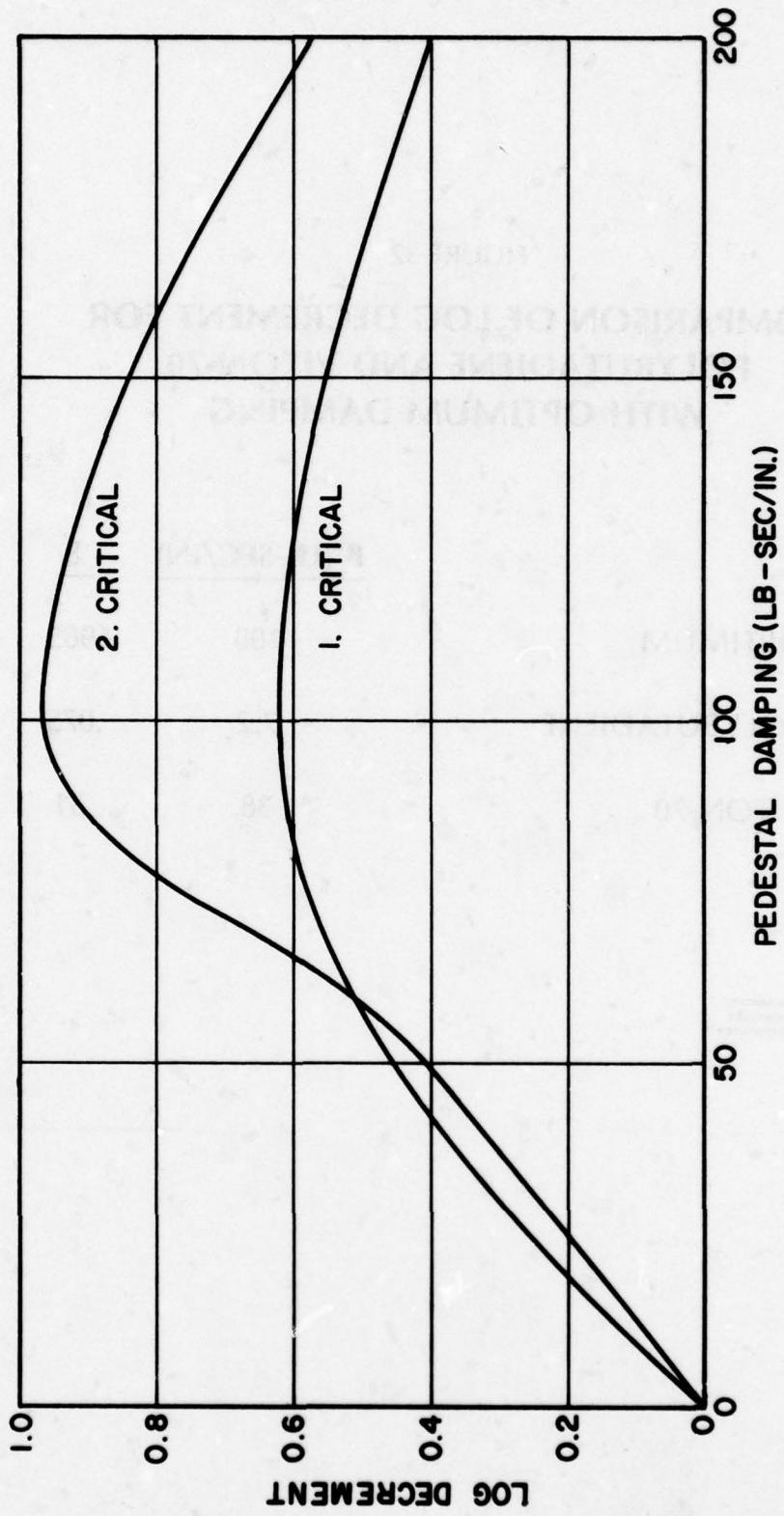


FIGURE 32

**COMPARISON OF LOG DECREMENT FOR
POLYBUTADIENE AND VITON-70
WITH OPTIMUM DAMPING**

	<u>B (LB-SEC/IN)</u>	<u>8</u>
(1) OPTIMUM	100	.965
(2) POLYBUTADIENE	7.2	.075
(3) VITON-70	38	.31

MTI MECHANICAL
TECHNOLOGY
INCORPORATED
78P61

FIGURE 33

**DRIVE TRAIN DYNAMICS TECHNOLOGY TEST RIG
Configured for High-Speed Interconnect
Shaft System Tests**

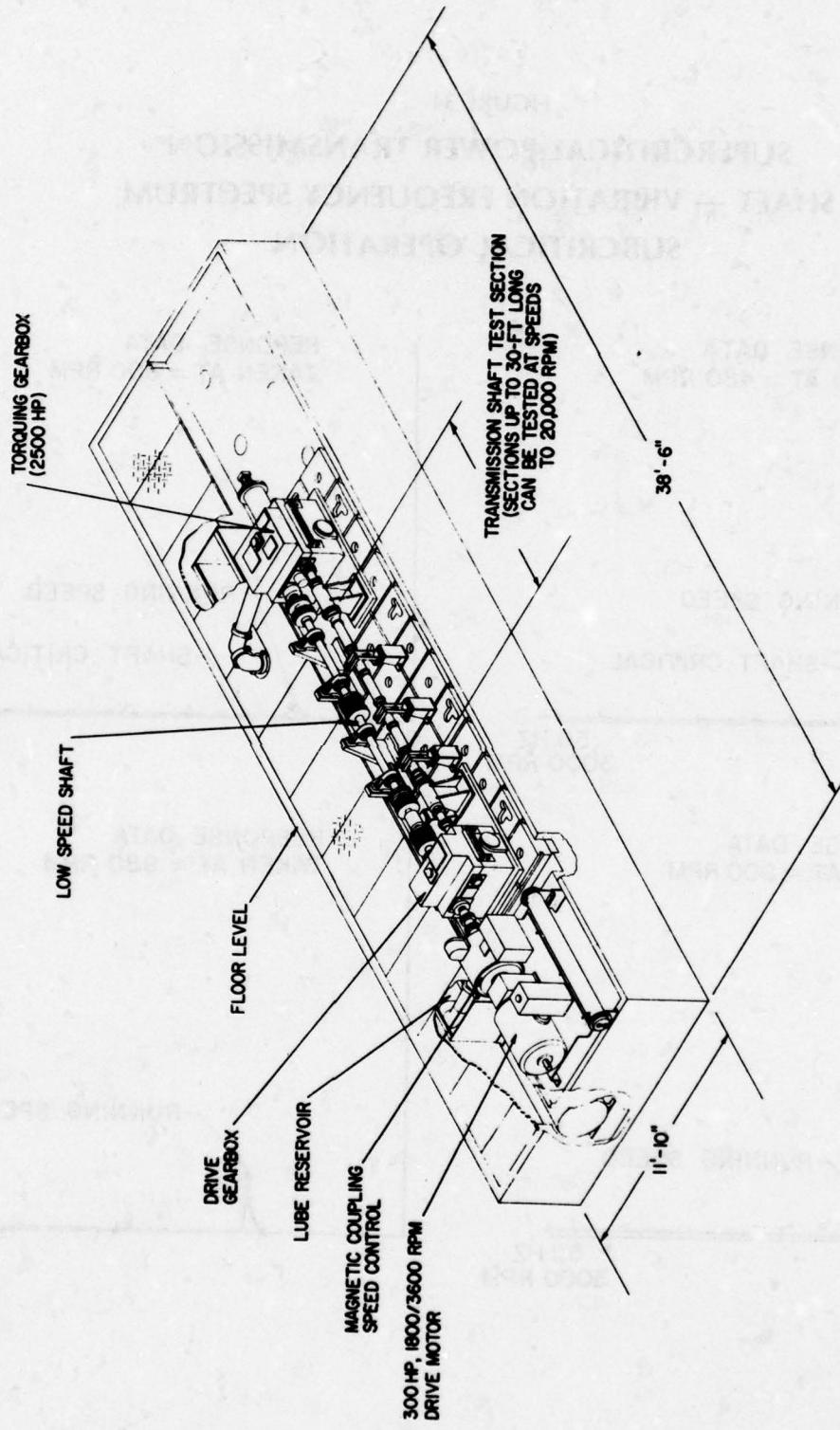


FIGURE 34

**SUPERCritical POWER TRANSMISSION
SHAFT — VIBRATION FREQUENCY SPECTRUM
SUBCRITICAL OPERATION**

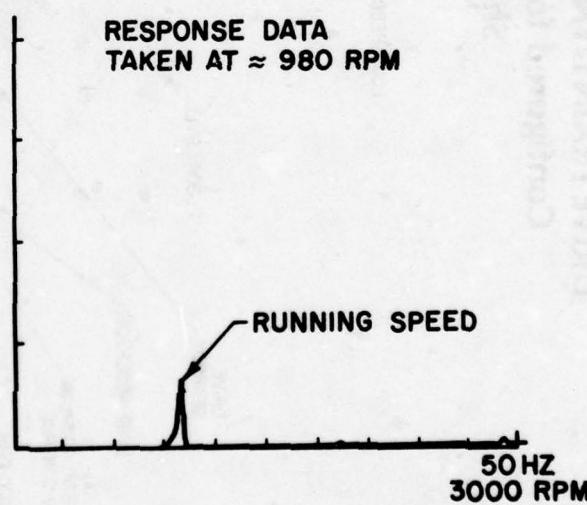
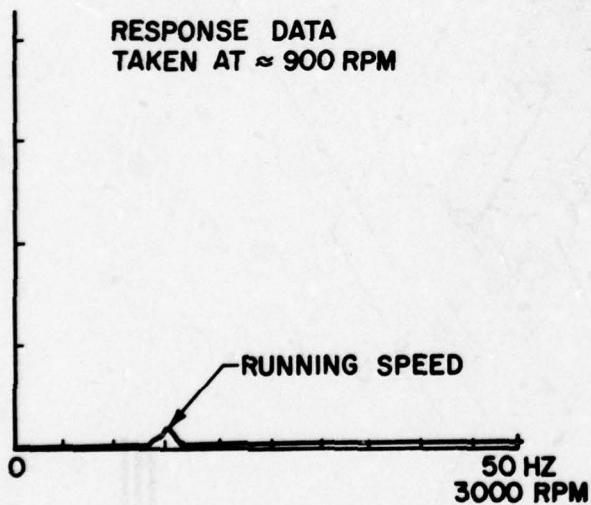
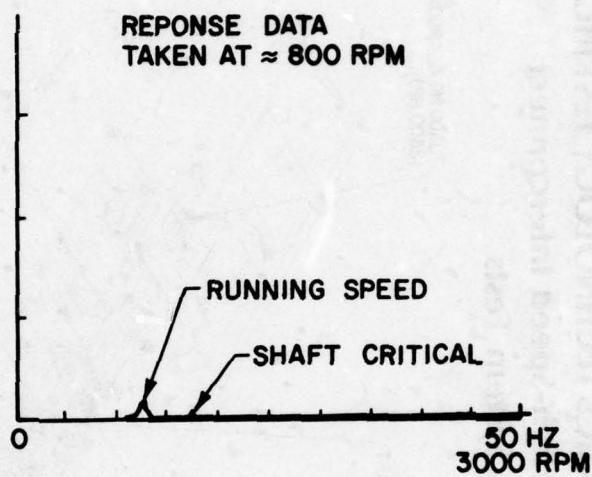
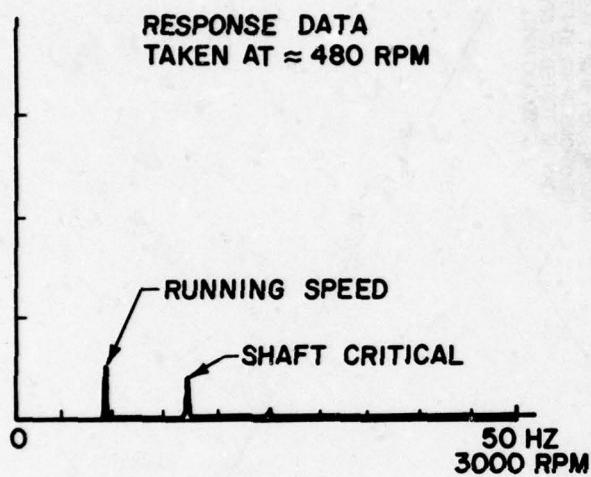


FIGURE 35

**SUPERCritical POWER TRANSMISSION
SHAFT — VIBRATION FREQUENCY SPECTRUM
SUPERCritical OPERATION**

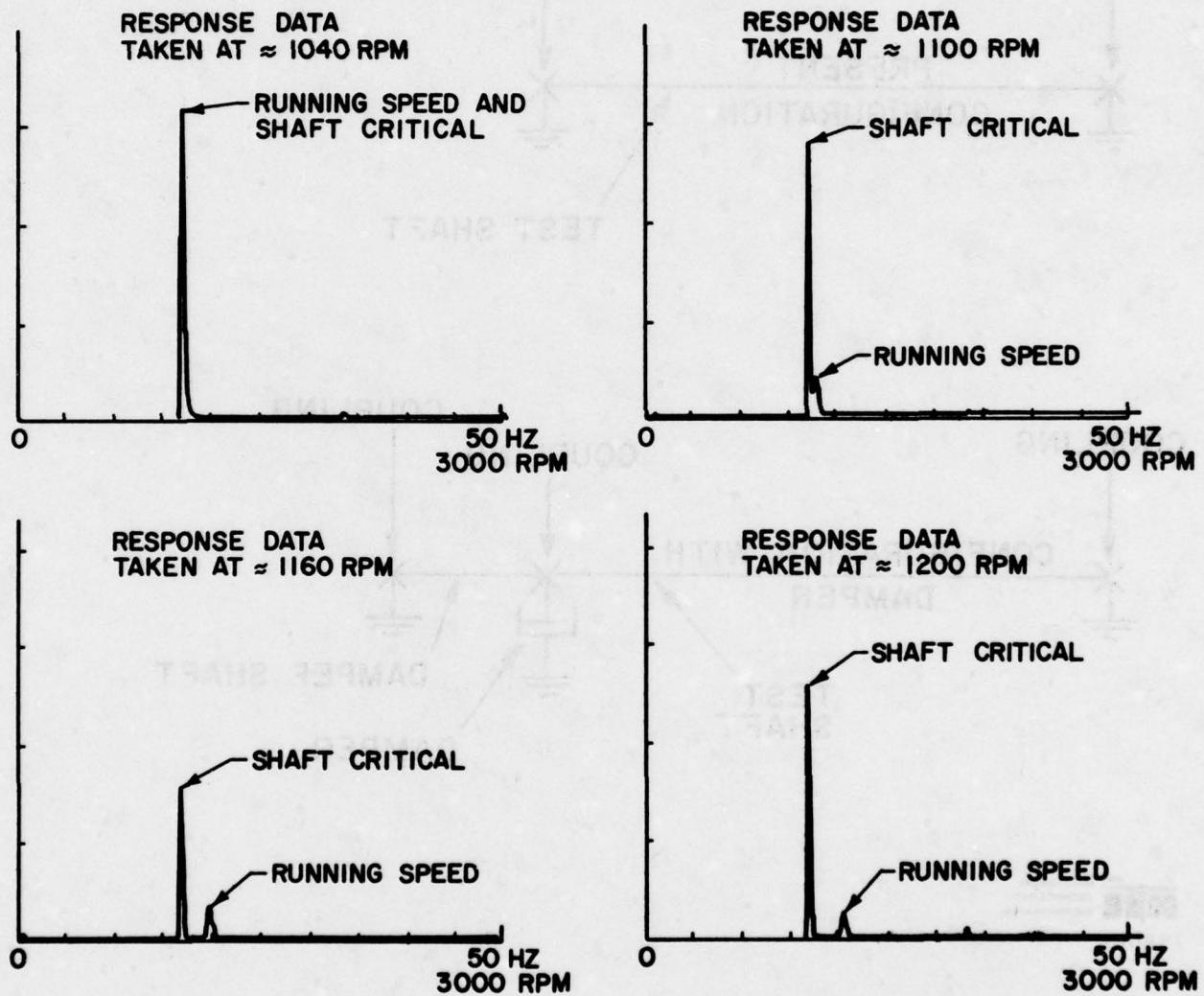
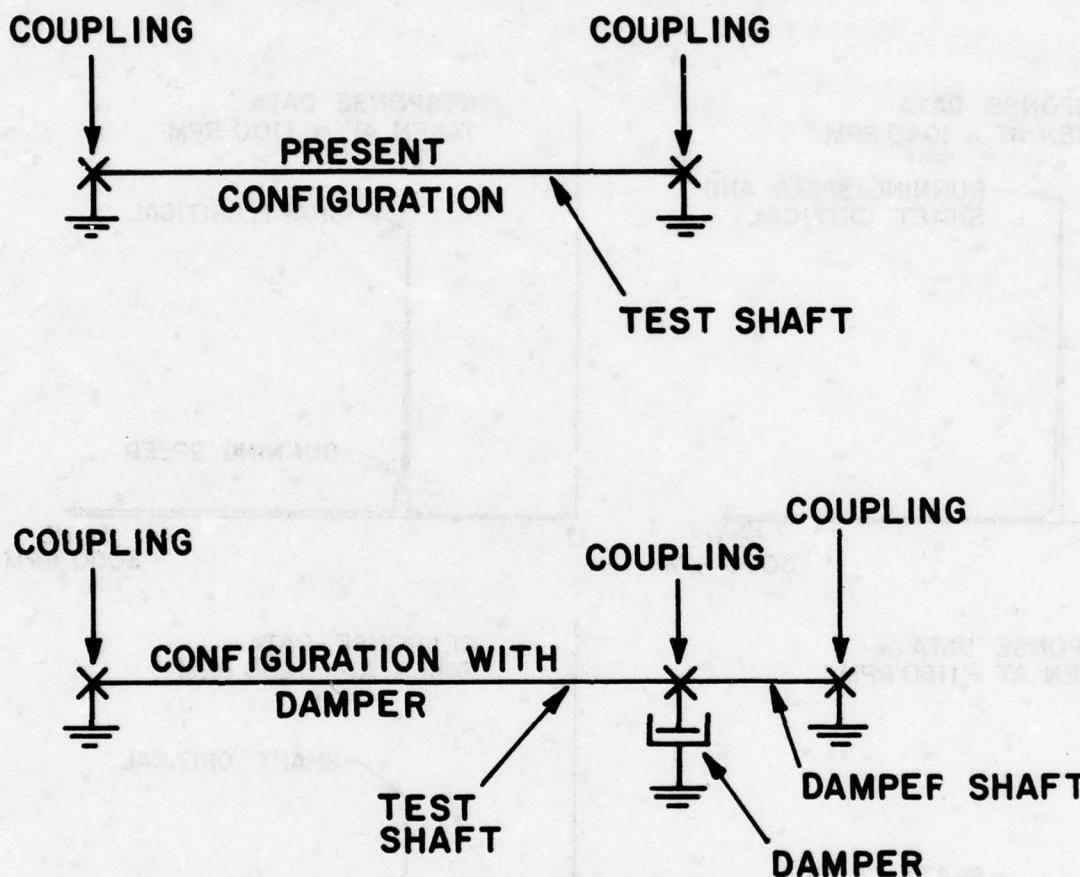


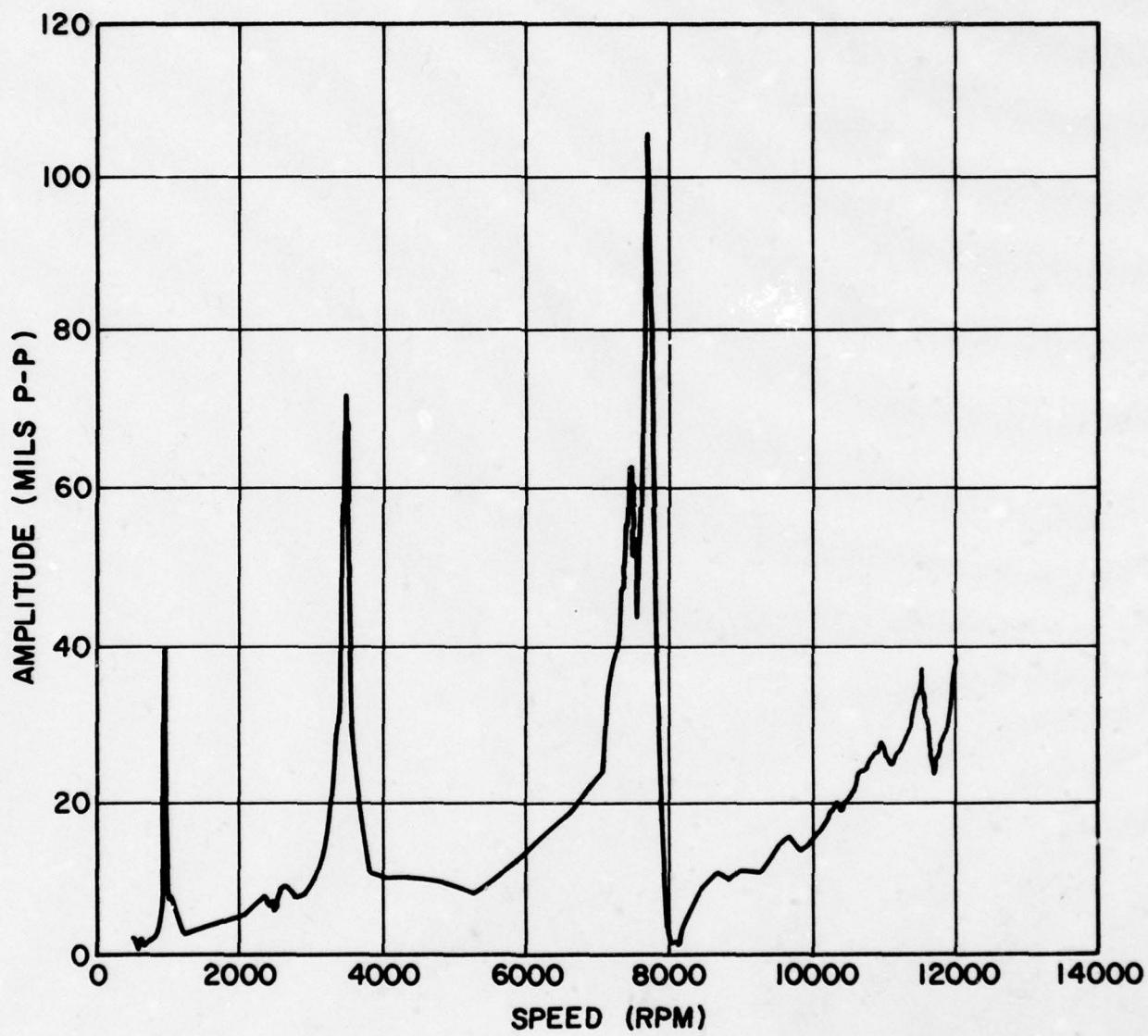
FIGURE 36
DAMPED SHAFT DESIGN CONFIGURATION



MTI MECHANICAL
TECHNOLOGY
INCORPORATED

78P61

FIGURE 37
**PLOT OF AMPLITUDE AS A FUNCTION OF
FREQUENCY FOR SUPER SHAFT RUN
0-12000 RPM PROBE 6**



MTI
MECHANICAL
TECHNOLOGY
INCORPORATED
78P61

**ASTM DAMPING MATERIALS
TESTING SPECIFICATION ACTIVITY**

E. E. Dennison
Gilbert/Commonwealth Association
Power Engineering Division
Jackson, Michigan

ASTM DAMPING MATERIALS
TESTING SPECIFICATION ACTIVITY

E. EARL DENNISON, P.E.
GILBERT/COMMONWEALTH, JACKSON, MICHIGAN

ABSTRACT

The American Society for Testing and Materials (ASTM) has initiated a Task Group charged with the responsibility of identifying a meaningful test method. This voluntary consensus standards writing body is proceeding to develop a standard at an early date. The decisions already determined by the Task Group are presented, together with an estimated schedule for completion of a standard.

ASTM DAMPING MATERIALS
TESTING SPECIFICATION ACTIVITY

INTRODUCTION

The American Society for Testing and Materials (ASTM) Committee E-33 on Environmental Acoustics is concerned with establishing a standardized test method for damping materials. This desire is based on the interest of the Committee in promoting the use of damping materials for the control of audible noise. Task Group E-33.03-M on Damping Materials was formed in April, 1977 to address this problem.

DISCUSSION:

ASTM E-33 Committee on Environmental Acoustics consists of approximately 150 members, including material suppliers, users and third party consultants. The committee meets every six months for three days. Task Groups meet on Monday, followed by Subcommittee meetings on Tuesday, and a meeting of the committee as a whole on Wednesday. Task Groups can (and do) meet more often. Much of the work of the Task Groups and Subcommittees is accomplished by telephone and correspondence.

The Task Group on Damping Materials functions under the E-33.03 Subcommittee on Transmission Loss. The test methods evolving from the actions of the Task Group, Subcommittee and committee of the whole represent a consensus-type standard with acceptance throughout industry.

Task Group E-33.03M on Damping Materials consists of approximately 20 members having diverse backgrounds. The Task Group has met twice and has developed certain operating procedures which are described herein. There are no major hurdles to the early development of a test method apparent at this time.

The procedure to be followed includes a written vote of the Task Group members on the proposed standard. The draft document is put to a vote first by the Subcommittee and then by the whole committee. Two or more of these votes may occur simultaneously, thereby speeding up the process. It is important to understand that in the ASTM scheme of operation, one does not have to be a member of ASTM in order to fully participate in the operation of a Task Group.

The relationship of the ASTM to other standards writing agencies, to the American National Standards Institute (ANSI) and to the international standards writing bodies is best shown in the following scheme:

International Standards
ISO/TC28 and ISO/TC43

ANSI Consensus Standards
ASTM E-33 and ASA (S1, S2, S3)

Prof/Trade/Gov't. Standards
ASHRAE, IEEE, EEI, ASME, Etc.

All professional, trade and governmental standards agencies are of course free to develop standards for submission to ANSI. However, ASTM and the Acoustical Society of America (ASA) prepare the bulk of the audible noise and vibration related standards.

A recently developed ASTM Proposed Standard program is designed to facilitate the rapid development of new test methods. The new Proposed Standard has a two year review cycle, versus the normal five year review cycle required of most ASTM standards. It is possible to establish a Proposed Standard and to have it reviewed in two years to incorporate the results during its' early use.

In the broadest sense, damping materials cover a multitude of damping concepts and products. In its first decision, the Task Group has set as its' Purpose, "to develop testing standards relating to uniform materials and/or material composites with joined interfaces". The proper interpretation of this stated Purpose will be found in the ASA Nomenclature Document to be discussed shortly. In practice, the Task Group Purpose is concerned with polymeric damping systems.

Next, the Task Group has accepted the Acoustical Society of America (ASA) STD 6-1976 (ANSI S2.9-1976), "Nomenclature for Specifying Damping Properties of Materials" for the conduct of Task Group business.

Common practice for a new ASTM Task Group is to prepare a White Paper on the Subject under investigation. With far more than 2,500 documents having been written on this subject during the past 20 years, what is not needed at this time is another White Paper!

ASTM policy does not require the preparation of a White Paper, provided that adequate records are maintained by the

Task Group during its' work. Therefore, a decision has been taken by the Task Group Chairman to forego the preparation of a White Paper. This decision will significantly shorten the preparation time of a test standard.

The Task Group is inclined to identify an existing test method, or one which may be slightly modified, rather than attempting to develop a new test method. There is recognition that none of the existing test methods, either for dynamic modulus or system loss factor, are entirely satisfactory. It is felt that by publishing a Proposed Standard with a two year review cycle, we may force the development of improved test methods for consideration by the ASTM or the ASA.

The first draft standard is expected to be distributed to the Task Group members within the next two months. Final ASTM approval is anticipated by April 1979. The results of this meeting today may conceivably alter this schedule. However, the efforts undertaken by ASTM make this target date of April, 1979 appear realistic, at this moment.

The next meeting of ASTM E-33.03-M Task Group on damping materials will be held on Monday, Tuesday and Wednesday, April 10, 11, 12, 1978 at ASTM Headquarters in Philadelphia, Pennsylvania. Again, anyone desiring to participate in the activities of this Task Group are invited to attend this meeting.

DAMP IT: A PROPOSED ADVANCED DEVELOPMENT PROGRAM

Dr. Lynn Rogers
Air Force Flight Dynamics
Laboratory
Wright-Patterson Air Force
Base, Ohio

DAMP IT: A PROPOSED ADVANCED DEVELOPMENT PROGRAM

Dr. Lynn Rogers
Air Force Flight Dynamics Laboratory

The Air Force Advanced Metallic Structures Advanced Development Program (AMS ADP) has as one of its primary objectives the systematic investigation of improvements in structural reliability and the verification of the structural reliability of new materials, processes, and designs. A technology area identified by the AMS ADP that has the potential of providing dramatic improvements in structural reliability is the area of damping technology (see Figure 1). The most significant payoff will be in the reliability of airframes, avionics, and accessories which are subject to a severe dynamics environment. This improved reliability will result in dramatic life cycle cost savings and improved operational readiness. Where vibratory stresses determine hardware lifetimes, tenfold increases in life with no weight or acquisition cost increases are anticipated.

A substantial body of successful research and development experience exists (References 1 - 5, and the rest of these proceedings), particularly with regard to additive damping treatments. This emerging technology, together with the existence of generic problems and areas where the design is governed by the dynamics environment, dictates that damping be integrated into design and manufacture to avoid reliability, cost, and weight penalties. The AMS ADP is defining an effort titled "Dynamics Abatement and Major Payoff through Integrated Technology (DAMP IT)."

For the uninitiated, an Advanced Development Program (ADP) is a hardware program consisting of design, manufacture, and test phases. These phases can result in hardware which is fully qualified for incorporation into a system with all integration aspects covered; or, the hardware may be limited to serving as a technology demonstrator with major advances in confidence. An ADP must be founded on both an existing technology base and an established payoff. The typical scope of an advanced development program is in the neighborhood of 30 man-years, with a range of four to 300 man-years and possibly beyond, depending on many factors.

The viability of viscoelastic damping technology to control vibration, noise, and resonant fatigue has been repeatedly demonstrated; further, a substantial technology base consisting of a body of successful research, development, and applications exists (see References 1 - 5 and the rest of these Proceedings). Materials are available and methods for engineering damping applications exist.

A number of projects have been plotted in Figure 2, which shows percent weight change vs. percent vibratory stress reduction

and approximate life extension. It is immediately obvious that additive damping is preferable to the beef-up or stiffening approach from a weight consideration; further, it has the added economic benefit of extending the life of existing hardware. It is also obvious that integral damping is even better than added damping, and saves appreciable weight provided the vibroacoustic condition is dominant. Figure 3 summarizes the possibilities of extending high cycle fatigue life and saving weight and cost by use of integral damping.

Granted that integral damping has significant payoff in high cycle fatigue life and other facets of reliability, how is increased use achieved? Figure 4 lists the ingredients. The factors of technology, requirements/incentives, and volume all must increase at nearly equal paces. Any increase in one area leads to increases in the other areas.

With the established damping technology base and the potential payoff in the use of integral damping concepts to control vibration, noise and/or resonant fatigue, an advanced development program to provide a major technology advancement is in order. Figure 5 gives the objective, approach, and payoff in most general terms.

It remains to select an appropriate project, quantify the potential payoff, develop management support, and secure funding. Possible projects include: airframe, avionics, accessories, equipment, secondary airframe structure, elevators, flaps, bombbay doors, nacelles, inlets, sheet metal near a gun, high energy lasers, wave guides, radar dishes, gimbals, heat exchangers, vidicons, TWT's, pods, avionics covers, circuit boards, components, spacecraft structure, etc. Figure 6 lists the criteria for selection and definition of a project. Systems window refers to the timing; technological opportunity signifies a general awareness in both technical and management personnel of limitations caused by use of conventional technology. Payoff must be in terms of the baseline system whether or not it is hoped to use the technology in the system production. It is obvious that the planned technology advancement must be generically applicable.

The very proper questions posed in Figure 7 should be borne in mind, and that is why an ADP is needed in the face of great interest in the technology. Of those reasons listed, probably the most basic is "Accelerate the application." An ADP is needed to break into the systems life cycle circle and incorporate integral damping into original manufacture. An offeror cannot choose to put in his proposal the use of a high technology such as integral damping without very substantial confidence in technical, schedule, and cost aspects because, if he did, his competitor would win. The Air Force cannot make the use of high technology a requirement unless it is well established. Hence, the need for an ADP to break the circle.

REFERENCES

1. M.D. Lamoree and W.L. LaBarge, "Sonic Fatigue Resistance of Structures Incorporating a Constrained Viscoelastic Core," The Shock and Vibration Bulletin, Bulletin 40 Part 5, December 1969, pp 49-60.
2. B.C. Nakra, "Vibration Control with Viscoelastic Materials," The Shock and Vibration Digest, Vol. 8, No. 6, June 1976, pp 3-12.
3. J.D. Sharp, Enhanced Durability Through Additive Damping Treatments, AIAA/SAE 13th Propulsion Conference, Orlando, Florida, 11-13 July 1977, Paper No. 77-881.
4. M. Ferrante, C.V. Stahle, and F.J. On, "Feasibility Study of an Acoustic Enclosure for Shuttle Payloads," The Shock and Vibration Bulletin, Bulletin 46 Part 2, August 1976, pp 209-227.
5. G. SenGupta, "Reduction of Low Frequency Cabin Noise During Cruise Condition by Stringer and Frame Damping," AIAA 19th Structural Dynamics Conference, Bethesda, Maryland, April 1978, Paper No. 78-504.

HOW DAMPING IMPROVES RELIABILITY IN A VIBROACOUSTIC ENVIRONMENT

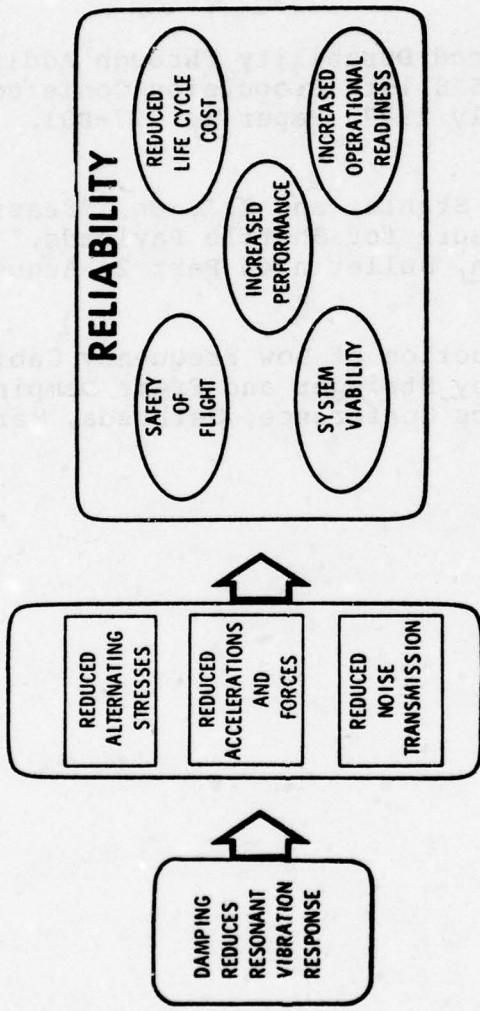


Figure 1

COMPARISON OF APPROACHES TO EXTENSION OF RESONANT FATIGUE LIFE

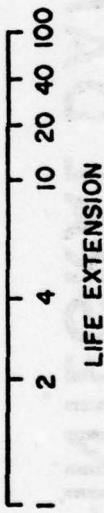
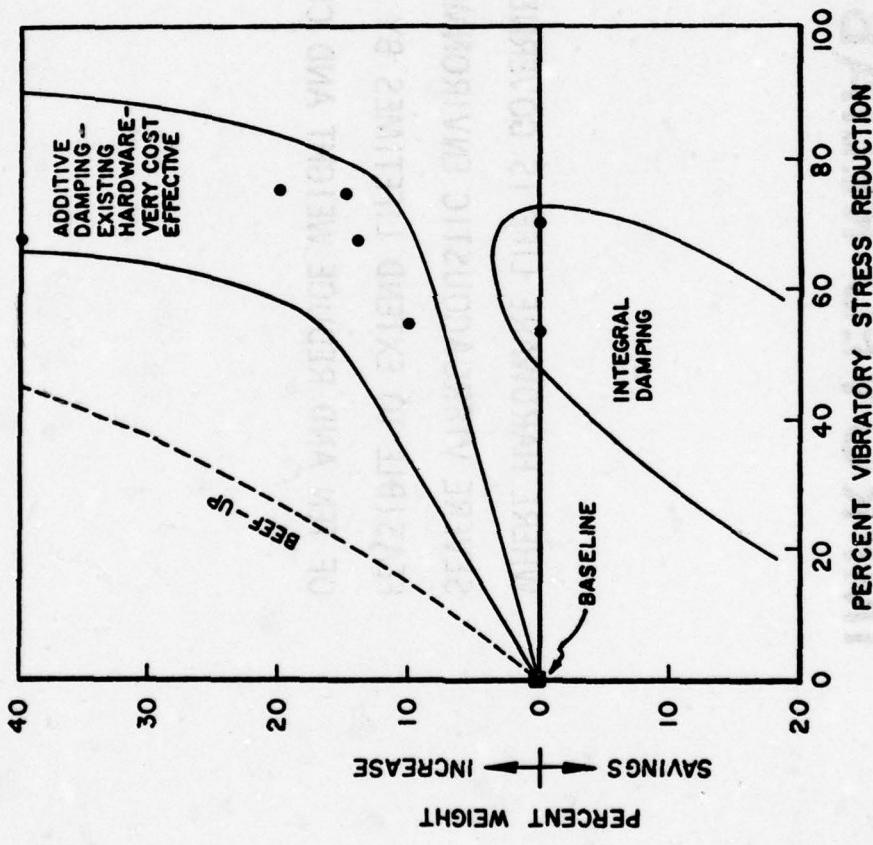


Figure 2

INTEGRAL DAMPING FOR IMPROVED RELIABILITY

WHERE HARDWARE LIFE IS GOVERNED BY A SEVERE VIBROACOUSTIC ENVIRONMENT, IT IS FEASIBLE TO EXTEND LIFETIMES BY A FACTOR OF TEN AND REDUCE WEIGHT AND COST.

Figure 3

INGREDIENTS OF INCREASED USE OF INTEGRAL DAMPING

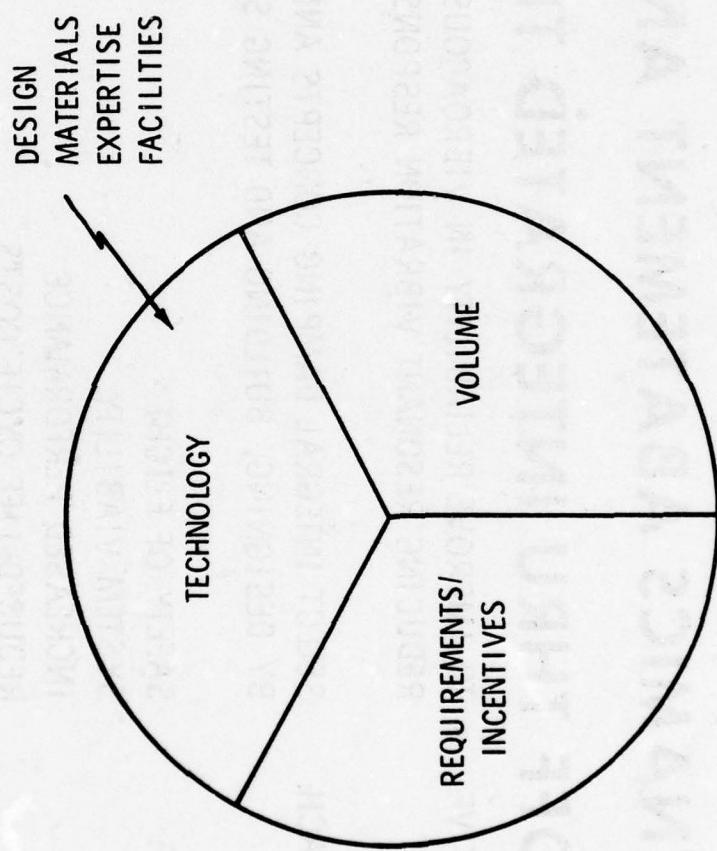


Figure 4

DAMP IT

DYNAMICS ABATEMENT AND MAJOR PAYOFF THRU INTEGRATED TECHNOLOGY

OBJECTIVE: TO IMPROVE RELIABILITY IN VIBROACOUSTIC ENVIRONMENTS BY REDUCING RESONANT VIBRATION RESPONSE

APPROACH: SELECT INTEGRAL DAMPING CONCEPTS AND DEMONSTRATE BY DESIGNING, BUILDING AND TESTING SELECTED COMPONENTS

PAYOUT: SAFETY OF FLIGHT
SYSTEM VIABILITY
INCREASED PERFORMANCE
REDUCED LIFE CYCLE COSTS
IMPROVED OPERATIONAL READINESS

CRITERIA FOR SELECTION OF DAMP IT AREAS

- SYSTEMS WINDOWS
- TECHNOLOGICAL OPPORTUNITY
- PAYOFF IN RELIABILITY AND COST AND WEIGHT SAVINGS
- GENERIC APPLICABILITY

GIVEN THE EXISTING, SUBSTANTIAL INDUSTRY INTEREST, WHY IS AN ADVANCED DEVELOPMENT EFFORT NEEDED?

- FUNDING LEVEL REQUIRED
- INVESTIGATE SENSITIVITY TO ALTERNATIVE CONTRACTURAL REQUIREMENTS/INCENTIVES
- ESTABLISH CONTRACTURAL REQUIREMENTS/INCENTIVES
- COMPLETE CONFIDENCE TECHNICAL SCHEDULE COST
- INFORMATION TRANSFER TO ENTIRE AEROSPACE COMMUNITY
- ACCELERATE THE APPLICATION

Figure 7

CONFERENCE SUMMARY

CONFERENCE SUMMARY

- 112 attendees
- Broad representation of industry and Government
- Profound interest exists
- Considerable interchange
- Some outstanding successful applications
- Some bared souls telling of poor results - should serve as a warning to others that applications must be adequately engineered
- Avionics, black box applications look attractive
- Applications tend to be interdisciplinary
- Better design procedures are needed to reduce amount of test and fix
- Education and information dissemination needed, including management-short course in vibration damping highly desirable
- Laminated metal panels are the visible successful applications
- Research into other forms of damping is needed
- A design guide is needed
- Current and active material file is needed
- Standardized material measurement techniques should be established
- Materials needed for 400 - 700°F range
- Finite element analysis methods needed
- Research is needed into mechanism and levels of inherent damping in conventional, bonded, and composite structure
- Research is needed on effects of damping on resonant fatigue and sound and vibration transmission of structure
- Application should be accelerated to broader use in hardware designed by a vibroacoustic environment
- Development is needed to advance technology and establish confidence in integrally damped concepts

AGENDA

AGENDA

MONDAY, 6 FEBRUARY 1978

1830 REGISTRATION

TUESDAY, 7 FEBRUARY 1978

0730 REGISTRATION

0900 KEYNOTE: THE ROLE OF DAMPING TECHNOLOGY IN RELIABILITY AND LIFE CYCLE COST OF FUTURE AIR FORCE SYSTEMS
G. P. Peterson
Air Force Wright Aeronautical Laboratories

INTRODUCTION

L. C. Rogers
Air Force Flight Dynamics Laboratory

EFFECTS OF DAMPING

L. C. Rogers
Air Force Flight Dynamics Laboratory

DAMPING IN AEROSPACE STRUCTURES

J. P. Henderson
Air Force Materials Laboratory

MATERIAL BEHAVIOR AND CHARACTERIZATION

D. I. G. Jones
Air Force Materials Laboratory

MEASUREMENT OF MATERIAL AND SYSTEM DAMPING

R. Plunkett
University of Minnesota

1040 COFFEE BREAK

LAYERED DAMPING TREATMENTS
J. P. Henderson
Air Force Materials Laboratory

DISCRETE DAMPING DEVICES
D. I. G. Jones
Air Force Materials Laboratory

SURVEY OF CONSTRAINING LAYER LITERATURE
R. A. DiTaranto
Widener College

VIBRATION DAMPING ANALYSIS BY FINITE ELEMENTS

F. Bogner and R. Brockman
University of Dayton Research Institute

DAMPED VIBRATION THEORY: A STATE-OF-THE-ART ASSESSMENT

F. C. Nelson
Tufts University

DESIGN OF DAMPING TREATMENTS BY DESK TOP COMPUTER

A. D. Nashif
Anatrol

1300 LUNCH

1415 OPENING OF AFTERNOON SESSIONS

SELECTED 3M MATERIALS, PROPERTIES, ENVIRONMENTAL RESISTANCE AND APPLICATIONS

D. B. Caldwell
3M Company

SELECTED SOUNDCOAT MATERIALS AND APPLICATIONS

F. Kirschner
Soundcoat

SELECTED ANTIPHON MATERIALS AND APPLICATIONS

E. O'Keefe
Specialty Composites

SELECTED EAR MATERIALS AND APPLICATIONS

E. H. Berger
EAR Corporation

STEPS FOR APPLICATION OF DAMPING TECHNOLOGY

L. C. Rogers
Air Force Flight Dynamics Laboratory

SPATIAL AND TEMPORAL TEMPERATURE DISTRIBUTIONS

D. Paul
Air Force Flight Dynamics Laboratory

**FOURIER ANALYSIS IN THE LAB AND IN THE
THE FIELD**

M. L. Drake
University of Dayton Research Institute

LOCAL MODES FROM HOLOGRAPHY

G. Maddux
Air Force Flight Dynamics Laboratory

**A THOROUGHLY ENGINEERED APPLICATION
OF DAMPING TECHNOLOGY TO JET ENGINE
INLET GUIDE VANES**

M. C. Parin
University of Dayton Research Institute

**HIGH MODULUS GRAPHITE FIBER CON-
STRAINED LAYER DAMPING TREATMENT
FOR HEAVY AEROSPACE STRUCTURES**

J. Soovere
Lockheed-California Company

SELECTED BOEING DAMPING PROJECTS

L. D. Jacobs
The Boeing Company

**SELECTED BOEING ANALYTICAL METHODS
AND EXPERIMENTAL RESULTS**

G. Sen Gupta
The Boeing Company

1700 ADJOURNMENT OF SESSION

1800 C. O. D. SOCIAL

1900 CONFERENCE BANQUET

WEDNESDAY, 8 FEBRUARY 1978

**0800 SELECTED LOCKHEED-GEORGIA
DAMPING PROJECTS**

H. W. Bartel
Lockheed-Georgia Company

SELECTED ROCKWELL DAMPING PROJECTS

A. Tipton
Rockwell International

**MODAL DAMPING MEASUREMENTS ON
BONDED AIRFRAME STRUCTURE**

R. Gordon
Air Force Flight Dynamics Laboratory
and
J. Sharp
Aeronautical Systems Division

**DAMPING FOR ENHANCED RELIABILITY
IN VIBROACOUSTIC ENVIRONMENTS**

R. N. Hancock
Vought Corporation

**SELECTED HAMILTON STANDARD
DAMPING PROJECTS**

W. Ammerman
Hamilton Standard

SELECTED DAMPING PROJECTS

C. M. Cannon
University of Dayton Research Institute

SPACECRAFT DAMPING APPLICATIONS

J. M. Medaglia and C. V. Stahle
General Electric Company

0930 COFFEE BREAK

**VISCOELASTIC DAMPING FOR ELECTRO-
OPTICAL SYSTEMS**

S. E. Asendorf
Westinghouse Electric Corporation

DAMPING OF INERTIAL GUIDANCE SYSTEMS

D. Sullivan
Charles Draper Lab

**THE INFLUENCE OF DAMPING ON
ACOUSTIC TRANSMISSION LOSS OF PANELS**

L. L. Faulkner
Battelle

DAMPING IN ELECTRO-OPTICAL SYSTEMS

C. Liu
Hughes Aircraft Company

**MEASUREMENT OF ELASTOMER PROPER-
TIES AND APPLICATION TO VIBRATION
CONTROL**

A. J. Smalley
Mechanical Technology, Inc.

CONSUMER AND INDUSTRIAL DAMPING

APPLICATIONS

A. D. Nashif

Anatrol

**THE INFLUENCE OF VIBROACOUSTICS ON
SPACECRAFT COST AND RELIABILITY**

C. V. Stahle and H. R. Gongloff

General Electric Company

and

W. B. Keegan and J. P. Young

NASA-Goddard

**ASTM DAMPING MATERIALS TESTING
SPECIFICATION ACTIVITY**

E. E. Dennison

Gilbert/Commonwealth

**ANSI DAMPING MATERIALS TESTING
SPECIFICATION ACTIVITY**

J. P. Henderson

Air Force Materials Laboratory

AFML PLANNED DAMPING EFFORTS

J. P. Henderson

Air Force Materials Laboratory

AFFDL PLANNED DAMPING EFFORTS

L. C. Rogers

Air Force Flight Dynamics Laboratory

1130 LUNCH

1300 OPENING OF AFTERNOON SESSION

**PLANNED ADVANCED DEVELOPMENT
PROGRAM DAMP IT EFFORTS**

L. C. Rogers

Air Force Flight Dynamics Laboratory

OPEN DISCUSSION

WORKING GROUP DISCUSSIONS

WORKING GROUP REPORTS

SUMMARY

1530 CONFERENCE ADJOURNMENT

ATTENDANCE LIST

CONFERENCE ON AEROSPACE POLYMERIC
VISCOELASTIC DAMPING TECHNOLOGY
FOR THE 1980's

7-8 FEBRUARY 1978

LIST OF ATTENDEES

Wesley B. Ammerman
Applied Mechanics/Mechanical Design
Hamilton Standard Electronics Depart.
Hamilton Road
Windsor Locks, CT 06096

James A. Bair
ASD/ENFSL
Wright-Patterson Air Force Base
Ohio 45433

Ronald L. Bagley
AFIT
Aero/Astro
Wright-Patterson Air Force Base
Ohio 45433

David Baker
EAR Corporation
7911 Zionsville Road
Indianapolis, IN 46268

Stanley Barrett
Martin-Marietta Corporation
Aerospace Division
P. O. Box 179, Mail Stop 0970
Denver, CO 80201

Harold W. Bartel
Lockheed-Georgia Company
Advanced Structures
72-26, Zone 329
Marietta, GA 30063

Jacob R. Beard, Jr.
Lockheed-Georgia Company
Advanced Technology Sales
86 South Cobb Drive
Marietta, GA 30063

Elliott H. Berger
EAR Corporation
Technical
7911 Zionsville Road
Indianapolis, IN 46268

Herman V. Boenig
Lord Kinematics, Div. of Lord Corp.
Manager, Material Sciences, Res & Dev Dept.
1635 West 12th Street
Erie, PA 16512

Fred K. Bogner
University of Dayton Research Institute
300 College Park Avenue
Dayton, OH 45469

Robert A. Brockman
University of Dayton Research Institute
300 College Park Avenue
Dayton, OH 45469

George Buchhalter
University of Dayton Research Institute
300 College Park Avenue
Dayton, OH 45469

Charles L. Budde
AFWL/LRO
Kirtland Air Force Base, NM 87117

Donald B. Caldwell
3M Company
Industrial Specialties Division
3M Center, Building 230-1F
St. Paul, MN 55101

Charles M. Cannon
University of Dayton Research Institute
300 College Park Avenue
Dayton, OH 45469

Richard P. Chartoff
University of Dayton Research Institute
300 College Park Avenue
Dayton, OH 45469

Toby M. Cordell
AFML/LTN
Wright-Patterson Air Force Base, OH 45433

Carl A. Dahlquist
3M Company
Central Research Department
3M Center
St. Paul, MN 55101

E. Earl Dehnison
Gilbert/Commonwealth Association
Power Engineering Division
209 E. Washington
Jackson, MI 49203

Thomas F. Derby
Barry Controls
700 Pleasant Street
Framingham, MA 02172

Gordon L. Getline
General Dynamics
Convair Division, MZ 32-6020
P. O. Box 80847
San Diego, CA 92138

Bennie F. Dotson
Boeing Military Airplane Development
Structures Dynamics
P. O. Box 3999
Seattle, WA 98124

Richard C. Goodman
University of Dayton Research Institute
300 College Park Avenue
Dayton, OH 45469

Michael L. Drake
University of Dayton Research Institute
300 College Park Avenue
Dayton, OH 45469

Don Gordon
Aerospace Corporation
Vehicle Integrity Subdivision
2350 East El Segundo Blvd.
El Segundo, CA 90245

Paul Dunn
Aerospace Corporation
Vehicle Integrity Subdivision
2350 East El Segundo Blvd.
El Segundo, CA 90245

Robert Gordon
AFFDL/FBA
Wright-Patterson Air Force Base, OH 45433

Thomas E. Dunning, Sr.
Boeing Military Airplane Development
Structures Technology - Stress
P. O. Box 3999
Seattle, WA 98124

James L. Graham
University of Dayton Research Institute
300 College Park Avenue
Dayton, OH 45469

Joseph H. Emme
H. L. Blachford, Inc.
1855 Stephenson Highway
Troy, MI 48084

James A. Groening
H. L. Blachford, Inc.
1855 Stephenson Highway
Troy, MI 48084

Lynn L. Faulkner
Battelle
Applied Dynamics & Acoustics
505 King Avenue
Columbus, OH 43017

Edward J. Hall
Charles Stark Draper Laboratory
Navy Mechanical Design Division
555 Technology Square
Cambridge, MA 02139

William G. Flannelly
Kaman Aerospace Corporation
Research Department
Old Windsor Road
Bloomfield, CT 06002

Preston S. Hall
AFFDL/FEE
Wright-Patterson Air Force Base, OH 45433

James C. Furlong
The Boeing Company
Aerospace
P. O. Box 3999, MS 44-66
Seattle, WA 98124

William Halvorsen
Anatrol Corporation
11305 Reed Hartman High, Suite 227
Cincinnati, OH 45241

Robert N. Hancock
Vought Corporation
Vibroacoustics
P. O. Box 5907
Dallas, TX 75222

William John Hanson
Liberty Mutual Insurance Co.
Loss Prevention, Research Center
71 Franisland Road
Hopkinton, MA 01748

Daniel Hayes
AFIT/ENY
Wright-Patterson Air Force Base
Ohio 45433

J. P. Henderson
AFML/LLN
Wright-Patterson Air Force Base
Ohio 45433

Harry Himelblau
Rockwell International Corporation
Space Division
D/380-301 AB 97
Downey, CA 90241

Alan K. Hopkins
Air Force Pram Program Office
Wright-Patterson Air Force Base
Ohio 45433

Loyd D. Jacobs
The Boeing Company
P. O. Box 3999
Seattle, WA 98124

Marcus J. Jacobson
Northrop Corporation, Aircraft Group
Structural Dynamics Research
3901 W. Broadway
Hawthorne, CA 90056

Conor D. Johnson
Anamet Labs.
Applied Mechanics Division
100 Industrial Way
San Carlos, CA 94070

D. I. G. Jones
AFML/LLN
Wright-Patterson Air Force Base
Ohio 45433

Carl S. King
University of Dayton Research Institute
300 College Park Avenue
Dayton, OH 45469

Donna Knighton
AFML/LLN
Wright-Patterson Air Force Base, OH 45433

Bernard J. Korites
Arthur D. Little Inc.
Applied Mechanics
Acorn Park
Cambridge, MA 02140

Edward D. Lakin
ASD/ENFSL
Wright-Patterson Air Force Base, OH 45433

Robert H. Lamb
3M Company
Federal Government Affairs
349 W. First St., Suite 102
Dayton, OH 45402

Neal R. Langley
Dow Corning Corporation
Elastomer Research
S. Saginaw Road
Midland, MI 48640

Roy M. Law
General Motors Corporation
Detroit Diesel Allison Division
13400 W. Outer Drive
Detroit, MI 48228

Michael J. Laughlin
Pratt & Whitney Aircraft Company
Government Products Division
P. O. Box 2691, M.S. E-26
West Palm Beach, FL 33402

Chi-Long Lee
Dow Corning Corporation
Research Department
S. Saginaw Road
Midland, MI 48640

Kenneth G. Lindh
Northrop Corporation
Aircraft Division
3901 W. Broadway
Hawthorne, CA 90250

Chang P. Liu
Hughes Aircraft Company
Laser Division, 5/B136
Centinela & Teale Streets
Culver City, CA 90230

Arthur E. Lohmeyer
ASD/YEAF
Wright-Patterson Air Force Base
Ohio 45433

Y. P. Lu
David W. Taylor Naval Ship R&D Center
Machinery Dynamics Division
Code 2744
Annapolis, MD 21402

James C. MacBain
AFAPL/TBP
Wright-Patterson Air Force Base
Ohio 45433

James W. McCormick
AFAL/RWF
Wright-Patterson Air Force Base
Ohio 45433

Gene E. Maddux
AFFDL/FBEC
Wright-Patterson Air Force Base
Ohio 45433

John M. Medaglia
General Electric Company
Space Division, M 4018
P. O. Box 8555
Philadelphia, PA 19101

Vincent R. Miller
AFFDL/FBE
Wright-Patterson Air Force Base
Ohio 45433

Otto Mueller
AFFDL/FBG
Wright-Patterson Air Force Base
Ohio 45433

Robert E. Mullans
McDonnell Aircraft Company
Structural Dynamics
P. O. Box 516
St. Louis, MO 63166

Ahid D. Nashif
Anatrol Corporation
11305 Reed Hartman High, Suite 227
Cincinnati, OH 45241

Frederick C. Nelson
Tufts University
Mechanical Engineering Department
Medford, MA 02155

Michael W. Obal
AFFDL/FBG
Wright-Patterson Air Force Base, OH 45433

Warren Painter
Lockheed-California Company
Flight Sciences
P. O. Box 551, Hollywood Way
Burbank, CA 91520

Mike M. Parin
University of Dayton Research Institute
300 College Park Avenue
Dayton, OH 45469

Don B. Paul
AFFDL/FBE
Wright-Patterson Air Force Base, OH 45433

Charles H. Parr
Lord Kinematics, Div. of Lord Corp.
Manager, Research & Development Dept.
1635 West 12th Street
Erie, PA 16512

Jerome Pearson
AFFDL/FBG
Wright-Patterson Air Force Base, OH 45433

Robert C. Peller
General Dynamics
Convair Division, MZ-43-6150
P. O. Box 80847
San Diego, CA 92138

Raymond P. Peloubet
General Dynamics
Fort Worth Division
P. O. Box 748
Fort Worth, TX 76101

G. P. Peterson
AFWAL/CD
Wright-Patterson Air Force Base, OH 45433

Larry D. Pinson
NASA/Langley Research Center
Structures & Dynamics Division
Mail Stop 230
Hampton, VA 23665

Robert Plunkett
University of Minnesota
Dept. of Aerospace Eng. & Mech.
107 Aero Engineering Building
Minneapolis, MN 55455

Henry C. Pusey
Naval Research Laboratory
Shock and Vibration Information Center
Code 8404
Washington, DC 20375

Ronald J. Reynolds
AFALD/PTEE
Wright-Patterson Air Force Base
Ohio 45433

Lynn C. Rogers
AFFDL/FBA
Wright-Patterson Air Force Base
Ohio 45433

Gautam SenGupta
The Boeing Company
Noise Staff, M.S. 73-16
Seattle, WA 98124

Cecil W. Schneider
Lockheed-Georgia Company
Advanced Structures Department
Department 72-26, Zone 329
Marietta, GA 30063

Ralph M. Shimovetz
AFFDL/FBED
Wright-Patterson Air Force Base
Ohio 45433

Tony Shipley
Anatrol Corporation
11305 Reed Hartman High, Suite 227
Cincinnati, OH 45241

Bill J. Simmons
AFOSR/FJSRL
U.S. Air Force Academy, CO 80840

Jaak Soovere
Lockheed-California Company
Aeromechanics Department
D75-71, Bldg. 63,
P. O. Box 551
Burbank, CA 91520

Clyde V. Stahle, Jr.
General Electric Company
Space Division/M4018
P. O. Box 8555
Philadelphia, PA 19101

William A. Stange
AFAPL/TBP
Wright-Patterson Air Force Base, OH 45433

Daniel F. Sullivan
Charles Stark Draper Laboratory
Navy Mechanical Design Division 20F
555 Technology Square
Cambridge, MA 02139

Ronald F. Taylor
University of Dayton Research Institute
300 College Park Avenue
Dayton, OH 45469

Al G. Tipton
Rockwell International
Los Angeles Division
Los Angeles, CA 90009

Peter J. Torvik
AFIT/ENY
Wright-Patterson Air Force Base, OH 45433

Eric E. Ungar
Bolt Beranek and Newman Inc.
50 Moulton Street
Cambridge, MA 02138

Maurice R. Valine
3M Company
Ind. Specialties Division
3M Center, Bldg. 230-1
St. Paul, MN 55101

Abraham Van Kooy
Rockwell International
Space (041), Department 190
12214 Lakewood Blvd.
Downey, CA 90241

John H. Wafford
ASD/ENFSL
Wright-Patterson Air Force Base, OH 45433

Joe W. White
3M Company
Industrial Specialties Division
3M Center, 230-1F
St. Paul, MN 55101

Dale H. Whitford
University of Dayton Research Institute
300 College Park Avenue
Dayton, OH 45469

Robert F. Wilkus
ASD/ENFSL
Wright-Patterson Air Force Base
Ohio 45433

John R. Williamson
AFFDL/FBA
Wright-Patterson Air Force Base, OH 45433

Howard F. Wolfe
AFFDL/FBED
Wright-Patterson Air Force Base, OH 45433

William E. Zins
Kaman Aerospace Corporation
Marketing Department
Old Windsor Road
Bloomfield, CT 06002

LATE REGISTRANTS

Pete Allen
Industrial Associates
8947 Lima Road
Fort Wayne, IN 46708

Stephen E. Asendorf
Westinghouse Electric Corporation
Mech. Des. & Dev.
System Dev. Div.
Box 746
Baltimore, MD 21203

Gunnar Ekstrand
Specialty Composites Corp.
Antiphon Products
650 Dawson Drive
Newark, DE 19713

Louis J. Kiraly
NASA/Structures Section
21000 Brookpark Road
Cleveland, OH 44135

Edmund J. O'Keefe
Specialty Composites Corp.
Acoustics R&D
Delaware Industrial Park
Newark, DE 19713

George W. Reynolds
Westinghouse Electric Corp.
SDD, P. O. Box 746
Baltimore, MD 21203

Anthony J. Smalley
Mechanical Technology Inc.
Machinery Dynamics Section
968 Albany-Shaker Road
Latham, NY 12110